

2011 Atomic, Molecular, Optical Sciences Research Meeting



**Airline Conference Center
Warrenton, Virginia
September 6-9, 2011**



U.S. DEPARTMENT OF
ENERGY

Office of
Science

Office of Basic Energy Sciences
Chemical Sciences, Geosciences &
Biosciences Division

Foreword

This volume summarizes the 31st annual Research Meeting of the Atomic, Molecular and Optical Sciences (AMOS) Program sponsored by the U. S. Department of Energy (DOE), Office of Basic Energy Sciences (BES), and comprises descriptions of the current research sponsored by the AMOS program. The participants of this meeting include all of the DOE laboratory and university principal investigators (PIs) within the BES AMOS Program. The purpose is to facilitate scientific interchange among the PIs and to promote a sense of program identity.

The BES/AMOS program is vigorous and innovative, and enjoys strong support within the Department of Energy. This is due entirely to our scientists, the outstanding research they perform, and the relevance of this research to DOE missions. FY 2011 has been an exciting year for BES and the research community. Continuing initiatives included the Early Career Research Program, the Energy Frontier Research Centers and the Energy Innovation Hubs. As illustrated in this volume, the AMOS community continues to explore new scientific frontiers relevant to the DOE mission and the strategic challenges facing our nation and the world.

We are deeply indebted to the members of the scientific community who have contributed their valuable time toward the review of proposals and programs, either by mail review of grant applications, panel reviews, or on-site reviews of our multi-PI programs. These thorough and thoughtful reviews are central to the continued vitality of the AMOS program.

We are privileged to serve in the management of this research program. In performing these tasks, we learn from the achievements of, and share the excitement of, the research of the scientists and students whose work is summarized in the abstracts published on the following pages.

Many thanks to the staff of the Oak Ridge Institute for Science and Education (ORISE), in particular Connie Lansdon, and Tim Ledford, and to the Airlie Conference Center for assisting with the meeting. We also thank Diane Marceau, Robin Felder, and Michaelena Kyler-King in the Chemical Sciences, Geosciences, and Biosciences Division for their indispensable behind-the-scenes efforts in support of the BES/AMOS program. We also appreciate Mark Pederson's coordination of computational resources and interactions with related DOE program offices.

Jeffrey L. Krause
Michael P. Casassa
Chemical Sciences, Geosciences and Biosciences Division
Office of Basic Energy Sciences
Department of Energy

**Cover Art Courtesy of Diane Marceau
Chemical Sciences, Geosciences and Biosciences
Division, Basic Energy Sciences, DOE**

**This document was produced under contract number DE-AC05-06OR23100
between the U.S. Department of Energy and Oak Ridge Associated Universities.**

**The research grants and contracts described in this document are supported by the
U.S. DOE Office of Science, Office of Basic Energy Sciences, Chemical Sciences,
Geosciences and Biosciences Division.**

Agenda

2011 Meeting of the Atomic, Molecular and Optical Sciences Program
Office of Basic Energy Sciences
U. S. Department of Energy

Airlie Center, Warrenton, Virginia, September 6-9, 2011

Tuesday, September 6

3:00-6:00 pm **** Registration ****
6:00 pm **** Reception (No Host) ****
7:00 pm **** Dinner ****

Wednesday, September 7

7:30 am **** Breakfast ****

8:45 am *Welcome and Introductory Remarks*
Jeff Krause, BES/DOE

Session I Chair: **Tom Weinacht**

9:00 am *Laser Control of Molecular Alignment and Bond Strength*
Phil Bucksbaum, SLAC National Accelerator Laboratory

9:30 am *Theory and Simulations of Nonlinear X-ray Spectroscopy of Molecules*
Shaul Mukamel, University of California, Irvine

10:00 am *Using Strong Optical Fields to Manipulate and Probe Coherent Molecular Dynamics*
Bob Jones, University of Virginia

10:30 am **** Break ****

11:00 am *Attosecond (IR/EUV Pump-Probe) Experiments using the Full Power of COLTRIMS*
Lew Cocke, Kansas State University

11:30 am *Ultrafast X-ray Probes of Laser-Controlled Molecules*
Elliot Kanter, Argonne National Laboratory

12:00 noon *Non-Born-Oppenheimer Dynamics in Electronically-Excited Polyatomic Molecules*
Ali Belkacem, Lawrence Berkeley National Laboratory

12:30 pm **** Lunch ****

Session II Chair: **Carlos Trallero**

4:00 pm *Resonant Nonlinear X-ray Interactions at High Intensity*

Bertold Krässig, Argonne National Laboratory

4:30 pm *Attosecond Transient Absorption Spectroscopy*

Zenghu Chang, Kansas State University

5:00 pm *Generation of Bright Soft X-ray Laser Beams*

Jorge Rocca, Colorado State University

5:30 pm *Atomic and Molecular Physics in Strong Fields*

Shih-I Chu, University of Kansas

6:00 pm ***** Reception (No Host) *****

6:30 pm ***** Dinner *****

Thursday, September 8

7:30 am ***** Breakfast *****

Session III Chair: **Dan Haxton**

8:30 am *Nonperiodic Imaging at the LCLS*

Mike Bogan, SLAC National Accelerator Laboratory

9:00 am *Structure and Dynamics from Ultralow Signal Random Sightings of Evolving Systems*

Abbas Ourmazd, University of Wisconsin-Milwaukee

9:30 am *High Intensity Femtosecond XUV Pulse Interactions with Atomic Clusters*

Todd Ditmire, University of Texas at Austin

10:00 am *Attosecond Science: Generation, Metrology and Application*

Lou DiMauro, Ohio State University

10:30 am ***** Break *****

11:00 am *Femtosecond EUV Photoelectron and Ion Imaging of Ultrafast Relaxation Dynamics in Helium Nanodroplets*

Oliver Gessner, Lawrence Berkeley National Laboratory

11:30 am *Coherent and Incoherent Transitions*

Francis Robicheaux, Auburn University

12:00 noon *Attosecond Time-Resolved Photoelectron Emission from Solids and Gases*

Uwe Thumm, Kansas State University

12:30 pm ***** Lunch *****

Session IV Chair: **Veit Elser**

- 4:00 pm *Inner-Valence Ionization and Dissociative Electron Attachment*
Tom Rescigno, Lawrence Berkeley National Laboratory
- 4:30 pm *Resonant and Nonresonant Photoelectron-Vibrational Coupling*
Robert Lucchese, Texas A&M University
- 5:00 pm *Theory of Atomic Collisions and Dynamics*
Joe Macek, University of Tennessee and Oak Ridge National Laboratory
- 5:30 pm *Reaction Imaging and the Molecular Coulomb Continuum*
Jim Feagin, California State University, Fullerton
- 6:00 pm ***** Reception (No Host) *****
- 6:30 pm ***** Dinner *****

Friday, September 9

- 7:30 am ***** Breakfast *****

Session V Chair: **Matthias Kling**

- 8:30 am *Femtosecond and Attosecond Laser-Pulse Energy Transformation and Concentration in Nanostructured Systems*
Mark Stockman, Georgia State University
- 9:00 am *Antenna-Coupled Emission from Single Quantum Systems*
Lukas Novotny, University of Rochester
- 9:30 am *Nonlinear Materials Spectroscopies Probed by Ultrafast X-rays*
Keith Nelson, MIT
- 10:00 am ***** Break *****
- 10:30 am *Control of Molecular Dynamics: Algorithms for Design and Implementation*
Hersch Rabitz, Princeton University
- 11:00 am *Heavy and Aligned: Rotational Wavepacket Dynamics with a Million Atom Spinor Bose-Einstein Condensate*
Chandra Raman, Georgia Tech
- 11:30 am *Closing Remarks*
Jeff Krause, BES/DOE
- 11:45 am ***** Lunch *****
- 1:00 pm Discussion
- 3:00 pm Adjourn

Table of Contents

Laboratory Research Summaries (by institution)

AMO Physics at Argonne National Laboratory	1
<i>Hidden Resonances and Nonlinear X-ray Processes at High Intensities</i> Elliot Kanter	2
<i>Nonlinear Atomic Response to Intense Ultrashort X-rays</i> Linda Young.....	3
<i>Measuring LCLS X-ray Pulse Duration using Two Color Laser–X-ray Pump Probe Methods</i> Gilles Doumy	4
<i>Double Core-Hole Electron Spectroscopy of Formamide</i> Steve Southworth	5
<i>Impact of Hollow-Atom Formation on Coherent X-ray Scattering at High Intensity</i> Robin Santra.....	6
<i>High-Order Harmonic Generation Enhanced by X-rays</i> Christian Buth.....	6
<i>Optical Control of X-ray Lasing</i> Christian Buth.....	7
<i>Ultrafast Absorption of Intense X-rays by Nitrogen Molecules</i> Christian Buth.....	8
<i>Time-Dependent Resonance Fluorescence</i> Christian Buth.....	9
<i>Decoherence in Attosecond Photoionization</i> Robin Santra.....	9
<i>X-ray Scattering from Laser-Aligned Molecules–Experiment</i> Bertold Krässig.....	10
<i>Development of High-Repetition-rate Laser Pump/X-ray Probe Methodologies for Synchrotron Facilities</i> Gilles Doumy	11
<i>Capturing Ultrafast Dynamics of Molecules with X-ray Absorption, X-ray Emission, and X-ray Scattering</i> Steve Southworth	12

<i>Optical Trapping and X-ray Imaging of Nanoparticles</i> Matt Pelton and Norbert Scherer	13
<i>Interatomic Coulombic Decay (ICD) in Deep Inner-Shell Vacancy Cascades</i> Bob Dunford	14
<i>Progress toward a Short Pulse X-ray Facility (SPX) at the Advanced Photon Source</i> Linda Young	15
J.R. Macdonald Laboratory - Overview 2011	21
<i>Structure and Dynamics of Atoms, Ions, Molecules, and Surfaces: Molecular Dynamics with Ion and Laser Beams</i> Itzik Ben-Itzhak	23
<i>Probing Sub-cycle Excitation Dynamics with Isolated Attosecond Pulses</i> Zenghu Chang	27
<i>Structure and Dynamics of Atoms, Ions, Molecules and Surfaces: Atomic Physics with Ion Beams, Lasers and Synchrotron Radiation</i> Lew Cocke	31
<i>Atoms and Molecules in Intense Laser Pulses</i> Brett Esry	35
<i>Control and Tracing of Attosecond Electron Dynamics in Atoms, Molecules and Nanosystems in Few-Cycle Laser Fields</i> Matthias Kling	39
<i>Controlling Rotations of Asymmetric Top Molecules: Methods and Applications</i> Vinod Kumarappan	43
<i>Strong Field Rescattering Physics and Attosecond Physics</i> Chii-Dong Lin	47
<i>Structure and Dynamics of Atoms, Ions, Molecules and Surfaces: Atomic Physics with Ion Beams, Lasers and Synchrotron Radiation</i> Uwe Thumm	51
<i>Strong-Field Time-Dependent Spectroscopy and Quantum Control</i> Carlos Trallero	55

Atomic, Molecular and Optical Sciences at Los Alamos National Laboratory.....	59
<i>Engineered Electronic and Magnetic Interactions in Nanocrystal Quantum Dots</i> Victor Klimov	59
Atomic, Molecular and Optical Sciences at LBNL	63
<i>Inner-Shell Photoionization and Dissociative Electron Attachment to Small Molecules</i> Ali Belkacem and Thorsten Weber	64
<i>Electron-Atom and Electron-Molecule Collision Processes</i> Tom Rescigno and Bill McCurdy	68
Ultrafast X-ray Science Laboratory at LBNL.....	73
<i>Soft X-ray High Harmonic Generation and Applications in Chemical Physics</i> Oliver Gessner	73
<i>Ultrafast X-ray Studies of Condensed Phase Molecular Dynamics</i> Robert Schoenlein	74
<i>Time-Resolved Studies and Nonlinear Interaction of Femtosecond X-rays with Atoms and Molecules</i> Thorsten Weber and Ali Belkacem	75
<i>Theory and Computation</i> Bill McCurdy and Martin Head-Gordon	77
<i>Attosecond Atomic and Molecular Science</i> Steve Leone and Dan Neumark	78
PULSE: The PULSE Institute for Ultrafast Energy Science at SLAC.....	83
<i>Strong Field Control of Coherence in Molecules and Solids</i> Phil Bucksbaum and David Reis	86
<i>High Harmonic Generation and Electronic Structure</i> Markus Gühr and Todd Martinez and Phil Bucksbaum.....	90
<i>Nonperiodic Imaging at the Stanford PULSE Institute</i> Mike Bogan.....	94
<i>Solution Phase Chemistry</i> Kelly Gaffney.....	98

University Research Summaries (by PI)

<i>Coherent Control of Electron Dynamics</i> Andreas Becker	101
<i>Probing Complexity using the LCLS and the ALS</i> Nora Berrah	105
<i>Reactive Scattering of Ultracold Molecules</i> John Bohn	109
<i>Ultrafast Electron Diffraction from Aligned Molecules</i> Martin Centurion	113
<i>Atomic and Molecular Physics in Strong Fields</i> Shih-I Chu	117
<i>Formation of Ultracold Molecules</i> Robin Côté	121
<i>Optical Two-Dimensional Spectroscopy of Disordered Semiconductor Quantum Wells and Quantum Dots</i> Steve Cundiff	125
<i>Theoretical Investigations of Atomic Collision Physics</i> Alex Dalgarno	129
<i>Understanding and Controlling Strong-Field Laser Interactions with Polyatomic Molecules</i> Marcos Dantus	133
<i>Production and Trapping of Ultracold Polar Molecules</i> Dave DeMille	137
<i>Attosecond and Ultrafast X-ray Science</i> Lou DiMauro and Pierre Agostini	141
<i>Imaging of Electronic Wave Functions during Chemical Reactions</i> Lou DiMauro, Pierre Agostini and Terry Miller	145
<i>High Intensity Femtosecond XUV Pulse Interactions with Atomic Clusters</i> Todd Ditmire	149
<i>Ultracold Molecules: Physics in the Quantum Regime</i> John Doyle	153

<i>Atomic Electrons in Strong Radiation Fields</i>	
Joe Eberly	157
<i>Algorithms for X-ray Imaging of Single Particles</i>	
Veit Elser	161
<i>Reaction Imaging and the Molecular Coulomb Continuum</i>	
Jim Feagin	165
<i>Studies of Autoionizing States Relevant to Dielectronic Recombination</i>	
Tom Gallagher	169
<i>Experiments in Ultracold Collisions and Ultracold Molecules</i>	
Phil Gould	173
<i>Physics of Correlated Systems</i>	
Chris Greene	177
<i>Using Strong Optical Fields to Manipulate and Probe Coherent Molecular Dynamics</i>	
Bob Jones	181
<i>Molecular Dynamics Probed by Coherent Electrons and X-rays</i>	
Henry Kapteyn and Margaret Murnane	185
<i>Imaging Multi-particle Atomic and Molecular Dynamics</i>	
Allen Landers	189
<i>Properties of Actinide Ions from Measurements of Rydberg Ion Fine Structure</i>	
Steve Lundeen	193
<i>Theory of Atomic Collisions and Dynamics</i>	
Joe Macek	197
<i>Photoabsorption by Free and Confined Atoms and Ions</i>	
Steve Manson	201
<i>Combining High Level Ab Initio Calculations with Laser Control of Molecular Dynamics</i>	
Spiridoula Matsika and Tom Weinacht	205
<i>Electron-Driven Processes in Polyatomic Molecules</i>	
Vince McKoy	209
<i>Electron/Photon Interactions with Atoms/Ions</i>	
Alfred Msezane	213
<i>Theory and Simulations of Nonlinear X-ray Spectroscopy of Molecules</i>	
Shaul Mukamel	217

<i>Nonlinear Photoacoustic Spectroscopies Probed by Ultrafast EUV Light</i> Keith Nelson	221
<i>Antenna-Coupled Light-Matter Interactions</i> Lukas Novotny	225
<i>Electron and Photon Excitation and Dissociation of Molecules</i> Ann Orel	229
<i>Low-Energy Electron Interactions with Liquid Interfaces and Biological Targets</i> Thom Orlando	233
<i>Structure from Fleeting Illumination of Faint Spinning Objects in Flight</i> Abbas Ourmazd and Peter Schwander	237
<i>Energetic Photon and Electron Interactions with Positive Ions</i> Ron Phaneuf	241
<i>Molecular Photoionization Studies of Nucleobases and Correlated Systems</i> Erwin Poliakoff and Robert Lucchese	245
<i>Control of Molecular Dynamics: Algorithms for Design and Implementation</i> Hersch Rabitz and Tak-San Ho	249
<i>Ultracold Sodium and Rubidium Mixtures: Collisions, Interactions and Heteronuclear Molecule Formation</i> Chandra Raman	253
<i>Coherent and Incoherent Transitions</i> Francis Robicheaux	255
<i>Generation of Bright Soft X-ray Laser Beams</i> Jorge Rocca	259
<i>Ultrafast Holographic X-ray Imaging and its Application to Picosecond Ultrasonic Wave Dynamics in Bulk Materials</i> Christoph Rose-Petruck	263
<i>New Directions in Intense-Laser Alignment</i> Tamar Seideman	267
<i>New Scientific Opportunities through Inelastic X-ray Scattering at 3rd- and 4th-Generation Light Sources</i> Jerry Seidler	271

<i>Dynamics of Few-Body Atomic Processes</i>	
Tony Starace	275
<i>Femtosecond and Attosecond Laser-Pulse Energy Transformation and Concentration in Nanostructured Systems</i>	
Mark Stockman	279
<i>Laser-Produced Coherent X-ray Sources</i>	
Don Umstadter	283
<i>Cold and Ultracold Polar Molecules</i>	
Jun Ye	287
Author Index	289
Participants	291

Laboratory Research Summaries
(by institution)

AMO Physics at Argonne National Laboratory

C. Buth, G. Doumy, R. W. Dunford, E. P. Kanter, B. Krässig, S. H. Southworth, and L. Young

Argonne National Laboratory, Argonne, IL 60439

cbuth@anl.gov, gdoumy@aps.anl.gov, dunford@anl.gov, kanter@anl.gov,

kraessig@anl.gov, southworth@anl.gov, young@anl.gov

Overview

The Argonne AMO physics program aims at a quantitative understanding of x-ray interactions with atoms and molecules from the weak-field limit explored at the Advanced Photon Source (APS) to the strong-field regime accessible at the Linac Coherent Light Source (LCLS). Tunable, polarized, high-repetition-rate x-ray pulses at the APS are used to probe the time-dependent response of atoms and molecules to ultrafast and intense optical laser pulses. Examples of the phenomena that are studied include strong-field ionization, spatial alignment of molecules in laser fields, and optical excitation of charge-transfer complexes in solution. To exploit the full x-ray flux available at the APS, we have developed a high-repetition-rate laser system for pump-probe experiments at MHz pulse rates. The first applications were to record x-ray absorption, x-ray emission, and x-ray diffuse scattering of metal-ligand charge-transfer in laser-excited, solvated molecules. Detailed characterizations result from the combined x-ray techniques. High-repetition-rate methods will optimize the use of picosecond x-ray pulses for time-resolved research at the Short Pulse X-ray (SPX) facility being developed within the APS-Upgrade project. SPX is progressing through a series of technical and scientific reviews of the beamlines, end stations, and research programs. Other APS projects include development of an x-ray scattering probe of laser-aligned molecules, studies of dissociative molecular ionization following deep inner-shell x-ray absorption, and diffuse x-ray scattering by laser-trapped and aligned nanoparticles in solution. Theory is a key component of our research program by predicting phenomena that motivate experiments and by simulating measured results.

Experimental activities at the LCLS include measurements of a two-photon/two-electron resonant process, observation of the nonlinear atomic response to intense ultrashort x rays, use of two-color optical-laser/x-ray techniques to characterize LCLS pulses, and electron spectroscopy studies of double core holes in molecules. Intense x-ray interactions with atoms and molecules provides fertile ground for theoretical exploration, particularly in combination with optical lasers. Several theoretical ideas are being developed that will lead to proposals for experimental investigations.

High-intensity x-ray experiments at LCLS

Hidden resonances and nonlinear x-ray processes at high intensities (E.P. Kanter, B. Krässig, G. Doumy, A. M. March, P. Ho, S.H. Southworth, L. Young, Y. Li,¹ N. Rohringer,² R. Santra,^{3,4} L. F. DiMauro,⁵ C. A. Roedig,⁵ N. Berrah,⁶ L. Fang,⁶ M. Hoener,⁶ P. H. Bucksbaum,⁷ S. Ghimire,⁷ D. A. Reis,⁷ J. D. Bozek,⁸ C. Bostedt,⁸ M. Messerschmidt⁸)

The first experiments at LCLS all studied photon-matter interactions in a continuum, in principle, far removed from resonances. In this later study, we focused instead on resonant interactions. Resonances provide interaction strengths that are more than 1000-fold larger than those in the continuum and the ability to selectively address quantum states. Specifically, with resonant x-rays at extreme intensities approaching 10^{18} W/cm², Rabi cycling can effectively compete with Auger decay and directly modify the branching between decay channels. Here, starting with a neutral neon target, we used ultraintense, high-fluence x-ray pulses from the LCLS to first reveal and subsequently drive the “hidden” $1s \rightarrow 2p$ resonance in singly-ionized neon and thus demonstrate the ability to modify femtosecond Auger decay. Our work illustrates the complexities associated with using ultraintense, high-fluence x-ray pulses as a controlled probe of matter and is a first step toward photonic control of inner-shell electrons.

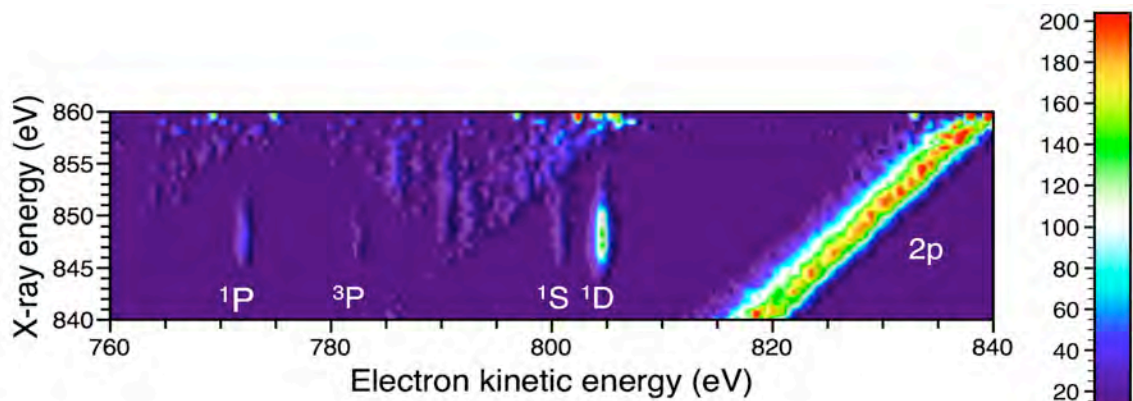


Fig. 1. Map of electron emission from neon vs. x-ray energy. X-ray pulses ($0.3 \text{ mJ} \times 20\%$, 8.5 fs) were focused to $\sim 2 \text{ } \mu\text{m}^2$ in a neon gas jet target. The prominent diagonal line is due to $2p$ photoelectron emission that creates a $2p$ hole in Ne^+ . The structures at fixed kinetic energies are formed by Auger decay electrons after creation of a $1s$ hole via the $\text{Ne}^+ 1s \rightarrow 2p$ resonance at 848 eV and are labeled by their final state configurations. The additional higher-lying vertical lines represent similar Auger decays in higher charge state ions while the diagonal features are photoelectron correlation satellites

Resonances can be used to enhance x-ray multiphoton processes. At photon energies less than the binding energy of the $1s$ electron, *resonant* two-photon absorption has a significantly larger cross section than *non-resonant* two-photon absorption; though both generate the same final state of the system - an atom with a $1s$ hole plus an *s*- or *d*- wave photoelectron. Capitalizing on this resonance phenomenon, we have studied two-photon absorption in neon at 848 eV , where, as we have demonstrated, the first photon ionizes the $\text{Ne } 2p$ electron and the second photon excites the $\text{Ne}^+ 1s-2p$ resonance, refilling that $2p$ vacancy. $\text{Ne}^+ 1s^{-1} K\text{-LL}$ Auger electrons are the signature of this resonant two-photon creation of a $1s$ hole (see Fig. 1). This generation of a $2p$ hole

orbital is advantageous for observing/studying the Rabi-cycling phenomenon; the Ne^+ $1s$ - $2p$ dipole matrix element is $5.6\times$ larger than that for the $1s$ - $3p$ transition in neutral Ne.

We have followed the response of the neon atom on this two photon resonance at 848 eV as a function of x-ray FEL pulse width. For narrow x-ray pulses, the signature of $1s$ hole creation is weak, but as the pulse width is raised, the Auger line appears and, at high intensity, is broadened as Rabi-oscillations become important in comparison to the normal diagram line (1D) measured far above threshold. Indeed, as expected for the $1s$ - $3p$ transition, no such broadening was detected. At high x-ray intensities, Rabi oscillations can be studied and at lower x-ray intensities alignment of the Ne^+ $2p$ hole state can be studied.

A report on this work is given in Ref. [1] and illustrates the nuances associated with using high-fluence, high-intensity femtosecond x-ray pulses for controlled investigations of material properties. We demonstrate that high-fluence x-ray pulses reveal otherwise hidden resonances through sequential valence ionization. The consequences of photoexciting these resonances are that they 1) break open inner shells, at unexpectedly low photon energies, i.e. below the $1s$ -threshold, and 2) can unleash damaging Auger electron cascades. These phenomena must be considered in the design of all future XFEL experiments. We further demonstrated that a strong, incoherent SASE pulse can induce Rabi-cycling on a deep inner-shell transition and thus modify Auger decay. Control of inner-shell electron dynamics should be markedly enhanced with soon-to-be-available longitudinally-coherent x-ray pulses.

Nonlinear atomic response to intense ultrashort x rays (G. Doumy, L. Young, E. P. Kanter, B. Krässig, S.-K. Son,³ R. Santra,^{3,4} N. Rohringer,² P. Agostini,⁵ L. F. DiMauro,⁵ C. A. Roedig,⁵ C. I. Blaga,⁵ A. DiChiara,⁵ N. Berrah,⁶ L. Fang,⁶ M. Hoener,⁶ M. Kuebel,⁹ G. G. Paulus,⁹ P. H. Bucksbaum,⁷ J. P. Cryan,⁷ S. Ghimire,⁷ J. M. Glowina,⁷ D. A. Reis,⁷ J. D. Bozek,⁸ C. Bostedt,⁸ M. Messerschmidt⁸)

Since the first demonstration of optical non linearity by Franken and collaborators 50 years ago, the study of non linear optics has been extended successfully from the microwave to the extreme UV. In the x-ray regime, dwindling cross-sections and the absence of suitable intense sources had confined it to purely theoretical considerations. With the LCLS delivering intense, ultrashort x-ray pulses reaching intensities above 10^{17} W/cm² with focusing optics, the situation has changed.

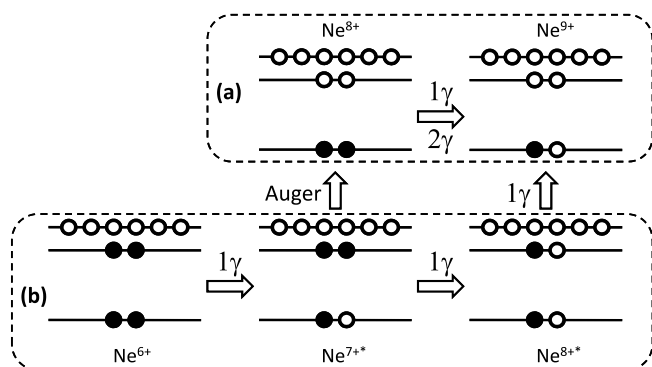


Fig. 2. Illustration of Ne^{9+} production. (a) Direct process through one-photon (1γ) or two-photon (2γ) ionization of Ne^{8+} , depending on the photon energy. (b) Indirect process first ionizes Ne^{6+} into Ne^{7+*} excited state. Before Auger decay occurs, which would otherwise direct through (a), a valence electron is photoionized to produce Ne^{8+*} that can also be subsequently ionized into Ne^{9+} .

In order to realize the first experimental study of nonlinearities in the x-ray regime, we used an atomic target, Neon, in order to keep a simple enough system, and because the electron binding energies were very well suited to the range offered by the AMO endstation where the

first experiments took place. Because a single x-ray pulse can easily strip several electrons from an atom, we also had to center our study on Helium-like Neon ions, which were produced during the x-ray pulse itself. There, we studied how the ionization of a K-shell electron from Ne^{8+} behaves as a function of pulse energy, for photon energies below and above the K-shell ionization threshold (1196 eV).

We clearly demonstrated how, above threshold, the behavior is linear, while below threshold, it becomes quadratic. Careful study of the mechanisms with the help of very accurate modeling including simple rate equations and shake-off processes identified 2 different competing nonlinear mechanisms below threshold. A dominant, direct 2-photon, one electron process, and a sequential, 2-photon 2-electron process involving transient excited states that becomes relevant because the pulse duration is short enough to compete with the Auger decay clock. In addition, we found that we needed to use a 2-photon cross section more than 2 orders of magnitude larger than previously calculated in order to reproduce completely our results. We attribute the discrepancy to a neglected effect of a nearby electronic resonance. This work has been published [5] and highlighted in Physics: <http://physics.aps.org/synopsis-for/10.1103/PhysRevLett.106.083002>

Measuring LCLS x-ray pulse duration using two color laser-x-ray pump probe methods (G. Doumy, S. Düsterer,¹⁰ P. Radcliffe,¹¹ C. Bostedt,⁸ J. Bozek,⁸ A. L. Cavalieri,³ R. Coffee,⁸ J. T. Costello,¹² D. Cubaynes,¹³ L. DiMauro,⁵ Y. Ding,⁸ W. Helml,^{14,15} W. Schweinberger,¹⁴ R. Kienberger,^{14,15} A. R. Maier,^{14,16} M. Messerschmidt,⁸ V. Richardson,¹² C. Roedig,⁵ T. Tschentscher,¹¹ M. Meyer^{11,13})

The first x-ray free electron laser, LCLS, has started delivering pulses with unprecedented intensities, in part because of the short pulse duration, in the range of a few to several hundred femtoseconds. Both for experiments involving only the x-ray pulse, and for pump-probe experiments studying time resolved phenomena on the femtosecond time scale, the x-ray pulse duration is a crucial parameter that is not yet experimentally accessible to users. A series of experiments carried out by a large collaboration has started exploring diagnostics methods involving the interaction of the x-ray pulses with atomic targets in the presence of a

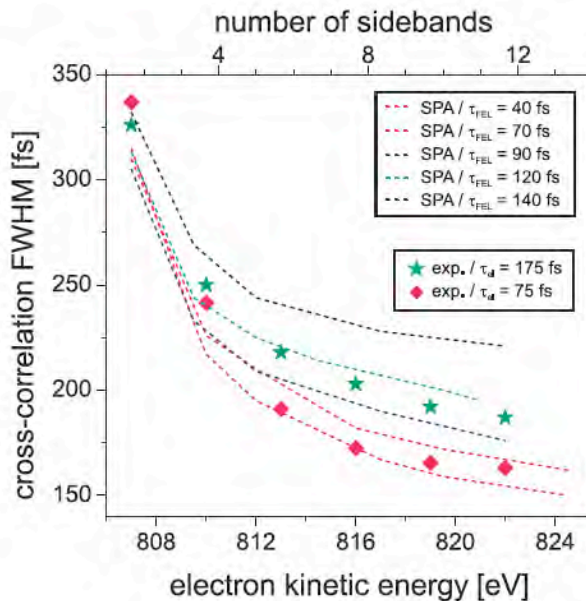


Fig. 3. Comparison of the experimentally obtained cross-correlation widths with those calculated using the soft-photon simulation using the following parameters (in FWHM): $\tau_{\text{FEL}} = 40 - 150$ fs, $\tau_{\text{NIR}} = 100$ fs, $\tau_{\text{JITTER}} = 140$ fs, $I_{\text{NIR}} = 1.2 \times 10^{12} \text{ Wcm}^{-2}$.

strong infrared laser field, in two different regimes of operation of the LCLS: so-called low bunch charge (20 pC), with expected pulses of less than 5 fs, and high bunch charge (250 pC), with pulse durations expected between 70 and 300 fs.

The common principle those experiments are based on is the ability of the strong infrared field to modulate the energy of electrons produced either by photoionization from the x-ray pulse, or from the subsequent Auger decay. In the long pulse regime, this modulation results in the production of spectral sidebands around the electron peak. The number and intensity of those sidebands depends on the laser intensity. Because the LCLS is a chaotic source, there are several sources of timing jitter between the x-ray and laser pulses. One consequence is that the number of sidebands varies shot to shot. A statistical analysis of the number of sidebands observed yielded a value of $t_{\text{jitter}} = 140$ fs. In addition, one can then also retrieve an average value for the pulse duration by comparing with modeling, as shown in Fig. 3, where the experimental results are compared with simulations using different values for the x-ray pulse duration. One interesting point is that the measurements suggest that the x-ray pulse duration is often shorter than the measured electron bunch pulse duration (40 fs instead of 75 fs, and 120 fs instead of 175 fs). Those results have been recently submitted to New Journal of Physics [2]. In the short pulse regime, the situation changes if the pulse duration can be of the order of a half period of the laser. Using an OPA delivering pulses at 2.4 mm (period of 8 fs), we were indeed able to demonstrate that regime. The timing jitter considerations here again limit the amount of information that can be extracted on a single shot basis, but we are still able to conclude on an upper value of 5 fs for the pulses in the low bunch charge regime. Those results are still under analysis, and publication is expected later this year.

Double core-hole electron spectroscopy of formamide (S. H. Southworth, G. Doumy, D. Ray, E. P. Kanter, B. Krässig, L. Young, Y. Li,¹ J. Kuepper,^{3,4} J. D. Bozek,⁸ C. Bostedt,⁸ M. Messerschmidt,⁸ N. Berrah,⁶ L. Fang,⁶ B. Murphy,⁶ T. Osipov,⁶ J. Cryan,⁷ J. Glowia,⁷ S. Ghimire,⁷ R. Santra,^{3,4} N. V. Kryzhevoi,¹⁷ L. S. Cederbaum¹⁷)

Several of the first LCLS experiments on atoms and molecules demonstrated that intense, femtosecond x-ray pulses produce double core holes (DCHs) by absorbing two photons sequentially prior to Auger decay. The lifetimes of single *K*-shell vacancies on C, N, and O are in the range $\sim 5 - 7$ fs. In LCLS experiments on atomic neon, we observed the double-core-hole/single-core-hole ratio to be as high as $\sim 10\%$, which is $\sim 30\times$ larger than the $\sim 0.3\%$ ratio produced by electron correlation in a one-photon process. In molecules, there are two types of DCHs - those on the same atomic site and those on different sites. The two-site DCHs are particularly interesting, because the two-hole electron binding energies are sensitive to the chemical environment and electron correlations. We conducted an LCLS experiment to search for DCHs in the electron spectra of formamide, HCONH_2 , to compare with calculated DCH binding energies at the C, O, and N sites of the molecule. It is challenging to experimentally measure DCH features in photoelectron and Auger-electron spectra due to the strong one-photon and shakeup/shakeoff contributions to the spectra. We varied the LCLS pulse energy, pulse duration, and x-ray micro-focusing to optimize observation of DCH features distinct from backgrounds. Data analysis is in progress, but the first results on the test molecule N_2 are encouraging. We observe distinct one-site and two-site DCH peaks in the photoelectron spectra of N_2 that agree well with calculated binding energies. The next step in the data analysis is to observe DCH features in the electron spectra of formamide for comparison with the *ab initio* calculated binding energies.

Impact of hollow-atom formation on coherent x-ray scattering at high intensity

(Sang-Kil Son,³ Linda Young, Robin Santra^{3,4})

X-ray free-electron lasers (FELs) are promising tools for structural determination of macromolecules via coherent x-ray scattering. During ultrashort and ultraintense x-ray pulses with an atomic-scale wavelength, samples are subject to radiation damage and possibly become highly ionized, which may influence the quality of x-ray scattering patterns. We develop a toolkit to treat detailed ionization, relaxation, and scattering dynamics for an atom within a consistent theoretical framework. The coherent x-ray scattering problem including radiation damage is investigated as a function of x-ray FEL parameters such as pulse length, fluence, and photon energy. We find that the x-ray scattering intensity saturates at a fluence of $\sim 10^7$ photon/ \AA^2 per pulse but can be maximized by using a pulse duration much shorter than the time scales involved in the relaxation of the inner-shell vacancy states created. Under these conditions, both inner-shell electrons in a carbon atom are removed, and the resulting hollow atom gives rise to a scattering pattern with little loss of quality for a spatial resolution $> 1\text{\AA}$. Our numerical results predict that in order to scatter from a carbon atom 0.1 photon per x-ray pulse, within a spatial resolution of 1.7\AA , a fluence of 1×10^7 photons/ \AA^2 per pulse is required at a pulse length of 1 fs and a photon energy of 12 keV. By using a pulse length of a few hundred attoseconds, one can suppress even secondary ionization processes in extended systems. The present published results [6] suggest that high-brightness attosecond x-ray FELs would be ideal for single-shot imaging of individual macromolecules.

High-order harmonic generation enhanced by x rays (C. Buth, M. C. Kohler,¹⁸ J. Ullrich,^{2,18} C. H. Keitel¹⁸)

We consider the case of x rays combined with an optical laser which is sufficiently intense to ionize krypton [3] or neon atoms. The atoms emit high harmonic generation (HHG) light produced by an initial tunnel ionization of a valence electron, a propagation of the liberated electron in the continuum, and eventual recombination with the hole under emission of a high-harmonic photon. Additional x rays, e.g., from the Linac Coherent Light Source (LCLS), are chosen to resonantly excite a core electron into the transient valence vacancy that is created in

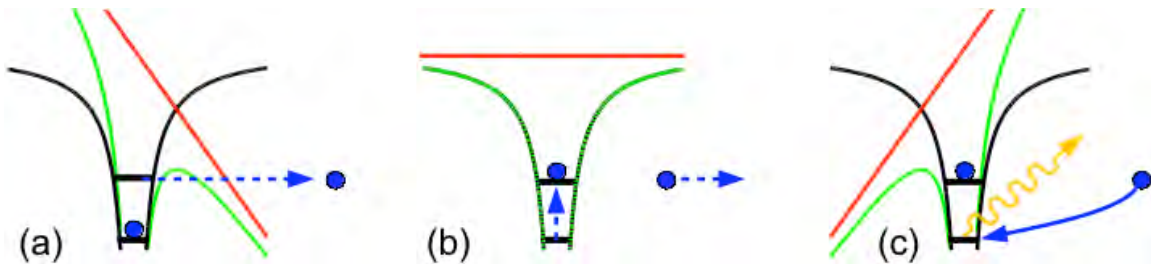


Fig. 4. Schematic of the three-step model for the HHG process augmented by x-ray excitation of a core electron [3]: (a) the atomic valence is tunnel ionized; (b) the liberated electron propagates freely in the electric field of the optical laser; (c) the direction of the optical laser field is reversed and the electron is driven back to the ion and eventually recombines with it emitting HHG radiation.

the course of the HHG process. Depending on the probability to find the core electron in the valence and the core, the returning continuum electron recombines with the valence and the core, emitting HHG radiation that is characteristic for the combined process. We devise a two-electron quantum theory for a single atom assuming no electron correlations between the two electrons. As HHG is the basis of attoscience and x-ray sources, our prediction opens perspectives for nonlinear x-ray physics, attosecond x rays, and HHG-based spectroscopy involving core orbitals. Large parts of the basic theory have been devised [3], however several cases need to be worked out further. A detailed computational study of the HHG light depending on the parameters of the x rays and the optical light shall be carried out.

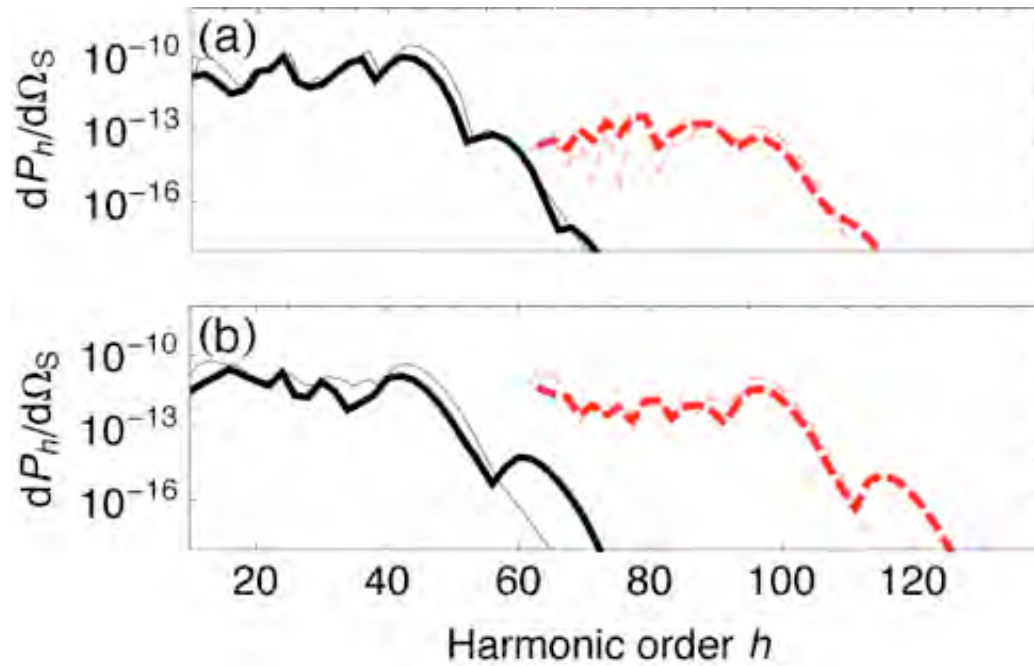


Fig. 5. Photon number of the h -th harmonic order for krypton atoms with x-ray intensities of (a) 10^{13} W/cm² and, (b) 10^{16} W/cm² [3]. The optical laser has a wavelength of 800 nm and an intensity of 3×10^{14} W/cm². The black solid lines show the contribution from recombination with a valence hole whereas the red dashed lines correspond to recombination with a core hole. The lines represent harmonic strengths obtained by integrating over peaks in the spectrum. The thin lines are spectra where ground-state depletion due to direct valence ionization by the x rays is neglected. The x-ray pulse duration is three optical laser cycles.

Optical control of x-ray lasing (G. Darvasi,¹⁸ C. Buth, C. H. Keitel¹⁸)

X-ray lasing has been predicted to occur when intense x rays from an x-ray free electron laser (FEL) core-ionize atoms [34-36]. Recent measurements at the Linac Coherent Light Source (LCLS) confirm these theoretical predictions. In core-ionized atoms, electrons in higher shells may fill the core vacancy and in the course of this emit x rays spontaneously. During the copropagation of a beam of FEL radiation and spontaneously emitted x rays through a macroscopic medium, the spontaneously emitted radiation stimulates emission, i.e., lasing in the x-ray regime. Based on this scheme, we have begun to investigate means for optical control of x-ray lasing. Namely, an optical laser is used to modify the x-ray absorption cross section in a way

that absorption is substantially enhanced for a chosen x-ray energy when the optical laser is present [37]. Then, the degree of core ionization depends on the presence of the optical laser and x-ray lasing is controlled by it. The optically controlled x-ray laser has been modeled and a computer program has been implemented to calculate its output radiation. First results look promising. A number of questions shall be examined in detail:

- a) Temporal structuring of x-ray laser pulses with attosecond precision by a shaped optical laser pulse which is imprinted on a longer x-ray pulse
- b) Spatial structuring of x-ray laser pulses by a spatially structured optical laser pulse
- c) Attosecond x-ray pulses by a nonlinear compression of the FEL x-ray pulse during the propagation in the medium
- d) Seeding of an x-ray laser with, e.g., HHG light to obtain clean and controlled output radiation

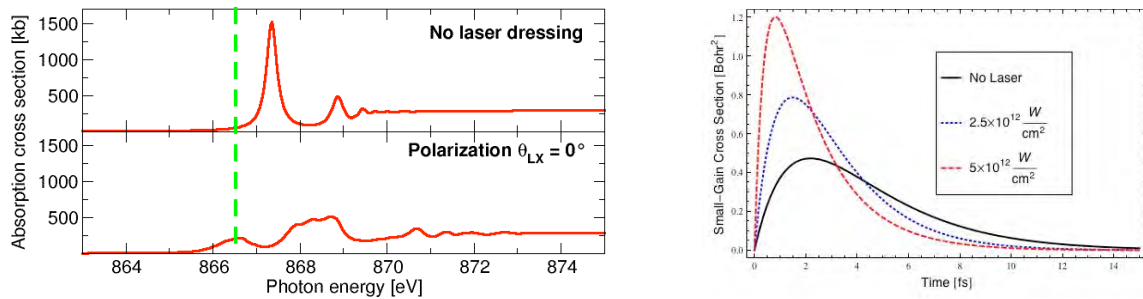


Fig. 6. (a) X-ray photoabsorption cross section of neon near the K edge with and without optical laser dressing. Here, θ_{LX} is the angle between the polarization vectors of the optical laser and the x rays. The optical laser operates at a wavelength of 800 nm and an intensity of 10^{13} W/cm². Figure adapted from Ref. [37]. (b) Small-gain cross section for x-ray lasing in neon depending on the strength of the optical laser.

Ultrafast absorption of intense x rays by nitrogen molecules (C. Buth, J.-C. Liu,^{18,19} M. H. Chen²⁰)

We devise a theoretical description for the response of nitrogen molecules (N₂) to ultrashort, intense x rays from the free electron laser (FEL) Linac Coherent Light Source (LCLS) [15-17]. We set out from a rate-equation description for the x-ray absorption by a nitrogen atom. The equations are formulated using all one-x-ray-photon absorption cross sections and the Auger and radiative decay widths of multiply-ionized nitrogen atoms. Cross sections are obtained with nonrelativistic one-electron theory and decay widths are determined from *ab initio* computations using the Dirac-Hartree-Slater (DHS) method. We also calculate all binding and transition energies of nitrogen atoms in all charge states with the Δ SCF method. To describe the interaction with N₂, a detailed investigation of intense x-ray-induced ionization and nuclear dissociation dynamics are carried out. As a figure of merit, we calculate ion yields and the average charge state measured in recent experiments at the LCLS. We use a series of phenomenological models of increasing sophistication to unravel the mechanisms of the interaction of x rays with N₂: first, the average charge state from a single atom, a fragmentation matrix model, and a lower limit model are computed; second, the hints from these models are used to devise molecular rate equations centered around the formation and decay of single and

double core holes, the metastable states of N_2^{2+} and molecular fragmentation which describe the experimental data [15] satisfactorily.

Time-dependent resonance fluorescence (S. Cavaletto,¹⁸ C. Buth, Z. Harman,¹⁸ C. H. Keitel¹⁸)

Resonance fluorescence is elastic scattering of photons by atoms for a photon energy that is tuned to an atomic resonance. It is one of the cornerstones of quantum optics. Resonance fluorescence becomes very intriguing when the atom is driven strongly by the light, leading to nonlinear effects (Mollow triplets in the stationary case). With the emerging x-ray free electron lasers (FELs), very intense x rays become accessible with, however, chaotic pulse shape due to the Self-Amplified Spontaneous Emission (SASE) principle that is used in present-day FELs. We would like to explore the potential of resonance fluorescence with FELs for diagnostics and spectroscopy. Therefore, we have devised a time-dependent theory of resonance fluorescence based on Ref. [38] for two-level and three-level atoms and molecules. First results for a two-level system look promising. Building on the first results of the resonance spectrum, a number of further questions shall be examined in detail:

- a) Time-dependent resonance fluorescence spectrum of LCLS pulses
- b) Time-dependent resonance fluorescence spectrum of pulse trains
- c) Optical control of resonance fluorescence in a three-level system; imprinting shapes on the fluorescence spectrum
- d) Investigation of the possibility for the retrieval of SASE pulse shapes from the time-dependent resonance fluorescence spectrum.

Control of x-ray interactions with strong laser fields

Decoherence in Attosecond Photoionization (S. Pabst,^{3,4} L. Greenman,²¹ P. J. Ho, D. Mazziotti,²¹ R. Santra^{3,4})

Atomic and molecular ions generated in a strong optical field generally are not in the electronic ground state. The ion hole dynamics for such ions is characterized by the electronic quantum-state populations and by the coherences among the electronic quantum states. Our previous work [30,39-42] focused on the ion hole dynamics associated with the most outer-valence single-hole states with a total angular momentum of $j = 1/2$ or $j = 3/2$. In Ref. [7], the creation of superpositions of hole states via single-photon ionization using attosecond extreme-ultraviolet pulses is studied with the time-dependent configuration-interaction singles (TDCIS) method [13]. Specifically, the degree of coherence between hole states in atomic xenon is investigated. We find that interchannel coupling not only affects the hole populations, but it also enhances the entanglement between the photoelectron and the remaining ion, thereby reducing the coherence within the ion. As a consequence, even if the spectral bandwidth of the ionizing pulse exceeds the energy splittings among the hole states involved, perfectly coherent hole wave packets cannot be formed. For sufficiently large spectral bandwidth, the coherence can only be increased by increasing the mean photon energy.

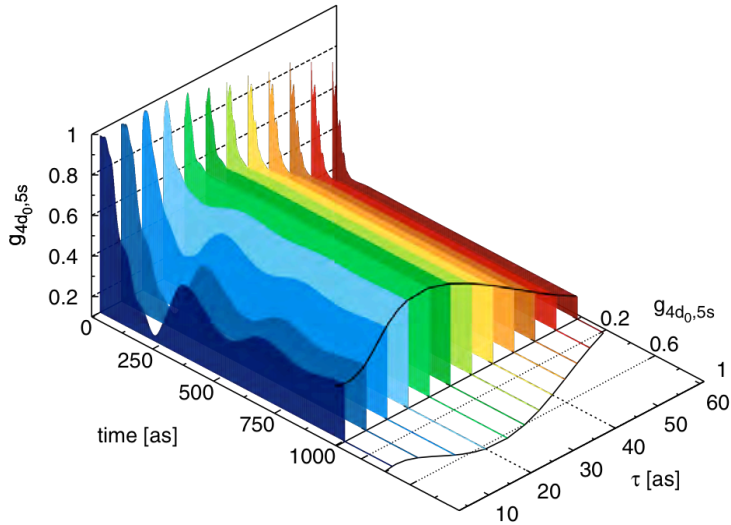


Fig. 7. The time evolution of the coherence between the $4d_0$ and $5s$ hole states in xenon is shown for the full Coulomb interaction model. The photon energy is 136 eV, and the pulse duration varies from 5 - 60 as.

Ultrafast x-ray probes of photoinduced dynamics

X-ray scattering from laser-aligned molecules—experiment (G. Doumy, P. J. Ho, E. P. Kanter, B. Krässig, A. M. March, D. Ray, S. H. Southworth, L. Young, T. J. Graber,²² R. W. Henning²²)

This work builds upon our previous demonstration of an x-ray microprobe of laser-aligned bromotrifluoromethane (CF_3Br) molecules [43]. As in the previous work, the duration of the x-ray probe pulse is ~ 100 ps, which is of similar magnitude as molecular rotational periods, and TW laser pulses with ~ 100 ps duration at 1 kHz are used to produce quasi-adiabatic molecular alignment in a gaseous sample cooled by supersonic expansion. Whereas in our previous work the x-ray probe was based on resonant x-ray absorption and fluorescence detection, the goal of this work is to collect diffraction patterns of coherently scattered x-rays from laser aligned ensembles of molecules, guided by theoretical predictions made in our group [21,27,44].

The cross section for coherent x-ray scattering is orders of magnitude lower than that of resonant absorption and a demonstration of coherent scattering from a molecular beam requires significantly higher x-ray flux and sample density than in the work of Ref. [43]. We have therefore built a new target chamber for use at the high flux beamline APS Sector 14-ID-B (two in-line undulators and pink beam operation, $\Delta E/E \sim 2\%$, 10^{10} photons per pulse). The chamber design incorporates a skimmed molecular beam target with a pulsed nozzle and a 60° viewing angle for forward scattered x-rays. Scattered x-rays are collected by the Sector 14 Mar 165 high-resolution CCD detector. The chamber is mounted on a specially designed table with 5 motorized degrees of freedom that can be wheeled into the tight space of the 14-ID-B hutch to straddle the existing table with minimal disturbance to the equipment for macromolecular crystallography located at this beam line. The setup incorporates a set of two 100-mm length Kirkpatrick-Baez mirrors to refocus the x-ray beam to about $20 \times 40 \mu\text{m}^2$ at the intersection of the x-ray beam and the molecular beam. The existing Spitfire Ti:Sapphire laser system was modified such that the uncompressed output could be directly transported to our new experimental setup, providing a beam of 800-nm, 4.5-mJ laser pulses of ~ 150 ps duration at 1 kHz. The first experimental runs with this setup, using both a cw and the pulsed gas nozzle, without the

aligning laser, provided x-ray scattering images that were dominated by scattered x-rays from sources other than the molecular beam. Tight collimation of the focused beam, the reduction of slit scattering by the beam halo components, and limiting backscattering from the beam stop are absolutely critical and need further improvement. We are planning to implement a collimation system of multiple apertures with individual motorized positioning. We will apply for beam time during the less oversubscribed 324-bunch periods at the APS to test the collimation system and to perform further characterizations of the pulsed nozzle. The goal of these tests will be to establish firm estimates for the signal-to-noise levels for molecular scattering achievable with the existing system.

Development of high-repetition-rate laser pump/x-ray probe methodologies for synchrotron facilities (A. M. March, G. Doumy, E. P. Kanter, B. Krässig, S. H. Southworth, L. Young, A. Stickrath,²³ K. Attenkofer,¹ C. A. Kurtz,¹ L. X. Chen^{23,24})

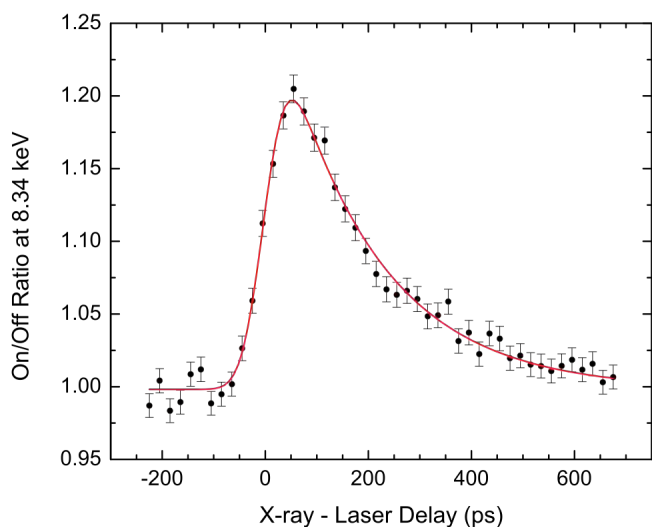


Fig. 8. Time evolution of the Ni 1s \rightarrow 4p_z resonance of the laser-excited T₁ state of NiTMP at 8.34 keV. The ratio of the laser-on and laser-off x-ray fluorescence yields is plotted. The solid line is a fit of a Gaussian function, that accounts for the 94-ps FWHM x-ray pulse, convoluted with an exponential decay function. The fit gives a decay time of 186 \pm 10 ps for the T₁ state. The data was collected for 20 sec per point at 135.8 kHz and the laser power was 0.7 W.

In the standard operating mode of the Advanced Photon Source (APS) storage ring, there are 24 equally spaced (153 ns) electron bunches (\sim 94 ps FWHM), each circulating at 271 kHz for a total x-ray pulse repetition rate of 6.52 MHz. To take advantage of the available x-ray flux for laser-pump/x-ray probe experiments, we have installed a Nd:YAG (1064 nm, 10 W) laser at APS beamline 7ID-D with variable repetition rate (54 kHz - 6.5 MHz) and selectable pulse durations of 10 and 130 ps. The laser is synchronized to the 352-MHz rf clock of the storage ring for precise control of the laser/x-ray time delay, and a pulse picker controls the repetition rate. The second and third harmonics (532 and 355 nm) of the fundamental are generated using nonlinear optical techniques with thermally stabilized crystals. At 54 kHz [6.52 MHz] we obtain pulse energies of 185 [2.5], 130 [1.5], and 45 [0.6] μ J at 1064, 532, and 355 nm, respectively. The first experiments were on 100- μ m-thick liquid jets of solvated molecules. Focusing the 532 nm light to \leq 40 μ m produces fluences that induce electronic excitations with high conversion efficiencies, even at the highest repetition rates. An optical transport system with position feedback maintains stable laser focusing through the liquid jet. A new x-ray focusing system, installed just upstream of the liquid jet, consists of two rhodium-coated silicon mirrors in Kirkpatrick-Baez (KB) geometry that are separately tilted (\sim 4-5 mrad) and dynamically bent to focus to \sim 8 μ m FWHM diameter within the laser focus. The KB mirrors have large acceptance

apertures ($> 1 \text{ mm} \times 1 \text{ mm}$), resulting in large x-ray fluxes on target, e.g., 2×10^{12} x rays/sec over $\sim 7\text{-}13 \text{ keV}$. The laser and x-ray pulses are initially overlapped spatially through a $50\text{-}\mu\text{m}$ pinhole and temporally with an MSM timing detector. This is sufficient to produce a transient excited state in the solvated molecules that is then used to optimize the spatial overlap and precisely determine the zero time delay. An external timing reference developed from the 352-MHz clock maintains timing control for different laser repetition rates. In the first demonstration experiment, the time-evolution of x-ray absorption spectra at the Ni *K*-edge were studied for laser-excited Ni(II)-tetramesitylporphyrin (NiTMP) in a 2 mM toluene solution. NiTMP is a model system for the class of molecules called metalloporphyrins, which constitute the active center of biologically relevant molecules such as chlorophylls and heme groups. Data were recorded by overlapping every other x-ray pulse from one of the 24 electron bunches with 532-nm laser pulses at 135.8 kHz. An avalanche photodiode recorded Ni *K*-fluorescent x-rays as the incident x-ray energy was scanned across the Ni *K* edge. The laser-on and laser-off fluorescence yields were measured by electronically gating the fluorescence pulses. Figure 8 shows a laser/x-ray time delay scan recorded at the Ni $1s \rightarrow 4p_z$ resonance at 8.34 keV. The lifetime of the laser-excited T_1 state was determined to be $186 \pm 10 \text{ ps}$. A recent report [4] gives a detailed description of the high-repetition-rate instrumentation along with results for the time-evolution of NiTMP x-ray absorption spectra. High-repetition-rate laser methods are also being developed at other synchrotron radiation facilities. At the APS, these methods will be exploited for the Short Pulse X-ray (SPX) facility that is described below.

Capturing ultrafast dynamics of molecules with x-ray absorption, x-ray emission, and x-ray scattering (A. M. March, G. Doumy, S. H. Southworth, E. P. Kanter, R. W. Dunford, D. Ray, L. Young, M. K. Haldrup,²⁵ A. Bordage,²⁶ G. Vankó,²⁶ J. Uhlig,²⁷ A. Galler,¹¹ W. Gawelda,¹¹ C. Bressler,¹¹ M. M. Nielsen,²⁸ K. Kjaer,²⁸ T. van Driel,²⁸ H. Lemke,⁸ S. Canton,²⁷ V. Sundström²⁷)

As described above, we have developed the capability of performing laser-pump and x-ray probe experiments on liquid jets of solvated molecules at repetition rates up to the full 6.52 MHz of the APS storage ring [4]. To take advantage of this capability, an international collaboration was assembled that brought together experts in the use of x-ray absorption (XAS), x-ray emission (XES), and x-ray diffuse scattering (XDS) techniques. Measurements were made using both hybrid-singlet and 24-bunch operating modes of the APS storage ring. In hybrid-single mode, a single, high-current electron bunch is well separated temporally from closely spaced multi-bunches. The singlet produces x-ray pulses at 271 kHz, and the laser was operated at 135 kHz to concurrently record laser-on and laser-off data. Signals from the remaining x-ray pulses were removed from the data stream by electronic gating. In 24-bunch mode, the laser was operated at 3.26 MHz, and alternate x-ray pulses contributed to the laser-on and laser-off data. Two molecular systems were studied in aqueous solutions: iron(II)-tris(bipyridine) and iron(II)-bis(terpyridine). Both systems are metal-ligand charge-transfer (MLCT) systems that transiently transfer an electron from the central Fe 3d orbitals to the ligands. The transferred electron returns to the Fe 3d orbitals, but produces a high spin state. Time-resolved x-ray absorption spectra were recorded in the form of x-ray fluorescence yields using a silicon drift detector, an avalanche photodiode (APD), or a scintillator/photomultiplier tube. The XAS detector recorded fluorescence from one side of the liquid jet, while fluorescence from the other side was dispersed by a 10-cm-diameter Si(111) crystal and detected by a gated APD to record the transient Fe $K\alpha_{1,2}$ spectrum with $\sim 1\text{-eV}$ resolution. The high-resolution $K\alpha_{1,2}$ spectrum clearly demonstrated the transition from a low-spin ground state to a high-spin transient excited state. Fe $K\beta$ x-ray

fluorescence spectra were also recorded as well as resonant x-ray emission spectra excited at the Fe 1s \rightarrow 3d resonance. A temporally gated position-sensitive x-ray detector (Pilatus 100K) was positioned just downstream of the liquid jet and a small x-ray beam block. Time-resolved, diffuse scattering patterns were recorded over scattering angles $2\theta \approx 0 - 80^\circ$. Variations of the scattering patterns with laser/x-ray delay characterized the transient structural modifications. By combining the XAS, XES, and XSD techniques, a much more detailed characterization of these MLCT systems will be obtained.

Optical trapping and x-ray imaging of nanoparticles (M. Pelton,²⁹ J. Sweet,²⁹ N. F. Scherer,²¹ M. Guffey,²¹ L. Young)

The central goal of this portion of the project is x-ray imaging of single trapped and aligned nanoparticles in solution. Progress towards this goal proceeded on two fronts: (1) x-ray imaging of single metal nanoparticles on a solid support, and (2) development of optical trapping and manipulation techniques for metal nanoparticles.

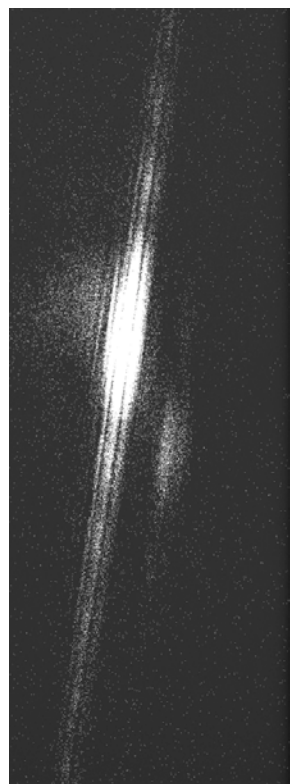


Fig. 9. Coherent x-ray diffraction from a single gold nanowire.

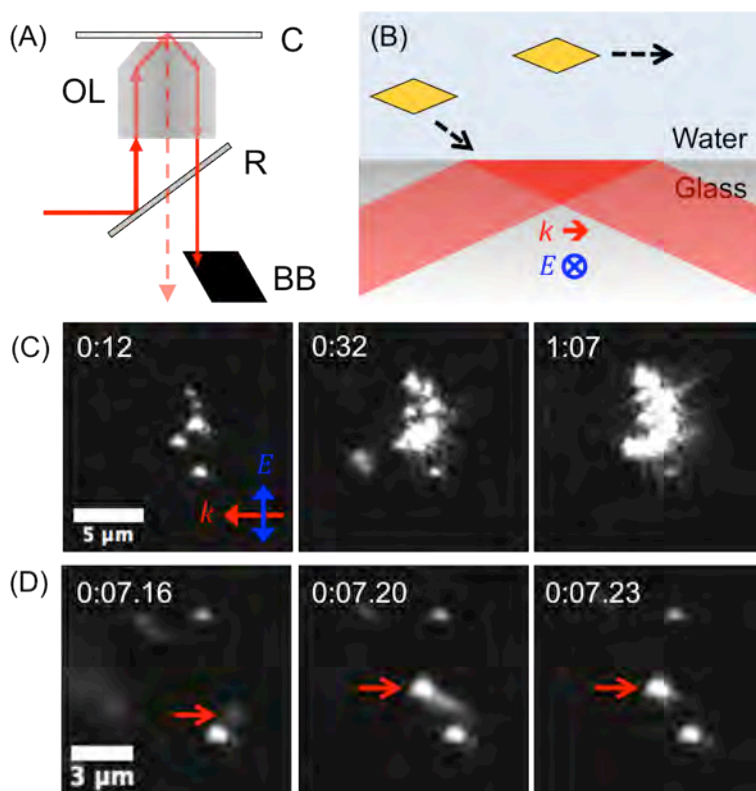


Fig. 10. (A) Schematic of the total-internal-reflection setup for optical manipulation of nanoparticles. "C," coverslip, "OL," 100 \times oil immersion objective lens, "R," incoherent-coated reflective neutral density filter, "BB," beam block. (B) Cartoon depicting observed particle trajectories; some particles deposit on the surface at the edge of the evanescent field area, while others stream past. (C) Dark-field optical images of bipyramid deposition at different times after the start of laser exposure (denoted as minutes:seconds). The laser propagation direction k and polarization E are indicated on the figure. (D) Three successive frames showing nanoparticle (highlighted with red arrow) accelerating towards the surface and depositing.

Initial x-ray scattering measurements were performed on single metal nanowires, whose large aspect ratios facilitate optical trapping as well as x-ray diffraction. The nanowires were deposited on silicon nitride membranes and were encapsulated with a thin alumina layer by atomic layer deposition; this layer is intended to protect the nanowires chemically against oxidation by the ambient environment and physically against damage by the incident x-rays. We found that, even with this layer, the silver wires were unstable under an intense x-ray flux, undergoing apparent melting and recrystallization within a few seconds. The gold wires were more stable and were able to produce coherent diffraction patterns when illuminated by a focused, coherent x-ray beam. Figure 9 shows an example of the diffraction patterns measured at Sector 34 of the APS around the [200] Bragg peak from a single nanowire. Measurement of several such images for a series of incident angles will allow nanometer-scale reconstruction of the internal structure of the nanowire using coherent-diffraction imaging (CDI) techniques. Our initial attempts at such measurements indicated some remaining instability for the gold wires over the ~1 hr. integration time required for such an experiment. We are currently working to improve imaging conditions and sample preparation in order to overcome this instability; in particular, we are investigating alternative methods of encapsulating the nanowires, such as sputtering thicker layers of amorphous oxides. As well as providing previously inaccessible information about strain distribution within the metal nanowires, the CDI technique will be directly transferrable to imaging of trapped nanoparticles in solution.

We have also completed design and begun construction of a compact, portable optical-trapping apparatus that can be used at the APS beamlines. Assembly and testing of this apparatus is being performed in a recently completed laser laboratory at Argonne's Center for Nanoscale Materials. In parallel, optical trapping techniques appropriate for metal nanoparticles are being developed at the University of Chicago. Previous work demonstrated the possibility of selectively trapping individual particles and depositing them on a substrate [10,11]. Recently, we complemented this with a multiplex approach, based on plasmon-selective, driven deposition of Au nanoparticles using total internal reflection (TIR) illumination [9]. As illustrated in Figure 10, near-IR laser light undergoing TIR at a glass-water interface causes colloidal Au bipyramids to irreversibly deposit onto the glass surface. We demonstrated that the deposition process has shape selectivity that is associated with resonant plasmon excitation. Our measurements and finite difference time domain simulations show that the optical forces that act on the particles are significant and cause the observed acceleration and directed motion of the bipyramids. The collective optical manipulation of multiple nanoparticles provides the opportunity to study optically induced interparticle interactions through x-ray scattering. In addition, we observed that resonant photothermal heating of the Au bipyramids causes an irreversible loss in colloidal stability, thus inducing them to adhere to the surface. Structural characterization of the deposited bipyramids revealed a slight reduction in aspect ratio relative to the ensemble, consistent with the proposed heating mechanism. Understanding and limiting the thermal instability and laser-induced structural modification will be critical if the nanoparticles are to be held stably in an optical trap long enough to make detailed structural measurements by coherent x-ray diffraction.

Interatomic Coulombic Decay (ICD) in deep inner-shell vacancy cascades (R. W. Dunford, S. H. Southworth, E. P. Kanter, B. Krässig, D. Ray, L. Young, R. Santra,^{3,4} O. Vendrell³)

The photoionization of an inner-shell electron in an atom sets off a cascade of x-ray and Auger transitions as the atom relaxes. The different possible decay paths lead to a range of final charge states. If the cascade occurs in an atom that is part of a molecule or cluster, it can also

lead to the removal of delocalized valence electrons and produce two or more ions, followed by a Coulomb explosion of the system. The role of delocalized electrons was emphasized by Cederbaum and co-workers, e.g., Ref. [45]. They predicted a new decay process for inner-valence vacancies in atoms or molecules that were part of a cluster and later identified similar processes in other systems. The new process was termed Interatomic Coulombic Decay (ICD) and, in general, leads to electronic decay of a vacancy which, in an isolated system, can only undergo radiative decay. The focus of our work is to explore ICD in a new regime in which the initial vacancy is a deep inner-shell electron in a heavy atom. This is a system in which x-ray emission is the dominant decay mode for the first step in the cascade. Our method is based on the notion that the ICD process tends to lead to an increase in the total charge of all of the fragments in the final state. To show this, we compare the total charge produced following *K*-shell photoionization of atomic Xe to the total charge produced by *K*-shell photoionization of the Xe atom in XeF₂ molecules. Analysis of the data is still in progress, the initial results show evidence that the ICD process plays a role in this regime. As an aid in understanding the dynamics of the ion breakup, we are carrying out simulations of the ion time-of-flight (TOF) spectrometer.

We will follow up on the initial ICD experiments by improving the apparatus and exploring other systems. In addition to gaining a further understanding of the ICD process in the hard x-ray regime, we will also explore the more general question of what are the most probable breakup modes for a molecule following deep inner-shell photoionization of a heavy atom constituent. Theoretical guidance is being provided by R. Santra and O. Vendrell. We are working with them to identify interesting molecules to study. It is clear that the theoretical calculations of molecular breakup modes can be most readily tested by studying asymmetric molecules such as bromiodomethane, CH₂BrI. Using APS x rays, *K*-shell holes can be created on either the Br atom at 13 keV or on the I atom at 33 keV. For future work we note that, in initial experiments, the ion fragments were identified by their times-of-flight only. While the multi-hit capability of the detection circuit allowed us to identify certain fragmentation channels, there were remaining ambiguities. The measurements were also plagued by excessive electronic dead time and low ion detection efficiencies. An improved apparatus is being designed that will utilize faster electronics, a multi-hit position-sensitive detector, and increased detection efficiency. Together these improvements will remove the ambiguities in the charge-state distributions, resulting in clearer determination of breakup channels and better tests of theoretical calculations.

Progress toward a Short Pulse X-ray Facility (SPX) at the Advanced Photon Source

(L. Young, P. Evans, L. X. Chen, H. Dürr, M. Beno, E. Dufresne, Y. Li, D. Keavney, B. Yang, M. Borland, R. Dejus, G. Navrotsky, D. Reis, R. Clarke, J. Wang, S. Southworth, V. Batista, F. Castellano, E. Castner, R. Crowell, C. Laperle, C. Rose-Petruck, R. Sension, D. Tiede, S. Vajda, D. Arena, P. Crowell, B. Bailey)

The proposed Short Pulse X-ray Facility at the Advanced Photon Source (APS) promises to be the world's first high-average-flux, tunable, polarized synchrotron-based x-ray source. The SPX is a central part of the APS Upgrade with an average flux that is comparable to the Linac Coherent Light Source (LCLS) and that far exceeds other accelerator-based ultrafast x-ray sources (slicing sources, e.g. at ALS, BESSY and the Swiss Light Source) and low alpha operation. The SPX facility features a variable pulse duration (1-100 ps), variable monochromatization ($10^{-4} - 10^{-2}$), variable repetition rate (up to 6.5 MHz) and photon energies in

the soft and hard x-ray regimes. With $10^4 - 10^6$ x rays/pulse focused to $\sim 1 \mu\text{m}^2$ the use of the SPX as a probe resides squarely in the standard one-photon regime and will be free from multiphoton processes so prevalent at the LCLS. This past year, we completed a conceptual design of the SPX facility consisting of three beamlines (two hard x-ray and one soft x-ray) that can operate simultaneously, and five independently operating endstations. One hard x-ray beamline will take a 1% vertical slice from the chirped electron beam, be fully tunable from 4 – 35 keV, with variable pulse duration, bandwidth, repetition rate and used for traditional spectroscopy and scattering experiments. The other hard x-ray beamline will explore novel uses of other characteristics of the chirped electron beam by accepting the full vertical fan for time-dispersed diffraction or wide field imaging. The soft x-ray beamline will operate from a bending magnet source from 200 eV to 2 keV and offer monochromatic radiation with variable circular polarization, modulated at a rapid repetition rate, for studies of magnetic systems. This past year, the team assembled a scientific case and a conceptual design and underwent four reviews (Technical Design Review, Scientific Advisory Committee Review, Argonne Director’s Review and DOE Independent Cost Estimate Review). The reviews endorsed the building of the SPX facility and offered useful advice. During the upcoming year, completion of a full preliminary design and costing for the three beamlines and laser infrastructure will be the primary activity.

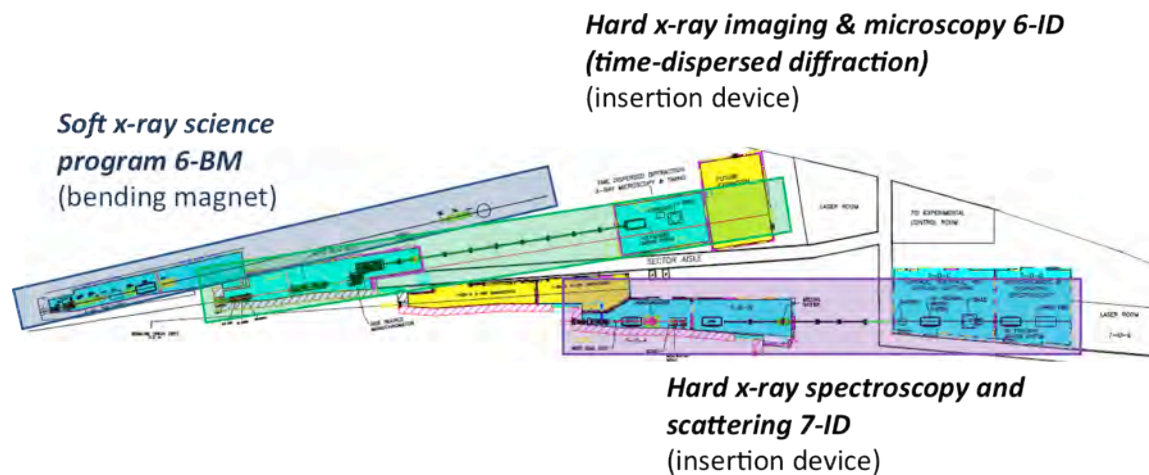


Fig. 11. Proposed layout for SPX Facility beamlines. Deflection cavities are to be located in the downstream ends of Sectors 5 and 7, both of which have long straight sections. Sector 6 has a standard-length straight section that can accommodate two 2.2-m undulators for later expansion. In the first phase, three independently operating beamlines are planned, two hard x-ray beamlines and one soft x-ray bending magnet beamline. The high repetition rate (6.5 MHz), medium fluence ($10^4 - 10^6$ x rays/pulse) tunable, polarized x-ray pulses will facilitate high precision x-ray measurements with picosecond and picometer resolution.

Affiliations of collaborators

- ¹X-Ray Science Division, Argonne National Laboratory
- ²Max-Planck Advanced Study Group at CFEL, Hamburg, Germany
- ³CFEL at DESY, Hamburg, Germany
- ⁴University of Hamburg, Germany
- ⁵Ohio State University, Columbus, OH
- ⁶Western Michigan University, Kalamazoo, MI
- ⁷PULSE Center, SLAC, Stanford, CA
- ⁸Linac Coherent Light Source, SLAC, Stanford, CA
- ⁹Institute of Optics, Jena, Germany
- ¹⁰DESY, Hamburg, Germany
- ¹¹European XFEL, Hamburg, Germany
- ¹²Dublin City University, Dublin, Ireland
- ¹³Université Paris Sud, Orsay, France
- ¹⁴Max Planck Institute for Quantum Optics, Garching, Germany
- ¹⁵Technical University, Munich, Germany
- ¹⁶Ludwig Maximilians University, Munich, Germany
- ¹⁷University of Heidelberg, Heidelberg, Germany
- ¹⁸Max-Planck-Institut für Kernphysik, Heidelberg, Germany
- ¹⁹North China Electric Power University, Beijing, China
- ²⁰Lawrence Livermore National Laboratory, Livermore, CA
- ²¹University of Chicago, Chicago, IL
- ²²BioCARS, University of Chicago, IL
- ²³Chemical Sciences and Engineering Division, Argonne National Laboratory
- ²⁴Northwestern University, Evanston, IL
- ²⁵Risoe National Laboratory, Technical University of Denmark
- ²⁶KFKI Research Institute for Particle and Nuclear Physics, Budapest, Hungary
- ²⁷Lund University, Sweden
- ²⁸University of Copenhagen, Denmark
- ²⁹Center for Nanoscale Materials, Argonne National Laboratory

Publications (2009 - 2011)

- [1] E. P. Kanter, B. Krässig, Y. Li, A. M. March, P. Ho, N. Rohringer, R. Santra, S. H. Southworth, L. F. DiMauro, G. Doumy, C. A. Roedig, N. Berrah, L. Fang, M. Hoener, P. H. Bucksbaum, S. Ghimire, D. A. Reis, J. C. Bozek, C. Bostedt, M. Messerschmidt, and L. Young, "Unveiling and driving hidden resonances with high-fluence, high-intensity x-ray pulses," submitted to Phys. Rev. Lett. (2011).
- [2] S. Düsterer *et al.*, "Femtosecond X-ray Pulse Length Characterization at the LCLS Free Electron Laser," submitted to New Journal of Physics (June 2011).
- [3] C. Buth, M. C. Kohler, J. Ullrich, and C. H. Keitel, "High-order harmonic generation enhanced by XUV light," submitted to Opt. Lett. (2011); arXiv:1012:4930.
- [4] A. M. March, A. Stickrath, G. Doumy, E. P. Kanter, B. Krässig, S. H. Southworth, K. Attenkofer, C. A. Kurtz, L. X. Chen, and L. Young, "Development of high-repetition-rate laser pump/x-ray probe methodologies for synchrotron facilities," Rev. Sci. Instrum., accepted (2011).

- [5] G. Doumy, C. Roedig, S.-K. Son, C. I. Blaga, A. D. Chiara, R. Santra, N. Berrah, C. Bostedt, J. D. Bozek, P. H. Bucksbaum, J. Cryan, L. Fang, S. Ghimire, J. M. Glowonia, M. Hoener, E. P. Kanter, B. Krässig, M. Kuebel, M. Messerschmidt, G. G. Paulus, D. A. Reis, N. Rohringer, L. Young, P. Agostini, and L. F. DiMauro, "Nonlinear atomic response to intense ultrashort x rays," *Phys. Rev. Lett.* **106**, 083002 (2011).
- [6] S.-K. Son, L. Young, and R. Santra, "Impact of hollow-atom formation on coherent x-ray scattering at high intensity," *Phys. Rev. A* **83**, 033402 (2011).
- [7] S. Pabst, L. Greenman, P. J. Ho, D. A. Mazziotti, and R. Santra, "Decoherence in attosecond photoionization," *Phys. Rev. Lett.* **106**, 053003 (2011).
- [8] E. Silver, J. D. Gilaspy, P. Gokhale, E. P. Kanter, N. S. Brickhouse, R. W. Dunford, K. Kirby, T. Lin, J. McDonald, D. Schneider, S. Seifert, and L. Young, "Work towards experimental evidence of hard x-ray photoionization in highly charged krypton," *AIP Conference Proceedings* **1336**, 146 (2011).
- [9] M. J. Guffey, L. Cao, S. Gray, and N. F. Scherer, "Plasmon-selective driven deposition of Au bipyramidal nanoparticles," *Nano Lett.*, in revision (2011).
- [10] M. J. Guffey and N. F. Scherer, "All-optical patterning of Au nanoparticles on surfaces using optical traps," *Nano Lett.* **10**, 4302 (2010).
- [11] M. J. Guffey and N. F. Scherer, "All-optical positioning of single and multiple Au nanoparticles on surfaces using optical trapping," *Proc. SPIE* **7762**, 77623H (2010).
- [12] A. Grigoriev, P. G. Evans, M. Trigo, D. Reis, L. Young, R. W. Dunford, E. P. Kanter, B. Krässig, R. Santra, S. H. Southworth, L. X. Chen, D. M. Tiede, K. Attenkofer, G. Jennings, X. Zhang, T. Graber, and K. Moffat, "Picosecond structural dynamics at the Advanced Photon Source," *Synch. Rad. News* **23** (2), 18 (2010).
- [13] L. Greenman, P. J. Ho, S. Pabst, E. Kamarchik, D. A. Mazziotti, and R. Santra, "Implementation of the time-dependent configuration interaction singles method for atomic strong-field processes," *Phys. Rev. A* **82**, 023406 (2010).
- [14] E. Goulielmakis, Z.-H. Loh, A. Wirth, R. Santra, N. Rohringer, V. S. Yakovlev, S. Zherebtsov, T. Pfeifer, A. M. Azzeer, M. F. Kling, S. R. Leone, and F. Krausz, "Real-time observation of valence electron motion," *Nature* **466**, 739 (2010).
- [15] M. Hoener, L. Fang, O. Kornilov, O. Gessner, S. T. Pratt, M. Gühr, E. P. Kanter, C. Blaga, C. Bostedt, J. D. Bozek, P. H. Bucksbaum, C. Buth, M. Chen, R. Coffee, J. Cryan, L. DiMauro, M. Glowonia, E. Hosler, E. Kukk, S. R. Leone, B. McFarland, M. Messerschmidt, B. Murphy, V. Petrovic, D. Rolles, and N. Berrah, "Ultraintense x-ray induced ionization, dissociation, and frustrated absorption in molecular nitrogen," *Phys. Rev. Lett.* **104**, 253002 (2010).
- [16] L. Fang, M. Hoener, O. Gessner, F. Tarantelli, S. T. Pratt, O. Kornilov, C. Buth, M. Gühr, E. P. Kanter, C. Bostedt, J. D. Bozek, P. H. Bucksbaum, M. Chen, R. Coffee, J. Cryan, M. Glowonia, E. Kukk, S. R. Leone, and N. Berrah, "Double core hole production in N₂: beating the Auger clock," *Phys. Rev. Lett.* **105**, 083005 (2010).
- [17] J. P. Cryan, J. M. Glowonia, J. Andreasson, A. Belkacem, N. Berrah, C. I. Blaga, C. Bostedt, J. Bozek, C. Buth, L. F. DiMauro, L. Fang, O. Gessner, M. Guehr, J. Hajdu, M. P. Hertlein, M. Hoener, O. Kornilov, J. P. Marangos, A. M. March, B. K. McFarland, H. Merdji, V. Petrovic, C. Raman, D. Ray, D. Reis, F. Tarantelli, M. Trigo, J. White, W. White, L. Young, P. H. Bucksbaum, and R. N. Coffee, "Auger electron angular distribution of double core hole states in the molecular reference frame," *Phys. Rev. Lett.* **105**, 083004 (2010).
- [18] J. M. Glowonia, J. Cryan, J. Andreasson, A. Belkacem, N. Berrah, C. I. Blaga, C. Bostedt, J. Bozek, L. F. DiMauro, L. Fang, J. Frisch, O. Gessner, M. Gühr, J. Hajdu, M. P. Hertlein, M. Hoener, G. Huang, O. Kornilov, J. P. Marangos, A. M. March, B. K. McFarland, H. Merdji, V. S. Petrovic, C. Raman, D. Ray, D. A. Reis, M. Trigo, J.

L. White, W. White, R. Wilcox, L. Young, R. N. Coffee, and P. H. Bucksbaum, "Time-resolved pump-probe experiments at the LCLS," *Optics Express* **18**, 17620 (2010).

[19] L. Young, E. P. Kanter, B. Krässig, Y. Li, A. M. March, S. T. Pratt, R. Santra, S. H. Southworth, N. Rohringer, L. F. DiMauro, G. Doumy, C. A. Roedig, N. Berrah, L. Fang, M. Hoener, P. H. Bucksbaum, J. P. Cryan, S. Ghimire, J. M. Glowia, D. A. Reis, J. D. Bozek, C. Bostedt, and M. Messerschmidt, "Femtosecond electronic response of atoms to ultra-intense x-rays," *Nature* **466**, 56 (2010).

[20] S. Pabst and R. Santra, "Alignment of asymmetric-top molecules using multiple-pulse trains," *Phys. Rev. A* **81**, 065401 (2010).

[21] S. Pabst, P. J. Ho, and R. Santra, "Computational studies of x-ray scattering from three-dimensionally-aligned asymmetric-top molecules," *Phys. Rev. A* **81**, 043425 (2010).

[22] T.E. Glover, M.P. Hertlein, S.H. Southworth, T.K. Allison, J. van Tilborg, E.P. Kanter, B. Krässig, H. R. Varma, B. Rude, R. Santra, A. Belkacem, and L. Young, "Controlling x-rays with light", *Nature Physics* **6**, 69 (2010).

[23] L. Young, C. Buth, R.W. Dunford, P. Ho, E.P. Kanter, B. Krässig, E.R. Peterson, N. Rohringer, R. Santra, and S.H. Southworth. "Using strong electromagnetic fields to control x-ray processes," *Rev. Mex. Fis. S* **56**, 11 (2010).

[24] C. Buth, R. Santra, and L. Young. "Refraction and absorption of x-rays by laser-dressed atoms," *Rev. Mex. Fis. S* **56**, 59 (2010).

[25] P. J. Ho and R. Santra, "Theory of x-ray diffraction from laser-aligned molecules," *Rev. Mex. Fis. S* **56**, 88 (2010).

[26] H. R. Varma, M. F. Ciappina, N. Rohringer, and R. Santra, "Above-threshold ionization in the x-ray regime," *Phys. Rev. A* **80**, 053424 (2009).

[27] P. J. Ho, D. Starodub, D. K. Saldin, V. L. Shneerson, A. Ourmazd, and R. Santra, "Molecular structure determination from x-ray scattering patterns of laser-aligned symmetric-top molecules," *J. Chem. Phys.* **131**, 131101 (2009).

[28] R. Santra, N. V. Kryzhevoi, and L. S. Cederbaum, "X-ray two-photon photoelectron spectroscopy: A theoretical study of inner-shell spectra of the organic para-aminophenol molecule," *Phys. Rev. Lett.* **103**, 013002 (2009).

[29] B. Krässig, R.W. Dunford, E. P. Kanter, E. C. Landahl, S.H. Southworth, and L. Young, "A simple cross-correlation technique between infrared and hard x-ray pulses," *Applied Physics Letters* **94**, 171113 (2009).

[30] N. Rohringer and R. Santra, "Multichannel coherence in strong-field ionization," *Phys. Rev. A* **79**, 053402 (2009).

[31] P. J. Ho, M. R. Miller, and R. Santra, "Field-free molecular alignment for studies using x-ray pulses from a synchrotron radiation source," *J. Chem. Phys.* **130**, 154310 (2009).

[32] L. Young, R. W. Dunford, E. P. Kanter, B. Krässig, R. Santra, S. H. Southworth, "Strong-field control of x-ray processes," In *Pushing the Frontiers of Atomic Physics: Proceedings of the XXI International Conference on Atomic Physics*, R. Côté, P.L. Gould, M. Rozman and W.W. Smith, Eds., World Scientific Publishing Co., NJ, Singapore (2009), p. 344-353.

[33] R. Santra, "Concepts in x-ray physics," *J. Phys. B* **42**, 023001 (2009).

Other cited references

- [34] M. A. Duguay and P. M. Rentzepis, "Some approaches to vacuum UV and x-ray lasers," *Appl. Phys. Lett.* **10**, 350 (1967).
- [35] J. Zhao, Q. L. Dong, S. J. Wang, L. Zhang, and J. Zhang, "X-ray lasers from inner-shell transitions pumped by the free-electron laser," *Opt. Express* **16**, 3546 (2008).
- [36] N. Rohringer and R. London, "Atomic inner-shell x-ray laser pumped by an x-ray free-electron laser," *Phys. Rev. A* **80**, 013809 (2009).
- [37] C. Buth, R. Santra, and L. Young, "Electromagnetically induced transparency for x rays," *Phys. Rev. Lett.* **98**, 253001 (2007).
- [38] J. H. Eberly and K. Wódkiewicz, "The time-dependent physical spectrum of light," *J. Opt. Soc. Am.* **67**, 1252 (1977).
- [39] L. Young, D. A. Arms, E. M. Dufresne, R. W. Dunford, D. L. Ederer, C. Höhr, E. P. Kanter, B. Krässig, E. C. Landahl, E. R. Peterson, J. Rudati, R. Santra, and S. H. Southworth, "X-Ray Microprobe of Orbital Alignment in Strong-Field Ionized Atoms," *Phys. Rev. Lett.* **97**, 083601 (2006).
- [40] C. Höhr, E. R. Peterson, N. Rohringer, J. Rudati, D. A. Arms, E. M. Dufresne, R. W. Dunford, D. L. Ederer, E. P. Kanter, B. Kraessig, E. C. Landahl, R. Santra, S. H. Southworth, and L. Young, "Alignment dynamics in a laser-produced plasma," *Phys. Rev. A* **75**, 011403(R) (2007).
- [41] Z.-H. Loh, M. Khalil, R. E. Correa, R. Santra, C. Buth, and S. R. Leone, "Quantum state-resolved probing of strong-field-ionized xenon atoms using femtosecond high-order harmonic transient absorption spectroscopy," *Phys. Rev. Lett.* **98**, 143601 (2007).
- [42] S. H. Southworth, D. A. Arms, E. M. Dufresne, R. W. Dunford, D. L. Ederer, C. Höhr, E. P. Kanter, B. Kraessig, E. C. Landahl, E. R. Peterson, J. Rudati, R. Santra, D. A. Walko, and L. Young, "K-edge x-ray absorption spectroscopy of laser-generated Kr^+ and Kr^{2+} ," *Phys. Rev. A* **76**, 043421 (2007).
- [43] E. R. Peterson, C. Buth, D. A. Arms, R. W. Dunford, E. P. Kanter, B. Krässig, E. C. Landahl, S. T. Pratt, R. Santra, S. H. Southworth, and L. Young, "An x-ray probe of laser-aligned molecules," *Appl. Phys. Lett.* **92**, 094106 (2008).
- [44] P. J. Ho and R. Santra, "Theory of x-ray diffraction from laser-aligned symmetric-top molecules," *Phys. Rev. A* **78**, 053409 (2008).
- [45] L. S. Cederbaum, J. Zobel, and F. Tarantelli, "Giant intermolecular decay and fragmentation of clusters," *Phys. Rev. Lett.* **79**, 4778 (1997).

J.R. MACDONALD LABORATORY – OVERVIEW 2011

The J.R. Macdonald Laboratory focuses on the interaction of intense laser pulses with matter – specifically, observing and controlling single atoms and molecules on short time scales. The eventual goal is to work at the natural time scale for electrons moving in matter. Doing so will add to our existing capability to trace nuclear motion in molecules using femtosecond laser pulses. All of these activities build toward the ultimate goal of understanding the dynamical processes of reactions well enough to control them. To this end, we are advancing theoretical modeling and computational approaches as well as experimental techniques and taking advantage of our expertise in particle imaging techniques (such as COLTRIMS, VMI, MDI, etc.). Most of our research projects are associated with one of the two themes: “Attosecond Physics” and “Control”. The boundary between these themes, however, is sometimes not well defined. A few examples are briefly mentioned below, while further details of typical projects are provided in the individual contributions of the PIs: *I. Ben-Itzhak, Z. Chang, C.L. Cocke, B.D. Esry, M.F. Kling, V. Kumarappan, C.D. Lin, U. Thumm and C. Trallero.*

Attosecond physics: The goal of the efforts under this theme is to follow, in real time, electronic motion in atoms and molecules. However, attosecond pulses can also serve as very precise triggers or probes of the femtosecond-scale nuclear motion in molecules. We have generated and characterized single 77 attosecond transform-limited pulses, then employed such pulses in studies of time resolved AC stark shifts of auto-ionizing states. Using an attosecond pulse train in an EUV/infrared pump-probe scheme, we have modified the fragmentation dynamics of autoionizing states of O_2^+ . The quantitative re-scattering (QRS) theory has been applied to Fano resonances initiated by an attosecond pulse in He, and it reproduces the recently measured electron spectra for the $2s2p$ (1P) state. We have also simulated high harmonic generation including propagation in the medium, to help extract better information about photoionization of atoms and molecules from measured HHG spectra. We have followed theoretically the time delay in photoelectron emission from surfaces and experimentally demonstrated attosecond control over electron emission from Ar and nanoparticles. We have applied the QRS theory to these experimental studies of non-sequential double ionization (NSDI).

Control: Methods for controlling the motion of heavy particles in small molecules continue to be developed. Theoretically, the ability to control the dissociation of molecules (e.g., H_2^+) into different final channels has been investigated using pulse pairs or the carrier-envelope (CE) phase. Experimentally, we have used a $\omega+2\omega$ field to orient heteronuclear diatomic molecules and then explored how the orientation affects the ionization rate – the favored orientation is in agreement with MOL-ADK expectations. We have experimentally observed nuclear wave packet propagation in both time and energy domains, and also modeled it by TDSE calculations. We have treated theoretically the correlated electron-nuclear motion in multiphoton dissociative ionization of H_2^+ . We have demonstrated control over the elusive “zero-photon dissociation” of an H_2^+ beam using the pulse bandwidth and chirp. Recently, we have observed a channel asymmetry in HD^+ dissociation that depends on the dissociation energy and laser parameters – theory support was essential for the interpretation of these unexpected phenomena. We have improved our ability to align asymmetric top molecules and measure their degree of alignment using optical methods as well as single-shot VMI. We have recently begun a program to investigate the dynamics of a polyatomic molecule near a conical intersection driven by an intense field.

In addition to the laser-related research, we have conducted some collision studies using our high- and low-energy accelerators. Some of this work is conducted in collaboration with visiting scientists (for example, S. Lundeen, J. Shinpaugh & L. Toburen).

Like the visitors benefiting from the use of our facilities, we pursue several outside collaborations at other facilities and with other groups (e.g., ALLS-INRS, ALS, Århus, Auburn University, University of Colorado, FLASH, Max-Planck Institutes for Quantum Optics and Kernphysik, Sao Carlos, Tokyo, Weizmann Institute of Science, and others).

Finally, it is worth mentioning the changes our group and laboratory are undergoing at present. With DOE funding, we have purchased a high-repetition-rate, high-power, CE phase-locked laser from KM Labs that is expected to be operational in our lab around the time of this meeting (mid- to late September). Specifically, this laser will provide about an order of magnitude improvement in count rates (10-20 kHz, 1 mJ/pulse, 790 nm, ≤ 21 fs FWHM), which are essential for most of our multi-parameter coincidence measurements (like COLTRIMS, MDI, etc). Moreover, the shorter pulses (than currently available from KLS) will allow us to generate sub 5 fs pulses by compression in hollow core fibers and to generate single attosecond pulses directly after the amplifier using the generalized double optical gating method – therefore increasing the EUV/XUV photon flux. In addition to the added laser capabilities, this new laser system will alleviate a shortage of beam time – hopefully allowing for more collaborations involving visiting scientists.

To make room for this new laser and the associated attosecond physics experimental setup, we have removed the LINAC, after about 20 years of service, and kept only a couple of beam-lines on the tandem van de Graaff accelerator, which should be sufficient to satisfy the reduced demand for high-energy ion beams.

On the personnel side, we have just received university approval for advertising a search for an AMO faculty to join our group by summer 2012 at the assistant or associate professor level. We are making an effort to hire an experimentalist with ultrafast science experience and interests that match the theme of the JRML research. We welcome any assistance in identifying and recruiting the bright talent we need.

The above search will complete the JRML hiring process and will establish the experimental component of our research group for years to come. We are looking forward toward this future and have started planning the addition of a third laser – a high power, long wavelength system, based on an upgrade of an existing, MURI supported, laser – specifically adding another amplification stage. We envision the three young faculty, *Vinod*, *Carlos* and *Matthias*, taking charge of the operation, scheduling, maintenance and upgrade of the three main laser systems, each responsible for one of them, while experiments conducted by all are allocated to the laser that fits them best.

**Structure and Dynamics of Atoms, Ions, Molecules, and Surfaces:
Molecular Dynamics with Ion and Laser Beams**

*Itzik Ben-Itzhak, J. R. Macdonald Laboratory, Kansas State University
Manhattan, KS 66506; ibi@phys.ksu.edu*

The goal of this part of the JRML program is to study and control molecular dynamics under the influence of ultrashort intense laser pulses or the swift Coulomb field of ions. To this end we typically use molecular ion beams as the subject of our studies and have a close collaboration between theory and experiment.¹ Examples of our recent work are given below.

Strong-field coherent control of molecular-ion-beam fragmentation

We have achieved control over the dissociation of the benchmark HD^+ molecule into either $H^+ + D$ or $H + D^+$, i.e. imposed channel asymmetry upon dissociation, using the pulse bandwidth and chirp as control knobs of the elusive “zero-photon dissociation” of H_2^+ – a process driven by “two colors” within the laser bandwidth.

Zero-photon dissociation (ZPD), B. Gaire, M. Zohrabi, J. McKenna, U. Ablikim, A.M. Saylor, N.G. Johnson, K.D. Carnes, F. Anis, J.J. Hua, D. Ursrey, J. Hernandez., B.D. Esry, and I. Ben-Itzhak – To explain a very low KER feature in their H_2^+ dissociation data, Posthumus *et al.* [1] suggested an intriguing mechanism, which they named “zero-photon dissociation” (ZPD), as it involves no net photon absorption. Recently, the same group repeated their measurements of dissociative ionization of H_2 by 263 nm (~150 fs) pulses, but this time they presented an alternative interpretation involving resonance-enhanced multiphoton ionization (REMPI) [2].

In order to eliminate the competing REMPI process we have studied the dissociation of H_2^+ and HD^+ beams in <10 fs, 790 nm laser pulses. We have measured very low kinetic energy release (KER) from the dissociation of H_2^+ using a crossed-beams coincidence three-dimensional momentum imaging method [3] – after an upgrade allowing KER measurements down to almost zero KER [4]. The combined experimental and theoretical results provide convincing evidence for dissociation with the net absorption of zero photons, i.e. the elusive ZPD process [5]. However, instead of involving vibrational trapping as the key ingredient of the mechanism, we suggest that ZPD is driven by the absorption of a somewhat more energetic photon followed by the stimulated emission of a less energetic photon (see Fig. 1), both within the laser bandwidth. This is consistent with our findings that broad-band pulses cause ZPD more efficiently, thus providing a control knob for the dissociation of highly excited vibrational states of H_2^+ .

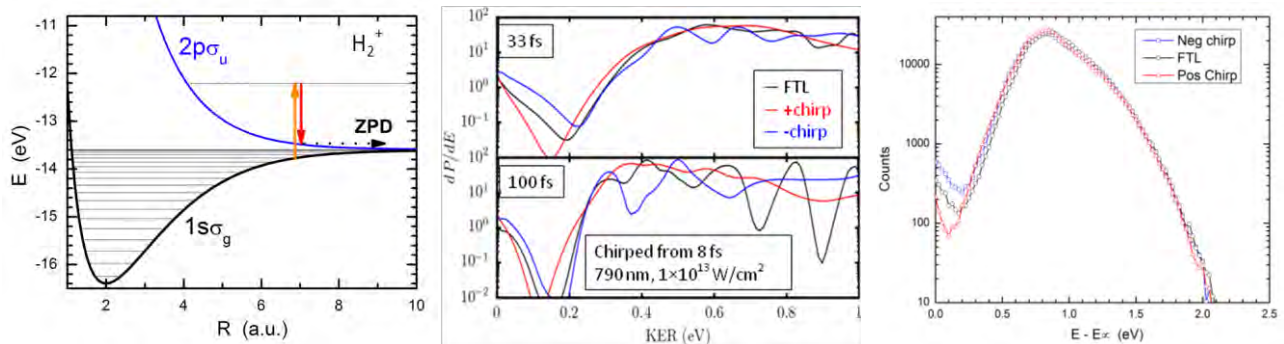


Figure 1. *Left:* A schematic view of ZPD as a two-color process within the laser bandwidth. *Center:* Theory: Probability density of H_2^+ dissociation in pulses chirped from an 8 fs Fourier transform limited (FTL) pulse. *Right:* Experiment: Dissociation of H_2^+ in 7 fs FTL pulses and pulses chirped to 15 fs. Both theory and experiment show the predicted effect of the pulse chirp (see text).

We have also demonstrated control over ZPD using the pulse chirp as a control knob. In our understanding of ZPD, a higher energy photon should precede a lower energy photon. This suggests that a negative chirp should enhance ZPD while a positive chirp should suppress it – a fact demonstrated by both our measurements and calculations in Fig. 1.

More intriguing is the study of ZPD in HD^+ , which has two distinguishable dissociation channels, H^+D and $\text{H}+\text{D}^+$. In ultrashort 7 fs (FTL) pulses we observe a preference for dissociation to the lower H^+D channel at very low KER (see figure to the right) in accord with ground state dissociation findings [6]. Surprisingly, this channel asymmetry, i.e. the preference for H^+D over $\text{H}+\text{D}^+$ or vice versa, is observed over a wide range of KER. Preliminary calculations and measurements indicate that this channel asymmetry depends strongly on the explicit conditions initiating dissociation of specific vibrational states and appears in a wide variety of pulses. It is curious to note that we observe this channel asymmetry in a single pulse where, in contrast, such asymmetry is not visible in asymmetric fields generated by mixing 2-colors (i.e. $\omega-2\omega$) [7,8]. This project was recently presented as an invited talk at DAMOP 2011, and we plan to pursue the study of this phenomenon further.

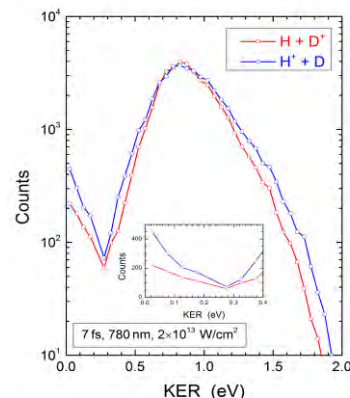


Figure 2. The KER distribution of HD^+ dissociation into H^+D and $\text{H}+\text{D}^+$.

Intense short pulse laser-induced ionization and dissociation of molecular-ion beams

The goal for these projects was to extend our knowledge of H_2^+ and apply it to more complex molecules in intense ultrafast laser pulses. – Studies of the benchmark H_2^+ and H_2 molecules provide the foundation for our understanding of the behavior of diatomic and somewhat more complex molecules in intense ultrashort laser pulses. For example, we have studied vibrational structure and suppression in O_2^+ dissociation (Pub. #23) following our similar work on H_2^+ (Pub. #11). Taking advantage of our new experimental capabilities we have extended our studies of dissociation of the benchmark polyatomic molecule, H_3^+ , down to almost zero KER. All these projects have benefited from the strong collaboration with the theory group of Esry.

Armed with better understanding of the benchmark systems above, we have explored more complex molecules. For example, in collaboration with the WIS group we have studied channel opening in I_2^+ and NO^+ dissociation. In another example, a summer project of an undergraduate student “*Strong-field dissociation dynamics of NO^{2+} : A multiphoton electronic or vibrational excitation?*”, was presented in the undergraduate student research session of DAMOP 2011.

Adaptive femtosecond control of isomerization dynamics in acetylene and ethylene, E.

Wells, M. Zohrabi, C. Rallis, B. Jochim, P. Andrews, U. Ablikim, B. Gaire, S. De, B. Bergues, K.D. Carnes, M.F. Kling, and I. Ben-Itzhak – Shaping ultrafast laser pulses using adaptive feedback is a proven technique for manipulating dynamics in molecular systems with no readily apparent control mechanism. Commonly employed feedback signals include fluorescence or ion yield, which do not always uniquely identify the final state. This ambiguity can further complicate the already difficult task of deciphering the control mechanism, which in turn leads to lower control fidelity and difficulties in understanding how to best parameterize the experimental search space for a particular problem (e.g. Pub. #13-14,22). By rapidly inverting 2D velocity map images to recover the three-dimensional photofragment momentum distribution and incorporating the complete three-dimensional information into the control loop, we improve our

ability to select and control specific final targets. The application of this strong-field closed-loop control technique is demonstrated by controlling isomerization dynamics in acetylene and ethylene, where we find that we can selectively enhance or suppress the production of CH_2^+ from C_2H_2 and CH_3^+ from C_2H_4 . In acetylene, the isomerization channel appears to be enhanced by restricting the relaxation back to the acetylene-like configuration following excitation to the vinylidene-like state using a train of pulses sequenced appropriately in time ($150 \text{ fs} < \Delta t < 250 \text{ fs}$) [9,10]. Pulse parameterization in either the frequency or time domain leads to similar optimal pulse features. This project was presented by Eric Wells as an invited talk at DAMOP 2011.

In addition to our laser studies, we have conducted a few collision experiments between keV molecular ion beams and atomic targets. For example, at present we are investigating collision induced dissociation accompanied by target ionization and have shown that target ionization and excitation very likely raises questions about the common practice of neglecting target excitation in theoretical treatments. This project will be presented as an invited talk in ISAC 2011.

Future plans: We will continue interrogating benchmark molecular ion beams, such as H_2^+ and H_3^+ , in particular taking advantage of the new capabilities of the PULSAR laser, specifically exploring challenging two-color, pump-probe and CEP dependence (see Pub. #21) experiments. We will carry on our studies of more complex molecules including polyatomic molecules and also continue some collision studies that will merge with our laser studies in the near future.

References:

1. J.H. Posthumus *et al.*, J. Phys. B **33**, L563 (2000).
2. J.H. Posthumus *et al.*, Phys. Rev. Lett. **101**, 233004 (2008).
3. I. Ben-Itzhak *et al.* Phys. Rev. Lett. **95**, 073002 (2005).
4. B. Gaire, Ph.D. Thesis, Kansas State University (2011).
5. B. Gaire *et al.*, submitted to Phys. Rev. Lett. (2011).
6. E. Wells *et al.* Phys. Rev. Lett. **86**, 4803 (2001).
7. B. Sheehy, B. Walker, and L. F. DiMauro, Phys. Rev. Lett. **74**, 4799 (1995).
8. E. Charron, A. Giusti-Suzor, and F. H. Mies, Phys. Rev. Lett. **75**, 2815 (1995).
9. Matsuda *et al.*, Phys. Chem. Chem. Phys. (2011), DOI: 10.1039/c0cp02333g.
10. Hishikawa *et al.*, Phys. Rev. Lett. **99**, 258302 (2007).

Publications of DOE sponsored research in the last 3 years:

24. "Effect of linear chirp on strong field photodissociation of H_2^{++} ", Vaibhav S. Prabhudesai, Uri Lev, Oded Heber, Daniel Strasser, Dirk Schwalm, Daniel Zajfman, Adi Natan, Barry D. Bruner, Yaron Silberberg, and Itzik Ben-Itzhak, Journal of Korean Physical Society (AISAMP proceedings) (2011) – accepted.
23. "Vibrationally resolved structure in O_2^+ dissociation induced by intense ultrashort laser pulses", M. Zohrabi, J. McKenna, B. Gaire, Nora G. Johnson, K.D. Carnes, S. De, I.A. Bocharova, M. Magrakvelidze, D. Ray, I.V. Litvinyuk, C.L. Cocke, and I. Ben-Itzhak, Phys. Rev. A **83**, 053405 (2011).
22. "Velocity map imaging as a tool for gaining mechanistic insight from closed-loop control studies of molecular fragmentation", Bethany Jochim, R. Averin, Neal Gregerson, J. McKenna, S. De, D. Ray, M. Zohrabi, B. Bergues, K.D. Carnes, M.F. Kling, I. Ben-Itzhak, and E. Wells, Phys. Rev. A **83**, 043417 (2011).
21. "single-shot carrier-envelope-phase-tagged ion-momentum imaging of nonsequential double ionization of argon in intense 4-fs laser fields", Nora G. Johnson, O. Herrwerth, A. Wirth, S. De, I. Ben-Itzhak, M. Lezius, B. Bergues, M.F. Kling, A. Senftleben, C.D. Schröter, R. Moshhammer, J. Ullrich, K.J. Betsch, R.R. Jones, A.M. Saylor, T. Rathje, K. Rühle, W. Müller, and G.G. Paulus, Phys. Rev. A **83**, 013412 (2011).
20. "Three-dimensional energy profile measurement of a molecular ion beam by coincidence momentum imaging compared to a retarding field analyzer", W. Wolff, J. McKenna, R. Vácha, M. Zohrabi, B. Gaire, K.D. Carnes, and I. Ben-Itzhak, Journal of Instrumentation **5**, 10006 (2010).
19. "Dynamic control of the fragmentation of CO^{q+} excited states generated using high-order harmonics", W. Cao, S. De, K.P. Singh, S. Chen, M. Schöffler, A. Alnaser, I. Bocharova, G. Laurent, D. Ray, M.F. Kling, I. Ben-Itzhak, I. Litvinyuk, A. Belkacem, T. Osipov, T. Rescigno, and C.L. Cocke, Phys. Rev. A **82**, 043410 (2010).

18. "Time-dependent dynamics in intense laser-induced above threshold Coulomb explosion", B.D. Esry and I. Ben-Itzhak, *Phys. Rev. A* **82**, 043409 (2010).
17. "Resonances in electron-capture total cross sections for C^{4+} and B^{5+} collisions with $H(1s)$ ", P. Barragán, L.F. Errea, F. Guzmán, L. Mández, I. Rabadán, and I. Ben-Itzhak, *Phys. Rev. A* **81**, 062712 (2010).
16. "Vibrationally-cold CO^{2+} in intense ultrashort laser pulses", J. McKenna, A.M. Saylor, F. Anis, Nora G. Johnson, B. Gaire, Uri Lev, M.A. Zohrabi, K.D. Carnes, B.D. Esry, and I. Ben-Itzhak, *Phys. Rev. A* **81**, 061401(R) (2010).
15. "Tracing the photodissociation probability of H_2^+ in intense fields using chirped laser pulses", Vaibhav S. Prabhudesai, Uri Lev, Adi Natan, Barry D. Bruner, Adi Diner, O. Heber, D. Strasser, D. Schwalm, I. Ben-Itzhak, J.J. Hua, B.D. Esry, Y. Silberberg, and D. Zajfman, *Phys. Rev. A* **81**, 023401 (2010).
14. "Closed-loop control of vibrational population in CO^{2+} ", E. Wells, J. McKenna, A.M. Saylor, Bethany Jochim, Neal Gregerson, R. Averin, M. Zohrabi, K.D. Carnes, and I. Ben-Itzhak, *J. Phys. B* **43**, 015101 (2009).
13. "Examining the feedback signals used in closed-loop control of intense laser fragmentation of CO^+ ", E. Wells, Michael Todt, Bethany Jochim, Neal Gregerson, R. Averin, Nathan G. Wells, N.L. Smolnisky, Nathan Jastram, J. McKenna, A.M. Saylor, Nora G. Johnson, M. Zohrabi, B. Gaire, K.D. Carnes, and I. Ben-Itzhak, *Phys. Rev. A* **80**, 063402 (2009).
12. "Controlling two-electron dynamics in double photoionization of lithium by initial state preparation", G. Zhu, M. Schuricke, J. Steinmann, J. Albrecht, J. Ullrich, I. Ben-Itzhak, T.J.M Zourus, J. Colgan, M. Pindzola, and A. Dorn, *Phys. Rev. Lett.* **103**, 103008 (2009).
11. "Suppressed dissociation of H_2^+ vibrational states by reduced dipole coupling", J. McKenna, F. Anis, B. Gaire, Nora G. Johnson, M. Zohrabi, K.D. Carnes, B.D. Esry, and I. Ben-Itzhak, *Phys. Rev. Lett.* **103**, 103006 (2009).
10. "Benchmark measurements of H_3^+ nonlinear dynamics in intense ultrashort laser pulses", J. McKenna, A.M. Saylor, B. Gaire, Nora G. Johnson, K.D. Carnes, B.D. Esry, and I. Ben-Itzhak, *Phys. Rev. Lett.* **103**, 103004 (2009).
9. "Dissociation and ionization of an HD^+ beam induced by intense 395-nm ultrashort laser pulses", J. McKenna, A.M. Saylor, B. Gaire, Nora G. Johnson, E. Parke, K.D. Carnes, B.D. Esry, and I. Ben-Itzhak, *Phys. Rev. A* **80**, 023421 (2009).
8. "Laser-induced multiple ionization of molecular ion beams: N_2^+ , CO^+ , NO^+ , and O_2^+ ", B. Gaire, J. McKenna, Nora G. Johnson, A.M. Saylor, E. Parke, K.D. Carnes, and I. Ben-Itzhak, *Phys. Rev. A* **79**, 063414 (2009).
7. "Permanent dipole transitions remain elusive in HD^+ strong-field dissociation", J. McKenna, A.M. Saylor, B. Gaire, Nora G. Johnson, M. Zohrabi, K.D. Carnes, B.D. Esry and I. Ben-Itzhak, *J. Phys. B* **42**, 121003 (2009) – Fast Track Communication.
6. "Rapid Formation of H_3^+ from ammonia and methane following 4 MeV proton impact", Bethany Jochim, Amy Lueking, Laura Doshier, Sharayah Carey, E. Wells, Eli Parke, M. Leonard, K.D. Carnes, and I. Ben-Itzhak, *J. Phys. B* **42**, 091002 (2009) – Fast Track Communication.
5. "Bond rearrangement following collisions between fast ions and ammonia or methane", E. Wells, E. Parke, Laura Doshier, Amy Lueking, Bethany Jochim, Sharayah Carey, Mat Leonard, K.D. Carnes, and I. Ben-Itzhak, *Application of Accelerators in Research and Industry*, edited by B.L. Doyle and F.D. McDaniel (AIP press, New York 2009), vol. **1099**, p. 133.
4. "Interrogating molecular-ion beams by ultra-short laser pulses", I. Ben-Itzhak, J. McKenna, A.M. Saylor, B. Gaire, Nora G. Johnson, E. Parke, and K.D. Carnes, *Application of Accelerators in Research and Industry*, edited by B.L. Doyle and F.D. McDaniel (AIP press, New York 2009), vol. **1099**, p. 146.
3. "Molecular ion beams interrogated with ultrashort intense laser pulses", Itzik Ben-Itzhak, *Progress in Ultrafast Intense Laser Science IV*, Series: Springer Series in Chemical Physics, Vol. **91**, edited by K. Yamanouchi, A. Becker, R. Li, and S.L. Chin (Springer, New York 2009) p. 67 – invited.
2. "Elusive enhanced-ionization structure for H_2^+ in intense ultrashort laser pulses", I. Ben-Itzhak, P.Q. Wang, A.M. Saylor, K.D. Carnes, M. Leonard, B.D. Esry, A.S. Alnaser, B. Ulrich, X.M. Tong, I.V. Litvinyuk, C.M. Maharjan, P. Ranitovic, T. Osipov, S. Ghimire, Z. Chang, and C.L. Cocke, "Elusive enhanced-ionization structure for H_2^+ in intense ultrashort laser pulses", *Phys. Rev. A* **78**, 063419 (2008).
1. "High kinetic energy release upon dissociation and ionization of N_2^+ beams by intense few-cycle laser pulses", B. Gaire, J. McKenna, A.M. Saylor, Nora G. Johnson, E. Parke, K.D. Carnes, B.D. Esry, and I. Ben-Itzhak, *Phys. Rev. A* **78**, 033430 (2008).

¹In addition to the close collaboration with the theory group of Brett Esry, some of our studies are done in collaboration with Lew Cocke's group, Matthias Kling's group, C.W. Fehrenbach, and others.

Probing Sub-Cycle Excitation Dynamics with Isolated Attosecond Pulses

Zenghu Chang

Kansas State University and University of Central Florida
Zenghu.Chang@ucf.edu

The goals of this aspect of the JRML program are (1) to generate and characterize ultrabroad bandwidth attosecond pulses, (2) to use the isolated attosecond pulses for studying electron dynamics in atoms on its natural time scale.

1. Characterization of Broadband Isolated 77 as Pulse. *Kun Zhao, Qi Zhang, Michael Chini, Steve Gilbertson, Sabih D. Khan, and Zenghu Chang.*

Due to the low-photon flux of the isolated attosecond XUV pulse at the present time, methods for characterization of femtosecond lasers that based on nonlinear optical gating, such as second order auto-correlator, are difficult to implement on the attosecond timescale [1]. Instead, attosecond pulses are typically characterized using an attosecond streak camera, whereby an electron replica of the XUV pulse produced through photoionization of atoms is accelerated in a delayed dressing near-infrared (NIR) laser field. The amplitude and phase of the attosecond pulse are retrieved from the delay-dependent streaked spectrogram using a technique known as FROG-CRAB (frequency-resolved optical gating for complete reconstruction of attosecond bursts) [8]. This method, however, are not appropriate for pulses whose spectral bandwidth is large than the center photon energy [3]. This is a serious deficiency since such attosecond pulse with small center photon energy (close to the ionization energy of atoms and molecules, ~ 10 to 20 eV) are very important for studying dynamics of chemical reactions and other processes. For generating pulses much shorter than the current record, 80 as, the bandwidth may also be much larger than the central photon energy. It is therefore desirable to develop methods for characterize isolated attosecond pulses whose bandwidth is larger than the center photon energy. We developed a new technique for characterizing attosecond pulses, whereby the spectral phase of the attosecond pulse is extracted from the oscillation component with the dressing laser frequency in the photoelectron spectrogram. This technique, termed PROOF (Phase Retrieval by Omega Oscillation Filtering), can be applied to characterizing attosecond pulses with ultrabroad bandwidths [9]. The spectral phase encoding in PROOF can be described by quantum interference of the continuum states caused by the dressing laser.

Recently, an improved PROOF algorithm which accounts for both the amplitude and phase of the interference oscillations has been employed to retrieve broadband attosecond pulses, which converges more robustly than that introduced previously. Two algorithms, PROOF and FROG-CRAB, were employed to retrieve attosecond pulses with spectra spanning 25 to 80 eV from the experimental spectrograms shown in Fig. 1. The attosecond pulses were generated using GDOG [2, 10, 18]. An isolated 77 as transform-limited pulse and a 115 as negatively-chirped pulse were reconstructed by PROOF, while FROG-CRAB gave flat spectral phases in both cases. This is the first experimental evidence that shows PROOF is able to retrieve broadband attosecond pulses even when FROG-CRAB is not.

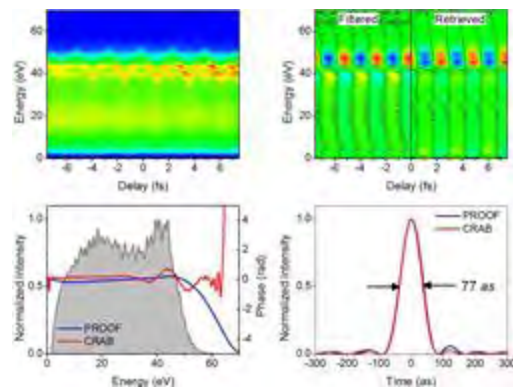


FIG. 1 Characterization of a nearly transform-limited 77 as XUV pulse.

2. Time resolved AC Stark shift and autoionization. *Michael Chini, He Wang, Yan Cheng, Baozhen Zhao, S. X. Hu, U. Thumm and Zenghu Chang.*

Single isolated attosecond pulse is a new powerful tool for studying dynamics of correlated electron motion in pump-probe experiments. Such pulses can now be routinely generated with the Generalized Double Optical Gating (GDOG) method. The broadband XUV supercontinuum spectrum of the attosecond pulse is particularly suitable for probing the time variation of the electronic states in transient absorption measurements [17].

We performed the first measurement of AC Stark shift of the helium $1snp$ manifold of excited states using isolated attosecond pulses. With this measurement, we can fully characterize the AC Stark shift of each excited state and observe dynamics of electrons in these states with unprecedented time resolution. The same method was also used to time-resolve the Fano profile which is the result of interference between the direct ionization and the decay from an autoionizing state due to configuration interaction [14].

The experiments were done using a Mach-Zehnder type pump-probe configuration and by detecting the transient absorption spectrum of the attosecond XUV pulse, as shown in Fig. 2.

1 mJ, 6 to 8 fs pulses centered at 750 nm were split into two parts. A portion of the beam was used to generate an isolated attosecond pulse using the generalized double optical gating technique. The XUV supercontinuum spectrum spanned photon energies from 20 eV to 40 eV and the isolated 140 as pulses were characterized using an attosecond streak camera.

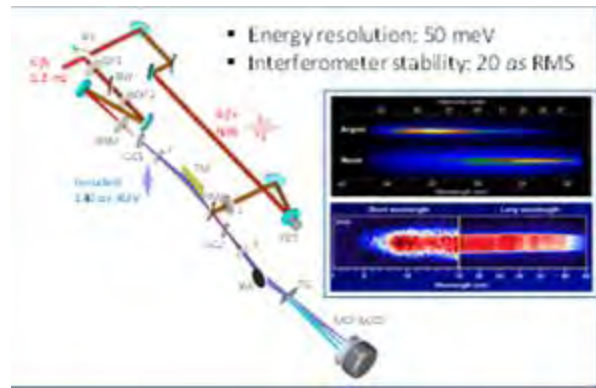


Fig. 2 Attosecond transient absorption setup.

As compared to other schemes for generating isolated attosecond pulses, the GDOG does not require the stabilization of the carrier-envelope phase of the driving laser, which significantly reduced the difficulties of the experiments.

The XUV light was then focused using a toroidal mirror to a second gas cell filled with the atomic gas. The gas density was adjusted to have $\sim 25\%$ transmission above the ionization potential (24.6 eV for helium). The other half of the NIR beam passed through an equal optical path length and was recombined collinearly with the XUV pulse using a hole-drilled mirror. Delay between the two pulses was introduced using a piezoelectric translation stage. The transmitted XUV spectrum of the attosecond pulse was measured using a transmission grating spectrometer (2000 l/mm) with <50 meV resolution in the energy region of interest and measured as a function of the time delay between the two pulses. The setup is all-optical, much simpler than the attosecond streak camera that has been a popular tool in attosecond experiments.

Helium atom was chosen for the AC Stark shift experiments. We measured the delay-dependent transmitted XUV spectrum with a NIR laser peak intensity of 10^{13} W/cm² when the delay was scanned over the entirety of the NIR laser pulse. Several of the $1snp$ excited states can be identified by their strong absorption. Each of the absorption lines traces out the NIR laser pulse profile. From the energy

shift, the NIR pulse shape and intensity on target can be determined in situ, which is important for analyzing data of other attosecond transient absorption experiments. By fitting the trace of the $1s3p$ state, the FWHM of the NIR pulse in the current experiments is 8 fs. Interestingly, the shifts of the individual excited states appear to occur on different time scales, which was unexpected. Moreover, the lines are broadened in the laser pulse, with the lower-lying states exhibiting larger energy shifts and broadened widths.

Most remarkably, when the two pulses overlap, a clear oscillation of the signal with a period of ~ 1.3 fs (half of the laser oscillation period) is observed, which extends above the ionization potential of 24.6 eV. Such half-cycle oscillations indicating sub-laser-cycle dynamics in the AC Stark effect have never been observed experimentally before.

We also studied the autoionization of argon atom, which is a process governed by electron-electron correlation. The Fano profile, which is the signature of the autoionization process, has widespread significance in many scientific disciplines. For decades, spectral-domain measurements with synchrotron radiation have served as a window into the rich dynamics of autoionization. However, the synchrotron pulse duration is too long (100 fs to 100 ps) to time-resolve the Fano resonances since the autoionization lifetimes can be as short as a few femtoseconds.

We measured the transmitted XUV signal at the energy of the unperturbed $3s3p64p$ (26.6 eV) and $3s3p65p$ (28.0 eV) peaks as a function of the delay. When the XUV and NIR overlap temporally, the transmitted signals are minimized, as shown in Fig. 3. The recovery of the signal is substantially faster when the delay is positive.

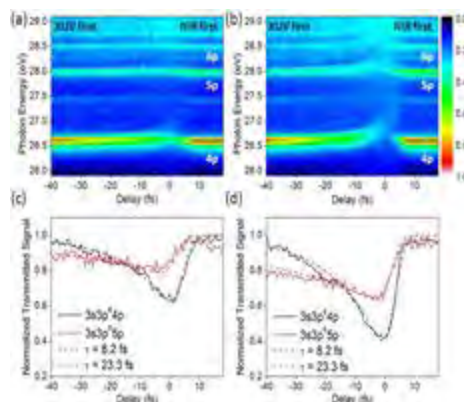


Fig. 3 Transmitted attosecond XUV spectra of argon in a strong NIR laser field with a peak intensity of (a)/(c) 5×10^{11} W/cm² and (b)/(d) 10^{12} W/cm².

The asymmetric weakening of the signal with respect to delay can be fit very well using a cross-correlation of an exponential function with the autoionization state lifetimes and a Gaussian laser pulse. At the NIR laser peak intensity of $\sim 10^{12}$ W/cm, the $3s3p65p$ and $3s3p66p$ states primarily exhibit an energy shift as well as broadening and weakening of the resonances, but the effects were enhanced compared with the results for the lower intensity in Fig. 3 (a). Most interestingly, $3s3p64p$ exhibits a dramatic splitting which is asymmetric with respect to zero delay. The upper branch extends nearly to the neighboring $3s3p65p$ peak, whereas the lower branch remains near the unperturbed energy. The observed phenomena suggest a dynamic control over the autoionizing states by the NIR laser.

Isolated attosecond pulses generated with GDOG allow direct measurement of the attosecond dynamics in the Stark shift of the excited states in helium atoms. The observed half-cycle oscillation indicates that the bound electrons are able to respond to the field oscillations on the attosecond time scale. Furthermore, control of the autoionization process in argon clearly demonstrates that isolated attosecond pulses are crucial tools for studying electron correlation dynamics. The time resolution is limited by the NIR laser. New schemes of GDOG are under development to produce more intense XUV attosecond pulses so that they can be used as both the pump and probe in the same experiment.

We have participated in studying dynamics in molecules [13, 20] (lead by Dörner at the University of Frankfurt) and on micro-machining using the ultrafast lasers lead by Lei at KSU.

PUBLICATIONS (2009-2011). Some papers in 2009 are not included.

1. (Book chapter) Zenghu Chang, "Chapter 20: Attosecond Optics," *Handbook of Optics* Vol. II, sponsored by Optical Society of America, Edition 3, 2009, McGraw Hill. ISBN: 9780071498906.
2. Ximao Feng, Steve Gilbertson, Hiroki Mashiko, He Wang, Sabih D. Khan, Michael Chini, Yi Wu, Kun Zhao, and Zenghu Chang, "Generation of isolated attosecond pulses with 20 to 28 femtosecond lasers," *Phys. Rev. Lett.* **103**, 183901 (2009).
3. Hiroki Mashiko, Steve Gilbertson, Ximao Feng, Chenxia Yun, Sabih D. Khan, He Wang, Michael Chini, Chen Shouyuan, and Zenghu Chang, "XUV supercontinua supporting pulse durations of less than one atomic unit of time," *Optics Letters* **34**, 3337 (2009).
4. Chenxia Yun, Shouyuan Chen, He Wang, Michael Chini and Zenghu Chang "Temperature feedback control for long-term carrier-envelope phase locking," *Applied Optics* **48**, 5127 (2009).
5. Steve Gilbertson, Ximao Feng, Sabih Khan, Michael Chini, He Wang, Hiroki Mashiko, and Zenghu Chang, "Direct measurement of an electric field in femtosecond Bessel-Gaussian beams," *Optics Letters* **34**, 2390 (2009).
6. He Wang, Eric Moon, Michael Chini, Hiroki Mashiko, Chengquan Li, and Zenghu Chang, "Coupling between energy and carrier-envelope phase in hollow-core fiber based f-to-2f interferometers," *Optics Express* **17**, 12082 (2009).
7. Eric Moon, He Wang, Steve Gilbertson, Hiroki Mashiko and Zenghu Chang, "Advances in Carrier-Envelope Phase Stabilization of Grating-Based Chirped-Pulse Lasers," *Laser and Photonics Reviews* **4**, 160 (2009).
8. He Wang, Michael Chini, Sabih D. Khan, Shouyuan Chen, Steve Gilbertson, Ximao Feng, Hiroki Mashiko and Zenghu Chang, "Practical issues of retrieving isolated attosecond pulses," *J. Phys.* **B42**, 134007 (2009).
9. Michael Chini, Steve Gilbertson, Sabih D. Khan, and Zenghu Chang, "Characterizing ultrabroadband attosecond lasers," *Opt. Express* **18**, 13006 (2010).
10. Steve Gilbertson, Yi Wu, Sabih D. Khan, Michael Chini, Kun Zhao, Ximao Feng, and Zenghu Chang, "Isolated attosecond pulse generation using multicycle pulses directly from a laser amplifier," *Phys. Rev. A* **81**, 043810 (2010).
11. He Wang, Michael Chini, Yi Wu, Eric Moon, Hiroki Mashiko and Zenghu Chang, "Carrier-envelope phase stabilization of 5 fs, 0.5 mJ, pulses from adaptive phase modulators," *Applied Physics B* **98**, 291 (2010).
12. Ximao Feng, Steve Gilbertson, Sabih D. Khan, Michael Chini, Yi Wu, Kevin Carnes, and Zenghu Chang, "Calibration of electron spectrometer resolution in attosecond streak camera," *Optics Express* **18**, 1316 (2010).
13. B. Ulrich, A. Vredenburg, A. Malakzadeh, M. Meckel, K. Cole, M. Smolarski, Z. Chang, T. Jahnke, and R. Dörner, "Double ionization mechanisms of the argon dimer in intense laser fields," *Phys. Rev. A* **82**, 013412 (2010).
14. Steve Gilbertson, Michael Chini, Ximao Feng, Sabih Khan, Yi Wu, and Zenghu Chang, "Monitoring and Controlling the Electron Dynamics in Helium with Isolated Attosecond Pulses," *Phys. Rev. Lett.* **105**, 263003 (2010).
15. Qi Zhang, Kun Zhao, and Zenghu Chang, "Determining time resolution of microchannel plate detectors for electron time-of-flight spectrometer," *Rev. Sci. Instrum.* **81**, 073112 (2010).
16. Zenghu Chang and P. Corkum, "Attosecond optics, the first decade and beyond," *J. Opt. Soc. Am. B* **27**, 9 (2010). (Invited).
17. He Wang, Michael Chini, Shouyuan Chen, Chang-Hua Zhang, Feng He, Yan Cheng, Yi Wu, Uwe Thumm, and Zenghu Chang, "Attosecond Time-Resolved Autoionization of Argon," *Phys. Rev. Lett.* **105**, 143002 (2010).
18. Steve Gilbertson, Sabih D. Khan, Yi Wu, Michael Chini, Zenghu Chang "Isolated attosecond pulse generation without the need to stabilize the carrier-envelope phase of driving lasers," *Phys. Rev. Lett.* **105**, 093902 (2010).
19. (Book chapter) Ximao Feng, Steve Gilbertson, Hiroki Mashiko, Sabih Khan, He Wang, Michael Chini, Yi Wu, and Zenghu Chang, "Chapter 5, Single Isolated Attosecond Pulses Generation with Double Optical Gating," *Progress in Ultrafast Intense Laser Science VI*, pp. 89-112. Series: Springer Series in Chemical Physics, Vol. 99, Yamanouchi, Kaoru; Gerber, Gustav; Bandrauk, Andre D. (Eds.), 1st Edition., 2010, XVI, 237 p., ISBN: 978-3-642-15053-1.
20. B. Ulrich, A. Vredenburg, A. Malakzadeh, L. Schmidt, T. Havermeier, M. Meckel, K. Cole, M. Smolarski, Zenghu Chang, T. Jahnke, R. Doerner, "Imaging of the Structure of the Argon and Neon Dimer, Trimer and Tetramer," *The Journal of Physical Chemistry*, DOI: 10.1021/jp1121245 (2011).
21. (Book) Zenghu Chang, *Fundamentals of Attosecond Optics*, CRC Press; 1 edition (February 16, 2011) ISBN-10: 1420089374.

Structure and Dynamics of Atoms, Ions, Molecules and Surfaces: Atomic Physics with Ion Beams, Lasers and Synchrotron Radiation

C.L.Cocke, Physics Department, J.R Laboratory, Kansas State University,
Manhattan, KS 66506, cocke@phys.ksu.edu

During the past year we have concentrated on three projects. We have used a pump/probe technique with 8 fs IR pulses and velocity map imaging to investigate the dynamics of wave packets in N_2 , O_2 and CO . We have used two-color (800 nm/400nm) pulses to investigate the favored orientation for strong-field ionization of CO and NO . We have used a EUV/IR pump/probe method to investigate the double ionization of O_2 and to follow the time dependence of the fragmenting wave packet in collaboration with the COLTIRMS group at the ALS.

Progress:

1) Observing the same wave packets in both time domain and energy domain in O_2 and CO with short infrared pulses, *S. De, M. Magrakvelidze, I. Bocharova, D. Ray, W. Cao, I. Znakovskaya, H. Li, Z. Wang, G. Laurent, U. Thumm, M. F. Kling, I. Litvinyuk, I. Ben-Itzhak and C. L. Cocke.* [1] We launch vibrational wave packets into excited states of various potential curves of charged oxygen and carbon monoxide molecules using 8 fs 790 nm pulses. After a delay up to 1.2 ps the wave packet is probed with a second 8 fs pulse. We record the kinetic energy release (KER) of the ions using a velocity-map-imaging system. We are able to distinguish fragments from final cation and dication molecules. For the case of the low energy cation fragments (KER below 2 eV) we observe vibrational structure in the KER spectrum of both molecules with a characteristic spacing ΔE . The pump-probe spectra of the same packets show oscillatory behavior with a period of ΔT . The product of ΔE and ΔT is found to be Planck's constant, indicating that we are observing the same physical process in both the energy and the time domain. The power spectra (Fourier transform of the time-versus-KER plot) show that the wave packets are chirped: higher KER is accompanied by smaller oscillation frequencies because the vibrational spacing is smaller. We have evaluated models for describing this chirp for both O_2 and CO . Good qualitative agreement is found, but the expected oscillation frequencies are lower than those observed. A coupled channel solution to Schrödinger's equation, within a two-state basis, has also been calculated for the oxygen case. This project will be presented orally.

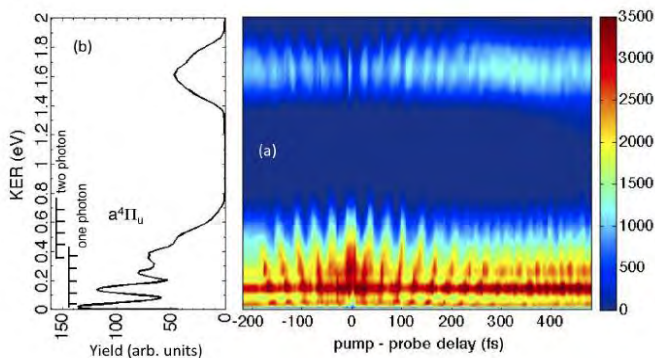


Fig. 1 The yield of O^+ ions as a function of pump-probe delay and KER. Vibrational structure is seen in the projection onto the energy axis, with a spacing near 0.12 eV. This approximately matches the expected ΔE for the $a^4\Pi_u$ state of O^+ . The oscillation period near 35 fs is similarly close to that expected for this state.

2) Orientation dependence of the ionization of CO and NO in an intense femtosecond two-color laser field, *H.Li, D. Ray, S.De, I. Znakovskaya, W.Cao, G.Laurent, Z.Wang, M. F. Kling,*

A.T.Le, and C. L. Cocke. [2] Two-color (800 nm and 400 nm) short (45 fs) linearly polarized pulses were used to ionize and dissociate CO and NO. The emission of C^{+q} , N^{+q} and O^+ fragments were measured with a velocity-map-imaging system. The data show that the ionization rate is dependent on the orientation of the molecules with respect to the laser polarization, with the higher rate occurring when the electric field points from the C to the O (for CO) or N to the O (for NO). The sign of the asymmetry is not dependent on kinetic energy release (KER). The asymmetry of emission is much higher for CO than for NO. The favored ionization orientation is in agreement with the expectations of MO-ADK [3] theory, but when the effective ionization potential is corrected for a linear Stark shift, this agreement is lost. A strong-field-approximation calculation, including the Stark shift, is found to be in agreement with the data.

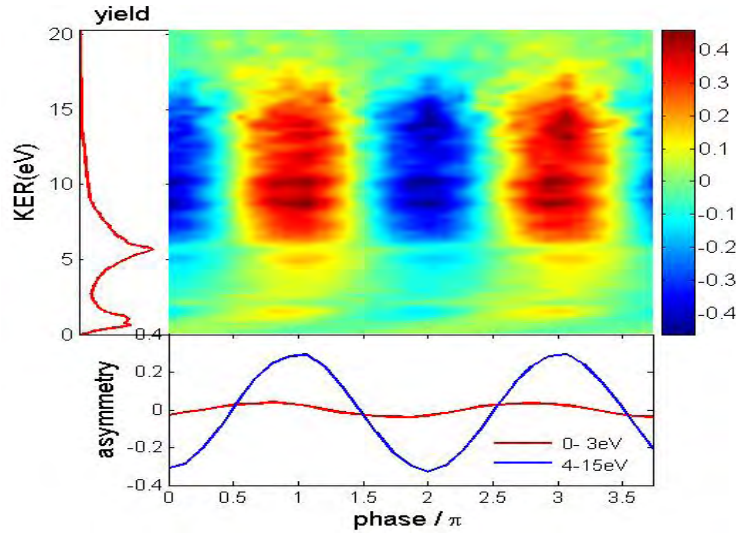


Fig. 2 Density plot of the asymmetry $(Y_{up}-Y_{down})/(Y_{up}+Y_{down})$, of emission of C^+ ions from CO at an intensity of 2×10^{14} W/cm² as a function of two-color phase and KER. A projection of the yield versus KER is shown in the left panel, while the lower panel shows plots of asymmetry versus phase for two chosen slices of the KER. A two color phase of zero corresponds to the maximum electric field pointing “up”.

3) Dynamic modification of the fragmentation of autoionizing excited states of O_2^+ , W. Cao, G. Laurent, S. De, M. S. Schöffler^{1,2}, T. Jahnke², A. Alnaser³, I. A. Bocharova¹, D. Ray, M. F. Kling⁴, I. Ben-Itzhak, T. Weber¹, A. Landers⁵, A. Belkacem¹, R. Dörner², A. Ore⁶, T. Rescigno¹ and C. L. Cocke,¹ Lawrence Berkeley National Laboratory, Berkeley, CA 94720, USA; ²Institut für Kernphysik, Univ. of Frankfurt, Max-von-Laue-Str. 1, D-60438 Frankfurt, Germany; ³Physics Department, American University of Sharjah, Sharjah, UAE, ⁴Max-Planck Institute of Quantum Optics, Hans-Kopfermann-Strasse 1, 85748, Garching, German; ⁵Department of Physics, Auburn University, Auburn, AL 36849, USA ; ⁶ Univ. Cal. Davis. [4] The dynamic process of fragmentation of excited states of molecular oxygen is investigated in a two-part study. First, using monochromatic 41 eV radiation from the Advanced Light Source and COLTRIMS detection of O^+/O^+ ion pairs and associated electrons, we establish that this channel is populated only by an indirect process enabled by autoionization of excited oxygen neutrals, and identify the final active molecular states involved. Second, we probe the dynamics of this process using an attosecond pulse train (APT) of 35-42 eV EUV, followed by an intense laser pulse (800 nm, up to 10^{12} W/cm²). As shown in Fig. 1 below, the KER in the O^+/O^+ channel is found to depend on the delay between the APT and the IR pulse. Our interpretation of this is that the IR removes the most weakly bound electron from the slowly dissociating autoionizing cation molecular state(s) and transforms the cation into a dication. The KER is increased by this removal because of the Coulomb energy in the dication fragmentation channel. A theoretical potential curve for this autoionizing molecule has been calculated and used with a solution to the

time dependent Schrödinger equation to calculate the expected KER versus delay. The result is in adequate agreement with experiment.

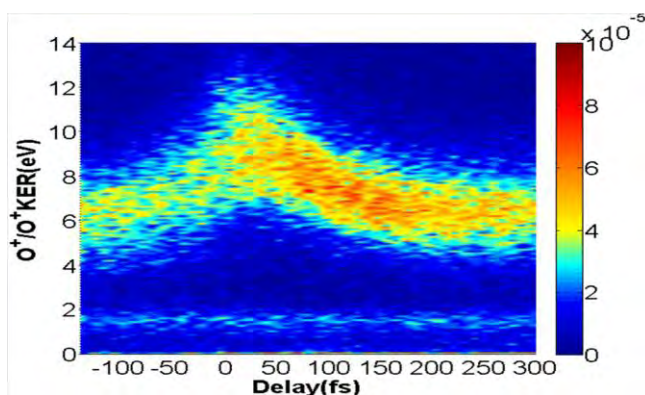


Fig. 3 The KER in the O^+/O^+ channel when an APT used to ionize and excite O_2 and an infrared pulse is used to modify the fragmentation dynamics after a certain

References:

- [1] S. De, M. Magrakvelidze, I. Bocharova, D. Ray, W. Cao, I. Znakovskaya, H. Li, Z. Wang, G. Laurent, U. Thumm, M. F. Kling, I. Litvinyuk, I. Ben-Itzhak and C. L. Cocke, submitted to Phys.Rev. A (2011).
- [2] , H.Li, D. Ray, S.De, I. Znakovskaya, W.Cao, G.Laurent, Z.Wang, M. F. Kling, A.T.Le, and C. L. Cocke, submitted to Phys.Rev. A (2011).
- [3] X.M.Tong,Z.X Zhao and C.D.Lin, Phys.Rev.A 66 , 033402 (2002).
- [4] W. Cao, G. Laurent, S. De, M. S. Schöffler, T. Jahnke, A. Alnaser, I. A. Bocharova, D. Ray, M. F. Kling, I. Ben-Itzhak, T.Weber, A Landers, A. Belkacem, R. Dörner, A.Orel , T.Rescigno and C. L. Cocke, to be submitted to Phys.Rev. A (2011).

Publications since 2010: (Earlier publications are available at

<http://www.phys.ksu.edu/personal/cocke>)

- 1) Tracking nuclear wave-packet dynamics in molecular oxygen ions with few-cycle infrared laser pulses, De, I. A. Bocharova, M. Magrakvelidze, D. Ray, W. Cao, B. Bergues, U. Thumm, M. F. Kling, I. V. Litvinyuk, and C. L. Cocke, Phys. Rev. A 82, 013408 (2010).
- 2) Carbon K-shell photoionization of fixed-in-space C_2H_4 , T. Osipov, M. Stener, A. Belkacem, M. Schöffler, Th. Weber, L. Schmidt, A. Landers, M. H. Prior, R. Dörner, and C. L. Cocke, Phys. Rev. A 81, 033429 (2010).
- 3) Carbon K-shell photoionization of fixed-in-space C_2H_4 , T. Osipov, M. Stener, A. Belkacem, M. Schöffler, Th. Weber, L. Schmidt, A. Landers, M. H. Prior, R. Dörner, and C. L. Cocke, Phys. Rev. A 81, 033429 (2010).
- 4) Control of Electron Localization in Deuterium Molecular Ions using an Attosecond Pulse Train and a Many-Cycle Infrared Pulse , K. P. Singh, F. He, P. Ranitovic, W. Cao, S. De, D. Ray, S. Chen, U. Thumm, A. Becker, M. M. Murnane, H. C. Kapteyn, I. V. Litvinyuk, and C. L. Cocke, Phys. Rev. Lett. 104, 023001 (2010).
- 5) Separation of Auger transitions into different repulsive states after K -shell photoionization of N_2 molecules , N. A. Cherepkov, S. K. Semenov, M. S. Schöffler, J. Titze, N. Petridis, T. Jahnke, K. Cole, L. Ph. H. Schmidt, A. Czasch, D. Akoury, O. Jagutzki, J. B. Williams, C. L. Cocke, T. Osipov, S. Lee, M. H. Prior, A. Belkacem, A. L. Landers, H. Schmidt-Böcking, Th. Weber, and R. Dörner, Phys. Rev. A 80, 051404 (2009).

- 6) Ion-Energy Dependence of Asymmetric Dissociation of D₂ by a Two-Color Laser Field , D. Ray, F. He, S. De, W. Cao, H. Mashiko, P. Ranitovic, K. P. Singh, I. Znakovskaya, U. Thumm, G. G. Paulus, M. F. Kling, I. V. Litvinyuk, and C. L. Cocke, *Phys. Rev. Lett.* 103, 223201 (2009).
- 7) Field-Free Orientation of CO Molecules by Femtosecond Two-Color Laser Fields , S. De, I. Znakovskaya, D. Ray, F. Anis, Nora G. Johnson, I. A. Bocharova, M. Magrakvelidze, B. D. Esry, C. L. Cocke, I. V. Litvinyuk, and M. F. Kling, *Phys. Rev. Lett.* 103, 153002 (2009).
- 8) Photoelectron and Auger-electron angular distributions of fixed-in-space CO₂ ,F. P. Sturm, M. Schöffler, S. Lee, T. Osipov, N. Neumann, H.-K. Kim, S. Kirschner, B. Rudek, J. B. Williams, J. D. Daughhetee, C. L. Cocke, K. Ueda, A. L. Landers, Th. Weber, M. H. Prior, A. Belkacem, and R. Dörner, *Phys. Rev. A* 80, 032506 (2009) .
- 9) Angular Correlation between Photoelectrons and Auger Electrons from K-Shell Ionization of Neon , A. L. Landers, F. Robicheaux, T. Jahnke, M. Schöffler, T. Osipov, J. Titze, S. Y. Lee, H. Adaniya, M. Hertlein, P. Ranitovic, I. Bocharova, D. Akoury, A. Bhandary, Th. Weber, M. H. Prior, C. L. Cocke, R. Dörner, and A. Belkacem, *Phys. Rev. Lett.* 102, 223001 (2009).
- 10) IR-assisted ionization of helium by attosecond extreme ultraviolet radiation , P. Ranitovic , X. M. Tong, B. Gramkow , S. De , B. DePaola , K. P. Singh , W. M. Magrakvelidze , D. Ray , I. Bocharova , H. Mashiko , A. Sandhu , E. Gagnon , M. M. Murnane , H.C. Kapteyn , I. Litvinyuk and C. L. Cocke , *New J. Phys.* 12, 013008 (2010).
- 11) Dynamic field-free orientation of polar molecules by intense two-color femtosecond laser pulses , I.V. Litvinyuk, S. De , D. Ray , N.G. Johnson , I. Bocharova , M. Magrakvelidze, F. Anis , B.D. Esry , C.L.Cocke, I. Znakovskaya and M. F. Kling , *J. Phys.: Conf. Ser.* 194, 032013 (2010).
- 12) Dynamic modification of the fragmentation of CO^{q+} excited states generated with high-order harmonics , W. Cao, S. De, K. P. Singh, S. Chen, M. S. Schöffler, A. S. Alnaser, I. A. Bocharova, G. Laurent, D. Ray, S. Zherebtsov, M. F. Kling, I. Ben-Itzhak, I. V. Litvinyuk, A. Belkacem, T. Osipov, T. Rescigno, and C. L. Cocke, *Phys. Rev. A* **82**, 043410 (2010).

Atoms and molecules in intense laser pulses

B.D. Esry

J. R. Macdonald Laboratory, Kansas State University, Manhattan, KS 66506

esry@phys.ksu.edu

<http://www.phys.ksu.edu/personal/esry>

Program Scope

The primary goal of my program is to quantitatively understand the behavior of simple benchmark systems in ultrashort, intense laser pulses. As we gain this understanding, we will work to transfer it to other more complicated systems. In this effort, my group works closely with the experimental groups in the J.R. Macdonald Laboratory, including, in particular, the group of I. Ben-Itzhak.

A second component of my program is to develop novel analytical and numerical tools to (i) more efficiently and more generally treat these systems and (ii) provide rigorous, self-consistent pictures within which their non-perturbative dynamics can be understood. The ultimate goal is to uncover the simplest picture that can explain the most.

1. Correlated electron-nuclear motion in multiphoton dissociative ionization

Recent Progress Some time ago in Ref. [1], we proposed a new mechanism for the dissociative ionization of molecules that we called “above threshold Coulomb explosion” (ATCE). The key feature of this process being peaks in the nuclear relative kinetic energy release (KER) spectrum spaced by a photon’s energy in analogy with well-known above threshold ionization and dissociation processes. We supported this proposal with a simple Floquet-based model that we used to explain the structure in experimental data also presented in [1]. More recently, we have applied this model to explain the experimental data of other groups in Pub. [P16]. Our explanation is not the only one that has been given, however [2,3].

We decided that the most unambiguous way to identify the correct explanation was to simply calculate the dissociative ionization spectrum. In a calculation, we can control the conditions perfectly and analyze the results at a level of detail not possible experimentally. Since a direct calculation including all degrees of freedom for this process has not yet been done for any molecule in an intense laser field — and to keep the calculation as simple as possible, but still retain the essential physics — we used H_2^+ including only nuclear vibration and electron motion along the polarization direction of the laser.

Having solved the time-dependent Schrödinger equation for this model system, we had to extract the physical observables from the joint electron-nuclear wave function. Dissociative ionization of H_2^+ results in a free electron along with two free protons and thus lies in the double continuum. The most direct way to obtain this spectrum is thus to project the joint wave function onto the system’s energy eigenstate with asymptotic nuclear energy E_N and electronic energy E_e , then integrate over all electron energies to account for the fact that the electron was not measured in the experiment. We calculated this double continuum eigenstate within the Born-Oppenheimer approximation which we expect to be a good approximation so long as the electron velocity is much larger than the nuclear velocity.

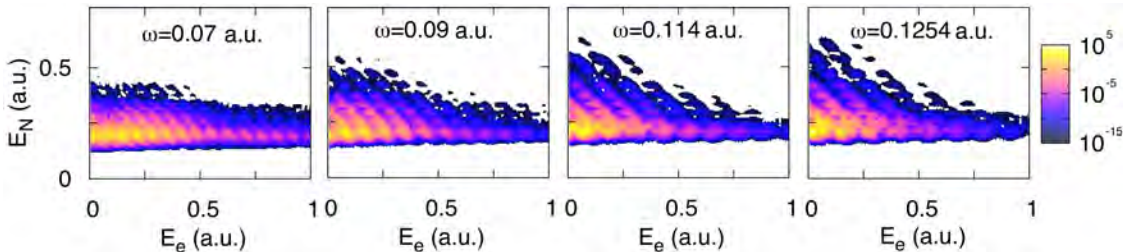


Figure 1: The joint electron-nuclear energy distribution for dissociative ionization of $\text{H}_2^+(v=7)$ in a 6×10^{13} W/cm², 10 cycle laser pulse at the photon energies indicated.

We quickly realized, however, that it was much more interesting to skip the integration over electron energies and look at the joint electron-nuclear energy distribution. Figure 1 shows why: the joint energy spectrum clearly shows the multiphoton nature of the interaction. The peaks that run diagonally through each panel simply reflect the expected energy conservation of a multiphoton process, $E_v + n\omega = E_N + E_e$ (E_v is the initial vibrational energy relative to the $p+p+e$ threshold), up to a possible pondermotive shift.

In two previous decades of similar computational studies, only the projected electron *or* nuclear spectra had been examined. The former shows photon peaks much less clearly when it shows them at all. The latter has only shown them at very low intensities in the ATCE peaks.

It turns out that plots like Fig. 1 reveal quite a lot of information. For instance, the minima at constant E_N seem to correspond to the nodes in the initial vibrational wave function, and this connection can be made quite concrete within the strong field approximation. A little additional analysis of these figures also shows that the simple reflection method for calculating the KER spectrum for ionization is not such a good approximation. Examination of the spectra for different initial vibrational states further shows that the dressed Floquet potentials we introduced in Ref. [1] for ionization can provide a convenient, consistent explanation of the spectrum. Moreover, in the limit of low laser intensity, the spectra tend to collapse towards $E_e=0$, leaving peaks along E_N separated by ω in apparent support of our ATCE explanation.

Future Plans Except for the pervasive influence of the Born-Oppenheimer picture which tends to lead people to consider nuclear observables separately from electronic — and the twenty or so years of study of this particular model without a figure like Fig. 1 — these figures are quite intuitive. A similar figure of electron-nuclear energy sharing following *single* photon dissociative ionization has been shown, for instance, in Ref. [4]. Figure 1 shows that the electron and nuclei interact and share the absorbed energy even in the multiphoton regime. This behavior certainly is not limited to H_2^+ , nor even the electron-nuclear joint spectrum. We expect similar multiphoton features in the joint energy spectrum for any three or more particle breakup in an intense laser field, including three-particle dissociation of a polyatomic molecule and multiple ionization of atoms [5] or molecules.

We are extending this study by looking for ways to manipulate the energy sharing between electrons and nuclei using multiple or shaped pulses. Preliminary results indicate that such manipulation is possible and maybe not even so difficult.

2. Supersymmetric phase-equivalent potentials for atoms in intense fields

Recent progress For multielectron atoms, the single active electron approximation (SAE) provides essentially the only means of calculating their response to intense laser pulses. Generally, the SAE assumes that the core electrons are frozen and do not respond to the laser field. A simple model potential can then be constructed for the one electron to be treated dynamically. While this potential can be calculated from the many-electron wave function, it is more often obtained by fitting the spectrum of a parametrized potential to the experimental spectrum of the atom in question.

One problem with such model potentials is that they support not only the allowed states of the valence electron, but also the Pauli-forbidden states of the core. The valence electron should not be allowed to occupy any of these core states at any point during the dynamics. Satisfying the exclusion principle thus requires that extra steps be taken.

Several methods of approximately excluding the occupied states have been used in the literature, including not excluding them. We have compared some of these methods in the past, and they give qualitatively — but not *quantitatively* — the same answer. Since theory is sometimes now being used to extract laser pulse parameters from experiment, it is critically important to pin down the magnitude of the errors in the theory itself and to find an accurate and efficient means of solving the problem.

One essentially exact approach involves expanding the wave function on the field-free eigenstates — minus the occupied orbitals — of the model potential. This close-coupling approach, however, is not nearly as computationally efficient as grid-based methods. But, grid methods have generally suffered from inexact removal of the occupied states and only partially reproduce the atom’s spectrum.

In a seeming stroke of luck, we recently come across supersymmetric phase equivalent potentials (PEPs). These PEPs let one use the one electron model potential to construct a new potential with the exact same bound spectrum and scattering phase shifts, but with one fewer bound state. The new potential is the PEP; it is local in radius, but is ℓ dependent. It thus works perfectly with a grid method and allows the occupied orbitals to be removed exactly.

Figure 2 compares the spectra calculated with close-coupling (V_0) and with PEPs (V_1). It is clear from the figure that although both methods have exactly the same bound spectra, exactly the same scattering phase shifts, and exactly remove the occupied orbitals, the intense field dynamics are different. To be sure, they match qualitatively, but even the total ionization probabilities differ at the 10% level. Based on our experience with close-coupling, we compared the transition dipole matrix elements for the two methods and

found that those for the PEPs are substantially different from the close-coupling.

Future plans Given the trend towards using theory to extract laser pulse parameters, it is important to be able to provide error bars for the approximations made in the theory. With the PEPs, though, we found that getting the intense field dynamics correct requires more than reproducing the spectral properties of the one-electron model potential in the SAE, it requires reproducing the transition dipole matrix elements as well. This is a substantial challenge and even calls into question the quantitative reliability of the SAE itself. We will continue to investigate methods to treat the multielectron dynamics efficiently and quantitatively, focusing especially on the connection with experiment.

3. Intense-field-driven dynamics near a conical intersection

Recent Progress We have recently begun a program to investigate the dynamics of a polyatomic molecule near a conical intersection driven by an intense field. Conical intersections abound between Born-Oppenheimer surfaces of polyatomics and are an important non-radiative decay path in many systems. Our focus will first be on H_3^+ since that is a simple system and one that we know can be experimentally studied in our Lab [P9]. Actually, our first focus will be on the singly ionized channels, H_3^{2+} , looking at the two- and three-body nuclear breakup problem.

Choosing H_3^{2+} keeps the quantum chemistry demands low, allowing us to focus on the nuclear dynamics. In fact, for our first steps, we lower the chemistry bar even more and consider simple pairwise model of the interaction potential based on the H_2^+ $1s\sigma_g$ (U_g^{ij}) and $2p\sigma_u$ (U_u^{ij}) potentials between atoms i and j :

$$H_e = |g_{12}\rangle U_g^{12} \langle g_{12}| + |u_{12}\rangle U_u^{12} \langle u_{12}| + |g_{31}\rangle U_g^{31} \langle g_{31}| + |u_{31}\rangle U_u^{31} \langle u_{31}| + |g_{23}\rangle U_g^{23} \langle g_{23}| + |u_{23}\rangle U_u^{23} \langle u_{23}|.$$

This diatomics-in-molecule-like interaction is written in terms of projections onto the H_2^+ molecular states $|(g, u)_{ij}\rangle$ for each pair ij . This form allows us to quickly explore different diabaticization schemes appropriate for treating the breakup of this molecule. Writing the dipole operator in a similar pairwise fashion in terms of the H_2^+ $1s\sigma_g$ - $2p\sigma_u$ transition dipole, for instance, shows that in the atomic orbital basis the dipole matrix is diagonal. This should not have been a surprise, but it does show that we ought to be able to take real Born-Oppenheimer potential and dipole surfaces, diagonalize the dipole operator, and use its eigenvectors to produce a diabatic representation that correlates to the atomic basis asymptotically.

Figure 3 shows one diabatic potential surface in the atomic basis for the interaction above in Smith-Whitten hyperspherical coordinates at a fixed hyperradius. These coordinates are convenient as they show all possible configurations of the system in a compact figure. Equilateral triangles, for instance, lie at $\theta=0$; and linear molecules, at $\theta=\pi/2$. The conical intersection (which only exists for the adiabatic surfaces) lies at the equilateral configuration.

The interatomic distances r_{ij} are zero along $\theta=\pi/2$ at $\phi=\pi/3, \pi, \text{ and } 5\pi/3$. The potential surface H_{11} in Fig. 3 shows strong repulsion at two of these three points, with the missing point corresponding to $r_{23}=0$. The other two diabatic surfaces look the same, except with the missing point obtained by cyclic permutation. The advantage of this representation is the lack of the diverging couplings that one finds in the usual Born-Oppenheimer representation.

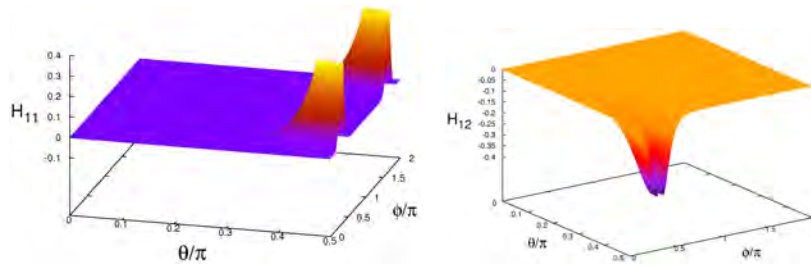


Figure 3: Diabatic potential surface H_{11} in the atomic basis and one of the diabatic coupling elements for H_3^{2+} .

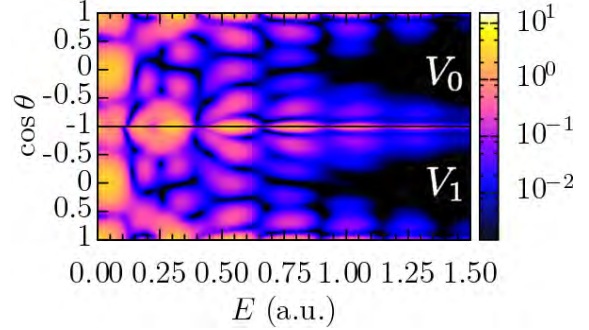


Figure 2: The photoelectron spectra for Ar in a 180 nm, 1.8 cycle, 8.75×10^{14} W/cm² laser pulse calculated using close-coupling (V_0) and grid method with PEPs (V_1). Note that the distributions are mirrored about $\cos\theta=-1$.

Future Plans We are just beginning to explore conical intersections by first identifying a good candidate representation for the electronic degrees of freedom. We believe the atomic basis (or the eigenstates of the dipole operator) will facilitate the solution of the time-dependent Schrödinger equation for the nuclear motion. This will be our next step and should allow us to start gaining insight into the Macdonald Lab experiments [P9]. In the longer term, we hope to design generic models of conical intersections so that a single calculation can apply to a wider range of systems.

References

1. B.D. Esry, A.M. Saylor, P.Q. Wang, K.D. Carnes, and I. Ben-Itzhak, *Phys. Rev. Lett.* **97**, 013003 (2006).
2. A. Staudte, *et al.*, *Phys. Rev. Lett.* **98**, 073003 (2007).
3. S. Chelkowski, A.D. Bandrauk, A. Staudte, and P.B. Corkum, *Phys. Rev. A* **76**, 013405 (2007).
4. W. Cao *et al.*, *Phys. Rev. A* **82**, 043410 (2010).
5. Parker *et al.*, *J. Phys. B* **34**, L69 (2001).

Publications of DOE-sponsored research in the last 3 years

- P17. “Protonium formation in collisions of antiprotons with atomic and molecular hydrogen: A semiclassical study,” R. Cabrera-Trujillo and B.D. Esry, *Radiation Effects and Defects in Solids* (2011).
- P16. “Time-dependent dynamics of intense laser-induced above threshold Coulomb explosion,” B.D. Esry and I. Ben-Itzhak, *Phys. Rev. A* **82**, 043409 (2010).
- P15. “Comparison of theoretical analyses of intense-laser-induced molecular dissociation,” B. Abeln, J.V. Hernández, F. Anis, and B.D. Esry, *J. Phys. B* **43**, 155005 (2010).
- P14. “Vibrationally-cold CO^{2+} in intense ultrashort laser pulses,” J. McKenna, A.M. Saylor, F. Anis, N.G. Johnson, B. Gaire, U. Lev, M.A. Zohrabi, K.D. Carnes, B.D. Esry, and I. Ben-Itzhak, *Phys. Rev. A* **81**, 061401(R) (2010).
- P13. “Tracing the photodissociation probability of H_2^+ in intense fields using chirped laser pulses,” V.S. Prabhudesai, U. Lev, A. Natan, B.D. Bruner, A. Diner, O. Heber, D. Strasser, D. Schwalm, I. Ben-Itzhak, J.J. Hua, B.D. Esry, Y. Silberberg, and D. Zajfman, *Phys. Rev. A* **81**, 023401 (2010).
- P12. “Field-free orientation of CO molecules by femtosecond two-color laser fields,” S. De, I. Znakovskaya, D. Ray, F. Anis, N.G. Johnson, I.A. Bocharova, M. Magrakvelidze, B.D. Esry, C.L. Cocke, I.V. Litvinyuk, and M.F. Kling, *Phys. Rev. Lett.* **103**, 153002 (2009).
- P11. “Enhancement of carrier-envelope phase effects in photoexcitation of alkali atoms,” F. Anis and B.D. Esry, *J. Phys. B* **42**, 191001(FTC) (2009).
- P10. “Suppressed dissociation of H_2^+ vibrational states by reduced dipole coupling,” J. McKenna, F. Anis, B. Gaire, N.G. Johnson, M. Zohrabi, K.D. Carnes, B.D. Esry, and I. Ben-Itzhak, *Phys. Rev. Lett.* **103**, 103006 (2009).
- P9. “Benchmark measurements of H_3^+ nonlinear dynamics in intense ultrashort laser pulses,” J. McKenna, A.M. Saylor, B. Gaire, N.G. Johnson, K.D. Carnes, B.D. Esry, and I. Ben-Itzhak, *Phys. Rev. Lett.* **103**, 103004 (2009).
- P8. “Intense 395 nm ultrashort laser-induced dissociation and ionization of an HD^+ beam,” J. McKenna, A.M. Saylor, B. Gaire, N.G. Johnson, E. Parke, K.D. Carnes, B.D. Esry, and I. Ben-Itzhak, *Phys. Rev. A* **80**, 023421 (2009).
- P7. “Laser-induced multiphoton dissociation branching ratios for H_2^+ and D_2^+ ,” J.J. Hua and B.D. Esry, *Phys. Rev. A* **80**, 013413 (2009).
- P6. “Permanent dipole transitions remain elusive in HD^+ strong-field dissociation,” J. McKenna, A.M. Saylor, B. Gaire, N.G. Johnson, M. Zohrabi, K.D. Carnes, B.D. Esry and I. Ben-Itzhak, *J. Phys. B* **42**, 121003(FTC)(2009).
- P5. “Rotational dynamics of dissociating H_2^+ in a short intense laser pulse,” F. Anis, T. Cackowski, and B.D. Esry, *J. Phys. B* **42**, 091001(FTC) (2009).
- P4. “The role of mass in the carrier-envelope phase effect for H_2^+ dissociation,” J.J. Hua and B.D. Esry, *J. Phys. B* **42**, 085601 (2009).
- P3. “Elusive enhanced ionization structure for H_2^+ in intense ultrashort laser pulses,” I. Ben-Itzhak, P.Q. Wang, A.M. Saylor, K.D. Carnes, M. Leonard, B.D. Esry, A.S. Alnaser, B. Ulrich, X.M. Tong, I.V. Litvinyuk, C.M. Maharjan, P. Ranitovic, T. Osipov, S. Ghimire, Z. Chang, and C.L. Cocke, *Phys. Rev. A* **78**, 063419 (2008).
- P2. “Isotopic pulse-length scaling of molecular dissociation in an intense laser field,” J.J. Hua and B.D. Esry, *Phys. Rev. A* **78**, 055403 (2008).
- P1. “High kinetic energy release upon dissociation and ionization of N_2^+ beams by intense few-cycle laser pulses,” B. Gaire, J. McKenna, A.M. Saylor, N.G. Johnson, E. Parke, K.D. Carnes, B.D. Esry, and I. Ben-Itzhak, *Phys. Rev. A* **78**, 033430 (2008).

Control and tracing of attosecond electron dynamics in atoms, molecules and nanosystems in few-cycle laser fields

Matthias F. Kling

J.R. Macdonald Laboratory, Kansas State University, Manhattan, KS 66506, USA

**E-mail: kling@phys.ksu.edu*

Scope:

Few-cycle laser light pulses with controlled electric field waveform are utilized to steer electronic motion in atoms, molecules and nanostructures. While before the start of this program, initial work on the control of single electrons in atoms and simple molecules was performed, our aim is to extend the control metrology to much more complex, highly-correlated systems. Our research is motivated by gaining fundamental insight into the real-time dynamics of many-electron systems. Furthermore, the control and observation of collective electron motion in molecules and nanomaterials is an important step towards the realization of lightwave (nano)electronics. An important part of our research program is to also visualize the control by attosecond time-resolved probing techniques, such as attosecond streaking and attosecond transient absorption spectroscopies.

Progress:

Waveform control of geometric and dynamic field-free molecular orientation:

Combining a fundamental frequency of a laser and its second harmonic with a definite relative phase results in an asymmetric electric field and broken inversion symmetry. Such field-asymmetric laser pulses can generate macroscopic orientation in polar molecules. We have performed the first experimental implementation of this technique. In our experiments we combined 800 nm pulses from a Ti:Sapphire laser with their second harmonic field of 400 nm wavelength. The resulting field-asymmetric two-color pulses were focused onto a supersonic jet of CO molecules inside a velocity-map imaging (VMI) spectrometer, which has been build within this external collaboration. Rotationally excited CO molecules were interrogated at a varying time delay by a more intense single-color (800 nm) laser pulse. The probe pulses Coulomb exploded the molecules and resulting C^{2+} fragments were momentum analyzed using the VMI.

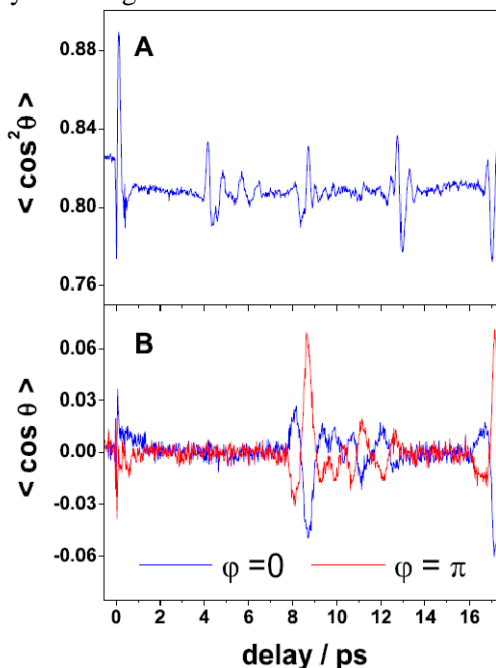


Fig. 1 Evolution of the (A) alignment parameter $\langle \cos^2 \theta \rangle$ and (B) orientation parameter $\langle \cos \theta \rangle$ with pump probe delay time for two opposite phases φ of the two-color pump. Time traces of $\langle \cos^2 \theta \rangle$ and $\langle \cos \theta \rangle$, where θ is the angle between the CO molecular axis

(represented by the momentum direction of C^{2+}) and the laser polarization are displayed in Fig. 1. $\langle \cos^2\theta \rangle$ represents the alignment of CO and the values of $\langle \cos \theta \rangle$ indicate a net macroscopic orientation of the molecular ensemble. The observed orientation exhibits rotational revivals after each rotational period. We studied the dependence of the degree of orientation on the pump pulse peak intensity and compared our experimental results to a series of theoretical calculations. The calculations confirm that the orientation of CO is dominated by an asymmetry in the molecular hyperpolarizabilities rather than the molecules' permanent dipole moment. The results demonstrate field-free orientation of CO [1], which might be used to study angle-differential properties of this and similar heteronuclear molecules, such as ionization and scattering cross-sections.

We have furthermore explored the geometric orientation of polar molecules by phase-stable few-cycle optical fields [8]. We studied the dissociative ionization of DCI in phase-stabilized, 5fs laser fields at $1.3 \times 10^{14} \text{ W cm}^{-2}$. The measured angular distributions of the resulting D^+ and Cl^+ ions are similar and exhibit an anti-correlated CEP dependence. Importantly, the angular distribution of the asymmetry of D^+ ions resembles the orientation-dependent ionization probability of the HOMOs of DCI (see Fig. 2). These findings indicate that mainly the ionization step is responsible for the asymmetry in the fragment emission. Preferential ionization of DCI molecules with suitable orientation towards the laser electric field permits the control over the orientation of DCI^+ ions, which is reflected in the ionic fragment emission. We believe that a similar control can be achieved in other heteronuclear molecules with potentially higher degree of orientation. Taking advantage of this control scheme, near single-cycle light fields may be used to produce samples of oriented molecular ions under field-free conditions (which are present after the ionization pulse has passed the sample) for studies on their dynamics in the molecular frame.

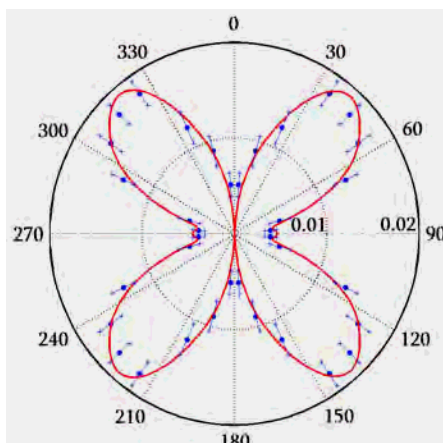


Fig 2: Polar plot of the energy-integrated asymmetry (blue dots) as compared to the calculated symmetric ionization probability from the HOMOs of DCI (red line). For better comparison, the data and calculated results (which are up-down and left-right symmetric) are shown over a range of 2π .

Attosecond control of correlated electron emission:

Using a reaction microscope (REMI) in combination with the recently developed single-shot carrier-envelope-phase (CEP) tagging technique, we investigated the control of the sub-cycle dynamics of the non-sequential double ionization process in rare gas atoms in near single-cycle laser pulses [5]. The pulses with a central wavelength of 750 nm, a duration of 4 fs are generated at a repetition rate of 3 kHz and focused into a cold atomic jet in the center of the REMI, which consists of two time-of-flight spectrometers for electrons and ions combined with position sensitive detectors to enable measuring the particles' three-dimensional momentum vectors. The peak intensities used in the present experiment are of the order of 10^{14} W/cm^2 . A small fraction of the beam is focused into a Stereo-ATI phase meter providing a measurement of the relative CEP for every laser shot. As an example, Fig. 3 shows the CEP-dependent recoil momentum spectra of Ar^{2+} , which exhibit a pronounced (± 0.7) asymmetry.

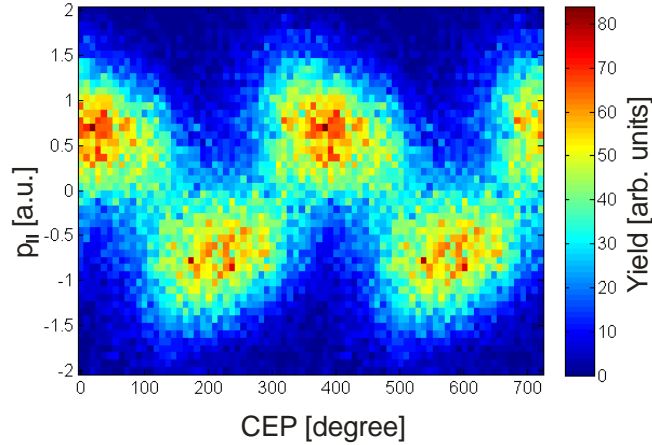


Fig. 3 Experimental results showing the CEP dependence of the Ar^{2+} momentum along the laser polarization axis.

Attosecond control of electron emission and acceleration in nanoparticles:

We demonstrate the emission and directional control of highly energetic electrons from isolated SiO_2 nanoparticles in few-cycle laser fields with well defined waveform at intensities close to the tunneling regime [9].

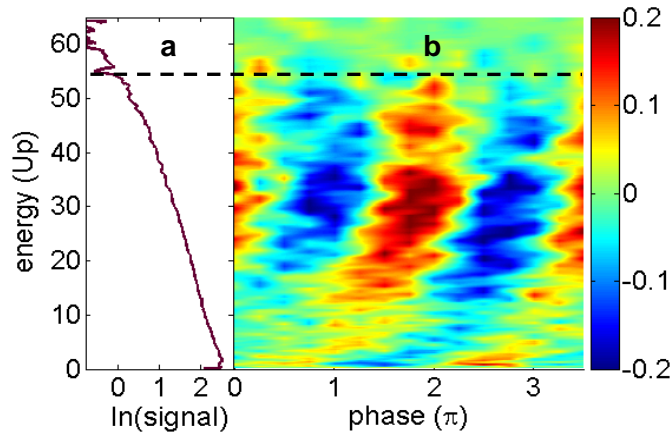


Fig. 4 Electron kinetic energy spectrum (a) and asymmetry in the electron emission along the polarization vector (b) measured in 109 nm diameter SiO_2 nanoparticles at a laser intensity of $1.9 \times 10^{13} \text{ W/cm}^2$. The black dashed line indicates the cutoff in the electron emission.

Intense ($1 - 4.5 \times 10^{13} \text{ W/cm}^2$) carrier-envelope phase (CEP) stabilized laser pulses with a central wavelength of 720 nm and 5 fs pulse duration were focused onto a nanoparticle beam. The nanoparticles were inserted into the gas phase by aerosol preparation and aerodynamic lens focusing [4]. The resulting full 3-D momentum distribution of the emitted electrons was obtained by a velocity-map imaging (VMI) spectrometer. High kinetic energy electrons up to 100 eV were observed. The asymmetry of the electron emission in the direction of the polarization vector shows a pronounced CEP dependence in the energy range up to the cutoff energy (see Fig. 4). The intensity dependent measurements show a nearly linear dependence of the cutoff energy on laser intensity with an average cutoff value of 53.0 U_p , which is more than a factor of five over the classical 10 U_p cutoff law for above-threshold ionization (ATI) in atoms. Here $U_p = e^2 E^2 / 4m\omega^2$ is the ponderomotive potential of an electron in the laser field. Comparison of the experiment to quasi-classical simulations indicate that the electron rescattering in the dielectrically enhanced near-field of the nanoparticle and the trapping potential produced by residual ions and other free electrons in the surface region is responsible for the

large energy gain. By using isolated nanoparticles we can also explore the regime near, at and beyond the material damage threshold. The extremely short pulse duration of only a few cycles in our studies ensures that the electron dynamics responsible for the observed phenomena occurs before any nuclear dynamics. The electron acceleration mechanism could also be of importance to other materials, including nanofilms, composite nanostructures, semiconductor and metal nanoparticles and nanotips in strong few-cycle laser fields.

Future plans:

We are particularly aiming at the implementation of attosecond tracing of electron dynamics in real-time using single attosecond XUV light pulses. The techniques to be utilized will include attosecond streaking spectroscopy, which we have recently applied to measure the photoemission in Ne and Auger decay in Ar via VMI [10]. The extension of the approach to probing the collective electron motion in nanoparticles may reveal completely novel insight into how nanolocalized fields are build-up and decay.

Publications 2009-2011:

11. S.L. Stebbings, F. Süßmann, Y.-Y. Yang, A. Scrinzi, M. Durach, A. Rusina, M.I. Stockman, M.F. Kling, Generation of isolated attosecond XUV pulses employing nanoplasmonic field enhancement: optimization of coupled ellipsoids, *New J. Phys.*, in press.
10. S. Zherebtsov, A. Wirth, T. Uphues, I. Znakovskaya, O. Herrwerth, J. Gagnon, M. Korbman, V.S. Yakovlev, M.J.J. Vrakking, M. Drescher, M.F. Kling, Attosecond imaging of XUV-induced atomic photoionization and Auger decay in strong laser fields, *J. Phys. B.* 44, 105601 (2011).
9. S. Zherebtsov, Th. Fennel, J. Plenge, E. Antonsson, I. Znakovskaya, A. Wirth, O. Herrwerth, F. Süßmann, C. Peltz, I. Ahmad, S. A. Trushin, V. Pervak, S. Karsch, M.J.J. Vrakking, B. Langer, C. Graf, M.I. Stockman, F. Krausz, E. Rühl, M.F. Kling, Controlled near-field enhanced electron acceleration from dielectric nanospheres with intense few-cycle laser fields, *Nature Phys.*, published online, DOI:10.1038/NPHYS1983 (2011).
8. I. Znakovskaya, P. von den Hoff, N. Schirmel, G. Urbasch, S. Zherebtsov, B. Bergues, R. de Vivie-Riedle, K.-M. Weitzel, M.F. Kling, Waveform control of orientation-dependent ionization of DCI in few-cycle laser fields, *Phys. Chem. Chem. Phys.* 13, 8653 (2011).
7. B. Jochim, R. Averin, N. Gregerson, J. McKenna, S. De, D. Ray, M. Zohrabi, B. Bergues, K.D. Carnes, M.F. Kling, I. Ben-Itzhak, E. Wells, Velocity map imaging as a tool for gaining mechanistic insight from closed-loop control studies of molecular fragmentation, *Phys. Rev. A* 83, 043417 (2011).
6. D. Ray, Z.J. Chen, S. De, W. Cao, I.A. Bocharova, I.V. Litvinyuk, A.T. Le, C.D. Lin, M.F. Kling, C.L. Cocke, Momentum spectra of electrons rescattered from rare gas targets following their extraction by one- and two-color short laser pulses, *Phys. Rev. A.* 83, 013410 (2011).
5. N.G. Johnson, O. Herrwerth, A. Wirth, S. De, I. Ben-Itzhak, M. Lezius, B. Bergues, M.F. Kling, A. Senftleben, C.D. Schröter, R. Moshhammer, J. Ullrich, K.J. Betsch, R.R. Jones, T. Rathje, K. Rühle, W. Müller, G.G. Paulus, Single-shot carrier-envelope-phase tagged ion momentum imaging of non-sequential double ionization of argon in intense 4-fs laser fields, *Phys. Rev. A.* 81, 013412 (2011).
4. W. Cao, S. De, K.P. Singh, S. Chen, M.S. Schöffler, A. Alnaser, I.A. Bocharova, G. Laurent, D. Ray, S. Zherebtsov, M. F. Kling, I. Ben-Itzhak, I.V. Litvinyuk, A. Belkacem, T. Osipov, T. Rescigno, and C.L. Cocke, Dynamic control of the fragmentation of CO^{q+} excited states generated with high-order harmonics, *Phys. Rev. A.* 82, 043410 (2010).
3. S. De, I.A. Bocharova, M. Magrakvelidze, D. Ray, W. Cao, B. Bergues, U. Thumm, M.F. Kling, I.V. Litvinyuk, and C.L. Cocke, Tracking nuclear wave packet dynamics in molecular oxygen ions with few-cycle infrared laser pulses, *Phys. Rev. A.* 82, 013408 (2010).
2. D. Ray, F. He, S. De, W. Cao, H. Mashiko, P. Ranitovic, K. P. Singh, I. Znakovskaya, U. Thumm, G. G. Paulus, M. F. Kling, I. V. Litvinyuk, and C. L. Cocke, Ion-Energy Dependence of Asymmetric Dissociation of D₂ by a Two-Color Laser Field, *Phys. Rev. Lett.* 103, 223201 (2009)
1. S. De, I. Znakovskaya, D. Ray, F. Anis, Nora G. Johnson, I.A. Bocharova, M. Magrakvelidze, B.D. Esry, C.L. Cocke, I.V. Litvinyuk, M.F. Kling, Field-free orientation of CO molecules by femtosecond two-color laser fields, *Phys. Rev. Lett.* 103, 153002 (2009).

Controlling rotations of asymmetric top molecules: methods and applications

Vinod Kumarappan

James R. Macdonald Laboratory, Department of Physics
Kansas State University, Manhattan, KS 66506
vinod@phys.ksu.edu

1 Program Scope

The goal of this part of the James R. Macdonald Laboratory's research program is to develop better methods of aligning and orienting polyatomic molecules for ultrafast AMO experiments, including high-harmonic generation and photoelectron spectroscopy. So far, almost all experiments that use aligned molecules have been carried out on linear molecules. The development of more effective alignment/orientation methods for asymmetric top molecules will allow these experiments to be extended to a much larger class of molecules. We use non-adiabatic alignment with non-resonant femtosecond laser pulses to align/orient molecules and velocity map imaging (VMI) and non-linear optical methods to quantify the degree of alignment.

2 Recent progress

2.1 Optical measurement of alignment:

(Xiaoming Ren, Varun Makhija, Vinod Kumarappan)

During the last two years, my group has concentrated on measuring alignment optically. The goals of developing such methods are: (a) to be able to measure alignment — including 3D alignment — rapidly so that a feedback algorithm can be efficiently used to optimize the degree of alignment, (b) to facilitate direct characterization of the alignment in a dense sample suitable for high harmonic generation, and (c) to be able to measure alignment of any molecules that can be aligned/oriented. Fragment ion detection techniques such as VMI fall short on all three requirements. Fragment ion imaging is slow compared to optical measurements, requires low target density to avoid space charge and detector saturation effects, and is suitable only for molecular fragments for which the axial recoil approximation holds true.

We continued the development of a degenerate four wave mixing (DFWM) probe of alignment in which an arbitrary pulse, or sequence of pulses, excites a rotational wavepacket and a DFWM probe in a folded boxCARS geometry measures the evolution of the third order non-linear susceptibility of the gas. The setup is shown in Figure 1. In this geometry, the DFWM signal is automatically phase-matched and background-free, allowing us to measure alignment even in a dilute (<0.1% sample fraction) jet-cooled target. We use a 1 kHz Even-Lavie valve [2] to rotationally cool the sample molecules seeded in a in a high-pressure helium jet. This setup also has the advantage that it is polarization sensitive. The pump can have arbitrary polarization, and the polarization of each probe pulse and the signal can be chosen independently. Coupled with a phase/amplitude/polarization shaper [3] for the pump pulse, we have a versatile setup for exciting and measuring rotational wavepackets in cold molecules.

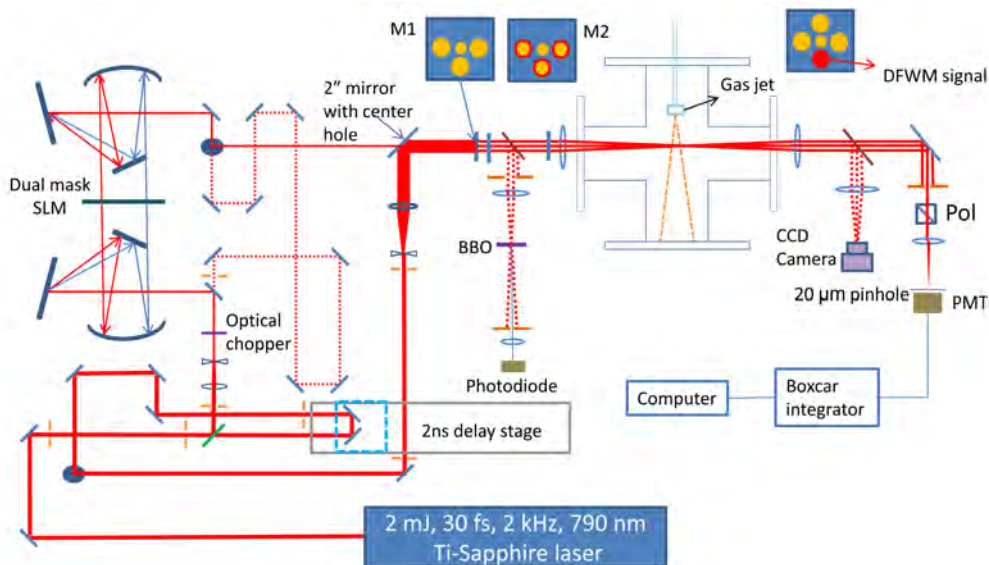


Figure 1: Pump-DFWM setup for measuring the rotational dynamics induced by polarization-shaped pulses. A 4f pulse shaper with a dual mask SLM can shape the pump phase, amplitude or polarization. The mask M1 is an aluminum plate with holes for the central pump pulse and to split the probe pulse into three beams. The mask M2 holds three achromatic wave-plates that can be rotated to change the component of the susceptibility tensor that is measured. The gas jet operates at 1 kHz, and is capable of cooling molecules to below 1 K rotational temperature.

2.2 One-dimensional alignment of benzene and iodobenzene

(Varun Makhija, Xiaoming Ren, Vinod Kumarappan)

Using the pump-DFWM scheme, we have measured the alignment of benzene (an oblate symmetric top where the symmetry axis has the lowest polarizability) and iodobenzene (a nearly prolate asymmetric top where the fastest axis is also the most polarizable). In both cases, the sample gas was seeded in 70 bar helium and cooled in the jet. The results are shown in Fig 2. The calculation for benzene does not include any intensity-averaging, and assumes that the probe does not induce any rotational motion. At the peak of the full revival at 88 ps, the calculated $\langle \cos^2 \theta \rangle$ is 0.45. In the case of iodobenzene, we find J-, C- and K-type revivals [4]. The first two have been observed in VMI experiments [5], but K-type revivals cannot be seen in such measurements. Thus, even in the case of 1D alignment the use of DFWM as a probe provides additional information not available from VMI measurements.

2.3 A new perspective on 3D alignment

(Xiaoming Ren, Varun Makhija, Vinod Kumarappan)

The alignment of asymmetric top molecules in all three dimensions has been characterized using cosines of the Euler angles [6] as well as the direction cosines [7] of molecular axes in the laboratory frame. In both these approaches, three or more expectation values must be evaluated in order to determine the degree of alignment of the molecules.

We have developed a new measure of 3D alignment based on the axis-angle description of rotations in space. As is well-known, any two arbitrarily oriented coordinate systems can be made to overlap by a single rotation. The angle of this rotation defines a metric on the group of rotations in 3D space ($SO(3)$). The expectation value of the cosine of this angle can, therefore, be used as a measure of 3D *orientation*. In the case of 3D *alignment*, there are four equivalent target orientations in the lab frame (three of these are obtained by rotating the lab frame by π around the three coordinate axes). To account for the presence of this additional symmetry, we have defined a

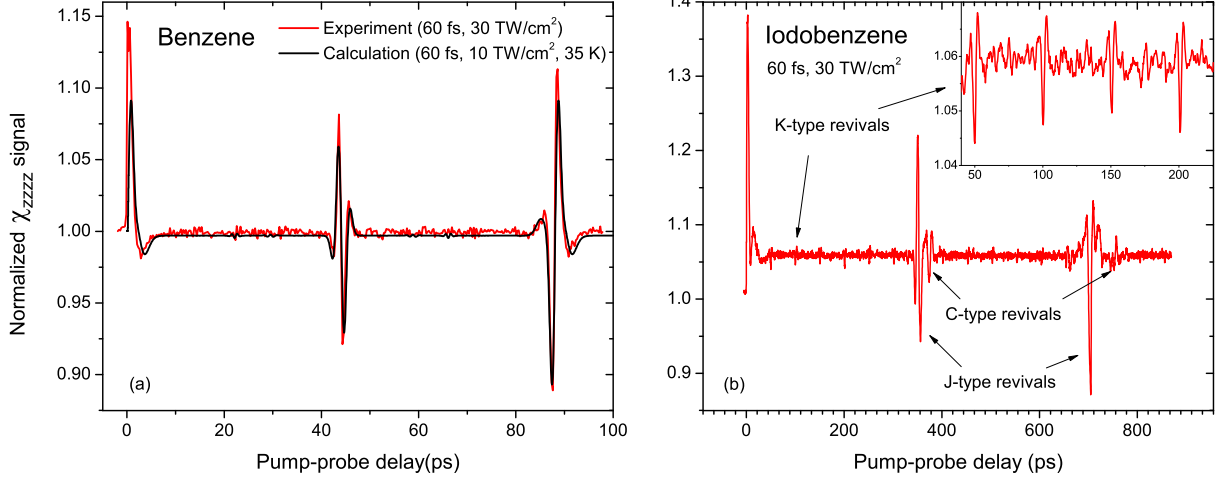


Figure 2: Pump-DFWM measurement of 1D alignment of (a) benzene and (b) iodobenzene. The signals are normalized with respect to the signal from the isotropic gas (in the absence of the pump pulse).

new measure in terms of the four angles of rotation to the four target orientations. This measure, which we call $\cos^2 \delta_{3d}$, characterizes the degree of 3D alignment.

The use of a single measure will help in the development of tools to produce and characterize 3D alignment, particularly in conjunction with genetic algorithms and feedback optimization schemes where it is essential to rank individuals in the correct order even when the alignment is very weak.

2.4 Calculation of 1D and 3D alignment of asymmetric tops:

(Varun Makhija, Xiaoming Ren, Vinod Kumarappan)

In order to help us understand experimental data and to guide future experiments, we have developed code to calculate alignment dynamics of rigid molecules during and after interaction with intense non-resonant laser pulses. We can now calculate 1D and 3D alignment dynamics, and the evolution of the pump-DFWM signal.

As an example, we show 3D alignment of SO_2 molecules by a sequence of linearly-polarized laser pulses in Fig. 3. We use a sequence of four pulses polarized along the lab-frame z -axis to strongly align one axis (following [10]) and then use a fifth pulse, polarized along the lab-frame x -axis, to align the two remaining axes. The rotational temperature is 10 K and the Gaussian laser pulses

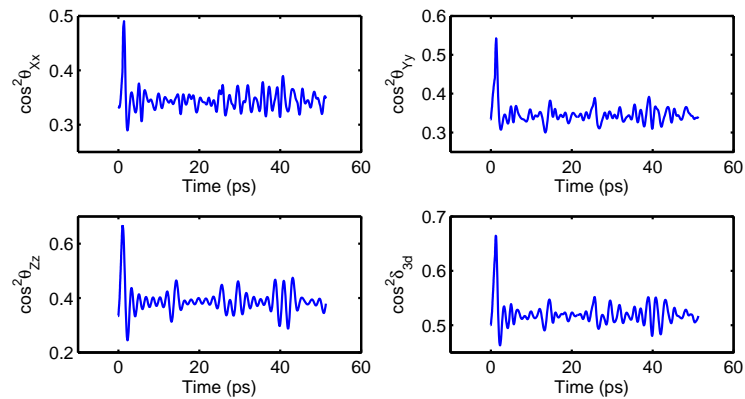


Figure 3: Calculated evolution of the alignment of SO_2 molecules. The lab frame is labeled XYZ and the molecular frame is xyz . See text for details about the pump pulse sequence.

are all 50 fs at full-width half-maximum. The intensity of the z-axis pulses is $20 \text{ TW}/\text{cm}^2$, and the x-polarized pulse is $40 \text{ TW}/\text{cm}^2$. The four panels show the degree of alignment of individual molecular frame axes with the corresponding lab frame axes, and the degree of 3D alignment as measured by $\langle \cos^2 \delta_{3d} \rangle$. The values of $\langle \cos^2 \delta_{3d} \rangle$ for perfect 3D alignment, isotropic distribution and perfect 3D anti-alignment are 1, 1/2 and 1/4, respectively. This scheme, where a pulse sequence is used to align one axis well before attempting to align the other axes, requires less laser energy and is more effective than the use of a sequence of elliptically polarized pulses. A pulse sequence like this can be produced by our polarization shaper, and we plan to do the experiment soon.

3 Work in progress and outlook

The experimental setup was moved next to the laser (from about 25 m away in a different room) earlier this year, resulting in substantial improvement in stability and signal-to-noise ratio. For instance, the noise in the iodobenzene measurements was large enough to obscure the K-type revivals completely. In the new location, these revivals are clearly seen even though we reduced the number of laser shots per data point by a factor of five. The system is also stable enough for a genetic algorithm (GA) to be used. In the old location, the noise level was so high that the GA was unable to reliably rank individuals and therefore could not find any solutions better than noise. With the installation of a new 10 kHz laser system in the Macdonald Lab later this year, the availability of laser time will also increase substantially.

We have started experiments using the pulse shaper and a genetic algorithm. At the moment we are using the shaper as a phase modulator for 1D alignment. Full 3D alignment experiments, using pulse sequences generated by the shaper, will begin soon. We have also made preliminary measurements of other components of the susceptibility tensor. These measurements will be required for 3D alignment experiments. Our alignment code will be extended to calculate the DFWM signal from asymmetric top molecules (at present we can do this calculation only for linear and symmetric top molecules).

The next step is to use the aligned molecules in high harmonic generation and photoelectron measurements with aligned asymmetric tops. We expect to start these measurements this year.

References

- [1] J. A. Shirley, R. J. Hall, and A. C. Eckbreth, *Optics Letters* **5**, 380 (1980).
- [2] U. Even, J. Jortner, D. Noy *et al.*, *Journal of Chemical Physics* **112**, 8068 (2000).
- [3] T. Brixner and G. Gerber, *Optics Letters* **26**, 557 (2001).
- [4] P. W. Joireman, L. L. Connell, S. M. Ohline *et al.*, *Journal of Chemical Physics* **96**, 4118 (1992).
- [5] L. Holmegaard, S. S. Viftrup, V. Kumarappan *et al.*, *Physical Review A* **75**, 051403 (2007).
- [6] M. Artamonov and T. Seideman, *Journal of Chemical Physics* **128**, 9 (2008).
- [7] J. G. Underwood, B. J. Sussman, and A. Stolow, *Physical Review Letters* **94**, 4 (2005).
- [8] V. Kumarappan, C. Z. Bisgaard, S. S. Viftrup *et al.*, *Journal of Chemical Physics* **125**, 7 (2006).
- [9] S. Pabst, P. J. Ho, and R. Santra, *Physical Review A* **81**, 043425 (2010).
- [10] S. Pabst and R. Santra, *Physical Review A* **81**, 065401 (2010).

Strong field rescattering physics and attosecond physics

C. D. Lin

J. R. Macdonald Laboratory, Kansas State University
Manhattan, KS 66506
e-mail: cdlin@phys.ksu.edu

Program Scope:

We investigate the interaction of ultrafast intense laser pulses, and of attosecond pulses, with atoms and molecules. Most notable accomplishments in the past year are: (1) Demonstration of femtoseconds temporal and sub-Angstroms spatial resolution in bond relaxation following tunneling ionization of O_2 and N_2 by Mid-infrared lasers. This is a collaboration with Lou DiMauro's group. (2) Incorporation of medium propagation in the HHG theory, thus enabling direct comparison with experiments. (3) Implement $(e,2e)$ and electron impact excitation cross sections of Ne^+ and Ar^+ into the rescattering theory to study nonsequential double ionization. (4) Theory of time-resolved autoionization dynamics of a Fano resonance and its control with IR pulses. Additional results and plans for the coming year will be summarized.

Introduction

When an atom or molecule is exposed to an intense infrared laser pulse, an electron which was released earlier may be driven back by the laser field to recollide with the parent ion. The collision of electrons with the ion may result in high-order harmonic generation (HHG), the emission of high-energy above-threshold-ionization (HATI) electrons and non-sequential double ionization (NSDI). Based on the quantitative rescattering theory (QRS) established in 2009 we are now capable of studying HHG, HATI and NSDI processes at the quantitative level such that they can be compared directly with experimental data. Using attosecond pulses generated from the HHG we also investigated attosecond electron dynamics such as the autoionization of a Fano resonance probed by another attosecond pulse or with an intense femtosecond IR laser.

1. Demonstration of sub-Angstrom bond length relaxation after tunneling ionization

Recent progress

Our earlier work has established the method to extract field-free elastic differential cross sections (DCS) of the target atomic or molecular ions from the HATI spectra. In 2010 we showed theoretically [A13] that DCS extracted from HATI spectra using mid-IR lasers can be used to retrieve the bond length of a molecule in a manner similar to the method used in gas-phase electron diffraction (GED). This new technique is called laser-induced electron diffraction (LIED). In collaboration with Lou DiMauro's group, HATI spectra from O_2 and N_2 at 2.0 μm , as well as from 1.7 and 2.3 μm lasers have been obtained and analyzed. For N_2 , the bond relaxation is small and the retrieved bond length is within the errors of the LIED. For O_2 , the experimental 2.0 μm data has shown clearly that the retrieved bond length is about 0.1 Å shorter than the bond length than the neutral O_2 . The retrieved bond lengths from different laser wavelengths reveal bond relaxation. After tunneling ionization, the readjustment of electrons in the molecule incurs bond relaxation. Since the recollision time is proportional to the laser's wavelength, the dynamics of bond relaxation is probed by using different wavelengths. This work demonstrates that bond relaxation of sub-Angstroms within a few femtoseconds can be obtained using MIR lasers. It further establishes that MIR can be used as a probe for a molecule under conformal transformation. A report on this work has been submitted for publication [B1].

Ongoing projects and future plan

Clearly the bond length relaxation demonstrated for O_2 should be continued for other molecules experimentally. The next step is to obtain HATI spectra for larger molecules, for molecules that are aligned, for molecules that are excited vibrationally (via stimulated Raman) or even electronically excited molecules. Since HATI signals are much smaller than direct electrons, dedicated experimental efforts will be needed. The retrieval of molecular structure from such data would also require additional theoretical tools. We are looking forward to more such data in the coming year.

2. Simulation of HHG including propagation effect for atoms and molecules

Recent progress

My graduate student C. Jin has incorporated HHG from single atoms or molecules using QRS with the macroscopic Maxwell Equation to account for the effect of propagation of IR and HHG in the medium. Thus the simulated HHG can be directly compared to experimental measurements. In the last year, he was able to show that experimental HHG spectra from Ar, Xe, and for aligned as well as unaligned N_2 and O_2 , can be well reproduced from his simulation. Since HHG spectra depend critically on the experimental parameters such as the gas pressure, position of the gas jet with respect to the laser focus, the focusing condition, the position of the detector and how the harmonics are collected, i.e., with a slit or not, comparison with experiments is possible only if these parameters are carefully specified. In the simulation, the laser intensity has to be adjusted from the reported value in general. Results from this work have appeared in A1, A2, A6, and the effect of multiple orbitals contributing to HHG from aligned CO_2 molecules has also been studied. In the latter, it was demonstrated that HHG also depends sensitively on the degree of alignment. This dependence will alter the interpretation of the experimental data.

To obtain HHG spectra experimentally there is a tendency to use intense laser fields. Due to medium propagation effect, when the field is near the saturation intensity, the IR field can be severely modified during the propagation. Using MIR and few-cycle pulses, the HHG spectra begin to display features that are similar to a supercontinuum. This has been observed experimentally (C. Travello) and the spectra have been reproduced theoretically. By analyzing the simulated HHG spectra in the time domain, it clearly confirms that indeed single attosecond pulses are generated if the HHG are synthesized at the far field. Thus we have the theoretical tools to analyze the conditions for the generation of single attosecond pulses.

Ongoing projects and future plan

Despite of our success so far in reproducing experimental HHG spectra, there are situations where we have failed; in particular, for short pulses near the saturation intensity regime. Our current theoretical model employs a laser pulse with Gaussian spatial profiles and that the gas pressure is uniform. For short pulses there are evidence that the pulse is closer to a Bessel beam. We are extending the code to include Bessel beams and nonuniform spatial distribution of the gas jet pressure. We will then check if discrepancies with experiments can be resolved.

3. QRS theory for NSDI

Recent progress

The QRS for nonsequential double ionization (NSDI) of He by lasers studied in the last year has now been extended to Ne and Ar targets where many experimental data are available for comparison. For this purpose, the $(e,2e)$ and electron impact excitation cross sections for Ne^+ and Ar^+ have to be fitted to some empirical form over a broad energy region, see A4. We have now implemented these cross sections into the QRS theory to obtain results that can be compared directly with experiments. In particular, we have examined the Ar data reported recently from Matthias Kling's group [Johnson et al, Phys. Rev. A83, 013412 (2001)] where NSDI of Ar were studied with a 4 fs laser pulse. Our simulation was able to reproduce their reported total NSDI

yield vs the carrier-envelope phase (CEP) as well as the ion spectra vs the CEP, but the pulse duration and peak laser intensity have to be adjusted from their reported values. We have also obtained the correlated electron spectra where the parallel (with respect to polarization) momentum spectra of the two electrons are measured against the CEP. They are to be compared to future measurements. Comparison also were made to the ion spectra at higher laser intensities for the NSDI of Ar for the long pulses reported from earlier measurements.

On-going projects and future plan

There are many NDSI studies on Ar and Ne from the past decade. Our QRS model is the only fully quantum mechanical theory. We intend to examine data from earlier experiments further in the coming year.

4. Attosecond Physics of Fano resonances

Traditionally atomic and molecular resonances are studied in the energy domain using high-precision spectroscopy. A Fano resonance is characterized by its position, width and the q parameter. Since a Fano resonance has a decay time, the question is how to probe its time evolution. This issue was addressed in paper A10. There we asked if a Fano resonance is initiated by an attosecond pulse, say, an 100 as pulse, how do we observe its autoionization within its lifetime? Since attosecond probe pulses are not yet available, presently intense IR pulses are used as the “probe”. However, the intense IR probe can strongly couple it with other resonances. The latter has been investigated analogous to a typical three-level atom where the IR couples two excited states, and the coupling is probe with an attosecond pulse. The resulting electron spectra for the 2s2p (¹P) of He has been reported in Gilberston et al [Phys. Rev. Lett. 105, 263003 (2011)] and we have provided a theoretical analysis of this experiment. The results of our analysis agree well with the measurement. A report of this work has been submitted for publication [B2].

Future plan

We will extend the XUV+IR studies to other situations, including transient absorption spectroscopy, where the XUV is a single attosecond pulse or a pulse train, and in the future, including the effect of the medium. For the latter, it would be based on the extension of the HHG propagation code we have developed in house.

5. Other topics

There are other works published in the last year (see the A-list below) that are not mentioned here due to space limitation.

Publications (19 more papers since 2009 not listed below)

A. Published papers

A1. Cheng Jin, Anh-Thu Le and C. D. Lin, “Analysis of effects of macroscopic propagation and multiple molecular orbitals on the minimum in high-order harmonic generation of aligned CO₂”, *Phys. Rev. A* **83**, 053409 (2011).

A2. Cheng Jin, Hans Jakob Wörner, V. Tosa, Anh-Thu Le, Julien B. Bertrand, R. R. Lucchese, P. B. Corkum, D. M. Villeneuve, and C. D. Lin, “ Separation of Target Structure and Medium Propagation Effects in High-Harmonic Generation”, *J. Phys. B* **44**, 095601 (2011)

A3. Junliang Xu, Yaqiu Liang, Zhangjin Chen and C. D. Lin, “Elastic scattering and impact ionization by returning electrons induced in a strong laser field”, *J. of Phys. Conf. series* **288**, 012017 (2011)

- A4 Yaqiu Liang, Zhangjin Chen, D. H. Madison, and C. D. Lin, “Calibration of distorted wave Born approximation for electron impact excitation of Ne and Ar at incident energies below 100 eV” *J. Phys. B* **44**, 085201 (2011).
- A5. Song-Feng Zhao, Cheng Jin, R. R. Lucchese, Anh-Thu Le, and C. D. Lin “ High-order-harmonic generation using gas-phase H₂O molecules”, *Phys. Rev. A* **83**, 033409 (2011)
- A6. Cheng Jin, A. T. Le and C. D. Lin, “Medium propagation effects in high-order harmonic generation of Ar and N₂”, *Phys. Rev A* **83**, 023411 (2011)
- A7. D. Ray, Z. J. Chen, S. De, W. Cao, I. V. Litvinyuk, A. T. Le, C. D. Lin, M. F. Kling and C. L. Cocke, “Momentum spectra of electrons rescattered from rare gas targets following their extraction by one- and two-color short laser pulses”, *Phys. Rev. A* **83**, 013410 (2011)
- A8. Song-Feng Zhao, Junliang Xu, Cheng Jin, Anh-Thu Le and C D Lin “ Effect of orbital symmetry on the orientation dependence of strong field tunneling ionization of nonlinear polyatomic molecules”, *J. Phys. B* **44**, 035601 (2011)
- A9. Zhangjin Chen, Yaqiu Liang and C. D Lin, “Quantitative rescattering theory of correlated two-electron momentum spectra for strong field nonsequential double ionization of helium”, *Phys. Rev. A* **82**, 063417 (2010)
- A10. W.C. Chu and C. D. Lin, “Theory of ultrafast autoionization dynamics of Fano resonances”, *Phys. Rev. A* **82**, 053415 (2010).
- A11. A. T. Le and C. D. Lin, Ultrafast Optics: Imaging a chemical reaction, *Nature Photonics*, **4**, 671 (2010) .
- A12. Song-Feng Zhao, Cheng Jin, A. T. Le and C. D. Lin, “Effect of an improved molecular potential on strong field tunneling ionization of molecules” *Phys. Rev. A* **82**, 035402 (2010).
- A13. Junliang Xu, Zhangjin Chen, A. T. Le and C. D. Lin, “Self-imaging of molecules from diffraction spectra by laser-induced rescattering electrons”, *Phys. Rev. A* **82**, 023814 (2010)
- A14. A. T. Le, R. Lucchese and C. D. Lin, “Polarization and ellipticity of high-order harmonics from aligned molecules generated by linearly polarized intense laser pulses”, *Phys. Rev. A* **82**, 023814 (2010)
- A15. N. N. Choi, T. F. Jiang, T. Morishita, M-H. Lee and C. D. Lin, “Theory of probing attosecond electron wave packets via two-path interference of angle-resolved photoelectrons”, *Phys. Rev. A* **82**, 013409 (2010)

Papers submitted for publication

- B1. Cosmin I. Blaga, Junliang Xu, Anthony D. DiChiara, Emily Sistrunk, Kaikai Zhang, Pierre Agostini, Terry A. Miller, Louis F. DiMauro, C. D. Lin, “Observation of femtosecond, sub-Angstrom molecular bond relaxation using laser-induced electron diffraction”, submitted to *Nature*.
- B2. Wei-Chun Chu, Song-Feng Zhao and C. D. Lin, “Probing transient photoelectron spectra by coherent coupling of two autoionizing states in helium with single-attosecond pulse”, submitted to *Phys. Rev. A*.
- B3. Zhangjin Chen, Y. Liang, D. H. Madison and C. D. Lin, “Strong Field nonsequential double ionization of Ar and Ne”, submitted to *Phys. Rev. A*.

Structure and Dynamics of Atoms, Ions, Molecules and Surfaces: Atomic Physics with Ion Beams, Lasers and Synchrotron Radiation

Uwe Thumm, J.R. Macdonald Laboratory, Kansas State University
Manhattan, KS 66506 thumm@phys.ksu.edu

1. Attosecond time-resolved photoelectron (PE) spectroscopy (with Chang-Hua Zhang)

Project scope: We model the time-resolved infra-red (IR)-assisted extreme ultraviolet (XUV) PE emission and Auger decay in pump-probe-delay-dependent streaking experiments with atoms and complex targets, such as clusters, carbon nanotubes, and surfaces.

Recent progress: We examined Wigner and streaking time delays [1-5,R1] and modeled the time-dependent autoionization [6,7] for the emission of PEs from atoms [3,5-7] and solid surfaces [1-4,6]. For atoms, we scrutinized the effect of the Coulomb interaction between PE and residual ion [5]. For photoemission from surfaces, we found that streaking delays are very sensitive to changes in the IR-skin depth and Fermi energy and deviate from Wigner time delays for non-zero IR-skin depths [1-4]. We modeled the excitation of bulk and surface plasmons during and after the release of PEs from metal surfaces and examined the influence of the dynamical plasmon response on PE spectra and photoemission time delays [4].

Example 1: Coulomb-laser coupling effects in attosecond time-resolved photoelectron spectra. Photoionization by attosecond XUV pulses into the laser-dressed continuum of the ionized atom is commonly approximated in strong-field approximation (SFA), i.e., by neglecting the Coulomb interaction between the emitted PE and the residual ion [1,2,6]. By solving the time-dependent Schrödinger equation (TDSE), we identified a temporal shift in streaked photoemission spectra that is due to the Coulomb-laser coupling in the final-state and exceeds 50 as at small PE kinetic energies. We expect the examination of this shift to enable (i) the experimental scrutiny of effects that are due to the combined action of Coulomb and laser forces on the PE and (ii) tests of theoretical approximations to the exact Coulomb-Volkov state of the PE. Within an eikonal (semiclassical) approximation, we derived an analytical expression for this effect and assessed its accuracy in comparison with full TDSE numerical results [2]. **Future plans:** We intend to (i) continue to investigate the effect of interactions that are not included in SFA and (ii) examine the influence of initial-state polarization in the streaking IR-laser field on PE spectra and time delays. We will seek contact with experimental groups to explore the feasibility of and ideal parameters for the observation of Coulomb-laser effects beyond the standard SFA in streaked photoemission spectra [5].

Example 2: Streaking and Wigner time delays in photoemission from atoms and surfaces. Streaked photoemission metrology allows the observation of an apparent relative time delay between the detection of PEs from different initial electronic states [1-3,R1,R2]. Theoretically, photoemission delays can be defined based on (i) the phase shift the photoelectron wavefunction accumulates during the release and propagation of the PE ("Wigner delay") and, alternatively, (ii) the streaking trace in the calculated photoemission spectrum ("streaking delay"), while experimentally time delays can only be deduced from streaked PE spectra [1,3,R1]. We investigated the relation between Wigner and streaking delays in the photoemission from atoms and solid surfaces. For surfaces and assuming a vanishing IR-skin depth, both Wigner and streaking delays can be interpreted as an average propagation time needed by photoelectrons to reach the surface, while the two delays differ for non-vanishing skin depths [3,4]. For atomic targets, the difference between Wigner and streaking delays depends on the range of the ionic potential [3]. **Future plans:** We hope to clarify the precise interpretation of and relations between different time-delay measures based on specific numerical examples for photoemission from atoms and surfaces.

Example 3: Dynamical image-charge effects in streaked photoelectron spectra of metal surfaces. The release of conduction-band electrons from a metal surface by a sub-femtosecond XUV pulse, and their propagation through and near the solid [1,2,6, R2], provokes a dielectric response in the solid that acts back on the PE wave packet. We modeled the response of the metal due to excitation of bulk and surface plasmons induced by the creation

and propagation of PEs in the solid in terms of an effective potential that depends on the velocity of the PE. We numerically calculated the (wake) potential associated with this PE self-interaction and showed that it induces a considerable XUV-frequency-dependent temporal shift in streaked-photoemission spectra [4], suggesting the observation of the ultrafast solid-state dielectric response in contemporary streaked photoemission experiments [R2]. We analyzed the dependence of this relative shift on the XUV frequency as well as on solid-state characteristics, such as the bulk plasmon frequency, the IR skin depth, and the PE transport in the solid [4].

Future plans: We plan to (1) further improve our modeling of the transport (including diffraction effects) of released PEs inside the substrate and (2) collaborate with experimental groups to explore the feasibility of and ideal parameters for the observation of plasmon response effects (i.e., the time-resolved creation of “image charges”) during and after the XUV-pulse-triggered release of PEs from metal surfaces [4, R2].

2. Time-resolved single and double ionization of atoms

Project scope: We attempt to model, calculate, and understand the excitation and ionization of atoms with sub-optical-cycle (T_{IR}) time resolution.

Recent progress: The role of laser-dressed highly excited energy levels in atomic excitation and ionization has been studied recently using attosecond technology [R3, R4]. We followed up on these studies and showed that this pump-probe technique also enables the measurement of *instantaneous* level shifts of bound atomic [8] (and molecular [9]) states in optical electric fields. We demonstrated how the control of instantaneous level shifts can be exploited to gate strong-field phenomena, such as non-sequential double ionization (NSDI) [8].

Example 1: Attosecond probing of instantaneous AC Stark shifts in helium atoms (with Feng He, Camilo Ruiz, and Andreas Becker). Based on numerical solutions of TDSE for either one or two active electrons, we proposed a method for observing time-dependent instantaneous level shifts in an oscillating strong IR field, using a single tunable XUV pulse to probe excited states of the perturbed atom. We assumed IR-laser fields with negligible distortion of the He ground state, that are, however, strong enough to couple low-lying excited and continuous states, inducing noticeable level splitting, shift, and decay. We fixed the number of XUV cycles and varied the central frequency ω_{XUV} of the XUV pulse. Key to our investigation is the observation that, for a given ω_{XUV} of the attosecond (SA) pulse and depending on the delay Δt between pump and probe pulse, the IR pulse may shift low-lying bound states into or out of resonance with one-photon excitations from the He ground state. The excited atom may then be easily ionized by the remaining IR pulse. If the SA pulse is applied while the instantaneous level energies are off (in) resonant with ω_{XUV} less (more) excitation and thus less (more) ionization out of excited states is expected to occur. This suggests that detection of the ionization probability as a function of ω_{XUV} and Δt can be used to experimentally track the instantaneous Stark shifts [7,8]. **Future plans:** We showed that this method (i) allows the detection of instantaneous atomic energy gaps with sub-laser-cycle time resolution and (ii) can be applied as an ultrafast gate for more complex processes such as NSDI [8]. We intend to continue to search for ideal laser parameters and targets for the observation, with sub-IR-cycle resolution, of AC Stark shifts in delay-dependent single and double ionization probabilities. This may lead to new schemes for the coherent control of NSDI, high harmonic generation, and molecular dissociation, for which we hope to find suitable proof-of-principle examples.

Example 2: Electron wave-packet interference in atomic photoionization by a single few-cycle IR laser pulse (with Aihua Liu). We analyzed recently measured [R5] interference patterns in momentum-resolved single-ionization PE spectra from He targets in terms of the interference of specific contributions to calculated PE spectra that originate from a few selected sub- T_{IR} time intervals during the laser-atom interaction. For contributions from just two such narrow time intervals that are centered at successive maxima of the laser-electric field with lengths of a few attoseconds, our calculations reproduce the measured interference structure in the momentum-resolved spectra. By selecting PE wave packets that are released with inter- or intra-IR-cycle spacings, we were able to distinguish known above-threshold-ionization (ATI) interferences and non-ATI interference structures in our simulated photoelectron spectra [10]. **Future plans:** We intend to provide a more complete interpretation of interferences in the momentum-resolved photoionization of atoms by single few-cycle IR pulses in terms of a semiclassical analysis of relevant electron trajectories.

3. Dissociation dynamics of diatomic molecules

Project scope: We develop numerical and analytical tools to (i) efficiently predict the effects of strong laser fields on the bound and free electronic and nuclear dynamics in small molecules and (ii) fully image the laser-controlled nuclear and electronic dynamics.

Recent progress: We designed a scheme for simulating the bound and dissociating nuclear dynamics in laser-excited molecular ions [11-14]. This scheme is based on the solution of the TDSE for either individual or a carefully selected set of dipole-coupled diabatic electronic states of the molecular ion and proceeds by comparing vibrational revival times, quantum-beat frequencies [15-17], and pump-probe-delay-dependent simulated fragment kinetic energy release (KER) spectra with experimental data. We completed full-dimensionality calculations [18] for the vibrational quenching of nuclear wave packets in H_2^+ that allowed us to scrutinize our previous reduced-dimensionality results [19].

Example 1: Full dimensional study of the heating and cooling of vibrational wave packets in oriented H_2^+ molecules (with Thomas Niederhausen and Fernando Martín). We investigated the control of the vibrational dynamics in H_2^+ with ultrashort IR laser pulses [18,19]. With the laser electric field being aligned along the molecular axis, we numerically solved the full vibronic TDSE and compared our results with H_2^+ model calculations that only include the lowest two coupled adiabatic potential curves [19]. We find that the precise timing between pump and control laser pulses allows the direct manipulation of the final vibrational state composition and dissociation dynamics of the molecular ion. We showed that a significant enhancement of the occupation of particular vibrational stationary state contributions can be achieved for laser intensities below the onset of strong ionization. **Future plans:** We plan to examine and optimize control schemes for quenching *ro*-vibrational nuclear wave packets in diatomic molecules using a sequence of control pulses. The quality of this Raman-control mechanism can be tested experimentally by Coulomb-explosion imaging [18].

Example 2: Time-resolved fragmentation dynamics in N_2 , O_2 , and CO (with Maia Magrakvelidze, Sankar De, Irina B ocharova, Christine A ikens, Matthias Kling, Itzik Ben-Itzhak, and Lew C ocke). We investigated the nuclear dynamics of electronically and vibrationally excited heavy diatomic molecular ions by applying intense ultrashort IR probe pulses and measuring the KER spectra as a function of the pump-probe delay [11-14]. To analyze these spectra, we performed wave-packet-propagation calculations on a diabatic molecular potential curves. First, to identify relevant transiently populated electronic states of the molecular ions, we modeled the pump step in Franck-Condon approximation and calculated the time evolution of initial vibrational wave packets *separately* for selected molecular potential curves. The comparison of calculated KER spectra as a function of delay, quantum-beat frequency, and vibrational revival times for one adiabatic curve at a time with experimental spectra served us as a guide for selecting relevant electronic states of the molecular ions. Next, we included probe-laser-induced dipole couplings between the relevant molecular potential curves and compared the improved calculated KER spectra with experimental data, in an attempt to reveal non-adiabatic effects in measured KER spectra [14]. We employed the quantum chemistry code GAMESS [R6] to calculate molecular potential curve and dipole couplings between them [14]. **Future plans:** Measured delay-dependent KER spectra of heavy diatomic molecules are difficult to simulate theoretically and not fully understood. We believe that the simultaneous study of measured and simulated KER spectra in both, time and energy domains provides a powerful tool that we intend to refine in order to disentangle the complicated *ro*-vibrational nuclear dynamics of laser-excited (and ionized) molecules.

Publications (2008-2011). References [1-19] are addressed in the abstract.

- [1] *Attosecond photoelectron spectroscopy of metal surfaces*, C.-H. Zhang and U. Thumm, Phys. Rev. Lett. **102**, 123601 (2009).
- [2] *Time-resolved IR laser-assisted XUV photoelectron spectroscopy of metal surfaces*, C.-H. Zhang and U. Thumm, invited paper, XXVI ICPEAC, Kalamazoo, Journal of Physics: Conf. Series **194**, 012055 (2009).
- [3] *Streaking and Wigner delays in photoemission from atoms and surfaces*, C.-H. Zhang and U. Thumm, Phys. Rev. A, submitted; <http://arxiv.org/abs/1106.1421>

- [4] *Probing dielectric response effects with attosecond time-resolved streaked photoelectron spectroscopy of metal surfaces*, C.-H. Zhang and U. Thumm, Phys. Rev. Lett., submitted; <http://arxiv.org/abs/1102.0751>
- [5] *Electron-ion interaction effects in attosecond time-resolved photoelectron spectra*, C.-H. Zhang and U. Thumm, Phys. Rev. A **82**, 043405 (2010).
- [6] *Time-resolved core-hole decay in laser-assisted photoemission from adsorbate-covered metal surfaces*, C.-H. Zhang and U. Thumm, Phys. Rev. A **80**, 032902 (2009).
- [7] *Attosecond time-resolved autoionization of argon*, H. Wang, M. Chini, S. Chen, C.-H. Zhang, F. He, Y. Cheng, Y. Wu, U. Thumm, and Z. Chang, Phys. Rev. Lett. **105**, 143002 (2010).
- [8] *Attosecond probing of instantaneous AC Stark shifts in helium atoms*, F. He, C. Ruiz, A. Becker, and U. Thumm, Phys. Rev. Lett., submitted; <http://arxiv.org/abs/1105.5204>
- [9] *Strong-field modulated diffraction effects in the correlated electronic-nuclear motion in dissociating H_2^+* , F. He, A. Becker, and U. Thumm, Phys. Rev. Lett. **101**, 213002 (2008).
- [10] *Momentum imaging of electron wave packet interference in few-cycle laser pulses*, A. Liu and U. Thumm, in preparation.
- [11] *Tracking dynamic wave packets in the O_2 dication using a pump/probe approach*, S. De, I. Bocharova, M. Magrakvelidze, D. Ray, W. Cao, B. Bergues, U. Thumm, M. F. Kling, I. V. Litvinyuk, and C. L. Cocke, Phys. Rev. A **82**, 013408 (2010).
- [12] *Time-resolved Coulomb explosion imaging of nuclear wave-packet dynamics induced in atomic molecules by intense few-cycle laser pulses*, I.A. Bocharova, A. S. Alnaser, U. Thumm, T. Niederhausen, D. Ray, C.L. Cocke, and I.V. Litvinyuk, Phys. Rev. A **83**, 013417 (2011).
- [13] *Quantum-beat imaging of the nuclear dynamics in D_2^+ : Dependence of bond softening and bond hardening on laser intensity, wavelength, and pulse duration*, M. Magrakvelidze, F. He, T. Niederhausen, I. V. Litvinyuk, and U. Thumm, Phys. Rev. A **79**, 033410 (2009).
- [14] *Following dynamic nuclear wave packets in N_2 , O_2 and CO with few-cycle infrared pulses*, S. De, M. Magrakvelidze, I. Bocharova, D. Ray, W. Cao, I. Znakovskaya, H. Li, Z. Wang, G. Laurent, U. Thumm, M. F. Kling, I. V. Litvinyuk, I. Ben-Itzhak, and C. L. Cocke, Phys. Rev. A, submitted.
- [15] *Multidimensional quantum-beat spectroscopy*, M. Winter, R. Schmidt, and U. Thumm, Phys. Rev. A **80**, 031401(R) (2009).
- [16] *Quantum-beat analyses of the rotational-vibrational dynamics in D_2^+* , M. Winter, R. Schmidt, and U. Thumm, New Journal of Physics, New J. of Phys. **12**, 023023 (2010).
- [17] *Time-series analysis of vibrational nuclear wave packet dynamics in D_2^+* , U. Thumm, T. Niederhausen, and B. Feuerstein, Phys. Rev. A **77**, 063401 (2008).
- [18] *Controlled vibrational quenching of nuclear wave packets in D_2^+* , T. Niederhausen and U. Thumm, Phys. Rev. A **77**, 013407 (2008).
- [19] *Full-dimensional study of the heating and cooling of vibrational wave packets in oriented H_2^+ molecules*, T. Niederhausen, U. Thumm, and F. Martin, PRA, submitted.
- [20] *Neutralization dynamics of H^- near (2×1) reconstructed $Si(100)$ surfaces*, B. Obreshkov and U. Thumm, Phys. Rev. A **83**, 062902 (2011).
- [21] *Steering the electron motion in H_2^+ by nuclear wave packet control*, B. Fischer, M. Kremer, B. Feuerstein, T. Pfeifer, V. Sharma, U. Thumm, C.D. Schröter, R. Moshhammer, and J. Ullrich, Phys. Rev. Lett. **105**, 223001 (2010).
- [22] *Dissociative ionization of H_2 in an XUV pulse train and delayed IR laser pulse*, F. He and U. Thumm, Phys. Rev. A **81**, 053413 (2010).
- [23] *Band-gap-confinement and image-state-recapture effects in the survival of anions scattered from metal surfaces*, A. Schmitz, J. Shaw, H. S. Chakraborty, and U. Thumm, Phys. Rev. A **81**, 042901 (2010).
- [24] *Control of electron localization in molecules using XUV and IR pulses*, K. P. Singh, W. Cao, P. Ranitovic, S. De, F. He, D. Ray, S. Chen, U. Thumm, A. Becker, M. M. Murnane, H. C. Kapteyn, I. Litvinyuk, and C. L. Cocke, Phys. Rev. Lett. **104**, 023001 (2010).
- [25] *Ion-energy dependence of asymmetric dissociation of D_2 by a two-color laser field*, D. Ray, F. He, S. De, W. Cao, H. Mashiko, P. Ranitovic, K. P. Singh, I. Znakovskaya, U. Thumm, G. G. Paulus, M. F. Kling, I. Litvinyuk, and C. L. Cocke, Phys. Rev. Lett. **103**, 223201 (2009).
- [26] *Electron localization in molecular fragmentation of H_2 with CEP-stabilized laser pulses*, M. Kremer, B. Fischer, B. Feuerstein, V. L. B. De Jesus, V. Sharma, C. Hofrichter, A. Rudenko, U. Thumm, C. D. Schröter, R. Moshhammer, and J. Ullrich, Phys. Rev. Lett. **103**, 213003 (2009).
- [27] *Angular dependence of the strong-field ionization of randomly oriented hydrogen molecules*, M. Magrakvelidze, F. He, S. De, I. Bocharova, D. Ray, I. Litvinyuk, and U. Thumm, Phys. Rev. A **79**, 033408 (2009).

References: [R1] M. Schultze *et al.*, Science **328**, 1658 (2010). [R2] A. L. Cavalieri *et al.*, Nature **449**, 1029 (2007). [R3] P. Johnsson *et al.*, Phys. Rev. Lett. **99**, 233001 (2007). [R4] P. Ranitovic *et al.*, New J. Phys. **12**, 013008 (2010). [R5] R. Gopal *et al.*, Phys. Rev. Lett. **103**, 053001 (2009). [R6] M. W. Schmidt *et al.*, J. Comput. Chem. **14**, 1347 (1993).

Strong-Field Time-Dependent Spectroscopy and Quantum Control

Carlos A. Trallero

J. R. Macdonald Laboratory, Kansas State University, Manhattan, KS 66506
carlos@phys.ksu.edu

Scope

The main scope of my program is to measure and control the state of molecular systems. In particular, I'm interested in observing molecules evolve with attosecond and/or femtosecond time resolution. For this purpose, my group has a very strong theory support from C.D. Lin's group.

1. Extracting photoionization cross sections from harmonic spectra

As mentioned above we are interested in extracting information about the quantum state of molecules or atoms using higher-order harmonic generation (HHG). In particular, we are interested in measuring photoionization cross sections (PICS) using HHG spectra. This method has several advantages compared to the standard use of synchrotron radiation. For example, we can have time resolved measurements of the PICS in a table top apparatus and perform the measurement in the molecular frame using alignment. Furthermore, the generation of harmonics gives us all the energies of the PICS in a single event rather than having to tune the ionization energy. However, since HHG is a macroscopic process it carries information not only about a particular emitter but also carries information of the properties of the bulk. Therefore, if we want to extract the PICS we need to isolate the influence of the medium. Usually, such effects are neglected and a simplistic single-atom model is used to describe HHG spectra obtained experimentally. Recently, at JRML C.D. Lin and collaborators were able to use a simple, but very accurate model to describe the emission of harmonics [1, 2, 3] and model the entire macroscopic process [4, 5, 6]. By making use of such simulations I believe we can fully characterize the influence of several macroscopic parameters and isolate the response of atoms and molecules.

As an example, in Fig. 1 we show HHG spectra obtained in atomic Xe with laser pulses of central wavelength $\lambda_0 = 1824$ nm and duration of 14fs which corresponds to 2.2 optical cycles. The appearance of the peak at $\tilde{80}$ eV has been explained already in [7]. However, the spectrum shown here under almost identical conditions show a much lower cutoff than then one originally presented in [7] although it was measured with the same laser parameters. In order to show the level of accuracy that we can obtain Figure 2 shows simulations in atomic Xe. Panel (a) shows the harmonic spectra for four peak intensities after propagation through the jet with parameters that closely resemble the experimental conditions. Such condition include not only the laser parameters but also the jet size ($500 \mu\text{m}$), the spectrometer slit opening ($190 \mu\text{m}$) and distance of the slit to the interacting region (455 mm). All spectra are averaged over random values of the CEP to simulate the lack of control on the phase in the experiment. The values for the peak intensities chosen are close to the measured in the experiment but not exactly matching since we are interested in describing the overall behaviour. The simulation involves the calculation of the single atom response using QRS and the photoionization cross section for Xe [8] which contains the multi-electron correlation effect. Details of this simulations can be seen in two forthcoming articles [9, 10]. CEP-averaged HHG spectra of the single atom response obtained with the same QRS method is shown in Fig. 2 (b). The color scheme used (online version) is the same as in panel (a), the spectrum with the lowest cutoff (red) is for a peak intensity of $I = 0.5 \times 10^{14} \text{W/cm}^2$ and the spectrum with the largest cutoff (green) is for $I = 1.0 \times 10^{14} \text{W/cm}^2$. By

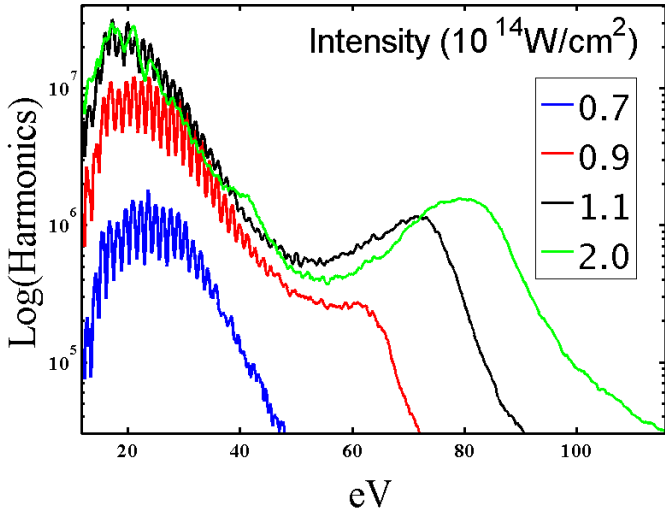


Figure 1: Experimentally measured (at ALLS-INRS, Canada) HHG spectra in Xe for four different intensities. Driving field has $\lambda_0 = 1825 \text{nm}$ and duration 14 fs.

comparing HHG spectra obtained for the single atom with the ones from a macroscopic simulation for the same peak intensities, we observe large discrepancies in the cutoff and the overall shape. Finally, panel (c) of the same figure shows harmonic spectra as in panel (a) for peak intensity $I = 2.0 \times 10^{14} W/cm^2$ at two different pressures showing that in order to retrieve the original spectrum shown in [7] a lower pressure had to be used. In addition to the pressure we studied the effect of the focusing conditions, slit, and pulse duration.

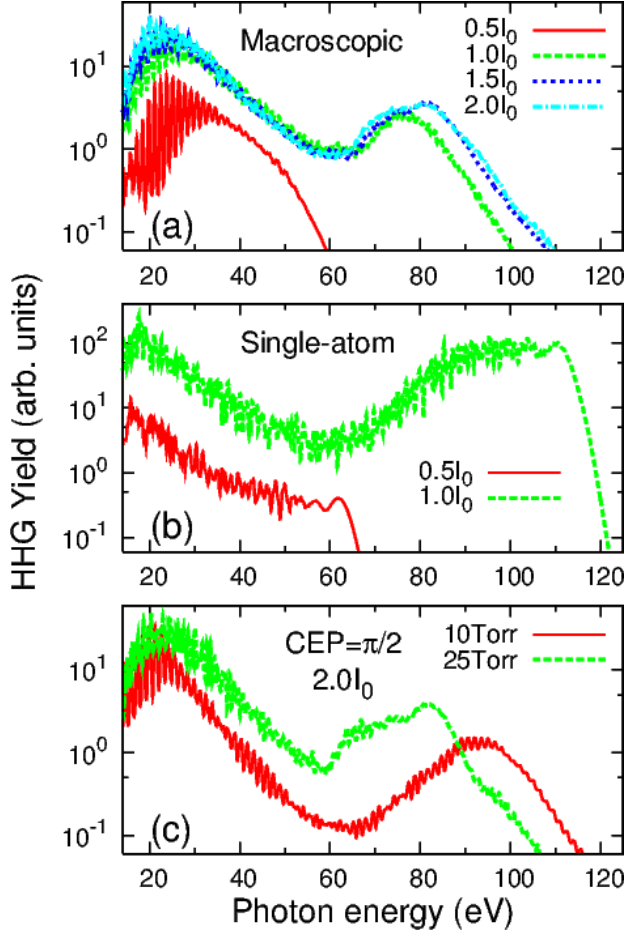


Figure 2: (color online) HHG spectra calculated using QRS theory for four different peak intensities as indicated where $I_0=10^{14} W/cm^2$. Panel (a) shows spectra when including propagation of both the fundamental and the XUV beams. Panel (b) shows spectra for a single atom response.

IR have two main advantages; tunability, and that the supercontinuum of frequencies occur at a much lower XUV energy compared to the case when HHG is driven by the typical 800nm field. In addition, the generation of few cycle mid-IR pulses have been demonstrated to be almost trivial since there is no need to use carefully engineered chirp compensating mirrors [11]. Furthermore, it has being demonstrated recently that the XUV flux can actually increase with wavelength if the right conditions for phase matching are exploited [12]. Therefore, having sources for IAP driven by mid-IR pulses could be feasible.

While we are able to reproduce the main features of the experimental HHG spectra with our macroscopic model, there is still no clear indication why the spectra becomes continuum. In addition to the ionization gating there has to be another process that is medium-related. To further clarify this, we followed the fundamental field in space and time through the simulation. The results are plotted in Fig. 3. In the figure we can see the fundamental field as a function of time at three different positions under the gas jet; at the entrance, at the focus, and just before exiting the jet.

Future work We plan to produce HHG with

different driving pulses and fully characterize the influence of different parameters such as the relative position of the focus and molecular jet, molecular axis angle, pressure, and pulse duration. All of these while changing the intensity. The laser will be properly characterized (spot size and duration) and all the parameters will enter in the full simulation using the HHG spectra as the observable that the theory will fit to. Once we understand how to isolate the response of the bulk in simple molecules, we will proceed to extract the photoionization cross section of more complicated molecules using the simple cases as reference.

2. Generation of attosecond pulses with mid-IR pulses

A closer look at Fig. 1 reveals the emergence of a continuum spectrum for high intensity values. Indeed, the macroscopic simulations also show a continuum HHG spectrum for the highest peak intensities, thus reproducing the behaviour observed experimentally. This is not the case for the single atom simulations, independently of peak intensity. Therefore we conclude that the supercontinuum is a consequence of the propagation in the medium of both the fundamental and the XUV beam. The presence of a continuum spectrum in the XUV is a necessary condition for the generation of isolated attosecond pulses (IAPs). While we do not provide an experimental characterization of the attosecond pulses, we carry out detailed macroscopic calculations to show that this scheme is capable of producing IAPs if a proper spatial filter is applied. Producing IAPs by using an optical parametric amplifier (OPA) in the mid-

As we can see, the driving field undergoes a very large chirp as it travels through the medium due to depletion [10]. A chirped pulse means that harmonics will be produced at different fundamental frequencies depending of where they are in the medium and in time thus creating harmonics of different driving frequencies ω_o . Therefore, the features we observe experimentally in the HHG of atomic Xe as a function of the driving field's intensity is a combined effect of the saturation of the ionization step under the half cycle (ionization gating) *and* of the large chirp suffered by the driving field. Fig. 4 (a) shows the attosecond pulses using harmonics 40 (27.2eV) to 80 (54.4 eV) for the same driving field ($\lambda_o = 1825nm$ duration (FWHM) = 14fs) with peak intensity of $I = 1.5 \times 10^{14} W/cm^2$ at the end of the interacting region (500 μm) or near field. The presence of an APT is evident. However, as proposed in [13], IAPs can be obtained in the far field by spatially filtering the XUV pulses. Panel (b) of Fig. 4 shows harmonics H40 to H80 in time domain, under the same conditions as panel (a), after putting a circular filter of radius $r_o = 300\mu m$ at the exit of the interacting region. The pulse is "measured" 455 mm away from the focus (far field). In this case, a single 390 as pulse is measured, thus proving that this observed XUV supercontinuum can indeed produce IAPs. An upcoming publication [10] will provide further details on how this IAPs can be manipulated by changing the CEP of the driving field and/or the spatial filter applied.

Future work We are planning on expanding the JRML capabilities to have high energy mid-IR laser pulses to study the generation of attosecond pulses.

3. Improving models for ionization rates

After the study of macroscopic behavior of HHG presented above it was clear that there is a great lack of measured optical properties in molecular systems, and that we need more accurate models for molecular ionization rates. While the first issue is more out of our hands, we can improve ionization models for molecular systems by combining our experimental and theoretical expertise. Theoretically we will make use of the molecular ADK rates [14] and improve the model by finding the optimal parameters that fit the experiment. Experimentally we will measure ionization yields in a VMI configuration for different atomic and molecular species with similar IPs as a function of peak intensity and for different pulse durations. For the atomic case ADK rates can be compared to other models [15]. All ionization simulations will be time and space average, therefore a careful characterization of the laser parameters is of most importance.

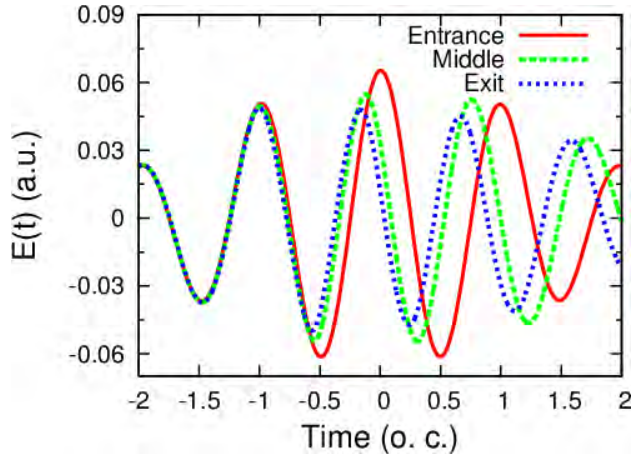


Figure 3: Driving electric field ($\lambda_o = 1825nm$) as a function of time (units of the optical cycle, o.c.) at three different positions relative to the atomic jet. All values are "measured" on axis. Laser parameters are $I = 1.5 \times 10^{14} W/cm^2$, CEP=0.

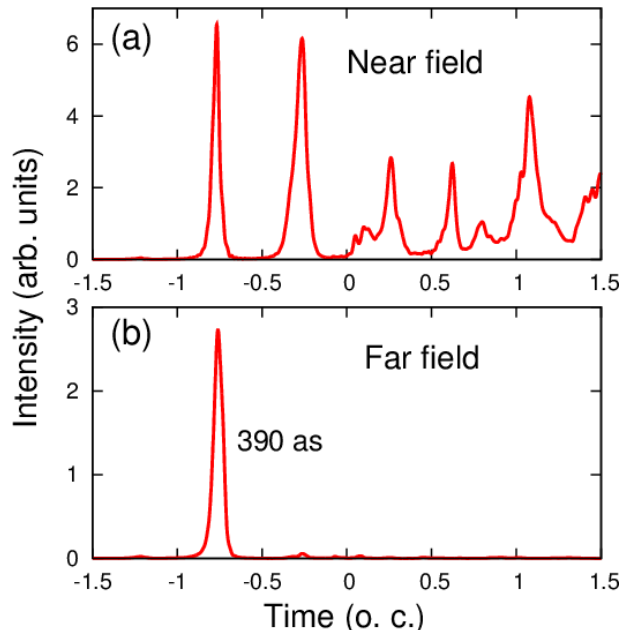


Figure 4: (a) Intensity of attosecond pulses in the near field. (b) Intensity of isolated attosecond pulses (IAPs) in the far field. The durations (FWHM) of IAPs are labeled.

In figure 5 we show the ratio of N_2^+ to Ar^+ measured in our VMI as a function of pulse energy. The energy of the laser is controlled by a polarizer beam splitter and a half wave plate to ensure that all beam parameters remain constant and only the energy changes. The background pressures for this particular measurement were, 4.7×10^{-8} Torr for N_2 and 1.0×10^{-8} Torr for Ar . We performed the same measurement at a large range of pressures in order to isolate possible saturation or non-linear responses from the detection.

Future work

We are in the process of measuring the ionization rates for several atom-molecule combination at 6fs and 30fs pulse durations. A strong collaboration with An-Thu Le and C. D. Lin is currently in progress and once the full measurements are finish they will proceed to implement the modification in the molecular ADK model. Once we have a robust ionization model for a particular molecular specie we can then proceed with macroscopic simulations as a function of intensity and alignment angle.

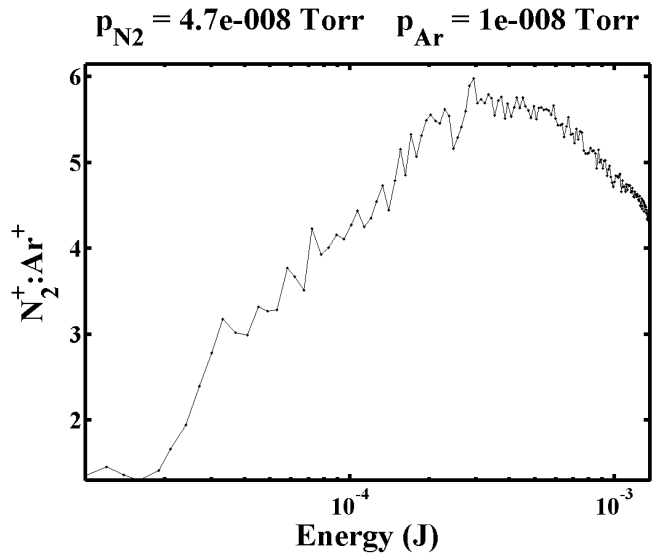


Figure 5: Ionization yield ratio of N_2^+/Ar^+ as a function of laser pulse energy for a 30 fs pulse. The pressure of each specie is indicated in the graph..

References

- [1] Z. Chen T. Morishita C. D. Lin, A. T. Le and R. R. Lucchese. *J. Phys. B*, 43:122002, 2009.
- [2] Z. Chen T. Morishita, A. T. Le and C. D. Lin. *Phys. Rev. Lett.*, 100:013903, 2008.
- [3] S. Tonzani T. Morishita .A. T. Le, R. R. Lucchese and C. D. Lin. *Phys. Rev. A*, 80:013401, 2009.
- [4] A. T. Le C. Jin and C. D. Lin. *Phys. Rev. A*, 79:053413, 2009.
- [5] A. T. Le C. Jin and C. D. Lin. *Phys. Rev. A*, 83:023411, 2011.
- [6] V. Tosa A. T. Le J. B. Bertrand R. R. Lucchese P. B. Corkum D. M. Villeneuve C. Jin, H. J. Wöner and C. D. Lin. *J. Phys. B.*, 44:095601, 2011
- [7] A. D. Shiner, B. E. Schmidt, C. Trallero-Herrero, H. J. Worner, S. Patchkovskii, P. B. Corkum, J-C. Kieffer, F. Legare, and D. M. Villeneuve. *Nat. Phys.*, 7(6):464–467, 2011.
- [8] V. Radojević M. Kutzner and H. P. Kelly. *Phys. Rev. A*, 40(9):5052, 1989.
- [9] C. A. Trallero-Herrero C. Jin, A. T. Le and C. D. Lin. *Phys. Rev. A*, in preparation.
- [10] C. Jin, A. T. Le C. A. Trallero-Herrero and C. D. Lin. *Phys. Rev. A*, submitted.
- [11] Bruno E. Schmidt, Pierre Béjot, Mathieu Giguère, Andrew D. Shiner, Carlos Trallero-Herrero, Éric Bissson, Jérôme Kasparian, Jean-Pierre Wolf, David M. Villeneuve, Jean-Claude Kieffer, Paul B. Corkum, and François Légaré. *Applied Physics Letters*, 96(12):121109, 2010.
- [12] T. Popmintchev, M.-C. Chen, A. Bahabad, M. Gerrity, P. Sidorenko, O. Cohen, I. P. Christov, M. M. Murnane, and H. C. Kaptelyn. *PNAS*, 106(26):10516–10521, 2009.
- [13] Mette B Gaarde, Jennifer L Tate, and Kenneth J Schafer. *J. Phys. B*, 41(13):132001, 2008.
- [14] X.M. Tong, Z.X. Zhao, and C.D. Lin. *Phys. Rev. A*, 66:033402, 2002.
- [15] Gennady L. Yudin and Misha Yu. Ivanov. *Phys. Rev. A*, 64(1):013409, Jun 2001.

Engineered Electronic and Magnetic Interactions in Nanocrystal Quantum Dots

Victor I. Klimov

Chemistry Division, C-PCS, MS-J567, Los Alamos National Laboratory
Los Alamos, New Mexico 87545, klimov@lanl.gov, <http://quantumdot.lanl.gov>

1. Program Scope

Using nanocrystal (NC) quantum dots one can produce extremely strong spatial confinement of electronic excitations not accessible with other types of nanostructures. Because of this confinement, electronic energies in nanocrystals are directly dependent upon their dimensions, which is known as the quantum-size effect. This effect has been a powerful tool for controlling spectral responses of NCs, enabling potential applications such as multicolor labeling, optical amplification and low-cost lighting. In addition to spectral tunability, strong spatial confinement results in a significant enhancement of carrier-carrier interactions that lead to a number of novel physical phenomena including large splitting of electronic states induced by electron-hole exchange coupling, ultrafast multiexciton decay via Auger recombination, and direct generation of multiple excitons by single photons via carrier multiplication. Confinement-induced mixing between the conduction and the valence band can also lead to interesting peculiarities in magnetic interactions such as switching of the sign of the g -factor in magnetically doped NCs. The major thrust of this project is to understand the physics of electronic and magnetic interactions under conditions of extreme quantum confinement, and to develop methods for controlling these interactions. Research topics explored here include: control of Auger recombination via engineered exciton-exciton interactions in heterostructured and alloyed NCs with a goal of realizing the regime of continuous-wave lasing; new functional behaviors via NC doping with optically active ions such as copper; control of single-exciton dynamics via tunable fine-structure excitonic splitting; and controlled exchanged interactions in magnetically doped NCs probed by steady state and time-resolved magneto-optical spectroscopies.

2. Recent Progress

During the past year, our work in this project has focused on elucidating the mechanisms for suppression of Auger recombination in thick-shell CdSe/CdS hetero-structures, the development of a new experimental methodology for evaluating the biexciton emission yields via single-NC measurements of two-photon correlations, and investigations of polarization properties of emission from Mn^{2+} ions in Mn:ZnSe/CdSe NCs. During 2009 - 2011, our studies resulted in 20 peer-reviewed articles including 1 *Nature Mater.* report, 1 *Nature Comm.* article, 4 *Phys. Rev. Letters*, 4 *J. Am. Chem. Soc.* papers, 5 *Nano Letters*, etc. Various aspects of this work were presented in 35 invited talks (including a Plenary talk, a Keynote talk and a Distinguished Lecture) at major research forums such as APS March meetings, Gordon Research Conferences, Spring and Fall MRS meetings, and ACS National meetings. Our studies of carrier multiplication and competing processes were highlighted in the *LANL Press Release* "Research Highlights Potential for Improved Solar Cells" (February 10, 2009) and reviewed in several popular science outlets, including publications in *Photonics* ("Nanocrystals Improve PV Cells," February 12, 2009) and *Nanowerk* ("Improving solar cells," February 10, 2009). Our work on tunable g -factors in Mn-doped hetero-NCs was reviewed in *Nature Mater.* (8, 8, 2009), while the studies of the effect of interfacial alloying on Auger decay in core/shell CdSe/CdS NCs were highlighted in *Chemical & Engineering News (C&N News 89, 32, 2011)*. Below, we provide a brief description of this latter piece of work, which represents an important milestone in the research on "Auger-recombination-free" colloidal nanostructures. Such nanostructures would be ideally suited for the realization of NC lasing under conditions of steady state pumping and eventually electrical injection.

Interfacial alloying and Auger recombination in core/shell semiconductor NCs. One consequence of strong confinement of electronic excitations in NCs is a significant enhancement in the rate of Auger recombination (AR), a nonradiative process in which an electron-hole pair transfers its energy to a third charge carrier. In conventional 'single-component' NCs, Auger decay lifetimes are proportional to NC volume, a seemingly universal trend that is observed for many different semiconductors including both direct- and indirect-gap materials. The time scales of AR in NCs are very short. For example, in CdSe particles, the biexciton Auger lifetime (τ_{2A}) is reduced from 360 ps to only 6 ps as the NC radius is decreased from 4.1 to 1.2 nm. Even in large single-component NCs, τ_{2A} is much less than the radiative lifetime (~ 20 ns at room temperature) implying that biexcitons and other multiexcitons of higher order are essentially non-emissive. The development of approaches for reducing AR rates, while still preserving a significant degree of spatial confinement, has been a long-standing goal in the field of NCs and especially NC lasing.

In the present work, we experimentally study the influence of NC volume, electron-hole spatial separation, and the shape of interfacial potential on the rate of Auger recombination in CdSe/CdS NCs with a shell of a variable thickness. In parallel, we analyze the composition of the CdSe/CdS interface by monitoring the intensity of the CdS, CdSe and CdSeS phonon replicas in low-temperature emission spectra recorded using a fluorescence line

narrowing (FLN) technique. We observe a marked increase of AR time that correlates with the formation of a CdSeS alloy layer at the core-shell interface (i.e., a region with a gradually changing confinement potential), which occurs in the range of shell thickness between 2 and 9 monolayers (MLs). These observations provide direct experimental evidence that the shape of the interfacial potential plays an important role in AR in semiconductor nanostructures.

We study core/shell CdSe/CdS NCs with a fixed core radius ($R_0 = 1.5\text{nm}$) and a shell thickness H varied from 0 to 19 MLs via a layer-by-layer deposition technique (1 ML = 0.4 nm). The emission energy of CdSe seed particles is $\sim 2.2\text{ eV}$. It shifts to the red by more than 200 meV upon deposition of the thick CdS shell. Based on the energy offsets at the CdSe/CdS interface, this shift occurs mostly as a consequence of electron delocalization into the shell region, while the hole remains primarily confined to the core.

To obtain biexciton dynamics (Fig. 1a), we subtract the low-fluence photoluminescence (PL) traces from the “tail-normalized” traces measured for $\langle N \rangle$ slightly above unity ($\langle N \rangle$ is the average NC excitonic occupancy). The biexciton lifetimes (τ_2) derived from the extracted decay curves are shown in Fig. 1b for two series of NCs. Both sets of data are in good agreement indicating an excellent sample-to-sample reproducibility of these measurements. Furthermore, importantly, the data reveal a dramatic, more than two orders of magnitude increase (from 60 ps to 23 ns) in τ_2 with increasing shell thickness from 0 to 14 ML. We use these results to extract the biexciton Auger decay times τ_{2A} (Fig. 1c). The extracted time constants indicate a dramatic increase in the AR lifetime with increasing shell thickness. It changes from 60 ps for core-only sample to 60 – 120 ns for the 14 ML sample.

First, we examine whether this increase can be entirely due to increasing volume of the NC, i.e., is similar to traditional “ V -scaling” observed for standard NCs. In the present case however, the V -scaling must be modified to account for a significant difference in the regions of electron and hole localization. The approach, which we use

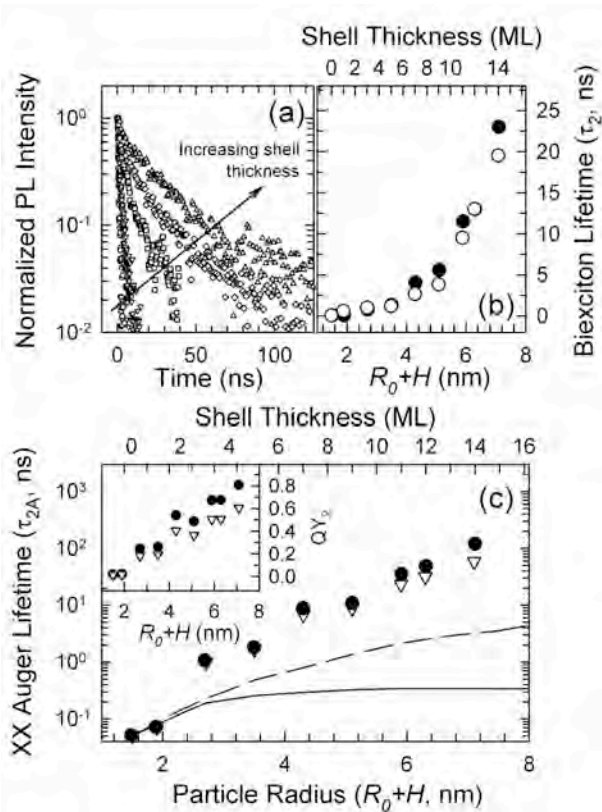


Fig. 1. (a) Biexciton recombination dynamics for samples with increasing shell thicknesses ($R_0 = 1.5\text{ nm}$ and $H = 0.8, 2.0, 3.6, 5.2$ and 6.0 nm). (b) Biexciton lifetimes (τ_2) as a function of total NC radius for two different batches of samples shown by open and solid circles ($R_0 = 1.5\text{ nm}$). (c) Biexciton AR lifetimes calculated using $\tau_{2A}^{-1} = \tau_2^{-1} - \beta \tau_{1r}^{-1}$ for $\beta = 3$ (open triangles) and $\beta = 4$ (solid circles); τ_{1r}^{-1} is the measured single exciton radiative decay rate. Lines show AR lifetimes expected for the cases of linear scaling with effective exciton volume (V_{exc} -scaling; solid line) and the V_{exc} -scaling corrected for electron-hole spatial separation (dashed line). The inset shows the “intrinsic” biexciton emission quantum yield calculated using $QY_2 = \beta \tau_{1r}^{-1} / \tau_2^{-1}$.

here, is to consider not the total volume of the NC but the effective excitonic volume (V_{exc}) estimated from the position of the 1S transition: $V_{\text{exc}} = (4\pi/3)R_{\text{exc}}^3$. We observe that the measured data indeed follow the V_{exc} -scaling (solid line in Fig. 1c) for thin shells, however, they experience progressive deviation from this scaling for $H > 3$ MLs. Next, we account for the effect of electron-hole separation that can also lead to reduced Auger decay rates. The V_{exc} -scaling corrected for reduced electron-hole overlap, Θ_{eh} , ($\tau_{2A} \propto V_{\text{exc}}/\Theta_{\text{eh}}$) is shown in Fig. 1c by the dashed line. It still significantly underestimates the τ_{2A} values derived from the measurements, indicating a contribution from some other effects besides the increased NC volume and electron-hole spatial separation.

One such effect is associated with the influence of the steepness of the interfacial potential on the AR rate. By considering Auger ionization (AR accompanied by charge ejection from the NC), one can show that the rate of this process scales as the square of the large-wave-vector (k_f) Fourier component of the ground-state wave function, $\psi_0(k_f)$ (k_f is determined by the energy of the ejected carrier). It turns out that $\psi_0(k_f)$ is much greater (exponentially) for a “sharp” step-like potential than for a “smooth” parabolic profile. As a result, the AR rates can be different by more than three orders of magnitude for structures with similar degrees of spatial confinement but different shapes of the confinement potential.

To elucidate the role of the shape of the confinement potential on AR in our core/shell NCs, we study the composition of the core-shell interface as a function of H . Since the growth of thick shells involves long reaction times and relatively high temperatures (4 hours per ML at $240\text{ }^\circ\text{C}$) one might expect it to be accompanied by inter-diffusion of S and Se ions at the core/shell interface, which would result in the CdSeS alloy layer with a smoothly varying potential. To analyze the composition of the NC interface, we use a FLN spectroscopy. In this method, the samples are excited with a narrowband cw laser on the red edge of the 1S absorption feature, which allows us to effectively narrow down the size distribution

in the photoexcited NC sub-ensemble by selecting only a small fraction of larger dots from the sample. As a result of this spectroscopic selection, using FLN we can clearly resolve features due to phonon-assisted transitions involving various longitudinal optical (LO) modes; based on the intensity of these modes we can analyze the composition of the NC within the volume sampled by a photoexcited exciton.

The FLN spectra indeed indicate the development of the CdSeS phonon replica due to a “combinatory” 60 meV mode, which represents the sum of CdS (35 meV) and CdSe (25 meV) LO phonon energies. The FNL data indicate that most of the interfacial alloying occurs until the shell thickness reaches ~9 MLs, while further shell growth is not accompanied by any significant expansion of the alloy region. Further, based on the quantitative analysis of the relative intensities of phonon replicas associated with CdSe, CdS and CdSeS, we obtain that the final thickness of CdSeS alloy layer is ~1.5 ML. Interestingly, the largest change in the Auger decay time also occurs in the range of shell thicknesses for which we observe the formation of the alloyed interface. Specifically, τ_{2A} changes by more than two orders of magnitude (from 250 ps to 31 ns), when H increases from 0 to 11 ML. This increase is about ten times larger than that predicted based on changes in the effective exciton volume and electron-hole spatial overlap (Fig. 1c). These results indicate that the formation of even a very thin (less than two MLs) graded layer is sufficient to produce a “smooth” potential profile resulting in greatly reduced rate of AR.

One important consequence of suppressed AR is a significant increase in emission efficiencies of multiexciton states. For example, in the core-only samples studied in this work, the emission quantum yield of biexcitons is ~1%. However, it reaches 40 – 50% in CdSe/CdS structures with shell thickness of 9 ML and is as high as 60 – 80% in samples with a 19 ML shell (Fig. 1c, inset). This dramatic increase in PL yields of multiexciton states can greatly benefit applications of NCs in technologies involving light emission such as lasing, optical amplification and solid-state lighting.

To summarize, we have investigated multiexciton dynamics in hetero-NCs composed of CdSe cores and CdS shells of tunable thickness. Thicker shells dramatically reduce AR rates, particularly during initial shell growth, which cannot be explained by traditional volume scaling alone. Rather, FLN studies indicate that the suppression of AR correlates with the formation of an alloy layer at the core-shell interface suggesting that this effect derives primarily from the “smoothing” of the confinement potential associated with interfacial alloying. These data highlight the importance of the NC interfacial structure in the AR process and provide general guidelines for the development of new nanostructures with suppressed AR for future applications in solution processable lasing media.

3. Future Plans

A new theme that will be explored in this project is the synthesis, spectroscopic characterization and application of NCs doped with “electronic” impurities, i.e., impurities that introduce into the NCs optically and potentially electrically active carriers. As a model system for our studies we will use Cu-doped NCs. Previous studies of bulk semiconductors indicate that substitutional doping of Cu into materials such as ZnS and ZnSe leads to formation of localized hole states that are optically active, as indicated by the development of new intra-gap emission lines. In this project, we will develop a new class of electronically doped NCs by combining the reported methods for Cu doping with strategies for complex heterostructuring previously explored in this project. Our initial focus will be on ZnSe/CdSe core/shell NCs, a system offering wide-range size-tunability, with Cu-doped cores. In these structures, by tuning the thickness of the CdSe shell we should be able to tune the position of the conduction band level while preserving the number and the original placement of the Cu ions. The use of this strategy, which decouples Cu incorporation into the nanostructure from the control of the degree of spatial confinement, should allow us to obtain a wide range of tunability for the Cu-related intra-gap transitions without losing the strength of these transitions.

Because of the temperature-dependent dynamics of Cu ions as mobile impurities in the semiconductor lattice of the NCs, the method we employ for synthesis of the doped core/shell structure must take into account the potentially deleterious effects of excessive reaction time and temperatures. To effectively sequester the Cu in the core, we will start with the fast-injection synthesis of a small Cu:ZnSe doped core in the presence of excess Se precursor, followed by slower growth of additional pure ZnSe at a lower temperature by addition of more Zn precursor. The desired thickness of CdSe can then be deposited by slow addition of Cd precursor. The average number of Cu ions per NC depends on the inclusion efficiency during core growth and the fraction that escape the core volume during additional ZnSe growth; these will have to be determined empirically for any given combination of core and shell dimensions by measuring Cu:Zn ratio by ICP post-synthesis.

We will use these structures to study the mechanism of intra-gap emission and will attempt to obtain conclusive evidence that it is indeed due to optically active holes associated with the Cu^{2+} state. The experiments to clarify this issue will involve “quenching” of optically generated holes with electron-donating surface ligands and excitation of doped wide-gap NCs with a single type of charge using electron transfer from an adjacent narrow-gap NC.

This initial spectroscopic work will be extended to studies of optical amplification in these novel doped materials. Our goal in this work will be to demonstrate the regime of a “zero-threshold” optical gain. We will also incorporate these doped NCs into LED structures and test them in the regime of alternating current, in which the

“negative” wave will be used to excite emission by injecting electrons that will recombine with “intrinsic” holes on the Cu^{2+} centers transforming them into the Cu^+ state. The positive “wave” will then be used to “refill” the copper centers with holes to prepare them for the next emission cycle. In such a device the processes of radiation and recombination are separated in time and can be optimized independently via separate optimization of electron and hole currents.

4. Publications (2009 - 2011)

1. R. Viswanatha, J. M. Pietryga, V. I. Klimov, and S. A. Crooker, *Circularly-polarized Mn^{2+} emission from Mn-doped colloidal nanocrystals*, Phys. Rev. Lett., in press (2011)
2. S. Brovelli, R. D. Schaller, S. A. Crooker, F. Garcia-Santamaria, Y. Chen, R. Viswanatha, J. A. Hollingsworth, H. Htoon, V. I. Klimov, *Nano-engineered electron-hole exchange interaction controls exciton dynamics in core-shell semiconductor nanocrystals*, Nature Comm. **2**, 280 (2011)
3. Y.-S. Park, A. V. Malko, J. Vela, Y. Chen, Y. Ghosh, F. Garcia-Santamaria, J. A. Hollingsworth, V. I. Klimov, H. Htoon, *Near-unity quantum yields of biexciton emission from CdSe/CdS nanocrystals measured using single-particle spectroscopy*, Phys. Rev. Lett. **106**, 187401 (2011)
4. L. Li, A. Pandey, D. J. Werder, B. P. Khanal, J. M. Pietryga, V. I. Klimov, *Efficient synthesis of highly luminescent indium sulfide based core/shell nanocrystals with surprisingly long-lived emission*, J. Am. Chem. Soc. **133**, 1176 (2011).
5. Garcia-Santamaria, F., S. Brovelli, R. Viswanatha, J. A. Hollingsworth, H. Htoon, S. Crooker, V. I. Klimov, *Breakdown of volume scaling in Auger recombination in CdSe/CdS heteronanocrystals: The role of the core-shell interface*, Nano Lett. **11**, 687 (2011).
6. Piryatinski, A. and K. A. Velizhanin, *An exciton scattering model for carrier multiplication in nanocrystals: Theory*, J. Chem. Phys. **133**, 084508 (2010).
7. McGuire, J. A., M. Sykora, I. Robel, L. A. Padilha, J. Joo, J. M. Pietryga, V. I. Klimov, *Spectroscopic signatures of photocharging due to hot-carrier transfer in solutions of semiconductor nanocrystals under low-intensity ultraviolet excitation*, ACS Nano **4**, 6087 - 6097 (2010).
8. Schaller, R. D., S. A. Crooker, D. A. Bussian, J. M. Pietryga, J. Joo, V. I. Klimov, *Revealing the exciton fine structure in PbSe nanocrystal quantum dots*, Phys. Rev. Lett. **105**, 067403 (2010).
9. Htoon, H., A. V. Malko, D. Bussian, J. Vela-Becerra, Y. Chen, J. A. Hollingsworth, V. I. Klimov, *Highly emissive multiexcitons in steady-state photoluminescence of individual “giant” CdSe/CdS core/shell nanocrystals*, Nano Lett. **10**, 2401 (2010).
10. Lee, D. C., I. Robel, J. M. Pietryga, V. I. Klimov, *Infrared-active heterostructured nanocrystals with ultralong carrier lifetimes*. J. Am. Chem. Soc. **132**, 9960 (2010).
11. Sykora, M., A. Y. Kuposov, J. A. McGuire, R. K. Schulze, O. Tretiak, J. M. Pietryga, V. I. Klimov, *Effect of air exposure on surface properties, electronic structure and carrier relaxation in PbSe nanocrystals*, ACS Nano **4**, 2021 (2010).
12. McGuire, J. A., M. Sykora, J. Joo, J. M. Pietryga, V. I. Klimov, *Apparent versus true carrier multiplication yields in semiconductor nanocrystals*, Nano Lett. **10**, 2049 (2010).
13. Glennon, J. J., R. Tang, W. E. Buhro, R. A. Loomis, D. A. Bussian, H. Htoon, V. I. Klimov, *Exciton localization and migration in individual CdSe quantum wires at low temperatures*, Phys. Rev. B **80**, 081303 (2009).
14. Joo, J., J. M. Pietryga, J. A. McGuire, S.-H. Jeon, D. J. Williams, H.-L. Wang, V. I. Klimov, *A reduction pathway in the synthesis of PbSe nanocrystal quantum dots*, J. Am. Chem. Soc. **131**, 10620 (2009).
15. Garcia-Santamaria, F., Y. Chen, J. Vela, R. D. Schaller, J. A. Hollingsworth, V. I. Klimov *Suppressed Auger recombination in “giant” nanocrystals boosts optical gain performance*, Nano Lett. **9**, 3482 (2009).
16. Robel, I., R. Gresback, U. Kortshagen, R. D. Schaller, V. I. Klimov, *Universal size-dependent trend in Auger recombination in direct-gap and indirect-gap semiconductor nanocrystals*, Phys. Rev. Lett. **102**, 177404 (2009).
17. Lee, D. C., J. M. Pietryga, I. Robel, D. J. Werder, R. D. Schaller, V. I. Klimov, *Colloidal synthesis of infrared-emitting germanium nanocrystals*, J. Am. Chem. Soc. **131**, 3436 (2009).
18. Sun, B., A. T. Findikoglu, M. Sykora, D. J. Werder, V. I. Klimov, *Hybrid Photovoltaics based on semiconductor nanocrystals and amorphous silicon*, Nano Lett. **9**, 1235 (2009)
19. Bussian, D., M. Ying, S. A. Crooker, M. Brynda, A. L. Efros, V. I. Klimov, *Tunable magnetic interactions in manganese-doped inverted core/shell ZnSe/CdSe nanocrystals*, Nature Mater. **8**, 35 (2009)
20. Bussian, D., A. Malko, H. Htoon, Y. Chen, V. I. Klimov, J. A. Hollingsworth, *Quantum optics with nanocrystal quantum dots in solution: Quantitative study of clustering*, J. Phys. Chem. C **113**, 2241 (2009).

Atomic, Molecular and Optical Sciences at LBNL

Ali Belkacem, Daniel J. Haxton, Clyde W. McCurdy, Thomas N. Rescigno and Thorsten Weber

Chemical Sciences Division, Lawrence Berkeley National Laboratory, Berkeley, CA 94720

Email: abelkacem@lbl.gov, djhaxton@lbl.gov, cwmcurdy@lbl.gov, tnrescigno@lbl.gov, tweber@lbl.gov

Objective and Scope

The AMOS program at LBNL is aimed at understanding the structure and dynamics of atoms and molecules using photons and electrons as probes. The experimental and theoretical efforts are strongly linked and are designed to work together to break new ground and provide basic knowledge in fundamental atomic and molecular processes that underpin energy research that is central to the programmatic goals of the Department of Energy. The current emphasis of the program is in three major areas with important connections and overlap: inner-shell photo-ionization and multiple-ionization of atoms and small molecules; low-energy electron impact and dissociative electron attachment of molecules; and time-resolved studies of atomic processes using a combination of femtosecond X-rays and femtosecond laser pulses. This latter part of the program is folded in the overall research program in the Ultrafast X-ray Science Laboratory (UXSL).

The experimental component at the Advanced Light Source makes use of the Cold Target Recoil Ion Momentum Spectrometer (COLTRIMS) to advance the description of the final states and mechanisms of the production of these final states in collisions among photons, electrons and molecules. Parallel to this experimental effort, the theory component of the program focuses on the development of new methods for solving multiple photo-ionization of atoms and molecules. This dual approach is key to break new ground and provide a new understanding how electronic energy channels into nuclear motion and chemical energy in polyatomic molecules as well as unravel unambiguously electron correlation effects in multi-electron processes.

Inner-Shell Photoionization and Dissociative Electron Attachment to Small Molecules

Ali Belkacem and Thorsten Weber

Chemical Sciences Division, Lawrence Berkeley National Laboratory, Berkeley, CA 94720

Email: abelkacem@lbl.gov, tweber@lbl.gov

Objective and Scope

This program is focused on studying photon and electron impact ionization, excitation and dissociation of small molecules and atoms. The first part of this project deals with the interaction of X-rays with atoms and simple molecules by seeking new insight into atomic and molecular dynamics and electron correlation effects. These studies are designed to test advanced theoretical treatments by achieving a new level of completeness in the distribution of the momenta and/or internal states of the products and their correlations. The second part of this project deals with the interaction of low-energy electrons with small molecules with particular emphasis on Dissociative Electron Attachment (DEA). Both studies are strongly linked to our AMO theoretical studies led by C.W. McCurdy and T.N. Rescigno and are designed to break new ground and provide basic knowledge that is central to the programmatic goals of BES in electron-driven chemistry. Both experimental studies (photon and electron impact) make use of the powerful COLd Target Ion Momentum Spectroscopy (COLTRIMS) method to achieve a high level of completeness in the measurements.

Kinematically complete experimental study of the dissociation pathways of the singly ionized CO molecule.

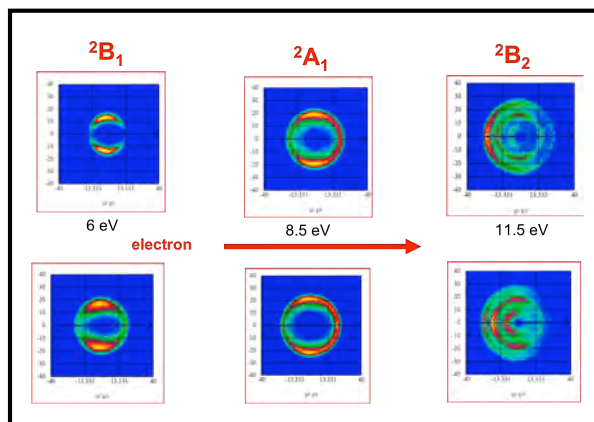
We studied the dissociation of the singly ionized carbon monoxide molecule, followed by subsequent autoionization of O^* , by detecting for the first time all four final fragments ($C^+ + O^+ + 2e$) in coincidence. In this experiment the supersonic jet of carbon monoxide was illuminated by the 43 eV x-ray beam at the Advanced Light Source. Although some direct double ionization of CO molecule was observed, the energetics dictated that most of the registered events must be attributed to single ionization followed by an autoionization in the atomic state of the oxygen. The energy of the slow electron is constant and independent of the first electron energy or of the nuclear kinetic energy release (KER) which is a clear signature of autoionization. The molecular dissociation of CO^+ ion followed by autoionization of the oxygen has been observed before. In this study we performed the most kinematically complete experiment where by simultaneously measuring the vector momenta of all particles we were able to extract the KER of the reaction together with the energies and complete angular distributions of photo-electron and autoionization electron in the body-fixed molecular frame. The study of these detailed angular distributions as a function of polarization and KER reveal a surprising dissociation dynamics. Comparison with theoretical calculations by colleagues Rescigno and Orel shine light on the molecular states involved in the initial process of photo-ionization. We observe a strong correlation between the polarization of the light and the angle of emission of the autoionization electron despite the fact that autoionization takes place in the atomic oxygen when the molecule has already fully dissociated. Further studies both experimental and theoretical are on-going to understand the origin of this unique photo and autoionization electron correlation.

Kinetic Energy Release dependence in the Photo Double Ionization of H₂.

In order to trace down electron-electron correlation in the initial-state wavefunction and understand asymmetry effects due to electron-nuclei interaction we chose to study the simplest molecular target (H₂) as a follow up to our successful double slit experiments. In the Photo Double Ionization (PDI) of hydrogen molecules with photon energies of 150eV we were able to probe the electronic two particle density as a function of the bond length, i.e. the Kinetic Energy Release (KER) of the ions, and the orientation of the molecular axis with respect to the polarization vector of the incoming light. For these investigations we performed and compared measurements with linear and circular polarized light while using our COLTRIMS technique measuring two electrons and two protons in coincidence. In the PDI with linear polarized light we found a shift in the KER for s and p transitions. While the KER is lower when the molecular axis is aligned parallel to the linear polarization vector (s-s), the KER for a perpendicular orientation (s-p) seems to be higher by a little more than 1eV. The different variation in the cross sections with the internuclear distance for the two different transitions is largely a reflection of the changes in the correlated initial state wave function. It can also be interpreted as a sensitive test for probing the two particle electron density wave function since for the s-p transitions smaller internuclear distances seem to be preferred and for s-s transitions an atomic like target, i.e. larger bondlengths appear to be more likely double ionized. The experiments were also carried out with circular polarized light. The Molecular Frame Angular Photoelectron Distributions (MFPADs) reveal a tilt for the circular polarization compared to the coherent sum of the angular distributions for linear polarized light. This again can be traced back to the different two-particle electron densities for s and p transitions resulting in different starting points of the outgoing p-waves, which is then reflected in a s-p phase shift.

Dissociative electron attachment to water molecules.

DEA to the deceptively simple H₂O molecule involves complex electronic and nuclear dynamics. In the gas phase, it proceeds via three transient anion states of ²B₁, ²A₁ and ²B₂ symmetries which are responsible for three distinct broad peaks in the DEA cross section at electron energies of 6.5, 9 and 12 eV. The negative ion states subsequently fragment to produce H⁻, O⁻ and possibly OH⁻, in various two-body as well as three-body breakup channels. As an example we show in the figure to the right a sample of momentum images we obtain for the H⁻ channel. D⁻ momentum images from DEA to D₂O look identical to these. A simple look at the images reveals that the symmetry of the resonance plays a major role. We produced similar momentum images at various electron energies as well as the O⁻ channel. Some of the key results either helped resolve some controversies found in the literature or bring completely new understanding of DEA to H₂O. We settled a long-standing discrepancy between theory and experiment with respect to the production of O⁻ for the ²B₁ resonance. We found that experimental measurements in the literature are most likely contaminated by O⁻ from background O₂. Our measurement can clearly see and separate O⁻ from DEA to H₂O and O⁻ from DEA to background O₂. The production of O⁻ from H₂O is extremely small supporting the calculations of our colleagues McCurdy and Rescigno.



We find that for the 2A_1 resonance O^- is produced predominantly via three-body breakup. However the most striking result for this resonance is the dissociation dynamics for the O^- channel. The contrast between the measured distribution and the axial recoil prediction suggests that after attachment, the molecule scissors backwards and ejects the oxygen through the mouth of the H-O-H bond, regardless of the direction of the incident electron, while the hydrogens recoil in the opposite direction. This interpretation of the dissociation dynamics, which is also supported by classical trajectory calculations, explains why O^- production for this resonance is most likely to proceed through three-body breakup. The most intriguing results for DEA to water are found in the H^- (D^-) channel of the 2B_2 . For this resonance the electron attaches to the molecule along the OH bond, impinging from the hydrogen side. Unlike 2B_1 and 2A_1 the momentum image for this resonance seen in the figure above exhibits three distinct rings (or kinetic energy releases). The middle ring corresponds to dissociation on the 2B_2 potential energy surface with OH fragment left in the $^2\Sigma$ excited-state. A dramatic observation here is the loss of equivalency of the two hydrogen atoms of H_2O . Dissociation favors breaking the OH bond opposite to the bond on which electron attachment happens. This effect is particularly dramatic at the lowest electron energy. This break of the equivalency of the two OH bonds suggests that the electron attachment is most likely taking place during an asymmetric stretch. Theory is not yet able to account for this strikingly strong effect. The outer ring corresponds to the OH fragment left in the $^2\Pi$ ground state giving a clear signature of funneling through a conical intersection and dissociation on the 2A_1 surface. Our theory group predicted the presence of this conical intersection. One remarkable aspect of this measurement is that we are able to control with high precision the fraction of the wave-packet that funnels through the conical intersection and dissociate on the lower 2A_1 state by tuning the energy of the electron around the 2B_2 .

Future Plans

We plan to continue application of the COLTRIMS approach to achieve complete descriptions of the single photon double ionization of CO, O_2 and their analogs. Of particular interest is an in-depth study of the “photoelectron and autoionization-electron” correlation and entanglement. We will also study double Auger decay of small molecules after photo excitation and photo ionization of inner shell electrons. The main scientific goals are to investigate the dissociation pathways and ionization mechanism during the double Auger decay. We plan to continue using our Dissociative Electron Attachment modified-COLTRIMS to study DEA to methanol and ethanol to unravel the OH functional group effects as well as some relevant molecules such as CO_2 or DNA bases such as uracil. This latter work will be done in collaboration and theoretical support from Vincent McKoy.

Recent Publications (2009-2011)

- 1) A.L. Landers, F. Robicheaux, T. Jahnke, M. Schoffler, T. Osipov, J. Titze, S.Y. Lee, H. Adaniya, M. Hertlein, P. Ranitovic, I. Bocharova, D. Akoury, A. Bhandary, Th. Weber, M.H. Prior, C.L. Cocke, R. Doerner and A. Belkacem, “*Angular correlation between photoelectrons and Auger electrons from K-shell ionization of neon*“, Phys. Rev. Lett. **102**, 223001 (2009).
- 2) F. Sturm, M. Schoeffler, S. Lee, T. Osipov, S. Kirschner, N. Neumann, H.-K. Kim, B. Rudek, J. Williams, J. Daughhete, C.L. Cocke, K. Ueda, A. Landers, Th. Weber, M.H. Prior, A. Belkacem, and R. Doerner. “*Photo and Auger electron angular distributions of fixed-in-space CO_2* “, Phys. Rev. A **80**, 032506 (2009).
- 3) N.A. Cherepkov, S.K. Semenov, M.S. Shoeffler, J. Titze, N. Petridis, T. Jahnke, K. Cole, L. Ph. Schmidt, A. Czasch, D. Akoury, O. Jagutzki, J.B. Williams, C.L. Cocke, T. Osipov, S. Lee, M.H. Prior, A. Belkacem, A.L. Landers, H. Schmidt-Bocking, Th. Weber and R. Doerner, “*Separation of Auger*

- transitions into different repulsive states after K-shell photoionization of N₂ molecules*” Phys. Rev. A **80**, 051404 (2009).
- 4) H. Adaniya, B. Rudek, T. Osipov, D.J. Haxton, T. Weber, T.N. Rescigno, C.W. McCurdy and A. Belkacem, “*Imaging the molecular dynamics of dissociative electron attachment to water*”, Phys. Rev. Lett. **103**, 233201 (2009).
 - 5) H. Adaniya, B. Rudek, T. Osipov and A. Belkacem, “*Experimental study for dissociative attachment to water molecule in the ²B₁ resonance*”, Journal of physics, conference series, volume **194**, pages 194-200 (2009).
 - 6) S.K. Semenov, M.S. Schoeffler, J. Titze, N. Petridis, T. Jahnke, K. Cole, L.P.H. Schmidt, A. Czasch, D. Akoury, O. Jagutzki, J.B. Williams, T. Osipov, S. Lee, M.H. Prior, A. Belkacem, A.L. Landers, H. Schmidt-Bocking, Th. Weber, N.A. Cherepkov, R. Doerner, “*Auger decay 1σ_g and 1σ_u hole states of the N₂ molecule: Disentangling decay routes from coincidence measurements*”, Phys. Rev. A **81**, 043426 (2010).
 - 7) T. Osipov, M. Stener, A. Belkacem, M. Schoeffler, Th. Weber, L. Schmidt, A. Landers, M.H. Prior, R. Doerner and C.L.Cocke, “*Carbon K-shell photoionization of fixed-in-space C₂H₄*”, Phys. Rev. A **81**, 033429 (2010).
 - 8) T. Osipov, Th. Weber, T.N. Rescigno, S.Y. Lee, A.E. Orel, M. Schoeffler, F.P. Sturm, S. Schoessler, U. Lenz, T. Havermeier, M. Kuhnel, T. Jahnke, J.B. Williams, D. Ray, A. Landers, R. Doerner and A. Belkacem, “*Formation of inner-shell autoionizing CO⁺ states below the CO²⁺ threshold*”, Phys. Rev. A **81**, 011402 (2010).
 - 9) N.A. Cherepkov, S.K. Semenov, M.S. Schoffler, J. Titze, N. Petridis, T. Jahnke, K. Cole, L. Ph. H. Schmidt, A. Czasch, D. Akoury, O. Jagutzki, J.B. Williams, T. Osipov, S. Lee, M.H. Prior, A. Belkacem, A.L. Landers, H. Schmidt-Bocking, R. Dorner, and T. Weber, “*Auger decay of 1σ_g and 1σ_u hole states of the N₂ molecule. II. Young-type interference of Auger electrons and its dependence on internuclear distance*”, Phys. Rev. A **82**, 023420 (2010).
 - 10) W. Cao, S. De, K.P. Singh, S. Chen, M.S. Schoeffler, A.S. Alnaser, I.A. Bocharova, G. Laurent, D. Ray, S. Zherebtsov, M.F. Kling, I. Ben-Itzak, I.V. Litvinyuk, A. Belkacem, T. Osipov, T. N. Rescigno, and C.L. Cocke, “*Dynamic modification of the fragmentation of CO^{q+} excited states generated with high-order harmonics*”, Phys. Rev. A **82**, 043410 (2010)
 - 11) T. Jahnke, H. Sann, T. Havermeier, K. Kreidi, C. Stuck, M. Meckel, M. Schoeffler, N. Neumann, R. Wallauer, S. Voss, A. Czasch, O. Jagutzki, A. Malakzadeh, F. Afaneh, T. Weber, H. Schmidt-Bocking, and R. Doerner, “*Ultrafast energy transfer between water molecules*”, Nature Physics **6**, 139 (2010).
 - 12) H. Adaniya, B. Rudek, T. Osipov, D. J. Haxton, T. Weber, T. N. Rescigno, C. W. McCurdy, and A. Belkacem, “*Reply to Comment on “Imaging the dynamics of dissociative electron attachment to water”*”, Phys. Rev. Lett. **106**, 049302 (2011).
 - 13) H. Sann, T. Jahnke, T. Havermeier, K. Kreidi, C. Stuck, M. Meckel, M. Schöffler, N. Neumann, R. Wallauer, S. Voss, A. Czasch, O. Jagutzki, Th. Weber, H. Schmidt-Böcking, S. Miyabe, D.J. Haxton, A.E. Orel, T. N. Rescigno, and R. Dörner, “*Electron diffraction self imaging of molecular fragmentation in two step double ionization of water*”, Phys. Rev. Lett. **106**, 133001 (2011)
 - 14) D. S. Slaughter, H. Adaniya, T. N. Rescigno, D. J. Haxton, A. E. Orel, C. W. McCurdy and A. Belkacem, “*Dissociative Electron Attachment to Carbon Dioxide via the 8.2eV Feshbach resonance*”, Phys. Rev. Lett. (submitted)
 - 15) D. J. Haxton, H. Adaniya, D. S. Slaughter, B. Rudek, T. Osipov, T. Weber, T. N. Rescigno, C. W. McCurdy and A. Belkacem, “*Observation of the dynamics leading to a conical intersection in dissociative electron attachment to water*”, Phys. Rev. A. (submitted).

Electron-Atom and Electron-Molecule Collision Processes

T. N. Rescigno and C. W. McCurdy

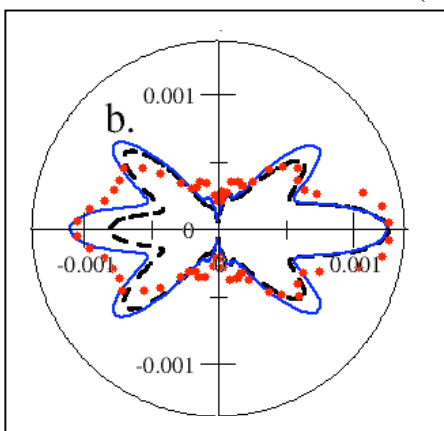
Chemical Sciences, Lawrence Berkeley National Laboratory, Berkeley, CA 94720

tnrescigno@lbl.gov, cwmccurdy@lbl.gov

Program Scope: This project seeks to develop theoretical and computational methods for treating electron processes that are important in electron-driven chemistry and physics and that are currently beyond the grasp of first principles methods, either because of the complexity of the targets or the intrinsic complexity of the processes themselves. A major focus is the development of new methods for solving multiple photoionization and electron-impact ionization of atoms and molecules. New methods are also being developed and applied for treating low-energy electron collisions with polyatomic molecules and clusters. A state-of-the-art approach is used to treat multidimensional nuclear dynamics in polyatomic systems during resonant electron collisions and predict channeling of electronic energy into vibrational excitation and dissociation.

Recent Progress and Future Plans:

The fixed-nuclei, complex Kohn variational method, which continues to serve as our principal tool for studying electron-molecule scattering, has been adapted to the study of molecular photoionization and photodetachment of negative ions and to compute cross sections both in the body- and laboratory frames. The complex Kohn method is particularly well suited to photoionization and photodetachment studies of polyatomic targets since it does not rely on single-center expansions and can handle elaborate correlated wavefunctions in both initial (bound) and final (continuum) states. Previously, we used the complex Kohn method to study C 1s ionization of CO₂ and to clarify the origin of recently observed asymmetry effects in the molecular-frame photoelectron angular distribution (MFPAD)(ref. 4). We have since refined the treatment by developing a semi-classical model to treat the molecular dynamics of the transient core-hole ionized cation prior to Auger decay and obtained quantitative agreement between the calculated and observed MFPADs (ref. 12).



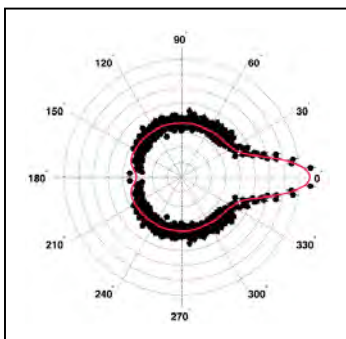
Molecular-frame photoelectron angular distribution for C 1s ionization of CO₂ computed with Auger lifetime set at 0 fs (black dotted curve) and 6 fs (green solid line). Red dots: experimental values of Liu et al. Phys. Rev. Lett. 101, 083001 (2008).

We also carried out (ref. 13) an extensive theoretical study of photodetachment of HOCO⁻. The HOCO⁻ anion has been the focus of several recent experiments since it can be used to obtain information about the HOCO radical, which is an important intermediate in combustion chemistry. Published experiments by Lu and Continetti revealed two sharp peaks in the photodetachment spectrum very close to threshold, which were interpreted to be s- and p-wave resonances. However, this interpretation took no account of the fact that HOCO has a large permanent dipole moment, which would make the presence of such resonances near threshold

unlikely. Indeed, our computed photodetachment amplitudes, which gave photoelectron angular distributions in good agreement with experiment, showed a complete absence of threshold resonances. Electronic structure calculations confirmed that the threshold peaks are most likely due to the decay of vibrationally excited states of a dipole-bound anion. Such dipole-bound anions have been observed in other systems with similarly large dipole moments.

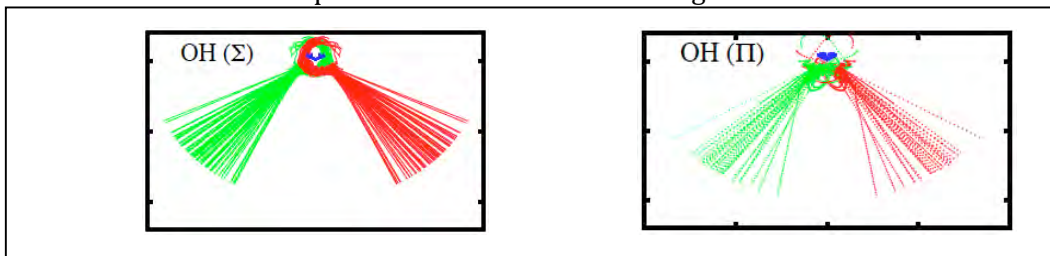
Photoionization of a diatomic molecule can be accompanied by the formation and subsequent decay of autoionizing states. Each electronically *excited* state of a molecular cation can support a series of neutral Rydberg states, many of which must necessarily lie in the electronic continuum and can thus autoionize. These states generally carry little oscillator strength, have narrow widths and have potential energy curves that simply track their parent ion states. Of particular interest are *non-Rydberg* doubly excited states which are expected to have much larger oscillator strengths, since their spatial overlap with the initial state is large. The N_2 and CO cases are particularly interesting since their doubly excited valence states, near the equilibrium target geometry, can decay into four open electronic channels. We have initiated a study of non-Rydberg autoionizing states in N_2 with electronic structure and coupled-channel, fixed-nuclei electron-ion scattering calculations to obtain the energies and lifetimes of these states as a function of nuclear geometry. The primary motivation for undertaking these studies is to see if these states are interesting candidates for XUV pump/probe experiments, which we expect they will be, especially if the calculations show a rapid change in the branching ratios with increasing internuclear distance. This work will also form a basis for further time-dependent studies of these states in the ultrafast program.

Because of the long-range repulsive interaction between singly charged ions, the vertical double ionization thresholds of small molecules generally lie above the dissociation limits corresponding to formation of singly charged fragments. This leads to the possibility of populating singly charged molecular ions by photoionization in the Franck-Condon region at energies below the lowest dication state, but above the dissociation limit into two singly charged fragment ions. These singly charged molecular ions can emit a second electron by autoionization, but only at large internuclear separations where the ionic state crosses into the electron+dication continuum. This process has been termed indirect double photoionization. Previously, we had studied this process in the case of CO and published a joint theoretical/experimental analysis of experiments carried out at the ALS (refs. 7 and 11). A similar study was carried out at BESSY for the case of water. *Ab initio* calculations carried out here showed that the indirect, sequential process in this case involves formation of an inner-shell excited state of H_2O^+ which subsequently dissociates into a proton and an autoionizing state of OH^* . These autoionizing states were found to be extremely long-lived, decaying when the H^+ and OH^* fragments were separated by several hundred angstroms. A simple classical trajectory model involving Rutherford scattering of the emitted slow electron by the distant proton gave a good description of the observed electron angular distribution in the body-frame. The results were published in Physical Review Letters (ref. 15).



Indirect DPI of water. Measured distribution of the angle between the electron and the proton direction for electron energies between 0.2 and 0.6 eV and KER between 2 and 5 eV. Black dots experiment, red line classical simulation for electron energy of 0.2–0.6 eV and internuclear distance $R = 1/4 \text{ 800 a.u.}$ at the instant of autoionization.

Dissociative electron attachment (DEA) is fundamentally important in electron-driven chemistry because it can induce chemical reactions with electrons whose energies lie below the threshold for ionization. In the case of water, COLTRIMS studies at LBNL showed that, in the minor channels, the H⁺ angular distributions deviated significantly from simple axial recoil predictions. We were previously able to successfully explain the observed angular distributions for the 8.5 eV ²A₁ peak by combining body-frame entrance amplitudes from ab initio calculations with classical trajectories on the anion potential surface that detail precisely how the water anion dissociates. We have now extended this treatment to study H⁺ angular distributions from the 12 eV ²B₂ peak where a conical intersection plays a significant role in the dissociation dynamics. This collaborative experimental/theoretical study, which has been submitted for publication (ref. 17), is the first to show how the geometry of the anion at the conical intersection is imprinted on the dissociation fragments. We have also initiated a



H⁺ production by DEA to H₂O via ²B₂. Trajectories leading through (right) the conical intersection recoil with a smaller angle than those which avoid the conical intersection (left).

study of dissociative electron attachment to CO₂. Our first efforts have targeted the main DEA peak at 8.2 eV, which our ab initio studies show involves attachment through a doubly excited (Feshbach) resonance of ²P_g symmetry and dissociated through a conical intersection with a lower energy shape resonance. This result is confirmed by COLTRIMS measurements and our joint study has been submitted to Physical Review Letters (ref. 16).

Exterior complex scaling (ECS) continues to provide the computational framework for our studies of strongly correlated processes that involve several electrons in the continuum. Recent efforts using ECS in time-independent studies have focused on 2-photon double ionization with both atomic and molecular 2-electron targets. In the case of helium, we predicted that sequential ionization should leave a clear signature on the magnitude and shape of the total, single- and triple-differential cross sections, even at energies below the sequential threshold (54.4 eV) where it is a virtual process. The qualitative predictions of our time-independent calculations have now been confirmed, although more elaborate time-dependent studies, which are described in the USXL review document, were needed to obtain quantitatively accurate results. We also undertook our first study of two-photon double ionization of a molecular target, with a study of 2-photon DPI of H₂ by 30 eV photons (ref. 1). As in the case of helium, this work will pave the way for elaborate time-dependent studies.

Publications (2009-2011):

1. J. Fernández, F. L. Yip, T. N. Rescigno, C. W. McCurdy and F. Martín, “Two-center effects in one-photon single ionization of H₂⁺, H₂ and Li₂⁺ with circularly polarized light”, *Phys. Rev. A* **79**, 043409 (2009).
2. Liang Tao, C. W. McCurdy and T. N. Rescigno, “Grid-based methods for diatomic quantum scattering problems: a finite-element, discrete variable representation in prolate spheroidal coordinates”, *Phys. Rev. A* **79**, 012719 (2009).

3. F. Morales, F. Martin, D. A. Horner, T. N. Rescigno and C. W. McCurdy, “Two-photon double ionization of H₂ at 30 eV using Exterior Complex Scaling”, *J. Phys. B* **42**, 134013 (2009).
4. S. Miyabe, C. W. McCurdy, A. E. Orel and T. N. Rescigno, “Theoretical study of asymmetric molecular-frame photoelectron angular distributions for C 1s photoejection from CO₂”, *Phys. Rev. A* **79**, 053401 (2009).
5. H. Adaniya, B. Rudek, T. Osipov, D. J. Haxton, T. Weber, T. N. Rescigno, C. W. McCurdy and A. Belkacem, “Imaging the dynamics of dissociative electron attachment to water”, *Phys. Rev. Lett.* **103**, 233201 (2009).
6. T. N. Rescigno, C. S. Trevisan and A. E. Orel, Comment on “Electron-induced bond-breaking at low energies in HCOOH and Glycine: The role of very short-lived s* anion states”, *Phys. Rev. A* **80**, 046701 (2009).
7. T. Osipov, Th. Weber, T. N. Rescigno, S. Y. Lee, A. E. Orel, M. Schöffler, F. P. Sturm, S. Schössler, U. Lenz, T. Havermeier, M. Kuehnel, T. Jahnke, J. B. Williams, D. Ray, A. Landers, R. Dörner and A. Belkacem, “Formation of inner-shell autoionizing CO⁺ states below the CO⁺⁺ threshold”, *Phys. Rev. A* **81**, 011402(R) (2010).
8. F. L. Yip, C. W. McCurdy and T. N. Rescigno “Hybrid Orbital and Numerical Grid Representation for Electronic Continuum Processes: Double Photoionization of Atomic Beryllium”, *Phys. Rev. A* **81**, 053407 (2010).
9. F. L. Yip, C. W. McCurdy and T. N. Rescigno, “Double Photoionization of excited Lithium and Beryllium”, *Phys. Rev. A* **81**, 063419 (2010).
10. L. Tao, C. W. McCurdy and T. N. Rescigno, “Grid-based methods for diatomic quantum scattering problems. III. Double photoionization of molecular hydrogen in prolate spheroidal coordinates”, *Phys. Rev. A* **82**, 023423 (2010).
11. W. Cao, S. De, K. P. Singh, S. Chen, M. S. Schöffle, A. Alnaser, I. A. Bocharov, G. Laurent, D. Ray, M. F. Kling, S. Zherebtso, I. Ben-Itzhak, I. V. Litvinyuk, T. N. Rescigno, A. Belkacem, T. Osipov and C. L. Cocke, “Dynamic modification of the fragmentation of CO^{q+} excited states generated with high-order harmonics”, *Phys. Rev. A* **82**, 043410 (2010).
12. S. Miyabe, D. J. Haxton, T. N. Rescigno and C. W. McCurdy, “Role of nuclear dynamics in the Asymmetric molecular-frame photoelectron angular distributions for C 1s photoejection from CO₂”, *Phys. Rev. A* **83**, 023404 (2011).
13. S. Miyabe, D. J. Haxton, K. V. Lawler, A. E. Orel, C. W. McCurdy and T. N. Rescigno, “Vibrational Feshbach resonances in near threshold HOCO⁻ photodetachment; a theoretical study”, *Phys. Rev. A* **83**, 043401 (2011).
14. H. Adaniya, B. Rudek, T. Osipov, D. J. Haxton, T. Weber, T. N. Rescigno, C. W. McCurdy, and A. Belkacem, “Reply to Comment on “Imaging the dynamics of dissociative electron attachment to water”, *Phys. Rev. Lett.* **106**, 049302 (2011).
15. H. Sann, T. Jahnke, T. Havermeier, K. Kreidi, C. Stuck, M. Meckel, M. Schöffler, N. Neumann, R. Wallauer, S. Voss, A. Czasch, O. Jagutzki, Th. Weber, H. Schmidt-Böcking, S. Miyabe, D. J. Haxton, A. E. Orel, T. N. Rescigno and R. Dörner, “Electron diffraction self-imaging of molecular fragmentation in two-step double ionization of water”, *Phys. Rev. Lett.* **106**, 133001 (2011).
16. D. S. Slaughter, H. Adaniya, T. N. Rescigno, D. J. Haxton, A. E. Orel, C. W. McCurdy and A. Belkacem, “Dissociative Electron Attachment to Carbon Dioxide via the 8.2eV Feshbach resonance”, *Phys. Rev. Lett.* (submitted).
17. D. J. Haxton, H. Adaniya, D. S. Slaughter, B. Rudek, T. Osipov, T. Weber, T. N. Rescigno, C. W. McCurdy and A. Belkacem, “Observation of the dynamics leading to a conical intersection in dissociative electron attachment to water”, *Phys. Rev. A.* (submitted).

Ultrafast X-ray Science Laboratory

C. William McCurdy (Director), Ali Belkacem, Oliver Gessner, Martin Head-Gordon, Stephen Leone, Daniel Neumark, Robert W. Schoenlein, Thorsten Weber

Chemical Sciences, Lawrence Berkeley National Laboratory, Berkeley, CA 94720

CWMcCurdy@lbl.gov, ABelkacem@lbl.gov, OGessner@lbl.gov, MHead-Gordon@lbl.gov,
SRLeone@lbl.gov, DMNeumark@lbl.gov, RWSchoenlein@lbl.gov, TWeber@lbl.gov

Program Scope: This program exploits short pulses of X-rays to provide basic knowledge of ultrafast dynamics of photo-excited molecules in the gas phase and condensed phase from the natural time scale of electron motion to the time scale of the chemical transformations. There five subtasks in the UXSL effort, outlined below.

Recent Progress and Future Plans:

1. Soft X-ray high harmonic generation and applications in chemical physics

This part of the laboratory is focused on the study of ultrafast chemical dynamics enabled by novel femtosecond VUV and soft x-ray light sources. Laboratory based setups centered around several high-order harmonic generation light sources operate at up to 3 kHz repetition rate. The light sources are complemented by state-of-the-art photoelectron and ion imaging techniques and a newly installed VUV spectrometer for transient absorption measurements.

Transient EUV photoelectron and ion imaging experiments have revealed a detailed picture of the coupling between electronic and nuclear dynamics in superfluid helium nanodroplets. The ejection of Rydberg atoms has been monitored in real-time and with quantum-state sensitivity. Significant differences in electronic alignment and kinetic energy distributions are observed for Rydberg fragments in different quantum states. A

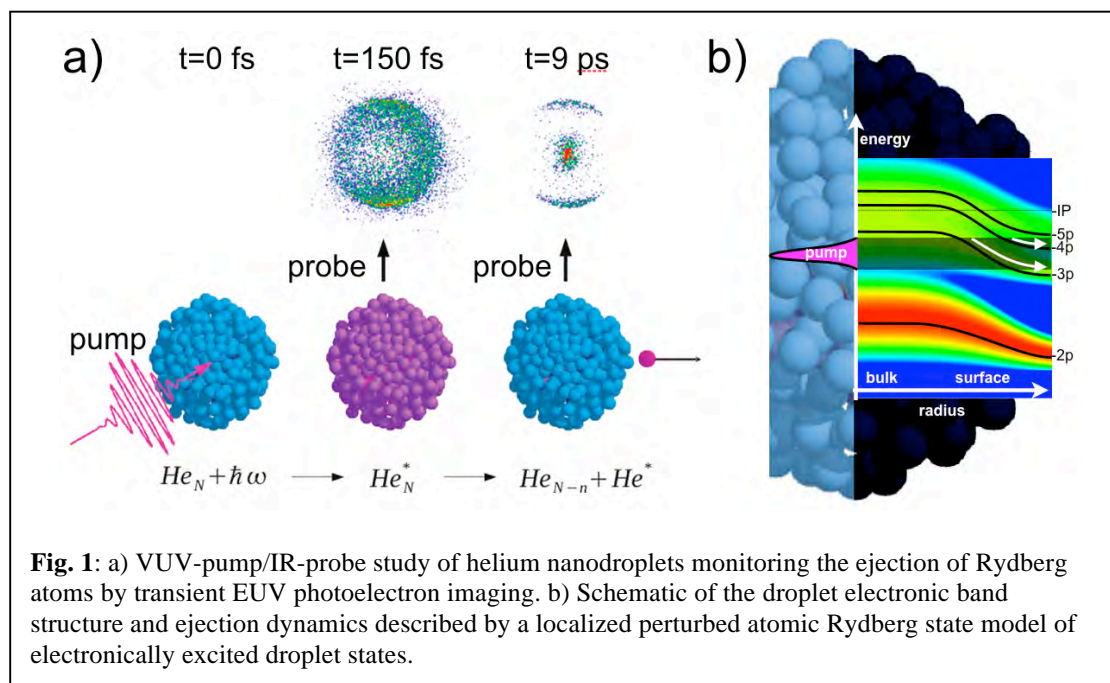


Fig. 1: a) VUV-pump/IR-probe study of helium nanodroplets monitoring the ejection of Rydberg atoms by transient EUV photoelectron imaging. b) Schematic of the droplet electronic band structure and ejection dynamics described by a localized perturbed atomic Rydberg state model of electronically excited droplet states.

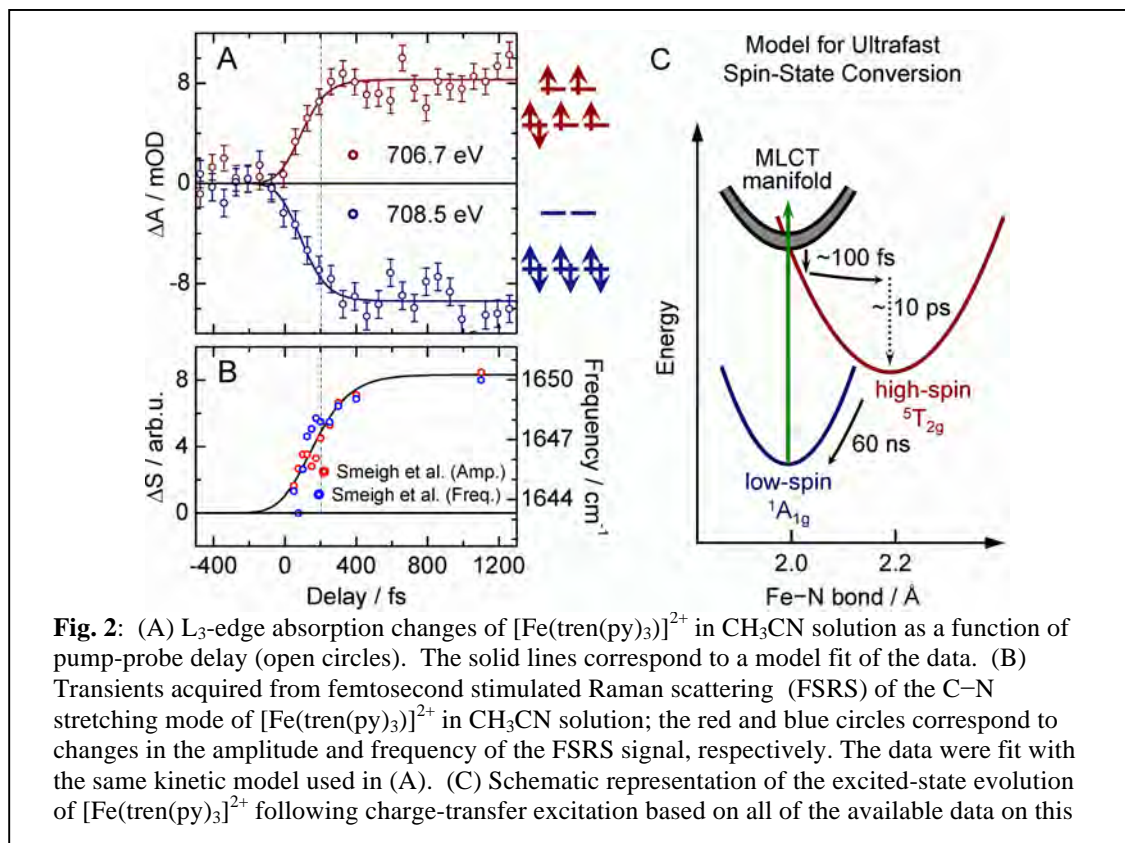
relatively simple theoretical model has been developed that reproduces the findings with encouraging accuracy based on a description of electronically excited droplet states in terms of localized perturbed atomic Rydberg states.

The construction of a VUV transient absorption setup is completed. An experimental time resolution of 25 fs has been demonstrated by monitoring strong-field ionization of Xe atoms with pump-probe delay dependent variations in inner-valence absorption lines using photon energies ranging from ~50 eV to ~70 eV. First transient absorption spectra during strong-field ionization of bromobenzene have been recorded at the bromine M-edge (~70 eV photon energy). The depletion of the neutral species as well as the emergence of the ionized species are clearly discernable.

A UXSL-lead proposal to conduct femtosecond time-resolved x-ray photoionization studies of charge transfer dynamics at interfaces between molecular dyes and nanoporous semiconductor substrates at the Linac Coherent Light Source (LCLS) has received a Tier 1 ranking and is scheduled for beam time in October 2011.

2. Ultrafast X-ray Studies of Condensed Phase Molecular Dynamics

The objective of this research program is to advance our understanding of solution-phase molecular dynamics using ultrafast x-rays as time-resolved probes of the evolving electronic and atomic structure of solvated molecules. Two beamlines have been



developed at the Advanced Light Source, with the capability for generating ~200 fs x-ray pulses from 200 eV to 10 keV. We have also developed a new capability for transmission XAS studies of thin liquid samples in the soft x-ray range, based on a novel Si_3N_4 cell design with controllable thickness <math><1 \mu\text{m}</math>.

Present research is focused on charge-transfer processes in solvated transition-metal complexes, which are of fundamental interest due to the strong interaction between electronic and molecular structure. In particular, Fe^{II} complexes exhibit strong coupling between structural dynamics, charge-transfer, and spin-state interconversions. This year we have focused on understanding the evolution of the valence electronic structure, and the influence of the ligand field dynamics on the Fe 3*d* electrons, using time-resolved XANES measurements at the Fe L-edge. Picosecond and femtosecond studies show a clear 1.7 eV dynamic shift in the Fe-L₃ absorption edge with the ultrafast formation of the high-spin state on a 200 fs time scale. This reflects the evolution of the ligand-field splitting, and is the first time-resolved solution-phase transmission spectra ever recorded in the soft x-ray region. Comparison with charge-transfer multiplet calculations reveals a reduction in ligand field splitting of ~1 eV in the high-spin state. A significant reduction in orbital overlap between the central Fe-3*d* and the ligand N-2*p* orbitals is directly observed, consistent with the expected 0.2 Å increase in Fe-N bond length upon formation of the high-spin state. The overall occupancy of the Fe-3*d* orbitals remains constant upon spin crossover, suggesting that the reduction in σ-donation is compensated by significant attenuation of π-back-bonding in the metal-ligand interactions.

A second area of focus is on the structural dynamics of liquid water following coherent vibrational excitation of the O-H stretch (in collaboration with A. Lindenberg et al. at Stanford). Time-resolved results at the O K-edge show distinct changes in the near-edge spectral region that are indicative of a transient temperature rise of 10K following laser excitation and rapid thermalization of vibrational energy. The rapid heating at constant volume creates an increase in internal pressure, ~8MPa, which is manifest by spectral changes that are distinct from those induced by temperature alone. Femtosecond studies of hydrogen bond dynamics reveal the dynamic conversion of strongly hydrogen-bonded water structures to more disordered structures with weaker hydrogen-bonding on a 700 fs time scale.

An important goal is to apply time-resolved X-ray techniques to understand the structural dynamics of more complicated reactions in a solvent environment. Future research will focus on charge-transfer, and ligand dynamics in bi-transition-metal complexes and porphyrins, as well as reaction dynamics of solvated halide molecules. Solvated metal carbonyls represent a model system where photo-induced ligand dissociation is strongly solvent dependent. In these complexes, the molecular intermediates and solvent exchange mechanisms are poorly understood. Time-resolved XAS will provide important new insight to the molecular dynamics.

3. Time-resolved studies and non-linear interaction of femtosecond x-rays with atoms and molecules:

Higher-order harmonic generation has reached intensities high enough as to induce multiphoton ionization processes. The design and construction of our intense XUV source is based on scaling-up in energy of the loose focusing high harmonic generation scheme. Pump/probe delay is achieved with a newly constructed split mirror interferometer (SMI). VUV and XUV wavelength selection in each arm of the SMI is achieved through a combination of transmission filters and coatings on the two D-shaped mirrors. We applied our two-color VUV/XUV pump-probe system to the study non-

Born-Oppenheimer dynamics in excited-state ethylene. In a first study we used a fifth harmonic pump-probe configuration to the study the excited state lifetime shown in Fig. 3 resolving a decade long discrepancy and controversy between theory and experiment. To follow the dynamics onto the ground state potential energy surface, we conducted experiments using 7.7 eV photons as a pump and in one case the 19th harmonic (29.45 eV) of the fundamental as a probe and in another case a band of EUV harmonics (17-23 eV) as a probe. These XUV probe photons

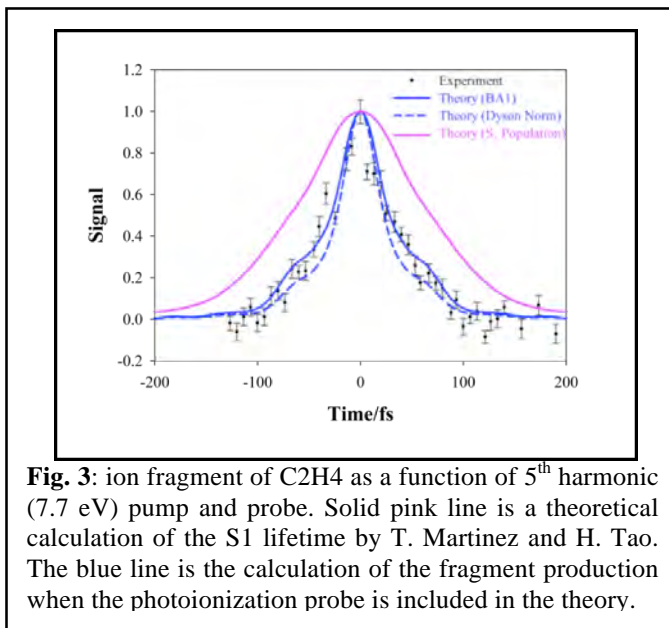


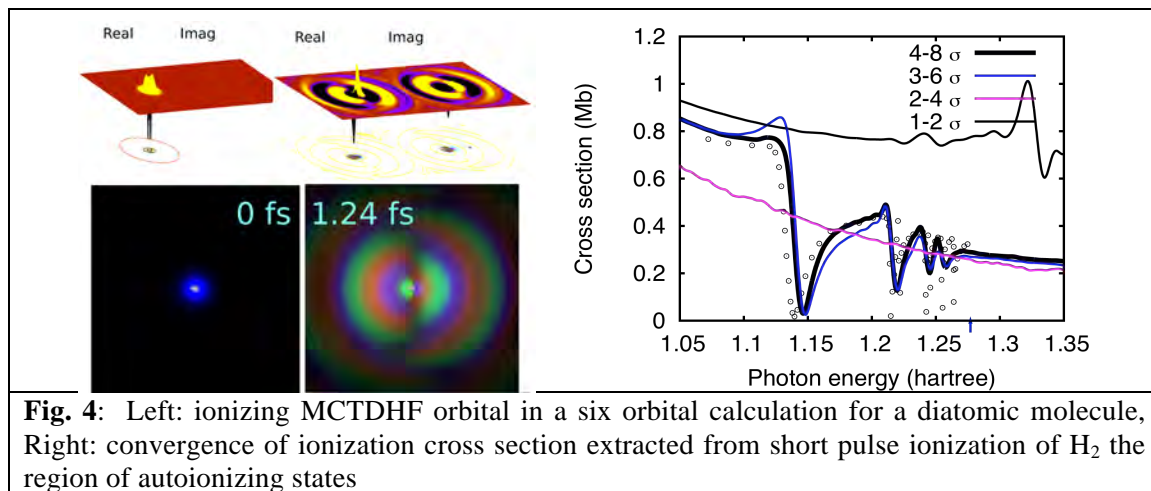
Fig. 3: ion fragment of C₂H₄ as a function of 5th harmonic (7.7 eV) pump and probe. Solid pink line is a theoretical calculation of the S1 lifetime by T. Martinez and H. Tao. The blue line is the calculation of the fragment production when the photoionization probe is included in the theory.

allow us to break the C-C bond and observe transient structures such as ethylidene. In both experiments, the pump and the probe act on the molecule perturbatively through single photon excitation. We observe a transient increase in the CH₃⁺ fragment production using ion time-of flight spectroscopy providing evidence for hydrogen migration in ethylene following $\pi\pi^*$ excitation. In a collaboration work with T. Martinez we show that a combination of theory and experiment clearly identifies the dynamics through two competing conical intersection.

For this coming fiscal year we are planning an upgrade of our HHG system from 10 Hz to higher repetition rate to enable the application of our successful COLTRIMS technique to time-resolved studies. The construction of the new Momentum Imaging Spectroscopy for Time Resolved Studies (MISTERS) apparatus began in the second half of 2008. The main chamber and the two stage super sonic gas jet as well as the differential pumping stage and a tip-tilt xyz split mirror back focusing unit are assembled and combined to one setup. After a debugging phase vacuum and jet tests were successfully performed. A reaction microscope was designed and is currently in fabrication. The components for the position and time sensitive multihit detectors were built and are assembled. Moreover, a dedicated and improved Split Mirror Interferometer as well as a dispersive spectrometer for diagnosing the high harmonics light next to the interaction region spawned by the back focused light and the supersonic gas jet are in the construction and testing phase. The latter components will improve the interface between the high harmonics beamline and the experimental endstation. In an initial phase the setup will be optimized for a startup program on two-color two-photon single ionization of rare gas atoms like He, Ne and Ar.

4. Theory and computation

We have developed computational methods that allow the accurate treatment of multiple ionization of atoms and molecules by short pulses in the VUV and soft X-ray regimes. We have extended our numerical methods based on the finite-element discrete variable representation to the essentially exact time-dependent treatment of two electron atoms in a radiation field, including the rigorous extraction of the amplitudes for ionization from these wave packets and separation of single and double ionization probabilities. These developments have been applied to short pulse single and double ionization of helium and have showed new effects that appear only for subfemtosecond pulses, including an intrinsically two-electron interference phenomenon, in which subfemtosecond UV pulses can be used to probe spin entanglement directly. Recently we have completed an entirely new implementation of the Multiconfiguration Time-dependent Hartree Fock (MCTDHF) method using prolate spheroidal coordinates for the treatment of general diatomics including nuclear motion without the Born-Oppenheimer approximation. Calculations on short pulse ionization and core hole dynamics of atoms and diatomics with this method are under way, the first results of which are illustrated in Fig. 4.



The crucial photochemical events in processes ranging from vision to light-harvesting to light emission involve ultrafast processes that involve multiple excited states. Experiments provide one window on the relevant states while first principles computations offers another, complementary view. For example, our efforts on the excited states of helium clusters provide information that is not directly accessible to experiment, as shown in Fig. 5. Furthermore, while there are established methods to calculate the potential surfaces for small molecules, it is an open challenge to develop appropriate methods for larger molecules and interface them to appropriate tools for finding reaction pathways and performing direct dynamics. We have reported promising developments towards this goal (through spin-flipping methods), and have also identified new areas where interesting challenges confront us (excited states of large clusters, and associated dynamics).

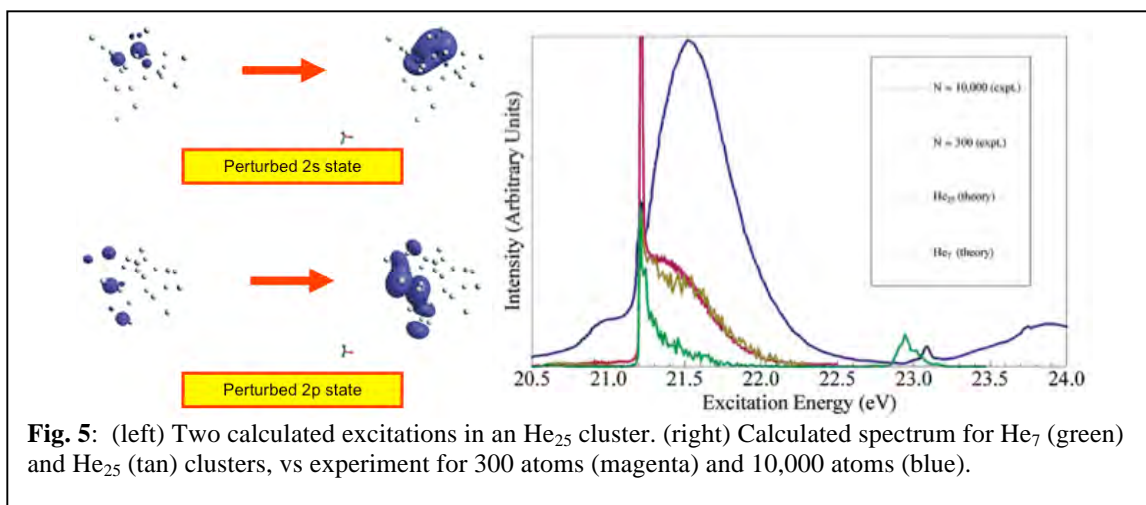


Fig. 5: (left) Two calculated excitations in an He_{25} cluster. (right) Calculated spectrum for He_7 (green) and He_{25} (tan) clusters, vs experiment for 300 atoms (magenta) and 10,000 atoms (blue).

5. Attosecond atomic and molecular science

Attosecond dynamics are explored experimentally, focusing on direct measurements of time scales for processes that are driven by electron-electron interactions like autoionization and Auger decay. Isolated attosecond pulses (IAP), approximately 120 as in duration, are generated over the spectral range of 15 eV to 80 eV via high harmonic generation and Double Optical Gating (DOG)) for use in time resolved photoelectron or mass spectroscopy measurements. Additionally, new experimental techniques including transient dispersion and the methods of detecting superpositions of atomic states via attosecond photoelectron and mass spectroscopy are being explored.

Design and implementation of a compact interferometer external to the vacuum system, with 50 as rms jitter over 24 hours, enables two-color, pump-probe experiments with an extreme ultraviolet IAP and a general optical field, which can be different from the conventional 800 nm field used to generate harmonics. For example, the first experimental streak trace with a 400 nm streak field is shown in Fig 6. Variation of wavelength or polarization of the optical field will allow additional dynamics to be accessed in experiments.

Experiments are underway to investigate the competition between autoionization and predissociation in superexcited states of molecular nitrogen. According to theoretical calculations lifetimes ranging from 10s of fs to <1 fs are expected. Isolated attosecond pulses (spectrally limited to 15-24 eV by a 200 nm thick Sn filter) access superexcited states of N_2 , which decay via autoionization to N_2^+ or predissociate to N and excited N atoms, N^* . An optical (800 nm or 400 nm) few-fs pulse ionizes N^* to N^+ which is then detected in the mass spectrometer. Preliminary pump-probe measurements of predissociation products suggest the lifetime of the superexcited state is approximately 10 fs. Complementary, photoelectron streaking measurements can

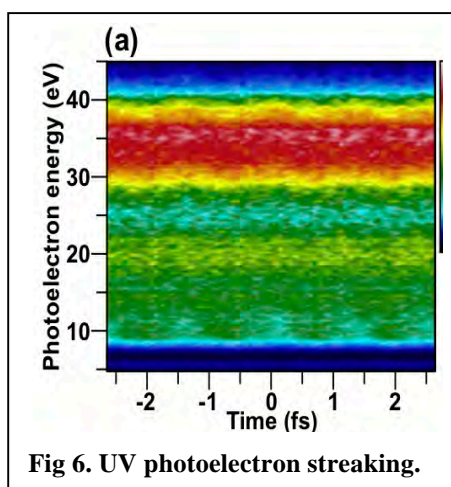


Fig 6. UV photoelectron streaking.

be used to determine the time at which autoionization electrons are born with sub-fs precision. Combination of the experiments will yield a more full characterization of the dynamics. In a collaborative effort, the AMO theory group has estimated the timescale of autoionization as 17 fs.

Construction of a transient dispersion spectrometer is nearly complete. Planned experiments will use spectral interferometry to detect phase shifts between time-delayed twin isolated attosecond pulses as a measure of changes in the index of refraction. For example, shifts in the index of refraction around the $4d \rightarrow 5p$ resonance region of Xe^+ (~ 55 eV) are expected as an electron is removed from Xe by strong field ionization. Transient absorption spectra of Xe and Xe^+ have been acquired with experimental spectral resolution of 0.42 eV. Neutral depletion and formation of Xe^+ cation by the strong 800 nm field are observed at ~ 65 ($4d \rightarrow 6p$) and ~ 55 eV ($4d \rightarrow 5p$), respectively.

Spin-orbit wave packets and alignment created by strong field ionization of atomic krypton will be probed with XUV photoionization to investigate alignment, coherence and phase information about the atomic superposition. Polarization control of optical fields will be critical for these experiments. The timescale of Auger decay of molecular species such as HBr will be measured with photoelectron streaking and compared to the analogous atomic case, krypton.

Publications, by Subtask (2009-2011)

1. Christer Z. Bisgaard, Owen J. Clarkin, Guorong Wu, Anthony M. D. Lee, Oliver Geßner, Carl C. Hayden, Albert Stolow, "Time-Resolved Molecular Frame Dynamics of Fixed-in-Space CS_2 Molecules", *Science* **323**, 1464 (2009).
2. Oleg Kornilov, Chia C. Wang, Oliver Bünermann, Andrew T. Healy, Mathew Leonard, Chunte Peng, Stephen R. Leone, Daniel M. Neumark, and Oliver Gessner, "Ultrafast Dynamics in Helium Nanodroplets Probed by Femtosecond Time-Resolved EUV Photoelectron Imaging", *J. Phys. Chem. A* **114**, 1437 (2010).
3. Oleg Kornilov, Russell Wilcox, and Oliver Gessner, "Nanograting-based compact VUV spectrometer and beam profiler for in-situ characterization of high-order harmonic generation light sources", *Rev. Sci. Instrum.* **81**, 063109 (2010).
4. M. Hoener, L. Fang, O. Kornilov, O. Gessner, S. T. Pratt, M. Gühr, E. P. Kanter, C. Blaga, C. Bostedt, J. D. Bozek, P. H. Bucksbaum, C. Buth, M. Chen, R. Coffee, J. Cryan, L. DiMauro, M. Glowonia, E. Hosler, E. Kuk, S. R. Leone, B. McFarland, M. Messerschmidt, B. Murphy, V. Petrovic, D. Rolles, and N. Berrah, "Ultra-intense X-ray Induced Ionization, Dissociation, and Frustrated Absorption in Molecular Nitrogen", *Phys. Rev. Lett.* **104**, 253002 (2010).
5. James M. Glowonia, J. Cryan, J. Andreasson, A. Belkacem, N. Berrah, C. I. Blaga, C. Bostedt, J. Bozek, L. F. DiMauro, L. Fang, J. Frisch, O. Gessner, M. Gühr, J. Hajdu, M. P. Hertlein, M. Hoener, G. Huang, O. Kornilov, J. P. Marangos, A. M. March, B. K. McFarland, H. Merdji, V. S. Petrovic, C. Raman, D. Ray, D. A. Reis, M. Trigo, J. L. White, W. White, R. Wilcox, L. Young, R. N. Coffee, and P. H. Bucksbaum, "Time-resolved pump-probe experiments at the LCLS", *Opt. Express* **18**, 17620 (2010).
6. L. Fang, M. Hoener, O. Gessner, F. Tarantelli, S. T. Pratt, O. Kornilov, C. Buth, M. Gühr, E. P. Kanter, C. Bostedt, J. D. Bozek, P. H. Bucksbaum, M. Chen, R. Coffee, J. Cryan, M. Glowonia, E. Kuk, S. R. Leone, and N. Berrah, "Double core hole production in N_2 : Beating the Auger clock", *Phys. Rev. Lett.* **105**, 083005 (2010).
7. James P. Cryan, J. M. Glowonia, J. Andreasson, A. Belkacem, N. Berrah, C. I. Blaga, C. Bostedt, J. Bozek, C. Buth, L. F. DiMauro, L. Fang, O. Gessner, M. Guehr, J. Hajdu, M. P. Hertlein, M. Hoener, O. Kornilov, J. P. Marangos, A. M. March, B. K. McFarland, H. Merdji, V. Petrovic, C. Raman, D.

- Ray, D. Reis, F. Tarantelli, M. Trigo, J. White, W. White, L. Young, P. H. Bucksbaum, and R. N. Coffee, "Auger electron angular distribution of double core hole states in the molecular reference frame", *Phys. Rev. Lett.* **105**, 083004 (2010).
8. O. Gessner, O. Kornilov, M. Hoener, L. Fang, and N. Berrah, "Intense Femtosecond X-ray Photoionization Studies of Nitrogen - How Molecules interact with Light from the LCLS" in *Ultrafast Phenomena XVII*, M. Chergui, D. M. Jonas, E. Riedle, R. W. Schoenlein, A. J. Taylor, Eds., Oxford University Press (2011).
 9. Oliver Bünermann, Oleg Kornilov, Stephen R. Leone, Daniel M. Neumark, and Oliver Gessner, "Femtosecond Extreme Ultraviolet Ion Imaging of Ultrafast Dynamics in Electronically Excited Helium Nanodroplets", *IEEE J. Sel. Top. Quantum Electron.* published online (2011), DOI: 10.1109/JSTQE.2011.2109054.
 10. Oleg Kornilov, Oliver Bünermann, Daniel J. Haxton, Stephen R. Leone, Daniel M. Neumark, and Oliver Gessner, "Femtosecond photoelectron imaging of transient electronic states and Rydberg atom emission from electronically excited He droplets", *J. Phys. Chem. A*, published online (2011), DOI: 10.1021/jp2004216.
 11. N. Huse, H. Wen, D. Nordlund, E. Szilagy, D. Daranciang, T.A. Miller, A. Nilsson, R.W. Schoenlein, and A.M. Lindenberg, "Probing the hydrogen-bond network of water via time-resolved soft x ray spectroscopy," *Phys. Chem. Chem. Phys.*, **11**, 3951–3957 (2009) – cover article.
 12. N. Huse, M. Khalil, T.-K. Kim, A.L. Smeigh, L. Jamula, J.K. McCusker, and R.W. Schoenlein, "Probing reaction dynamics of transition-metal complexes in solution via time-resolved x-ray spectroscopy," *J. Phys. Conf.*, **148**, 012043 (2009).
 13. N. Huse, T.-K. Kim, M. Khalil, L. Jamula, J.K. McCusker, and R.W. Schoenlein, "Probing reaction dynamics of transition-metal complexes in solution via time-resolved soft x-ray spectroscopy," in **Ultrafast Phenomena XVI**, Springer Series in Chemical Physics, **92**, P. Corkum, S. De Silvestri, K.A. Nelson, E. Riedle, R.W. Schoenlein, Eds., Springer-Verlag, (2009).
 14. H. Wen, N. Huse, R.W. Schoenlein, and A.M. Lindenberg, "Ultrafast conversions between hydrogen bond structures in liquid water observed by femtosecond x-ray spectroscopy," *J. Chem. Phys.*, **131**, 234505 (2009).
 15. N. Huse, T.-K. Kim, L. Jamula, J.K. McCusker, F.M.F. de Groot, and R.W. Schoenlein, "Photo-Induced Spin-State Conversion in Solvated Transition Metal Complexes Probed via Time-Resolved Soft X-ray Spectroscopy," *J. Am. Chem. Soc.*, **132**, 6809-6816 (2010).
 16. N. Huse, H. Cho, T.K. Kim, L. Jamula, J.K. McCusker, F.M.F. de Groot, and R.W. Schoenlein, "Ultrafast spin-state conversion in solvated transition metal complexes probed with femtosecond soft x-ray spectroscopy," in **Ultrafast Phenomena XVII**, M. Chergui, D.M. Jonas, E.Riedle, R.W. Schoenlein, A.J. Taylor, Eds., Oxford University Press, New York, p. 370-372, (2011)
 17. N. Huse, H. Wen, H. Cho, T.K. Kim, R.W. Schoenlein, and A.M. Lindenberg, "Ultrafast conversions of hydrogen-bonded structures in liquid water observed via femtosecond soft x-ray spectroscopy," in **Ultrafast Phenomena XVII**, M. Chergui, D.M. Jonas, E.Riedle, R.W. Schoenlein, A.J. Taylor, Eds., Oxford University Press, New York, p. 460-462, (2011)
 18. N. Huse, H. Cho, K. Hong, L. Jamula, F.M.F. de Groot, T.K. Kim, J.K. McCusker, and R.W. Schoenlein, "Femtosecond soft x-ray spectroscopy of solvated transition metal complexes: Deciphering the interplay of electronic and structural dynamics," *J. Phys. Chem. Lett.* **2**, 880–884 (2011).
 19. J. van Tilborg, T.K. Allison, T.W. Wright, M.P. Hertlein, R.W. Falcone, Y. Liu, H. Merdji and A. Belkacem, "Femtosecond isomerization dynamics in the ethylene cation measured in an EUV-pump NIR probe configuration", *J. Phys. B: At. Mol. Opt. Phys.* **42** (2009) 081002.
 20. T.K. Allison, J. van Tilborg, T.W. Wright, M.P. Hertlein, R.W. Falcone, and A. Belkacem, "Separation of high order harmonics with fluoride windows", *Optics Express* **17**, (2009) 8941.

21. K. Motomura, H. Fukuzawa, L. Foucar, X-J Liu, G. Prumper, K. Ueda, N. Saito, H. Iwayama, K. Nagaya, H. Murakami, M. Yao, A. Belkacem, M. Nagasono, A. Higashiya, M. Yabashi, T. Ishikawa, H. Ohashi, and H. Kimura, "Multiple ionization of atomic argon irradiated by EUV free-electron laser pulses at 62 nm: evidence of sequential electron strip" *J. Phys. B: At. Mol. Opt. Phys.* **42**, Fast Track Communication, (2009) 221003
22. J. van Tilborg, T. Allison, T.K. Wright, M.P. Hertlein, Y. Liu, H. Merdji, R. Falcone, and A. Belkacem, "EUV-driven femtosecond dynamics in ethylene", *Journal of Physics, Conference Series* **194**, 012015 (2009).
23. T.E. Glover, M.P. Hertlein, S.H. Southworth, T.K. Allison, J. van Tilborg, E.P. Kanter, B. Krassig, H.R. Varma, B. Rude, R. Santra, A. Belkacem and L. Young, "Controlling X-rays with light", *Nature Physics* **6**, 69 (2010)
24. Y.H. Jiang, A. Rudenko, J.F. Perez-Torres, O. Herrwerth, L. Foucar, M. Kurka, K. U. Kuhnel, M. Toppin, E. Plesiat, F. Morales, F. Martin, M. Lezius, M.F. Kling, T. Jahnke, R. Doerner, J.L. Sanz-Vicario, J. van Tilborg, A. Belkacem, M. Schultz, K. Ueda, T.J.M. Zouros, S. Dusterer, R. Treusch, C.D. Schroter, R. Moshhammer, and J. Ullrich, "Investigating two-photon double ionization of D2 by XUV-pump-XUV-probe experiments", *Phys. Rev. A* **81**, 05140(R) (2010).
25. Y.H. Jiang, A. Rudenko, E. Plesiat, L. Foucar, M. Kurka, K. U. Kuhnel, Th. Ergler, J.F. Perz-Torres, F. Martin, O. Herrwerth, M. lezius, M.F. Kling, J. Titze, T. jahnke, R. Doerner, J.L. Sanz-Vicario, M. Schoffler, J. van Tilborg, A. Belkacem, K. Ueda, T.J.M. Zouros, S. Dusterer, R. Treusch, C.D. Schroter, R. Moshhammer, and J. Ullrich, "Tracing direct and sequential two-photon double ionization of D2 in femtosecond extreme-ultraviolet laser pulses", *Phys. Rev. A* **81**, 021401 (R) (2010).
26. A. Palacios, T. N. Rescigno and C. W. McCurdy, "Time-dependent treatment of two-photon resonant single and double ionization of helium by ultrashort laser pulses" , *Phys. Rev. A* **79**, 033402 (2009).
27. Liang Tao, W. Vanroose, B. Reys, T. N. Rescigno, and C. W. McCurdy, "Long-time solution of the time-dependent Schrödinger equation for an atom in an electromagnetic field using complex coordinate contours" *Phys. Rev. A* **80**, 063419 (2009).
28. A. Palacios, T. N. Rescigno and C. W. McCurdy, "Two-electron time-delay interference in atomic double ionization by attosecond pulses," *Phys. Rev. Lett.* **103**, 253001 (2009).
29. M Kurka , J Feist , D A Horner , A Rudenko , Y H Jiang , K U Kühnel , L Foucar , T N Rescigno , C W McCurdy , R Pazourek , S Nagele , M Schulz , O Herrwerth , M Lezius , M F Kling , M Schöffler , A Belkacem , S Dusterer , R Treusch , B I Schneider , L A Collins , J Burgdörfer , C D Schröter , R Moshhammer and J Ullrich, "Differential cross sections for non-sequential double ionization of He by 52 eV photons from the Free Electron Laser in Hamburg, FLASH" *New J. Phys.* **12**, 073035 (2010).
30. D. J. Haxton, K. Lawler and C. W. McCurdy, "Multiconfiguration Time-dependent Hartree-Fock Treatment of Electronic and Nuclear Dynamics in Diatomic Molecules," *Phys. Rev. A* **83**, 063416 (2011).
31. Y.M. Rhee and M. Head-Gordon, "Quartic-scaling analytical gradient of quasidegenerate scaled opposite spin second order perturbation corrections to single excitation configuration interaction", *J. Chem. Theor. Comput.* **5**, 1224 (2009).
32. Y.M. Rhee, D. Casanova, and M. Head-Gordon, "Performance of quasi-degenerate scaled opposite spin perturbation corrections to single excitation configuration interaction for excited state structures and excitation energies with application to the stokes shift of 9-methyl-9,10-dihydro-9-silaphenanthrene", *J. Phys. Chem. A* **113**, 10564 (2009).
33. D. Casanova and M. Head-Gordon, "The spin-flip extended single excitation configuration interaction method", *J. Chem. Phys.* **129**, 064104 (2008).
34. D. Casanova, L.V. Slipchenko, A.I. Krylov, and M. Head-Gordon, "Double spin-flip approach within equation-of-motion coupled cluster and configuration interaction formalisms: Theory, implementation and examples" *J. Chem. Phys.* **130**, 044103 (2009).

35. D. Casanova, and M. Head-Gordon, "Restricted active space spin-flip configuration interaction approach: Theory, implementation and examples", *Phys. Chem. Chem. Phys.* **11**, 9779 (2009).
36. Y. Kurzweil, and M. Head-Gordon, "Improving approximate-optimized effective potentials by imposing exact conditions: Theory and applications to electronic statics and dynamics", *Phys. Rev. A* **80**, 012509 (2009).
37. K.D. Closser and M. Head-Gordon, "Ab initio calculations on the electronically excited states of small helium clusters", *J. Phys. Chem. A* **114**, 8023-8032 (2010).
38. F. Bell, D. Casanova and M. Head-Gordon, "Theoretical study of substituted PBPB dimers: Structural analysis, tetraradical character and excited states", *J. Am. Chem. Soc.* **132**, 11314–11322 (2010)
39. M. J. Abel, T. Pfeifer, A. Jullien, P. M. Nagel, M. J. Bell, D. M. Neumark, and S. R. Leone, "Carrier-envelope phase-dependent quantum interferences in multiphoton ionization," *J. Phys. B: At. Mol. Opt. Phys.* **42**, 075601 (2009).
40. T. Pfeifer, M. J. Abel, P. M. Nagel, W. Boutu, M. J. Bell, Y. Liu, D. M. Neumark, and S. R. Leone, "Measurement and optimization of isolated attosecond pulse contrast," *Opt. Lett.* **34**, 1819 (2009).
41. M. J. Abel, T. Pfeifer, P. M. Nagel, W. Boutu, M. J. Bell, C. P. Steiner, D. M. Neumark, and S. R. Leone, "Isolated attosecond pulses from ionization gating of high harmonic emission," *Chem. Phys.* **366**, 9 (2009).
42. E. Goulielmakis, Z.-H. Loh, A. Wirth, R. Santra, N. Rohringer, V. S. Yakovlev, S. Zherebtsov, T. Pfeifer, A. M. Azzeer, M. F. Kling, S. R. Leone, and F. Krausz, "Real-time observation of valence electron motion," *Nature* **466**, 739 (2010).
43. H. Mashiko, M. J. Bell, A. R. Beck, M. J. Abel, P. M. Nagel, C. P. Steiner, J. Robinson, D. M. Neumark, and S. R. Leone, "Tunable frequency-controlled isolated attosecond pulses characterized by either 750 nm or 400 nm wavelength streak fields," *Opt. Exp.* **18**, 25887 (2010).
44. M. J. Abel, D. M. Neumark, S. R. Leone, and T. Pfeifer, "Classical and Quantum Control of Electrons using the Carrier-Envelope Phase of a Strong Field." *Laser Photonics Rev.* **25**, 1 (2011).

The PULSE Institute at SLAC

M. Bogan, P.H. Bucksbaum (Director), H. Dürr, K. Gaffney, M. Gühr, A. Lindenberg, T. Martinez, D. Reis (Deputy Director), J. Stohr, SLAC National Accelerator Laboratory, phb@slac.stanford.edu

PULSE Vision Statement: The ultrafast laser science initiative underway now at the SLAC National Accelerator Laboratory, has as its centerpiece the Linac Coherent Light Source. LCLS, has been conducting user operations now for nearly two years. It routinely exceeds its original design goals, and reaches new milestones regularly in both tuning capability and instrumentation. Its x-rays are a billion times more brilliant than any other laboratory source. This new class of x-ray sources is revolutionizing many areas of science by making it possible for the first time to see atomic scale structures and simultaneously track atomic motions of the underlying nanoscale processes of energy conversion and transport.

The PULSE mission is to advance the frontiers of ultrafast science at SLAC with particular emphasis on discovery and Grand Challenge energy-related research enabled by LCLS. The PULSE Institute initiates and leads multidisciplinary collaborative research programs in studies of atoms, molecules, and nanometer-scale systems, where motion and energy transfer occurs on picosecond, femtosecond, and attosecond time scales. Ultrafast energy research at PULSE combines the disciplines of atomic and molecular physics, ultrafast chemistry and biochemistry, ultrafast condensed matter and materials science, ultrafast x-ray science, nanoscale x-ray imaging science, and the enabling science for next-generation ultrafast light and electron sources. Our metrics of success are the level of the ultrafast science challenges we address, and our progress toward and impact on their solution.

SLAC Photon Science Directorate Placement of PULSE: The PULSE has the status as a Stanford University Independent Laboratory, organized under the office of the Stanford Associate Provost and Dean of Research. The DOE component of PULSE research is organized by SLAC through two research divisions. Approximately 35% of the PULSE DOE research portfolio is managed by the SLAC Materials Science Division, while the remaining 65% is managed by a SLAC Chemical Science Division. This annual summary concerns the Chemical Science component, which operates under a Field Work Contract from the AMOS program.

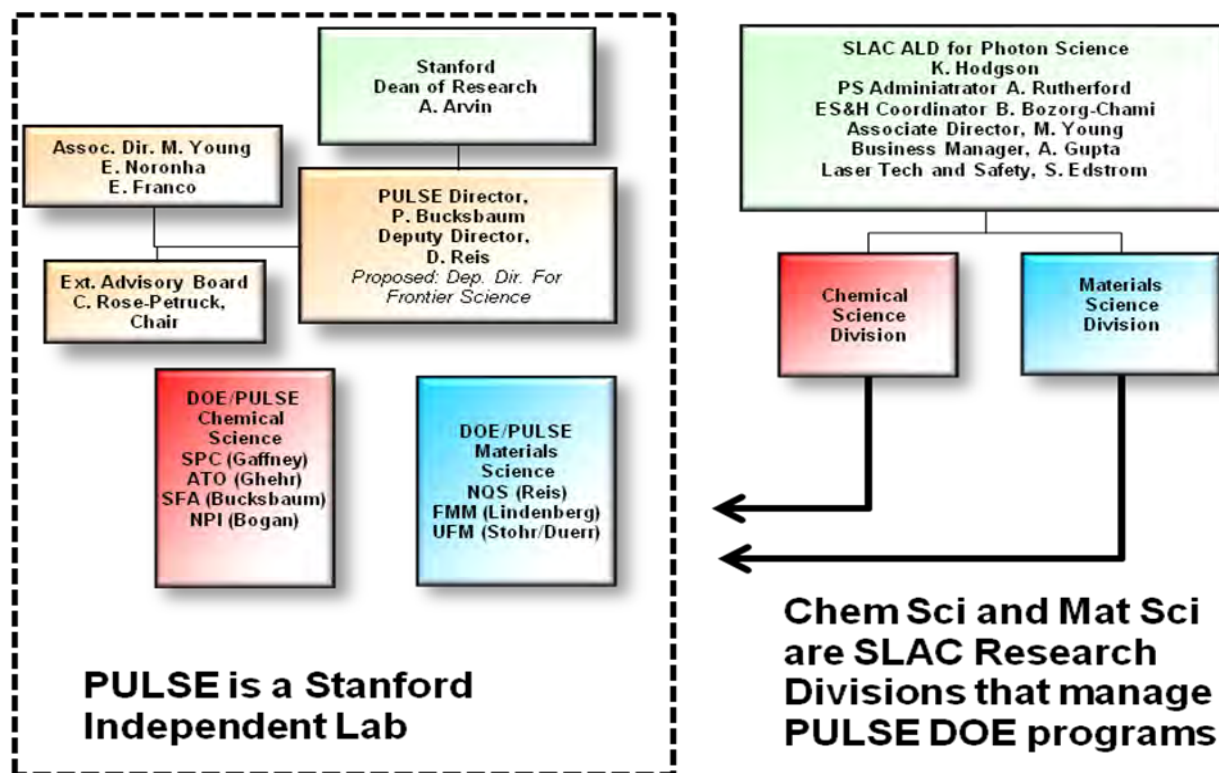
The PULSE Institute Laboratory Building at SLAC: PULSE occupies a recently renovated 18,000 sf laboratory and office building, formerly known as the SLAC Central Lab. This is SLAC's first venue for laboratory-scale research, and is a basis for future program expansion at SLAC in the performing research areas. The renovated space enables us to develop close collaborations in important ultrafast areas such as time-resolved photoemission, time-resolved x-ray scattering, support for ultrafast biological imaging, and multidimensional spectroscopy.

PULSE also has strong research connections to SSRL and to LCLS in laser science and accelerator science. PULSE research utilizes the capabilities of LCLS, but also goes beyond this. For example, PULSE has a vigorous program on high harmonics generation and associated measurement techniques for atoms and molecules on the sub-femtosecond timescale. PULSE research extends to the research floor of the SPEAR3 synchrotron at SLAC, where ultrafast lasers can create transient conditions that are probed by synchrotron radiation. Finally, PULSE develops frontier research that makes use of technologies such as ultrafast imaging of biological and nanoscale materials, and ultrafast x-ray studies of matter in extreme environments. Our aim is to establish the leadership of SLAC research in these areas to solve fundamental challenges in basic energy science.

Education and Outreach: The major educational, physical research, engineering research, and medical research activities at Stanford provide strong support for all of our activities in PULSE. In addition, PULSE continues to run a successful international ultrafast X-ray Summer School. **The Ultrafast X-ray Summer School** is a five day residential program organized annually by PULSE, and starting this year, co-organized by CFEL at DESY in Hamburg, Germany. The goal is to disseminate information and train students and post-docs on new opportunities in ultrafast science, particularly using X-ray Free Electron Lasers. Lectures are presented by expert scientists in this exciting new field. The attendees are expected to participate in the

discussions and quizzes. This year's Ultrafast X-ray Summer School was co-directed by Robin Santra from CFEL and Hermann Durr from PULSE. Next year the summer school will return to SLAC.

PULSE maintains a **visitors program** to enable researchers from around the world to work in our center. These visitors are extremely valuable to the PULSE primary research program. Visitors are given an office, access to PULSE laboratories and institute services, and some expense reimbursement, according to SLAC rules. PULSE extends to them the Stanford designation of Visiting Scientist or Visiting Professor (in line with their rank at their home institution), which entitles them to access to the Stanford Housing Office and the use of the Stanford Library. The budget for this program is relatively modest, particularly when one considers that a senior investigator with major talents and established abilities can be associated as a sabbatical visitor for a year, for less than the cost of a Postdoc. In 2010-2011 a sabbatical visitor was Yaron Silberberg from Weizmann Institute. We also had a number of extended visits.



Organization Chart for the PULSE Institute

Tasks supported by the Chemical Sciences FWP: These tasks are aimed at the control and imaging of chemical dynamics, from electrons in small molecules to atoms in clusters. The emphasis is on grand challenges for energy science. The proposed research utilizes our core strengths in molecular theory (Martinez), ultrafast spectroscopy (Gaffney), quantum control (Bucksbaum), ultrafast x-ray-matter interactions (Reis) and strong field AMO physics (Gühr and Bucksbaum). The imaging expertise in PULSE includes biological imaging (Bogan) with laser manipulation of targets for imaging (Bucksbaum) and our special abilities to capture and image ultrafast processes as they happen. Tasks in this area utilize the PULSE Institute building as well as SPEAR3 and the LCLS AMO, SXR, CXI, and XPP end stations. Subtasks:

- **Attosecond Coherent Electron Dynamics (ATO)** Task Leaders Markus Gühr, Todd Martinez, and P. Bucksbaum. This task studies the fastest timescales in chemical physics involved with electron correlation, and nonradiative chemical processes, connecting LCLS research to the new field of attophysics.

- **Strong Fields in Molecules (SFA)** Task Leader Phil Bucksbaum and David Reis. This task incorporates and extends strong-field quantum control to LCLS experiments in molecular dynamics and molecular imaging. Strong field effects in atoms and molecules can be studied using ultrafast x rays, or employed to create targets for x -ray imaging. In addition, LCLS is itself the world's first source of coherent volt/Ångstrom fields of x-ray radiation. A separate component of this program in ultrafast x-ray scattering is in the Nonequilibrium Dynamics in Solids task.
- **Solution-Phase Chemical Dynamics (SPC)** Task Leader Kelly Gaffney. This task explores ultrafast chemical processes in solutions, utilizing LCLS, synchrotrons, and the PULSE labs. Emphasis is on the ultrafast dynamics of energy conversion in chemistry.
- **Nonperiodic Imaging (NPI)** Task Leader Michael Bogan. This task studies nonperiodic nanoscale imaging, one of the greatest new opportunities for LCLS. The frontier science questions under study range from nanobiology to aerosol chemistry to combustion.

Find out more: <http://pulse.slac.stanford.edu>



Students relax on a boat cruise down the Elbe during the outing at the Ultrafast X-ray Summer School, 2011

Strong Field Control of Coherence in Molecules and Solids

Philip H. Bucksbaum and David Reis, Stanford PULSE Institute for Ultrafast Energy Science, SLAC National Accelerator Laboratory, Menlo Park, CA 94025, phb@slac.stanford.edu

(Staff and students: A. Natan, S. Ghimire, J. Cryan, J.M. Glowonia, D. Broege, G. Ndabashimiye) This is subtask concerns strong field control of molecules and solids (SFA). Our efforts are directed towards investigations of strong-field induced coherent processes in atoms and molecules that are of value as either LCLS experiments or ultrafast x-ray diagnostics, as well as ultrafast hard x-ray studies of coherently excited phonons in solids.

Recent Progress: Progress this year continued to surround our LCLS experiments, as well as laboratory work that supports current and future work with ultrafast x-rays.

X-ray Timing. Our timing tool based on laser dissociation of nitrogen dications has now been employed successfully in several LCLS user experiments. Meanwhile, there are three significant advances in our x-ray-laser ultrafast timing work: First, we are working with LCLS on a simple timing tool related to our very early work on transient x-ray scattering and absorption:

Pump-probe timing tool using transient absorption in silicon nitride: (Mina Bionta, James Cryan, Mike Glowonia, Ryan Coffee) We have developed a new technique for measuring the relative delay between a soft x-ray FEL pulse and an optical laser. We use a femtosecond Ti:Sapphire amplified laser system to produce a smooth continuum spanning 600nm-700nm, chirped to cover 3ps of delay. This optical pulse and the x-ray beam interact in a semiconductor material (Si₃N₄) such that the timing of the x-ray beam can be determined from a modulation of the spectrum of the optical pulse. This method yields sub 20fs RMS resolution of timing and allows for in-situ measurements of the relative time of arrival of the x-rays and optical laser pulses. Initial experiments are under analysis, and a research paper will be written on this.

A very powerful potential tool for timing is post-run analysis of transient phenomena such as molecular excitation or dissociation. Sophisticated statistical correlations can reveal timing:

New analysis tools for extracting transient state information at LCLS: (Russell Fung, Mike Glowonia, James Cryan, Adi Natan, Phil Bucksbaum, Abbas Urmaz) We have been working with Russell Fung from the Urmaz group at Wisconsin-Milwaukee on data sorting of our LCLS nitrogen x-ray absorption and dissociation experiment. The goal is to sort different decay channels, remove jitter, and reveal transient processes. The work appears to be able to successfully reveal heretofore hidden transient processes related to laser-induced alignment, dication formation, and transient state dissociation. This will be described in more detail in the Urmaz contribution to the AMOS progress report. The work is still under analysis.

At the same time, we are developing new timing tools for the future based on quantum control of rotational wave packets. Our hope is that these advanced experiments will eventually supplant other timing methods, because they are non-destructive of the x-ray beam, and also can work even for femtosecond or sub-femtosecond applications. Here is a first step on this path:

A molecular stopwatch, (James Cryan, James M. Glowonia, Douglas W. Broege, Yue Ma, and Philip H. Bucksbaum) We have developed a method to create non-dispersing rotational quantum states in an ensemble of linear molecules with a well defined rotational speed in the laboratory frame. Using a sequence of transform limited laser pulses, we show that these states can be established through a process of rapid adiabatic passage. Coupling between the rotational and pendular motion of the molecules in the laser field can be used to control the detailed angular shape of the rotating ensemble. We have published a paper to describe applications of these rotational states in molecular dissociation and ultrafast metrology. This work has been accepted by Physical Review X for one of its first issues.

Strong-field x-ray spectroscopy: We are continuing to analyze data from our first LCLS run, which yielded two publications last year plus a major contribution to a third. Still in preparation is this contribution to Auger spectra of previously inaccessible transient states:

Auger Electron Angle-resolved Spectrum in the Molecular Frame (James Cryan, James M. Glowonia, Phil Bucksbaum, Ryan Coffee) We have developed a novel approach to angle-resolved Auger electron spectroscopy (ARAES) that is equally effective for bound final states as it is for dissociative final states. In molecules with low-Z atomic constituents, photo-ionization of a K-shell electrons is predominantly followed by KLL-Auger electron emission. The result of this process is a molecular dication with two vacancies in the valence shell. In many cases, the dication rapidly dissociates into fragment ions via the steep ionic potential energy surface. Auger electron emission generally proceeds anisotropically in the frame of the molecule. This anisotropy is a result of: (i) the angular shape of the wavefunctions involved in the decay process, (ii) two-center interference effects, and (iii) scattering of the Auger outgoing electron by the molecular potential. For these high energy Auger electrons, the latter two effects are less important. Until now, ARAES have only been measured for rapidly dissociative final electronic states, because the dissociation of such molecules shows the orientation of the molecular frame. Our approach is to use strong laser fields to align the molecules in the lab frame, so that laboratory Auger spectra display the same angular dependence as the molecular frame. This work will be submitted for publication within the next few weeks.

Strong field processes in solids: (S. Ghimire, G. Ndabashimiye and D. A. Reis) We are interested in the fundamental response of solids to high fields from THz to x-ray, including the effect that periodicity has on high-harmonic generation, photon-assisted tunneling and wave-mixing.

Nonperturbative HHG in Solids: In last year's abstract we described preliminary results on the first observation of nonperturbative high order harmonic generation in solids (single crystal ZnO) in collaboration with the Lou DiMauro group at OSU. We were interested in how the HHG process in crystalline solid would differ from the atomic case, given the large density and periodicity of the lattice. We have since demonstrated that the process differs fundamentally from the case of atomic HHG. Most notably, we found that the cutoff scales linearly with applied electric field, in contrast to the quadratic scaling for atoms. Up to the 25th harmonic was observed for a field approaching 0.6 V/Å. We are able to describe the salient features of the harmonics in terms of a two step model comprising tunnel ionization followed by nonlinear acceleration of the electrons in the conduction band. Because the process repeats twice a laser cycle, odd harmonics are emitted. In this model, the cutoff occurs at multiples of the Bloch Frequency ($\omega_B = 2\pi eEd/h$, where d is the lattice spacing) depending on the detailed shape of the conduction band (see Figure 1). In this picture, electron trajectories are nonsinusoidal and become localized by the periodic Bragg scattering off the Brillouin zone boundaries. Thus, the emission is distributed over the laser cycle, even if ionization occurs only at the peak. Unlike the standard three-step model of the atomic case, the electrons can never get far from the atomic cores. Here the periodicity is key because it supplies a built in coherence between the sites.

Strong-field induced below band-gap absorption: We have also studied the optical response of crystalline ZnO to strong electromagnetic radiation in the limit when the electric field amplitude approaches the ratio of the band-gap to the lattice spacing. In this limit the ponderomotive energy well exceeds the photon energy and is comparable to (and in fact confined by) the electronic bandwidth. The strong field response in solids in this regime remains relatively unexplored. As described above (and in ref [1]) one response of periodic solids to strong field mid-infrared (MIR) excitation is the production of high-order harmonics that could not be understood within a perturbative framework. Because the interaction term in the Hamiltonian can compete with the periodic potential, we expect that the basic characteristics of the solid, including the electronic structure itself, in the presence of the field could be altered dramatically. In particular, we have found that the optical absorption is strongly affected by the presence of the MIR laser. Figure 2a. shows that there is a substantial shift in the absorption edge to lower energies with increasing intensity. Up to about 1TW/cm², the redshift scales with the cube-root in the intensity. The effect exists only during overlap of the MIR and the optical probe. The cube-root scaling is what would be expected for photon assisted tunneling in a DC

field (Franz-Keldysh effect) in the effective mass approximation, suggesting that the absorption occurs on a sub-cycle time-scale (and thus that it cannot be explained through a multiphoton absorption process). Above $1\text{TW}/\text{cm}^2$ the effect saturates at well with a reduction of more than 10% of the band gap. Interestingly, the saturation occurs at the same intensity at which we see a knee in the scaling of the MIR harmonics (see Figure 2b), and where the Bloch frequency of electrons at the peak of the field is approximately twice the drive frequency. At this intensity electrons are accelerated throughout the entire Brillouin zone and one expects to see substantial changes in both the photo-assisted and direct tunneling rates due to dispersion and periodicity of the band effective mass.

X-ray-Optical mixing: In a collaboration led by Ernie Glover at LBNL, we have studied x-ray optical mixing in single crystal diamond using the hard x-rays at LCLS. We have observed optical sidebands on the x-ray diffraction, shifted in both energy and momentum from the elastic diffraction peak. The data are currently under analysis.

Future work: We are continuing efforts to understand the strong field effects in solids using thinner ZnO crystals as well as looking at the response of other solids including Argon films. In conjunction with Materials Science funding we are also looking at the high-field THz response of solids using coherent transition radiation from the LCLS electron beam, in collaboration with Aaron Lindenberg and others. Initial results are promising (Darancing 2011). In addition, we have received beamtime at LCLS to look at nonlinear Compton and Thomson scattering in the x-ray regime.

Papers, last three years

1. Broege, D., R.N. Coffee, and P.H. Bucksbaum, 2008a, "Strong-field impulsive alignment in the presence of high temperatures and large centrifugal distortion," *Phys. Rev. A*, 78, 035401.
2. Broege, D. W., Coffee, R., Bucksbaum, P.H. (2009). "Impulsive longitudinal molecular alignment." *Bull. Am. Phys. Soc.* 54:7: B6.04.
3. Broege, D. W., R. N. Coffee, et al. (2008). "Strong-field impulsive alignment in the presence of high temperatures and large centrifugal distortion." *Physical Review A (Atomic, Molecular, and Optical Physics)* 78(3): 035401-3. <http://link.aps.org/abstract/PRA/v78/e035401>
4. Bucksbaum, P. H. (2009). *AMO Research at the LCLS X-Ray Laser*. Conference on Lasers and Electro-Optics/International Quantum Electronics Conference, Optical Society of America.
5. Coffee, R. N., Cryan, J., Bucksbaum, P.H. (2009). "Rotational decoherence in a dense gas of multiply kicked N_2 ." *Bull. Am. Phys. Soc.* 54:7: B6.2.
6. Coffee, R. N., J. P. Cryan, et al. (2009). "Impulsive Alignment of N_2 with a Train of 8 Pulses." *Conference on Lasers and Electro-Optics/International Quantum Electronics Conference*: IWB1. <http://www.opticsinfobase.org/abstract.cfm?URI=IQEC-2009-IWB1>
7. Cryan, J. P., Coffee, R., Bucksbaum, P.H. (2009). "High Degrees of Impulsive Alignment in Repetitively Excited N_2 at STP." *Bull. Am. Phys. Soc.* 54:7: Q5.09.
8. J. P. Cryan, J. M. Glowina, J. Andreasson, A. Belkacem, N. Berrah, C. I. Blaga, C. Bostedt, J. Bozek, C. Buth, L. F. DiMauro, L. Fang, O. Gessner, M. Guehr, J. Hajdu, M. P. Hertlein, M. Hoener, O. Kornilov, J. P. Marangos, A. M. March, B. K. McFarland, H. Merdji, V. S. Petrović, C. Raman, D. Ray, D. Reis, F. Tarantelli, M. Trigo, J. L. White, W. White, L. Young, P. H. Bucksbaum, and R. N. Coffee. Auger electron angular distribution of double core-hole states in the molecular reference frame. *Phys. Rev. Lett.*, 105(8):083004, Aug 2010.
9. Cryan, J. P., P. H. Bucksbaum, et al. (2009). "Field-free alignment in repetitively kicked nitrogen gas." *Physical Review A (Atomic, Molecular, and Optical Physics)* 80(6): 063412-5. <http://link.aps.org/abstract/PRA/v80/e063412>
10. D. Daranciang, J. Goodfellow, S. Ghimire, H. Loos, D. Reis, A. S. Fisher, and A. M. Lindenberg. Generation of >100 uJ Broadband THz Transients with >10 MV/cm Fields via Coherent Transition Radiation at the Linac Coherent Light Source. In *CLEO:2011 - Laser Applications to Photonic Applications*, page CMW7. Optical Society of America, 2011.
11. Ding, Y., Z. Huang, et al. (2009). "Generation of attosecond x-ray pulses with a multicycle two-color enhanced self-amplified spontaneous emission scheme." *Physical Review Special Topics - Accelerators and Beams* 12(6): 060703. <http://link.aps.org/abstract/PRSTAB/v12/e060703>

12. A. D. DiChiara, S. Ghimire, C. I. Blaga, E. Sistrunk, E. P. Power, A. M. March, T. A. Miller, D. A. Reis, P. Agostini, and L. F. DiMauro. Scaling of high-order harmonic generation in the long wavelength limit of a strong laser field. *IEEE Journal of Selected Topics in Quantum Electronics*, to be published, 2011.
13. Doumy G., C. Roedig, S.-K. Son, C. I. Blaga, A. D. DiChiara, R. Santra, N. Berrah, C. Bostedt, J. D. Bozek, P. H. Bucksbaum, J. P. Cryan, L. Fang, S. Ghimire, J. M. Glowina, M. Hoener, E. P. Kanter, B. Kraessig, M. Kuebel, M. Messerschmidt, G. G. Paulus, D. A. Reis, N. Rohringer, L. Young, P. Agostini & L. F. DiMauro, (2011) "Nonlinear Atomic Response to Intense Ultrashort X Rays," *Phys. Rev. Letters* 106, 10.1103/PhysRevLett.106.083002.
14. EmmaP, AkreR, et al. (2010). "First lasing and operation of an angstrom-wavelength free-electron laser." *Nat Photon* advance online publication. <http://dx.doi.org/10.1038/nphoton.2010.176>
15. Gabrysch, M., E. Marklund, et al. (2008). "Formation of secondary electron cascades in single-crystalline plasma-deposited diamond upon exposure to femtosecond x-ray pulses." *Journal of Applied Physics* 103(6): 064909. <http://link.aip.org/link/?JAP/103/064909/1>
16. S. Ghimire, A. D. DiChiara, E. Sistrunk, P. Agostini, L. F. DiMauro, and D. A. Reis. Observation of high-order harmonic generation in a bulk crystal. *Nature Physics*, 7(2):138–141, 2011
17. S. Ghimire, A. D. DiChiara, E. Sistrunk, U. Szafruga, P. Agostini, L. F. DiMauro, and D. A. Reis. Strong-field electroabsorption near the limit of crystal bonding. under consideration, *Phys. Rev. Lett.*, 2011.
18. S. Ghimire, D. A. Reis, A. DiChiara, E. Sistrunk, L. F. DiMauro, and P. Agostini. Strong-field induced optical absorption in zno crystal. In *Quantum Electronics and Laser Science Conference*, page QMF6. Optical Society of America, 2011.
19. S. Ghimire, A. D. DiChiara, E. Sistrunk, L. F. DiMauro, P. Agostini, and D. A. Reis. High-harmonic generation in strongly driven bulk periodic solid. In *Lasers and Electro-Optics (CLEO) and Quantum Electronics and Laser Science Conference (QELS)*, 2010 Conference on, pages 1–2, May 2010.
20. J. M. Glowina, J. Cryan, J. Andreasson, A. Belkacem, N. Berrah, C. I. Blaga, C. Bostedt, J. Bozek, L. F. DiMauro, L. Fang, J. Frisch, O. Gessner, M. Gühr, J. Hajdu, M. P. Hertlein, M. Hoener, G. Huang, O. Kornilov, J. P. Marangos, A. M. March, B. K. McFarland, H. Merdji, V. S. Petrovic, C. Raman, D. Ray, D. A. Reis, M. Trigo, J. L. White, W. White, R. Wilcox, L. Young, R. N. Coffee, and P. H. Bucksbaum. Time-resolved pump-probe experiments at the lcls. *Opt. Express*, 18(17):17620–17630, 2010.
21. Alexei Grigoriev; Paul G. Evans; Mariano Trigo; David Reis; Linda Young; Robert W. Dunford; Elliot P. Kanter; Bertold Krässig; Robin Santra; Stephen H. Southworth; Lin X. Chen; David M. Tiede; Klaus Attenkofer; Guy Jennings; Xiaoyi Zhang; Timothy Graber; Keith Moffat , *Picosecond Structural Dynamics at the Advanced Photon Source Synchrotron Radiation News*, 1931-7344, Volume 23, Issue 2, 2010, Pages 18 – 25
22. Hoener, M., L. Fang, et al. (2010). "Ultraintense X-Ray Induced Ionization, Dissociation, and Frustrated Absorption in Molecular Nitrogen." *Phys. Rev. Lett.* 104(25): 253002. 10.1103/PhysRevLett.104.253002
23. E. P. Kanter, B. Krässig, Y. Li, A. M. March, P. Ho, N. Rohringer, R. Santra, S. H. Southworth, L. F. DiMauro, G. Doumy, C. A. Roedig, N. Berrah, L. Fang, M. Hoener, P. H. Bucksbaum, S. Ghimire, D. A. Reis, J. D. Bozek, C. Bostedt, M. Messerschmidt, and L. Young. Unveiling and driving hidden resonances with high-fluence, high-intensity x-ray pulses. submitted to *Phys. Rev. Lett.*, 2011.
24. J. Li, J. Chen, D. A. Reis, S. Fahy, and R. Merlin. Measuring the lifetime of ultrashort electronic coherences with long light pulses: The fragile eg state in sb and bi. In *Quantum Electronics and Laser Science Conference*, page QTuN7. Optical Society of America, 2011.
25. Lindenberg, A. M., S. Engemann, et al. (2008). "X-Ray Diffuse Scattering Measurements of Nucleation Dynamics at Femtosecond Resolution." *Physical Review Letters* 100(13): 135502. <http://link.aps.org/abstract/PRL/v100/e135502>
26. D. A. Reis. Squeezing more out of ultrafast x-ray measurements. *Physics*, 2:33, Apr 2009.
27. M. Trigo, J. Chen, V. H. Vishwanath, Y. M. Sheu, T. Graber, R. Henning, and D. A. Reis. Imaging nonequilibrium atomic vibrations with x-ray diffuse scattering. *Phys. Rev. B*, 82(23):235205, Dec 2010.
28. M. Trigo and D. Reis. Time-resolved x-ray scattering from coherent excitations in solids. *MRS Bulletin*, 35:514–519, 2010.
29. Young, L., E. P. Kanter, et al. (2010). "Femtosecond electronic response of atoms to ultra-intense X-rays." *Nature* 466(7302): 56-61. <http://dx.doi.org/10.1038/nature09177>

High harmonic generation and electronic structure

Markus Gühr, Todd Martinez and Philip H. Bucksbaum

Stanford PULSE Institute, SLAC National Accelerator Laboratory, Menlo Park, CA 94025

Scope: The goal of this task is to investigate non-adiabatic molecular processes and electronic dynamics using high harmonic spectroscopy (HHS) as a probe. We have for the first time in our lab observed attosecond transients of molecules using high harmonic spectra. The results of this research will have a big impact on attosecond physics and multi-orbital high harmonic generation. Furthermore, we have studied the sensitivity of the high harmonic spectroscopy technique macroscopic parameters in harmonic generation and performed first pump-probe experiments with XUV pulses from harmonic sources. Apart from our table top based activities we also have invested a considerable effort into LCLS experiments, as collaborators in PULSE and WMU lead initiatives. We have learned about the opportunities of LCLS and this together with our fruitful collaborations has resulted into an accepted beamtime proposal in September 2011.

Recent Progress P. H. Bucksbaum, J. P. Farrell, M. Guehr, T. Martinez, Brian McFarland, L. Spector *Attosecond dynamics in water (in collaboration with S. Petretti, J. Foerster, Y. V. Vanne and A. Saenz, HU Berlin and P. Declava, Universita Trieste):* We observe a nuclear and electronic motion of the water molecule on the attosecond time scale. This is possible by comparing high harmonic spectra of water (H_2O) and heavy water (D_2O).

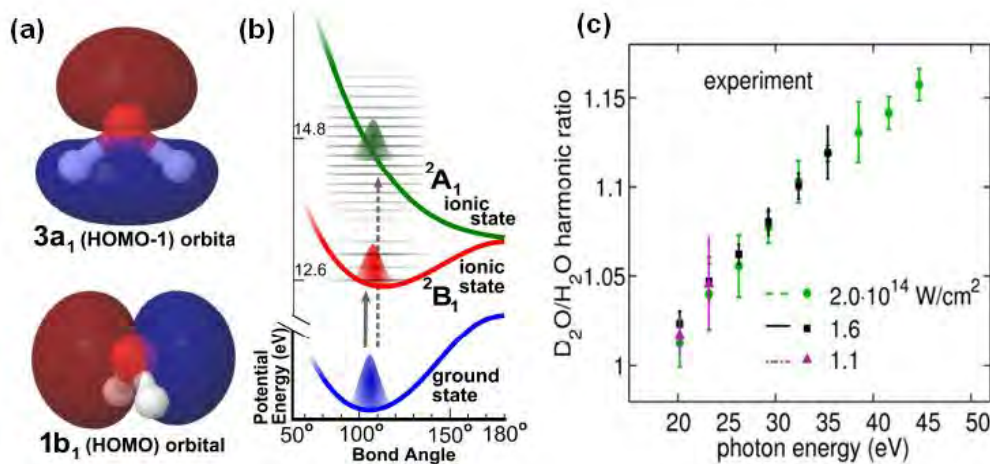


Fig. 1: a) HOMO and HOMO-1 of water. The corresponding neutral and ionic surfaces are shown in b). Upon tunnel ionization the ionic states are populated. The vibrational wavepacket on the ground ionic state (HOMO ionized) does not move, while the HOMO-1 ionized nuclear wavepacket changes the bond angle of the molecule considerably already on a sub-femtosecond timescale. This motion is encoded in the relative harmonic yield of water with respect to heavy water shown in c) (see text).

Figure 1a shows the geometric structure of water and the HOMO and HOMO-1 orbitals. We have shown in 2008, that in the process of high harmonic generation, both the HOMO and HOMO-1 can be ionized via strong field ionization. The fast ionization of the molecular orbital (either HOMO or HOMO-1 in Fig. 1a) launches a vibrational wave packet on an ionic potential energy surface in Fig. 1c (red and green, respectively). The harmonic light is emitted as the returning electron recombines with the molecular ion, thereby forming a molecule in its electronic and vibrational ground state. The efficiency of this process is governed by the spatial overlap of the ionic state nuclear wave packet and the neutral vibrational ground state. As the ionic state nuclear wave packet moves, overlap with the ground state is reduced. The nuclear wave packet for the heavy isotope is slow, thus a stronger overlap is maintained compared to the lighter, faster isotope. This gives a larger harmonic yield for the heavier isotope. The timescale of the nuclear motion is mapped onto the energy of different harmonics as shown by the Marangos group in 2006.

The ionization of the HOMO does not result in a moving nuclear wave packet, since the neutral and ionic ground state surfaces (HOMO ionization, red in Fig. 1 b) have equal equilibrium bond angles.

This results from the fact that the HOMO orbital has lone pair character and thereby does not contribute to the molecular bond. In contrast, the HOMO-1 ionization results in a fast nuclear motion as indicated by the steep green excited ionic surface in Fig. 1b.

The experimental results in Fig. 1c show that harmonic generation of heavy water results in a stronger harmonic efficiency than the water HHG. This clearly states that ionic nuclear dynamics is imprinted on the harmonic yield. Therefore, we deduce that a considerable amount of ionization stems from the lower lying HOMO-1 orbital, since only that ionic state produces a difference in harmonics from D₂O and H₂O. We have quantified these results in a collaboration with the group of A. Saenz in Berlin. The findings have important consequences. First, we confirm that HHG from multiple orbitals is the rule, not the exception for molecular HHG. Second, it is relatively easy to create a coherent superposition of ionic states in molecules, which automatically results in an attosecond electronic transient. We will observe these transients in the future using extreme UV spectroscopy. Third, we can achieve multi orbital ionization even without preparing the molecules in vibrational or rotational coherences in the neutral state. This was thought to be a prerequisite based on our former research and the contributions of other groups.

High harmonic spectroscopy and phase matching (in collaboration with M. Gaarde and K. Schafer, LSU):

The goal of high harmonic spectroscopy is to deduce information about electronic structure of target atoms or molecules from the shape and phase of a harmonic spectrum generated on that particular target. A general problem in this method is that the spectral information contains both the response of the single molecule/atom as well as the macroscopic sample response originating from the phase matching of harmonics. While phase matching is necessary to observe the harmonics, it is possibly hazardous in the interpretation of harmonic spectra in terms of single molecule/atom response.

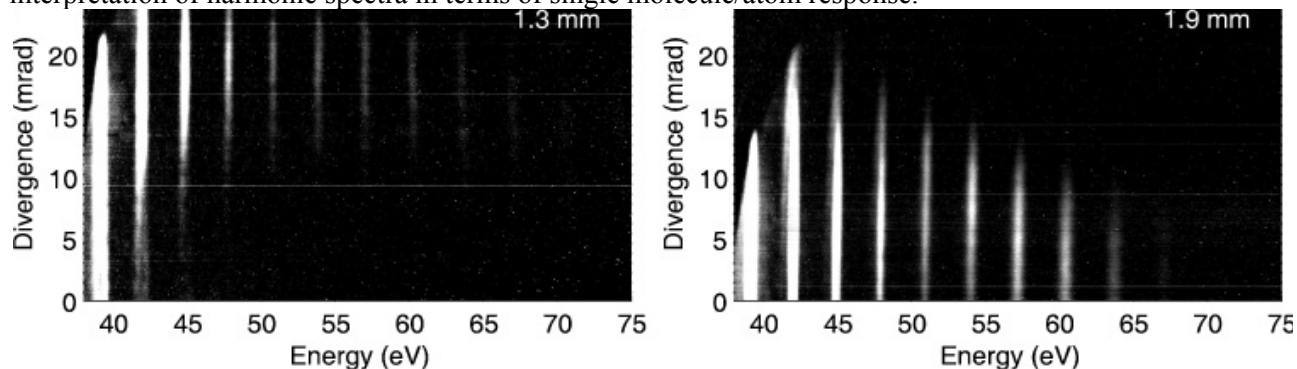


Fig. 2: Harmonic spectra of argon dispersed with respect to wavelength while preserving the divergence of the harmonic beam. The left and right panels are recorded with different positions of the target gas with respect to the laser focus (1.3 and 1.9mm respectively), which changes the phase matching.

We have studied the influence of phase matching on spectral information using the Cooper minimum of argon as a spectral marker. We have developed a new spectrometer in our lab to observe the wavelength content and divergence of a harmonic spectrum (see Fig. 2). The positions of the harmonic target with respect to the laser focus (1.3 and 1.9 mm in the two graphs) lead to different phase matching conditions manifested in dramatically different spectral shape and divergence. The Cooper minimum is absent in the left panel, whereas it is pronounced at 51 eV in the right panel (harmonic at 51 eV is less intense than the neighboring ones). We have collaborated with M. Gaarde and K. Schafer (both at Louisiana State University) to find the origins for that behavior. We found that the interference of s and d channels in the recombination together with phase matching effects lead to different modulation depth and energy location, or also the complete absence of the Cooper minimum structural feature. However, the spectral phase of the d-channel, also reflecting the Cooper minimum, is not altered by phase matching effects.

The study cautions interpreting harmonic spectra solely in terms of electronic structure. Comparing two spectra with similar phase matching but different excitation conditions or isotope content of the target (as in our N₂ or water studies) protects against artifacts from phase matching.

High harmonic spectroscopy – SO₂: We apply our high harmonic spectroscopy expertise to image excited electronic state dynamics on SO₂, presenting a prototypical system for non-adiabatic molecular dynamics. We have commissioned the apparatus and the gas handling in the lab. First harmonic spectra of the SO₂ ground state have been collected and within the next couple of weeks we will implement an excitation beam that will promote molecular population from the electronic ground state to covalent excited states. On those excited states, the molecule will undergo rapid electronic symmetry changes as a consequence of a conical intersection passage. We expect that the harmonic spectrum will contain information about the symmetry changes that reflect the conical intersection. Our past studies of transient gratings for the extreme UV domain provide the basis for contrast enhancement in the SO₂ experiments.

Time resolved XUV spectroscopy – first experiments (in collaboration with H. Duerr, SLAC and C. Back, Uni Regensburg): The extreme UV (XUV) spectral range provides two clear advantages for probing chemical dynamics. First, the transitions for different elements are clearly spectrally separated, thus element sensitivity in probing chemical processes can be obtained. Second, the dipole matrix element contains an initial state of core character with rather small spatial extension and a valence state with large extension. This allows the probing of electronic valence processes with high spatial electronic resolution.

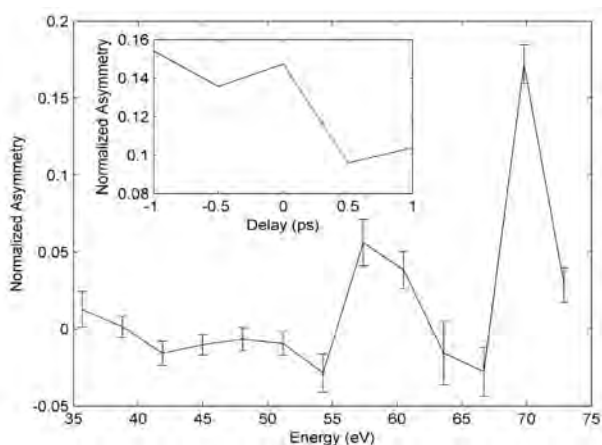


Fig. 3: Normalized asymmetry of XUV radiation reflected from a permalloy sample in a transverse magneto-optical Kerr effect geometry. The reflection R is recorded for two different magnetic field directions up and down. The normalized asymmetry is $R_{up} - R_{down} / (R_{up} + R_{down})$. The characteristic peaks at 57 and 70 eV are due to the M edges of Fe and Ni, respectively. A femtosecond IR pulse diminishes the asymmetry as shown in the inset as a function of delay between IR pulse and XUV pulse.

High harmonic generation provides pulses in the XUV range with femto- to attosecond duration. Our program has analyzed the pulses to learn about the HHG target structure. Now we are extending into the domain of using the broadband XUV pulses for time resolved experiments. To start with the rather complex experiments we have chosen a solid ferromagnetic FeNi sample (so called permalloy) with support from H. Durr at PULSE and Ch. Back from Regensburg, Germany. The reflection of the XUV pulse from the sample is spectrally dispersed. The normalized reflection under two different external magnetic field symmetries is shown in Fig. 3. One pulse covers the whole range from 35 eV to 75 eV. The two features at 57 and 70 eV are due to the M edges of Fe and Ni respectively. When shining an intense IR pulse on the sample and measuring the normalized XUV reflection in a time dependent fashion, the asymmetry changes on a picoseconds time scale (see inset in Fig. 3). This is indicative for a phase transition of the material.

Nucleobase photoprotection studies at LCLS: Towards the end of this fiscal year, we will lead an LCLS collaboration dedicated to study the electronic photoprotection mechanism of nucleobases. The nucleobases in DNA encode genetic information. Although the bases absorb strongly in the near ultraviolet region transmitted by the Earth's atmosphere, the UV excitation does surprisingly and fortunately not lead to destruction of the base molecules. Theory and previous experiments indicate that the photoprotection of the nucleobases proceeds via a fast (femtoseconds to picoseconds) non-adiabatic transitions, but understanding of the energy transfer mechanisms and the detailed relaxation pathways is currently a matter of debate. In particular it is not understood if the relaxation occurs through a reaction barrier. For thymine, models assuming the barrier predict a non-adiabatic transition to the optically dark

n^* state within a few picoseconds after photoexcitation whereas the models without barrier predict ~ 100 femtoseconds for this process. We propose to directly determine the transient electronic occupation during photoprotection by a UV-pump – LCLS probe experiment on thymine. The UV light starts the photoprotection mechanism, whereas the soft x-ray LCLS pulse leads to photo- and Auger electrons. Auger electrons emitted from the oxygen atoms in the photoexcited base sensitively display the n^* state occupation. Measuring the time constants of the Auger channel associated with the n^* state will therefore allow a direct experimental statement about the reaction barrier in the photoprotection pathway.

Future Progress

Nucleobase photoprotection studies at LCLS: We will start the FY2012 by analyzing our LCLS data and performing the theory on the right level to explain them.

Time resolved XUV spectroscopy: We will insert molecules in the interaction region of strong IR fields and XUV pulses and perform femtosecond resolved XUV absorption experiments aiming at the coherent superposition of vibrational states in the ion. We will drive our time resolution into the few to sub-femtosecond domain to study electronic wavepackets on simple diatomic and triatomic molecules. We will aim at the molecules that we studied by harmonic generation spectroscopy since we have already developed an understanding for those.

High harmonic spectroscopy – SO_2 : We will analyze data and push the time resolution to 10-20 fs by using hollow core fiber technology.

Publications over the past 3 years

1. J. P. Farrell, S. Petretti, J. Foerster, B. K. McFarland, L.S. Spector, Y. V. Vanne, P. Decleva, P. H. Bucksbaum, A. Saenz, and M. Gühr, Strong field ionization to multiple ionic states of water, arXiv: 1103.4423 [phys.atom-ph] (2011) submitted to Phys. Rev. Lett.
2. J. P. Farrell, L. S. Spector, B. K. McFarland, P. H. Bucksbaum, M. Gühr, M. Gaarde, K. Schafer, Influence of Phase Matching on the Cooper Minimum in Ar High Harmonic Spectra, Phys. Rev. A, **83**, 023420 (2011)
3. L. Fang, M. Hoener, et al., Double core hole production in N_2 : Beating the Auger clock, Phys. Rev. Lett., **105**, 083005 (2010)
4. J. P. Cryan, J. M. Glowia, et al., Auger electron angular distribution of double core hole states in the molecular reference frame, Phys. Rev. Lett., **105**, 083004 (2010)
5. J. M. Glowia, J. Cryan, et al., Time resolved pump-probe experiments at the LCLS, Optics Express, **18**, 17620 (2010)
6. M. Hoener, L. Fang, et al., Ultraintense X-Ray Induced Ionization, Dissociation, and Frustrated Absorption in Molecular Nitrogen, Phys. Rev. Lett., **104**, 253002 (2010)
7. J. P. Farrell, L. S. Spector, M. B. Gaarde, B. K. McFarland, P. H. Bucksbaum and M. Gühr, Strongly Dispersive Transient Bragg Grating for High Harmonics, Optics Letters, **35**, 2028 (2010)
8. J. P. Farrell, B. K. McFarland, P. H. Bucksbaum, and M. Gühr, Calibration of a high harmonic spectrometer by laser induced plasma emission, Optics Express **17**, 15134-15144 (2009)
9. B. K. McFarland, J.P. Farrell, P. H. Bucksbaum and M. Gühr, High harmonic phase of nitrogen, Phys. Rev. A, **80**, 033412 (2009)
10. J.P. Farrell, B. K. McFarland, M. Gühr, and P. H. Bucksbaum, Relation of high harmonic spectra to electronic structure in N_2 , Chem. Phys., **366**, 15-21 (2009)
11. M. Gühr, B. K. McFarland, J.P. Farrell and P. H. Bucksbaum, High harmonic generation from multiple molecular orbitals of N_2 , Ultrafast Phenomena XVI, Springer (2008)
12. B. K. McFarland, J.P. Farrell, P. H. Bucksbaum and Markus Gühr, High Harmonic Generation from multiple orbitals N_2 , Science **322**, 1232 (2008)

Non-Periodic Imaging at the Stanford PULSE Institute
Michael J. Bogan
Stanford PULSE Institute for Ultrafast Energy Science
SLAC National Accelerator Laboratory, Menlo Park, CA 94025
Email: mbogan@slac.stanford.edu

PROGRAM SCOPE From complex biological systems to ubiquitous airborne particulate matter regulating our climate, nanoscale non-periodic structures dominate our natural world. Over the past six years, we have helped pioneer the serial femtosecond x-ray diffractive imaging (XDI) approach to view this nanoscale world using ultrafast x-ray free-electron lasers (FELs). XDI utilizes the ultrafast and ultrabright x-ray pulses to overcome resolution limitations in x-ray microscopy imposed by x-ray induced damage to the sample by “diffracting before destroying” the sample on sub-picosecond timescales. XDI is elegant in its experimental simplicity: a coherent x-ray beam illuminates the sample and the far-field diffraction pattern of the object is recorded on an area detector. These measured diffraction intensities are proportional to the modulus squared of the Fourier transform of the wave exiting the object. An inversion of the diffraction pattern to an image in real space requires the retrieval of the phases of the diffraction pattern using the particularly robust and practical shrink-wrap algorithm. The algorithm reconstructs images ab initio which overcomes the difficulty of requiring knowledge of the high-resolution shape of the diffracting object. XDI overcomes the restrictions of limited-resolution x-ray lenses, offering a means to produce images of general non-crystalline objects at a resolution only limited in principle by the x-ray wavelength and by radiation-induced changes of the sample during exposure. The Non-periodic imaging program has shifted emphasis from early demonstration experiments at the FLASH free electron laser facility in Hamburg, where we experimentally verified “diffract and destroy” science and pioneered the experimental XDI methods, to the first hard x-ray FEL XDI experiments at the Linac Coherent Light Source (LCLS) at the SLAC National Accelerator Laboratory. The program’s near-term goals include development of new algorithms for interpreting structure from single-shot diffraction patterns, solving time-resolved protein structures at atomic resolution using LCLS serial crystallography, and experimental demonstration of our proposed x-ray morphometry of airborne particulate matter.

RECENT PROGRESS

First-ever 3D reconstruction from single particle x-ray diffraction data collected with an FEL: A proposed scheme for 3D, high-resolution imaging of single particles first involves collecting a large number of 2D diffraction patterns/data from an ensemble of nearly identical particles, one particle at a time. We reached a key milestone on this path by recording the first data set of identical particles in random orientations at FLASH using our aerodynamic focusing inlet. Each of these diffraction data results from a FEL pulse diffracting off a single particle at a random and unknown orientation before this particle suffers irreversible damage. A framework (named the EMC) for reconstructing the 3D electron densities from unoriented, noisy 2D diffraction data, extensively studied through realistic simulations of various experimental and sample conditions by Loh and Elser in 2009, was used to create the first-ever 3D reconstruction by single particle XDI. This was the first clear indication that such a synthesis can be productive, even if it were applied only to simple iron oxide nano ellipsoids (Figure 1). Experimentally, we demonstrated a reliable deliverance of nearly mono-disperse, aerosolized particles into the path of a train of FEL pulses. Theoretically, it was shown that the EMC reconstruction framework could be extended to unknown noise distributions beyond the simplest Poissonian photon-noise and also accommodate the unmeasured FEL pulse fluences (two conditions unexplored in all associated theoretical studies prior to this experiment). Besides recovering the average ellipsoid's 3D intensities, we were able to estimate the FEL pulse fluence distribution in our data, the ellipsoid’s most probable

orientations and also recover the symmetry axis and dimensions of the iron oxide ellipsoid; these measurements used only the most basic, sample-independent assumptions (Loh, Bogan et al. 2010). Subsequently, the first author of this study, Duane Loh, joined the NPI team as a postdoc and is now fully engaged in analysis of LCLS data from FY2010/2011.

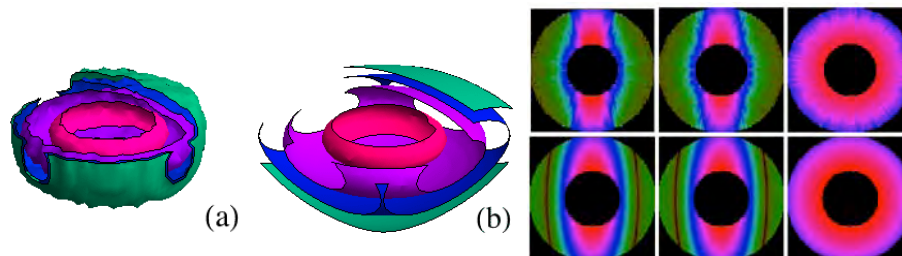


Figure 1. Comparing reconstructed intensities to those of an ideal ellipsoidal particle I_{ellip} . (a) Cutaway view of choice 3D isointensity surfaces of a reconstruction which show an oblate intensity distribution and (b) those of I_{ellip} with the best R-factor fit to this reconstruction; (top row) mutually perpendicular cross sections of this reconstruction; (bottom row) same cross sections of I_{ellip} in (b). Logarithm of intensities is shown as hues (See Loh, et al 2010 for color bar). Intensities in reconstructions span 3 orders of magnitude.

LCLS first results: Recent experimental research efforts were dominated by LCLS experiments that relied heavily on our new lab space occupied in June 2009. We staged the first ever LCLS experiments scheduled in December 2009, including optimization of gas dynamic virtual nozzles developed at Arizona State University for nanocrystal delivery and growth of photosystem I membrane protein nanocrystals. Results from these experiments were published back-to-back in a single issue of Nature in February 2011. Within a month, these two papers occupied position 1 and 5 in the Faculty 1000 for biochemistry, a prestigious listing of influential manuscripts.

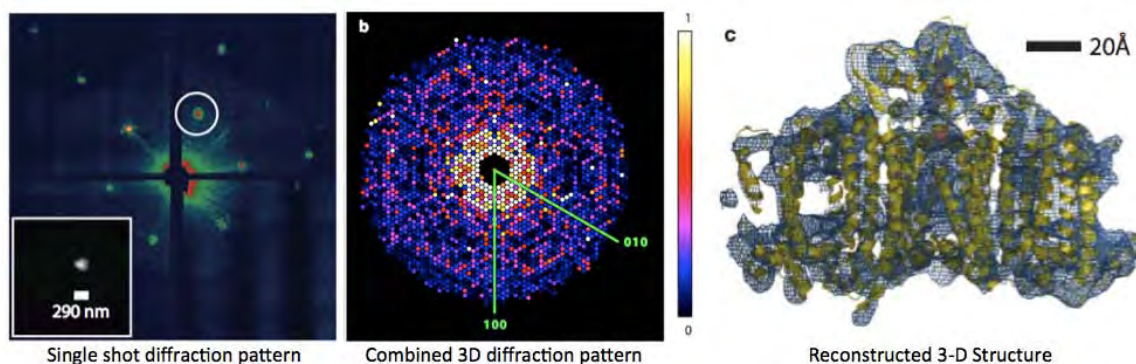


Figure 2. Femtosecond nanocrystallography at LCLS. A single shot diffraction pattern from a photosystem I nanocrystal showing Bragg scattering at low q (left). The inset depicts the real space image of the nanocrystal obtained by iterative phase retrieval from an isolated Bragg spot. The combined 3D diffraction map from $\sim 100,000$ patterns (middle) and the reconstructed 3D structure of the protein fit to a model of a synchrotron-solved structure (right).

LCLS femtosecond x-ray protein nanocrystallography: We measured the structure factors of membrane protein complexes using LCLS for the first time. Diffraction images at a resolution limited only by the early-operation beamline optics were obtained from photosystem I (PS I) crystals of only 6 unit cells across ($a=b=281 \text{ \AA}$, $c=165 \text{ \AA}$) using a liquid jet delivery system. Refinement of the PS I structure against $\sim 100,000$ individual LCLS diffraction images produced electron density maps at $\sim 9 \text{ \AA}$. These experiments demonstrate exciting new possibilities in macromolecular crystallography, especially for crystals that are too small for conventional data

collection at synchrotrons (*i.e.* nanocrystals) and for systems that suffer severe x-ray radiation damage at the active site (*i.e.* metalloproteins). Although the LCLS pulse vaporizes crystalline samples, this happens after the extremely short x-ray pulse has given rise to a diffraction pattern while inertia keeps the atoms in place long enough not to “blur” the pattern. Thus, the radiation damage limit is extended beyond what is possible with a conventional synchrotron and a given sample may be exposed to more photons than possible at synchrotron stations.

LCLS XDI of viruses: This study culminated years of single particle XDI development at FLASH for biological samples with the first single-shot diffraction patterns of viruses captured in a substrate-free manner. Our results showed that high quality diffraction data can be obtained with a single X-ray pulse from a non-crystalline biological sample, a single Mimivirus particle, which was injected into the pulsed beam of the LCLS (Seibert, Ekeberg et al. 2011) (Figure 3). The far-field diffraction pattern of each particle hit by an X-ray pulse is recorded on a pair of fast pnCCD detectors housed in the CAMP apparatus developed and operated by our Max Planck Institute collaborators. Calculations indicate the energy deposited into the virus by the pulse heated the particle to over 100,000 K after the pulse had left the sample. The reconstructed exit wave front (image) yielded 16 nm optical resolution from the single exposure and shows no measurable damage. The reconstruction reveals a compartmentalized interior inside the virion with a distinct arrangement of dense material (presumably the DNA genome) that has never been reported before. Resolution in such experiments can be extended from a redundant data set, similar to the example of the ellipsoidal nanoparticles from FLASH (Loh, Bogan et al 2010). Work is under way at the LCLS to reduce the amount of missing low-resolution data and to increase the photon flux on the sample. Mimiviruses are the largest known viruses, so a significant and ongoing effort remains to extend these experiments to typical viruses that are much smaller (by often an order of magnitude in diameter).

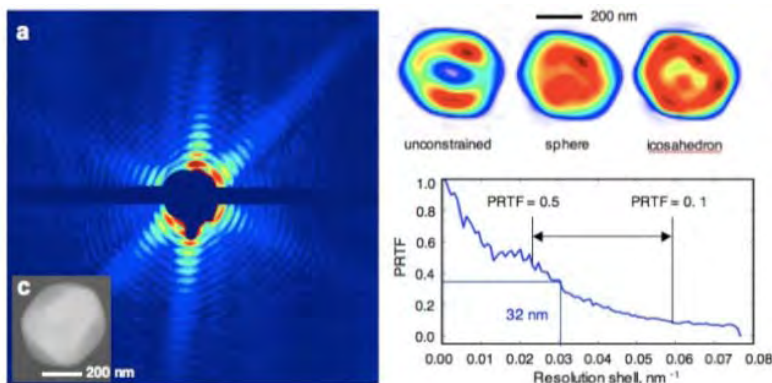


Figure 3. Single shot diffraction patterns on single virus particles give interpretable results. **a**, Experimentally recorded far-field diffraction pattern in false color representation from an individual virus particles. Deep blue = low intensity; yellow to red = high intensity. **c**, TEM of a uranyl acetate-stained Mimivirus particle with pseudo-icosahedral appearance. The bar corresponds to 200 nm.

b, Reconstructed images after iterative phase retrieval with the Hawk software package. The size of a pixel corresponds to 9 nm in the images. Three different reconstructions are shown: A averaged reconstruction with unconstrained Fourier modes, followed by averaged images after fitting unconstrained low-resolution modes to a spherical or an icosahedral profile. The orientation of the icosahedron was determined from the diffraction data. The results show small differences between the spherical and icosahedral fits. **d**, The phase retrieval transfer function (PRTF) for the reconstruction where the unconstrained low-resolution modes were fitted to a sphere. Resolution is defined by the point where the PRTF drops to 1/e 20 (about 16 nm optical resolution in both exposures).

LCLS XDI of non-periodic matter: Whereas high-resolution, three-dimensional imaging of identical single particles is expected from FELs (13, 43, 49), there remains the obvious question of what we can learn about sub-micron particles that are non-identical. Imaging single

nanoparticles that are non-identical are especially challenging, even if illuminated by FELs of very high photon fluences, since they will still scatter few photons (13). Although signal-limited measurements of non-identical nanoparticles will not provide atomic-resolution snapshots, high-resolution morphology may still be accessible (49). Because they are generally disordered and show a range of interesting morphologies, complex airborne particulate matter (PM) are particularly well-suited candidates to test capability of XDI morphometry to probe single particles in their native state (12). In an invited article to the *J. Phys. B: At. Opt. Phys.* special issue on science from the last 5 years of FLASH we described the potential for single particle coherent x-ray diffractive imaging to probe the non-periodic structure of airborne particulate matter such as soot (Bogan, Starodub et al. 2010). This extension of single particle XDI parallels the concept of imaging non-reproducible biological objects such as cells. In June 2010 we demonstrated for the first time the ability to capture single shot diffraction from individual soot particles with FELs, (1.2keV x-rays, 150fs pulses). Data analysis is ongoing.

FUTURE PLANS Our experimental campaign at LCLS continues with the first XDI experiments with hard x-rays at the CXI endstation focusing on time-resolved nanocrystallography, the structure of water and electrohydrodynamic processes. Data analysis efforts will include new algorithm developments for 3D and 2D structures. We will continue to develop the particle beam generation and diagnostics instrumentation necessary to perform any experiments utilizing laser interactions with single particles.

COLLABORATIONS: This work is done with colleagues from SLAC, Stanford, LLNL, Uppsala, LBNL, Arizona State University, Max Planck Biomedical Heidelberg, CFEL@DESY and others.

SELECTED PUBLICATIONS FROM DOE SPONSORED RESEARCH IN 2010-2011

1. Yoon, C. H. *et al.* Unsupervised classification of single-particle X-ray diffraction snapshots by spectral clustering. *Optics Express* submitted (2011).
2. Seibert, M. M. *et al.* Single Mimivirus particles intercepted and imaged with an X-ray laser *Nature* **470**, 78-81 (2011).
3. Saldin, D. K. *et al.* New Light on Disordered Ensembles: Ab-Initio Structure Determination of One Particle From Scattering Fluctuations Of Many Copies. *Physical Review Letters* **106**, 115501 (2011).
4. Pedersoli, E. *et al.* Multipurpose Modular Experimental Station for the DiProI Beamline of Fermi@Elettra Free Electron Laser. *Review of Scientific Instruments* **82**, 043711 (2011).
5. Frank, M. *et al.* in *Rapid Characterization of Microorganisms by Mass Spectrometry* p. 161-196 (ed Demirev) (American Chemical Society, 2011).
6. Chapman, H. *et al.* Femtosecond x-ray protein nanocrystallography. *Nature* **470**, 73-77 (2011).
7. Seibert, M. M. *et al.* Femtosecond diffractive imaging of biological cells. *Journal of Physics B: Atomic, Molecular and Optical Physics* **43**, 194015 (2010).
8. Saldin, D. K. *et al.* Structure of a single particle from scattering by many particles randomly oriented about an axis: a new route to structure determination? *New Journal of Physics* **12**, 035014 (2010).
9. Loh, N. T. D. *et al.* Cryptotomography: Reconstructing 3D fourier intensities from randomly oriented single-shot diffraction patterns. *Physical Review Letters* **104**, 225501 (2010).
10. Hau-Riege, S. P. *et al.* Sacrificial tamper slows down sample explosion in ultrafast x-ray diffraction experiments. *Physical Review Letters* **104**, 064801 (2010).
11. Bogan, M. J., Starodub, D., Hampton, C. Y. & Sierra, R. G. Single particle coherent diffractive imaging with a soft X-ray free electron laser: Towards soot aerosol morphology *Journal of Physics B: Atomic, Molecular and Optical Physics* **43**, 194013 (2010).
12. Bogan, M. J. *et al.* Aerosol imaging with a soft x-ray free electron laser. *Aerosol Science and Technology* **44**, 1-6 (2010).
13. Bogan, M. J. *et al.* Single-shot femtosecond X-ray diffraction from ellipsoidal nanoparticles in random orientations. *Physical Review Special Topics - Accelerators and Beams* **13**, 094791 (2010).

SPC–Solution Phase Chemistry

K. Gaffney, W. Zhang, Z. Sun, M. Ji, R. Hartsock

Overview

During the past year of the solution phase chemical dynamics program we have made progress on numerous research fronts, moved our laser laboratory from Building 130 to the Building 40 and begun commissioning of a second laser laboratory and a chemical preparation laboratory. Our activities in the Solution Phase Chemical Dynamics sub-task split into two complementary areas of investigation: studies of thermal fluctuation driven chemical dynamics and studies of photoinduced electron transfer dynamics in coordination chemistry.

Thermal fluctuation driven chemical dynamics

Hydrogen bond dynamics in ionic solutions: The mechanism for hydrogen bond (H-bond) switching in solution has remained subject to debate despite extensive experimental and theoretical studies. We have applied polarization-selective multidimensional vibrational spectroscopy to investigate the H-bond exchange mechanism in aqueous NaClO₄ solution. The results show that a water molecule shifts its donated H-bonds between water and perchlorate acceptors by means of large, prompt angular rotation. Using a jump-exchange kinetic model, we extract an average jump angle of 49±4°, in qualitative agreement with the jump angle observed in molecular dynamics simulations of the same aqueous NaClO₄ solution. This provides strong experimental support for the angular jump model of H-bond exchange proposed by Laage and Hynes.

Dynamics of ligand exchange, ion pairing, and ion assembly in solution: We have extended our studies of H-bond dynamics in aqueous ionic solutions to the study of ion pairing and assembly in polar solvents. Our efforts have focused on the mechanism of ligand exchange for solvated Mg²⁺ ions in water and lithium thiocyanate ion assembly in aprotic solvents. Our studies of the exchange of ligands into and out of the first coordination sphere of Mg²⁺ occur via a dissociative mechanism. The predominance of dissociative mechanisms for Mg²⁺ ligand exchange reactions had been predicted by molecular dynamics simulations, but never demonstrated experimentally. Our studies of Li⁺ NCS⁻ ion assembly demonstrate that the short ranged ion-solvent interaction dominates the chemical dynamics of the system, and cannot be accounted for with traditional solvation models.

Photoinduced electron transfer dynamics in coordination chemistry

Structural dynamics and bond isomerization in photocatalytic coordination compounds: We have utilized femtosecond-resolution optical pump-probe spectroscopy of bimetallic d⁸-d⁸ Ir(I)₂ metal cores held together by four diisocynoalkane ligands. These complexes have the dual attraction of a large structural difference between the ground and excited state and photo-catalytic, such as hydrogen gas production from 2-propanol, and interesting photo-physical. The length of the metal-metal bond in the molecular crystal depends sensitively on the steric properties of the alkyl component of the bridge and the nature of the counter ion. For 1,8-diisocyno-menthane bridging ligands, these molecules can form weak metal-metal bonds with bond lengths as large as 4.5 Å and eclipsed 1,8-diisocyno-menthane ligands. In solution, the electronic absorption spectrum indicates that the Ir(I)₂-dimer forms two bond isomers with Ir-Ir bond lengths of roughly 3.5 Å and 4.5 Å. Upon excitation to the lowest energy electronic excited state, the metal-metal bond length has been proposed to shrink significantly and only result in a single bond conformation since visible excitation promotes an electron from a metal-metal anti-bonding state to a bonding state.

While prior studies have proposed a general picture for the ground state structure, and a partial picture of the excited state structure, no experimental investigations have characterized the dynamic evolution of the Ir₂[1,8-diisocyno-menthane]₄ structure following electronic excitation. We have initiated femtosecond resolution

pump-probe measurements of the bi-metallic d^8-d^8 coordination complex $\text{Ir}_2[1,8\text{-diisocyano-menthane}]_4$. The signal peaked around 600 nm corresponds to the ground state bleach and the stimulated emission at very small time delays. The signal peaked at 710 nm corresponds to the stimulated emission signal. These preliminary results demonstrate that we will be able to learn a significant amount about the excited state dynamics of the bi-metallic photo-catalysts with optical pump-probe measurements and also gives us confidence that these materials will be amenable to time resolved x-ray scattering measurements which we will perform at the LCLS in the winter of 2012.

Ultrafast x-ray spectroscopy studies in coordination chemistry: We have participated in the commissioning of both the solution phase soft x-ray spectroscopy endstation and the hard x-ray pump-probe endstation at the Linac Coherent Light Source (LCLS). For the soft x-ray spectroscopy endstation, we have investigated the photodissociation dynamics of $\text{Fe}(\text{CO})_5$ with time resolved resonant inelastic x-ray scattering measurements at the $\text{Fe L}_{3\text{-edge}}$. With hard x-rays, we have used time resolved XANES measurements at the Fe K-edge to investigate the dynamics of photo-induced spin crossover in $\text{Fe}(\text{II})(\text{bipyridine})_3$ and $\text{Fe}(\text{II})(\text{phenanthroline})_3$. Getting this work in print and preparing for the next round of LCLS experiments will be a focus for the next year.

Publications:

1. Efficient Multiple Exciton Generation Observed in Colloidal PbSe Quantum Dots with Temporally and Spectrally Resolved Intraband Excitation: M. Ji, S. Park, S.T. Connor, T. Mokari, Y. Cui, K.J. Gaffney, *Nano. Lett.* **9**, 1217 (2009).
2. Ultrafast Dynamics of Hydrogen Bond Exchange in Aqueous Ionic Solutions: S. Park, M. Odelius, K.J. Gaffney, *J. Phys. Chem. B* **113**, 7825 (2009).
3. Characterization of Charge Transfer Excitations in hexacyanomanganate(III) with Mn K-Edge Resonant Inelastic X-ray Scattering, D.A. Meyer, U. Bergmann, X. Zhang, K.J. Gaffney, *J. Chem. Phys.* **132**, 134502 (2010).
4. Ligand Exchange Dynamics in Aqueous Solution Studied with 2DIR Spectroscopy: S. Park, M. Ji, K.J. Gaffney, *J. Phys. Chem. B* **114**, 6693 (2010).
5. Large Angular Jump Mechanism Observed for Hydrogen Bond Exchange in Aqueous Perchlorate Solution: M. Ji, M. Odelius, K.J. Gaffney, *Science* **328**, 1003 (2010). *see also* – Following the Motions of Water Molecules in Aqueous Solutions: J.L. Skinner *Science* **328**, 985 (2010).
6. Dynamics of Ion Assembly in Solution: 2DIR Spectroscopy Study of LiNCS in Benzonitrile: M. Ji, S. Park, K.J. Gaffney, *J. Phys. Chem. Lett.* **1**, 1771 (2010).
7. Orientational Relaxation Dynamics in Aqueous Ionic Solution: Polarization-selective two-dimensional infrared study of angular jump-exchange dynamics in aqueous 6M NaClO_4 : M. Ji, K.J. Gaffney, *J. Chem. Phys.* **134**, 044516 (2011).
8. H-bond Switching and Ligand Exchange Dynamics in Aqueous Ionic Solution: K.J. Gaffney, M. Ji, M. Odelius, S. Park, Z. Sun, **frontiers article Chem. Phys. Lett.** **504**, 1 (2011).
9. Characterizing the deformational isomers of bi-metallic [dimen = 1, 8-diisocyano-*p*-menthane] with vibrational wavepacket dynamics: R.W. Hartsock, W. Zhang, M.G. Hill, B. Sabat, K.J. Gaffney, *J. Phys. Chem. A* **115**, 2920 (2011).

University Research Summaries
(by PI)

DOE-SISGR: Coherent Control of Electron Dynamics

Principal Investigator: Andreas Becker

Jing Su, Daniel Weflen, Shaohao Chen, Norio Takemoto, Antonio Picoń,
Agnieszka Jaroń-Becker

JILA and Department of Physics, University of Colorado at Boulder,
440 UCB, Boulder, CO 80309-0440

andreas.becker@colorado.edu

Introduction

Advances in laser technology and computing power, that have been made recently, enable us to enter a fundamentally new regime, where the correlated electron-nucleus interaction in molecules can be observed and controlled in real time. Aspects, such as on which time scale energy is transferred between electronic and nuclear motion or how light can be used to monitor ultrafast electronic dynamics in a molecule, can now be studied both in experiment and theory. In this project we theoretically analyze how electron dynamics in a molecule can be observed and controlled using new laser technologies on a sub-femtosecond time scale

Recent Progress and Future Goals

Our activities in the project can be summarized in the following three sub-projects.

A. Time-dependent analysis of few-photon coherent control schemes

Coherent control schemes in the perturbative intensity regime are often analyzed in the frequency domain, which provides the opportunity to understand the control over the transition probability in terms of interference effects between different pathways [1]. In view of the application of these control schemes using ultrashort pulses we developed a complementary view on these control schemes in the temporal domain. To this end, we solved the time-dependent Schrödinger equation for a hydrogen atom interacting with an (ultraviolet) laser field. Results were obtained for two-photon excitation from the ground state of the hydrogen atom to the 2s state for symmetric and antisymmetric phase distributions leading to so-called dark and bright pulses, for which the temporal field distributions consist of many subpulses. It was found that the maxima (minima) in the final excitation probabilities are due to constructive (destructive) interferences between the amplitudes induced by the sub-pulses in the temporal domain [2].

We then extended our studies to the molecular case. Our analysis in the temporal domain shows in an intuitive way that control schemes for atoms often fail for molecules. For example, few-photon coherent control of the transition between the ground and the first excited (dissociative) state in the hydrogen molecular ion cannot

lead to a cancelation of the transition probability. Since any dark pulse, suggested so far, consists of a sequence of sub-pulses, the wave packets pumped to the excited dissociative state starts to immediately evolve to larger internuclear distances, and wave packets pumped at different times cannot destructively interfere with each other. Next, we developed molecular models (potential energy schemes) in order to study the control of transitions between two bound states. Here, the transition probability can, in general, be controlled (maximized as well as minimized) via the time delay and the carrier-to-envelope phase difference between consecutive subpulses. In case of a population of a superposition of vibrational states in the upper bound state the time delay between the different sub-pulses in a pulse need to match with the revival time of the vibrational wave packet induced in order to effectively control the transition probability.

In future, we will test our general findings in view of the application of pulse forms used before in experiments with atoms (e.g.[1]).

B. Control and imaging of electron localization

The control of the localization of the electron on one of the protons in a dissociating hydrogen molecular ion using intense ultrashort laser pulses has become a topic of active research (e.g. [3]). The electronic dynamics driven by a strong field is found to be complex and potentially even counterintuitive. Depending on the laser intensity, the direction of the electron's motion between the two nuclei follows or opposes the classical laser-electric force. This sensitive dependence of the correlated electronic-nuclear motion was explained in terms of the diffracting electronic momentum distribution of the dissociating two-center system [4]. This leads to the surprising effect that the electron can transiently localize at the same proton several times over one half cycle of the laser pulse on an attosecond time scale and induce multiple bursts of ionization instead of one bursts at the maximum of the field [5]. This theoretical prediction is in contradiction with the widely-used (tunnel) ionization picture for atoms and molecules.

Recently, we examined this attosecond electron dynamics in collaboration with the experimental group of Reinhard Dörner (University Frankfurt, Germany). To this end, we studied electron emission from the hydrogen molecular ion by a circularly polarized laser pulse (800 nm, 6×10^{14} W/cm²). The electron momentum distribution in the body fixed frame of the molecule is experimentally obtained by a coincident detection of electrons and protons. The experimental data are compared to a solution of the time-dependent Schrödinger equation in two dimensions. Indeed, the observed radial and angular distributions are at odds with the tunnel ionization model. In the theoretical analysis we could trace back how the unexpected momentum distribution is related to the previously predicted complex laser driven electron dynamics which influences the time instants of ionization and initial momentum of the emitted electron. In a broader context our work shows the exciting

prospect that the (sometimes counter-intuitive) dynamics of an electron inside a molecule on the attosecond time scale can be mapped onto the momenta in the continuum where they become observable.

In future, we will extend our studies of the imaging of the intramolecular electron dynamics on the attosecond time scale. To this end, we have developed models for planar molecules. Besides the application to the dynamics in higher excited states in the hydrogen molecular ion we will also consider other single-active electron molecules such as H_3^{2+} .

C. Multiphoton coherent control of vibrational excitation in non-polar molecules

Much progress in the preparation and manipulation of the internal quantum state (vibration, rotation) of neutral diatomic polar molecules and molecular ions has been achieved recently (e.g. [6]), among others based on optical schemes such as stimulated Raman adiabatic passage [7]. Control and manipulation of the quantum state of nonpolar molecules and/or molecules with many excited dissociative states pose a challenge, since the well-known control methods are often limited in efficiency. We proposed an alternative coherent control scheme for the population distribution of the vibrational states of this class of molecules [8]. Our theoretical analysis and results of numerical simulations for the interaction of the hydrogen molecular ion in its electronic ground state with an infrared laser pulse revealed a selective two-photon transition between the vibrational states via a coupling with the first excited dissociative state. We demonstrated that for a given temporal intensity profile the population transfer between vibrational states, or a superposition of vibrational states, can be made complete for a single chirped pulse or a train of chirped pulses, which accounts for the accumulated phase difference due to the AC Stark effect. In particular, we showed how a superposition of excited vibrational states can be “cooled” to the vibrational ground states. We further considered a potential energy scheme of a model molecule (with bound and dissociative states) in order to show that the results found for the hydrogen molecular ion hold in more general. The limits of the control scheme in view of the peak intensity and duration of the applied pulse (or, pulse sequence) as well as effects of spatial intensity (or focal) averaging were analyzed.

As mentioned above, the control scheme between vibrational states in the same electronic state is based on a transfer of excited electronic states. In future, we will analyze how the transient population of these excited electronic states can be observed in an experiment. Since the transient population changes on the attosecond time scale, we study in particular the application of single attosecond pulses as well as trains of those pulses for the detection.

References

- [1] D. Meshulach and Y. Silberberg, *Nature* **396**, 239 (1998).
- [2] S. Chen, A. Jaroń-Becker, and A. Becker, *Phys. Rev. A* **82**, 013414 (2010).
- [3] M. F. Kling et al., *Science* **312**, 246 (2006).
- [4] F. He, A. Becker and U. Thumm, *Phys. Rev. Lett.* **101**, 213002 (2008).
- [5] N. Takemoto and A. Becker, *Phys. Rev. Lett.* **105**, 203004 (2010).
- [6] K.-K. Ni et al., *Science* **322**, 231 (2008).
- [7] K. Bergmann, H. Theuer, and B.W. Shore, *Rev. Mod. Phys.* **70**,1003 (1998).
- [8] A. Picon et al., *Phys.Rev. A* **83**, 023412 (2011).

Publications of DOE sponsored research

Shaohao Chen, Agnieszka Jaroń-Becker, and Andreas Becker, *Time-dependent analysis of few-photon coherent control schemes*, *Physical Review A* **82**, 013414 (2010).

Antonio Picon, Jens Biegert, Agnieszka Jaroń-Becker, and Andreas Becker, *Coherent control of the vibrational state population in a nonpolar molecule*, *Physical Review A* **83**, 023412 (2011).

Probing Complexity using the LCLS and the ALS

Nora Berrah

Physics Department, Western Michigan University, Kalamazoo, MI 49008

e-mail:nora.berrah@wmich.edu

Program Scope

The objective of our research program is to investigate *fundamental interactions between photons and gas-phase systems* to advance our understanding of correlated and many body phenomena. Our research investigations focus on non-linear physics and probe multi-electron interactions and energy transfer processes from electromagnetic radiation. Most of our work is carried out in a strong partnership with theorists.

Our current interests include: 1) The study of non linear and strong field phenomena in the x-ray regime using the linac coherent light source (LCLS), the first x-ray ultra-fast free electron laser (FEL) facility at the SLAC National Laboratory. Our investigations focus on the interaction of intense and short LCLS pulses with atoms, molecules and clusters. 2) The study of correlated processes in select anions using advanced techniques with vuv-soft x-rays from the Advanced Light Source (ALS) at Lawrence Berkeley Laboratory. We present here results completed and in progress this past year and plans for the immediate future.

Recent Progress

1) Double core hole production in N₂: Beating the Auger clock

Twenty five years ago, it was theoretically predicted that DCH spectroscopy would provide a richer and more sensitive technique than inner-shell photoelectron spectroscopy (PES), amplifying and rendering observable subtle differences between similar chemical systems [a]. DCH spectroscopy studies are now possible with the development of intense x-ray FELs like the LCLS. Our 2009 LCLS beamtime allowed us to explore multiple atomic sites in a molecule i.e., double core holes with both vacancies on a single site (DCHSS) and double core holes with a single vacancy on two different sites (DCHTS).

Our work investigated and reported on the observation of DCH produced via sequential two-photon absorption [1-3]. The production and decay of these states was characterized by using photoelectron spectroscopy, Auger electron spectroscopy, and mass spectrometry. The experimental results were interpreted with the help of *ab-initio* Green's function calculations of the energies of the DCH states and of the Auger decay energies. These results will serve not only as a basis for understanding double- and multiple- core hole states in more complex molecules, but also for producing selective configurations with single or double core holes on specific atoms, ultimately controlling how these states decay and how the molecule fragment. A new technique based on the x-ray two-photon photoelectron spectroscopy (XTPPS) of such DCHSS and DCHTS states has recently been proposed [b], and the present observations also provide the first experimental test for the method.

A new regime of light-matter interaction: Sequential x-ray multiphoton ionization

The interaction of intense x-rays with matter is dominated by core-shell excitation, and in particular by the competition between Auger relaxation and multiple inner-shell ionization events that become feasible at extreme x-ray intensities. For N₂, the Auger lifetime for a single core hole

is ~6.4 fs. Our experiment has measured the electron spectra revealing the creation of highly charged atomic and molecular states by ultraintense, femtosecond x-ray pulses at photon energies above the core shell ionization threshold (409.9 eV). With increasing molecular charge state, dissociation is expected to compete with electronic relaxation, and the ionization dynamics will transition from molecular to atomic behavior. With photon energies 600 - 700 eV above the K edge of N₂ and pulse durations longer (80, 280 fs) than the Auger-decay lifetimes (6.4 fs), many pathways are possible resulting in charge states up to N⁷⁺ which we measured [4-5].

Molecular DCHSS states

Our work clearly measured the DCHSS Auger spectra for N₂ and details are shown in refs [1-2]. The experimental spectra were collected with electron time-of-flight spectrometers positioned along axes perpendicular to the polarization axis to minimize contributions from direct photoionization. Our data was compared to calculations and the latter confirmed that we indeed observed the DCHSS as well as its shake-up satellite. We estimated the DCHSS signal intensity to be ~1% of the main Auger peak signal between 355eV-370 eV (\pm 5eV).

Molecular DCHTS states

The detection and assignment of electrons associated with the production of the uniquely molecular DCHTS states was difficult, even though we used the best resolution we could with our electron time-of-flight spectrometers. Our data was analyzed by taking into account the contributions from single-photon shake-up/off (SUO) processes as previously determined using synchrotron radiation [c], convoluted with the experimental energy resolution of the current study. In order to disentangle the major contributions generated by multiple photon ionization, a non-linear least-squares fit was performed [1]. Our global fit showed that one spectral component was consistently found exactly at the position of the expected DCHTS photoline. Unfortunately, this spectral region is also marked by the strongest SUO contributions. Additionally, the N1s⁻¹ photoline from inner shell ionization of excited N⁺(1s²2s¹2p³) fragments coincides with the DCHTS photoline within the theoretical and experimental uncertainties. Our analysis lead only to an upper bound for DCHTS contributions in the photoelectron spectrum of 4% relative to the intensity of the N₂(1s⁻¹) main photoline. Details can be found in our published work [1-2]. The good news is that our 2010 beamtime allowed us to unambiguously measure the elusive DCHTS in small molecules and our work will be submitted to publication this year.

2) Inner-shell photodetachment from Fe⁻

We have reported absolute inner-shell photodetachment cross-section data for the Fe⁻ negative ion near and above the 3*p*-excitation region, providing needed reference data for astrophysics and plasma physics. In the photon energy range 48–72 eV, the Fe⁻ photodetachment spectrum is dominated by shape resonances, which can be assigned to the 3*p* → (3*d* + ϵ *d*) excitation lying just above the 3*p* threshold. In the near-threshold region, the single-photodetachment cross section can be accurately fit using shape-resonance profiles with *l* = 2. The Wannier law was observed and fit well to the near-threshold region of the extracted Fe⁻ double photodetachment cross section, observed in the Fe²⁺ production channel. Furthermore, the absolute photodetachment cross sections for Fe⁻ leading to Fe⁺ and Fe²⁺ were measured at four photon energies. Details can be found in our published work [6].

Future Plans.

The principal areas of investigation planned for the coming year are:

1) Prepare and carry out the LCLS approved experiment consisting of ionizing C₆₀ with the x-rays from the LCLS. The experiment will be schedule in 2012. 2) Prepare and carry out three

collaborative LCLS-based experiments in August and September 2010. **3)** Continue the analysis of our LCLS data generated through our 2009 beamtime. **4)** Carry out the photodetachment experiment of H. **5)** Finish the photodetachment experiments in the carbon anions cluster chain at the ALS and continue the analysis of the K-shell photodetachment of C_{60}^- (conducted in collaboration with the UNR, DU, ALS and Giessen groups).

References:

- [a] L. S. Cederbaum, et al., J. Chem. phys. 85, 6513-6523 (1986).
 [b] R. Santra, et al., Phys. Rev. Lett. 103, 013002-013005 (2009).
 [c] S. Svensson et al., J. Phys. B 25, 135-144 (1992); T. Kaneyasu et al., J. Phys. B: 41, 135101 (2008).

Publications from DOE Sponsored Research

1. L. Fang, M. Hoener, O. Gessner, F. Tarantelli, S.T. Pratt, O. Kornilov, C. Buth, M. Guehr, E.P. Kanter, C. Bostedt, J.D. Bozek, P.H. Bucksbaum, M.Chen, R. Coffee, J. Cryan, M. Glowonia, E. Kukuk, S.R. Leone, and N. Berrah, "Double core hole production in N_2 : Beating the Auger clock", Phys. Rev. Lett. **105**, 083005 (2010).
2. J. P. Cryan, J. M. Glowonia, J. Andreasson, A. Belkacem, N. Berrah, C. I. Blaga, C. Bostedt, J. Bozek, C. Buth, L. F. DiMauro, L. Fang, O. Gessner, M. Guehr, J. Hajdu, M. P. Hertlein, M. Hoener, O. Kornilov, J. P. Marangos, A. M. March, B. K. McFarland, H. Merdji, V. Petrovic, C. Raman, D. Ray, D. A. Reis, F. Tarantelli, M. Trigo, J. White, W. White, L. Young, P. H. Bucksbaum, and R. N. Coffee, "Auger electron angular distribution of double core hole states in the molecular reference frame", Phys. Rev. Lett; **105**, 083004 (2010),
3. J. M. Glowonia, J. Cryan, J. Andreasson, A. Belkacem, N. Berrah, C. I. Blaga, C. Bostedt, J. Bozek, L. F. DiMauro, L. Fang, J. Frisch, O. Gessner, M. Gühr, J. Hajdu, M. P. Hertlein, M. Hoener, G. Huang, O. Kornilov, J. P. Marangos, A. M. March, B. K. McFarland, H. Merdji, V. S. Petrovic, C. Raman, D. Ray, D. A. Reis, M. Trigo, J. L. White, W. White, R. Wilcox, L. Young, R. N. Coffee, and P. H. Bucksbaum, "Time-Resolved Pump-Probe Experiments at the LCLS" Optics Express, **18**, Issue 17, 17620 (2010).
4. M. Hoener, L. Fang, O. Kornilov, O. Gessner, S.T. Pratt, M. Guehr, E.P. Kanter, C. Blaga, C. Bostedt, J.D. Bozek, P.H. Bucksbaum, C. Buth, M. Chen, R. Coffee, J. Cryan, L. DiMauro, M. Glowonia, E. Hosler, E. Kukuk, S.R. Leone, B. McFarland, M. Messerschmidt, B. Murphy, V. Petrovic, D. Rolles, and N. Berrah, "Ultra-intense X-ray Induced Ionization, Dissociation and Frustrated Absorption in Molecular Nitrogen" Phys. Rev. Lett. **104**, 253002 (Published June 23, 2010). First published work from LCLS.
5. O. Gessner, O. Kornilov, M. Hoener, L. Fang, and N. Berrah, "Intense Femtosecond X-ray Photoionization Studies of Nitrogen - How Molecules interact with Light from the LCLS" in Ultrafast Phenomena XVII, M. Chergui, D. M. Jonas, E. Riedle, R. W. Schoenlein, A. J. Taylor, Eds., Oxford University Press, 47 (2011).
6. I. Dumitriu, R. Bilodeau, D. Gibson, W. Walter, A. Aguilar E. Reed and N. Berrah "Photoionization of Fe^{+} ", Phys. Rev. A, **81**, 053404 (2010).
7. N. Berrah, R.C. Bilodeau, I. Dumitriu, D. Toffoli, and R. R. Lucchese, "Shape and Feshbach Resonances in Inner-Shell Photodetachment of Negative Ions, J. Elect. Spectr. and Relat. Phen. Kai Siegbahn Memorial Volume **183**, 64 (2011)

8. G. Doumy, C. Roedig, S.-K. Son, C. I. Blaga, A. D. DiChiara, R. Santra, N. Berrah, C. Bostedt, J. D. Bozek, P. H. Bucksbaum, J. P. Cryan, L. Fang, S. Ghimire, J. M. Glowia, M. Hoener, E. P. Kanter, B. Krässig, M. Kuebel, M. Messerschmidt, G. G. Paulus, D. A. Reis, N. Rohringer, L. Young, P. Agostini, and L. F. DiMauro, *Phys. Rev. Lett.* **106**, 083002 (2011).
9. I. Dumitriu, R. C. Bilodeau, T. W. Gorczyca, C. W. Walter, N. D. Gibson, Z. D. Pesic, D. Rolles and N. Berrah, “Inner-shell photodetachment from Ru⁺”, *Phys. Rev. A.* **82**, 043434 (2010).
10. N. Berrah, J. Bozek, J. T. Costello, S. Düstererd, L. Fanga, J. Feldhausd, H. Fukuzawae, M. Hoenera, Y. H. Jiang; P. Johnsson, E. T. Kennedy, M. Meyer,; R. Moshhammer, P. Radcliffed, M. Richter, A. Rouzée; A. Rudenko, . A. Sorokind, K. Tiedtke, K. Ueda, Ullrich, M. J. J. Vrakking “Non-linear processes in the interaction of atoms and molecules with intense EUV and X-ray fields from SASE free electron lasers (FELs)” *Journal of Modern Optics, Topical Review*, **57**, Issue 12, 1015 (2010).
11. L. Young, E. P. Kanter, B. Krässig, Y. Li, A. M. March, S. T. Pratt, R. Santra, S. H. Southworth, N. Rohringer, L. F. DiMauro, G. Doumy, C. A. Roedig, N. Berrah, L. Fang, M. Hoener, P. H. Bucksbaum, J. P. Cryan, S. Ghimire, J. M. Glowia, D. A. Reis. J. D. Bozek, C. Bostedt, M. Messerschmidt, “Femtosecond electronic response of atoms to ultraintense x-rays” *Nature* **466**, 56-61 (2010).
12. M. Hoener, D. Rolles, A. Aguilar, R. C. Bilodeau, D. Esteves, P. Olalde Velasco, Z. D. Pesic, E. Red, and N. Berrah, “Site-selective ionization and relaxation dynamics in heterogeneous nanosystems”, *Phys. Rev. A.* **81**, 021201(R) (2010).
13. R. C. Bilodeau, I. Dumitriu, N. D. Gibson, C. W. Walter and N. Berrah, “Promoting a core electron to fill a d-shell: Threshold law and shape and Feshbach resonances” *Phys. Rev. A.* **80**, 031403R (2009)
14. Berrah, D. Rolles, Z. D. Pesic, M. Hoener, H. Zhang, A. Aguilar, R. C. Bilodeau, E. Red, J. D. Bozek, E. Kuk, R. Dies Muino and G. ed Abajo, *Proceedings of Advances in X-ray and Inner-Shell Processes, Euro. Phys. J. Special Topics (EPJ) ST*, **169**, 59 (2009).
15. D Rolles, G Prumper, H Fukuzawa, X-J Liu, J Harries, K. Ueda, Z D Pešić, I Dumitriu and N Berrah , “Molecular-frame angular distribution of normal and resonant Auger electrons” *J. Phys Conf Series*, **212**, 012009 (2010).
16. Z. D. Pesic, D. Rolles, I. Dumitriu, and N. Berrah “Fragmentation Dynamics of Gas-Phase Furan Following K-shell Ionization” *Phys. Rev. A* **82**, 013401 (2010).
17. D. Rolles, H. Zhang, Z. D. Pešić, J. D. Bozek, and N. Berrah “ Emergence of Band Structure in Valence Photoemission from Rare Gas Clusters” *Chem. Phys. Lett.* **468**, 148 (2009).
18. N. Berrah, D. Rolles, Z. D. Pesic, M. Hoener, H. Zhang, A. Aguilar, R. C. Bilodeau, E. Red, J. D. Bozek, E. Kuk, R. Dies Muino and G. Abajo, “Probing free Xe clusters from within” *Euro. Phys. J. Special Topics (EPJ) ST*, **169**, 59 (2009).
19. H. Zhang, D. Rolles, J. D. Bozek R. Bilodeau and N. Berrah, “ Photoionization of argon clusters in the Ar 3s→np Rydberg resonance region”, *J. Phys. B: At. Mol. Opt. Phys.*, **42**, 105103, (2009).

Reactive Scattering of Ultracold Molecules

Principal Investigator

John Bohn
JILA, UCB 440
University of Colorado
Boulder, CO 80309
Phone (303) 492-5426
Email bohn@murphy.colorado.edu

Program Scope

Upon renewal last year, this program has made a major shift in emphasis, from studying the many-body physics of quantum gases with strong anisotropic interactions, to understanding the collision dynamics of pairs of ultracold molecules. The unprecedented energy resolution afforded by molecular gases at sub-milliKelvin temperatures should enable new insights into the physics of the elementary chemical act. In these experiments, the incident channel of the reactants can be completely specified in terms of the internal state, as well as an extremely low relative translational energy that, in favorable cases, allows probing the reactivity of a single partial wave in the incident channel. The slowly-moving reactants are susceptible to probing and manipulation via electric, magnetic, optical, and microwave fields; dependence of reaction rates on these many variables may offer novel insights into the reaction.

Recent Progress

As a prelude to deciphering chemical reaction dynamics, it is worthwhile to appreciate the complexity of *nonreactive* collision partners. To this end we have begun with the nonreactive scattering of Rb atoms with KRb molecules, both prepared in their ground states, and colliding with translational kinetic energies in the neighborhood of 1 μ K. The Rb-K-Rb collision complex is expected to be quite rich with resonances, owing to virtual excitations into ro-vibrational states. This is not the case in the widely-studied case of cold collisions of molecules with helium atoms, because there the potentials are far shallower and the density of resonance states far lower.

Resonances, especially those that can be tuned with electric and magnetic fields, represent the primary means in ultracold scattering to deliver information on the collision complex. It is therefore worthwhile to see the effect of a large density of resonant states on the situation. To this end we have developed a qualitative model of the Rb+KRb collision system. The model is based on the conceptual division between ro-vibrational resonant states that occur at small values of the intermolecular separation R , versus threshold scattering and the effects of magnetic fields, which occur at large R . The latter are treated exactly by means of a quantum defect treatment of long-range matching functions. The former are treated within a statistical model borrowed from nuclear physics,

whereby the scattering is assumed to be chaotic and the distribution of levels satisfies the statistics of the Gaussian Orthogonal Ensemble.

For a realistic density of states, the kind of resonant structure that may be qualitatively expected is shown in the figure below. These represent possible ro-vibrational resonances for incident s-wave collisions of Rb+KRb, as a function of magnetic field. The large number of such resonances suggests that identifying individual resonances may be an extremely difficult task. Rather, it may be that a statistical treatment of scattering may be all that is possible for such collision partners. For example, accounting for a finite magnetic field resolution, the resonances are not individually identifiable (black line). They nevertheless exhibit fluctuations (Ericson fluctuations) whose statistical properties are understood. Thus in experiments, the emphasis may have to shift from identifying and exploiting individual resonances, to using statistical information to glean something of the short-range interaction.

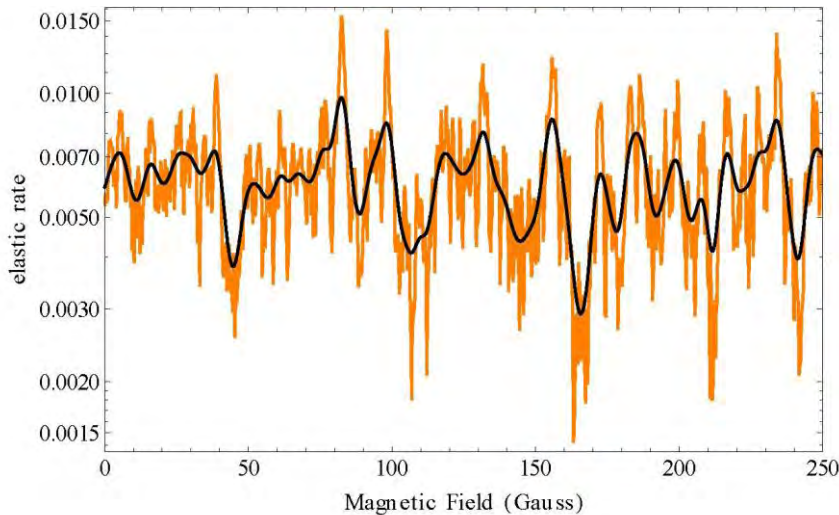


Figure. Model spectrum of Rb atoms colliding with KRb molecules in a $T=1 \mu\text{K}$ gas, as a function of applied magnetic field. The spectrum is filled wall-to-wall with ro-vibrational resonances of the Rb-K-Rb complex. At finite magnetic field resolution of 1 Gauss (black line), the spectrum consists of fluctuations around a mean value, rather than individually resolvable resonances.

A second project developing along with similar lines seeks to understand the cold collision dynamics of dysprosium, which has recently been successfully cooled and trapped at the University of Illinois. In this context dysprosium represents a useful way station between simpler atoms like alkalis, whose cold collision dynamics is well-understood; and molecular scattering, where, as noted above, resonant scattering may be hard to interpret in detail. The Dy_2 interaction resolves at short-range into 153 distinct born-Oppenheimer potential energy curves. We have written the close-coupling code for these collisions, using potential energies developed by Svetlana Kotochigova at Temple University, we and are beginning to characterize the scattering, again relying heavily on quantum defect methods to simplify computation and analysis.

Finally, there remains a last project from the previous funding cycle. In this case, we have considered the anisotropy of the Landau superfluid critical velocity in the presence of anisotropic dipole-dipole forces. This anisotropy can likely be seen by an experiment that slowly moves a probe, such as a blue-detuned laser beam, through a dipolar Bose-Einstein condensate. A probe moving above the critical velocity will excite vortices, corresponding to a drag force on the probe, whereas a more slowly-moving probe spins off no vortices and feels no such force. We have shown that at a given velocity the drag force may occur for a probe moving in one direction but not the other.

Future Plans

Immediate plans are to bring the Dy-Dy collisions on line to assess their resonant structure and sensitivity to short-range parameters. Are scattering lengths for all 153 born-Oppenheimer curves required, or only a subset? Also, for molecules, we will continue to explore the influence of a high density of states on such things as the Wigner threshold laws and observable transition rates. This will all need to be translated to the case of molecule-molecule scattering, where the density of states is much higher.

DOE-supported publication in the past three years

How Does a Dipolar Bose-Einstein Condensate Collapse?

J. L. Bohn, R. M. Wilson, and S. Ronen, Proceedings of the 17th International Laser Physics Conference, published in Laser Physics **19**, 547 (2009).

Angular Collapse of Dipolar Bose-Einstein Condensates

R. M. Wilson, S. Ronen, and J. L. Bohn, Phys. Rev. A **80**, 023614 (2009).

Critical Superfluid Velocity in a Trapped Dipolar Gas

R. M. Wilson, S. Ronen, and J. L. Bohn, Phys. Rev. Lett. **104**, 094501 (2010).

Zero Sound in Dipolar Fermi Gases

S. Ronen and J. L. Bohn, Phys. Rev. A **81**, 033601 (2010).

Anisotropic Superfluidity in a Dipolar Bose Gas

C. Ticknor, R. M. Wilson, and J. L. Bohn, Phys. Rev. Lett. **106**, 065301 (2011).

Emergent Structure in a Dipolar Bose Gas in a One-Dimensional Lattice

R. M. Wilson and J. L. Bohn, Phys. Rev. A **83**, 023623(2011).

Ultrafast Electron Diffraction from Aligned Molecules

Martin Centurion

Department of Physics and Astronomy, University of Nebraska, Lincoln, NE 68588-0299
mcenturion2@unl.edu

Program Scope or Definition

The aim of this project is to record time-resolved electron diffraction patterns of aligned molecules and to reconstruct the 3D molecular structure. The molecules will be aligned non-adiabatically using a femtosecond laser pulse. A femtosecond electron pulse will then be used to record a diffraction pattern while the molecules are aligned. The experiment consists of a laser system, a pulsed electron gun, a gas jet that contains the target molecules and a detector to capture the diffraction patterns. The diffraction patterns will then be processed to obtain the molecular structure.

Introduction

The experiment will consist of three main components: the electron gun, the laser system and the experimental chamber. First, a seeded supersonic gas jet is used to introduce the target molecules into the experiment and to cool the rotational temperature. A sample of molecules with a low rotational temperature will lead to a higher degree and duration of the alignment. Then, a femtosecond laser pulse intersects the molecules and aligns them along the direction of the laser polarization. The alignment survives only for a short time after the laser traverses the gas jet. A short electron pulse is then used to probe the molecules. The electron pulse is generated using an electron gun that is synchronized with the laser pulses. A small fraction of the laser energy is used to trigger electron emission from a photocathode, and the electrons are accelerated in a static field and collimated before reaching the target. The diffraction pattern from the aligned molecules is captured in a custom-made detector, and the image is stored on the computer for analysis.

A key to the success of the experiment is to capture the diffraction pattern during the short time in which the molecules are aligned. Previous experiments have shown that it is possible to observe conformational changes in isolated molecules with picosecond resolution using gas electron diffraction [1,2]. Recent experiments have shown that a temporal resolution of 3 ps is sufficient to detect the alignment following a dissociation reaction [3]. However, in order to extract 3D structural information from the diffraction patterns it is necessary to reach a higher degree of alignment. This can be achieved by using non-adiabatic alignment and improving the temporal resolution. A resolution of < 1 ps will allow us to capture the diffraction pattern while the distribution of molecules still shows a high degree of alignment. The current setup will also feature a detector with single-electron sensitivity. The detector consists of a phosphor screen, image intensifier and CCD which are all fiber coupled to maximize the transmission through each element. The phosphor screen converts each incident electron into photons which are

transmitted to the image intensifier and multiplied before reaching the CCD. Each incident electron will generate sufficient counts on the CCD to be detected. In addition, the current experiment will be performed at a repetition rate of 10 kHz, compared to 1 kHz of previous experiments, which will result in a significant improvement in the signal to noise ratio of the diffraction patterns.

Recent Progress

The main components of the experiment are operational, and we have performed several preliminary experiments for calibration. A stable electron beam with energy of 25 keV is now available. The home-made solenoid lens used to focus the electron beam has been tested and performs according to our calculations. We have also made progress in two key areas of the experiment: detector calibration and finding of time-zero. On the theory side, we have developed the tools to numerically simulate diffraction patterns from aligned molecules.

Detector calibration: The detector has been calibrated by reducing the electron current to the point where we can detect individual electrons. We have measured the average number of counts on the CCD by a single electron hitting the detector, as a function of the gain on the image intensifier. We can now calculate the electron current from the total intensity in the detector. We estimate that with a current of 1000 electrons per pulse it will take 20 minutes to record a diffraction pattern, which means that it will be possible to do a time-scan in a single day. With this charge, our simulations predict a pulse duration of 300 fs at the target.

Time zero: We have experimentally determined the temporal and spatial overlap of the electron and laser pulses. Given that it takes several minutes to capture a diffraction pattern, it is necessary to have an independent method to determine the overlap of laser and electrons spatially and temporally (time-zero). We have achieved both using the laser to ionize a gas target. The gas is introduced in a 100 micrometer gas jet using a Laval nozzle. We had success with both nitrogen and helium as the target. After the laser ionizes the target atoms, some electrons are accelerated to sufficiently high energies to escape from the plasma region. This effect was studied in a previous publication [4]. The separation between plasma electrons and the resulting positively charged plasma core creates transient electric and magnetic fields that deflect the incoming electron pulse. Figure 1 shows two images of the electron beam, with the electron beam arriving (a) 5 ps before and (b) 5 ps after the laser. In this case the electron beam is not focused and it has a diameter of 4 mm on the detector. The shadow near the top of the image is the nozzle from which the gas jet is introduced. After the laser ionized the gas, plasma electrons move away from the focus, which results in a deflection of the incoming electron pulse away from the plasma region, as seen in part (b). The position of the laser beam with respect to the nozzle can be determined by observing the position of the plasma. The temporal overlap (time-zero) can be determined by measuring the changes in the electron beam. Figure 1c shows the intensity of the electron beam at the position of the laser focus. The intensity decreases to a half after 6 ps, with this time constant determined by the plasma dynamics and not the pulse duration.

The time-zero can be determined more accurately by looking at the region where the effect is first seen. We expect that this will determine the time-zero to within 1 ps.

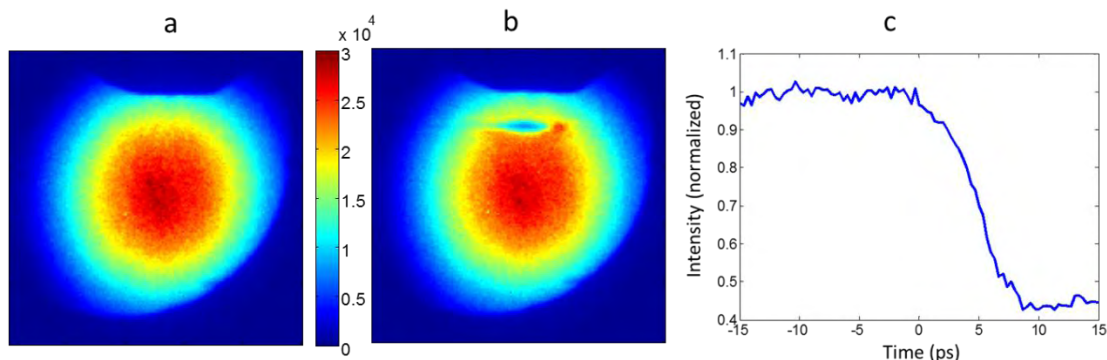


Figure 1. Finding the spatial and temporal overlap between electron and laser pulses. a) Image of the electron beam for the case of the electron pulse arriving at the target 5 ps before the laser pulse ($T = -5$ ps). b) Image of the electron beam for the case of the electron pulse arriving 5 ps after the laser pulse ($T = 5$ ps). In the images, the laser propagates from left to right. c) Intensity of the electron beam at the laser focus as a function of time delay. The laser-induced plasma deflects the electrons away from the plasma region.

Simulations: We have simulated the electron diffraction pattern of aligned molecules by calculating the electron scattering from a molecule. Figure 2 shows, as an example, the diffraction patterns calculated for Ozone (O_3). The O_3 molecule is bent with an angle of 116.8° . The figure shows the scattering intensity of the O_3 molecule divided by the scattering intensity of isolated oxygen atoms $I_S(O_3)/3I_S(O)$. The rescaling was necessary to visualize the diffraction rings in the case of randomly oriented molecules, where the modulation depth due to the interference is very weak. Figure 2a shows the resulting pattern for random orientation of the molecules, while Figure 2b shows the pattern for the case of aligned molecules. In this example the molecules are perfectly aligned, so the modulation of the diffraction pattern is maximized. We can now also calculate the diffraction pattern for any given degree of alignment by superimposing the diffraction pattern of molecules with a distribution of orientations.

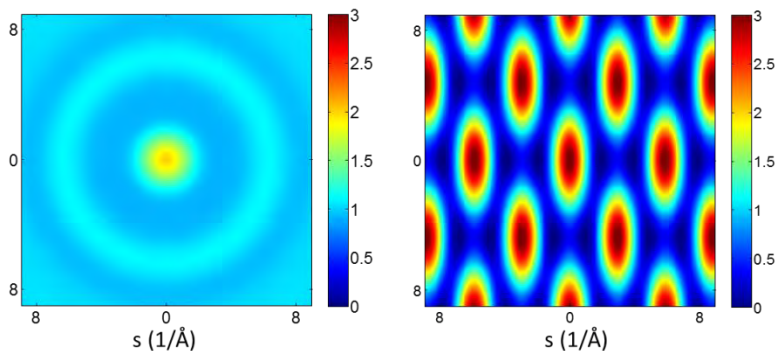


Figure 2. Simulations of diffraction patterns of ozone (O_3) molecules. Total scattering intensity of the ozone molecule divided by the scattering intensity of isolated atoms $I_S(O_3)/3I_S(O)$. a) Randomly oriented molecules (gas phase). b) Aligned (fixed in space) molecules.

Future Plans

We plan to take time-resolved diffraction patterns over the next few months. The target will be prepared by mixing the molecule of interest with helium and then using a Laval nozzle to create a supersonic gas jet in the chamber. We have already installed the Laval nozzles, which have an inner diameter of 30 μm and outer diameter of 90 μm , and the gas mixing setup is under construction. A laser pulse will be used to create a sample of non-adiabatically aligned molecules. We will then record diffraction patterns as a function of the delay between laser and electrons. There are several candidate molecules for first experiments, linear molecules such as carbon dioxide or carbon disulfide would be interesting because they would clearly show the effect of the laser, and the diffraction patterns will be relatively simple to analyze. A more complex molecule such as CF_3I would also be a good candidate because it will provide an example of a non-planar molecule.

We expect to see a large anisotropy in the diffraction pattern when the molecules are at the highest degree of alignment. In parallel to these experiments, we will work to develop the tools to analyze and recover structural information from the diffraction patterns. The reconstruction of structure from anisotropic diffraction patterns is currently an active area of research [5-6], and we expect to build on the existing work. Future experiments will also include extending the alignment method to 3D alignment by using a pair of alignment pulses (or elliptically polarized pulses), diffracting from larger molecules and studying ultrafast conformational changes in molecules.

References

- [1] H. Ihee, V. A. Lobastov, U. M. Gomez et al., "Direct imaging of transient molecular structures with ultrafast diffraction", *Science* 291, 458 (2001)
- [2] S. T. Park, A. Gahlmann A, Y. G. He et al., "Ultrafast Electron Diffraction Reveals Dark Structures of the Biological Chromophore Indole", *Angew. Chem. Int. Ed* 47, 9496 (2008)
- [3] P. R. Reckenthaeler, M. Centurion, W. Fuss et al., "Time-resolved electron diffraction from selectively aligned molecules" *Phys. Rev. Lett.* 102, 213001 (2009)
- [4] M. Centurion et al *Nature Photonics*
- [5] D. K. Saldin, V. L. Shneerson, D. Starodub D et al., "Reconstruction from a single diffraction pattern of azimuthally projected electron density of molecules aligned parallel to a single axis", *ACTA CRYSTALLOGR A* 66, 32 (2010).
- [6] P. J. Ho, D. Starodub, D. K. Saldin, et al., "Molecular structure determination from x-ray scattering patterns of laser-aligned symmetric-top molecules", *J. of Chem. Phys.* 131, 131101 (2009).

References to publications of DOE sponsored research that have appeared in the past 3 years or that have been accepted for publication.

None.

Atomic and Molecular Physics in Strong Fields

Shih-I Chu

Department of Chemistry, University of Kansas

Lawrence, Kansas 66045

E-mail: sichu@ku.edu

Program Scope

In this research program, we address the fundamental physics of the interaction of atoms and molecules with intense ultrashort laser fields. The main objectives are to develop new theoretical formalisms and accurate computational methods for *ab initio* nonperturbative investigations of multiphoton quantum dynamics and very high-order nonlinear optical processes of one-, two-, and many-electron quantum systems in intense laser fields, taking into account detailed electronic structure information and many-body electron-correlated effects. Particular attention will be paid to the exploration of the effects of electron correlation on high-harmonic generation (HHG) and multiphoton ionization (MPI) processes, multi-electron response and underlying mechanisms responsible for the strong-field ionization of diatomic and small polyatomic molecules, time-frequency spectrum, coherent control of HHG processes for the development of tabletop x-ray laser light sources, and for the exploration of attosecond AMO processes, etc.

Recent Progress

1. Probing the Origin of Elliptical High-order Harmonic Generation from Aligned Molecules in Linearly Polarized Laser Field

For ensembles of atoms or unaligned molecules, the polarization of the harmonics is expected to be the same as the polarization of the driving laser field. For aligned molecules, however, the harmonic radiation has two components: one parallel and another perpendicular to the laser polarization direction. Experiments showed that the linear polarization state of HHG driven by linearly polarized laser fields is tilted due to the nonvanishing perpendicular component of HHG. A recent experiment [1] has demonstrated that elliptically polarized high-order harmonic generation (HHG) can be produced from linearly polarized driving fields for aligned molecular systems. In order to reveal the underlying physical mechanisms of elliptical harmonics, we present fully *ab initio* and high-precision calculations and analyses of the amplitude, phase, and polarization state of the harmonic radiation from molecular hydrogen ions with arbitrary orientation [2]. We find that high ellipticity arises from molecular orbital symmetry and two-center interference effects. Our *ab initio* exploration and findings lead to a general rule that the ellipticity becomes high for molecular orbitals represented by a symmetric combination of atomic orbitals, whereas it becomes low for molecular orbitals represented by an antisymmetric combination. This finding also applies to the general case of aligned linear molecules [2].

2. Accurate Treatment of Above-Threshold-Ionization Spectra from Core Region of Time-Dependent Wave Packet: A New *ab initio* Time-Dependent Approach

The phenomenon of multiphoton above-threshold ionization (ATI) and the investigation of the resulting electron angular distributions have attracted much recent interest. This is related to advances in laser technology which made possible generation of ultrashort and intense laser pulses. For such pulses, the absolute or carrier-envelope phase (CEP) plays an important role and properties of the ejected electrons momentum (or energy–angular) distributions differ significantly from those for long pulses. Recent experiments were able to measure high-resolution fully differential data on ATI of noble gases. Thus accurate theoretical description of the electron distributions becomes an important and timely task.

In a recent work, we develop a new method for the accurate treatment of TDSE and electron energy and angular distributions after above-threshold multiphoton ionization [3]. The procedure does not require propagation of the wave packet at large distances, making use of the wave function in the core region. It is based on the extension of the Kramers–Henneberger picture of the ionization process while the final expressions involve the wave function in the laboratory frame only. The approach is illustrated by a case study of above-threshold ionization of the hydrogen atom subject to intense laser pulses. The ejected electron energy and angle distributions have been calculated and analyzed. We explore the electron spectrum dependence on the duration of the laser pulse and carrier-envelope phase [3].

3. High Precision Study of the Orientation Effects in MPI/HHG of H_2^+ in Intense Laser Fields

Recently we have developed a time-dependent generalized pseudospectral (TDGPS) method for accurate and efficient treatment of the time-dependent Schrödinger equation (TDSE) of two-center diatomic molecules systems in prolate spheroidal coordinates [4,5,6]. This method naturally accounts for the symmetry of diatomic molecules and provides accurate description of Coulomb singularities due to non-uniform distribution of the grid points. The GPS method delivers high accuracy while using only moderate computer resources; it is easy to implement since no calculation of potential matrix elements is required, and kinetic energy matrices have simple analytical expressions. The method is applied to a fully *ab initio* 3D study of the orientation effects in MPI and HHG of H_2^+ subject to intense laser pulses. We discuss the multiphoton resonance and two-center interference effects in the HHG spectra which can lead both to enhancement and suppression of the harmonic generation [5,6].

4. Exploration of the Role of the Electronic Structure and Multi-electron Response in the MPI and HHG Processes of Diatomic Molecules in Intense Laser Fields

There have been much recent experimental and theoretical interests in the study of strong-field molecular ionization and HHG. Most theoretical studies in the recent past are based on approximate models such as the ADK model, strong-field approximation, etc. The effects of detailed electronic structure and multi-electron responses are often ignored. Although these models have some partial success in weaker field processes, they cannot provide an overall consistent picture of the ionization and HHG behavior of different molecules.

We have recently extended the *self-interaction-free* TDDFT [7] for nonperturbative investigation of the ionization mechanisms and the HHG power spectra of homonuclear (N_2 , O_2 , and F_2) and heteronuclear (CO) diatomic molecules in intense ultrashort lasers [8] for the case that the laser polarization axis parallels the molecular axis. Our studies reveal several intriguing behaviors of the nonlinear responses of molecules to intense laser fields: (a) It is found that detailed electron structure and correlated multielectron responses are important factors for the determination of the strong-field ionization behavior. Further, it is not adequate to use only the highest occupied MO (HOMO) for the description of the ionization behavior since the inner valence electrons can also make significant or even dominant contributions. (b) We predict substantially different nonlinear optical response behaviors for homonuclear (N_2) and heteronuclear (CO) diatomic molecules. In particular, we found that the MPI rate for CO is higher than that of N_2 . Furthermore, while laser excitation of the N_2 molecule can generate only odd harmonics, both even and odd harmonics can be produced from the CO molecule [8].

More recently, we have further extended the *all-electron* TDDFT approach [7,8] to the study of the effect of correlated multielectron responses on MPI and HHG of homonuclear diatomic molecules N_2 , O_2 , and F_2 [9,10] and heteronuclear diatomic molecules (CO, BF, and HF) [11] in intense short laser pulses with arbitrary molecular orientation. We show that the contributions of inner molecular orbitals to the total MPI and HHG rates can be significant or even dominant over the HOMO, depending upon detailed electronic structure and symmetry, laser field intensity, and orientation angle. Furthermore, we found that the HHG spectrum for homonuclear molecules features a destructive interference of MO contributions while heteronuclear molecules show mostly constructive interference of orbital contributions [11].

5. Theoretical study of Orientation-dependent MPI of Small Polyatomic Molecules in Intense Ultrashort Laser Fields: A New Time-Dependent Voronoi-Cell Finite Difference Method

We develop a new grid-based time-dependent method for accurate investigation of multiphoton ionization (MPI) of small polyatomic molecules in intense ultrashort laser fields [12,13]. The electronic structure of polyatomic molecules is treated by the density-functional theory (DFT) with proper long-range potential and the Kohn–Sham equation is accurately solved by means of the Voronoi-cell finite difference (VFD) method on non-uniform and highly adaptive molecular grids utilizing geometrical flexibility of the Voronoi diagram. This method is generalized to the time-dependent problems with the split-operator time-propagation technique in the energy representation, allowing accurate and efficient non-perturbative treatment of attosecond electronic dynamics in strong fields [12]. The new procedure is applied to the study of MPI of N_2 and H_2O molecules in intense linearly-polarized and ultrashort laser fields with arbitrary field–molecule orientation [12]. Our results demonstrate that the orientation dependence of MPI is determined not just by the HOMO but also by the symmetries and dynamics of other contributing MOs. In particular, the inner MOs can show dominant contributions to the ionization processes when the molecule is aligned in some specific directions w.r.t. the field polarization. This feature suggests a new way to selectively probe individual orbitals in strong-field electronic dynamics.

More recently, we have extended the TDVFD method to the study of multi-electron effects on the orientation dependence and photoelectron angular distribution (PAD) of multiphoton ionization of CO_2 in strong laser fields [13]. We performed TDDFT calculations for CO_2 by means of the TDVFD method with highly adaptive molecular grids. Calculated orientation-dependent plot of CO_2 MPI shows the center-fat propeller shape with 40° maximum, which is mainly contributed by two perturbed HOMOs. Our prediction agrees well with the recent experiments [14,15]. The PAD with various orientations illustrates characteristics of the HOMO symmetry including the nodal shapes and the peak spot at the field direction, explaining suppression and enhancement of MPI at corresponding orientation. It supports the relation between the orientation dependence of MPI and the orbital symmetry.

6. Precision Calculation of Above-threshold Multiphoton Ionization in Intense Short-wavelength Laser Fields: The Momentum-space Approach and Time-dependent Generalized Pseudospectral Method

We develop a new approach in momentum (P) space for the accurate study of multiphoton and above-threshold ionization (ATI) dynamics of atomic systems driven by intense laser fields [16]. In this approach, the electron wave function is calculated by solving the P -space time-dependent Schrödinger equation (TDSE) in a finite P -space volume under a simple zero asymptotic boundary condition. The P -space TDSE is propagated accurately and efficiently by means of the time-dependent generalized pseudospectral method (TDGPS) with optimal momentum grid discretization and a split-operator time propagator in the *energy* representation. The differential ionization probabilities are calculated directly from the continuum-state wave function obtained by projecting the total electron wave function onto the continuum-state subspace using the projection operator constructed by the continuum eigenfunctions of the unperturbed Hamiltonian. As a case study, we apply this approach to the nonperturbative study of the multiphoton and ATI dynamics of a hydrogen atom exposed to intense shortwavelength laser fields. High-resolution photoelectron energy-angular distribution and ATI spectra have been obtained. We find that with the increase of the laser intensity, the photoelectron energy-angular distribution changes from circular to dumbbell shaped and is squeezed along the laser field direction. We also explore the change of the maximum photoelectron energy with laser intensity and strong-field atomic stabilization phenomenon in detail [16].

7. Generalized Floquet Treatment of Multiphoton Quantum Interference in a Superconducting Qubit Driven by a Strong ac Field.

We extend a generalized Floquet formulation [17] for the nonperturbative treatment of multiphoton quantum interference in a strongly driven superconducting flux qubit [18]. The periodically time-dependent Schrödinger equation can be reduced to an equivalent time independent infinite-dimensional Floquet matrix eigenvalue problem. For resonant or nearly resonant multiphoton transitions, we extend the generalized Van Vleck (GVV) nearly degenerate high-order perturbation theory for the treatment of the Floquet Hamiltonian, allowing the reduction of the infinite-dimensional Floquet matrix to an $N \times N$ effective Hamiltonian, where N is the number of eigenstates under consideration. The GVV approach allows accurate treatment of ac Stark shift, power broadening, time-dependent and time-averaged transition probability, etc., well beyond the rotating wave approximation. We extend the Floquet and GVV approaches for numerical and analytical studies of the multiphoton resonance processes and quantum interference phenomena for the superconducting flux qubit system ($N=2$) driven by intense ac fields.

Future Research Plans

In addition to continuing the ongoing researches discussed above, we plan to initiate the following several new project directions: (a) Further development of TDVFD method to the study of HHG in triatomic molecular systems. (b) Development of time-dependent *localized* Hartree-Fock (LHF)-DFT method for the study of singly, doubly, and triply excited states of Rydberg atoms and ions, inner shell excitations [19], as well as photoionization of atomic excited states [20]. (c) Extension of the TDGPS method in momentum space to the study of HHG processes in intense ultrashort laser fields. (d) Development of coupled coherent-state approach [21] and coherent-state Ehrenfest trajectory (CSET) approach [22] for probing atomic and molecular processes in intense long-wavelength laser fields. (e) Coherent control of rescattering and attosecond phenomena in strong ultrashort fields.

References Cited (* Publications supported by the DOE program in the period of 2009-2011.)

- [1] Xibin Zhou, Robynne Lock, Nick Wagner, Wen Li, Henry C. Kapteyn, and Margaret M. Murnane, Phys. Rev. Lett. **102**, 073902 (2009).
- *[2] S. K. Son, D. A. Telnov, and S. I. Chu, Phys. Rev. A **82**, 043829 (2010).
- *[3] D. Telnov and S. I. Chu, Phys. Rev. A **79**, 043421 (2009).
- [4] X. Chu and S. I. Chu, Phys. Rev. A **63**, 023411 (2001).
- [5] D. A. Telnov and S. I. Chu, Phys. Rev. A **76**, 043412 (2007).
- *[6] D. A. Telnov and S. I. Chu, Computer Phys. Comm. **182**, 18 (2011).
- [7] S. I. Chu, J. Chem. Phys. **123**, 062207 (2005). (Invited review article).
- [8] J. Heslar, J. Carrera, D. Telnov, and S. I. Chu, Int. J. Quantum Chem. **107**, 3159 (2007).
- *[9] D. A. Telnov and S. I. Chu, Phys. Rev. A **79**, 041401(R) (2009).
- *[10] D. A. Telnov and S. I. Chu, Phys. Rev. A **80**, 043412 (2009).
- *[11] J. Heslar, D. Telnov, and S. I. Chu, Phys. Rev. A **83**, 043414 (2011).
- *[12] S. K. Son and S. I. Chu, Chem. Phys. **366**, 91 (2009).
- *[13] S. K. Son and S. I. Chu, Phys. Rev. A **80**, 011403(R) (2009).
- [14] I. Thomann *et al.*, J. Phys. Chem. A **112**, 9382 (2008).
- [15] D. Pavičić, K. F. Lee, D. M. Rayner, P. B. Corkum, and D. M. Villeneuve, Phys. Rev. Lett. **98**, 243001 (2007).
- *[16] Z. Y. Zhou and S. I. Chu, Phys. Rev. A **83**, 013405 (2011).
- [17] S. I. Chu and D. A. Telnov, Phys. Rep. **390**, 1-131 (2004).
- *[18] S. K. Son, S. Y. Han, and S. I. Chu, Phys. Rev. A **79**, 032301 (2009).
- [19] Z. Y. Zhou and S. I. Chu, Phys. Rev. A **75**, 014501 (2007).
- *[20] Z. Y. Zhou and S. I. Chu, Phys. Rev. A **79**, 053412 (2009).
- *[21] J. Guo, X. S. Liu, and S. I. Chu, Phys. Rev. A **82**, 023402 (2010).
- *[22] Z. Y. Zhou and S. I. Chu, Phys. Rev. A **83**, 033406 (2011).

Formation of Ultracold Molecules

Robin Côté

Department of Physics, U-3046
University of Connecticut
2152 Hillside Road
Storrs, Connecticut 06269

Phone: (860) 486-4912
Fax: (860) 486-3346
e-mail: rcote@phys.uconn.edu
URL: <http://www.physics.uconn.edu/~rcote>

Program Scope

Current experimental efforts to obtain ultracold molecules (*e.g.*, photoassociation (PA), buffer gas cooling, or Stark deceleration) raise a number of important issues that require theoretical investigations and explicit calculations.

This Research Program covers interconnected topics related to the formation of ultracold molecules. We propose to investigate schemes to form ultracold molecules, such as homonuclear dimers (alkali or alkaline earth) using stimulated and spontaneous processes. We will also study heteronuclear molecules, in particular those with large dipole moments like alkali hydrides or some bi-alkali dimers (*e.g.* LiCs or LiRb). In addition, we will investigate the enhancement of the formation rate via Feshbach resonances, paying special attention to quantum degenerate atomic gases. Finally, we will explore the possible formation of a new and exotic type of molecules, namely ultralong-range Rydberg molecules.

Recent Progress

Since the start of this Program (August 1st 2005), we have worked on several projects. We limit ourselves to work published over the last three years (since 2008).

• Formation of homonuclear and heteronuclear molecules

In two previous papers sponsored by DOE [E. Juarros *et al.*, Phys. Rev. A **73**, 041403(R) (2006), and E. Juarros *et al.*, J. Phys. B **39**, S965 (2006)], we explored the formation of LiH and NaH in their $X^1\Sigma^+$ ground electronic state from one- and two-photon photoassociative processes. Recently, we extended this work to the formation of LiH molecules in the $a^3\Sigma^+$ electronic state [1]. It is predicted to support one ro-vibrational level, leading to a sample in a pure single ro-vibrational state. We found that very large rate coefficients can be obtained by using the $b^3\Pi$ excited state, which supports only seven bound levels. Because of the extreme spatial extension of their last “lobe”, the wave functions of the two uppermost bound levels have large overlap with the ($v = 0, J = 0$) bound level of $a^3\Sigma^+$, leading to branching ratios ranging from 1% to 90%. This property implies that large amounts of LiH molecules could be produced in a single quantum state, a prerequisite to study degenerate molecular gases [1]. In this work, we also discuss the implication of the statistics of the components of LiH (fermions or bosons) on the chemical reaction rates when colliding with H, Li, or LiH.

We also extended our earlier studies of PA in ^{86}Sr and ^{88}Sr atoms, together with Killian’s group at Rice University, and analyzed results from two-photon photoassociative spectroscopy of the least-bound vibrational level ($v = 62$) of the $X^1\Sigma_g^+$ state of the $^{88}\text{Sr}_2$ dimer [2]. By combining measurements of the binding energy with an accurate short range potential and calculated van der Waals coefficients, we were able to determine the *s*-wave scattering length $a_{88} = -1.46a_0$. We also modeled the observed Autler-Townes resonance splittings. Through mass scaling, we determined the scattering lengths for all other isotopic combinations. These measurements provide confirmation of atomic structure calculations for alkaline-earth atoms and provide valuable input for future experiments with ultracold strontium.

We suggested and analyzed a technique for efficient and robust creation of dense ultracold molecular ensembles in their ground rovibrational state [3]; a molecule is brought to the ground state through a series of intermediate vibrational states via a multistate chainwise stimulated Raman adiabatic passage technique. We studied the influence of the intermediate states decay on the transfer process and suggested an approach that minimizes the population of these states, resulting in a maximal transfer efficiency. As an example, we analyzed the formation of $^{87}\text{Rb}_2$ starting from an initial Feshbach molecular state and taking into account major decay mechanisms due to inelastic atom-molecule and molecule-molecule collisions. Numerical analysis suggests a transfer efficiency $> 90\%$, even in the presence of strong collisional relaxation.

• **Rydberg-Rydberg interactions**

We extended our previous work Rydberg-Rydberg interactions explaining spectral features observed in ^{85}Rb experiments, namely a resonance correlated to the $69p_{3/2} + 71p_{3/2}$ asymptote [J. Stanojevic *et al.*, *Eur. Phys. J. D* **40**, 3 (2006)], to the case of strong resonances near the $69d + 70s$ asymptote [4] when exciting $70p$ atoms. We found that such resonances are again attributed to strong ℓ -mixing. In this particular case, the resonances occur at energies corresponding to excited atom pairs $(n-1)d + ns$. We also obtained the n -scaling of both the position and size of the resonances, n^{-3} and $n^{8.5}$, respectively. Our results agree well with measurements.

In a more recent work [5], we investigate the interaction between two rubidium atoms in highly excited Rydberg states, and show the existence of potential wells for 0_g^+ symmetry of doubly-excited atoms due to ℓ -mixing. These wells are shown to be robust against small electric fields [6], and to support many bound states. We calculated their predissociation and show that their lifetimes are limited by the lifetime of the Rydberg atoms themselves. We also study how these vibrational levels could be populated via photoassociation, and how the signature of the ad-mixing of various ℓ -character producing the potential wells becomes apparent in photoassociation spectra [5,6].

• **Influence of Feshbach resonances on formation rates**

We have started to investigate the formation of polar molecules using photoassociation (PA) of atoms in mixtures in the vicinity of Feshbach resonances [7]. We focused our attention on heteronuclear dimers for which the presence of a permanent dipole moment allows transitions from the continuum directly to a rovibrational level v of the ground electronic molecular states. The corresponding photoassociation rate coefficient $K_{\text{PA}}^v = \langle v_{\text{rel}} \sigma_{\text{PA}}^v \rangle$ depends on v_{rel} , the relative velocity of the colliding pair, and on σ_{PA}^v , the PA cross section. The bracket stands for an average over the distribution of v_{rel} : for heteronuclear systems, it is a Maxwell-Boltzmann distribution characterized by the temperature T . We calculated the rate coefficients to form singlet molecules of LiNa using this Feshbach Optimized Photoassociation (FOPA) mechanism. To do so, we adapted our computer codes to not only calculate the scattering problem with all hyperfine couplings in a magnetic field, but also to give the wave functions for all channels, and their projection on the singlet electronic state $X^1\Sigma^+$. We found that the rate coefficients increase by 10^{3-4} when compared to the off-resonance rate coefficients [7]). We also gave a simple analytical expression based on a two-channel model relating the rate coefficient to the off-resonance rate coefficient and parameters of the resonance (such as its position and width); the model reproduces very well the results of our fully-coupled numerical problem.

We expanded this work to take into account the effect of saturation on the rate coefficient [8]. We computed rate coefficients and showed that new double-minima features would appear at large laser intensity near the resonance. We compared our theoretical results with recent experimental measurements on ^7Li obtained by Hulet and co-workers at Rice University, and found a good agreement without any adjustable parameters.

We combined this idea of FOPA with our previous work using STIRAP [9]. We showed that it is possible to enhance the Rabi frequency between the continuum and an intermediate state so that the efficient transfer of a pair of atoms directly from the continuum into the ro-vibrational ground state becomes achievable with moderate laser intensities and pulse durations. This approach opens interesting perspectives, since it does not require degenerate gases to work efficiently.

Finally, we also explored the role of Feshbach resonance and spin-orbit coupling in the formation of ultracold LiCs molecules [10]. We analyzed the experimental data of our co-workers, and found that even in the case of unpolarized atomic spin states (*i.e.* a mixture of all m_f states), hyperfine coupling can modify the formation rate measurably.

• Energy surfaces and reactions

A recent effort in my group towards reactive scattering involving cold molecules and molecular ions has started with the calculation of potential energy surfaces (PES) for trimers, such as for Li_3 , where we study an energy surface necessary in the photoassociation of Li_2 with Li to form the Li_3 trimer. For example, we obtained PES for the lowest doublet electronic state of Li_3 ($1^2A'$) [11], using the valence electron FCI method with atomic cores represented using an effective core potential, and investigated the Jahn-Teller splitting of the $1^2E'$ surface into the 1^2A_1 and 1^2B_2 states. We also calculated the lowest $^2A''$ surface arising from the $\text{Li}_2[\text{X}^1\Sigma_g^+] + \text{Li}[^2P]$ interaction [12]. We also analyzed the long range behavior of this surface by fitting the *ab initio* calculations at long range with a functional series of the form $-C_n/R^n$.

Together with my collaborators, we have studied the collisions of trapped molecules with slow beams, particularly of $\text{OH}(J = \frac{3}{2}, M_J = \frac{3}{2})$ molecules with ^4He atoms [13]. We found that the calculated cross sections are consistent with recent experimental observations at low beam energies, and demonstrated the importance of including the effects of non-uniform trapping fields in theoretical simulations of cold collision experiments with trapped molecules and slow atomic beams.

We also calculated the structure and thermochemistry relevant to $\text{KRb} + \text{KRb}$ collisions and reactions [14]. We found that the K_2Rb and KRb_2 trimers have global minima at higher energies than $\text{KRb} + \text{KRb}$, preventing the formation of those trimers by collisions, and that K_2Rb_2 tetramers and have two stable planar structures. We have calculated the minimum energy reaction path for the reaction $\text{KRb} + \text{KRb}$ to $\text{K}_2 + \text{Rb}_2$ and found it to be barrierless.

Finally, we have started a new effort on molecular ions. In order to study their formation, we carefully calculate their energy surface and transition dipole moments. We started with alkaline-earth elements, since they can be cool to very low temperatures. In [15], we report *ab initio* calculations of the $X^2\Sigma_u^+$ and $B^2\Sigma_g^+$ states of the Be_2^+ dimer. We found two local minima, separated by a large barrier, for the $B^2\Sigma_g^+$: we computed the spectroscopic constants and found good agreement with the recent measurements. We also calculated bound vibrational levels, transition moments and lifetimes in this state.

Future Plans

In the coming year, we plan to continue the alkali hydride work, and extend it to other polar molecules relevant to the experimental community, such as LiCs, LiRb, LiK, etc. We also plan to continue our work on FOPA, by expanding our treatment to the time domain.

We expect to carry more calculations on Rydberg-Rydberg interactions and explore the possibility of forming metastable long-range *macrotrimers* made of three Rydberg.

Finally, we will extend our work on surfaces of atom-diatom and diatom-diatom systems, as well as for molecular ions. Such systems are studied intensively in experiments, and theoretical guidance will become ever more important.

Publications sponsored by DOE

1. E. Juarros, K. Kirby, and R. Côté, *Formation of ultracold molecules in a single pure state: LiH in $a^3\Sigma^+$* . Phys. Rev. A **81**, 060704 (2010).
2. Y.N. Martinez de Escobar, P.G. Mickelson, P. Pellegrini, S.B. Nagel, A. Traverso, M. Yan, R. Côté, and T.C. Killian, *Two-photon photoassociative spectroscopy of ultracold ^{88}Sr* . Phys. Rev. A **78**, 062708 (2008).
3. E. Kuznetsova, P. Pellegrini, R. Côté, M.D. Lukin, and S.F. Yelin, *Formation of deeply bound molecules via adiabatic passage*. Phys. Rev. A **78**, 021402(R) (2008).
4. J. Stanojevic, R. Côté, D. Tong, S.M. Farooqi, E.E. Eyler, and P.L. Gould, *Long-range potentials and $(n-1)d + ns$ molecular resonances in an ultracold Rydberg gas*. Phys. Rev. A **78**, 052709 (2008).
5. N. Samboy, J. Stanojevic, and R. Côté, *Formation and properties of Rydberg macrodimers*, Phys. Rev. A **83**, 050501(R) (2011).
6. N. Samboy and R. Côté, *Rubidium Rydberg macrodimers*, Submitted to J. Phys. B.
7. P. Pellegrini, M. Gacesa, and R. Côté, *Giant formation rates of ultracold molecules via Feshbach Optimized Photoassociation*. Phys. Rev. Lett. **101**, 053201 (2008).
8. P. Pellegrini, and R. Côté, *Probing the unitarity limit at low laser intensities*. New J. Phys. **11**, 055047 (2009).
9. E. Kuznetsova, M. Gacesa, P. Pellegrini, S.F. Yelin, and R. Côté, *Efficient formation of ground state ultracold molecules via STIRAP from the continuum at a Feshbach resonance*. New J. Phys. **11**, 055028 (2009).
10. J. Deiglmayr, A. Grochola, M. Repp, R. Wester, M. Weidemüller, O. Dulieu, P. Pellegrini, and R. Côté, *Influence of a Feshbach resonance on the photoassociation of $LiCs$* . New J. Phys. **11**, 055034 (2009).
11. J.N. Byrd, J.A. Montgomery (Jr.), H.H. Michels, and R. Côté, *Potential energy surface of the $1^2A'$ Li_2+Li doublet ground state*, Int. J. of Quantum Chem., **109**, Issue 13, pp. 3112-3119, 5 November (2009).
12. J.N. Byrd, J.A. Montgomery (Jr.), H.H. Michels, and R. Côté, *Electronic Structure of the Li_2 [$X^1\Sigma_g^+$] + $LI^*[P_2]$ Excited A'' Surface*, Int. J. of Quantum Chem **109**, 3626 (2009).
13. T. V. Tscherbul, Z. Pavlovic, H. R. Sadeghpour, R. Côté, and A. Dalgarno, *Collisions of trapped molecules with slow beams*, Phys. Rev. A **82**, 022704 (2010).
14. J.N. Byrd, J.A. Montgomery (Jr.), and R. Côté, *Structure and thermochemistry of K_2Rb , KRb_2 and K_2Rb_2* , Phys. Rev. A **82**, 010502 (2010).
15. S. Banerjee, J. N. Byrd, R. Côté, H. H. Michels, J. A. Montgomery, Jr. *Ab initio potential curves for the $X^2\Sigma_u^+$ and $B^2\Sigma_g^+$ states of the Be_2^+ : Existence of a double minimum*, Chem. Phys. Lett. **496**, 208 (2010).

Optical Two-Dimensional Spectroscopy of Disordered Semiconductor Quantum Wells and Quantum Dots

Steven T. Cundiff

JILA, University of Colorado and NIST, Boulder, CO 80309-0440
cundiff@jila.colorado.edu

July 5, 2011

Program Scope: The goal of this program is to implement optical 2-dimensional Fourier transform spectroscopy and apply it to electronic excitations, including excitons, in semiconductors. Specifically of interest are quantum wells that exhibit disorder due to well width fluctuation and quantum dots. In both cases, 2-D spectroscopy will provide information regarding coupling among excitonic localization sites.

Progress: One of the powerful features of 2DFT spectroscopy is its ability to separate homogeneous and inhomogeneous broadening and measure both linewidths. This capability is not surprising as 2DFT spectroscopy is closely related to photon echo spectroscopy. In prior work, we had used an approach developed by our theory collaborators, namely measuring the frequency difference between positive and negative peaks in a phase resolved spectra with the overall phase set to give a maximally dispersive profile [1]. Applying this to the rephasing spectrum, $S_I(\omega_\tau, T, \omega_t)$, gives a value proportional to the homogeneous linewidth, whereas applying it to the non-rephasing spectrum, $S_{II}(\omega_\tau, T, \omega_t)$ gives a value proportional to the inhomogeneous width, in the limit of strong inhomogeneity.

An alternate approach is to use the projection-slice theorem of multi-dimensional Fourier transforms. This approach had been used previously to determine the lineshapes and widths of diagonal and cross-diagonal slices in the limits of pure homogeneous broadening and strong inhomogeneous broadening [2]. However, semiconductor quantum wells are often in the intermediate regime, where the homogeneous and inhomogeneous widths are comparable. To address this case, we extended the analysis to the intermediate regimes [3]. A significant advantage of this approach over our previous method was the ability to fit an entire lineshape which improves the confidence in the values.

We then used these results to analyze 2DFT spectra of the heavy-hole and light-hole exciton resonances in quantum wells broadened by weak disorder due to well width fluctuation [4]. The analysis provided the surprising result that the light-hole resonance actually had a narrower inhomogeneous width than the heavy-hole resonance. Since both experience the same disorder landscape, at first thought, it would seem that they should have identical inhomogeneous widths. However, the difference in hole mass does change how the excitons sense the disorder. The simpler effect is simply that a lighter particle actually sees a greater change in energy for a given change in spatial confinement which would suggest that the light-hole exciton should have a greater inhomogeneous width. However, a competing effect can arise due to the fact that excitons are most sensitive to interface roughness that has spatial frequencies comparable to the inverse of the Bohr radius [5]. Roughness that occurs on shorter length scales is averaged out. Thus we conclude that the interface roughness that occurs in the quantum wells must be stronger on length scales that correspond to the heavy hole exciton Bohr radius as compared to length scales that correspond to the light-hole exciton Bohr radius.

Another powerful capability of 2DFT spectroscopy is its ability to access coherences that are not optically active. These coherences are created by the first two pulses and then allowed to evolve during the time T . They set the initial phase of the signal emitted during time t . Thus by measuring the phase of the signal, scanning T and taking a Fourier transform with respect to T , it is possible to observe these coherences. During the previous grant period we had implemented this concept for measuring “Raman” coherences between the heavy-hole and light-hole exciton resonances in $S_I(\tau, \omega_T, \omega_t)$ [6]. During the most recent grant period, by measuring $S_{III}(\tau, \omega_T, \omega_t)$, we implemented it for two-quantum coherences between the ground state and two-exciton states [7, 8].

Prior work had measured the magnitude spectrum for two biexcitonic two quantum coherences [9]. We measured the real part of the spectrum and compared it to theory [8]. The theoretical results were able to reproduce the experimental observations, which showed dispersive resonances at the unbound two-exciton frequencies, which was reproduced in other measurements [10]. Interestingly, the theoretical results showed that these terms appear at a mean-field level of approximation. Thus comparison of $S_I(\omega_\tau, T, \omega_t)$ and $S_{III}(\tau, \omega_T, \omega_t)$ spectra could provide a quantitative comparison of the different many-body contributions to the nonlinear optical response of semiconductors.

If GaAs quantum wells are grown to be very thin and the with long growth interruptions to allow the interface fluctuation to form into large, flat islands, the localized states can be energetically well separated from the delocalized states [11]. These localized states are confined in all three spatial directions and thus have been dubbed “natural quantum dots”. The transverse localization, in the plane of the quantum well, is quite weak, which is a disadvantage for most applications. However, they interact strongly with light because their large physical size corresponds to a large dipole moment.

As a first demonstration of 2DFT spectroscopy of quantum dots, we chose to work on natural quantum dots because of their large dipole moment. In general, obtaining nonlinear signals from MBE grown quantum dots is challenging because they are embedded in a matrix that can give a non-resonant signal and scattering that masks the nonlinear signal. We have succeeded in obtaining clear 2DFT spectra of natural quantum dots, see Fig. 1. We studied the temperature and excitation density dependence [12] of the homogeneous linewidth. The temperature dependence displayed an activation-like behavior, where the activation energy and coupling coefficient varied across the ensemble, both increasing for smaller dots. Extrapolating to zero temperature and excitation density, yielded a linewidth that decreased for smaller dots, due to a reduction in radiative broadening for smaller dots due to their smaller dipole moment.

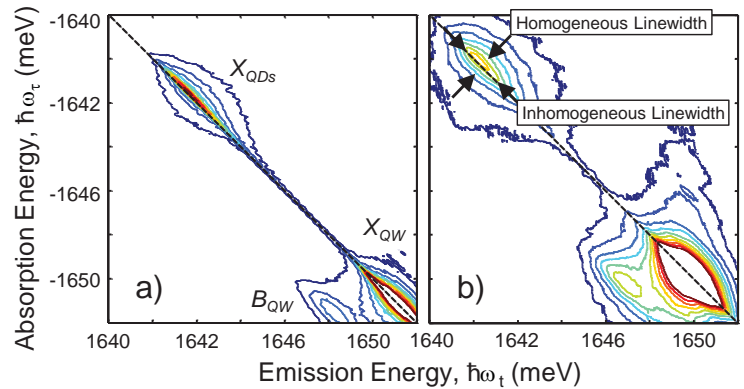


Figure 1: Amplitude 2DFT spectrum (normalized to the QW peak and truncated to emphasize the QD signal) of QW and QD ensemble for $T_L = 6$ K (a) and 50 K (b). The QW and QD homogeneous linewidths increase and the spectral features redshift with temperature.

By tuning the laser to excite both the localized quantum dot states and the delocalized quantum well states, it is possible to study the transfer of excitation between them [13]. Transfer of excitation is evident as cross-peaks that grow as T is increased. The dominant process is relaxation of quantum well states into quantum dot states, however, at elevated temperature the reverse process begins to happen. Studying the dynamics of these peaks allowed us to develop a rate equation model that described the transfer of excitation between the various states. To get agreement with the experimental results, it was critical to include dark excitons that are formed when only one carrier (typically the hole) undergoes a spin flip. This rate equation model simply includes fixed rates for the various processes. Actually calculating these rates due to effects like phonon-carrier interactions will require a more extensive theoretical effort.

Future Plans: We plan to concentrate on 3 topics in the future. The first topic is studying large ensembles of self-assembled InGaAs quantum dots using the current apparatus and a new light source. The second topic is building a new apparatus that will enable the study of single or small ensembles of quantum dots embedded in a photodiode structure. The final topic is studying colloidal quantum dots with the existing apparatus and new light source. Each of these topics is described in more detail in the following sections.

This selection of topics shows a shifting of emphasis towards quantum dots away from quantum wells. This shift is occurring for two reasons. First because the basic results have been obtained on quantum wells which establish a good understanding of their nonlinear optical response and a connection to the extensive body of prior work on quantum wells using methods such as transient four-wave-mixing. The second reason is that we have improved our methods to the point where studying the weaker signals from quantum dots is possible, as demonstrated in the work described

above.

Publication during the last 3 years from this project:

- A. L. Yang, T. Zhang, A.D. Bristow, S.T. Cundiff and S. Mukamel, "Isolating excitonic Raman coherence in semiconductors using two-dimensional correlation spectroscopy," *J. Chem. Phys.* **129**, 234711 (2008).
- B. A.D. Bristow, D. Karauskaj, X. Dai and S.T. Cundiff, "All-optical retrieval of the global phase for two-dimensional Fourier-transform spectroscopy," *Opt. Express* **16**, 18017 (2008).
- C. X. Li, T. Zhang, S. Mukamel, R.P. Mirin and S.T. Cundiff, "Investigation of Electronic Coupling in Semiconductor Double Quantum Wells using Optical Two-dimensional Fourier Transform Spectroscopy," *Sol. State Commun.* **149**, 361-366 (2008).
- D. I. Kuznetsova, P. Thomas, T. Meier, T. Zhang, and S. T. Cundiff, "Determination of homogeneous and inhomogeneous broadenings of quantum-well excitons by 2DFTS: An experiment-theory comparison," to appear in *Physica Status Solidi (c)* **6**, 445 (2009).
- E. A.D. Bristow, D. Karauskaj, X. Dai, R.P. Mirin and S.T. Cundiff, "Polarization dependence of semiconductor exciton and biexciton contributions to phase-resolved optical two-dimensional Fourier-transform spectra," *Phys. Rev. B* **79**, 161305(R) (2009).
- F. S.T. Cundiff, T. Zhang, A.D. Bristow, Denis Karauskaj and X.Dai, "Optical Two-Dimensional Fourier Transform Spectroscopy of Semiconductor Quantum Wells, *Acct. Chem. Res.* **42**, 1423 (2009).
- G. A.D. Bristow, D. Karauskaj, X. Dai, T. Zhang, C Carlsson, K.R. Hagen, R. Jimenez and S.T. Cundiff, "A Versatile Ultra-Stable Platform for Optical Multidimensional Fourier-Transform Spectroscopy," *Rev. Sci. Instr.* **80**, 073108 (2009).
- H. D. Karauskaj, A.D. Bristow, L. Yang, X. Dai, R.P. Mirin, S. Mukamel and S.T. Cundiff, "Two-Quantum Many-Body Coherences in Two-Dimensional Fourier-Transform Spectra of Exciton Resonances in Semiconductor Quantum Wells," *Phys. Rev. Lett.* **104**, 117401 (2010).
- I. M.E. Siemens, G. Moody, H. Li, A.D. Bristow and S.T. Cundiff, "Resonance lineshapes in two-dimensional Fourier transform spectroscopy," *Opt. Express* **18**, 17699 (2010).
- J. G. Moody, M. E. Siemens, A. D. Bristow, X. Dai, D. Karauskaj, A. S. Bracker, D. Gammon, and S.T. Cundiff, "Spectral broadening and population relaxation in a GaAs interfacial quantum dot ensemble and quantum well nanostructure," *Phys. Stat. Sol. (b)* **248**, 829-832 (2011).
- K. G. Moody, M. E. Siemens, A. D. Bristow, X. Dai, D. Karauskaj, A. S. Bracker, D. Gammon, and S. T. Cundiff, "Exciton-exciton and exciton-phonon interactions in an interfacial GaAs quantum dot ensemble," *Phys. Rev. B* **83**, 115324 (2011). [This paper was selected as an "**Editors Suggestion**" in Physical Review B]
- L. A.D. Bristow, T. Zhang, M.E. Siemens, S.T. Cundiff and R.P. Mirin, "Separating homogeneous and inhomogeneous line widths of heavy- and light-hole excitons in weaklydisordered semiconductor quantum wells," *J. Phys. Chem. B* **115**, 5365-5371 (2011).
- M. G. Moody, M. E. Siemens, A. D. Bristow, X. Dai, A. S. Bracker, D. Gammon, and S. T. Cundiff, "Exciton relaxation and coupling dynamics in a GaAs/AlGaAs quantum well and quantum dot ensemble," *Phys. Rev. B* **83** 245316 (2010).

References

- [1] I. Kuznetsova, T. Meier, S. T. Cundiff, and P. Thomas, “Determination of homogeneous and inhomogeneous broadening in semiconductor nanostructures by two-dimensional Fourier-transform optical spectroscopy,” *Phys. Rev. B* **76**, 153,301 (2007).
- [2] A. Tokmakoff, “Two-dimensional line shapes derived from coherent third-order nonlinear spectroscopy,” *J. Phys. Chem. A* **104**(18), 4247–4255 (2000).
- [3] M. E. Siemens, G. Moody, H. Li, A. D. Bristow, and S. T. Cundiff, “Resonance lineshapes in two-dimensional Fourier transform spectroscopy,” *Opt. Express* **18**(17), 17,699–17,708 (2010). URL <http://www.opticsexpress.org/abstract.cfm?URI=oe-18-17-17699>.
- [4] A. D. Bristow, T. Zhang, M. E. Siemens, S. T. Cundiff, and R. P. Mirin, “Separating homogeneous and inhomogeneous line widths of heavy- and light-hole excitons in weakly disordered semiconductor quantum wells,” *J. Phys. Chem. B* **115**, 5365–5371 (2011).
- [5] I. Kuznetsova, N. Gogh, J. Foerstner, T. Meier, S. T. Cundiff, I. Varga, and P. Thomas, “Modeling excitonic line shapes in weakly disordered semiconductor nanostructures,” *Phys. Rev. B* **81**(7), 075307 (2010).
- [6] L. Yang, T. Zhang, A. D. Bristow, S. T. Cundiff, and S. Mukamel, “Isolating excitonic Raman coherence in semiconductors using two-dimensional correlation spectroscopy,” *J. Chem. Phys.* **129**, 234,711 (2008).
- [7] S. T. Cundiff, T. Zhang, A. D. Bristow, D. Karaiskaj, and X. Dai, “Optical Two-Dimensional Fourier Transform Spectroscopy of Semiconductor Quantum Wells,” *Acc. Chem. Res.* **42**, 1423–1432 (2009).
- [8] D. Karaiskaj, A. D. Bristow, L. Yang, X. Dai, R. P. Mirin, S. Mukamel, and S. T. Cundiff, “Two-Quantum Many-Body Coherences in Two-Dimensional Fourier-Transform Spectra of Exciton Resonances in Semiconductor Quantum Wells,” *Phys. Rev. Lett.* **104**(11), 117401 (2010).
- [9] K. W. Stone, K. Gundogdu, D. B. Turner, X. Li, S. T. Cundiff, and K. A. Nelson, “Two-quantum 2D FT electronic spectroscopy of biexcitons in GaAs quantum wells,” *Science* **324**, 1169–1173 (2009).
- [10] K. W. Stone, D. B. Turner, K. Gundogdu, S. T. Cundiff, and K. A. Nelson, “Exciton-Exciton Correlations Revealed by Two-Quantum Two-Dimensional Fourier Transform Optical Spectroscopy,” *Acc. Chem. Res.* **42**, 1452–1461 (2009).
- [11] D. Gammon, E. Snow, B. Shanabrook, D. Katzer, and D. Park, “Homogeneous linewidths in the optical spectrum of a single gallium arsenide quantum dot,” *Science* **273**, 87–90 (1996).
- [12] G. Moody, M. E. Siemens, A. D. Bristow, X. Dai, D. Karaiskaj, A. S. Bracker, D. Gammon, and S. T. Cundiff, “Exciton-exciton and exciton-phonon interactions in an interfacial GaAs quantum dot ensemble,” *Phys. Rev. B* **83**, 115,324 (2011).
- [13] G. Moody, M. E. Siemens, A. D. Bristow, X. Dai, A. S. Bracker, D. Gammon, and S. T. Cundiff, “Exciton relaxation and coupling dynamics in a GaAs/AlGaAs quantum well and quantum dot ensemble,” accepted for publication in *Phys. Rev. B* (2011).

Theoretical Investigations of Atomic Collision Physics

A. Dalgarno

Harvard-Smithsonian Center for Astrophysics, Cambridge, MA 02138

adalgarno@cfa.harvard.edu

We have been exploring a range of atomic and molecular processes with an emphasis on collisions in cold and ultracold gases. As interest in cold ion-atom collisions is increasing, we have continued studies of near resonance charge exchange with emphasis on the effects of non-adiabatic perturbation on collision processes governed by a strong polarization potential and on the applicability of the prototypical two-state description of the charge exchange. The case of Be^+ in Be has been the subject of our theoretical investigation



where A and B label the isotopes. Effectively, as we have shown in our earlier research, the charge exchange process is controlled by the lowest ${}^2\Sigma_g^+$ and ${}^2\Sigma_u^+$ states of the molecular ion, where the g and u symmetries is labeled according to the center of the nuclear charge. A distinct and interesting feature arises for Be_2^+ because a third state, ${}^2\Pi$, is involved in the collision process even at very low scattering energies since it crosses the two lowest Σ^+ states in the inner regions of their potential wells. We have carried out refined electronic structure calculations of the interaction potentials and non-adiabatic corrections to the Born-Oppenheimer approximation. The accuracy of our computed non-Born-Oppenheimer potentials has been validated with the known isotope shift ΔE (5.6×10^{-5} eV) and measured vibrational spectra. The scattering theory we have constructed leads to coupled equations of three channels. The coupling operator between the Σ^+ states connect nuclear and electronic motions and are proportional to the difference in mass of the isotopes. The corresponding potential energy curves are modified in such a way that they separate at large distance to the correct energetic limits, $\pm 1/2\Delta E$. The interaction between Σ^+ and Π states originates from the electronic angular momentum operator. We have demonstrated that the near resonance charge exchange cross section in the low-energy limits follows Wigner's threshold law, varying as the inverse of the initial velocity. The limiting charge exchange rate coefficient is determined to be $4.5 \times 10^{-10} \text{ cm}^3\text{s}^{-1}$. In comparison, the resonance charge exchange ($\Delta E = 0$) rate tends to zero. When the collision energy is much higher than the threshold energy arising from the isotope shift, near resonance charge exchange becomes identical to resonance charge exchange. Close agreement with the Langevin charge model is found over a wide energy range. These results are consistent with findings in our earlier investigations of the isotopic ion-atom collision of HD^+ and Li_2^+ .

More importantly, our theoretical analysis showed that in the low energy regime the effects due to the Π state on the elastic and the charge exchange processes in both near resonance charge exchange and resonance charge exchange cases are negligible. Not only because the Π - Σ coupling is weak, but more importantly, because the low energy scattering dynamics is dominated by the strong long-range polarization interaction. The majority of the scattering phase is accumulated in the long-range part of the potential. The contribution from the short range is small and insensitive to the details of the interaction potentials. Above 0.1 meV of collision energy, the effects due to the Π state are still relatively small and mainly caused by the appearance of resonances due to the presence of quasi-bound states of the Π state. Of course, if there existed quasi-bound states at suitable positions, this type of resonances could also take

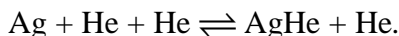
place below 0.1 meV. Nonetheless, we have explicitly demonstrated that the two-state approximation for the slow ion-atom collision is largely valid even in this case.

A critical issue in the scattering of an ion and its parent atom is the energy separation of the Σ_g and Σ_u states. Particularly, an accurate theoretical characterization of collisions at ultracold temperatures requires the precise energy separation at large internuclear distances. For light systems, such as Li_2^+ and Be_2^+ , conventional variational calculations of the kind we have carried out can achieve the required accuracy, but for more complex systems they become challenging. We have carried out an algebraic perturbation theory for efficient evaluations of localized states and hence exchange energies. The perturbation parameter is a function of internuclear distance and the energy E of the state considered. For the homonuclear case, the Herring-Holstein formula expresses the energy difference directly in terms of polarized wave functions. The formula yields the energy difference as an integral over the median plane, corrected for normalization. From Herring-Holstein formula, we have obtained analytical expansion of the exchange energy and applied it in the calculations of the exchange energy for Li_2^+ , Na_2^+ , K_2^+ , Rb_2^+ , and Cs_2^+ . Particularly, for Li_2^+ , we have performed the eighth-order perturbation analysis (PT8) and compared with our elaborated variational calculations. Table I lists the comparison of the two calculations.

Table I

R (a_0)	20	30	40	50	70	90
PT8 (au)	3.20×10^{-4}	1.43×10^{-6}	4.92×10^{-9}	1.47×10^{-11}	1.04×10^{-16}	6.06×10^{-22}
Variational	3.34×10^{-4}	1.46×10^{-6}	4.96×10^{-9}	1.47×10^{-11}	1.03×10^{-16}	6.05×10^{-22}

Responding to recent experiments (J. Doyle at Harvard) on the trapping of van der Waals molecules (XHe, X=N, P, Cu, Ag, Au) in a cryogenic buffer gas, particularly for AgHe, we have explored the spin relaxation of those molecules in buffer-gas-loaded magnetic trap and identified a loss mechanism based on Landau-Zener transition arising from the anisotropic hyperfine interaction. We have used *ab initio* calculations of the interaction potentials and hyperfine interactions, quantum collision calculations and Monte Carlo trap simulations to compare our model with experiment. We found close quantitative agreement, providing indirect evidence for molecule formation in a buffer-gas trap. The formation of AgHe goes through a three-body collision process



The typical trap used for buffer-gas cooling is a magnetic quadrupole, with $|\mathbf{B}|=0$ at the center, linearly increasing to a few Tesla at the edge. The weak-field-seeking state of both atoms and molecules are stably confined in such a trap. Collisions with free He atoms can cause loss of the trapped AgHe. The coherence of the precessing electronic spin is lost in the collision, and the internal $\mathbf{N}-\mathbf{S}$ and $\mathbf{I}_{\text{He}}-\mathbf{S}$ interactions can cause spin relaxation with the Zeeman energy release into the kinetic energy of the collision complex, where \mathbf{N} is the rotational angular momentum, \mathbf{S} is the electron spin, and \mathbf{I}_{He} is the nuclear spin of ^3He . We showed that the experimental observed loss rates cannot be explained by atom-atom and atom-molecule collisions. We demonstrated that the trapped AgHe molecules can make adiabatic transitions between the avoided crossings, which result from the low-field-seeking $N=0$ and high-field-seeking $N=2$ Zeeman levels and coupled by the anisotropic hyperfine interactions at a magnetic field of 1.06 T. The trapped AgHe molecules crossing this magnetic field can experience a spin flip, causing the molecules to be expelled from the magnetic trap.

In an effort to address the efficiency of spin-exchange optical pumping (SEOP) experiment

due to the anisotropic hyperfine interaction, we have carried out *ab initio* calculations of molecular interactions in combination with exact quantum scattering theory to quantify the role of the anisotropic hyperfine interaction in spin-exchange collisions of alkali-metal atoms with ^3He . Using the K-He system as a representative example we have showed that the maximum ^3He spin polarization attainable in SEOP experiments with K atoms is limited by the anisotropic hyperfine interaction. The maximum ^3He spin polarization of 81% achieved so far with SEOP experiments can be significantly improved. In addition, we have showed that spin-exchange in Ag-He collisions occurs much faster than in K-He collisions, suggesting that it may be advantageous to perform SEOP experiments with Ag atoms at low temperature to reduce the time scale for the production of hyperpolarized ^3He nuclei. The accuracy and validity of our calculations have been ensured by the quantitative agreement with recent measurements of frequency shift enhance factors and the rate constants for spin-exchange K- ^3He collisions.

In another study responding to the recent experiment efforts on the sympathetic cooling of open shell molecules by cold N atoms, we have performed quantum scattering calculations of Zeeman relaxation in N+NH collisions in a magnetic trap. We have demonstrated the ratio of N+NH elastic-to-inelastic collisions remains large (>100) over the temperature range ~ 10 mK–1K, which indicates that it is possible to sympathetically cool NH down to the millidegree Kelvin regime via elastic collisions with spin-polarized N. This conclusion may hold for other paramagnetic molecules such as the highly polar CaH and SrF. Additionally, we have carried out a rigorous theoretical analysis of low-temperature collisions polyatomic molecular radicals with close-shell atoms in the presence of an external magnetic field. We have showed the spin-relaxation in $^3\text{He}+\text{CH}_2$ collisions occurs at a remarkable slow rate of 1.2×10^{-14} cm^3s^{-1} at $T=0.5$ K, thereby making $\text{CH}_2(X^3B_1)$ an ideal candidate for sympathetic cooling experiments using cold ^3He gas. We have further extended our calculation to other polyatomic molecules and predicted two $S=1$ molecules (CH_2 and CHF) and eight $S=1/2$ molecules (NH_2 , PH_2 , AsH_2 , HO_2 , NF_2 , NO_2 , ClO_2 , and CH_3) should be amenable to cryogenic buffer-gas cooling and magnetic trapping with long lifetimes.

To assist the ongoing experimental work on the preparation and characterization of cold beams of polar molecules, we have investigated the temperature dependence of the diffusion for ThO in He gas. We have showed that the cross section is a monotonously decreasing function of temperature. The magnitude of the calculated cross section is consistent with a recent experimental measurement of YbF diffusion in He gas at 20K. Both the integral and momentum-transfer cross sections are sensitive to small variations of the molecular interaction potential at low collision energies, but become more robust against these variations at higher collision energies. The diffusion cross sections are far less sensitive to inaccuracies in the PES because of the thermal and rotational state averaging. We have examined the effects of an external electric field on j -changing and m_j -changing transitions in cold He+ThO collisions. We found that the cross sections for both type of transitions are sensitive to the magnitude of the external field, which indicates that rotational depolarization in low-temperature collisions of $^1\Sigma$ state molecules with 1S_0 -state atoms can be stimulated with electric fields.

We have continued our research on the thermalization of an initially energetic parcel of gas traversing a uniform bath gas and extended from the case of atom-atom collisions to the atom-diatom collisions, specifically, $\text{O}+\text{H}_2$. We have applied our theory and numerical algorithm in applications of planetary atmospheric science. We have proposed and evaluated a He escape mechanism from the Martian atmosphere due to collisions with hot $\text{O}(^1\text{D}, ^3\text{P})$ produced in the dissociative recombination of O_2^+ . Our predicted rate of escape agrees closely with the data

derived from the observation. We are currently extending our theory and model to the molecular escape (H_2), for which ro-vibrational degrees of freedom participate in the translational energy redistribution.

Publications (2010-2011):

1. N. Brahm, T.V. Tscherbul, P. Zhang, J. Klos, R.C. Forrey, Y.S. Au, H.R. Sadeghpour, A. Dalgarno, J.M. Doyle and T.G. Walker, Formation and dynamics of van der Waals molecules in buffer-gas trap, *Phys. Chem. Chem. Phys.* 2011, in press.
2. P. Zhang, A Dalgarno, E. Bodo, and R. Cote, Charge exchange in collisions of Beryllium with its ion, *Phys. Chem. Chem. Phys.* 2011, in press.
3. S. Bovino, P. Zhang, V. Kharchenko and A. Dalgarno, Relaxation of energetic S(1D) atoms in Xe gas: Comparison of ab initio calculations with experimental data, *J. Chem. Phys.* 135, 024304, 2011.
4. T.V. Tscherbul, P. Zhang, H.R. Sadeghpour, and A. Dalgarno, A Fundamental limit to the efficiency of spin-exchange optical pumping of 3He nuclei, *Phys. Rev. Lett.* 107, 023104, 2011.
5. T.V. Tscherbul, E.R. Sayfutyarova, A.A. Buchachenko and A. Dalgarno, He-ThO($1\Sigma^+$)interactions at low temperatures: Elastic and inelastic collisions, transport properties, and complex formation in cold 4He gas, *J. Chem. Phys.* 134, 144301, 2011.
6. T.V. Tscherbul, H.G. Yu and A. Dalgarno, Sympathetic Cooling of Polyatomic Molecules with S-State Atoms in a Magnetic Trap, *Phys. Rev. Lett.* 106, 073201, 2011.
7. M. T. Hummon, T.V. Tscherbul, J. Klos, H.-I. Liu, E. Tsikata, W.C. Campbell, A. Dalgarno and J. M. Doyle, Cold N + NH Collisions in a Magnetic Trap, *Phys. Rev. Lett.* 106, 053201, 2011.
8. S. Bovino, P. Zhang, F.A. Gianturco, A. Dalgarno and V. Kharchenko, Energy Transfer in O collisions with He isotopes and Helium Escape from Mars, *Geophys. Res. Lett.* 38, L02203, 2011.
9. N. Brahm, T.V. Tscherbul, P. Zhang, J. Klos, H.R. Sadeghpour, A. Dalgarno, J. M. Doyle and T. J. Walker, Formation of van der Waals molecules in buffer-gas-cooled magnetic traps, *Phys. Rev. Lett.* 105, 033001, 2010.
10. T.V. Tscherbul, J. Klos, A. Dalgarno, B. Zygelman, Z. Pavlovic, M.T. Hummon, H.-I. Lu, E. Tsikata, and J.M. Doyle Collisional properties of cold spin-polarized nitrogen gas: Theory, experiment, and prospects as a sympathetic coolant for trapped atoms and molecules, *Phys. Rev. A* 82, 042718, 2010.
11. B. L. Burroughs, A. Dalgarno and M. Cohen, Calculation of exchange energies using algebraic perturbation theory, *Phys. Rev. A* 81, 042508, 2010.
12. P. Zhang, H.R. Sadeghpour, and A. Dalgarno, Structure and spectroscopy of ground and excited states of LiYb, *J. Chem. Phys.* 133, 044306, 2010.
13. T. V. Tscherbul, Z. Pavlovic, H. R. Sadeghpour, R. Côté, and A. Dalgarno, Collisions of trapped molecules with slow beams, *Phys. Rev. A* 82, 022704, 2010.
14. J. L. Nolte, B. H. Yang, P. C. Stancil, Teck-Ghee Lee, N. Balakrishnan, R. C. Forrey and A. Dalgarno, Isotope effects in complex scattering lengths for He collisions with molecular hydrogen, *Phys. Rev. A* 81, 014701, 2010.

SISGR: Understanding and Controlling Strong-Field Laser Interactions with Polyatomic Molecules

DOE Grant No. DE-SC0002325

Marcos Dantus, dantus@msu.edu

Department of Chemistry and Department of Physics, Michigan State University, East Lansing MI 48824

We formally request continued funding for this project.

1. Program Scope

When intense laser fields interact with polyatomic molecules, the energy deposited leads to fragmentation, ionization and electromagnetic emission. The objective of this project is to determine to what extent these processes can be controlled by modifying the phase and amplitude characteristics of the laser field according to the timescales for electronic, vibrational, and rotational energy transfer. Controlling these processes will lead to order-of-magnitude changes in the outcome from laser-matter interactions, which may be of technical interests.

The proposed work involves experiments in which intense shaped laser pulses as short as 5fs in duration interact with a series of polyatomic molecules. Products of these interactions such as electrons, ions and photons, will be detected in order to provide valuable detailed information relevant to the electronic (<50 fs), vibrational (10-1000 fs) and rotational (1-100 ps) coherence time scales, as well as for intramolecular vibrational redistribution process (1-100 ps). The proposed work is unique because it seeks to combine knowledge from the field of atomic-molecular-optical physics with knowledge from the field of analytical chemistry, in particular ion chemistry. This multidisciplinary approach is required to understand to what extent the shape of the field affects the outcome of the laser-molecule interaction and to which extent the products depend on ion stability. The information resulting from the systematic studies will be used to construct a theoretical model that tracks the energy flow in polyatomic molecules following interaction with an ultrafast pulse.

2. Recent Progress

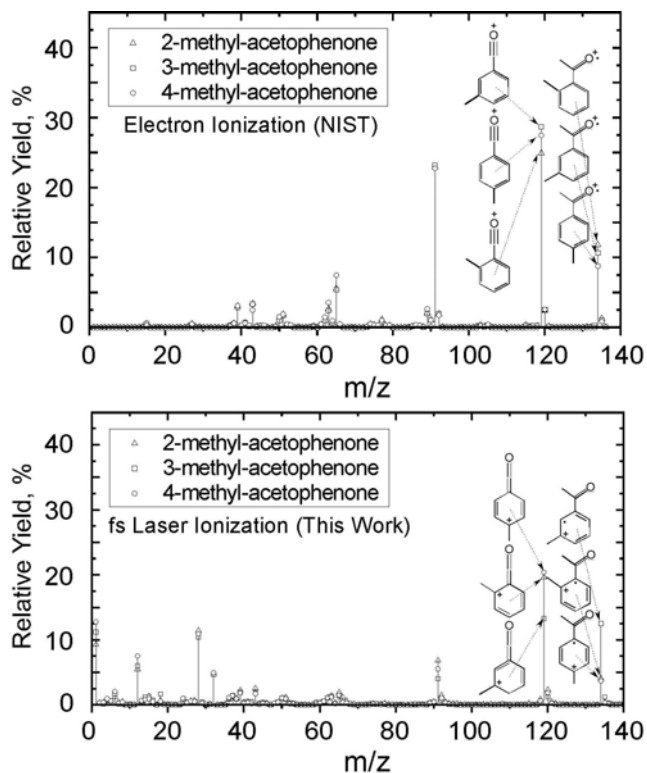


Fig. 1. Electron impact (obtained from NIST) and femtosecond laser induced dissociation mass spectra for three methyl substituted acetophenone compounds.

Our first project focused on the fragmentation of acetophenone and its derivatives. This molecule has been the subject of a number of studies aimed at controlling its fragmentation with shaped ultrafast pulses. Previous work from our group focused on the identity of the fragments and inconsistencies with published data. Here we focused on ultrafast dynamics that determine the formation of the major fragments.

First we compared the electron impact (70eV) and femtosecond induced fragmentation of methylated acetophenone molecules, see Figure 1. We find that electron impact causes few differences in fragmentation; however, femtosecond pulse ionization causes a large difference for 3-methyl acetophenone which has the methyl group in the meta (intermediate) position with respect to the carbonyl group. 3-methyl-acetophenone is found to fragment significantly less than the other two methylated isomers. In particular, the amplitude of the peak at m/z 134 for ortho and para substituted isomers is one third the amplitude of the meta substituted isomer. The decreased likelihood to fragment can be explained in terms of resonance structures of the long-lived radical ion species.

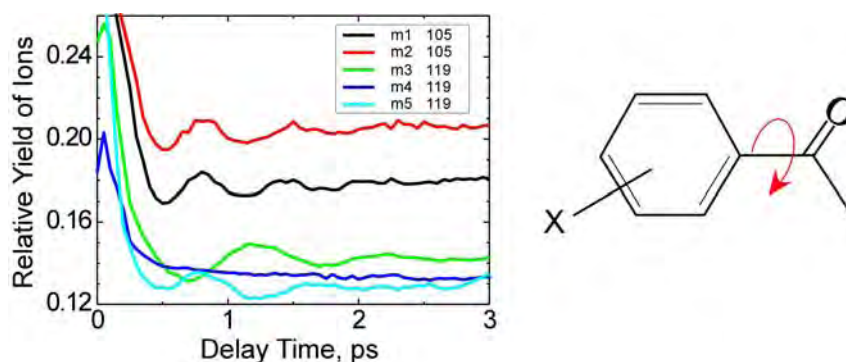


Fig. 2. Yields of benzoyl ion from acetophenone, d3-acetophenone, and three methyl acetophenone isomers plotted with respect to the delay between TL pump pulse and Chirped probe pulse. Molecules are m1: acetophenone; m2: d3-acetophenone; m3: 2-methyl-acetophenone; m4: 3-methyl-acetophenone; m5: 4-methyl-acetophenone. A schematic of the torsional vibration of the phenyl ring is shown on the right.

From the change in ion abundances with respect to the time delay between two pulses, we are able to elucidate a number of ladder climbing and ladder switching pathways and their time constants.¹ The yield of benzoyl ions, with m/z 105, was found to oscillate in time. By examining deuterated acetophenone and methyl-substituted acetophenone isomers, we confirmed the oscillations were caused by the torsional motion of the carbonyl group and not by vibration of the methyl group. We found that both ortho and para substituted methyl acetophenone had the same period but different phase (see Figure 2), therefore we conclude that the change in the period was caused by the electron donating property of the methyl fragment and not by the change in the moment of inertia. These findings have been published in the Journal of Physical Chemistry.¹

Improvements in the laser setup and molecular beam have allowed acquisition with better time resolution. We show in Figure 3 results for *o*- and *p*-methylacetophenone and *o*- and *p*-fluoroacetophenone. Methyl is an electron donating and fluoro is an electron withdrawing group. We find that the torsional oscillations are out-of-phase when comparing the ortho-methyl with the ortho-fluoro substituted constituents. We are exploring if the oscillations correlate with changes in different resonant structure configurations.

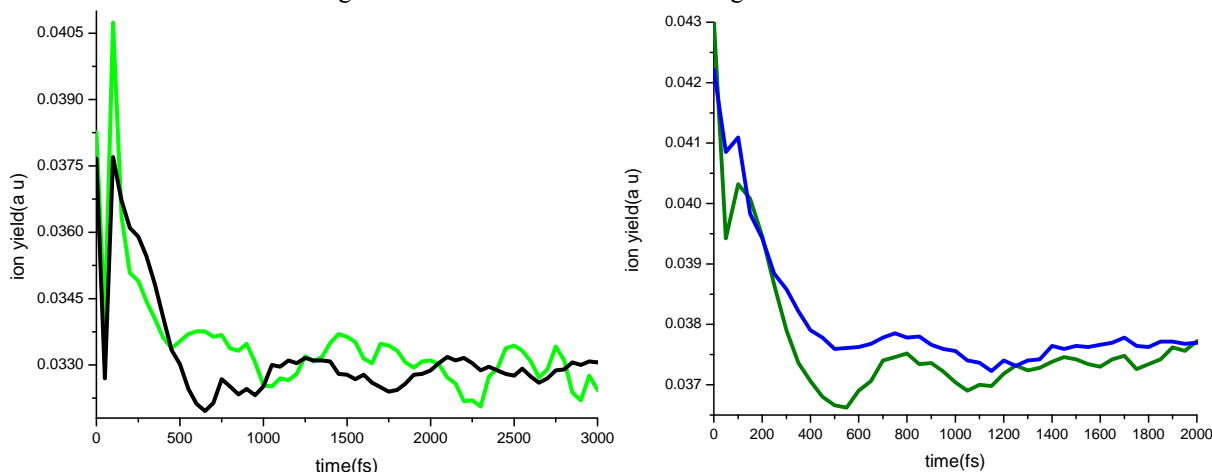


Fig. 3. Yields of fluoro-benzoyl (green) and methyl-benzoyl (black/blue) ions from ortho substituted (left) and para substituted (right) acetophenones. The early feature around 50fs is real and is found to be prominent only in substituted acetophenone. Note that the oscillations are out of phase for the ortho substituted compounds and in phase for the para substituted compounds.

NEW EXCITING RESULTS: In the field of Coherent Control, there has always been some ambiguity related to the word Coherent. When a laser pulse interacts with a molecule, the coherent response of the molecule may include rotational, vibrational and electronic quantum state coherence. Determining if electronic coherence plays a role in Coherent Control experiments has been very difficult because of the short timescales for electronic coherence, and because it is difficult to unravel the interference between the electric fields of the pump and probe laser pulses. For example, when two ultrashort pulses are scanned collinearly, they interfere, and this interference dominates the short time response of the molecule with the laser field in the timescale of the pulse duration.

The Dantus Group introduced in 2010 a novel method for creating replica pulses that have no frequencies in common and therefore exhibit no first-order interaction. The method is known as Multiple Independent Comb Shaping, and it is based on the selection of independent sets of comb lines in the spectrum of the original laser pulse, and introducing a phase that delays one set of comb lines with respect to the other. With proper selection of the subset of comb lines, two pulses are created that have the same carrier frequency and bandwidth, but have no comb lines in common. The method is illustrated in Figure 4 (left). In the right hand, the interferometric signal is collected at the fundamental frequency (red) and at the frequency doubled signal (blue). Note that the fundamental frequency does not show sign of interference in this unique measurement.³ This allows us to un-entangle the contribution of the optical interference inherent in other time-resolved methods, with the true electronic coherence which involves molecular quantum mechanical states. The MICS method is now being used to study the fragmentation of acetophenone following field ionization with intense ultrashort pulses. The results from these experiments are shown in Figure 5. Note that interference is measured even at time delays of 200fs, when the pulses have no temporal overlap.

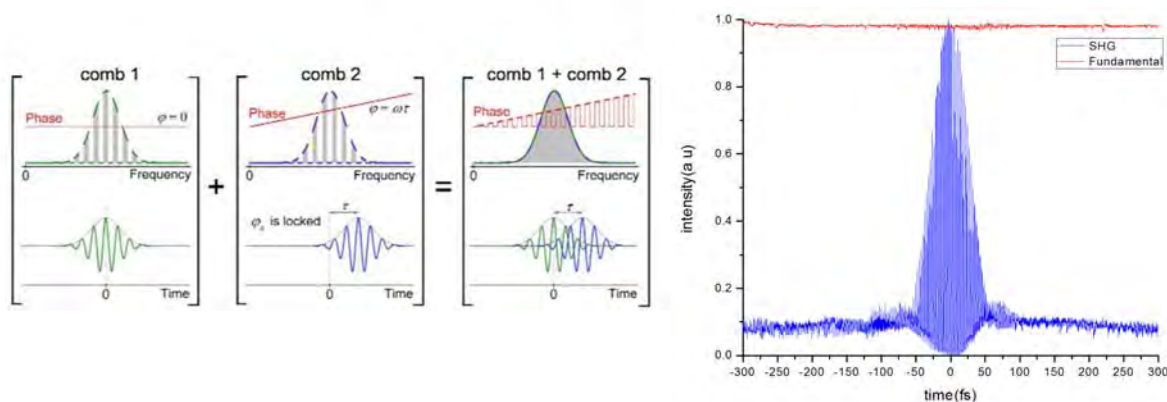


Figure 4: Left: Pulse shaping scheme for interferometric multiple independent comb shaping. Right: interferometric autocorrelation of SHG (blue), and the interferometric autocorrelation of the fundamental spectrum (red).

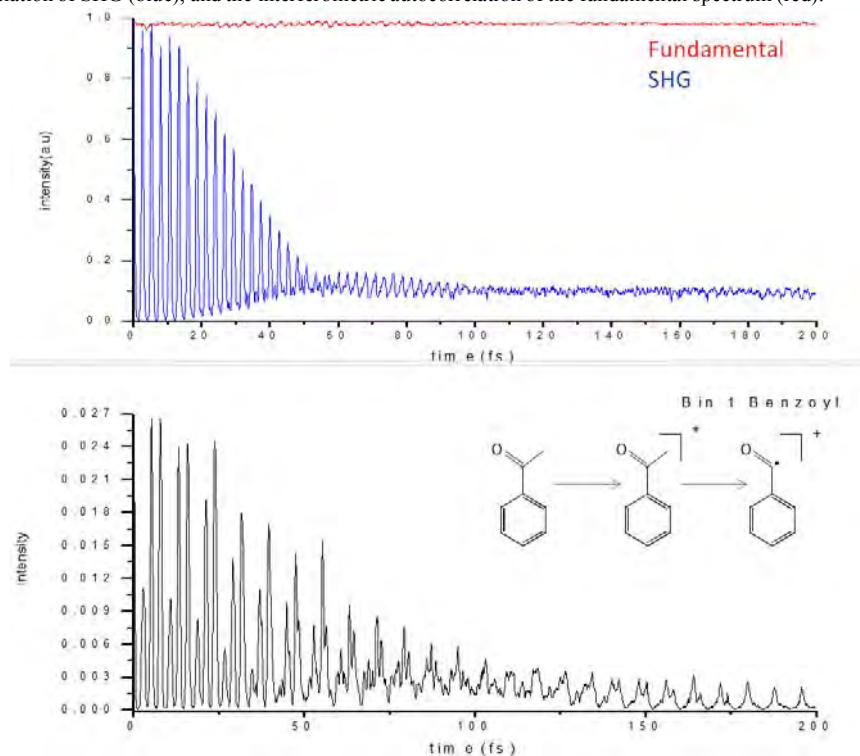


Figure 5: Top: interferometric autocorrelation of SHG (blue), and the fundamental spectrum (red) in the same range showing minimal interference. Bottom: Detected benzoyl ion yield in the mass spectrometer as a function of time delay of the two intense laser pulses centered at 800nm. Note that the interference signal reports on an electronically coherent transient species that is neutral and lives for times longer than 200fs.

The complexity of the reaction dynamics following field ionization of the acetophenone derivatives is presently challenging our ability to provide a simple explanation to the observed MICS transient data. In order to simplify the physics and gain a better perspective of the physical processes that can be studied by MICS, we turned our attention to an organic dye molecule, IR144, which has a well-known single photon excitation that is resonant with the central frequency of the laser pulses. Results from this quasi-two-level system, see figure 6, are much simpler to interpret.

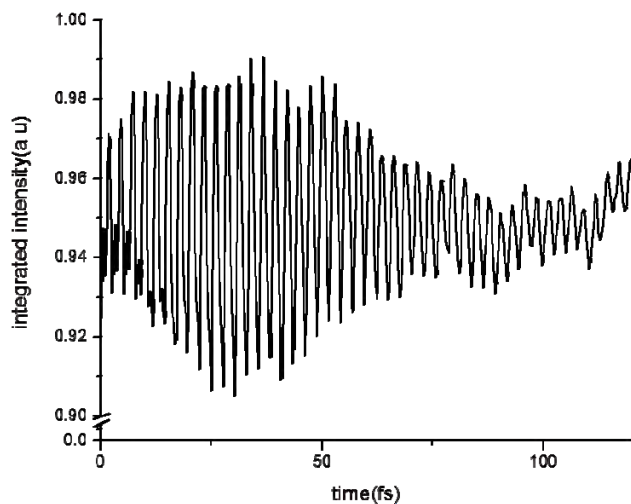


Figure 6: Left: MICS data on IR144 in solution. This is a one-photon transition between the ground and the first excited state of this molecule. The amplitude of the interference tracks the maximum transition probability for the stimulated emission back to the ground state.

Summary:

- (a) We have developed a new method to explore electronic coherence that involves pairs of replica ultrafast pulses. The method can be used with ultrashort pulses at any wavelength and can be applied to study dynamics in gas, liquid, solid and plasma states of matter.
- (b) We have found a way to measure resonance-structure dynamics in substituted benzene compounds. This is a very significant observation that represents the first direct measurement of resonance structures as have been postulated by chemists for over 100 years. Resonance structures involve flow of electron density that is schematically shown as changes in the electronic structure of molecules. One paper has been published and a second is being prepared.
- (c) We have made direct measurements of the extent of electronic coherence during strong-field excitation of polyatomic molecules. These measurements will lead to robust coherent control schemes.
- (d) We are building a PEPICO instrument that will give us additional information about the electronic states involved in the strong field experiments.

3. Future Plans

- (a) We plan to complete the studies of IR144 in solution and to collaborate with a group that will simulate the initial wave packet dynamics.
- (b) We plan to report on the electronic coherence involved in laser control of chemical reactions, in particular intense non-resonant fields. We have measured this for small molecules like oxygen and nitrogen, and for large molecules like indole. Our findings indicate that small molecules without resonant states (one-, two- or three-photon) show very short coherence time, but large molecules with two- or three-photon resonance states show longer coherence times (up to 600fs for indole).
- (c) We plan to complete a set of measurements for a number of substituted acetophenones with electron withdrawing and electron donating groups.

One of the important goals of our proposed work was to upgrade our molecular beam in order to be able to carry out experiments in which photoelectron and photoions are detected in coincidence (PEPICO). The advantage of PEPICO will be that we will be able to determine how much energy was deposited in the molecule by the laser field to produce each of the different fragment ions. We will also be able to correlate the origin of the ejected electron with a specific fragment. The parts for that instrument have started to arrive and we have started the construction of the equipment.

¹X. Zhu, V. V. Lozovoy, J. D. Shah and M. Dantus, "Photodissociation dynamics of acetophenone and its derivatives with intense nonresonant femtosecond pulses," *J. Phys. Chem. A* **115**, 1305–1312 (2011).

Production and trapping of ultracold polar molecules

D. DeMille

Physics Department, Yale University, P.O. Box 208120, New Haven, CT 06520

e-mail: david.demille@yale.edu

Program scope: The goal of our project is to produce and trap polar molecules in the ultracold regime. Once achieved, a variety of novel physical effects associated with the low temperatures and/or the polar nature of the molecules should be observable. We now form ultracold, vibrationally excited RbCs molecules in an optical lattice trap. We are investigating methods to transfer these trapped molecules into their absolute internal ground state. Once there, the molecules will be stable to collisions and hence suitable for further study and manipulation. We also will investigate a variety of techniques for manipulating and probing this sample. Once in place, we will study chemical reactions at ultracold temperatures.

Our group has pioneered techniques to produce and state-selectively detect ultracold heteronuclear molecules. These methods yielded RbCs molecules at translational temperatures $T < 100 \mu\text{K}$, in any of several desired rovibronic states—including the absolute ground state, where RbCs has a substantial electric dipole moment. Our method for producing ultracold, ground state RbCs consists of several steps. In the first step, laser-cooled and trapped Rb and Cs atoms are bound into an electronically excited state via photoassociation (PA).¹ These states decay rapidly into a few, weakly bound vibrational levels in the ground electronic state manifold.² We demonstrated the ability to transfer population from these high vibrational levels, into the lowest vibronic states $X^1\Sigma^+(v=0,1)$ of RbCs³ using a laser “pump-dump” scheme.⁴ We state-selectively detect ground-state molecules with a two-step, resonantly-enhanced multiphoton ionization process (1+1 REMPI) followed by time-of-flight mass spectroscopy. More recently, we incorporated a CO₂-laser based 1D optical lattice into our experiments. This has made it possible to trap vibrationally-excited RbCs molecules as they are formed. The precursor Rb and Cs atoms can also be trapped with long lifetimes (>5 s). We used this capability to measure inelastic (trap loss) cross-sections for individual RbCs vibrational levels on both Rb and Cs atoms in the ultracold regime, and also developed a simple theoretical model for these collisions.⁵

We are currently working to transfer the trapped molecules to their absolute internal ground state, $X(v=0, J=0)$. In this state the molecules should be immune to all (two-body) inelastic collisional loss processes, including the chemical reaction $2\text{RbCs} \rightarrow \text{Rb}_2 + \text{Cs}_2$ recently predicted to be endothermic⁶, and they should also possess a sizeable dipole moment (~ 1.3 D). We will accomplish the transfer using an improved version of our initial method, where “pump-dump” scheme is replaced by a coherent STIRAP (Stimulated Raman Adiabatic Passage) process. This requires narrow laser linewidths and high Rabi frequencies, which are obtained by the use of extended cavity diode lasers that can be tightly focused due to the small size of our sample. A similar STIRAP technique has now been demonstrated for producing ultracold trapped KRb molecules by the JILA group,⁷ validating our basic approach.

A crucial step towards STIRAP transfer is to map out the rotational and hyperfine structure of the molecular levels used. To this end we have performed spectroscopy of the RbCs $a^3\Sigma^+ \rightarrow c^3\Sigma^+$ transition. We create molecules in a few rovibrational and hyperfine states via PA as described above. Before the detection pulse, we illuminate the sample with cw laser light which,

if resonant with an $a^3\Sigma^+ \rightarrow c^3\Sigma^+$ transition, depletes the sample. Fig. 1 shows preliminary spectra obtained with this method. Identification of the transitions seen there is ongoing.

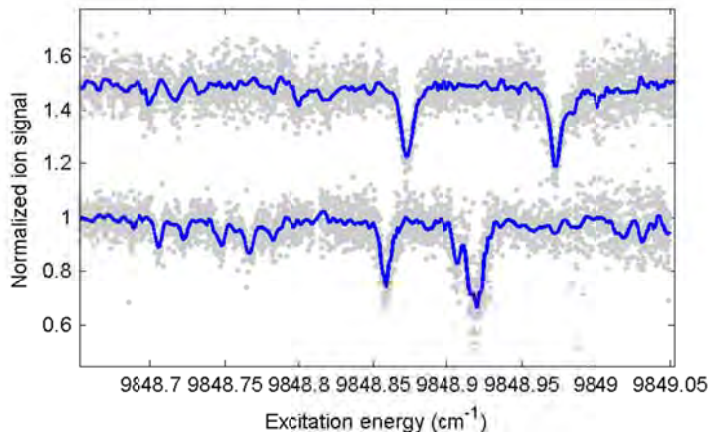


Figure 1: Depletion spectra of the RbCs $a^3\Sigma^+(v=37) \rightarrow c^3\Sigma^+(v=36)$ transition, with the $a^3\Sigma^+$ molecules created by photoassociation on a $J=0$ (lower) or $J=1$ (upper) line of an $\Omega=0'$ state.

In analogy to our recent experiments studying the level structure of deeply-bound Cs_2 ground-state molecules,⁸ we have determined that efficient ground-state molecule production via STIRAP almost certainly requires full control of all degrees of freedom, including nuclear spins. To address this issue, we now optically pump our trapped atoms to extreme M sublevels of the atomic hyperfine states, and plan to use appropriate laser polarizations and transitions to remain in such extreme states throughout the PA and STIRAP processes. This is made simpler by a new photoassociation protocol, where we create molecules out of atomic samples that are already trapped in the optical lattice, rather than by MOTs as in our previous work. The optical lattice affords long trapping times for robust spin-polarization as well as colder atomic samples. We note here that we have so far been unable to see evidence of photoassociation in the fully spin-stretched configuration. Instead, for now we spin-polarize the atoms in their lower hyperfine states, which still affords considerable control over the nuclear spin distribution.

Along with this main focus of our work, we are pursuing several additional directions. For example, we have begun developing methods for imaging detection of the small molecular samples. This is far more difficult than for atoms, because of the lack of cycling optical transitions. However, the utility of imaging detection in the study of atomic gases merits its extension to molecular systems. We have constructed an auxiliary system incorporating an imaging ion detection setup (microchannel plate + phosphor screen + fiber optic image conduit + CCD camera),⁹ which is currently being tested using rubidium atoms. Following resonant ionization, pulsed electric fields will be used to rapidly expand the ions and then accelerate them towards the detector, hence minimizing the effect of Coulomb self-expansion of the ion cloud. Simulations of the system have been performed and indicate that excellent spatial resolution and detection efficiency should be possible. Once this method is established, we can effectively study the variety of interesting two-body and many-body physics associated with polar molecules, including possibly the direct detection of product species resulting from ultracold chemical reactions.

In other related work, we have recently investigated in more detail the behavior of polar molecules held in optical traps, in the presence of DC electric fields E to polarize the molecules¹⁰. We find that the DC field modifies the optical tensor polarizability and at certain

values of E different pairs of rotational states experience the same trap potential. Similarly, for a particular “magic angle” between the light polarization and \mathbf{E} , the tensor shifts vanish and all rotational sublevels experience the same trap potential. In addition, we are now completing an analysis of the full set of our Cs_2 two-color PA data (described in part in Ref. [8]), with the goal to provide a more complete description of the coupled $a^3\Sigma_u^+$ and $X^1\Sigma_g^+$ ground state potentials in Cs_2 .

References

- ¹A.J. Kerman *et al.*, Phys. Rev. Lett. **92**, 033004 (2004).
- ²T. Bergeman *et al.*, Eur. Phys. J. D **31**, 179 (2004).
- ³J.M. Sage, S. Sainis, T. Bergeman, and D. DeMille, Phys. Rev. Lett. **94**, 203001 (2005).
- ⁴A.J. Kerman *et al.*, Phys. Rev. Lett **92**, 153001 (2004).
- ⁵ E. R. Hudson, N.B. Gilfoy, S. Kotochigova, J.M. Sage, and D. DeMille. Inelastic collisions of ultracold heteronuclear molecules in an optical trap. Phys. Rev. Lett. **100**, 203201 (2008). [DOE SUPPORTED]
- ⁶ P. S. Zuchowski and J. M. Hutson, Phys. Rev. A **81**, 060703(R) (2010).
- ⁷ K.-K. Ni *et al.*, Science **322**, 231 (2008).
- ⁸ D. DeMille, S. Sainis, J. Sage, T. Bergeman, S. Kotochigova, and E. Tiesinga. Enhanced sensitivity to variation of m_e/m_p in molecular spectra. Phys. Rev. Lett. **100**, 043202 (2008). [DOE SUPPORTED]
- ⁹ D.W. Chandler and P.L. Houston, J. Chem. Phys. **87**, 1445 (1987); A.J.R. Heck and D.W. Chandler, Annu. Rev. Phys. Chem. **46**, 335 (1995).
- ¹⁰ S. Kotochigova and D. DeMille. Electric-field-dependent dynamic polarizability and state-insensitive conditions for optical trapping of diatomic polar molecules. Phys. Rev. A **82**, 063421 (2010). [DOE SUPPORTED]

ATTOSECOND AND ULTRA-FAST X-RAY SCIENCE

Louis F. DiMauro
Co-PI: Pierre Agostini
Department of Physics
The Ohio State University
Columbus, OH 43210
dimauro@mps.ohio-state.edu
agostini@mps.ohio-state.edu

1.1 PROJECT DESCRIPTION

This document describes the BES funded project (grant #: DE-FG02-04ER15614) entitled “Attosecond & Ultra-Fast X-ray Science” at The Ohio State University (OSU). Attosecond light pulses from gases offer a transition to a new time-scale and open new avenues of science while complementing and directly contributing to the efforts at the LCLS. The main objectives of this grant is the development of competency in generation and metrology of attosecond pulses using mid-infrared drivers and a strategy of employing these pulses for studying multi-electron dynamics in atomic systems. It focuses on applications in which attosecond pulses are produced and transported to a different region of space and applied to a different target, thus providing the greatest degree of spectroscopic flexibility. The proposal has also a thrust at the LCLS for studying the scaling of strong-field interactions into a new regime of x-ray science.

Progress over the past year includes (1) measurement of the wavelength dependence of the attochirp using the RABBITT method, (2) initial studies on phase-dependent structural effects, (3) investigation of nonlinear excitation with intense x-rays and (4) preliminary measurement of time-resolved Auger decay using a two-color streaking method at the LCLS XFEL.

1.2 PROGRESS IN FY11: THE ATTOSECOND PROGRAM

The technical approach of the Ohio State University (OSU) group is the use of long wavelength ($\lambda > 0.8 \mu\text{m}$) driving lasers for harmonic generation. The objective is to create sufficiently short wavelength attosecond pulses to allow access to core level transitions. This is accomplished by exploiting the favorable scaling of the harmonic cutoff energy $\propto \lambda^2$, which results in attosecond pulses with higher central frequency. An additional benefit is the scaling of the attochirp $\propto \lambda^{-1}$, which leads to inherently shorter attosecond pulses at longer wavelength. Conversely, it has been shown that the single atom harmonic efficiency decreases with longer wavelength [1] but recent work [2] has demonstrated that effective phase-matching conditions can be realized. Using this approach, the OSU group has the ability to produce ~ 100 as pulses spanning 20-200 eV photon energies.

Spectral phase measurement. Measuring the spectral amplitude of XUV light is relatively easy, XUV spectrometers are available commercially, but measuring the spectral phase is nontrivial. Prior experiments at OSU designed to measure the spectral phase of high harmonics were adopted from an all-optical *in situ* method proposed by Dudovich *et al* [3]. In this case, a two-color harmonic field (ω and 2ω) is used to generate delay-dependent sidebands in the harmonic spectrum. Comparison of the sideband spectrogram with theory that describes the generation process allows the extraction of the spectral phase.

Alternately, the RABBITT (Reconstruction of Attosecond Beating By Interference of Two-photon Transitions) method is a direct measure (not theory dependent) of the average spectral phase of a train of attosecond pulses. This method was developed by Agostini and collaborators and was used to measure the first attosecond pulses [4]. The RABBITT method consists of a Mach-Zehnder interferometer with the harmonics in one arm and a small fraction of the IR field in the other arm. Photoionization of a suitable noble gas supplies the nonlinear medium necessary to mix the IR and harmonic fields, producing even-

order sidebands in the photoelectron energy distribution. By delaying the phase of the weak dressing IR field, the sidebands modulate producing a spectrogram (see Fig. 1(c)) that is used to extract the relative phase of the harmonics. The value measured is the discrete phase difference between consecutive harmonic orders which is proportional to the group delay and thus proportional to the emission time of the harmonics.

It is important to stress that the RABBITT and the *in situ* method do not measure the same thing. The RABBITT measures the spectral phase at the place of detection including all the macroscopic effects of absorption and linear and nonlinear dispersion of the fundamental and harmonic fields in the gas, ionization, saturation, phase-matching, propagation and dispersion induced by the spectral and spatial filters in the far field. Conversely, the *in situ* method measures the spectral phase of the microscopic single-atom response at the place of generation and is unaltered by macroscopic effects [5]. Most importantly, the *in situ* method is strongly dependent on the theory for its interpretation and extraction of the spectral phase and is known to fail in the region of the cutoff. Over the past year, we have been comparing these two methods in order to understand the differences in the information.

RABBITT measurements using driving laser wavelengths of 0.8 μm , 1.3 μm , and 2.0 μm . Over the past year we have performed RABBITT measurements using the recently commissioned attosecond beamline at OSU. We measured the spectral phase of high-order harmonics generated in noble gases with the three laser wavelengths available in our laboratory, 0.8 μm , 1.3 μm and 2.0 μm . The investigations aimed at characterizing the phase-matching conditions that produce good harmonic yield and short pulses. Ultimately, we were able to produce comparable count rates in our RABBITT apparatus for the different wavelength sources. Thus we have been able to show that the scaling of the single-atom response does not impose a limit on the macroscopic photon yield. The studies examine the effects of changing the laser intensity, beam waist, Rayleigh range, gas species, gas density, medium length, and the position of the focus relative to the gas medium on the photon yield and phase.

These studies are still in progress. However, it is clear that the macroscopic effects of phase-matching and propagation play a significant role in distorting the spectral phase, as well as the spectral amplitude, away from the microscopic single-atom result. Of special interest is the influence of the atomic structure, i.e. Cooper Minimum, Fano Resonances, etc., plays in shaping the phase. In the future, understanding the role of the atomic structure on phase-measurements could lead to new insights and methods. As part of this work, we have established a theoretical collaboration with Mette Gaarde (LSU).

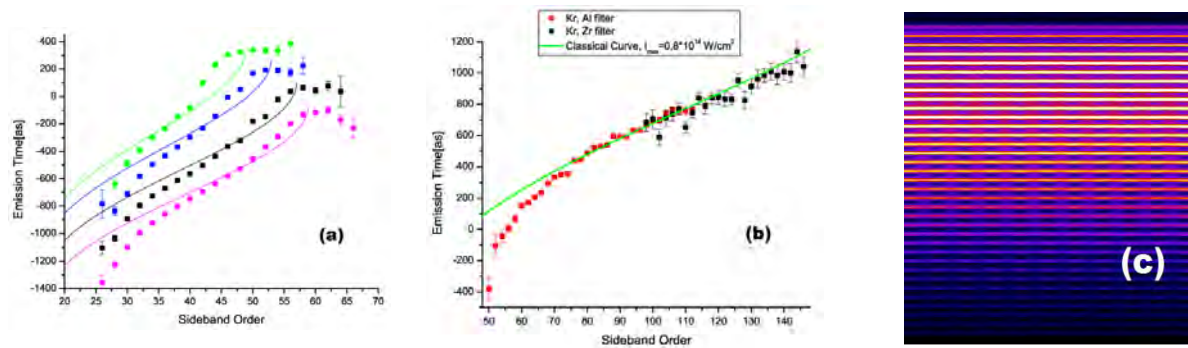


Figure 1: Examples of the relative harmonic emission times extracted from RABBITT scans using (a) a 1.3 μm fundamental field at four different intensities (aluminum filter) and (b) a 2 μm pump (aluminum and zirconium filters). Both (a) and (b) are generated in krypton and detected in neon. The GDD from the metal filters has been subtracted out and the emission times are shifted arbitrarily in time since the RABBITT does not give access to the absolute emission time. Note that spectral measurements extend to 150-order. The continuous lines are the classical emission times fitted to the corresponding cutoff harmonics. Plot (c) is a typical spectrogram at 2 μm used to extract the emission time. The abscissa spans several cycles of the MIR period and the ordinate is harmonic photon energy.

1.3 PROGRESS IN FY11: NONLINEAR INVESTIGATIONS AT THE LCLS XFEL

The nonlinear response to high intensity X-Ray pulses were explored at the LCLS XFEL by exposing neon and helium atoms to the focused LCLS beam using the AMOS end-station. Studies in helium showed that the presence of second-harmonic contamination in the LCLS beam and the expected low cross-sections made observations of above-threshold ionization impossible. Alternately, the photon energies achievable at the AMO beamline are ideal the study K-shell processes in neon. The possibility of producing completely stripped Neon was demonstrated in a prior experiment [6] at LCLS. A feasible system for the study of multiphoton absorption in neon is helium-like neon. The ground state of Ne^{8+} is a two-electron system with an ionization energy of 1196eV. This ionization threshold results in a sufficiently high ionization cross-section for photon energies achievable at the LCLS. Using longer LCLS pulses (~100 fs) neon was ionized to the Ne^{8+} state. The duration of the pulse allowed the remaining two electrons to relax to the K-shell via a series of Auger processes. The remainder of the X-Ray pulse drives the ionization to Ne^{9+} . To confirm the nonlinear response, the XFEL was tuned to above (1225eV) and below (1110eV) the ionization threshold. The ion charged state distribution was measured at various pulse energies, above and below the threshold. A quadratic response of the Ne^{9+} channel at photon energies below 1196eV provided the first evidence of a 2-photon absorption in the X-ray regime. Figure 2 shows the pulse energy dependence of the $\text{Ne}^{9+}/\text{Ne}^{8+}$ ratio. The data taken below the Ne^{8+} ionization threshold show a clear nonlinear dependence. Model calculations were performed by our collaborators (Santra and Son) and supported the interpretation as direct 2-photon absorption. The results from this experiment, together with the supporting theory were published in Physical Review Letters.

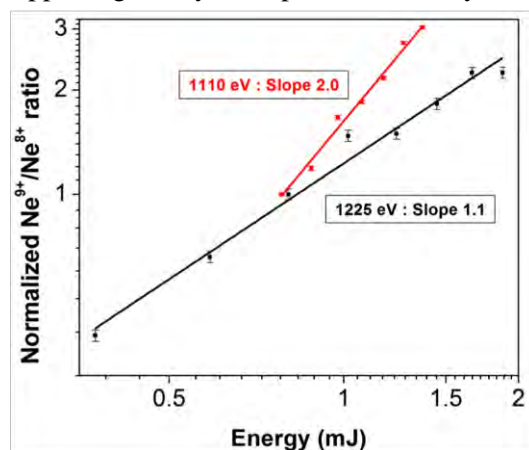


Figure 2: Dependence of $\text{Ne}^{9+}/\text{Ne}^{8+}$ ion yield on FEL pulse energy. Solid red line: XFEL photon energy tuned below Ne^{8+} ionization threshold. Solid black line: XFEL photon energy tuned above Ne^{8+} ionization threshold.

Time Resolved Measurement of the KLL Auger Decay in Neon. The concept of this investigation is to combine the high-energy X-Ray pulses of the XFEL with methods in attosecond science to measure Auger decays in a direct time resolved fashion. The short FEL pulse would promote a neon 1s electron (K-shell) to the continuum. A mid-infrared field (2.3 μm) from a conventional laser system would provide a phase dependent momentum kick to the resulting photoelectron and Auger electron. The problem is that the XFEL and MIR pulses cannot be synchronized on a few-femtosecond time scale. Thus, an approach is needed to measure the timing for each shot. This can be accomplished by recognizing that an electron ionized in the presence of the MIR field receives a momentum kick which depends on the relative phase between the MIR and X-ray pulses. The momentum shift of the photoelectron provides the start time to the decay measurement, while the momentum shift of the Auger electron provides information on the decay itself.

The experiment was performed during a beamtime in the summer of 2010. The data is currently undergoing analysis. Some preliminary results show simultaneous observation of the 1s and Auger

electron with MIR laser driven momentum shifts. The overall signal rate was lower than expected and analysis as well as simulation is ongoing to develop the data extraction techniques for this type of measurement. Monte Carlo simulations suggest that even with the observed signal rates, extraction with the time resolved data should be possible.

1.4 REFERENCES CITED

- [1] J. Tate *et al.*, Phys. Rev. Lett. **98**, 013901 (2007).
- [2] T. Popmintchev *et al.*, PNAS **106**, 10516 (2009).
- [3] N. Dudovich *et al.*, Nature Phys. **2**, 781 (2006).
- [4] P. Paul *et al.*, Science **292**, 1689 (2001).
- [5] M. Dahlström *et al.*, Phys. Rev. A **80**, 033836 (2009).
- [6] L. Young *et al.*, Nature **466**, 56 (2010).

1.5 PUBLICATION RESULTING FROM THIS GRANT

1. G. Doumy *et al.*, “Attosecond synchronization of high harmonics from mid-infrared drivers”, Phys. Rev. Lett. **102**, 093002 (2009).
2. G. Doumy *et al.*, “The frontiers of attosecond physics”, in Proceedings of the International Conference on Atomic Physics, (World Scientific Press, Singapore, 2009) 333-343.
3. G. Doumy *et al.*, “High order harmonics from mid-infrared drivers for attosecond physics”, in 16th International Conference on Atomic Processes in Plasmas (AIP Conference Proceedings, NY, 2009), 260-269.
4. E. Power *et al.*, “XFROG phase measurement of threshold harmonics in a Keldysh scaled system”, Nature Photonics, **4**, 352-356 (2010).
5. L. Young *et al.*, “Femtosecond electronic response of atoms to ultraintense x-rays”, Nature **466**, 56-61 (2010).
6. M. Hoener *et al.*, “Ultra-intense x-ray induced ionization, dissociation and frustrated absorption in molecular nitrogen”, Phys. Rev. Lett. **104**, 253002 (2010).
7. J. M. Glowia *et al.*, “Time-resolved pump-probe experiments at the LCLS”, Opt. Exp. **18**, 17620 (2010).
8. J. P. Cryan *et al.*, “Auger electron angular distribution of double core-hole states in the molecular reference frame”, Phys. Rev. Lett. **105**, 083004 (2010).
9. S. Ghimire *et al.*, “Observation of high-order harmonic generation in a bulk crystal”, Nat. Phys. **7**, 138 (2011).
10. G. Doumy *et al.*, “Nonlinear atomic response to intense ultrashort x-rays”, Phys. Rev. Lett. **106**, 083002 (2011).

IMAGING OF ELECTRONIC WAVE FUNCTIONS DURING CHEMICAL REACTIONS

Louis F. DiMauro

Department of Physics

The Ohio State University

Columbus, OH 43210

dimauro@mps.ohio-state.edu

co-PIs: Pierre Agostini (OSU Physics) & Terry A. Miller (OSU Chemistry)

1.1 ACCOMPLISHMENTS

This document is a request for continuing funding of BES funded project (grant #: DE-FG02-06ER15833) entitled “Imaging of Electronic Wave Functions during Chemical Reactions” at The Ohio State University (OSU). To date, accomplishments of critical elements of molecular imaging include (1) implementation of high harmonic generation (HHG) from aligned N₂ molecules at long wavelength ($0.8 \leq \lambda \leq 2 \mu\text{m}$), (2) implementation of the RABBITT method for spectral phase measurements of high harmonic light at long wavelength, (3) novel study of high harmonics generated from condensed-phase water and (4) time-resolved laser-induced electron diffraction imaging of bond relaxation.

The proposal strategy is the continual utilization of the long wavelength fundamental fields to drive the ionization into the strong-field tunnel limit, a crucial prerequisite to retrieve molecular or atomic structure. Two approaches are being evaluated: (1) laser-driven electron diffraction (LIED) and (2) high harmonics from aligned molecules.

1.1 PROGRESS IN FY11

Laser-driven electron diffraction on isolated molecules. As outlined in the renewal proposal, an alternative, and perhaps more promising, method to imaging based on HHG is high resolution photoelectron angular distributions (PAD). As previously reported for atomic targets using near-infrared pulses (Okunishi *et al.*, Phys. Rev. Lett. **100**, 143001 (2008)), the angular distribution of rescattered electrons carries the fingerprint of a diffraction pattern from which it is possible to extract structural information about the target ions. We have established collaboration with the group of Prof. C.D. Lin at Kansas State University.

During the last year, we have recorded and analyzed momentum distributions of N₂ and O₂ using $\sim 2 \mu\text{m}$, 50 fs pulses at intensities of 10^{14} W/cm^2 . For these experimental parameters, the returning electronic wave packets can have a de Broglie wavelength comparable or smaller than the intramolecular distances, thus ensuring the necessary spatial resolutions required in molecular imaging. In our initial studies accurate electron-ion elastic differential cross sections (DCS) were extracted and compared with electron scattering DCS measured for neutral targets (DuBois and Rudd, J. Phys. B **9**, 2657 (1976)) using conventional electron guns. The agreement was excellent and indicated that recollision energies above 100 eV were achieved using the long wavelength drivers and confirmed that the short range part of the potential plays a central role in determining the shape of the DCS, an observation recently confirmed by Prof. C.D. Lin’s group.

Our study verified two important principles needed for imaging that are enabled by long wavelength ionization. For sufficiently high energy returning electrons ($> 100 \text{ eV}$) (1) backscattering results in a large momentum exchange and (2) the short range interaction allows for the use of an independent atom model of scattering. Together these principles allow one to retrieve relative atomic positions, e.g. bond lengths, from a LIED experiment in a manner similar to conventional electron diffraction measurements. Figure 1 is a summary of the main finding of our study and the paper is under consideration for publication in Nature.

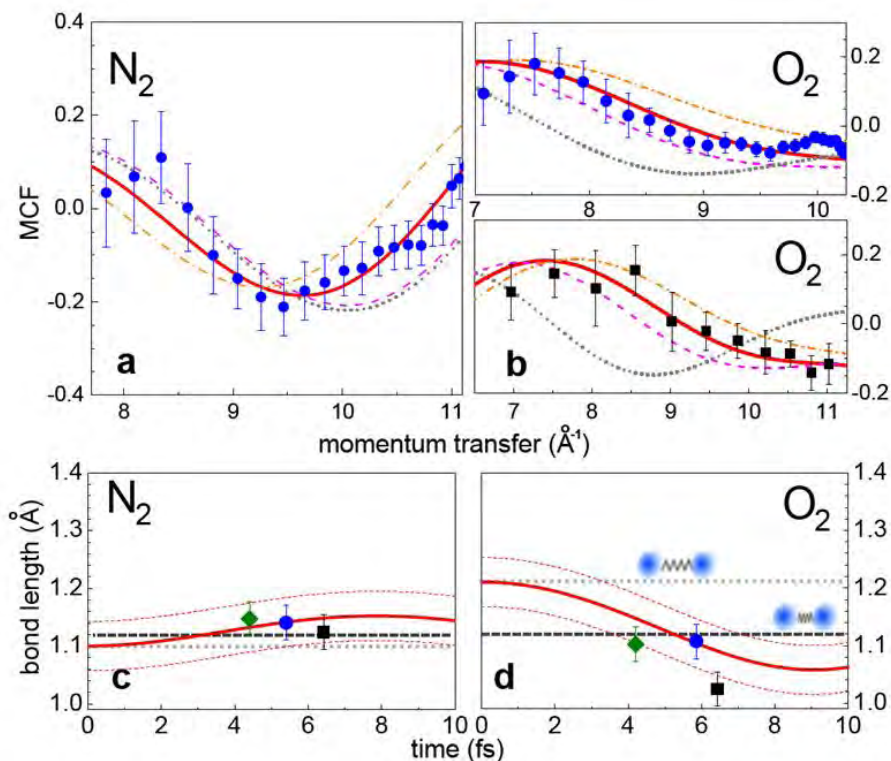


Figure 1: Comparison of experiment and theory for time-resolved LIED of bond relaxation. (a) The molecular contrast factor (MCF) extracted from the measured momentum distribution resulting from ionization of unaligned N_2 molecules by 260 TW/cm^2 , $2.0 \mu\text{m}$ pulses (blue circles). The analysis is performed for a return momentum of 2.97 a.u. (120 eV) and the error bars are statistical obeying a Poisson distribution. The solid red line is the genetic algorithm best fit to the experimental data. The gray dotted line is the calculated MCF assuming the equilibrium bond length for the neutral molecule. The dash-dotted orange and dashed magenta lines are the calculated MCF curves for $+5 \text{ pm}$ and -5 pm , respectively, around the best fit. (b) The experimental MCF for O_2 is shown for 133 TW/cm^2 , $2.0 \mu\text{m}$ (upper panel, blue circles) and 150 TW/cm^2 , $2.3 \mu\text{m}$ (lower panel, black squares). The corresponding return momenta are 2.71 a.u. (100 eV) and 2.97 a.u. (120 eV), respectively. The calculated lines have the same meaning as (a). Note that the calculated neutral MCF has a large shift compared to the experiment. (c) The LIED retrieved bond length as a function of time for N_2 ionized for $1.7 \mu\text{m}$ (green diamonds), $2.0 \mu\text{m}$ (blue circles) and $2.3 \mu\text{m}$ (black squares). The points are the values of R extracted from the experimental momentum distribution using the LIED procedure and the time is the classical correspondence between wavelength and wave packet propagation time. The dark grey dashed line is the equilibrium internuclear distance for N_2^+ . The red line is the calculated time-evolution of a vibrational wave packet assuming instantaneous excitation and the Franck-Condon principle. The error bars are the standard deviation ($\sigma_{\text{avg}} = 3 \text{ picometers}$) that result from the analysis. The analysis is performed at momentum varying between $2.57\text{-}4.02 \text{ a.u.}$ or $90\text{-}220 \text{ eV}$ energy. For the $1.7 \mu\text{m}$, $2.0 \mu\text{m}$ and $2.3 \mu\text{m}$ data the intensities are 170 TW/cm^2 , 260 TW/cm^2 and 290 TW/cm^2 , respectively. Taking into account laser intensity and spectrometer calibration uncertainties the estimated overall spatial resolution is 5 pm , comparable in size with the full width of half maximum of the vibrational wave packet.

(d) The bond length as a function of time for O_2 ionized by varying mid-infrared wavelengths. The symbols and lines are identical analysis to (c). The momentum varies between $2.57\text{-}3.09 \text{ a.u.}$ or $90\text{-}130 \text{ eV}$ energy. For the $1.7 \mu\text{m}$, $2.0 \mu\text{m}$ and $2.3 \mu\text{m}$ data the intensities are 130 TW/cm^2 , 133 TW/cm^2 and 150 TW/cm^2 , respectively. Within 4-6 fs following ionization, the change in R in the case of N_2 is only $\sim 2 \text{ pm}$, too small to be resolved with the 3-5 pm resolution achieved in the experiment. In the case of O_2 however, within 4-6 fs following ionization the bond length shortens by $\sim 10 \text{ pm}$, an amount large enough to be reflected in all three data sets, demonstrating that using mid-infrared wavelengths the LIED approach at long wavelengths accurately captures the relaxation dynamics as the bond compresses over a 5 fs time-scale. At near infrared wavelengths ($0.8 \mu\text{m}$), bond length retrieval is less accurate, mainly due to the smaller momentum transfers. This work was performed in collaboration with Prof. C.D. Lin and Junliang Xu (Kansas State University).

Time-resolved molecular imaging of a chemical reaction using high harmonic generation. As discussed in our renewal proposal the NO molecule is an ideal and practical system for testing the ideas of molecular imaging. The long wavelengths offer a viable means for pushing the ionization into the tunnel regime. The ground state is an open-shell system and the A and B states are accessible with a DUV source. The ultimate aim is to imagine the NO excited state during a photodissociation process.

We have begun the ground work for performing this experiment using HHG as the probe. A 4-pulse stacker is being tested for improved molecular alignment. Using more than one pulse has been demonstrated to improve the degree of alignment in samples even with limited cooling due to expansion. [Cryan *et al.*, PRA **80**, 063412 (2009)]. Previously in our own work, we were only able to demonstrate adequate alignment using a static *cw*-gas jet which placed a limitation on the target density due to insufficient pumping. Our goal is to replace this *cw*-jet with an existing pulsed gas jet that allows for increased harmonic intensities due to the higher gas densities. However, we know that the pulse valve will not be as effective in rotational cooling, thus impacting the overall alignment. However, the stacker should overcome this limitation resulting in enhanced harmonic response due to both improved alignment and increased density.

1.2 TECHNICAL ISSUES

We had significant problems associated with the reliability of our 2 μm source due to aging components (12 years in operation). Through DOE funding we have been able to upgrade these components and implementation of these changes are now in progress. This will have a large benefit on our harmonic generation experiments.

1.3 PROJECT PERSONNEL

A new post-doctoral research associate, Dr. Manuel Kremer, joined the group in January 2011. Dr. Kremer was a student at MPI Heidelberg under the supervision of Prof. Ulrich and Dr. Moshhammer. Dr. Kremer is overseeing the 2 μm source upgrade and the high harmonic tomography of NO. Dr. Cosmin Blaga (NSF supported) and Kaikai. Zhang, a third year graduate student, have conducted the laser-driven electron diffraction experiments.

1.4 PUBLICATION RESULTING FROM THIS GRANT

1. “Attosecond Synchronization of High Harmonics from Mid-Infrared Drivers”, G. Doumy *et al.*, Phys. Rev. Lett. **102**, 093002 (2009).
2. “The Frontiers of Attosecond Physics”, G. Doumy *et al.*, in Proceedings of the International Conference on Atomic Physics [ICAP 2009] (World Scientific Press, Singapore, 2009), 333-343.
3. “High Order Harmonics from Mid-Infrared Drivers for Attosecond Physics”, G. Doumy *et al.*, in the Proceedings of Atomic Processes in Plasmas [APiP 2009] (American Institute of Physics, New York, 2009), 1574–1580.
4. “Harmonic generation from the near-resonant excitation of liquid H₂O and D₂O from an intense mid-infrared laser”, A. DiChiara, E. Sistrunk, T. A. Miller, P. Agostini and L. F. DiMauro, Opt. Lett., **17**, 113357 (2009).
5. S. Ghimire *et al.*, “Observation of high-order harmonic generation in a bulk crystal”, Nat. Phys. **7**, 138 (2011).

6. “Observation of femtosecond, sub-Angstrom molecular bond relaxation using laser-induced electron diffraction”, C. I. Baga, Junliang Xu, A. D. DiChiara, E. Sistrunk, K. Zhang, P. Agostini, L.F. DiMauro and C. D. Lin, Nature, in review.

High Intensity Femtosecond XUV Pulse Interactions with Atomic Clusters

Project DE-FG02-03ER15406

Progress Report to Dr. Jeff Krause - 7/11/11

Principal Investigator:

Todd Ditmire

The Texas Center for High Intensity Laser Science

Department of Physics

University of Texas at Austin, MS C1600, Austin, TX 78712

Phone: 512-471-3296

e-mail: tditmire@physics.utexas.edu

Collaborators: J. W. Keto and K. Hoffman

Program Scope:

The nature of the interactions between high intensity, ultrafast, near infrared laser pulses and atomic clusters of a few hundred to a few thousand atoms have been well studied by a number of groups world wide. Such studies have found that these interactions are more energetic than interactions with either single atoms or solid density plasmas and that clusters explode with substantial energy when irradiated by an intense laser. Under the previous phase of BES funding we extended investigation in this interesting avenue of high field interactions by undertaking study of the interactions of intense extreme ultraviolet (XUV) pulses with atomic clusters, and more recently, interactions with intense x-ray pulses from the Linac Coherent Light Source (LCLS). Our current work, funded under our recently renewed grant, builds on our previous work with a high energy high harmonic (HHG) femtosecond XUV source and seeks to study these XUV/cluster interactions at two to three orders of magnitude higher XUV intensity than we obtained in the laser phase. This is being accomplished by upgrading our HHG beam line to much higher drive energies on our new THOR Petawatt laser.

The goal of our experimental program has been to extend experiments on the explosion of clusters irradiated at 800 nm to the short wavelength regime (1 to 50 nm). The clusters studied range from a few hundred to a few hundred thousand atoms per cluster (i.e. diameters of 1-30 nm). Our studies with XUV light are designed to illuminate the mechanisms for intense pulse interactions in the regime of high intensity but low ponderomotive energy by measurement of electron and ion spectra. This regime of interaction is very different from interactions of intense IR pulses with clusters where the laser ponderomotive potential is significantly greater than the binding potential of electrons in the cluster. Most of our previous studies have been conducted with an XUV source created by converting a high-energy (0.1 J) femtosecond laser to the short wavelength region through high order harmonic generation in a gas jet. Soon we will be able to generate short wavelength pulses with up to 30 J of laser drive energy in a much longer focal length geometry than previously employed.

Our main interest with this upgraded HHG beam line is to continue experiments in Ar and Xe clusters augmented by experiments in solid material clusters of a range of low- to high Z materials. We are working to confirm a hypothesis about the origin of the high charge states seen in XUV irradiated exploding clusters. We assessed from our first experiments that the photo-ionization of the atoms and ions in each cluster is strongly affected by plasma continuum lowering (ionization potential depression) in a cluster nano-plasma. This effect, which is well known in plasma physics, leads to a depression of the ionization potential enabling direct photo-ionization of ion charge states which would otherwise have ionization energies which are above the photon energy employed in the experiment. In our present work we intend to confirm this

hypothesis by performing experiments in which XUV pulses of carefully chosen wavelength irradiate clusters composed, on one hand, of only low-Z atoms and, on the other hand, clusters with a mixture of this low-Z atom with higher Z atoms. The latter clusters will exhibit higher electron densities and will see greater ionization potential lowering than in the clusters composed only of low Z atoms. By measuring the charge state distribution we can see if direct single photon photo-ionization channels open for higher charge states when there is a higher plasma density in the cluster. The other major aspect of our new work is an exploration of the transition of explosions in these XUV irradiated clusters from hydrodynamic expansion to Coulomb explosion. Initial experiments on the THOR HHG beamline at 38 nm suggested that Xe and Ar clusters exhibited different explosion mechanisms. The work we intend with the upgraded HHG beam line will explore clusters of a range of atoms, including clusters from van der Waals bonded gas atoms and molecules (Xe, Kr, Ar, Ne, N₂ and CH₄) as well as clusters from solids (eg. SiO₂ and SnO₂). Experiments on clusters from solids will be enabled by development during the past grant period in which we constructed and tested a cluster generator based on the Laser Ablation of Microparticles (LAM) method. Using a LAM device we will explore oxide clusters as well as metal clusters chosen such that the intense XUV pulse rests at a wavelength that coincides with the giant plasma resonance of the metallic cluster.

Progress During the Past Year

Work during this past year has concentrated in three areas. First we are completing the analysis of results from the LCLS run on exploding clusters that we led during the previous funding period. Second we have designed and began construction of the high energy HHG beam line on the upgraded THOR Petawatt laser. Finally, we have planned and scheduled an experiment on the Texas Petawatt laser designed to demonstrate XUV pulse production with per pulse energies in excess of 1 mJ.

Femtosecond LCLS X-ray pulse interactions with Methane clusters

We are concluding the analysis of data from the LCLS in which we examined explosions of various clusters irradiated by intense pulses of 860 eV and 1.7 keV photons. In these experiments we examined ion and electron energy spectra as well as ion charge state distributions. Our recent focus was on understanding the data from methane clusters. Figure 1 shows ion time-of-flight data from various sized methane clusters irradiated by 150 pulses from the LCLS tuned to 860 eV. The peak intensity was $\sim 10^{17}$ W/cm². The most salient feature we observed in this particular species at the LCLS was the strong predominance of protons when compared to carbon ions, particularly in the largest clusters. What is more, the proton peak grows broader with increasing cluster size which would imply increased proton kinetic energy.

Our working hypothesis was that the methane clusters absorb the x-ray photons through ionization of the carbon, with subsequent ionization of the protons occurring while the carbon recombines. We therefore expect a shell of protons to be ejected leaving behind nearly neutral carbon atoms. To aid in confirming this hypothesis we are now working with the group of J. M. Rost in Dresden who have been simulating our experiment with molecular dynamics type simulations. Figure 1 reproduces one of their calculations, which confirms our exploding proton shell picture of the methane cluster in the LCLS beam.

Upgrade of the HHG XUV beamline

Our principal work in the past year has been in the design and development of a high energy HHG XUV beam line. In our past experiments on intense XUV irradiation of noble gas clusters we produced harmonic radiation by loosely focusing 40 fs pulses with a MgF f/60 lens from our THOR Ti:sapphire laser into an Ar gas jet.

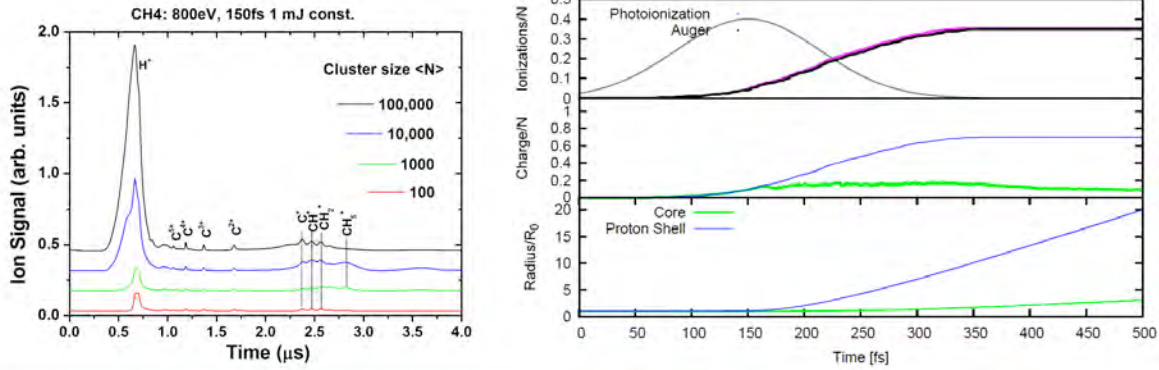


Figure 1: Time of flight spectra from methane clusters irradiated by the LCLS pulse at 860 eV (left). Results of the Dresden MD simulation of methane in the LCLS pulse. The third plot down shows the rapid expansion of the proton shell with time during the 150 fs pulse.

We separated the harmonics from the IR by imaging an annular beam mask in the infrared beam before the focusing lens onto an aperture after the focus, taking advantage of the fact that the XUV harmonics have substantially less divergence than the infrared beam. To reject scattered infrared light and to pass high harmonics with the energies between 15 eV and 73 eV an additional a 200 nm thin Al filter was used. To select a single XUV harmonic we then employed a specially designed Sc/Si short focal length multilayer mirror optimized for the 21st harmonic at 32.5 eV (38.1 nm) at close to normal incidence. These data showed that we were able to produce an 8μm spot with the 38 nm pulse, yielding a focal intensity of $\sim 10^{11}$ W/cm² assuming an XUV pulse duration of 20 fs. These harmonics were then focused into the plume of a second, low density cluster jet. This cluster interaction region was located in a separate vacuum chamber. A Wiley McLaren time-of-flight (TOF) spectrometer was used to extract positive ions after photoionization of the Xe clusters. The main limitation of this apparatus was that pulse energy was limited to ~ 100 mJ by the use of lens and focal geometry constrained by the lab space. This greatly limit the XUV energy produced to only ~ 10 nJ.

We are now working to improve this beamline. Figure 2 shows the new configuration of the beam line which now spans three rooms permitting focusing with a mirror. This will allow us to focus nearly the entire 30 J from our upgraded laser, improving the HHG intensity by at least two orders of magnitude.

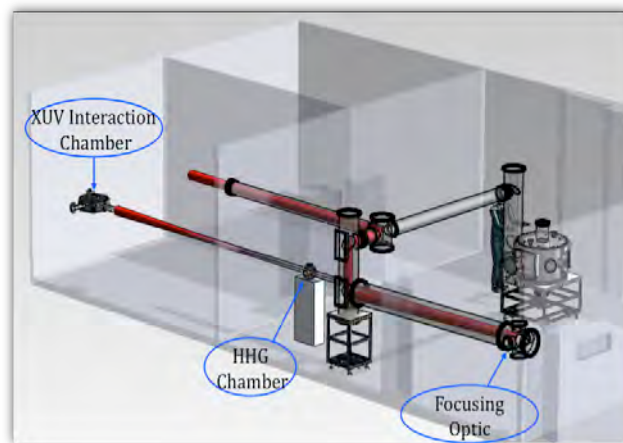


Figure 2: Schematic of the new 30 J HHG XUV beamline on the THOR Petawatt laser.

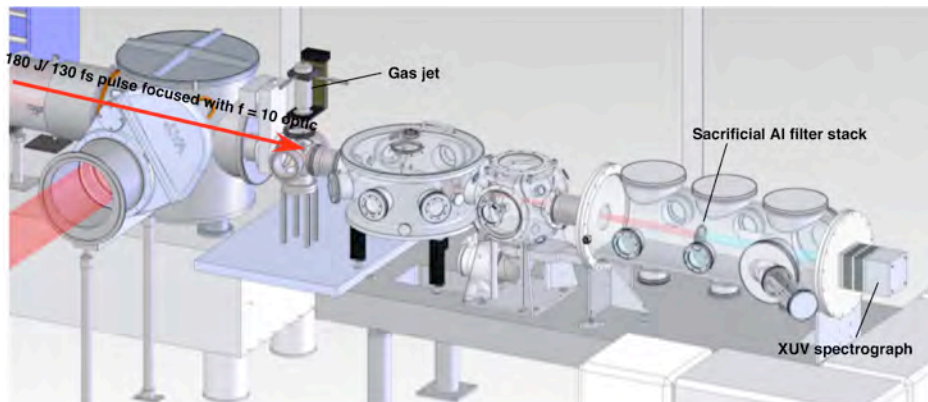


Figure 3: CAD design of the high energy HHG experiment planned on the Texas Petawatt laser.

We are pushing this idea even further in an experiment pictured in figure 3. Our plans are to use the 180 from the Texas Petawatt laser to generate HHG pulses. We estimate producing over 1 mJ per pulse at ~ 30 nm in this way.

Future Research Plans

Our future plans involve studying continuum lowering in mixed species clusters. We have previously finished the construction of a micro-particle laser ablation beam to be installed on the beam line in figure 2. This will allow us to study continuum lowering in mixed low and high Z clusters. These new experiments will commence on the upgraded THOR laser at the ~ 2 J level early this fall and will move to 30 J drive pulses next year. We also have scheduled later this fall the Texas Petawatt run on HHG.

Refereed papers published or submitted on work supported by this grant during the past three years

- 1) H. Thomas, A. Helal, K. Hoffmann, N. Kandadai, J. Keto, J. Andreasson, B. Iwan, M. Seibert, N. Timneanu, J. Hajdu, M. Adolph, T. Gorkhover, D. Rupp, S. Schorb, T. Möller, G. Doumy, L.F. DiMauro, M. Hoener, B. Murphy, N. Berrah, M. Messerschmidt, J. Bozek, C. Bostedt and T. Ditmire, "Explosions of Xe-clusters in ultra-intense femtosecond x-ray pulses from the LCLS Free Electron Laser" *Phys. Rev. Lett.* submitted.
- 2) N. Kandadai, K. Hoffmann, A. Helal, H. Thomas, J. Keto, J. Andreasson, B. Iwan, M. Seibert, N. Timneanu, J. Hajdu, M. Adolph, T. Gorkhover, D. Rupp, S. Schorb, T. Möller, G. Doumy, L.F. DiMauro, M. Hoener, B. Murphy, N. Berrah, J. Bozek, C. Bostedt and T. Ditmire, "Explosion of Methane Clusters in Intense X-ray FEL Pulses" *Phys. Rev. Lett.* submitted.
- 3) K. Hoffmann, B. F. Murphy, N. Kandadai, B. Erk, A. Helal J. Keto, and T. Ditmire, "Rare-gas-cluster explosions under irradiation by intense short XUV pulses" *Phys. Rev. A*, **83**, 043203 (2011).
- 4) B. Erk, K. Hoffmann, N. Kandadai, A. Helal, J. Keto, and T. Ditmire "Observation of shells in Coulomb explosions of rare-gas clusters" *Phys. Rev. A* **83**, 043201 (2011).
- 5) K. Hoffmann, B. Murphy, B. Erk, A. Helal, N. Kandadai, J. Keto, and T. Ditmire "High intensity femtosecond XUV pulse interactions with atomic clusters" *J. of High En. Den. Phys.*, **6**, 185 (2010).
- 6) A. P. Higginbotham, O. Semonin, S. Bruce, C. Chan, M. Maindi, T. D. Donnelly, M. Maurer, W. Bang, I. Churina, J. Osterholz, I. Kim, A. C. Bernstein, and T. Ditmire, "Generation of Mie size microdroplet aerosols with applications in laser-driven fusion experiments", *Rev. Sci. Instr.* **80**, 063503 (2009).
- 7) B. F. Murphy, K. Hoffmann, A. Belilopetski, J. Keto, and T. Ditmire, "Explosion of Xenon Clusters Driven by Intense Femtosecond Pulses of Extreme Ultraviolet Light" *Phys. Rev. Lett.* **101**, 203401 (2008).
- 8) S. Kneip, B. I. Cho, D. R. Symes, H. A. Sumeruk, G. Dyer, I. V. Churina, A. V. Belolipetski, A.S. Henig, T. D. Donnelly, and T. Ditmire "K-shell Spectroscopy of Plasmas Created by Intense Laser Irradiation of Micron-scale Cone and Sphere Targets" *J. High Energy Density Physics*. **4**, 41 (2008)

Ultracold Molecules: Physics in the Quantum Regime

John Doyle

Harvard University

17 Oxford Street

Cambridge MA 02138

doyle@physics.harvard.edu

1. Program Scope

Our research encompasses a unified approach to the trapping of diverse chemical species of both atoms and molecules. Our current goal is to study both CaH to NH and approach the ultracold regime. Our plan is to trap and cool NH and CaH molecules and measure elastic and inelastic collisional cross sections. Cooling to the ultracold regime will be attempted. We note that as part of this work, we are continuing to develop an important trapping technique, buffer-gas loading.

2. Recent Progress

NH and CaH, like many of the diatomic hydrides, have several advantages for molecular trapping including large rotational constant and relatively simple energy level structure. Some of the several key questions before us when this project began were: Could we produce enough NH using a pulsed beam? Is it possible to introduce a large number of NH molecules into a buffer gas? Would the light collection efficiency be enough for us to adequately detect fluorescence from NH? Could we get absorption spectroscopy to work so that absolute number measurements could be performed? Could we achieve initial loading of NH into the magnetic trap? Will the spin relaxation rates with helium be low enough for us to remove the buffer gas? We have now answered these questions, all to the positive. In addition, we have added several new features to the project including co-trapping of N with NH and the addition of CaH to our program.

Recently, we have made measurements of both NH-N and N-N collision rates. There are still key questions as we move forward. What will be the nature of an ultracold dense sample of heteronuclear molecules? Specifically, what about the hydrides, with their large rotational constants? Can metastable molecular states be used to switch between atom-like objects and molecular-like objects? These questions are still partially open and answering them are some of the long-term goals of this work.

Summary of Status of Project

The heart of the apparatus is a beam machine that we used to produce pulsed NH – alone or in combination with atomic N – in a beam (see figure 1). (Figure 3 shows a photo of the internals of the apparatus.) We have used two types of sources successfully, an “RF Plasma Source (CW)” and a “Glow Discharge Source (Pulsed)”. The plasma source is a commercial source used typically in MBE machines. The design of the pulsed source is based on the production of OH via DC discharge as executed by Nesbitt.

This beam is directed toward our trapping magnet, inside of which is a cryogenic buffer-gas cell. This cell can be cooled to as low as 500 mK by a He³ refrigerator. An entrance orifice of a few mm in diameter to allow the beam of NH to enter the cell. In a new addition to our apparatus, at the opposite end is a much larger orifice that allows for a new cold pulsed beam of helium to enter. The idea is that the helium pulse arrives simultaneously with the NH/N pulse, thermalizes the N/NH (leading to trapping), and then quickly exits. Thus, buffer-gas cooling and trapping of the NH and/or N takes place.

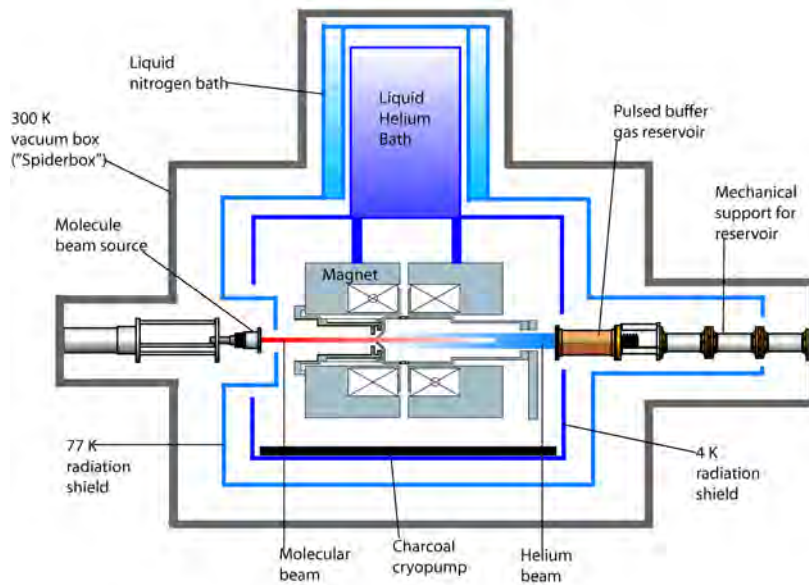


Figure 1: Schematic of current molecule trapping apparatus. The NH molecules and N atoms travel into the trapping region from the molecular beam source, where they are thermalized with the buffer gas and trapped. Simultaneous detection of NH and N is done spectroscopically.

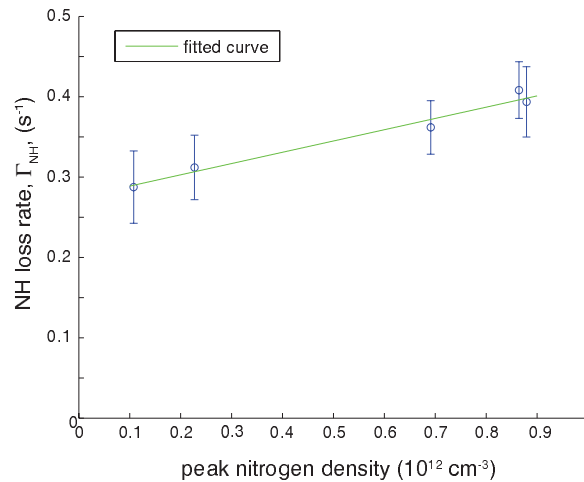


Figure 2: NH lifetime as a function of co-trapped Nitrogen atom density in our magnetic trap. This represents a first measurement of N-NH inelastic cold collision properties.

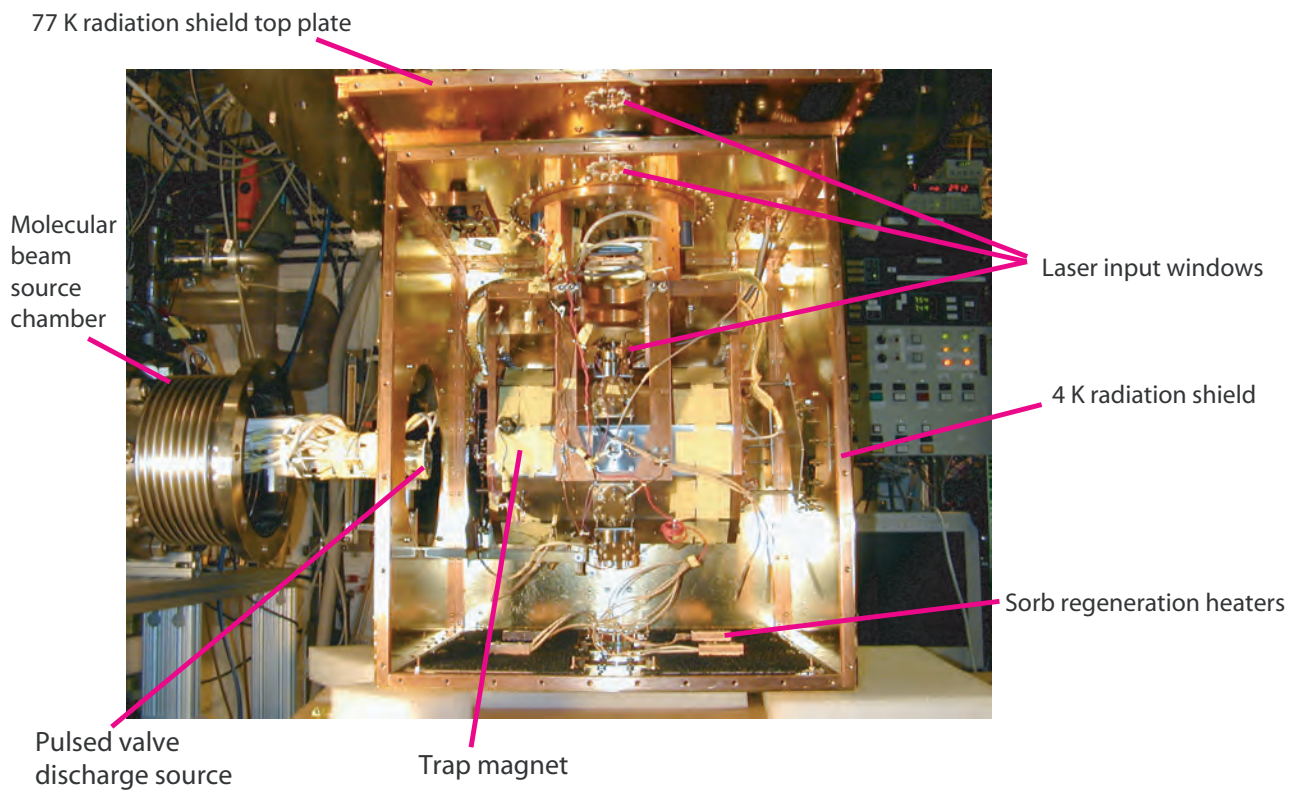
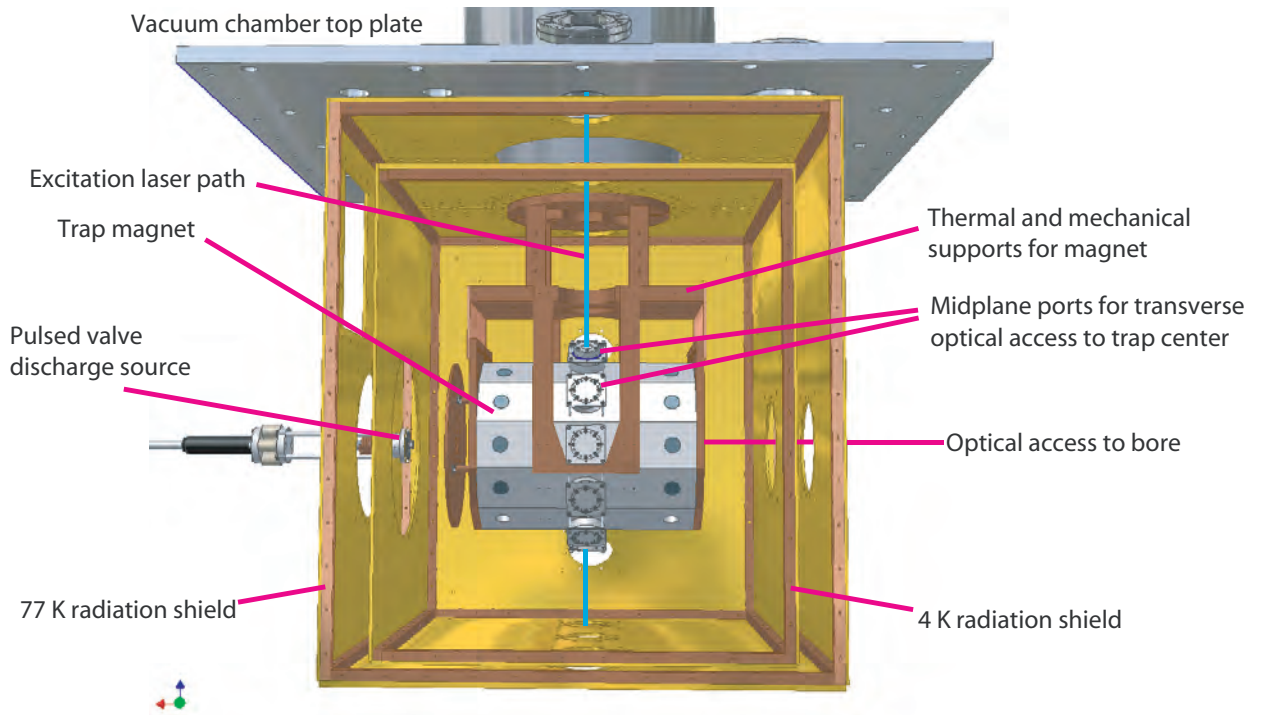
The basic experimental procedure is as follows. The source beam is directed toward the trap for times from about 10-100 ms. This long pulse beam travels about 10 cm to the face of the cell where some portion enter through the orifice and into the cell. The NH and/or N are then cooled by the buffer gas to their ground state by the helium resident in the cell. In our latest experiments we have been using fluorescence and absorption spectroscopy to detect trapped NH pulsed TALIF to simultaneously detect trapped atomic N. We have been able to observe trapped NH molecules and N for many seconds. Figure 2 shows condensed data of NH trapped lifetimes

versus co-trapped N density. As will be described in my talk, this indicates a measurement of N-NH inelastic processes. We have published one combined theory/experiment paper on trapped N-N collisions *Collisional properties of cold spin-polarized nitrogen gas: theory, experiment, and prospects as a sympathetic coolant for trapped atoms and molecules*, T.V. Tscherbul, J. Klos, A. Dalgarno, B. Zygelman, Z. Pavlovic, M.T. Hummon, H. Lu, E. Tsikata, and J.M. Doyle,, Physical Review A, **82**, 042718 (2010) and another, on N-NH collisions *Cold N+NH Collisions in a Magnetic Trap*, M.H. Hummon, T.V. Tscherbul, J. Klos, H.-I Lu, E. Tsikata, W.C. Campbell, A. Dalgarno, and J.M. Doyle,, Physical Review Letters, **106**, 053201 (2011). Publications from earlier in the past grant period include studies of NH-He collisions, *Magnetic Trapping and Zeeman Relaxation of NH*, W.C. Campbell, E. Tsikata, H. Lu, L.D. van Buuren, and J.M. Doyle, Physical Review Letters, **98**, 213001 (2007) and *Mechanism of Collisional Spin Relaxation in $^3\Sigma$ Molecules*, W.C. Campbell, T.V. Tscherbul, Hsin-I Lu, E. Tsikata, R.V. Krems, and J.M. Doyle, Physical Review Letters **102** 013003 (2009).

3. Future Plans

We continue on our program of trapping of NH with N and have embarked on a new approach to trap CaH, using combinations of optical and buffer-gas methods. With both species the technical challenge is to create high enough density to see collisions with a low background pressure.

Figure 3:



Atomic Electrons in Strong Radiation Fields

J. H. Eberly
Department of Physics and Astronomy
University of Rochester, Rochester, NY 14627
eberly@pas.rochester.edu

July 1, 2011

Scope: Electron Correlation under Strong Laser Fields

We are interested to understand how very intense laser light couples to atoms and molecules. Theoretical study faces substantial challenges in this domain. These arise from the combination of high intensity, fully phase-coherent character and short-time nature of the laser pulses in use, where the laser's electric-field force roughly matches the Coulomb forces among electrons and the nucleus. An important additional challenge arises when there is a need to account for more than one dynamically active electron.

Our work builds on earlier results obtained from numerical experiments [1, 2]. These were studies of two, three and four active atomic electrons in strong time-dependent and phase-coherent fields, using very large ensembles of classical multi-electron trajectories. The technique is capable of unique theoretical exploration. For example, it has achieved what we believe is the only direct comparison of ion-momentum distribution data between theory [3] and experiment [4] in triple ionization. Examples of topics where we expect similar advances will be possible are (i) multiple-electron ionization, (ii) effects arising from finite ellipticity, $\varepsilon \neq 0$, (iii) breakdown of the single-active electron approximation, and (iv) coherence in multi-electron pre-ionization joint-memory.

Elliptical Polarization and Ion-Momentum Distributions

A quick summary is this. Almost all NSDI experiments have been carried out with linearly polarized laser pulses, but elliptically polarized light has recently been proposed and used in a number of applications related to NSDI in high-field and attosecond environments. The recollision model for NSDI [5], as usually understood, naturally argues against successful e-e correlation with any substantial amount of ellipticity, because the orbits of an ionized electron that experience a transverse push are not able to revisit the ion to collide. Early experiments (Fittinghoff, et al., and Dietrich, et al., [6, 7]) confirmed that NSDI production drops rapidly as a function of ellipticity ε , and was not detectable beyond $\varepsilon \approx 0.25$. However, in clear conflict with the recollision scenario, several observations of NSDI have been reported under circular polarization [8, 9]. Preliminary explanations from our work and from phase-space analyses are just beginning to be reported [10, 11].

The lack of cylindrical symmetry defeats essentially all available methods for integrating the time-dependent Schrödinger equation (TDSE) to obtain a useful non-perturbative wave function in an elliptically polarized laser field. However, our classical TDNE trajectory approach provides another non-perturbative numerical method, and by using 1-million to 10-million member ensembles we undertook a trajectory study of the high-field effects of an elliptically polarized field over a wider range. By applying a sine-squared or trapezoidal envelope pulse:

$$\vec{E}(t) = E_0 f(t) [\hat{e}_x \sin(\omega t + \phi) + \hat{e}_y \varepsilon \cos(\omega t + \phi)], \quad (1)$$

we obtained numerical ion-momentum distributions over the entire range of ellipticities from linear to circular, in the high-field regime. No such similar TDSE or quantum SFA calculation appears currently to be feasible. A view of some results is provided in Fig. 1, where novel and non-trivial structural features are evident.

Features of most interest in the distributions occur in the mid-range near $\varepsilon = 0.5$. Four distinct bands give peaks in p_y for ellipticities $\varepsilon = 0.3 - 0.7$, whereas near to $\varepsilon = 0$ and $\varepsilon = 1$ the distributions are without significant internal structure. The first question is whether the four-band structure for ε around 0.5 in Fig. 1 is real, i.e., can it be observed experimentally? We were surprised to find a positive answer quickly. Such bands can be seen in experimental work reported earlier by the Heidelberg-Kansas State collaboration [12]. Our calculation and this data are both shown in Fig. 2. The calculated longitudinal distribution shows a single peak, while the transverse distribution shows four peaks. These are also visible in the experimental record. The poorer definition of the experimental peaks makes them harder to pick out. This is also consistent with the calculated distributions, which show poorer resolution (see Fig. 1) for high values of ε beyond 0.5. The experimental pulses were close to circular, with $\varepsilon \sim 0.8$ or possibly higher.

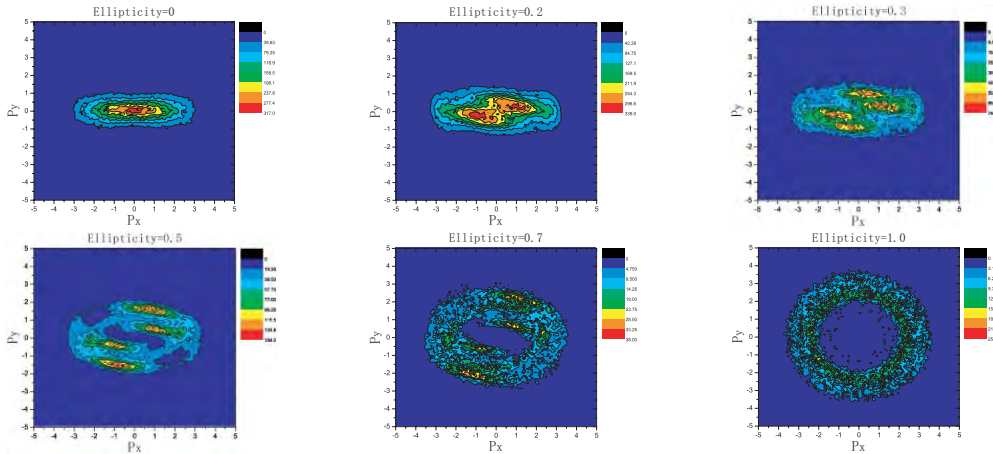


Figure 1: End-of-pulse x - y momentum correlation distributions for doubly ionized ions with ellipticities from 0 to 1, as indicated by the top label of each panel. From Wang and Eberly (2009) [10].

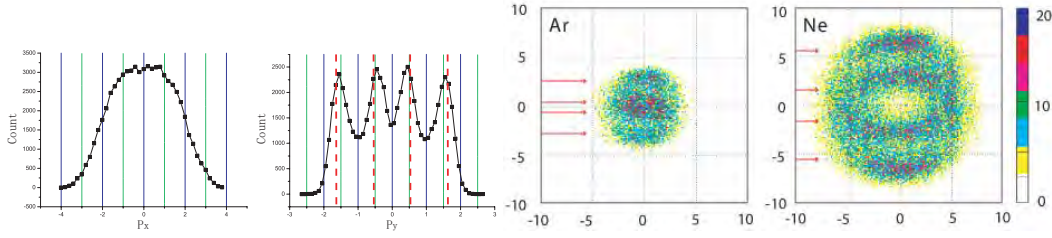


Figure 2: Momentum correlation distributions (from Wang and Eberly [10] for $\varepsilon = 0.5$) for SDI electrons along the major and minor (x and y) polarization axes, are shown along with experimental results (from Maharjan, et al. [12]) for Ne and Ar atoms and $\varepsilon \sim 0.8$. Red arrows indicate peak predictions obtained from an over-barrier estimate of ionizing field strengths.

Ellipticity and the Single Active Electron Approximation

Now we are directing attention to a regime where a breakdown in the SAE approximation has been suggested by the ETH-Zurich group [13]. Existing calculations of ours [14] appears to support a breakdown, with evidence for “knee” obtained from trajectories experiencing no recollision at all. This is shown in the first panel of Fig. 3.

A wide range of first ionization field strengths (as reported in [11]) implies that in a strong enough laser field the Coulomb barrier height is not really fixed or static. Additionally, what we have called “precollisions” during the pre-ionization interval also appear important. Precollisions allow ionization at field strengths both higher and lower than the SAE over-barrier value. It has been reasonably suggested (C.L. Cocke) that in a quantum interpretation the result of classical recollisions may be equivalent to weak coherences in the joint two-electron quantum state. SAE breakdown would require an interesting re-examination of Keldysh’s near-optical tunneling theory, a prospect which has often been suggested is long overdue.

We should anticipate species effects. It appears from the preliminary calculations with a magnesium model atom (see right two panels in Fig. 3) that we may even be able to untangle the various contributions to double ionization.

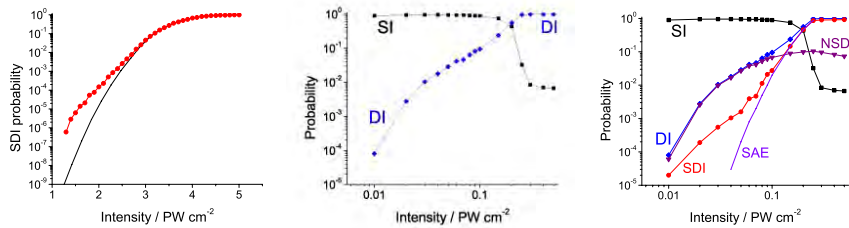


Figure 3: In pure SDI events an NSDI-type knee pattern is obtained from double ionization of an argon model atom with $\varepsilon = 0.5$. Back-analysis confirms that no recollisions occurred. In the right two panels one sees for a low- I_P atom such as Mg, that there is predicted to be an SDI knee, but buried under a much stronger collisional NSDI knee. The dashed SAE curves are sketched by hand. From Wang and Eberly (2011) [14].

Publications supported by DOE Grant DE-FG02-05ER15713 are marked with *** in the listing below.

References

- [1] R. Panfili, S.L. Haan and J.H. Eberly, *Phys. Rev. Lett.* **89**, 113001 (2002).
- [2] Phay J. Ho, R. Panfili, S. L. Haan and J. H. Eberly, *Phys. Rev. Lett.* **94**, 093002 (2005). See also Phay J. Ho, *Phys. Rev. A* **74**, 045401 (2005), ***Phay J. Ho and J.H. Eberly, *Phys. Rev. Lett.* **95**, 193002 (2005), ***Phay J. Ho and J.H. Eberly, *Phys. Rev. Lett.* **97**, 083001 (2006), and ***S.L. Haan, L. Breen, A. Karim, and J. H. Eberly, *Phys. Rev. Lett.* **97**, 103008 (2006).
- [3] ***P.J. Ho and J. H. Eberly, *Optics Expr.* **15**, 1845 (2007).
- [4] K. Zrost, A. Rudenko, Th. Ergler, B. Feuerstein, V. L. B. de Jesus, C. D. Schröter, R. Moshhammer, and J. Ullrich, *J. Phys. B* **39**, 40 (2006).
- [5] P. B. Corkum, *Phys. Rev. Lett.* **71**, 1994 (1993).
- [6] D.N. Fittinghoff, P. R. Bolton, B. Chang, and K. C. Kulander, *Phys. Rev. A* **49**, 2174 (1994).
- [7] P. Dietrich, N. H. Burnett, M. Yu. Ivanov, and P. B. Corkum, *Phys. Rev. A* **50**, R3585 (1994).
- [8] C. Guo, et al., *Phys. Rev. A* **58**, R4271 (1998), and C. Guo and G.N. Gibson, *Phys. Rev. A* **63**, 040701(R) (2001).
- [9] G. D. Gillen et al., *Phys. Rev. A* **64**, 043413 (2001).
- [10] ***Xu Wang and J.H. Eberly, *Phys. Rev. Lett.* **103**, 103007 (2009). See also Xu Wang and J.H. Eberly, *Laser Phys.* **19**, 1518 (2009).
- [11] ***Xu Wang and J.H. Eberly, *Phys. Rev. Lett.* **105**, 083001 (2010). See also, ***Xu Wang and J.H. Eberly, *New J. Phys.* **12**, 093047 (2010)
- [12] C.M. Maharjan, A. S. Alnaser, X. M. Tong, et al., *Phys. Rev. A* **72**, 041403(R) (2005).
- [13] ***A.N. Pfeiffer, et al., *New J. Phys.* **xx**, yyyyyy (2011).
- [14] ***Xu Wang and J.H. Eberly, arXiv:1102.0221 (2011).

Algorithms for X-ray Imaging of Single Particles

Office of Basic Energy Sciences
Division of Chemical Sciences, Geosciences, and Biosciences
Program in Atomic, Molecular, and Optical Sciences

Veit Elser, Department of Physics
PSB 426, Cornell University
Ithaca, NY 14853
(607) 255-2340
ve10@cornell.edu

Program Scope

The many-orders-of-magnitude gains in X-ray brightness recently achieved by free-electron laser sources such as the LCLS are driving a fundamental review of the data analysis methods in X-ray science. It is not just a question of doing the old things faster and with greater precision, but doing things that previously would have been considered impossible. My group at Cornell is working closely with experimental groups at LCLS and FLASH to develop data analysis tools that exploit the full range of opportunities made possible by the new light sources.

Recent Progress

One of the most ambitious proposals[1] stimulated by the new sources is the possibility of imaging individual particles, with an emphasis on biological particles that do not crystallize. Even with the full fury of the LCLS trained on a single protein complex, the diffraction pattern produced by a single laser pulse — the limit of what the particle can scatter before it explodes — looks like pure noise. It will test the faith of the experimental team to take millions of data of the kind shown simulated in Figure 1 (on near-identical particles), on the promise that the few hundred or so photons per data can tell us the structure! The unknown particle orientation in each measurement presents a random 2D structure projection to the beam, making simple signal averaging impossible.

Using the cryotomography approach introduced for a simple theoretical model[2] we were able to carry out particle reconstructions from simulated data of the quality in Figure 1 using the EMC algorithm developed specifically for this problem[3]. On the single computer available to us at the time we were limited to low resolution reconstructions, such as the one shown in Figure 1 (right panel). In the summer of 2011 we plan to double the resolution, again with simulated data, using the computing cluster at SLAC. Perhaps by next year the first actual single-particle data will become available at the CXI end station of LCLS.

Many of the ideas developed for dealing with noise in single particle imaging also apply to other targets. Although magnetic domains in thin film samples are by comparison macroscopic, the contrast mechanism is very weak and signal averaging is not an option when one is interested in tracking dynamics with one pulse per frame. Due to the high interest in magnetic phenomena, we made a comprehensive study of the theoretical noise limits in magnetic imaging[4, 5] (Figure 2) and developed algorithms that perform well even when the number of scattered photons is a few per pixel of resolved contrast.

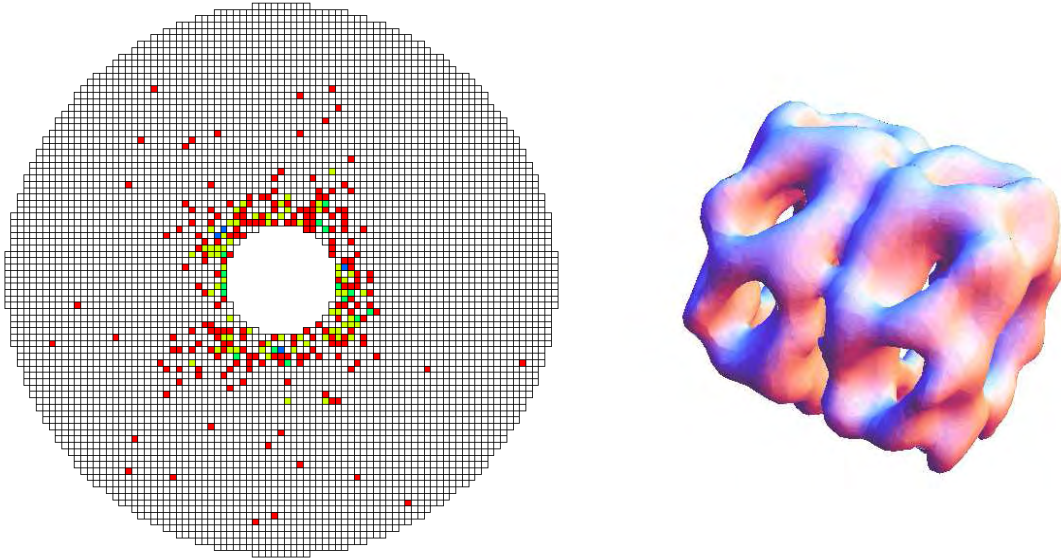


Figure 1: *Left*: Simulated diffraction pattern in a single particle imaging experiment, where color (white, red, green, blue) represents recorded photon counts (0, 1, 2, 3). *Right*: GroEL (a molecular chaperone) reconstructed from simulated data such as shown on the left. The resolution is estimated at 2 nm [3].

Future Plans

We will continue to augment our EMC single-particle reconstruction algorithm to address experimental realities. These include background photon counts and shot-to-shot X-ray fluence fluctuations. The background level is at this time a great unknown, and we hope that experiments this year will provide an estimate. Our simulation run at SLAC this summer will test how much background can be tolerated. Assuming the background is within tolerable limits, we will work with the experimental group at LCLS to develop a standard for compressing the data files which, in the absence of strong background, will be sparse. This is probably the single most significant way in which data processing will change: a move away from diffraction “images” to records of photon “events”.

Given the risks, we are also working on alternative strategies for imaging non-crystallized particles. One of these, originally proposed by Kam[6] and more recently studied by Dilano and coworkers, involves measuring intensity-intensity correlations from an ensemble of identical particles (in solution or gas phase). Whereas we showed that 3D reconstructions from a non-oriented ensemble is impossible[7], more recently we developed a complete 3D reconstruction method that requires only partial orientation, *i.e.* alignment with respect to a single axis. Proteins supported and aligned by a synthetic membrane and rotationally diffusing about its surface normal would be an obvious target addressed by this method. There are actually two “phase problems” encountered in this type of reconstruction and the method we have developed appears more promising than earlier methods in that the phases in the contrast and the phases in the intensity pattern are reconstructed in tandem. Figure 3 shows the reconstruction process applied to simulated intensity correlation data from the diffraction produced by an ensemble of spinning α 's.

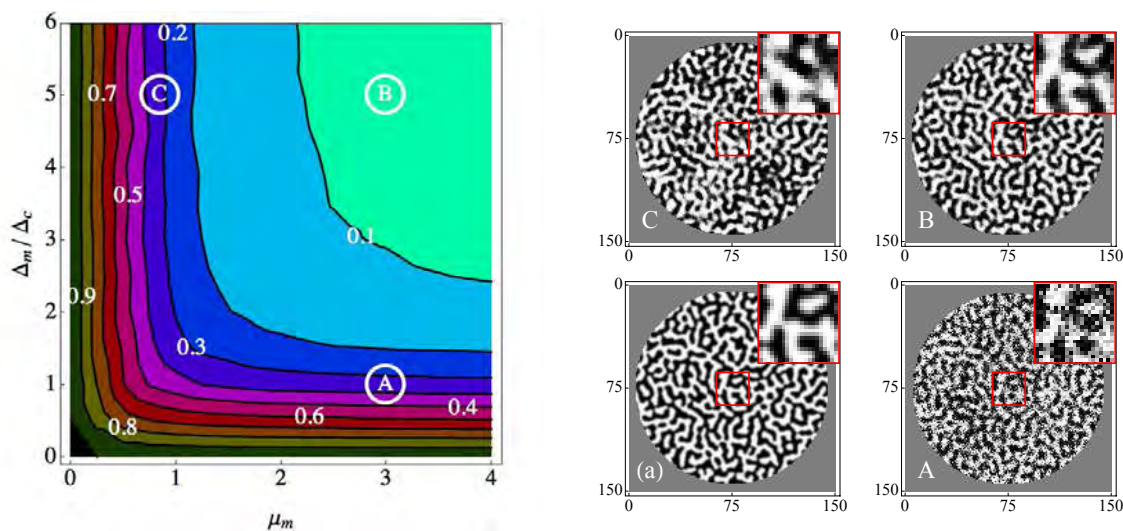


Figure 2: *Left:* Contour plot giving the fidelity of magnetic domain reconstructions as a function of shot noise (μ_m) and background (Δ_m/Δ_c) [5]. Small contour values correspond to high fidelity. *Right:* The magnetic contrast of the circular sample is shown in (a) and A-C are reconstructions at the corresponding points of the contour plot on the left. Panel A is an example of extreme charge background; reconstruction C is at the shot-noise limit — about 1 photon per pixel.

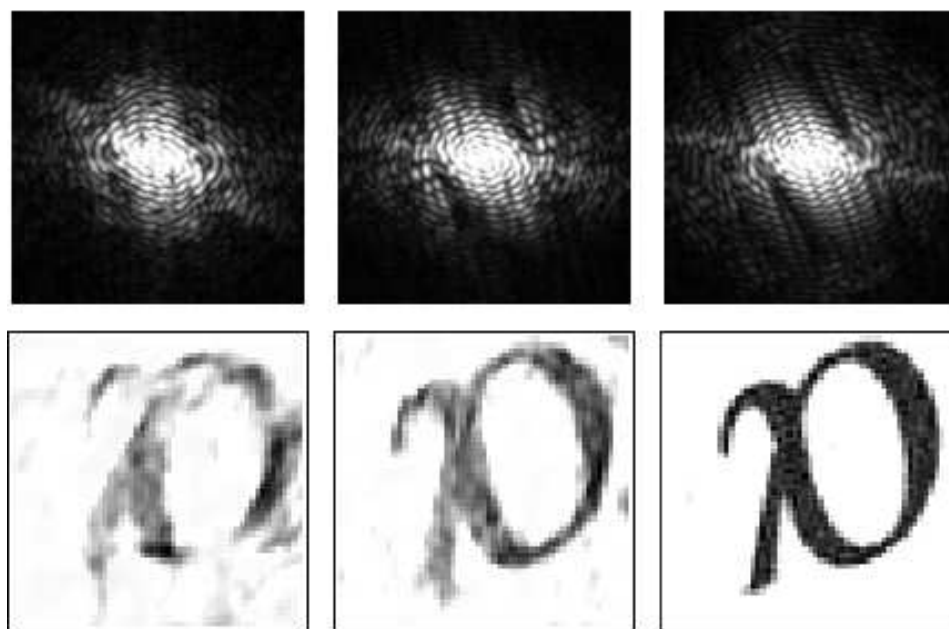


Figure 3: Iterations 40, 70, and 200 in the simultaneous reconstruction of the intensity (top) and contrast (bottom) of a test particle (the letter α) where the raw (simulated) data is intensity-intensity correlations from an ensemble of non-oriented particles.

References

- [1] R. Neutze, R. Wouts, D. van der Spoel, E. Weckert & J. Hajdu, *Potential for biomolecular imaging with femtosecond X-ray pulses*, Nature **406**, 752-757 (2000).
- [2] V. Elser, *Noise limits on reconstructing diffraction signals from random tomographs*, IEEE Trans. Information Theory **55**, 4715-4722 (2009).
- [3] N.-T. D. Loh & V. Elser, *Reconstruction algorithm for single-particle diffraction imaging experiments*, Phys. Rev. E **80**, 026705 (2009).
- [4] V. Elser & S. Eisebitt, *Uniqueness transition in noisy phase retrieval*, New J. Phys. **13**, 023001 (2011).
- [5] N.-T. D. Loh, S. Eisebitt, S. Flewett & V. Elser, *Recovering magnetization distributions from their noisy diffraction data*, Phys. Rev. E **82**, 061128 (2010).
- [6] Z. Kam, *Determination of macromolecular structure in solution by spatial correlation of scattering fluctuations*, Macromolecules **10**, 927-934 (1977).
- [7] V. Elser, *Strategies for processing diffraction data from randomly oriented particles*, Ultramicroscopy **111**, 788-792 (2011).

Reaction Imaging and the Molecular Coulomb Continuum

Department of Energy 2011-2012

James M Feagin

Department of Physics

California State University–Fullerton

Fullerton CA 92834

jfeagin@fullerton.edu

We continue work to extract basic understanding and quantum control of few-body microscopic systems based on our long-time experience with more conventional studies of correlated electrons and ions. Given the enormous advances over the past 20 years to our understanding of quantum correlations with photon interferometry, AMO collision science generally is ready to move beyond the one-particle, single-port momentum detection that has dominated collision physics since Rutherford. A recent beautiful example that much impresses is a direct measurement of the real and imaginary parts of a photon's transverse wavefunction reported in Nature.¹ These sorts of observations involving 'quantum weak measurements' (Aharonov-Vaidman) should in principle be just as doable with massive particles.² Nevertheless, our familiar theoretical tools for collision theory will need to be upgraded to incorporate these more generalized measurement formalisms and ultimately to provide incentive for a new generation of experiments.

On a broader scale, fresh insight into few-body science at molecular nano levels will be a critical component of ongoing national and international efforts to establish sustainable energy and environmental resources. The varied research paths to be taken will require the development of basic science on broad fronts with increasingly flexible views to crossover technologies.

Although the work described in this report is theoretical, our interest in these topics remains strongly motivated by the recent surge in and success of experiments involving few-body atomic and molecular fragmentation and the collection of all the fragments. We accordingly continue two parallel efforts with (i) emphasis on *reaction imaging* while (ii) pursuing longtime work on *collective Coulomb excitations*. As in the past, we continue to place strong priority on research relevant to experiment.

Two-Center Interferometry

For the past few years, we have been working to develop a robust, albeit approximate, framework for describing two-center interferometry readily adaptable to either photon or charged-particle scattering.^{3,4} We have thus formulated an impulse-approximation description that allows one to track the relatively sluggish external center-of-mass motion of the target atoms and ions and thereby ensure momentum conservation explicitly while describing the excitation of the target's internal states. These projects continue to link to our more conventional longtime work in the AMO field of collective Coulomb excitations,^{5,6} although we have been particularly interested recently in characterizing the resulting entanglements among the recoiling reaction fragments and the scattered particle.

¹ J. S. Lundeen et al., Nature **474**, 188 (2011).

² Y. Aharonov, S. Popescu, and J. Tollaksen, Physics Today, 27 (November, 2010).

³ J. M. Feagin, Phys. Rev. A **69**, 062103 (2004), Phys. Rev. A **73**, 022108 (2006)

⁴ R. S. Utter and J. M. Feagin, Phys. Rev. A **75**, 062105 (2007). *This work was highlighted in the June 2007 issue of the Virtual Journal of Quantum Information, vjquantuminfo.org. Utter was a CSUF masters degree student.*

⁵ A. Knapp et al., J. Phys. B: At. Mol. Opt. Phys. **35**, L521 (2002). (*Feagin is a coauthor.*)

⁶ Th. Weber et al., Phys. Rev. Lett. **92**, 163001 (2004) and references therein. (*Feagin is a coauthor.*)

Electron-Pair Excitations

One of the surprises of early observations of photo double ionization of molecular hydrogen was the close similarity with the corresponding electron-pair angular distributions well established in helium, especially for relatively low-energy electron pairs.⁷ Gisselbrecht et al. have identified equal-energy-sharing electron-pair configurations in the molecular fragmentation⁸ for which the helium-like description categorically fails. Their observations were a follow-on to somewhat earlier experiments at the ALS by Th. Weber, R. Dörner, A. Belkacem, and coworkers.⁹ These anomalous angular distributions are noncoplanar and occur when one electron is observed perpendicular to the plane of the other and the polarization direction with the ion-pair direction \mathbf{K}_- either parallel or perpendicular to the polarization. Gisselbrecht et al. termed these and related configurations *frozen-correlation*, since the electron-pair angular separation $\hat{\mathbf{k}}_1 \cdot \hat{\mathbf{k}}_2$ is held fixed in all three cases.

Parallel to these experimental achievements, the community has seen decisive advancement in the *ab initio* computation of Coulomb few-body fragmentation, in particular from two groups, T. Rescigno, W. McCurdy, and coworkers at LBNL¹⁰ using a time-*independent* close-coupling approach, and J. Colgan, M. Pindzola and F. Robicheaux at Los Alamos and Auburn¹¹ using a time-*dependent* close-coupling approach. Their abundant ‘virtual data’ are in excellent agreement in both magnitude and angular distribution with a wide variety of experimentally measured cross sections.¹²

Analysis of the close-coupling results, albeit as expansions in individual electronic angular momenta, show evidence for contributions to the fragmentation from higher electron-pair angular momenta. We have thus begun a collaboration with J. Colgan, A. Huetz, and T. Reddish to generalize the helium-like molecular description to higher *total* angular momentum of the electron-pair. In the molecular ground state, the electron-pair total angular momentum $\mathbf{L} = \mathbf{l}_1 + \mathbf{l}_2$ is not a good quantum number, so the helium-like dipole selection rule $^1S^e \rightarrow ^1P^o$ generalizes to $^1S^e, ^1P^e, ^1D^e, \dots \rightarrow ^1P^o, ^1D^o, ^1F^o, \dots$. Based on our longtime experience with electron-pair excitations in helium and H^- ,¹³ it turns out to be advantageous—perhaps surprisingly so—to define states of total L by quantizing rotations of the momentum plane of the electron pair based on a z axis along their relative momentum direction $\mathbf{k}_- = (\mathbf{k}_1 - \mathbf{k}_2)/2$. One thus introduces symmetric-top wavefunctions $\tilde{D}_{Mm}^L(\hat{\mathbf{k}}_-)$ defined by projections $\hbar m = \mathbf{L} \cdot \hat{\mathbf{k}}_-$ and $\hbar M = \mathbf{L} \cdot \hat{\mathbf{z}}_M$, where $\hat{\mathbf{z}}_M$ is a *molecular-frame* z axis, which we take to be along the ion-pair relative momentum direction \mathbf{K}_- .

As depicted in Fig. 1, we have thus found that superpositions of just three molecule symmetrized electron-pair states, $^1P^o + ^1D^o + ^1F^o$, give a remarkably robust description of the molecular fragmentation distributions including the anomalous out-of-plane *frozen-correlation* configurations.¹⁴ We also find that molecules require special axial-vector geometries in the momenta of the outgoing electron-pair, which are not seen in atoms, and we presented evidence for them in the fragmentation cross section.

Electron-Pair Vortex Kinematics

⁷ T. J. Reddish and J. M. Feagin, J. Phys. B: At. Mol. Opt. Phys. **32**, 2473 (1999); J. M. Feagin, J. Phys. B: At. Mol. Opt. Phys. **31**, L729 (1998).

⁸ M. Gisselbrecht et al., Phys. Rev. Lett. **96**, 153001 (2006).

⁹ Th. Weber et al., Nature (London) **431**, 437 (2004).

¹⁰ W. Vanroose, F. Martin, T. N. Rescigno, and C. W. McCurdy, Phys. Rev. **A70**, 050703 (R) (2004); Science **310**, 1787 (2005).

¹¹ J. Colgan, M. S. Pindzola and F. Robicheaux, J. Phys. B: At. Mol. Opt. Phys. **37**, L377 (2004); Phys. Rev. Lett. **98**, 153001 (2007).

¹² Th. Weber, private communication.

¹³ M. Walter, J. S. Briggs and J. M. Feagin, J. Phys. B: At. Mol. Opt. Phys. **33**, 2907 (2000).

¹⁴ J. M. Feagin, J. Colgan, A. Huetz, and T. J. Reddish, Phys. Rev. Lett. **103**, 033002 (2009).

Some years ago, Murray and Read¹⁵ pioneered the detection of electron pairs scattered by incident electrons fired obliquely to the detection plane. At various energies and for certain electron gun angles and relative angular separation of the scattered electron pair, they observed pronounced minima in the cross section, which over the years have stubbornly resisted a consistent theoretical interpretation, although modern close-coupling calculations can accurately describe their structure and pinpoint their location.¹⁶ Very recently, however, Macek and Ovchinnikov¹⁷ have traced these observed $(e, 2e)$ deep minima to the occurrence of vortices in the wavefunction of the continuum electron pair. They have thus demonstrated the existence of nonzero electron-pair angular momentum about a line through the singularity and out of the detection plane.

This past year, we have worked to establish an accurate analytic form of the cross section near a vortex in the electron-pair continuum by connecting with the angular momentum of the electron-pair center of mass (CM) about the vortex singularity. Following closely our electron-pair excitation work described above, we thus introduce the relative momentum wavevectors $\mathbf{k}_- = (\mathbf{k}_1 - \mathbf{k}_2)/2$ and $\mathbf{k}_+ = \mathbf{k}_1 + \mathbf{k}_2$ to describe the relative and center of mass (CM) motion, respectively, of the outgoing electron pair. Here, \mathbf{k}_1 and \mathbf{k}_2 are the electron wavevectors relative to the ion. We do not predict where a vortex is, or why, but given that it exists provide instead a compact description of its *kinematics*. In the equal-energy sharing experiments of Murray and Read, one has that $\mathbf{k}_+ \cdot \mathbf{k}_- = E_1 - E_2 = 0$, and the vortex line establishes itself along the relative momentum axis \mathbf{k}_- through a point \mathbf{k}_{+v} . Accordingly, we also introduce the projection $\hbar\lambda = \mathbf{L} \cdot \hat{\mathbf{k}}_-$ of the electron-pair total angular momentum $\mathbf{L} = \mathbf{L}_1 + \mathbf{L}_2$ along \mathbf{k}_- and use $\mathbf{k}'_+ \equiv \mathbf{k}_+ - \mathbf{k}_{+v}$ to describe the momentum of the electron-pair CM relative to the vortex singularity.

Our key notion is to move the angular-momentum origin from the helium ion to the vortex singularity with a momentum boost. Since the scattering amplitude is a momentum-space function, the boost is trivially introduced by the replacement $\mathbf{k}_+ \rightarrow \mathbf{k}'_+ \equiv \mathbf{k}_+ - \mathbf{k}_{+v}$. However, a shift of angular-momentum origin changes $\mathbf{L} \rightarrow \mathbf{L}'$ and moves the centrifugal barrier along with it, and the centrifugal barrier dominates the analytic form of the amplitude near the new origin. We thus derive¹⁸ a threshold-like analytic expansion of the scattering amplitude in

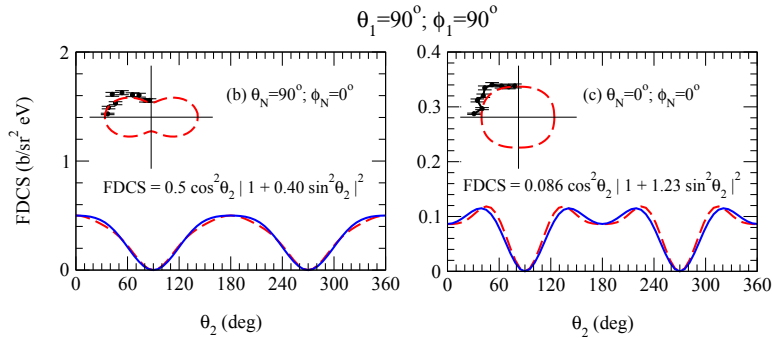


FIG. 1: Fits (solid curves) based on a three-state superposition ${}^1P_{\lambda=1} + {}^1D_{\lambda=1} + {}^1F_{\lambda=1}$ to the H_2 photo double ionization cross sections measured by Gisselbrecht et al. Here, the dashed curves show the TDCC results from J. Colgan.

¹⁵ A. J. Murray and F. H. Read, Phys. Rev. A **47**, 3724 (1993).

¹⁶ J. Colgan, O. Al-Hagan, D. H. Madison, A. J. Murray, and M. S. Pindzola, J. Phys. B: At. Mol. Opt. Phys. **42**, 171001 (2009).

¹⁷ J. H. Macek, J. B. Sternberg, S. Y. Ovchinnikov, and J. S. Briggs, Phys. Rev. Lett. **104**, 033201 (2010).

¹⁸ J. M. Feagin, J. Phys. B: At. Mol. Opt. Phys. **44**, 011001 (2011).

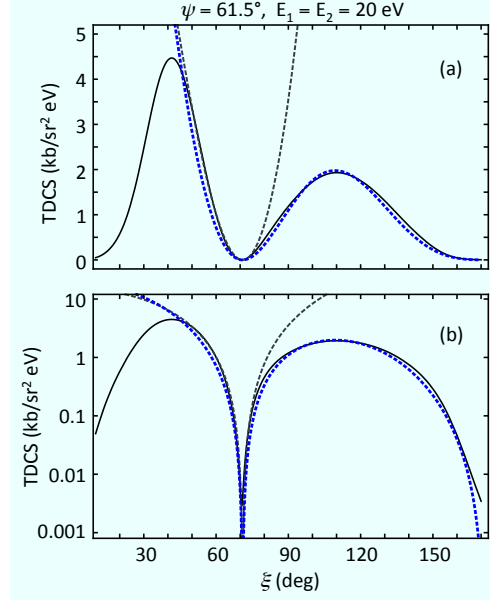


FIG. 2: The triple differential cross section for electron-impact ionization of helium as a function of angular separation $\xi \equiv \theta_{12}/2$ of the outgoing electron pair for fixed incident-electron beam angle $\psi = \psi_v$ and equal energy sharing $E_1 = E_2 = 20$ eV. Panel (b) shows the more conventional semilog plot of the linear results given in panel (a). In both panels, the solid black curves show the *ab initio* close-coupling calculation of Colgan and the dashed (gray) curves the lowest-order $\lambda = 1$ ($c_0 \equiv 0$) analytic approximation from Eq. (1) arbitrarily scaled using best-estimate values $\xi_v = 71^\circ$, $\psi_v = 61.5^\circ$. The dotted (blue) curves show the $\lambda = 1$ and 2 contributions from Eq. (1) and fitted with $c_2/c_1 = -0.275$.

cylindrical partial waves $\lambda = 0, 1, 2, \dots$ of the electron-pair about the vortex

$$f \sim c_0 + c_1 k'_+ \cos \psi' + c_2 k'^2_+ \cos 2\psi' + \dots, \quad (1)$$

where ψ' is the angle \mathbf{k}'_+ makes with incident electron beam and the coefficients c_λ are undetermined but otherwise independent of the momenta. As Fig. 2 demonstrates, good fits to the $(e, 2e)$ cross section near the vortex can be obtained with just the lowest two partial waves about the vortex.

Recent Publications

Vortex Kinematics of a Continuum Electron Pair, J. M. Feagin, J. Phys. B: At. Mol. Opt. Phys. **44**, 011001 (2011).

Electron-Pair Excitations and the Molecular Coulomb Continuum, J. M. Feagin, J. Colgan, A. Huetz, and T. J. Reddish, Phys. Rev. Lett. **103**, 033002 (2009).

Electron Pairs in the Molecular Coulomb Continuum, J. M. Feagin, Invited Talk to the International Symposium on $(e, 2e)$, Double Photoionization, and Related Topics, Lexington, KY, July (2009).

Trapped-Ion Realization of Einstein's Recoiling-Slit Experiment, R. S. Utter and J. M. Feagin, Phys. Rev. A **75**, 062105 (2007). (Utter was a CSUF masters degree student. This work was highlighted in the June 2007 issue of the Virtual Journal of Quantum Information, vjquantuminfo.org.)

Two-Center Interferometry and Decoherence Effects, J. M. Feagin, Phys. Rev. A **73**, 022108 (2006).

Studies of Autoionizing States Relevant to Dielectronic Recombination

T.F. Gallagher
Department of Physics
University of Virginia
P.O. Box 400714
Charlottesville, VA 22904-4714
tfg@virginia.edu

This research program has been focused on doubly excited autoionizing atomic states and the effects of intense low frequency radiation on atomic photoionization. The direct relevance of the former to the Department of Energy is that a systematic study of autoionization allows us to understand the reverse process, dielectronic recombination (DR), the recombination of ions and electrons via intermediate autoionizing states. DR provides an efficient recombination mechanism for ions and electrons in astrophysical and laboratory plasmas.¹⁻⁴ It is important in fusion plasmas because the ions, with the captured electrons, radiate power from the plasma, negating efforts to heat the plasma. The most important pathway for DR is through the autoionizing Rydberg states converging to the lowest lying excited states of the parent ion. As a result, DR rates are profoundly influenced by other charged particle collision processes and very small electric and magnetic fields, both of which are often present in a plasma.^{5,6} Charged particle collisions can be thought of as transient fields, and a major thrust of this program has been understanding how autoionization rates and DR are affected by external fields. This understanding is more widely applicable; DR exhibits the same physics as found in other contexts, notably zero kinetic energy electron (ZEKE) spectroscopy,⁷ dissociative recombination,⁸ and fluorescence yield spectroscopy.⁹ The use of a microwave field to mimic the rapidly varying fields which occur in electron collisions has led quite naturally to laser photoionization of atoms in moderately strong microwave fields, and we are exploring this problem to understand it more fully. An atom in a microwave field exposed to visible radiation is analogous to an atom in an intense infrared field exposed to a train of attosecond xuv pulses, a problem being vigorously investigated.^{10,11}

During the past year we have worked on projects in both of the areas mentioned above. First we describe the optical excitation in the presence of the microwave field. When an atom is exposed to laser photons more energetic than the ionization limit a photoelectron is produced which quickly leaves the ion core. If, however, a microwave field is present the electron can remain bound in the combined atom-microwave field system.¹² We have developed a simple classical model to show that the electron remains bound if the laser excitation occurs at the phase of the microwave field such that it removes energy from the photoelectron. The phase is $\pi/6$ after the positive going zero crossing of the field. The model is a classical model which is an extension of the "Simpleman's Model" in which we take into account the fact that the photoelectron is produced in a coulomb potential, not in a flat potential.^{13,14} In the past year we have shown this model to be correct by photoionizing the atoms with a ps laser pulse at a controllable phase of the microwave field. A report of this work has been published.¹⁵

According to the model, just as excitation at the correct phase of the microwave field leads to removal energy from the photoelectron, in the case of excitation at the phase $\pi/6+\pi$ the

microwave field gives energy to the photoelectron. To test this prediction we have produced bound wave packets with the ps laser pulse in the presence of the microwave field and analyzed the resulting final states by selective field ionization. As predicted, we see microwave phase dependent increases and decreases in the final state energy, indicating the phase dependent absorption of energy from and loss of energy to the microwave field. We are presently finishing the analysis of the data and preparing a report of this work.

We have observed the anisotropic up/down field asymmetry in the ejection of electrons from autoionizing Stark states. What we mean by the up/down asymmetry is as follows. Light linearly polarized in the z direction leads to more or fewer photoelectrons ejected in the +z direction than in the -z direction. Such an anisotropy is not possible for electric dipole photoionization of a state of good parity, but it is possible from a Stark state which does not have a well defined parity. A Stark state is a superposition of even and odd parity states, and the Rydberg electron is more likely to be on the downfield (upfield) side of the atom in a red (blue) Stark state.

Creating a well defined Stark state in any atom other than hydrogen usually requires a substantial, >100 V/cm, electric field, which makes it impossible to observe the angular distribution of the photoelectrons. We have circumvented the high field problem by using a microwave Stark switching approach which enables us to produce Stark states at very low fields of 0-20 V/cm. Using fields from 5 to 10 V/cm we have observed the up/down asymmetry of electron ejection from the Ba $6p_{1/2}nk$ Stark states. As expected, the up/down asymmetry reverses as we change the Stark state from red to blue.¹⁶ In the red Stark states the electron is ejected in the downfield direction while in the blue Stark states the electron is ejected in the upfield direction.

We are starting to conduct spectroscopy of the Ba $6p_{1/2}nk$ Stark states in very low electric fields, where the Stark shifts are comparable to the autoionization rates of the $6p_{1/2}ng$ states, and the higher states have autoionization rates far less than the $6p_{1/2}ng$ states and often less than 1 GHz. Using the microwave Stark switching technique we can produce $6sn\ell$ states of $\ell \geq 4$ for $n > 16$. A new aspect of these measurements is the use of a pulse amplified single frequency continuous wave laser to drive the transition from the bound $6snk$ states to the autoionizing $6pnk$ states. We have developed a reliable method for wavelength calibration based on absorption by I_2 lines and transmission through a Fabry Perot etalon. We are about to begin collecting spectroscopic data.

Our plans for the coming year are to complete analysis of the ps laser-microwave experiment and conduct the spectroscopy of the $6p_{1/2}nk$ Stark states in low field. We also plan to investigate the possibility repeating the microwave – laser excitation experiments using a laser which is amplitude modulated synchronously with the microwave field.

References

1. A. Burgess, *Astrophys. J.* **139**, 776 (1964).
2. A.L. Merts, R.D. Cowan, and N.H. Magee, Jr., Los Alamos Report No. LA-62200-MS (1976).
3. S. B. Kraemer, G. J. Ferland, and J. R. Gabel, *ApJ.* **604** 556 (2004).
4. N. R. Badnell, M. G. O'Mullane, H. P. Summers, Z. Altun, M. A. Bautista, J. Colgan, T. W. Gorczyca, D. M. Mitnik, M. S. Pindzola, and O. Zatsarinny, *Astronomy and Astrophysics*, **406**, 1151 (2003).
5. A. Burgess and H. P. Summers, *Astrophysical Journal* **157**, 1007 (1969).
6. V. L. Jacobs, J. L. Davis, and P. C. Kepple, *Phys. Rev. Lett.* **37**, 1390 (1976).
7. E. W. Schlag, *ZEKE Spectroscopy* (Cambridge University Press, Cambridge, 1998).
8. V. Kokoouline and C. H. Greene, **68**, 012703 (2003).
9. C. Sathe, M. Strom, M. Agaker, J. Soderstrom, J. E. Rubenson, R. Richter, M. Alagia, S. Stranges, T. W. Gorczyca, and F. Robicheaux, *Phys. Rev. Lett.* **96**, 043002 (2006).
10. P. Johnsson, R. Lopez-Martens, S. Kazamias, J. Mauritsson, C. Valentin, T. Remetter, K. Varju, M. B. Gaarde, Y. Mairesse, H. Wabnitz, P. Salieres, Ph. Balcou, K. J. Shafer, and A. L'Huillier, *Phys. Rev. Lett.* **95**, 013001 (2005).
11. P. Ranitovic, X. M. tong, B. Gramkow, S. De, B. DePaola, K. P. Singh, . . Cao, M. Majrakilidze, D. Ray, I. bocharova, H. Mashiko, A. Sandhu, E. Gagnon, M. M. Murnane, H. C. Kapteyn, I. Litvinyuk, and C. L. cocke, *New J. Phys.* **12**, 013008 (2010).
- 12.. E. S. Shuman, R. R. Jones, and T. F. Gallagher, *Phys. Rev. Lett.* **101**, 263001 (2008).
13. H. B. van Linden van den Heuvell and H. G. Muller, in *Multiphoton Processes*, edited by S. J. Smith and P. L. Knight (Cambridge University Press, Cambridge, 1988).
14. T. F. Gallagher, *Phys. Rev. Lett.* **61**, 2304 (1988).
15. K. R. Overstreet, R. R. Jones, and T. F. Gallagher, *Phys. Rev. Lett.* **106**, 033002 (2011).
16. J. Nunkaew and T. F. Gallagher, *Phys. Rev. A* **82**, 033413 (2010).

Publications 2009-2011

1. J. Nunkaew, E. S. Shuman, and T. F. Gallagher, "Indirect spin-orbit K splittings in strontium," *Phys. Rev. A* **79**, 054501 (2009).
2. J. Nunkaew and T. F. Gallagher, "Dielectronic recombination and autoionization yields in weak static electric fields," *Phys. Rev. A* **81**, 054501 (2009).
3. J. Nunkaew and T. F. Gallagher, "Up-down asymmetry of the electrons ejected from barium $6p_{1/2}nk$ autoionizing states," *Phys. Rev. A* **82**, 033413 (2010).
4. K. R. Overstreet, R. R. Jones, and T. F. Gallagher, "Phase-Dependent Electron-Ion Recombination in a microwave field," *Phys. Rev. Lett.* **106**, 033002 (2011).

Experiments in Ultracold Collisions and Ultracold Molecules

Phillip L. Gould
Department of Physics U-3046
University of Connecticut
2152 Hillside Road
Storrs, CT 06269-3046
<phillip.gould@uconn.edu>

Program Scope:

Recent advances in the production of ultracold atoms and molecules have enabled important progress not only in atomic, molecular and optical (AMO) physics, but also in other fields such as quantum information, condensed-matter physics, fundamental symmetries, and chemistry. Although their manipulation is more challenging, molecules have garnered a great deal of recent attention because they possess a number of internal degrees of freedom covering a wide range of energy scales. In addition, heteronuclear molecules can have permanent dipole moments, leading to long-range and anisotropic interactions that can have profound effects at low temperatures. Various techniques for producing and manipulating cold molecules have been developed, including buffer gas cooling, electrostatic slowing, photoassociation, Feshbach-resonance magnetoassociation, optical trapping, magnetic trapping, and electrostatic trapping. Applications of ultracold molecules include: quantum degenerate gases (bosons, fermions, and mixtures); simulations of condensed-matter systems; quantum computation; fundamental symmetries and fundamental constants; dipolar gases and novel quantum phases; ultracold chemistry; and ultracold collisions. The main thrust of our experimental program is to use pulses of laser light, frequency-chirped on nanosecond time scales, to coherently control the collision dynamics of ultracold atoms, including the process of photoassociative formation of ultracold molecules.

Our experiments utilize a sample of ultracold Rb atoms in a magneto-optical trap (MOT). We have chosen to work with Rb for several reasons: 1) the resonance lines of Rb (780 nm and 795 nm) are easily accessed with commercially available diodes lasers; 2) there exist two stable and abundant isotopes (^{85}Rb and ^{87}Rb); 3) ^{87}Rb is often the atom of choice in BEC experiments; and 4) the spectroscopy relevant to photoassociative formation and ionization detection of ultracold Rb_2 has been extensively studied here at UConn and elsewhere. Our experiments utilize a phase-stable MOT for improved stability. This MOT is loaded from a separate “source” MOT in order to maintain long trapping times. The experiments involve illuminating the cold atoms with pulses of frequency-chirped light. We either measure inelastic collisions via the resulting loss from the trap, or we directly detect, by pulsed-laser ionization, the ground-state molecules resulting from photoassociation.

Recent Progress:

Recent progress has been made in several areas: measurements and simulations of the influence of frequency chirp nonlinearity on the rate of ultracold trap-loss collisions;

resonance-enhanced multiphoton ionization (REMPI) detection of ultracold ground-state molecules produced by either MOT light or by chirped photoassociation light; investigation of the influence of chirp direction on photoassociative molecule production; use of a high-speed (4 GHz) arbitrary waveform generator to produce faster chirps; and the production of arbitrary line spectra with our electro-optic phase modulator.

When frequency-chirped light is used to induce a collision between a pair of atoms, the excitation radius changes with time. This Condon radius, R_c , is the atomic separation R at which the light resonantly excites the ground-state atom pair to the long-range attractive molecular potential. A larger detuning of the laser light below the atomic resonance results in excitation at smaller R . If the laser frequency changes on the appropriate time scale, the resonance condition can follow the motion of the atoms on this attractive potential. If the excited atom pair picks up sufficient kinetic energy by rolling inward on this potential, the atoms can be lost from the trap, a process we can easily detect.

We have previously addressed the question of how the trap-loss collisional rate depends on the direction of a linear chirp. We found that for certain center detunings of the chirp, the positive (red-to-blue) chirp yields a significantly larger collision rate than the negative (blue-to-red) chirp. We attribute this difference to the fact that the attractive potential causes the excited atom pair to always accelerate inward (towards smaller R), while the Condon radius R_c can either increase (positive chirp) or decrease (negative chirp). For the positive chirp, the atom pair can only undergo a single excitation because the atom separation and the Condon radius move in opposite directions following the resonant interaction with the light. For the negative chirp, however, the Condon radius and the trajectory of the excited atom pair both proceed inward and further interactions, returning the atom pair to the ground state, can occur. This results in less excited-state collisional flux reaching short range, and therefore a reduced trap-loss collisional rate.

Recently, we have added nonlinearity to the frequency chirps to examine the dependence of the trap-loss collision rate on the detailed shape of the chirp. In order to isolate the effects of the chirp shape, we fix the beginning and ending frequencies of the chirp, as well as the total time duration. Starting with a linear chirp, we superimpose either positive curvature (concave-up) or negative curvature (concave-down) to the temporal variation of the laser frequency. For negative chirps, we find a small but significant difference in collision rates for the concave-up versus concave-down shapes. In collaboration with Shimshon Kallush at ORT Braude and Ronnie Kosloff at Hebrew University (both in Israel), we have developed quantum simulations of the collisions induced by chirped light. Results of these simulations, in terms of the trends with respect to nonlinearity, are consistent with the experimental observations.

Besides exploring the effects of chirped light on trap-loss collisions, we have also applied these pulses to the process of photoassociation. We directly detect the resulting ground-state Rb_2 molecules using resonance-enhanced multiphoton ionization (REMPI) with a pulsed dye laser at ~ 600 nm, followed by ion time-of-flight analysis. We have seen that the MOT light itself produces a significant number of ground-state molecules and that the rate is higher for ^{85}Rb than for ^{87}Rb . Since this constitutes a background signal in our ultracold molecule experiments, we have switched to ^{87}Rb . Applying pulses of chirped photoassociation light, we see production of ground-state molecules. Interestingly, we see a significant dependence on chirp direction, with the positive chirp

yielding larger signals than the negative chirp. We also see that these chirp-produced ground-state molecules are slowly destroyed by successive chirps. Since the molecules are in high vibrational levels of the ground-state, we believe that this destruction is due to off-resonant excitation to states which dissociate into free atoms.

We continue to improve our system for producing fast and arbitrarily-shaped chirped pulses. Using our new 4 GHz arbitrary waveform generator (AWG) to drive our electro-optic phase modulator, we have been able to chirp approximately 1 GHz in 2 ns. We have also demonstrated <1 ns pulses by driving our electro-optic intensity modulator with the AWG.

Another interesting application of our fast phase modulation is to the production of arbitrary line spectra. Since frequency is the time derivative of phase, a linear phase ramp gives a fixed frequency offset. By applying a sequence of voltage ramps to the phase modulator, we generate a sequence of peaks whose offsets from the carrier are determined by the slopes of the corresponding ramps. Such multi-frequency light may prove useful in the efficient excitation of complex atomic or molecular systems.

Future Plans:

We will increase the intensities of our rapidly chirped pulses using a tapered amplifier and then incorporate these pulses into our molecule formation experiments. In order to simplify the photoassociation spectrum and avoid fine-structure predissociation of the excited molecules, we will switch from using light near the $5p_{3/2}$ resonance (780 nm) to light near the $5p_{1/2}$ resonance (795 nm). We will continue to explore the effects of chirped light on the production (and destruction) of ground-state molecules. One specific goal is to vary parameters of the chirped pulses in order to optimize the production of ground-state molecules in a target vibrational level. This will require the incorporation of state-selective REMPI detection. In general, we will take advantage of our nanosecond-time-scale control of laser frequency and amplitude to manipulate the dynamics of ultracold molecule formation.

Recent Publications:

“Characterization and Compensation of the Residual Chirp in a Mach-Zehnder-Type Electro-Optical Intensity Modulator”, C.E. Rogers III, J.L. Carini, J.A. Pechkis, and P.L. Gould, *Opt. Express* **18**, 1166 (2010).

“Coherent Control of Ultracold ^{85}Rb Trap-Loss Collisions with Nonlinearly Frequency-Chirped Light”, J.A. Pechkis, J.L. Carini, C.E. Rogers III, P.L. Gould, S. Kallush, and R. Kosloff, *Phys. Rev. A* **83**, 063403 (2011).

“Creation of Arbitrary Time-Sequenced Line Spectra with an Electro-Optic Phase Modulator”, C.E. Rogers III, J.L. Carini, J.A. Pechkis, and P.L. Gould, *Rev. Sci. Instrum.*, accepted for publication.

Physics of Correlated Systems

Chris H. Greene

Department of Physics and JILA, University of Colorado, Boulder, CO 80309-0440

chris.greene@colorado.edu

Program Scope

This research program aims to develop theoretical techniques capable of handling paradigmatic quantum systems that exhibit strong, nonperturbative correlations. Such correlations involve multiple electrons, or a single electron whose motion is coupled with that of one or more nuclear coordinates, or even a single electron in combined internal and external electromagnetic fields. The project focuses primarily on atoms or molecules for which the usual paradigms based on either perturbation theory or else the independent particle approximation are highly limited and struggle to describe the essential physics. The types of systems that have received attention in the most recent report period include the photoabsorption and collision physics of a Jahn-Teller or Renner-Teller triatomic molecular ion plus a continuum or Rydberg electron. Another major thrust has been initiated during the past year, namely the description of singly- or doubly-excited Rydberg states of two-electron atoms exposed to a strong radiation field.

Recent Progress and Immediate Plans

(i) Low energy electron-molecular ion collisions

The most notable progress in this project during the past year was the development of methods to calculate radiative transition frequencies and Einstein B-coefficients for low-lying Rydberg state nd to np transitions in H_3 . This project was motivated specifically by an experiment carried out in the Berkeley group of Rich Saykally, which observed lasing transitions in the inverse wavelength) range of approximately 1200-1600 wavenumbers that proved difficult to interpret and classify. While some possible interpretations were initially considered that involved vibrational overtones of the water molecule, this began to seem increasingly unlikely once it became clear that these lasing lines are observed even in a pure hydrogen gas with no oxygen added.

With graduate student Jia Wang taking the lead, new computer calculations combined a rovibrational frame transformation treatment of the np states with a perturbative multipole expansion for the nd levels. The resulting transition frequencies of many lines were found to span the approximate frequency range where lasing transitions were observed in the Saykally group experiment. While this initial study did not reach sufficiently high spectroscopic accuracy to definitively pin down the individual transition classifications, it did at least give suggestive evidence that the likely origin of the observed lasing transitions appears to be the $4d$ to $3p$ transitions of H_3 . To achieve lasing, of course, one also needs a population inversion. Ref.[1] argues that such an inversion is expected for this system because the states of lower orbital angular momentum (np) are more rapidly predissociated than nd levels. This part of the project resulted in two publications [1] and [2], the second of which presented the theoretical formulation and tested it against previous spectroscopic studies, and the first of which was a joint theoretical-experimental study published with Saykally's group on the application of the theory to suggest an interpretation of the previously unexplained lasing lines. Some of our future plans in this area include a test of this mechanism for the deuterated species, to see whether theory and

experiment are also in approximate accord for that system, also planned for exploration in the Saykally group in the near future.

The greatest puzzle in H_3^+ dissociative recombination has been solved during the past decade, through the development of a theoretical treatment that includes Rydberg intermediate state pathways excited through the Jahn-Teller effect. This theoretical development, in concert with improved understanding of the experimental systematic issues in storage ring collision experiments, finally produced a consensus concerning the gas-phase dissociative recombination rate at low energies. There remains room for improved understanding, however, because agreement between theory and experiment has not yet been achieved at the level of individual resonances. Some studies at improved resolution have been completed and were published recently [3,4], which compare our most recent theoretical work with experimental results from the Heidelberg TSR experiments. These have given the sharpest test to date of the detailed and richly complicated resonance spectrum of low-energy dissociative recombination for this simplest prototype polyatomic molecule. One of the main conclusions from that work has been that the rotational temperature in the experiment was apparently close to 400K, far hotter than had originally been believed. This recognition helps to resolve some of the residual discrepancies between experimental measurements and our theory, which now begins to look quite respectable at electron collision energies above 50 meV. However, at lower collision energies significant discrepancies between theory and experiment remain and will require further study to resolve more satisfactorily. In another study with long-time collaborator V. Kokoouline, as well as J. Tennyson and A. Faure, our Jahn-Teller-based theory was applied last year[5] to calculate low energy rotational and vibrational excitation of H_3^+ by electron impact. This study yielded more comprehensive and more reliable predictions for this process than have been produced by previous experiment or theory.

A more serious difficulty that has taken somewhat longer to resolve has been the fact that afterglow experiments have often measured H_3^+ recombination rates that differ tremendously from the values extracted from storage ring measurements. One of the developments that has been pursued by this project in a joint collaboration with Glosik's experimental group in Prague and Kokoouline's theory group in Orlando has been an exploration of a new mechanism that appears to explain part of the mystery as to why afterglow experiments yield a different apparent rate than storage ring experiments. The two types of experiments are now consistent with each other, and the past year saw an extension of the model developed in this collaboration, namely an application to D_3^+ that continues to show consistency between theory and experiments.[6]

An extension of these calculations to tackle the chemically-interesting and atmospherically-relevant molecule NO_2^+ has been a subject of investigation off and on for several years, and this has proven to be a particularly stringent test for theory. This is in part because there are tight chemical bonds and numerous electronic potential surfaces that are coupled strongly. Because there has been no previous theory or experiment on the DR rate of NO_2^+ , the theoretically predicted rate from this project will provide the first known information about this process in this ion. Our preliminary results suggest that indirect Rydberg state pathways play a comparatively small role. The collaborative effort with D. Haxton continued at a slower pace this past year since he left for a position at Lawrence Berkeley National Laboratory, but we hope to resume the effort and publish in the coming year our prediction of the overall recombination rate. Another system receiving attention is our first study of dissociative recombination in electron collisions

with a tetra-atomic species, namely H_3O^+ . The first pilot results obtained in a collaboration with the Kokoouline group will probably be published sometime during 2011.

(ii) Strong-field physics that ensues when an intense light pulse from a laser strikes an atom, molecule, or cluster.

A new project initiated during the past year has been a study of the combined effect of coherent infrared and XUV radiation pulses that are subjected to a two-electron atom. While one-electron systems are reasonably well understood in their transient absorption spectra, as the time delay between the two pulses are varied, two-electron atoms with their possibilities for autoionization are only beginning to receive attention for this process. We have started an exploration of this system using time-dependent methods, which has required a retooling of our existing computer programs. This has begun to produce reliable theoretical results in our time-dependent calculations, and we hope to finalize and report our results this year for the simplest two-electron atom, helium.

It is not anticipated that there will remain unexpended funds at the end of this year of the funding cycle. There have been one postdoc and two part-time graduate students supported during the past year by this grant.

Papers published since 2009 that were supported at least in part by this grant.

[1] *Recombination-pumped triatomic hydrogen infrared lasers*, R J Saykally, E A Michael, J Wang, and C H Greene, *J. Chem. Phys.* **133**, 234302-1 to -9 (2010).

[2] *Quantum-defect analysis of 3p and 3d H_3 Rydberg energy levels*, J Wang, C H Greene, *Phys. Rev. A* **82**, 022506-1 to -8 (2010).

[3] *Resonant structure of low-energy H_{3+} dissociative recombination*, A Petrigiani, S Altevogt, M H Berg, D Bing, M Grieser, J Hoffmann, B Jordon-Thaden, C Krantz, M B Mendes, O Novotny, S Novotny, D A Orlov, R Repnow, T Sorg, J Stuetzel, A Wolf, H Buhr, H Kreckel, V Kokoouline, C H Greene, *Phys. Rev. A* **83**, 032711-1 to -10 (2011). See also the Publisher's Note, *Phys. Rev. A* **83**, 049906 (2011).

[4] *Breaking bonds with electrons: Dissociative recombination of molecular ions*, V Kokoouline, N Douguet, and C H Greene, *Chem. Phys. Lett. (Frontiers Article)* **507**, 1-10 (2011).

[5] *Temperature dependence of binary and ternary recombination of D_3^+ ions with electrons*, T Kotrik, P Dohnal, I Korolov, R Plasil, S Roucka, J Glosik, C H Greene, V Kokoouline, *J. Chem. Phys.* **133**, 034305-1 to -8 (2010).

[6] *Calculation of rate constants for vibrational and rotational excitation of the H_3^+ ion by electron impact*, V Kokoouline, A Faure, J Tennyson, and C H Greene, *Mon. Not. R. Astron. Soc.* (2010).

[7] *Vibrational interference of Raman and high harmonic generation pathways*, Z B Walters, S Tonzani, and C H Greene, *Chem. Phys.* **366**, 103-114 (2009).

[8] *Low-energy electron scattering from DNA including structural water and base-pair irregularities*, L Caron, L Sanche, S Tonzani, and C H Greene, Phys. Rev. A **80**, 012705-1 to -6 (2009).

[9] *Ab initio frame-transformation calculations of direct and indirect dissociative recombination rates of $HeH^+ + e$* , D Haxton and C H Greene, Phys. Rev. A **79**, 022701 (2009).

[10] *Theoretical study of the quenching of $NH(1\Delta)$ molecules via collisions with Rb atoms*, D J Haxton, S A Wrathmall, H J Lewandowski, and C H Greene, Phys. Rev. A **80**, 022708-1 to -10 (2009).

[11] *Use of partial-wave decomposition to identify resonant interference effects in the photoionization-excitation of argon*, T J Gay, C H Greene, J R Machacek, K W McLaughlin, H W van der Hart, O Yenen, and D H Jaecks, J. Phys. B **42**, 044008-1 to -17 (2009).

Using Strong Optical Fields to Manipulate and Probe Coherent Molecular Dynamics

Robert R. Jones, Physics Department, University of Virginia
382 McCormick Road, P.O. Box 400714, Charlottesville, VA 22904-4714
bjones@virginia.edu

I. Program Scope

This project focuses on the exploration and control of dynamics in small molecules driven by strong laser fields. Our goal is to exploit strong-field processes to implement novel ultrafast techniques for manipulating and probing coherent electronic and nuclear motion within molecules. Ultimately, through the application of these methods, we hope to obtain a more complete picture of the non-perturbative response of molecules to intense laser pulses.

Optical pulses with up/down field asymmetry or pulse sequences with well-defined relative phase are particularly useful for this effort. Such fields can induce and probe time-dependent, laboratory-fixed directionalities. This capability, especially when used in combination with preferentially oriented molecular targets, can enable experiments in which electrons are driven in specific directions within molecules to influence and probe time-dependent molecular structure and dynamics.

II. Recent Progress

During the past year we have (i) continued to explore directional multi-electron dissociative ionization (MEDI) of small molecules driven by asymmetric fields; (ii) began an investigation of non-sequential double ionization of atoms and molecules in the sub-two optical cycle regime; and (iii) characterized the non-negligible role of the Coulomb binding potential in the continuum dynamics of photoelectrons ionized near threshold in a phase-locked low frequency field. Brief summaries of these projects are provided below.

i) Pump-probe Studies of MEDI with Few-Cycle Pulses of known CE-Phase

When molecules are exposed to strong laser fields, the emission of electron and ion fragments is the result of the coupled electron-nuclear dynamics in the field. In an asymmetric field, this emission can be directional and, as such, can provide a more rigorous test of theoretical models of strong field phenomena. Previously we coherently combined 35 fs laser pulses with 800nm and 400nm wavelengths to explore and control the directional emission of multiply-charged ion fragments from a variety of diatomic and triatomic molecules. Based on an initial, independent 2-color phase calibration from directional MEDI of CO [1], our measurements appeared to be at odds with the standard model, enhanced ionization, for MEDI in small molecules. These results prompted (in part) a re-evaluation of the method used to determine the 2-color optical phase from asymmetries in the above threshold ionization yield from noble gas atoms [2]. Based on this re-assessment, the enhanced ionization model accurately predicts the directionality of all ion fragments observed in our 2-color experiments.

In the enhanced ionization model, strong field ionization launches a dissociating molecular wavepacket which undergoes additional ionization at an enhanced rate once the internuclear separation has increased to a critical value, R_c . Although the directional MEDI observed with 2-

color fields is consistent with the enhanced ionization model, a number of important questions remain unanswered. First, does the asymmetry arise solely from the final ionization step near R_c , or does the initial dissociation event play a role as well? Second, is ionization at R_c optimal for directional fragment control, or does it simply give the largest contribution to the MEDI yield? To answer these questions ultrashort (< 10 fs) pump and probe pulses could be used to isolate the initial dissociation and final ionization events. The prospect of such measurements begs additional questions. Can a level of directional control similar to that realized with 2-color fields be obtained with asymmetric few-cycle laser pulses? If so, can directional Coulomb explosion be used as a robust single shot CE-phase detector?

To address these questions we, and the other members of a collaboration headed by Matthias Kling at MPQ [Matthias Kling (MPQ and KSU), Gerhard Paulus (Friedrich-Schiller-Universität), Robert Moshammer and Joachim Ullrich (MPI, Heidelberg), and Itzik Ben-Itzhak (KSU)], have explored MEDI in N_2 , O_2 , NO , and CO using sub-5fs pulses with known CE-phase. The experiments were performed in a standard COLTRIMS apparatus and utilized a piezo-driven split mirror to create time-delayed pump and probe pulses from a single input beam and focus them to a single spot within the vacuum chamber. The CE-phase of the few-cycle pulses was not locked, but instead, was measured on each laser shot using a stereo ATI optical phase retrieval instrument [3].

Our initial experiments focused on N^{2+} and O^{2+} fragments from N_2 and O_2 , respectively. In the following, the label (p,q) denotes the dissociation of molecule AB into $A^+ + B^+$. We observed no directional asymmetry in the $(2,0)$ or $(2,1)$ yields for single pulse experiments, suggesting that, for these species, the initial ionization step does not contribute to the asymmetry. The pump-probe results show signatures of enhanced ionization in both species, with an increase in the $(2,1)$ yield and depletion of $(2,0)$ signal at pump-probe delays corresponding to internuclear separations near the predicted value for R_c . Surprisingly, in contrast to the longer pulse, 2-color measurements, we find no asymmetry in the directionality of the N^{2+} and O^{2+} dissociation fragments, for any kinetic energy release or pump-probe delay. This is not due to the lack of asymmetry in the few-cycle pump-probe pulses, as strong, directional recoil momentum transfer is observed in the non-sequential ionization of atomic targets in the same apparatus [3]. The conspicuous absence of any asymmetry at any pump-probe delay coupled with the fact that enhanced ionization should not be required to produce $(2,1)$ from $(2,0)$ (at the intensities used, ionization of neutral fragments produced by the pump pulse should be possible at any pump-probe delay) again brings into question whether enhanced ionization plays the primary role in the MEDI dynamics for these channels [3]. Clearly additional measurements are needed to unambiguously identify the mechanisms responsible for directional MEDI in these homonuclear species.

Our single pulse measurements on MEDI of NO and CO show phase-dependent directional emission in to all $(1,1)$, $(2,0)$, and $(2,1)$ channels observed. Thus, for these molecules, an asymmetry in the initial ionization step likely plays some role in the directional MEDI. The CE-phase at which maximum asymmetry is observed differs for different dissociation channels and different molecules. Thus, it is unclear at this time if a common mechanism is responsible for the asymmetry. Interestingly, our results for CO do not agree with those recently obtained by another

group using a nearly identical laser system [4]. In particular, our measurements do not support the recollision depletion model they propose.

ii) Probing Electron Correlation through Non-sequential Double Ionization in 2-cycle Pulses

With the same group of collaborators, we have begun to explore (at MPQ) non-sequential double ionization (NSDI) of atoms and molecules in a regime where the ionizing laser has fewer than two optical cycles. In the standard recollision model, an electron liberated via tunneling ionization from an atom or molecule, can be driven back to its parent ion by the ionizing field. Upon colliding with the ion, the returning electron can ionize another electron directly (e,2e) or promote a second electron to an excited state of the ion from which it is subsequently ionized in the intense laser field (RESI). Both processes result in what is typically called NSDI, but which is the dominant mechanism?

In the experiments, electron-ion coincidence detection in a COLTRIMS spectrometer is used to measure correlated 2-electron momentum distributions resulting from NSDI of Ar, N₂, O₂, and CO. The CE-phase of each sub-2-cycle laser pulse is measured simultaneously with the experiment. The final momenta of the electrons is found to depend strongly on the CE-phase. Moreover, preliminary analysis suggests that comparisons of measured distributions with those simulated using semi-classical calculations can be used to identify the primary NSDI mechanism.

iii) Phase-dependent Electron-Ion Recombination in a Low-Frequency Field

Experiments utilizing XUV pulses for probing attosecond electronic processes within atoms, molecules, or condensed systems are typically performed in the presence of an infrared laser field. The infrared field acts as a streaking field, modifying the momenta of photoelectrons produced directly or indirectly from the XUV pulse. The magnitude and direction of the momentum transferred to the electron depends on the phase of the infrared field at the instant of ionization. For large photoelectron energies, the influence of the electron binding potential on the electron's motion is negligible. In this high energy limit, it is straightforward to extract, with attosecond precision, the time of ionization from the final electron momentum.

Conversely, for low energy electrons, the electron binding potential can have an enormous effect on the momentum transfer between the field and the photoelectron. This makes extraction of the emission time more complicated but, in principle, the difference in the momentum transfer to high- and low-energy photoelectrons might be used to probe the instantaneous binding potential experienced by a departing electron. Accordingly, we have been working to understand momentum and energy transfer from a low-frequency dressing field to near threshold photoelectrons.

While we are acquiring the necessary hardware to perform experiments with attosecond XUV pulses, we have entered into a collaboration with Tom Gallagher's group to study this problem in a scaled system. Specifically, we have recently measured the recombination of picosecond photoelectron wavepackets from Li as a function of the phase of a microwave dressing field. The net energy/momentum transfer as well as the recombination probability show a pronounced phase-dependence that is well described by a closed form expression which takes into account the influence of the Coulomb potential on the escaping electron. The same formalism should

accurately describe the phase-dependent momentum transfer to atto second wavepackets ionized at threshold in an infrared dressing field.

III. Future Plans

Currently we are developing new experimental capabilities to enable our next experiments. First, we are characterizing a new intense THz source based on optical rectification of high-energy, 100 fs, 800nm laser pulses in MgO-doped LiNbO₃ [5]. We are assembling a new molecular beam chamber equipped with an Even-Lavie valve which should enable us to achieve sufficient rotational cooling (~ 1K) to produce transiently oriented molecules by direct THz excitation of rotational wavepackets. Second, we are assembling a hollow-core fiber compressor to generate intense few-cycle pulses. We will use these pulses to continue our exploration of MEDI in asymmetric fields. These few-cycle pulses will also be used to generate sub-femtosecond XUV pulses, allowing us to explore the use of field-dressed, near-threshold photo-electrons for monitoring changes in molecular binding potentials on sub-femtosecond time-scales.

IV. Publications from Last 3 Years of DOE Sponsored Research (since July 1, 2008)

i) K.R. Overstreet, R.R. Jones, and T.F. Gallagher, "Phase-dependent Electron-Ion Recombination in a Microwave Field," *Phys. Rev. Lett.* **106**, 033002 (2011).

ii) Nora G. Johnson, O. Herrwerth, A. Wirth, S. De, I. Ben-Itzhak, M. Lezius, B. Bergues, M.F. Kling, A. Senfleben, C.D. Schröter, R. Moshhammer, J. Ullrich, K.J. Betsch, R.R. Jones, A.M. Saylor, T. Rathje, Klaus Rühle, Walter Müller, and G. G. Paulus, "Single-shot Carrier-Envelope-Phase Tagged Ion-momentum Imaging of Non-sequential Double Ionization of Argon in Intense 4-fs Laser Fields," *Phys. Rev. A* **83**, 013412 (2011).

iii) K.J. Betsch, D.W. Pinkham, and R.R. Jones, "Directional Emission of Multiply-Charged Ions During Dissociative Ionization in Asymmetric Two-Color Laser Fields," *Physical Rev. Lett.* **105**, 223002 (2010).

iv) Brett A. Sickmiller and R.R. Jones, "Effects of Phase-Matching on High Harmonic Generation from Aligned N₂," *Phys. Rev. A* **80**, 031802(R) (2009).

v) E. S. Shuman, R. R. Jones, and T. F. Gallagher, "Multiphoton Assisted Recombination," *Phys. Rev. Lett.* **101**, 263001 (2008).

vi) D. Pinkham, T. Vogt, and R.R. Jones, "Extracting the Polarizability Anisotropy from the Transient Alignment of HBr," *J. Chem. Phys.* **129**, 064307 (2008).

References

[1] S. De *et al.*, *Phys. Rev. Lett.* **103**, 153002 (2009).

[2] C.L. Cocke (private communication).

[3] Nora G. Johnson *et al.*, *Phys. Rev. A* **83**, 013412 (2011).

[4] Y. Liu *et al.*, *Phys. Rev. Lett.* **106**, 073004 (2011).

[5] J. Hebling, K.-L. Yeh, M.C. Hoffmann, B. Bartal, and K.A. Nelson, *J. Opt. Soc. Am. B* **25**, B6 (2008).

Molecular Dynamics Probed by Coherent Electrons and X-Rays

P.I.s: Henry C. Kapteyn and Margaret M. Murnane
University of Colorado at Boulder, Boulder, CO 80309-0440
Phone: (303) 492-8198; E-mail: kapteyn@jila.colorado.edu

The goal of this work is to develop novel short wavelength probes of molecules. We made exciting advances in several experiments that probe complex molecular dynamics using ultrafast, coherent, x-rays and electrons emitted during the high harmonic generation process.

Understanding high harmonic generation from molecules

We performed the first accurate polarimetry measurement of high harmonic emission (HHG) from aligned molecules. In work published in *PRL*, we found that harmonic emission from N_2 molecules can be strongly elliptically polarized even when driven by linearly polarized laser fields. These findings have broad implications for understanding molecules in strong fields because they cannot be explained by simple theories based on the strong field approximation and single active electron models.

We also demonstrated experimentally and theoretically (through a collaboration with Tamar Seideman) that the high-order nature and sensitivity of HHG to molecular structure make it particularly attractive as a means of studying molecular rotational coherences. We showed for the first time using any probe that many higher order fractional rotational revivals can be observed (up to order 12). Most significantly, by fitting our data to an exact theory of HHG from aligned molecules, we could extract the underlying electronic dipole elements for high harmonic emission, revealing new insights regarding electron dynamics in a strong laser field i.e. that the electron in the continuum can absorb angular momentum from the photon field.

Finally, in work in collaboration with Albert Stolow, we showed that HHG from large-amplitude vibrations in an N_2O_4 dimer molecule can reveal cation state dynamics. In initial work, we generated very large amplitude vibrations and observed a very large oscillation in the HHG yield that was correlated with the vibration of the dimer (bright at the outer turning points and dim at the inner turning points). More recent work at NRC Canada generated vibrations in the dimer using mid-IR pulses, and used weak fields to probe the ionization step separately.

X-ray driven dynamics in molecules: radiation femtochemistry

In a series of experiments in collaboration with Lew Cocke and Robin Santra, we combined HHG with a COLTRIMS momentum imaging apparatus to drive simple ionization-induced reactions. In this work, we were able for the first time to observe directly the chemical dynamics initiated by ionizing radiation i.e. *radiation femtochemistry*. This work immediately yielded new and unanticipated findings - exploring which shake-up states are responsible for dissociation of N_2 , and explaining why autoionization is delayed in O_2 .

More recent work is exploring how to use laser pulses to control non-Born-Oppenheimer dynamics in x-ray driven triatomics. N_2O is a simple linear triatomic molecule with an asymmetric bond. Using a few-femtosecond 43 eV XUV pulse, we can create an exotic excited-state target where a simple Born-Oppenheimer picture breaks down. The resultant decay dynamics involves a competition between two decay channels that occur on very fast, 20 fs, timescales and illustrated in Fig. 1: molecular autoionization by ejecting a second electron

($\text{N}_2\text{O}^{+*} \rightarrow \text{N}_2\text{O}^{2+} + e^-$), or dissociation without electron emission - including two-body dissociation to one singly charged atomic (molecular) ion plus another molecular (atomic) neutral fragment, or three-body dissociation to one singly charged atomic ion and two atomic neutral fragments. For the Coulomb explosion channel that involves the emission of a second electron, the transient intermediate doubly charged state then decays by breaking either the N-N or N-O bond. i.e. $\text{N}_2\text{O}^{2+} \rightarrow \text{N}_2^+ + \text{O}^+$ or $\text{N}_2\text{O}^{2+} \rightarrow \text{N}^+ + \text{NO}^+$. In the presence of a moderately intense infrared (IR) field, we can interrupt the neutral-ion dissociation channel and strongly enhance the double-ion channel yield, because the excited N_2O^{+*} is very fragile in the laser field and can easily lose a second electron. Moreover, with the addition of an IR field, breaking the N-O bond can be enhanced more than breaking the N-N bond (Fig. 1), indicating the presence of laser-induced non-adiabatic electron motion.

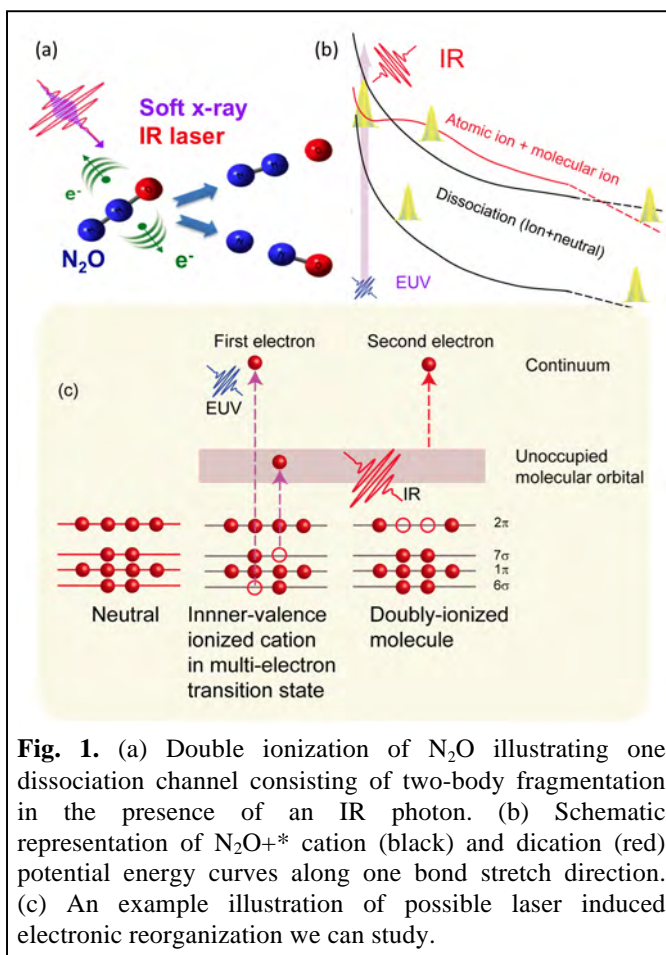


Fig. 1. (a) Double ionization of N_2O illustrating one dissociation channel consisting of two-body fragmentation in the presence of an IR photon. (b) Schematic representation of N_2O^{+*} cation (black) and dication (red) potential energy curves along one bond stretch direction. (c) An example illustration of possible laser induced electronic reorganization we can study.

Strong field ionization (SFI) and HHG in molecules using mid-IR driving lasers

The favorable λ^2 scaling in the cutoff motivated studies of HHG from atoms with mid-IR driving pulses, since the laser intensity required to generate a given harmonic is less than for 800nm lasers. This opens up the possibility of dramatically extending the number of harmonics that can be generated from molecules, which would allow more tomographic information about the molecular structure to be extracted from shorter wavelength recolliding electrons. The first requisite is to be able to *experimentally observe* HHG at very short wavelengths. Fortunately, in very recent work, we increased the HHG yield in atoms and molecules driven by mid-IR fields by phase-matching the conversion process at very high gas pressures. Because the process is phase matched, the HHG emission from all the molecules in the medium is coherent. This allowed us to observe record HHG emission from N_2 molecules at photon energies > 0.4 keV (Fig. 2).

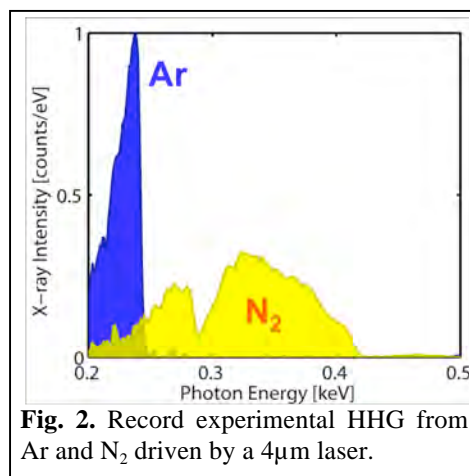


Fig. 2. Record experimental HHG from Ar and N_2 driven by a $4\mu\text{m}$ laser.

Finally, we have developed a velocity map imaging (VMI) apparatus to probe strong field ionization in atoms and molecules, particularly using mid-infrared (IR) driving fields with high

electron energy. The experimentally observed photoelectron distributions are extremely complicated, and in general it has proven challenging to date to reliably extract information about molecular structure. However, by utilizing a large range of laser wavelengths and several different detection schemes, a combination unique to our laboratory, we may be able to carefully benchmark theory and tell how reliable SFI is as a general probe technique. The intricate

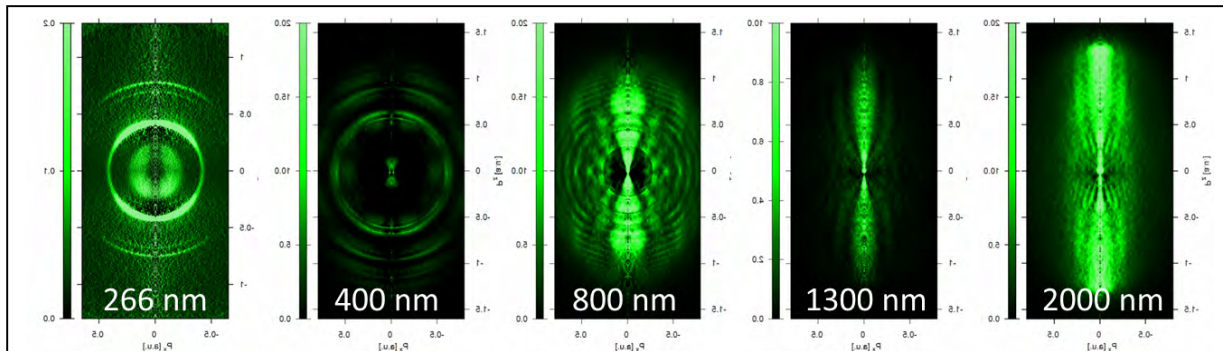


Fig. 3. Experimental photoelectron spectra collected with our VMI spectrometer, showing different structure at various wavelengths with the same laser intensity ($\sim 1 \times 10^{14}$ W/cm²). The structure encodes information about ionization dynamics, wavepacket propagation dynamics, and the structure of the parent ion, and graphically shows the transition from a multiphoton to a tunnel regime with increasing laser wavelength.

angular interference seen in the above-threshold ionization spectra from atoms and molecules is due to the scattering of an electron wavepacket with the ion. Thus, the resulting photoelectron distribution is governed by the structure of the wavepacket when it is born, the evolution of the wavepacket in the laser field, as well as the structure of the ion, which is recorded during electron rescattering. A general question to be addressed in collaboration with the theory AMOS groups is exactly what information is encoded by both the low and high energy photoelectrons.

Highlights in related DOE AMOS and other DOE-funded collaborations

In exciting recent work in collaboration with Andrius Baltuska in Vienna, we demonstrated full phase matching of high harmonic generation at photon energies > 1keV for the first time. This work extends bright attosecond pulses into the soft x-ray region for the first time. Early results that

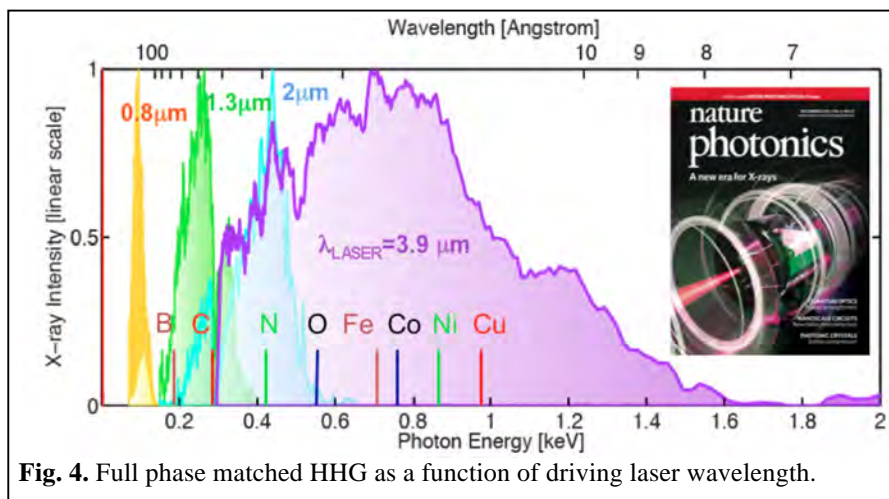


Fig. 4. Full phase matched HHG as a function of driving laser wavelength.

demonstrated full phase matching up to 0.5 keV were highlighted on the cover of Nature Photonics (Dec 2010) with DOE acknowledgement.

In work done in collaboration with Keith Nelson, we observed quasi-ballistic thermal transport in nanostructures for the first time, by using spatially coherent HHG beams. Finally, in work in

collaboration with John Miao (UCLA), we demonstrated 3D imaging from a single view using coherent diffractive imaging, published in Nature in 2010.

Publications with DOE AMOS support since 2008

1. P. Ranitovic, X. M. Tong, C. W. Hogle, X. Zhou, Y. Liu, N. Toshima, M. M. Murnane, and H. C. Kapteyn, "Laser-Enabled Auger Decay in Rare-Gas Atoms," *Physical Review Letters* **106**, 053002 (2011).
2. T. Popmintchev, M.-C. Chen, P. Arpin, M. M. Murnane, and H. C. Kapteyn, "The attosecond nonlinear optics of bright coherent X-ray generation," *Nature Photonics* **4**, 822 (2010).
3. W. Li, A. Jaron-Becker, C. Hogle, V. Sharma, X. Zhou, A. Becker, H. Kapteyn, M. Murnane, "Visualizing electron rearrangement in space and time during the transition from a molecule to atoms," *PNAS* **107**, 20219 (2010).
4. K. P. Singh, F. He, P. Ranitovic, W. Cao, S. De, D. Ray, S. Chen, U. Thumm, A. Becker, M. M. Murnane, H. C. Kapteyn, I. V. Litvinyuk, and C. L. Cocke, "Control of Electron Localization in Deuterium Molecular Ions using an Attosecond Pulse Train and a Many-Cycle Infrared Pulse," *Phys. Rev. Lett.* **104**, 023001 (2010).
5. P. Ranitovic, Xiao-Min Tong, B. Gramkow, S. De, B. DePaola, K. P. Singh, W. Cao, M. Magrakvelidze, D. Ray, I. Bocharova, H. Mashiko, A. Sandhu, E. Gagnon, M. M. Murnane, H. C. Kapteyn, I. Litvinyuk, C.L. Cocke, "IR-Assisted Ionization of Helium by Attosecond XUV Radiation," *New J. Phys.* **12**, 013008 (2010).
6. K. S. Raines, S. Salha, R. L. Sandberg, H. D. Jiang, J. A. Rodriguez, B. P. Fahimian, H. C. Kapteyn, J. C. Du, and J. W. Miao, "Three-dimensional structure determination from a single view," *Nature* **463**, 214 (2010).
7. M. Siemens, Q. Li, M. Murnane, H. Kapteyn, R. Yang, E. Anderson, K. Nelson, "High-Frequency Acoustic Waves in Nanostructures Characterized by Coherent EUV Beams", *Appl. Phys. Lett.* **94**, 093103 (2009).
8. M. Siemens, Q. Li, R. Yang, K. Nelson, E. Anderson, M. Murnane, H. Kapteyn, "Measuring quasi-ballistic heat transport across nanoscale interfaces using ultrafast coherent soft x-rays", *Nature Materials* **9**, 26 (2010).
9. P. Arpin, T. Popmintchev, N. Wagner, A. Lytle, O. Cohen, H. Kapteyn, M. Murnane, "Enhanced HHG from Multiply Ionized Ar > 500eV through Laser Pulse Self-Compression," *Phys. Rev. Lett.* **103**, 143901 (2009).
10. R. M. Lock, X. B. Zhou, W. Li, M. M. Murnane, and H. C. Kapteyn, "Measuring the intensity and phase of high-order harmonic emission from aligned molecules," *Chemical Physics* **366**, 22 (2009).
11. M.C. Chen, M. Gerrity, S. Backus, T. Popmintchev, X. Zhou, P. Arpin, X. Zhang, H. Kapteyn, M. Murnane, "Spatially coherent, phase matched, EUV beams at 50 kHz," *Optics Express* **17**, 17376 (2009).
12. T. Popmintchev, M. C. Chen, A. Bahabad, M. Gerrity, P. Sidorenko, O. Cohen, I. P. Christov, M. M. Murnane, and H. C. Kapteyn, "Phase matching of high harmonic generation in the soft and hard X-ray regions of the spectrum," *PNAS* **106**, 10516 (2009).
13. R. Sandberg, D. Raymondson, C. La-o-Vorakiat, A. Paul, K. S. Raines, J. Miao, M. Murnane, H. Kapteyn, W. Schlotter, "Tabletop soft-x-ray Fourier transform holography with 50nm resolution," *Opt. Lett.* **34**, 1618 (2009).
14. X.B. Zhou, R. Lock, N. Wagner, W. Li, H.C. Kapteyn, M.M. Murnane, "Elliptically Polarized High-Order Harmonic Emission from Molecules in Linearly Polarized Laser Fields," *Phys. Rev. Lett.* **102**, 073902 (2009).
15. A.S. Sandhu, E. Gagnon, R. Santra, V. Sharma, W. Li, P. Ho, P. Ranitovic, C.L. Cocke, M.M. Murnane, H.C. Kapteyn, "Observing the Creation of Electronic Feshbach Resonances in Soft X-ray-Induced O₂ Dissociation," *Science* **322**, 1081 (2008).
16. W. Li, X. Zhou, R. Lock, H. C. Kapteyn, M. M. Murnane, S. Patchkovskii, and A. Stolow, "Time-Resolved Dynamics in N₂O₄ Probed Using High Harmonic Generation," *Science* **322**, 1207 (2008).
17. I. Thomann, R. Lock, V. Sharma, E. Gagnon, S. Pratt, H. Kapteyn, M. Murnane, W. Li, "Direct measurement of the angular dependence of single-photon ionization of N₂ and CO₂," *J. Phys. Chem. A* **112**, 9382 (2008).
18. E. Gagnon, A.S. Sandhu, A. Paul, K. Hagen, A. Czasch, T. Jahnke, P. Ranitovic, C.L. Cocke, B. Walker, M.M. Murnane, H.C. Kapteyn, "Time-resolved momentum imaging system for molecular dynamics studies using a tabletop ultrafast extreme-ultraviolet light source," *Rev. Sci. Instrum.* **79**, 063102 (2008).
19. X. B. Zhou, R. Lock, W. Li, N. Wagner, M. M. Murnane, and H. C. Kapteyn, "Molecular recollision interferometry in high harmonic generation," *Physical Review Letters* **100**, 073902 (2008).

Imaging Multi-particle Atomic and Molecular Dynamics

Allen Landers

landers@physics.auburn.edu

Department of Physics
Auburn University
Auburn, AL 36849

Program Scope

We are investigating phenomena associated with ionization of an atom or molecule by single photons (weak field) with an emphasis on ionization-driven atomic and molecular dynamics. Of particular interest is untangling the complicated electron-correlation effects and molecular decay dynamics that follow an initial photoionization event. We perform these measurements using variations on the well established COLTRIMS technique. The experiments take place at the Advanced Light Source at LBNL as part of the ALS-COLTRIMS collaboration with the groups of Reinhard Dörner at Frankfurt and Ali Belkacem and Thorsten Weber at LBNL. Because the measurements are performed in “list mode” over a few days where each individual event is recorded to a computer, the experiments can be repeated virtually with varying gate conditions on computers at Auburn University over months. We continue to collaborate closely with theoreticians also funded by DOE-AMOS including most recently the groups of F. Robicheaux and C.W. McCurdy.

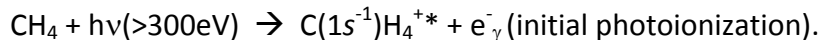
We present below one very new and exciting example of our current progress. We have recently measured the decay dynamics of C(1s) core photoionized methane, and we are in close collaboration with the McCurdy group to understand the many complex pathways that lead to the dissociative final states of the doubly or triply charged molecular ion.

Recent Progress: Decay Dynamics following Core Photoionization of Methane

1. Overview:

Methane is one of the simplest polyatomic molecules, and as such provides a useful laboratory to study molecular dynamics. Its complexity is sufficient for exhibiting interesting decay behaviors and for challenging theory, but perhaps just at the boundary so there is great promise for expanding our fundamental understanding of how such complex systems can evolve over short time scales. Methane is a neon analogue with 10 electrons, two of which are deeply bound in the core of the carbon atom. Prompt photoionization of one of these C(1s) electrons leads to a highly excited molecular cation that has valence electronic structure nearly identical to the neutral ground state. We have just begun to explore how this state decays and to investigate the mechanisms that lead to the many dissociative pathways.

Our experiment uses the standard COLTRIMS approach, where we measure in coincidence up to four particles resulting from the photoionization and subsequent decay (one photoelectron and up to three ions). The initial photoionization reaction is given by



The dipole absorption of the photon promotes the essentially atomic C(1s) electron into a continuum *sp* state that can be strongly influenced by the molecular potential. Following this photoionization, the molecule can decay through multiple pathways, which we organize here into groups corresponding to three of the final fragment states (in bold) that we have measured in the experiment:

- (1) $\text{C}(1s^{-1})\text{H}_4^{+*} + e_{\gamma}^{-} \rightarrow \mathbf{CH_3^+} + \mathbf{H^+} + e_{\gamma}^{-} + e_{\text{Auger}}^{-}$ (Auger, dication, [$\mathbf{H^+}, \mathbf{CH_3^+}$])
- (2) $\text{C}(1s^{-1})\text{H}_4^{+*} + e_{\gamma}^{-} \rightarrow \mathbf{CH_2^+} + \mathbf{H_2^+} + e_{\gamma}^{-} + e_{\text{Auger}}^{-}$ (Auger, dication, [$\mathbf{H_2^+}, \mathbf{CH_2^+}$])
- (3) $\text{C}(1s^{-1})\text{H}_4^{+*} + e_{\gamma}^{-} \rightarrow \mathbf{CH_2^+} + \mathbf{H^+} + \mathbf{H^+} + e_{\gamma}^{-} + 2e_{\text{A}}^{-}$ (Double Auger, trication, [$\mathbf{H^+}, \mathbf{H^+}, \mathbf{CH_2^+}$])

There are additional dissociative states, but we will limit the current presentation to cases (1) and (3).

2. Two-body breakup, $[H^+, CH_3^+]$:

The first step in understanding this decay mode is to see whether or not the axial recoil approximation holds, i.e. that measurement of the H^+ fragment momentum vector is equivalent to measurement of a bond axis. This will be the case for those events where the dissociation time is substantially faster than either the rotation period of the molecule or, more importantly, the timescales of conformation changes during the decay. We show data here for the case of 2.4 eV photoelectron energy.

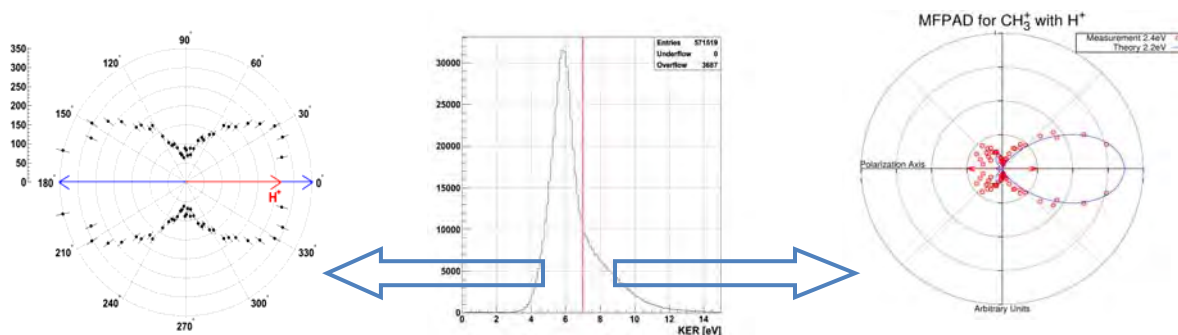


Figure 1: Kinetic energy release for the $[H^+, CH_3^+]$ channel (center) corresponding to axial-recoil breakdown (left) or axial-recoil valid (right) molecular frame photoelectron angular distributions with theory.

The center panel of figure 1 shows the fragment kinetic energy release for this two body breakup channel, which has a fairly sharp peak at ~ 5.5 eV and a long energetic tail. If we gate the data on the lower energy peak we get the molecular frame photoelectron angular distribution (MFPAD) shown to the left, whereas gating on the tail leads to the MFPAD shown to the right. In both cases we have confined the H^+ momentum vector to the positive horizontal axis along the photon polarization. The interesting result here is that on the left you get what is a nearly dipole distribution for the photoelectron, which is what you would expect for a randomly oriented molecule or breakdown of axial recoil. On the right, however, you see a strongly asymmetric MFPAD that is consistent with calculations by C. Trevisan and the group of C.W. McCurdy and T.N Rescigno.

The above result is quite fortunate, because we are able to identify at least two decay pathways: one prompt dissociation where axial recoil holds and a different pathway where axial recoil breaks down. This provides us a tool for exploring dynamics; by measuring the amount of axial-recoil breakdown when comparing the left and right spectrum and consulting with theory, we plan to determine the specific decay channels and associated timescales. This kind of information will be critical in interpreting future experiments with ultra-fast sources such the LCLS or the envisioned NGLS where event mode experiments might be possible.

This data set is enormously rich, because we can look at MFPADs associated with any of the many molecule orientations or tied to specific dissociative states. At the time of this writing, we have developed some preliminary theory-based interpretations about which channels are populating which dissociative states, and we anticipate new detailed results soon. In the meantime, we have also taken the next step in this type of measurement, where we have measured (as far as we know) the first fully three-dimensional molecular frame photoelectron angular distributions. These results are presented below.

2. Three-body breakup, $[H^+, H^+, CH_2^+]$:

As mentioned in the overview, methane is an electronic analogue to the neon atom. Our previous work on correlation effects in the core-photoionization of neon included an investigation of the double-Auger channel which leads to a triply charged Ne^{3+} . This channel is not only possible, but probable because there are no cascade pathways for a core-hole to decay to Ne^{3+} . We have found the exciting result that this appears to also be the case in methane. Furthermore, we have confirmed that when double Auger occurs in the molecule, the triply charged molecular ion is extremely unstable and dissociates rapidly along the bond axes. We show data here for the case of 4.5 eV photoelectron energy.

Ions: This axial-recoil result is illustrated in figure 2. The top left panel shows the momentum distribution of the two protons in the plane defined by their momentum vectors and that of the CH_2^+ ion, which defines the positive horizontal axis. The upper half of the figure shows the first measured proton in the plane it forms with the CH_2^+ ion, and the lower half shows the second measured proton in its plane with the heavy fragment. The large exterior islands correspond to protons ejected roughly along the bond axes (shown in red) but distorted from the CM to lab frame change and by “post-collision interaction” with the doubly charged heavy fragment. We currently interpret that the interior islands arise from the coincidence of a light and heavy ion with a random hit corresponding to a neutral, which is demonstrated in the lower left panel where we’ve gated on the island for the first hit and get a roughly random distribution for the second. We believe these events correspond to the $[\text{H}^0, \text{H}^+, \text{CH}_2^+]$ decay pathway, but have yet to pursue analysis of this channel.

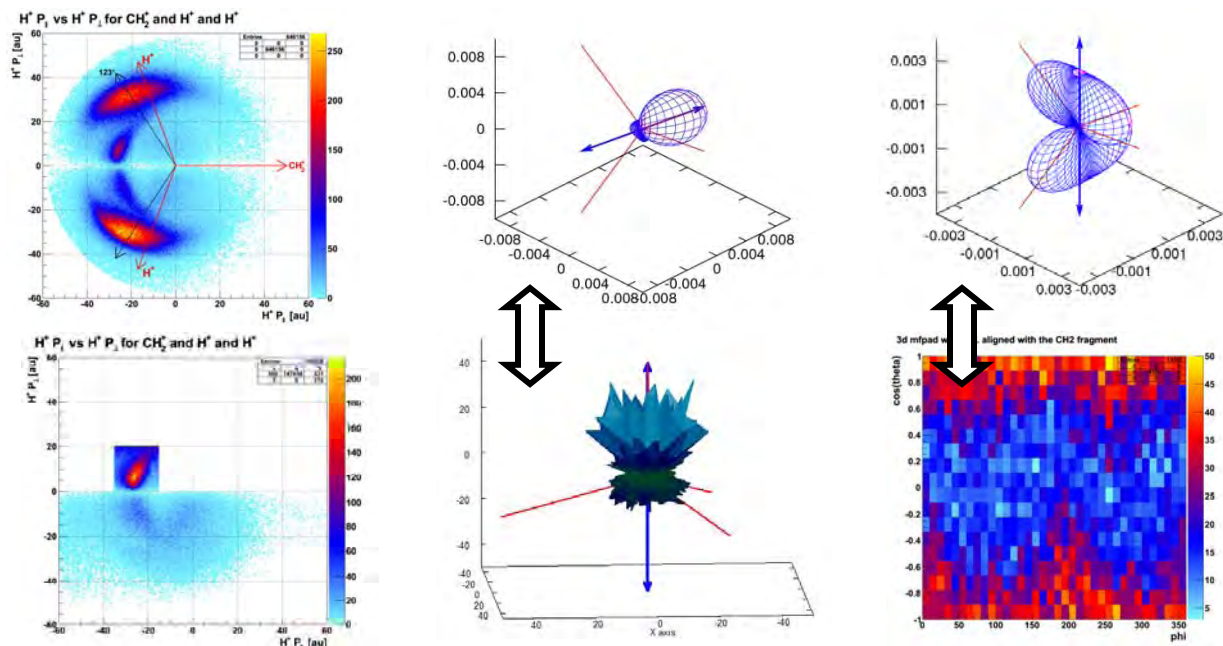


Figure2: Fragment ion momenta in for the three body breakup (left) and three-dimensional MFPADS (mid & right).

Electrons: The mid-top and mid-bottom panels show theory (top) and experiment (bottom), where electrons have a propensity to emerge along a bond aligned with the polarization axis. The statistics are limited, but the strong asymmetry is evident. Even more interestingly, the right panels show a comparison between theory (top) and experiment (bottom) with experiment plotted as a density plot in ϕ and $\cos(\theta)$ to plainly emphasize the kidney shaped structure arising when the polarization axis bisects a bond. We are currently pursuing clearer and more enlightening comparisons between these recent experimental results and theory. In brief, we believe there is a strong potential for 3D-MFPADS to become a powerful tool in furthering our understanding of molecular structure and dynamics.

Future Plans: Further Analysis and Future Experiments

- **Continued Analysis:** Explore the $[\text{H}_2^+, \text{CH}_2^+]$ and $[\text{H}^0, \text{H}^+, \text{CH}_2^+]$ channels, working closely with theory to help understand this rich system.
- **New experiments:**
 - Measure the Auger electrons in coincidence with fragments to produce molecular frame angular distributions for Auger electrons in order to better identify dissociative pathways.
 - Fluoromethane or similar molecules with broken symmetry should provide a new fertile testing ground for additional studies.
 - Use larger polyatomic molecules beginning slowly with ethane to explore the possibilities of extending these measurements to systems of increasing complexity.

Refereed Publications: Supported by DOE-AMOS (2008-present)

1. **Production of excited atomic hydrogen and deuterium from H₂, HD and D₂ photodissociation** R Machacek , V M Andrianarijaona , J E Furst , A L D Kilcoyne , A L Landers , E T Litaker , K W McLaughlin and T J Gay *J. Phys. B: At. Mol. Opt. Phys.* **44** 045201 (2011)
2. **Auger decay of 1σ_g and 1σ_u hole states of N₂ molecule: II. Young type interference of Auger electrons and its dependence on internuclear distance** N. A. Cherepkov, S. K. Semenov, M. S. Schöffler, J. Titze, N. Petridis, T. Jahnke, K. Cole, L. Ph. H. Schmidt, A. Czasch, D. Akoury, O. Jagutzki, J. B. Williams, T. Osipov, S. Lee, M. H. Prior, A. Belkacem, A. L. Landers, H. Schmidt-Böcking, R. Dörner and Th. Weber, *Phys. Rev. A* **82**, 023420 (2010).
3. **Auger decay of 1σ_g and 1σ_u hole states of the N₂ molecule: Disentangling decay routes from coincidence measurements** S. K. Semenov, M. S. Schöffler, J. Titze, N. Petridis, T. Jahnke, K. Cole, L. Ph. H. Schmidt, A. Czasch, D. Akoury, O. Jagutzki, J. B. Williams, T. Osipov, S. Lee, M. H. Prior, A. Belkacem, A. L. Landers, H. Schmidt-Böcking, Th. Weber, N. A. Cherepkov, and R. Dörner, *Phys. Rev. A* **81**, 043426 (2010).
4. **Carbon K-shell photoionization of fixed-in-space C₂H₄** T. Osipov, M. Stener, A. Belkacem, M. Schöffler, Th. Weber, L. Schmidt, A. Landers, M. H. Prior, R. Dörner, and C. L. Cocke, *Phys. Rev. A* **81**, 033429 (2010) .
5. **Formation of inner-shell autoionizing CO⁺ states below the CO₂⁺ threshold** T. Osipov, Th. Weber, T. N. Rescigno, S. Y. Lee, A. E. Orel, M. Schöffler, F. P. Sturm, S. Schössler, U. Lenz, T. Havermeier, M. Kühnel, T. Jahnke, J. B. Williams, D. Ray, A. Landers, R. Dörner, and A. Belkacem, *Phys. Rev. A* **81**, 011402 (2010).
6. **Separation of Auger transitions into different repulsive states after K-shell photoionization of N₂ molecules** N. A. Cherepkov, S. K. Semenov, M. S. Schöffler, J. Titze, N. Petridis, T. Jahnke, K. Cole, L. Ph. H. Schmidt, A. Czasch, D. Akoury, O. Jagutzki, J. B. Williams, T. Osipov, S. Lee, M. H. Prior, A. Belkacem, A. L. Landers, H. Schmidt-Böcking, R. Dörner and Th. Weber, *Phys. Rev. A* **80**, 051404(R) (2009).
7. **Photo and Auger Electron Angular Distributions of Fixed-in-Space CO₂** F.P. Sturm, M. Schöffler, S. Lee, T. Osipov, N. Neumann, H.-K. Kim, S. Kirschner, B. Rudek, J.B. Williams, J.D. Daughhetee, C.L. Cocke, K. Ueda, A.L. Landers, Th. Weber, M.H. Prior, A. Belkacem, and R. Dörner, *Phys. Rev. A* **80**, 032506 (2009).
8. **Angular Correlation between Photo- and Auger electrons from K-Shell Ionization of Neon** A.L. Landers, F. Robicheaux, T. Jahnke, M. Schöffler, T. Osipov, J. Titze, S.Y. Lee, H. Adaniya, M. Hertlein, P. Ranitovic, I. Bocharova, D. Akoury, A. Bhandary, Th. Weber, M.H. Prior, C.L. Cocke, R. Dörner, and A. Belkacem, *Phys. Rev. Lett.* **102**, 223001 (2009).
9. **Fragmentation pathways for selected electronic states of the acetylene dication** T Osipov, T N Rescigno, T Weber, S Miyabe, T Jahnke, A S Alnaser, M P Hertlein1, O Jagutzki, L Ph H Schmidt, M Schöffler, L Foucar, S Schössler, T Havermeier, M Odenweller, S Voss, B Feinberg, A L Landers, M H Prior, R Dörner, C L Cocke and A Belkacem, *J. Phys. B*, **41** 091001 (2008).
10. **Ultrafast Probing of Core Hole Localization in N₂** M. S. Schöffler, J. Titze, N. Petridis, T. Jahnke, K. Cole, L. Ph. H. Schmidt, A. Czasch, D. Akoury, O. Jagutzki, J. B. Williams, N. A. Cherepkov, S. K. Semenov, C. W. McCurdy, T. N. Rescigno, C. L. Cocke, T. Osipov, S. Lee, M. H. Prior, A. Belkacem, A. L. Landers, H. Schmidt-Böcking, Th. Weber, and R. Dörner, *Science*, **320**, 920 (2008).
11. **Photo-double-ionization of H₂: Two-center interference and its dependence on the internuclear distance** M. S. Schöffler, K. Kreidi, D. Akoury, T. Jahnke, A. Staudte, N. Neumann, J. Titze, L. Ph. H. Schmidt, A. Czasch, O. Jagutzki, R. A. Costa Fraga, R. E. Grisenti, M. Smolarski, P. Ranitovic, C. L. Cocke, T. Osipov, H. Adaniya, S. Lee, J. C. Thompson, M. H. Prior, A. Belkacem, Th. Weber, A. Landers, H. Schmidt-Böcking, and R. Dörner *Phys. Rev. A* **78**, 013414 (2008).
12. **Interference in the collective electron momentum in double photoionization of H₂** Kreidi K, Akoury D, Jahnke T, Weber T, Staudte A, Schöffler M, Neumann N, Titze J, Schmidt LPH, Czasch A, Jagutzki O, Costa Fraga RA, Grisenti RE, Smolarski M, Ranitovic P, Cocke CL, Osipov T, Adaniya H, Thompson JC, Prior MH, Belkacem A, Landers AL, Schmidt-Böcking H, and Dörner R., *Phys. Rev. Lett.*, **100**, 133005 (2008).

Program Title:

"Properties of actinide ions from measurements of Rydberg ion fine structure"

Principal Investigator:

Stephen R. Lundeen
Dept. of Physics
Colorado State University
Ft. Collins, CO 80523-1875
lundeen@lamar.colostate.edu

Program Scope:

This project determines certain properties of chemically significant Uranium and Thorium ions through measurements of fine structure patterns in high-L Rydberg ions consisting of a single weakly bound electron attached to the actinide ion of interest. The measured properties, such as polarizabilities and permanent moments, control the long-range interactions of the ion with the Rydberg electron or other ligands. The ions selected for initial study in this project, U^{6+} , U^{5+} , U^{4+} , Th^{4+} , and Th^{3+} , all play significant roles in actinide chemistry, and are all sufficiently complex that *a-priori* calculations of their properties are suspect until tested. The measurements planned under this project serve the dual purpose of 1) providing data that is directly useful to actinide chemists and 2) providing benchmark tests of relativistic atomic structure calculations. In addition to the work with U and Th ions, which takes place at the J.R. Macdonald Laboratory at Kansas State University, a parallel program of studies with stable singly-charged ions takes place at Colorado State University. These studies are aimed at clarifying theoretical questions connecting the Rydberg fine structure patterns to the properties of the free ion cores, thus directly supporting the actinide ion studies. In addition, they provide training for students who can later participate directly in the actinide work.

Recent Progress:

Progress towards the goals of this project began in earnest in Nov. 2008 with the installation of a new ECR source at Kansas State University that was capable of producing the necessary beams of U and Th ions. With the installation completed, our first RESIS signals with U^{6+} ions were seen in March 2009. As we worked towards optimization of the new RESIS beamline, we took advantage of the opportunity to carry out two relatively simple measurements on ions of Pb and Ba, leading to publications 3) and 4) listed below. For most of 2009, our major effort was directed at RESIS spectra of UVI, i.e. Rydberg electrons bound to Rn-like U^{6+} . This effort has, so far, been unsuccessful. The data we collected reveals several features that suggest that the underlying problem is a high metastable content in the U^{6+} beam extracted from the ECR source. The main symptoms are two: 1) The size of the resolved RESIS signals, relative to the unresolved signal we call the high-L peak, is at least a factor of ten smaller than we expected based on the previous study of KrVI. 2) In spite of magnetic separation of the U^{5+} beam after charge capture, there is a substantial U^{6+} beam observed in the detector and a large background of U^{6+} ions at the energy expected for voltage tagged U^{6+} ions created by Stark ionization after RESIS excitation. The background dominates the noise level in the measurement of small RESIS signals. Both of these symptoms could

plausibly be attributed to metastable Rydberg U^{5+} ions that contribute to the high-L signal, diluting the relative size of the resolved RESIS signals, and also producing the U^{6+} beams in the detector by autoionization.

In March of 2010, discouraged by lack of progress with U^{6+} , we decided to try Th beams. The Rn-like Th^{4+} beam was first. In spite of the fact that Th^{4+} and U^{6+} are isoelectronic, the results were dramatically different. We immediately saw resolved RESIS signals with much lower background, and we rather quickly had a result based on optical RESIS spectra that was comparable in precision to our earlier study of KrVI and is represented by publication 5) listed below. Furthermore, when we changed to Fr-like Th^{3+} , we quickly obtained optical RESIS spectra for the ThIII ion. Both of these optical spectra, Th IV and Th III, were pictured in our abstract for the 2010 AMOS Workshop. While this work was going in at the KSU site, we had also completed analysis of the optical RESIS spectra for neutral Ni Rydberg states at our CSU laboratory, and that is now represented in publication 2) listed below.

In late 2010 and early 2011, we completed the analysis of the ThIII optical spectra, represented in publication 6) listed below. This resulted in measurement of several properties of the Fr-like ion Th^{3+} , including its electric quadrupole moment and scalar and tensor dipole polarizabilities. The analysis of the spectra was complicated by the low excitation energies of the $6^2D_{3/2}$ and $6^2D_{5/2}$ levels, which introduced significant non-adiabatic corrections. Fortunately, our experience with similar effects in studies of Ba Rydberg levels, represented in publications 1) and 4) below, provided guidance in treating these effects.

With optical RESIS studies complete in ThIV, ThIII, and Ni, our efforts in 2011 turned to RF spectroscopy which promises much more precise results in each system. We began ThIV RF spectroscopy in April 2011. Six fine structure intervals within the $n=28$ manifold of ThIV were measured with sub-MHz precision, defining the fine structure pattern a hundred times more precisely than the optical study. The higher precision revealed slight curvature in the polarization plot of the results, a feature of the pattern that was not seen in the optical data. This introduces a complication in the analysis since, while the dominant higher term is expected to be proportional to r^{-8} , there could possibly be terms with L-dependence similar to r^{-7} . We discussed this problem in analysis of SiIII spectra (Phys. Rev. A 75, 062512 (2007)). The slight slope in the data pattern can be fit by including only the r^{-8} terms, but the intermediate r^{-7} terms can, if they are significant, alter the interpretation of the fitted parameters. In the case of ThIV we were able to determine, with theoretical assistance from Donald Beck and Marianna Safronova, that the intermediate terms were of minor importance relative to experimental errors. The final report of ThIV RF spectroscopy, represented in publication 7) below, reports dipole and quadrupole polarizabilities of Rn-like Th^{4+} with precision of 0.1% and 18% respectively.

Table I shows the properties of Th^{4+} and Th^{3+} determined to date from our studies, and compares them with theoretical calculations when available.

Table I. Properties of Thorium ions obtained from Rydberg ion fine structure measurements during the present grant period. Also shown are various theoretical calculations, most obtained by private communication. Although the uncorrelated wavefunctions calculated with the Hartree-Fock (HF) and Dirac-Fock (DF) methods are not expected to be extremely accurate, some results obtained with these methods are included for comparison to more precise calculations. Since HF and DF methods are standard, results calculated with these methods are not attributed to individuals.

Ion and Property	Measurement	Prediction
Th ⁴⁺ : α_D (a.u.)	7.61(6) ^a	7.699 ^c (RCCSD(T))
	7.720(7) ^b	7.75 ^d (RRPA)
		8.96 (DF)
		10.26 (HF)
Th ⁴⁺ : α_Q (a.u.)	47(11) ^a	28.8 ^d (RRPA)
	21.5(3.9) ^b	24.5 (DF)
Th ³⁺ : Q (a.u.)	0.54(4) ^e	0.62 ^f (RMBPT)
		0.91 (DF)
Th ³⁺ : $\alpha_{D,0}$ (a.u.)	15.42(17) ^c	15.073 ^f (RMBPT)
Th ³⁺ : $\alpha_{D,2}$ (a.u.)	-3.6(1.3) ^e	-6.166 ^f (RMBPT)
Th ³⁺ : $\langle 5^2F_{5/2} D 6^2D_{3/2} \rangle$	1.435(10) ^e	1.530 ^f (RMBPT)
		2.428 (DF)
Th ³⁺ : $\langle 5^2F_{5/2} D 6^2D_{5/2} \rangle$	0.414(24) ^e	0.412 ^f (RMBPT)
		0.639 (DF)

a Optical RESIS study, Hanni et. al. (Hanni, 2010)

b rf RESIS study. Keele et. al. (Keele, 2011)

c Relativistic Couple Cluster, Schwerdtfeger and Borschevsky (Borschevsky, 2010)

d Relativistic Random Phase Approximation, M. Safronova (Safronova M, 2010)

e Optical RESIS study, Keele et. al (Keele, 2011b)

f Relativistic Many Body Perturbation Theory, M. Safronova (Safronova M, 2010)

Immediate Future Plans

We are now focusing on RF spectroscopy of the other two systems for which optical RESIS studies have been completed, ThIII and Ni. Both systems are of comparable complexity since both the Th³⁺ and Ni⁺ ions have $J_C=5/2$. The absence of strong non-adiabatic effects in Ni promises to make that analysis simpler, and the comparison with ThIII, where these effects are more important, should be instructive. We have begun both studies. In Ni, 14 RF transitions have been seen in preliminary studies, while in ThIII, 6 transitions have been seen to date. We expect to complete both experiments by summer 2012, but final reports will require extensive analysis.

After completion of the ThIII RF studies at KSU, we plan to turn back to the more difficult studies of U ions. By that time, we hope to have more insight into the problem of metastable ions, and possible methods to reduce the metastable content in the U^{6+} beam. We will also look carefully at Rydberg levels bound to Fr-like U^{5+} , and compare the signal sizes and background rates encountered there with the comparable values for U^{6+} . This could be instructive since it seems improbable that metastable content would be similar in U^{5+} and U^{6+} . In our initial work with U ions, very little time was spent with U^{5+} , since it was expected to be much more difficult than U^{6+} due to the higher core angular momentum. After the successful studies of Th^{3+} , however, it seems possible that U^{5+} studies could actually be easier than U^{6+} studies.

Recent Publications:

- 1) "Dipole and quadrupole transition strengths in Ba^+ from measurements of K-splittings in high-L barium Rydberg levels", Shannon L. Woods, S.R. Lundeen, and Erica L. Snow, Phys. Rev. A 80, 042516 (2009)
- 2) "Optical spectroscopy of high-L Rydberg states of nickel", Julie A. Keele, Shannon L. Woods, M.E. Hanni, S.R. Lundeen, and W.G. Sturuss, Phys. Rev. A 81, 022506 (2010)
- 3) "Polarizabilities of Pb^{2+} and Pb^{4+} and Ionization Energies of Pb^+ and Pb^{3+} from spectroscopy of high-L Rydberg states of Pb^+ and Pb^{3+} . M.E. Hanni, Julie A. Keele, S. R. Lundeen, C.W. Fehrenbach, and W.G. Sturuss, Phys. Rev. A 81, 042512 (2010)
- 4) "Dipole transition strengths in Ba^+ from Rydberg fine structure measurements in Ba and Ba^+ ", Shannon L. Woods, M.E. Hanni, S.R. Lundeen, and Erica L. Snow, Phys. Rev. A 82, 012506 (2010)
- 5) "Polarizabilities of Rn-like Th^{4+} from spectroscopy of high-L Rydberg levels of Th^{3+} ", M.E. Hanni, Julie A. Keele, S.R. Lundeen, and C.W. Fehrenbach, Phys. Rev. A 82, 022512 (2010)
- 6) "Properties of Fr-like Th^{3+} from spectroscopy of high-L Rydberg levels of Th^{2+} ", Julie A. Keele, M.E. Hanni, Shannon L. Woods, S.R. Lundeen, and C.W. Fehrenbach, Phys. Rev. A 83, 062501 (2011)
- 7) "Polarizabilities of Rn-like Th^{4+} from rf spectroscopy of Th^{3+} Rydberg levels", Julie A. Keele, S.R. Lundeen, and C.W. Fehrenbach, Phys. Rev. A 83, 062509 (2011).

Publications in Preparation

- 8) "Effective Potential Model for high-L Rydberg atoms and ions", Shannon L. Woods and S.R. Lundeen

Other Reports

"Rydberg Spectroscopy of Fr-like Thorium and Uranium Ions", Mark E. Hanni, PhD thesis Colorado State University, Fall 2010

Theory of Atomic Collisions and Dynamics

J. H. Macek

*Department of Physics and Astronomy,
University of Tennessee, Knoxville, Tennessee and
Oak Ridge National Laboratory, Oak Ridge, Tennessee
email:jmacek@utk.edu*

1 Program scope

Our project seeks to characterize [1-4] atomic dynamics by the exchange of physical quantities such as energy, momentum, and angular momentum between various constituents of atoms, molecules and ions. Recent effort has concentrated on the exchange of angular momentum. Such exchange involving bound states has long been studied in connection with the states produce by photoexcitation and charged particle impact. The angular momentum properties of such states are expressed in terms of the Fano-Macek orientation parameter. A major accomplishment [4] of our research has been the recognition that vortices in atomic wave functions are closely connected with angular momentum transfer and that such vortices provide a means to experimentally investigate orientation of continuum states of quantum systems. This insight has wide application for essentially all atomic, molecular and optical processes. Up till now vortices in atoms has been of theoretical interest only. Our research has concentrated on experimental aspects of vortex detection and observation [2-4].

We also continue our research into structure related to threshold phenomena. The projects listed in this abstract are sponsored by the Department of Energy, Division of Chemical Sciences, through a grant to the University of Tennessee. The research is is carried out in cooperation with Oak Ridge National Laboratory under the ORNL-UT Distinguished Scientist program.

2 Recent progress

Our Previous work with the Regularized Lattice-Time-Dependent-Schrödinger equation (RLTDSE) method [7] has shown that time dependent wave functions $\psi(\mathbf{r}, t)$ have vortices at isolated points in coordinate space where the

real and imaginary parts of the wave function vanish. We atomic wave functions with non-zero mean angular momentum $\langle \mathbf{j} \rangle$ exhibit two types of rotation, namely rotation of the wave function about the center of mass or the charge center and rotations about isolated zeros or vortex points. These latter rotations are observable as zeros of electron momentum distributions $P(\mathbf{k})$ since such distributions image *coordinate* space wave functions according to

$$P(\mathbf{k}) = \lim_{t \rightarrow \infty} \left[\left| t^3 \psi(\mathbf{r}, t) \right|^2 \right]_{\mathbf{r}=\mathbf{k}t} \quad (1)$$

where it is understood that $\mathbf{r} \neq \mathbf{r}_Q$ and \mathbf{r}_Q is any potential center. This equation, called the "imaging theorem" allows structure in $P(\mathbf{k})$ to be traced to structure in $\psi(\mathbf{r}, t)$ at earlier times. Using the RLTDSE method and the imaging theorem we have shown that "holes" in highly accurate momentum distributions are due to free vortices [4]. The focus of our research this past year has been to see how these theoretical discoveries can be verified experimentally.

Professor J. S. Briggs has pointed out to us that unexplained minima appear triply differential cross sections (TDCS) in (e,2e) measurements of electron impact on atomic helium. His theoretical work has shown that there is an exact zero near a measured minima. In general, exact minima for (e,2e) are not expected since measured TCS are incoherent superpositions of singlet and triplet couplings of the two electrons a and b in the final state. For the special case of symmetric geometry with equal energies for the outgoing electrons, only the singlet couplings contributes. Then, there may be exact zeros in the TDCS. Using a 3C correlated final state, as in the previous calculations that found the minimum, we have computed the (e,2e) TDCS for helium targets. The calculations show a minimum similar to the observed minimum [2].

This minimum correlates with a vortex in the space of momentum variables $\mathbf{k}_+ = (\mathbf{k}_a + \mathbf{k}_b)/2$ and $\mathbf{k}_{ab} = (\mathbf{k}_a - \mathbf{k}_b)/2$ appropriate to the symmetric geometry. A contour plot of the ionization amplitude on a grid in the plane defined by \mathbf{k}_+ and the incident momentum \mathbf{K}_i , with the z -axis along the incident momentum and the x -axis in this plane plot shows a zero at a specific value of \mathbf{k}_+ . This is further confirmed by plotting the direction of the velocity $\mathbf{w} = \Im[\nabla_{\mathbf{k}_+} \log A]$ which circulate around the zero. Integration of the current around the zero gives 2π as is should for a first order zero. This confirms that the zero in (e,2e) distributions seen by Murray and Read [2]

corresponds to a vortex. To our knowledge this is the first observation of vortices in two-electron atomic wave functions.

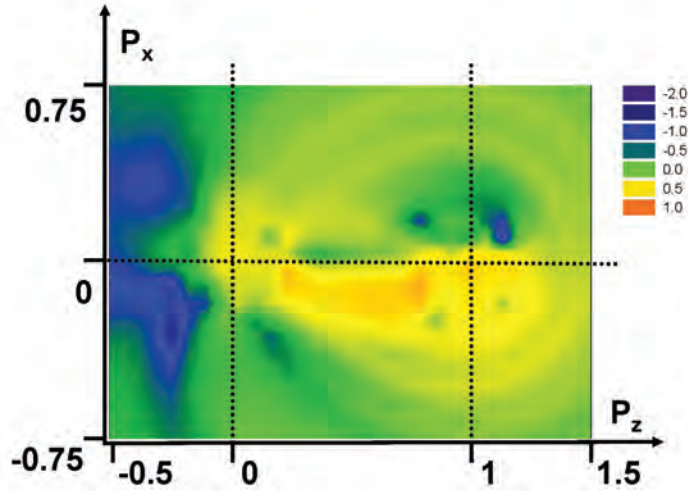


Figure 1. Contour plot on a logarithmic scale of the ejected electron momentum distribution near the projectile and target momenta from the present 4D RLTDSE calculations of the ejected electron spectrum for 10 keV/u $\text{He}^{2+} + \text{He}$ collisions with an impact parameter (along x) of 1 a.u.

It may be possible to observe the vortices predicted by time-dependent LTDSE calculations where they were first discovered. It turns out that the COLTRIMS technique is sufficiently sensitive that the zeros in the transfer ionization electron distributions in collisions of alpha particles with He may be observed. To check this possibility we have developed a two-electron version of the lattice-time-dependent-Schrodinger-equation method (LTDSE). Owing to memory requirements for these calculations we have developed a model for two electrons in a two-dimensional space. The model has been checked by comparing 2d and 3d one-electron wavefunctions where the results are essentially identical. This model was then used to search for vortices in transfer ionization in $\text{He}^{++} + \text{He}$ collisions. Figure 1 shows a contour plot in the electron momentum distribution in the scattering plane for 10 keV alpha particle impact on atomic helium. The contour plot shown in Fig. 1 shows several vortices located near the projectile center at $v_e/v = 1$. Prelim-

inary experimental distributions support the observation of deep minima in the region of the vortices.

Other projects investigate structure that appears in elastic scattering [4,5], charge exchange reactions [3], low energy three-body interactions [3,6] and ionization by positron impact [7]. The threshold ionization cross section obeys the extended threshold law proposed earlier by us and verified by convergent close coupling model calculations. We find some unanticipated structure owing to hidden crossings of hyperspherical adiabatic potential energy curves.

3 References to DOE sponsored research that appeared in 2008-2010

1. Creating and Manipulating Vortices in Atomic Wave Functions with Short Electric Field Pulses, Sergey Y. Ovchinnikov, Joseph H. Macek, James B. Sternberg, Teck-Ghee Lee, and David R. Schultz, *Phys. Rev. Lett.* **105**, 203005 (2010).
2. Theory of Deep Minima in $(e,2e)$ Measurements of Triply Differential Cross Sections, J. H. Macek, J. B. Sternberg, S. Y. Ovchinnikov, and J. S. Briggs, *Phys. Rev. Lett.*, **104**, 033201 (2010).
3. Evolution of Quantum Systems from Microscopic to Macroscopic Scales, Sergey Y. Ovchinnikov, Joseph H. Macek, James S. Sternberg, Teck-Ghee Lee, and David R. Schultz, *CAARI 2008 Proceedings AIP Conference Proceedings*, **1099**, 164 (2009).
4. Origin, evolution, and imaging of vortices in atomic processes, J.H. Macek J.S. Sternberg and S.Y. Ovchinnikov, T-G. Lee and D.R. Schultz, *Phys. Rev. Lett.*, **102**, 143201(2009).
5. Multiparticle interactions of zero-range potentials, J. H. Macek, *Few-Body Syst*, **45**,207 (2009).
6. Feshbach resonances in atomic structure and dynamics, J. H. Macek, *Proceedings of the JointPhysics/Mathematics Workshop on Quantum Few-Body Systems*, *AIP Conf. Proc.* **998**, 59 (2008).
7. Near-threshold positron impact ionization of hydrogen, S. J. Ward, Krista Jansen, J. Shertzer, and J. H. Macek, *Nuc. Inst. Meth. B*, **266**, 410 (2008).

Photoabsorption by Free and Confined Atoms and Ions

Steven T. Manson, Principal Investigator

Department of Physics and Astronomy, Georgia State University, Atlanta, Georgia 30303
(smanson@gsu.edu)

Program Scope

The goals of this research program are: to provide a theoretical adjunct to, and collaboration with, the various atomic and molecular experimental programs that employ latest generation light sources, particularly ALS, APS and LCLS; to generally enhance our understanding of the photoabsorption process; and to study the properties (especially photoabsorption) of confined atoms and ions. To these ends, calculations are performed employing and enhancing cutting-edge methodologies to provide deeper insight into the physics of the experimental results; to provide guidance for future experimental investigations; and seek out new phenomenology, especially in the realm of confined systems. The general areas of programmatic focus are: manifestations of nondipole effects in photoionization; photodetachment of inner and outer shells of atoms and atomic ions (positive and negative); studies of atoms endohedrally confined in buckyballs, C_{60} , particularly dynamical properties. Flexibility is maintained to respond to opportunities that present themselves as well.

Highlights of Recent Progress

1. Confined Atoms

The study of confined atoms just beginning. There are a number of theoretical investigations of various atoms endohedrally confined in C_{60} [1,2], but experimental studies are sparse [3-5]. Thus, we are conducting a program of calculations at various levels of approximation, aimed at delineating the properties of such systems, especially photoionization, to guide the experimental community. Among our recent results, we have found that a huge transfer of oscillator strength from the C_{60} shell, in the neighborhood of the giant plasmon resonance, to the encapsulated atom for both $Ar@C_{60}$ [6] and $Mg@C_{60}$ [7]. In addition, confinement resonances [8], oscillations that occur in the photoionization cross section of an endohedral atom owing to the interferences of the photoelectron wave function for direct emission with those scattered from the surrounding carbon shell have been predicted in a broad range of cases; within the past year, the existence of confinement resonances has been confirmed experimentally [5]. In addition, the photoionization of endohedral atoms within nested fullerenes, called buckyonions, has shown that, as a result of the multi-walled confining structures, the confinement resonances become considerably more complicated [9].

Considering a Xe atom endohedrally confined in C_{60} the formation of a new type of atom-fullerene hybrid state was discovered [10]. These dimer-type states arise from the near-degeneracy of inner levels of the confined atom and the confining shell, in contrast to the known overlap-induced hybrid states around the Fermi level of smaller compounds. The photoionization cross sections of these hybrid states exhibit rich structures and are radically different from the cross sections of free atomic or fullerene

states. This also occurs in buckyonions, nested fullerenes. A study of $C_{60}@C_{240}$ reveals strong hybridization between the plasmon excitations of the individual fullerenes leading to a photoionization cross section of the nested system being dramatically different from the sum of the individual constituents [11]. This result suggests the possibility of creating buckyonions with plasmons of specified character, i.e., *designer resonances*.

We have made an initial attempt to consider fast charged-particle impact ionization of atoms, looking at the $He@C_{60}$ system [12]. The motivation here is that there are experimental results in this area, along with a search for the possible existence of nondipole plasmon resonances. Our first results indicate that confinement resonances appear in the ionization of endohedrals by charged particle impact as well as in photoionization.

While these various effects have been computationally demonstrated in particular cases, their importance is that they are, in fact, quite general and it is expected that they will arise in many confined atom systems.

2. Atomic/Ionic Photoionization

The study of photoionization of atoms/ions at high resolution leads to results of great complexity. Our effort is to perform state-of-the-art calculations, in concert with high-resolution synchrotron experiments, to understand this complexity. Using our upgraded relativistic Breit-Pauli R-matrix methodology we have completed a study of the four-electron Be isoelectronic sequence [13]. Aside from showing that the calculations produce excellent agreement with experiment for five different members of the sequence, we have found that relativistic interactions are crucial for quantitative accuracy, even for the lowest member of the sequence; quite surprising for $Z=4$! A study of the behavior of satellite lines, ionization plus excitation, along the isoelectronic sequence was also performed [14] and exhibited a variety of interesting behaviors as a function of energy, nuclear charge and principal quantum number. In addition, an investigation of how resonance series begin to overlap with increasing Z showed that distinct resonances in the neutral become more and more mixed until they are no longer identifiable [15].

Calculations of some of the higher members of the K isoelectronic series were performed [16]. It was found that the giant $3p \rightarrow 3d$ resonances dominated the threshold region for Ti^{3+} (in excellent agreement with experiment) but lay below the ionization threshold for the higher members of the series. It would be expected that the calculation would be even more accurate for higher Z , but a recent experiment on Fe^{7+} [17] does not show good agreement with theory. This is not understood as yet.

3. Nondipole Effects in Atoms

Up until relatively recently, the conventional wisdom was that nondipole effects in photoionization were of importance only at photon energies of tens of keV or higher, despite indications to the contrary more than 35 years ago [18]. The last decade has seen an upsurge in experimental and theoretical results [19] showing that nondipole effects in photoelectron angular distributions could be important down to hundreds [20] and even tens [21] of eV. Our recent work included a study of Cl [22] which revealed that there are strong correlation effects in quadrupole channels, and these effects show up in the nondipole contribution to the photoelectron angular distribution at a level predicted to be measurable at rather low energies. We have also found a case where the quadrupole

cross section actually dominates the dipole cross section in the 10 eV range [22], in the Cooper minimum region of Mg 3s. The results also show a dramatic change in the photoelectron angular distribution over a small energy range. This study indicates that laboratory investigations in the neighborhood of dipole Cooper minima (which is now possible owing to high intensity light sources such FEL's) could prove quite fruitful and interesting.

Future Plans

Fundamentally our future plans are to continue on the paths set out above. In the area of confined atoms, we will perform many-body calculations on charged particle impact ionization of endohedral atoms and free fullerene molecules in an effort to elucidate any new insights inherent in the nondipole channels thus produced. In addition, we shall upgrade our theory to include relativistic interactions to be able to deal with heavy endohedrals with quantitative accuracy. The study of the photodetachment of C^- shall move on to the photoabsorption in the vicinity of the K-shell edge of both the ground 4S and excited 2D states in order to understand how the slight excitation of the outer shell affects the inner-shell photoabsorption and to pave the way for experiment, in addition to further study of Na^- and K^- . Further, build upon our previous work, we shall attack the problem of inner-shell photoionization of the Sc atom. Additionally, nondipole effects the inner subshells of Hg will be investigated to try to unravel the combined effects of many-body correlation effects and relativistic interactions. In addition, the search for cases where nondipole effects are likely to be significant, as a guide for experiment, and quadrupole Cooper minima, will continue.

Publications Citing DOE Support Since 2010

- “Quadrupole matrix element zeros and their effect on photoelectron angular distributions,” L. A. LaJohn, S. T. Manson and R. H. Pratt, *Nuc. Instr. Meth. A* **619**, 7-9 (2010).
- “Photoionization of Xe inside C_{60} : atom-fullerene hybridization, giant enhancement and interchannel oscillation transfer,” M. E. Madjet, D. Hopper, M. A. McCune, H. S. Chakraborty, J.-M. Rost and S. T. Manson, *Phys. Rev. A* **81**, 013202-1-8 (2010).
- “Effects of the fullerene (C_{60}) potential and position of the atom (A) on spectral characteristics of endohedral atoms $A@C_{60}$,” A. S. Baltenkov, U. Becker, S. T. Manson, and A. Z. Msezane, *J. Phys. B* **43**, 115102-1-9 (2010).
- “Satellite Lines in the Photoionization of Ions: The Be Isoelectronic Sequence,” W.-C. Chu, H.-L. Zhou, A. Hibbert and S. T. Manson, *Phys. Rev. A* **81**, 053412-1-5 (2010).
- “Interior static polarization effect in $A@C_{60}$ photoionization,” V. K. Dolmatov and S. T. Manson, *Phys. Rev. A* **82**, 023422-1-3 (2010).
- “Photoionization of the Be-like O^{4+} ion: Total and partial cross sections for the ground $2s^2$ and excited $2s2p\ ^{1,3}P$ states,” D.-S. Kim and S. T. Manson, *J. Phys. B* **43**, 155205-1-12 (2010).
- “Variation of photoelectron angular distributions along Ar and Ca isonuclear sequences,” G. B. Pradhan, J. Jose, P. C. Deshmukh, V. Radojević, and S. T. Manson, *Phys. Rev. A* **81**, 063401-1-4 (2010).
- “Overlapping Resonances in Atomic Ions,” W.-C. Chu, H.-L. Zhou, A. Hibbert and S. T. Manson, *Phys. Rev. A* **82**, 013417-1-4 (2010).

- “Inner Shell Photodetachment of Na^- Using the Multi-Configuration Tamm-Dancoff Approximation,” J. Jose, G. B. Pradhan, V. Radojević, S. T. Manson, and P. C. Deshmukh, *Publ. Astron. Obs. Belgrade* **89**, 29-32 (2010).
- “Photoionization of potassium-like transition metal ions: Ti^{3+} to Fe^{7+} ,” A. M. Sossah, H.-L. Zhou, S. T. Manson, *Phys. Rev. A* **82**, 043416-1-13 (2010).
- “Electron-Impact Ionization of Atoms: Secondary Electron Angular Distributions and Drag Currents,” A. S. Baltenkov, S. T. Manson and A. Z. Msezane, *Cent. Eur. J. Phys.* (in press).
- “Valence photodetachment of Li^- and Na^- using relativistic many-body techniques,” J. Jose, G. B. Pradhan, V. Radojević, S. T. Manson, and P.C. Deshmukh, *Phys. Rev. A* **85**, 053419-1-7 (2011).
- “Cooper Minima: A Window on Nondipole Photoionization at Low Energy,” G. B. Pradhan, J. Jose, P. C. Deshmukh, L. A. LaJohn, R. H. Pratt, and S. T. Manson, *Phys. Rev. Letters* (submitted).
- “Electron correlation effects near the photoionization threshold: The Ar isoelectronic sequence,” J. Jose, G. B. Pradhan, V. Radojević, S. T. Manson, and P.C. Deshmukh, *Phys. Rev. A* (submitted).
- “Plasmon-plasmon coupling in nested fullerenes: Creation of interlayer plasmonic cross modes,” M. A. McCune, R. De, M. E. Madjet, H. S. Chakraborty, and S.T. Manson, *Phys Rev. Letters* (submitted).

References

- [1] V. K. Dolmatov, A. S. Baltenkov, J.-P. Connerade and S. T. Manson, *Radiation Phys. Chem.* **70**, 417 (2004) and references therein.
- [2] V. K. Dolmatov, *Advances in Quantum Chemistry*, **58**, 13 (2009) and references therein.
- [3] A. Müller *et al*, *Phys. Rev. Lett.* **101**, 133001 (2008).
- [4] R. Phaneuf *et al*, *Bull. Am. Phys. Soc.* **55**(5), 40 (2010) and private communication.
- [5] A. L. D. Kilcoyne, A. Aguilar, A. Müller, S. Schippers, C. Cisneros, G. Alna'Washi, N. B. Aryal, K. K. Baral, D. A. Esteves, C. M. Thomas, and R. A. Phaneuf, *Phys. Rev. Lett.* **105**, 213001 (2010)
- [6] M. E. Madjet, H. S. Chakraborty and S. T. Manson, *Phys. Rev. Letters* **99**, 243003 (2007).
- [7] M. E. Madjet, H. S. Chakraborty, J. M. Rost and S. T. Manson, *Phys. Rev. A* **78**, 013201-1-4 (2008).
- [8] V. K. Dolmatov and S. T. Manson, *J. Phys. B* **41**, 165001 (2008).
- [9] V. K. Dolmatov and S. T. Manson, *J. Phys. Rev. A* **78**, 013415 (2008).
- [10] H. S. Chakraborty, M. E. Madjet, T. Renger, J.-M. Rost and S. T. Manson, *Phys. Rev. A* **79**, 061201(R) (2009).
- [11] M. A. McCune, R. De, M. E. Madjet, H. S. Chakraborty, and S.T. Manson, *Phys Rev. Letters* (submitted).
- [12] A. S. Baltenkov, V. K. Dolmatov, S. T. Manson, and A. Z. Msezane, *Phys. Rev. A* **79**, 043201 (2009).
- [13] W.-C. Chu, H.-L. Zhou, A. Hibbert and S. T. Manson, *J. Phys B* (submitted).
- [14] W.-C. Chu, H.-L. Zhou, A. Hibbert and S. T. Manson, *Phys. Rev. A* **81**, 053412 (2010).
- [15] W.-C. Chu, H.-L. Zhou, A. Hibbert and S. T. Manson, *Phys. Rev. A* **82**, 013417-1-4 (2010).
- [16] A. M. Sossah, H.-L. Zhou, S. T. Manson, *Phys. Rev. A* **82**, 043416-1-13 (2010).
- [17] A. Müller, R. Phaneuf, private communication (2011).
- [18] M. O. Krause, *Phys. Rev.* **177**, 151 (1969).
- [19] O. Hemmers, R. Guillemin and D. W. Lindle, *Rad. Phys. and Chem.* **70**, 123 (2004) and referenxces therein.
- [20] O. Hemmers *et al*, *Phys. Rev. Letters* **91**, 053002 (2003).
- [21] V. K. Dolmatov and S. T. Manson, *Phys. Rev. Letters* **83**, 939 (1999).
- [22] J. Jose, G. B. Pradhan, P. C. Deshmukh, V. Radojević and S. T. Manson, *Phys. Rev. A* **80**, 023405-1-6 (2009).
- [23] G. B. Pradhan, J. Jose, P. C. Deshmukh, L. A. LaJohn, R. H. Pratt, and S. T. Manson, *Phys. Rev. Letters* (submitted).

Combining High Level *Ab Initio* Calculations with Laser Control of Molecular Dynamics

Thomas Weinacht
Department of Physics and Astronomy
Stony Brook University
Stony Brook, NY
tweinacht@sunysb.edu

Spiridoula Matsika
Department of Chemistry
Temple University
Philadelphia, PA
smatsika@temple.edu

1 Program Scope

We use intense, shaped, ultrafast laser pulses to follow and control molecular dynamics and high level *ab initio* calculations to interpret the dynamics and guide the control. We are applying the techniques and understanding we have developed to dissociative ionization pump-probe spectroscopy and pulse shape spectroscopy.

2 Recent Progress

We have developed an approach to probe molecular dynamics on an excited electronic surface via strong field dissociative ionization. Conical intersections (CIs) play an important role in the excited state dynamics of most polyatomic molecules, but there are frequently multiple energetically accessible relaxation pathways and our technique enables us to probe which ones play an important role in a given molecule. Our approach is based on the idea that molecular fragment ions created by the probe pulse carry information about the relaxation channels on the neutral surface. An ultrafast UV pulse is used to excite the neutral molecules followed by an intense IR probe which ionizes and fragments them. Different fragments display different ion yields as a function of pump-probe delay, and can be used to label different pathways involved in the neutral relaxation, giving us separate timescales for individual pathways rather than an average or a collective lifetime.

Ab initio calculations are used to establish this connection between the fragments and the excited state relaxation pathways. Initially they provide information on the $S_1/S_2 \rightarrow S_0$ relaxation pathways of the neutral molecules. In order to understand what final states are accessed by the probe, the ionic states that can be reached upon ionization are calculated. Information on how these ionic states can subsequently fragment is necessary to determine the final connection between ionic fragments and neutral pathways. This step is the most complicated one.

Our pump-probe approach has been applied to explore the excited state dynamics in the DNA/RNA bases uracil, cytosine and adenine. All of these systems have been found to exhibit ultrashort excited state lifetimes due to radiationless decay through CIs. This is important because of the biological relevance of the nucleobases and their interaction with UV radiation. The details for each molecule are quite different, and extensive experimental and theoretical efforts have been devoted to understand these phenomena. The lower panels of Figure 1 show energy level diagrams of the main features involved in the excited state dynamics obtained previously for these systems¹⁻³.

We have already studied in detail the excited state dynamics in cytosine. Cytosine absorbs in the UV, but as with all of the nucleobases, the excited state lifetime is very short due to radiationless decay to the ground state. As seen in Figure 1 previous calculations have identified two different relaxation pathways that can lead from S_1 to the ground state, but it is hard to distinguish their importance based just on the electronic structure calculations. Based on our pump-probe measurements and ionic state calculations, we were able to show that both of these pathways participate in the relaxation, and thus the wavepacket is delocalized during relaxation to the ground state. Details of how we made this interpretation can be found in the original publication.

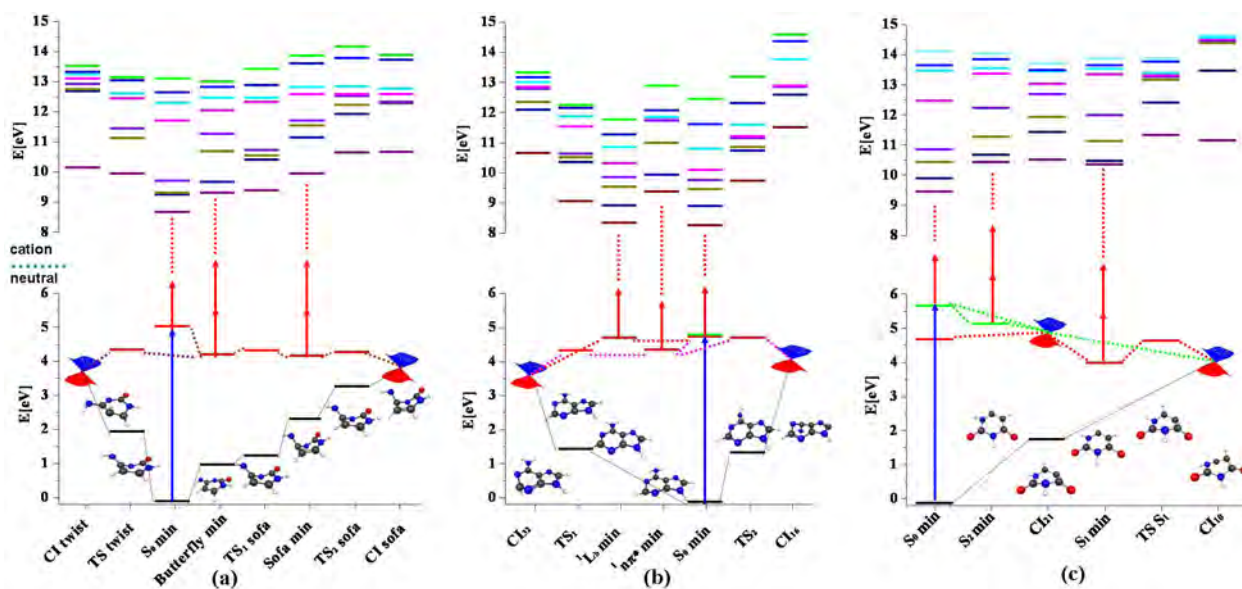


Figure 1: Neutral and ionic energies along some of the important features of the relaxation pathway on the S_1 (and S_2 for uracil) PES of the neutral molecule for (a) cytosine, (b) adenine, and (c) uracil. Lower panel: Energies for neutral states taken from¹⁻³ (black: ground state, red: S_1 state, green: S_2 state). Upper panel: Energies for the eight lowest-lying ionic states. Dotted lines are used to mark predicted connections between the states.

We are currently studying uracil and adenine. A snapshot of the different dynamics involved in these systems can be seen in Figure 2. The figure shows the ion signal for each molecule as a function of pump probe delay for two different fragments in each case: the parent ion and a smaller fragment that provides important complementary information.

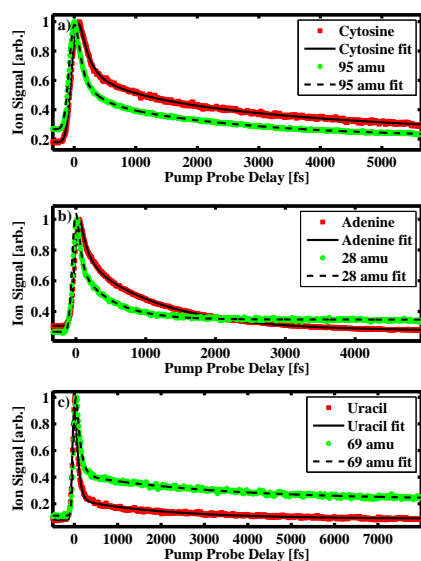


Figure 2: Parent and one selected fragment ion yield vs pump probe delay for cytosine, adenine and uracil.

Proper interpretation of the fragmentation requires information about how the cation fragments. This is a very difficult task. We have undertaken it for uracil. In uracil the most important fragments observed in TOFMS are 69, 41, 42 and 28. We have identified pathways on the ground ionic state that can lead to these fragments. This information is useful in understanding how these

Some features are common in all fragments. For example, there is always a sharp increase at time zero. This is because as the probe pulse comes during or after the pump pulse, the ionization potential is lowered by about 4.7 eV as compared with the probe pulse arriving before the pump pulse. The reduced ionization potential (IP) for a molecule in the S_1/S_2 state leads to a large increase in the ion yield since the ionization process is much lower order and requires the absorption of fewer probe photons. After some time passes, the IP can increase again as shown in Figure 2 and population is leaving the S_1 surface as well. This is what we are interested in measuring. The signal decays and lifetimes for each molecule are different as a signature of their unique PESs. The decays are also different between the parent ion and the fragments indicating that they can be used to label different dynamical processes.

fragments are generated from the parent ion.

Once we have identified specific ionic states from which a given fragment is produced, we can identify from which orbital(s) an electron was removed via ionization, by projecting the initial excited neutral state of the molecule onto the final cationic state. By varying the time delay and angle between the pump and probe pulses, we can measure the ionization from specific molecular orbitals with temporal and angular resolution.

As an example, we have measured the angle resolved ionization yields for several different fragments in uracil as a function of pump-probe delay. Based on our calculations, we have established that the parent molecular ion comes from ionization to one of the first two states of the ion (D_0 or D_1), corresponding to ionization from the LUMO orbital, whereas fragments 28,41 and 42 come from ionization to D_5 or D_6 , and correspond to ionization from the HOMO or HOMO-2 orbitals. Figure 3 shows the angular distributions for fragment 42 and the parent ion as a function of time along with the orbitals involved in ionization.

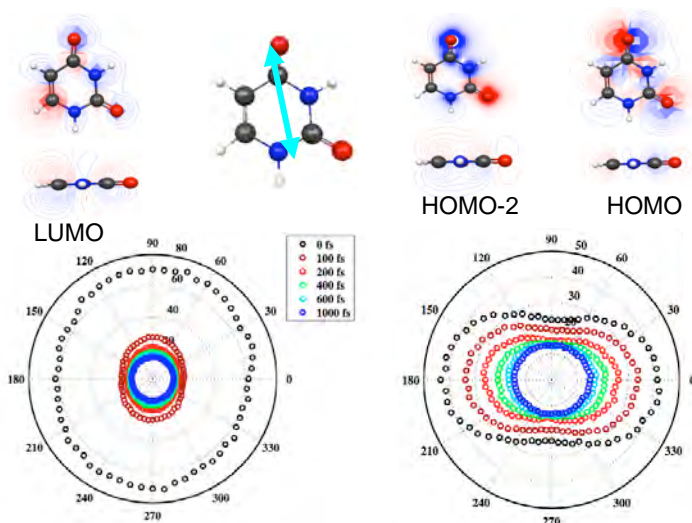


Figure 3: Pump-probe ion yield vs pump polarization and pump-probe delay, Left panel: for the parent ion, right panel: for fragment 42 amu. The azimuth angle corresponds to relative polarization between the pump and the probe beams, while the radial distance is the ion count in arbitrary units. The orbitals from which ionization is expected to occur in each case are shown in the top panels. The direction of the transition dipole moment for $S_1 \rightarrow S_2$ transition is also shown.

The angular distribution for the parent and fragment ions show opposite behavior, with the parent ion distribution being maximum for perpendicular pump and probe polarizations, while the fragment shows a maximum for parallel pump and probe polarizations. We note that the angular distributions for 28, 41 and 42 are identical for all delays. The parent ion distribution is consistent with ionization from the LUMO orbital being suppressed along the nodal plane of the π LUMO orbital^{4;5}, whereas the fragment ion angular distribution is not consistent with a simple interpretation in terms of the nodal planes of the HOMO or HOMO-2 orbitals. This indicates that the ionization of more extended molecular systems is more complicated than for diatomics and we suspect that the Stark shifts and mixing of different orbitals play an important role.

3 Future Plans

We have several goals for the immediate future:

1. We are interested in comparing our angle, time and state resolved ionization measurements with high level calculations of strong field ionization (carried out by Michael Spanner at the National Research Council of Canada). This comparison will allow us to explicitly check for violations of Koopmans' correlations in ionization of excited states and it will give us a more quantitative understanding of the ionization which will in turn be very useful for tracking

molecular dynamics in the excited state.

2. We are currently completing a comparison between molecules where our measurements indicate that the relaxation dynamics are local with molecules where the relaxation is non-local - i.e. the wave packet becomes extended, or breaks up into multiple spatially separated components during relaxation.
3. We would like to extend our study of excited neutral state dynamics to ionic states in order to probe how ionic dissociation proceeds.
4. We are trying to see whether we can achieve control over how the wavepacket moves towards the pathways to CIs in the molecules we are studying. Initial results indicate that it is difficult to achieve control and we are exploring this further.

References

- [1] K. A. Kistler and S. Matsika, *J. Phys. Chem. A*, 2007, **111**, 2650–2661.
- [2] S. Matsika, *J. Phys. Chem. A*, 2004, **108**, 7584.
- [3] S. Perun, A. L. Sobolewski and W. Domcke, *J. Am. Chem. Soc.*, 2005, **127**, 6257–6265.
- [4] A. S. Alnaser, C. M. Maharjan, X. M. Tong, B. Ulrich, P. Ranitovic, B. Shan, Z. Chang, C. D. Lin, C. L. Cocke and I. V. Litvinyuk, *Physical Review A.*, 2005, **71**, 031403.
- [5] D. Pavicic, K. F. Lee, D. M. Rayner, P. B. Corkum and D. M. Villeneuve, *Physical Review Letters*, 2007, **98**, 243001.

4 Publications of DOE Sponsored Research

- “Interpreting Ultrafast Molecular Fragmentation Dynamics with *ab initio* Calculations”, C. Trallero, B. J. Pearson, T. Weinacht, K. Gilliard and S. Matsika, *J. Chem. Phys.*, **128**, 124107, (2008)
- “Closed-Loop Learning Control of Isomerization using Shaped Ultrafast Laser Pulses in the Deep Ultraviolet”, M. Kotur, T. Weinacht, B. J. Pearson and S. Matsika *J. Chem. Phys.*, **130**, 134311, (2009)
- ”Two Dimensional Ultrafast Fourier Transform Spectroscopy in the Deep Ultraviolet C. Tseng, S. Matsika and T. C. Weinacht, *Optics Express* **17**, 18788 (2009)
- “Distinguishing Between Relaxation Pathways by Combining Dissociative Ionization Pump Probe Spectroscopy and *ab initio* Calculations: A Case Study of Cytosine ”, M. Kotur, T. Weinacht, C. Zhou, K. A. Kistler, and S. Matsika, *JCP*, **134**, 184309, (2011)
- “Following Ultrafast Radiationless Relaxation Dynamics With Strong Field Dissociative Ionization: A Comparison Between Adenine, Uracil, and Cytosine”, M. Kotur, T. Weinacht, C. Zhou, and S. Matsika, *IEEE Journal of selected topics in Quantum Electronics*, accepted, (2011)
- “Combining dissociative ionization pump probe spectroscopy and *ab initio* calculations to explore excited state dynamics involving conical intersections”, S. Matsika, C. Zhou, M. Kotur and T. Weinacht, *Faraday Discussions*, accepted, (2011)
- “Nonadiabatic Events and Conical Intersections”, S. Matsika and P. Krause, *Annu. Rev. Phys. Chem.*, **62**, 621 - 643, (2011)

ABSTRACT

ELECTRON-DRIVEN PROCESSES IN POLYATOMIC MOLECULES

Investigator: Vincent McKoy

A. A. Noyes Laboratory of Chemical Physics

California Institute of Technology

Pasadena, California 91125

email: mckoy@caltech.edu

PROJECT DESCRIPTION

The focus of this project is the development, extension, and application of accurate, scalable methods for computational studies of low-energy electron–molecule collisions, with emphasis on larger polyatomics relevant to electron-driven chemistry in biological and materials-processing systems. Because the required calculations are highly numerically intensive, efficient use of large-scale parallel computers is essential, and the computer codes developed for the project are designed to run both on tightly-coupled parallel supercomputers and on workstation clusters.

HIGHLIGHTS

The past year has seen progress both on applications and code development. In the area of applications, we continue to collaborate with leading experimental groups and, where appropriate, other theoretical groups on problems of mutual interest. Code development is focused on expanding the capabilities of our electron-molecule collision software by allowing more flexibility in the choice of target wavefunctions, as well as improving performance by exploiting graphical processors (GPUs) to accelerate key steps of the calculations. Specific accomplishments include:

- A study of low-energy elastic electron collisions with isomers of butanol, which revealed intriguing correlations between the molecular structure and the angular pattern of scattering
- A joint experimental-computational study of elastic electron scattering by the pyrimidine molecule, a prototype for DNA nucleobases
- A joint experimental-computational study of intermediate-energy electron collisions with fullerene, C₆₀
- A joint experimental-computational study of electron collisions with diacetylene, a molecule of technological and astrophysical interest
- Initial applications of a fully parallelized version of our electron collision code to an open-shell system, the CF₃ radical

ACCOMPLISHMENTS

We pursued our interest in electron collisions relevant to ignition of biofuels with a study of elastic collision processes involving the four isomers of butanol, *n*-butanol, 2-butanol, isobutanol, and *t*-butanol [1]. Butanols, which can be synthesized through bacterial fermentation and which have combustion properties closer to those of gasoline, have attracted interest as possible “second-generation” alternatives to the lighter alcohol biofuels, methanol and ethanol. Basic data about collision processes involving butanols will be needed in any numerical models of their ignition and combustion chemistry. From a fundamental point of view, a study of isomers provides insight into how the arrangement of atoms within the target molecule influences the scattering behavior. Our calculations, carried out in collaboration with Prof. Márcio Bettega of the Federal University of Paraná (Brazil), revealed a striking difference between the angular scattering patterns of the straight-chain and branched-chain isomers within a particular range of collision energies, roughly 6 to 10 eV: the straight-chain butanols yield a mostly *f*-wave pattern, while the branched isomers show a *d*-wave pattern. Though the details are not yet clear, the difference appears to reflect the shapes of

virtual orbitals into which the projectile electron is briefly captured to form a shape resonance. Interestingly, similar trends have been seen in the alkanes, indicating that the OH group plays a limited role.

In the area of electron collisions relevant to DNA damage in living systems, we undertook a joint computational and experimental study of pyrimidine, the prototype molecule for the DNA bases thymine and cytosine as well as the RNA base uracil. The experiments, carried out by the groups of Profs. Stephen Buckman (Australian National University) and Michael Brunger (Flinders University), involved measurement of the differential elastic scattering cross section over a wide range of collision energies. Our calculated differential cross sections show generally excellent agreement with the measurements, particularly at the lower collision energies. This work is currently being prepared for publication.

In conjunction with experiments carried out by the group of Prof. Birgit Lohmann (University of Adelaide, Australia), we extended our earlier low-energy calculations of elastic electron cross sections for C_{60} up to collision energies of 500 eV [2]. Agreement between the calculated and measured differential cross sections was excellent at energies up to 200 eV. At higher energies, the calculated results fall off too slowly with increasing scattering angle but continue to reproduce well the maxima and minima in the experimental cross section. Comparison with an independent-atom model demonstrates that the observed maxima and minima, even at energies as low as 100 eV, are essentially diffractive in origin.

We studied elastic scattering of slow electrons by diacetylene, C_4H_2 , in collaboration with Prof. Michael Allan (University of Fribourg, Switzerland), who carried out corresponding measurements [3]. Our calculations show both of the expected $^2\Pi^*$ shape resonances, although the first ($^2\Pi_u$) is placed somewhat too low in energy, and also revealed a $^2\Sigma_u$ resonance at about 9 eV that has an unusual profile (a step down, rather than a peak, in the cross section). Interestingly, the calculations do not show the presence of the broad Σ resonance near 4 eV that was postulated on the basis of vibrational-excitation measurements [4]. Detailed comparison of the calculated and measured differential cross sections shows generally quite good agreement except in the vicinity of the $^2\Pi_u$ resonance.

Part of our code development effort has included removing the restriction to closed-shell singlet ground states originally built into our computer programs. Although most stable molecules do indeed have singlet ground states, there are prominent exceptions (e.g., O_2); more importantly, however, dissociation processes involve stretched bonds and radical products requiring multi-configurational and/or open-shell wavefunctions. As an initial application of the extended code, we have been studying collisions with the CF_3 radical, in support of an experimental effort at the Flinders University, where a novel apparatus is being used to measure electron cross sections for radical targets. Initial results have been obtained at the static-exchange level, and we will be incorporating polarization effects in future work.

PLANS FOR COMING YEAR

In applications, one major focus will be electronic excitation of water. As the main constituent of living tissue, water plays a fundamental role in the interaction of biosystems with radiation. In particular, the electron cross sections of water are critical to modeling electron transport, energy deposition, and the generation of reactive species. We are collaborating with the group of Prof. Murtadha Khakoo (California State University, Fullerton), where measurements of electron-impact excitation cross sections are being carried out. To date we have generated vibrational overlap envelopes to aid in the unfolding of overlapping energy-loss peaks and carried out pilot calculations of electronically inelastic cross sections. Over the coming year we will be carrying out much more extensive cross section calculations with a view to obtaining reliable differential and integral cross sections for several of the low-lying electronic states.

A second major focus will be coupling electron collision calculations more directly to dissociation chemistry through a study of dissociative attachment to a polyatomic system. Although our ultimate interest is dissociative attachment in biomolecules, we will first, as a prototype, look at a methyl halide such as CH_3Cl . By comparing the results of single-mode calculations, in which only the carbon-halogen bond distance is varied, with those of two- or multimode calculations that add the “umbrella” and perhaps the

C–H stretching modes, we hope to gain experience as well as insight into what is required to obtain reliable results. This work will be carried out in collaboration with Prof. Márcio Varella (University of São Paulo, Brazil) and coworkers, who have developed numerical methods for treating the nuclear dynamics.

We will also be continuing work on electron collisions with large biomolecules by studying elastic collision with selected amino acids. As the basic building blocks of proteins, amino acids are ubiquitous in living tissue, and their electron collision properties are consequently of interest in understanding radiation damage. Further, we have held initial discussions with Dr. Ali Belkacem (LBNL) to plan collaborative studies of dissociative electron attachment to the nucleobase uracil.

In code development, we will continue to improve the ability of the recently parallelized sections of our program system to deal with more flexible (multiconfigurational, open-shell) wavefunctions. We are also beginning a major effort to port key computational steps to graphical processing units (GPUs), which offer the potential of enormous gains in speed at very low cost. To this end we have acquired a new server system containing two nVIDIA Tesla GPU cards, to be used for code development and validation, and are just beginning to explore code redesign. Our initial focus will be on an integral-transformation step. In our current code, this involves the multiplication of large, dense matrices and is parallelized using a distributed-memory, message-passing model. We aim to add a second level of parallelization by using GPUs to carry out the multiplication of the local matrix blocks. Our next target will be GPU acceleration of the evaluation of two-electron integrals. These two kernels make up the great bulk of our scattering calculations.

REFERENCES

- [1] M. H. F. Bettgega, C. Winstead, and V. McKoy, *Phys. Rev. A* **82**, 062709 (2010).
- [2] L. R. Hargreaves, B. Lohmann, C. Winstead, and V. McKoy, *Phys. Rev. A* **82**, 062716 (2010).
- [3] M. Allan, C. Winstead, and V. McKoy, *Phys. Rev. A* **83**, 062703 (2011).
- [4] M. Allan, O. May, J. Fedor, B. C. Ibănescu, and L. Andric, *Phys. Rev. A* **83**, 052701 (2011).

PROJECT PUBLICATIONS AND PRESENTATIONS, 2009–2011

1. “Differential and Integral Cross Sections for Elastic Electron Scattering from CF₂,” J. R. Francis-Staite, T. M. Maddern, M. J. Brunger, S. J. Buckman, C. Winstead, V. McKoy, M. A. Bolorizadeh, and H. Cho, *Phys. Rev. A* **79**, 052705 (2009).
2. “Vibrational Excitation of Water by Electron Impact,” M. A. Khakoo, C. Winstead, and V. McKoy, *Phys. Rev. A* **79**, 052711 (2009).
3. “Low-Energy Electron Collisions with Biomolecules,” C. Winstead, Fortieth Annual Meeting the Division of Atomic, Molecular, and Optical Physics of the American Physical Society (DAMOP 2009), Charlottesville, Virginia, 20–23 May, 2009 (*invited talk*).
4. “Improved Nonlocal Resonance Model for Electron–HCl Collisions,” J. Fedor, P. Kolorenč, M. Čížek, J. Horáček, C. Winstead, and V. McKoy, XXVI International Conference on Photonic, Electronic, and Atomic Collisions, Kalamazoo, Michigan, 22–28 July, 2009.
5. “Elastic Electron Scattering by Ethyl Vinyl Ether,” M. A. Khakoo, L. Hong, B. Kim, C. Winstead, and V. McKoy, *Phys. Rev. A* **81**, 022720 (2010).
6. “Electron Scattering in HCl: An Improved Nonlocal Resonance Model,” J. Fedor, C. Winstead, V. McKoy, M. Čížek, K. Houfek, P. Kolorenč, and J. Horáček, *Phys. Rev. A* **81**, 042702 (2010).
7. “Low-Energy Electron Scattering from C₄H₉OH Isomers,” M. H. F. Bettgega, C. Winstead, and V. McKoy, *Phys. Rev. A* **82**, 062709 (2010).
8. “Elastic Scattering of Intermediate Energy Electrons from C₆₀ Molecules,” L. R. Hargreaves, B. Lohmann, C. Winstead, and V. McKoy, *Phys. Rev. A* **82**, 062716 (2010).

9. "Measurement and Calculation of Absolute Single and Multiple Charge Exchange Cross Sections for Fe^{q+} Ions Impacting H_2O ," J. Simcic, D. R. Schultz, R. J. Mawhorter, J. B. Greenwood, C. Winstead, B. V. McKoy, S. J. Smith, and A. Chutjian, *Ap. J.* **722**, 435 (2010).
10. "Absolute Angle-Differential Elastic Cross Sections for Electron Collisions with Diacetylene," M. Allan, C. Winstead, and V. McKoy, *Phys. Rev. A* **83**, 062703 (2011).
11. "Low-Energy Electron Interactions with Biomolecules," V. McKoy, Physics Department Seminar, Federal University of Amazonas, Manaus, Brazil, June 13, 2011.
12. "Low-Energy Electron Interactions with Biomolecules," C. Winstead, XXVII International Conference on Photonic, Electronic, and Atomic Collisions, Belfast, UK, July 27–August 2, 2011 (*invited talk*).
13. "Anomalously Large Low-Energy Elastic Cross Sections for Electron Scattering from the CF_3 Radical," J. R. Brunton, L. R. Hargreaves, M. J. Brunger, S. J. Buckman, G. Garcia, F. Blanco, O. Zatsarinny, K. Bartschat, C. Winstead, and V. McKoy, XXVII International Conference on Photonic, Electronic, and Atomic Collisions, Belfast, UK, July 27–August 2, 2011.
14. "Cross Sections for Electronic Excitation of Water by Low-Energy Electrons," L. R. Hargreaves, K. Ralphs, M. A. Khakoo, C. Winstead, and V. McKoy, XXVII International Conference on Photonic, Electronic, and Atomic Collisions, Belfast, UK, July 27–August 2, 2011.
15. "Electron and Positron Scattering from Pyrimidine," P. D. Palihawadana, J. R. Machacek, C. Makochekanwa, J. P. Sullivan, M. J. Brunger, C. Winstead, V. McKoy, G. Garcia, F. Blanco, S. J. Buckman, XXVII International Conference on Photonic, Electronic, and Atomic Collisions, Belfast, UK, July 27–August 2, 2011.
16. "Absolute Cross Sections for Electron Collisions with Diacetylene: Elastic Scattering, Vibrational Excitation and Dissociative Attachment," M. Allan, O. May, J. Fedor, B. C. Ibanescu, L. Andric, C. Winstead, and V. McKoy, XXVII International Conference on Photonic, Electronic, and Atomic Collisions, Belfast, UK, July 27–August 2, 2011.

ELECTRON/PHOTON INTERACTIONS WITH ATOMS/IONS

Alfred Z. Msezane (email: amsezane@cau.edu)

Clark Atlanta University, Department of Physics and CTSPS
Atlanta, Georgia 30314

PROGRAM SCOPE

The project's primary objective is to gain a fundamental understanding of the near-threshold electron attachment mechanism and determine accurate electron affinities (EAs). The elegant Mulholland formula, implemented within the complex angular momentum (CAM) description of scattering, wherein resonances are rigorously defined as singularities of the S-matrix, is used for the investigations [1]. Regge trajectories allow us to probe electron attachment at its most fundamental level near threshold, thereby uncovering new manifestations and possibilities as well as determine the reliable EAs of tenuously bound and complicated atomic and molecular systems [2]. To date calculating accurate EAs still ranks among the most challenging problems for theoretical atomic and molecular physics.

The development and application of the Random Phase Approximation with Exchange (RPAE) method to atoms (ions) with unfilled sub-shells continue. The theory has been extended also to open outer-shell and inner open-shell atoms (ions) and applied to photoionization, including of Ce^{3+} @ C_{82} [3]. Methods are developed for calculating the generalized oscillator strength, useful in probing the intricate nature of the valence- and open-shell as well as inner-shell electron transitions. Standard codes such as CIV3 of Hibbert and the Belfast R-matrix are used to generate sophisticated wave functions for investigating configuration interaction (CI) mixing and relativistic effects in atomic ions. The wave functions are also used to explore correlation effects in dipole and non-dipole studies.

SUMMARY OF RECENT ACCOMPLISHMENTS

A. Complex Angular Momentum Analysis of Low-Energy Electron Scattering by Complex Atoms

The mechanisms of electron-electron correlations and core-polarization interaction are crucial for the existence and stability of most negative ions. In our calculations of the cross sections using the Regge-pole methodology the vital electron-electron correlation effects are accounted for through the Mulholland formula. This formula converts the infinite discrete sum into a background integral plus the contribution from a few poles to the process under consideration. The important core-polarization interaction is incorporated through the well-investigated Thomas-Fermi type model potential [4]. The power of the method lies in that it extracts the binding energies (BEs) of tenuously bound and complex negative ions from the resonances in the near threshold elastic total cross sections (TCSs), requiring no *a priori* knowledge of the experimental or other theoretical data. The “*Novel Mechanism for Nanoscale Catalysis*” [5] is the most important accomplishment in this funding cycle of our research.

A.1 Multiple excited negative ion formation in slow electron collisions with Tm, Lu and Hf atoms

Recently, the formation of ground and excited negative ions through slow electron collisions with the lanthanide and Hf atoms has been investigated using the CAM method [2]. From the calculated elastic TCSs the EAs and the BEs of the excited anions were extracted. For Hf the obtained EA was 0.525 eV. In contrast, Pan and Beck [6] obtained an EA value of 0.114 eV using Relativistic configuration interaction calculations. Here we predict, using the CAM method, the formation of multiple excited negative ionic states in low-energy $0 \leq E \leq 1.0$ eV electron elastic scattering from Tm, Lu and Hf atoms. Their BEs are extracted from the calculated elastic total and differential cross sections [7]. Ramsauer-Townsend (R-T) minima and shape resonances are determined as well. We conclude that the recently calculated BE value of 0.114 eV for the Hf^- anion [6] actually corresponds to an excited state.

A.2 Slow electron collisions with Mn, Zn and Cd atoms: First prediction of stable negative ions

The appearance of a large peak in low energy electron-atom elastic scattering TCSs facilitates considerably the identification of the binding energies of negative ions, formed during the collision as resonances [8]. Both relativistic and non-relativistic calculations and coupled cluster and multireference methods [9], supported by general beliefs, concluded contrary to the measurement [8], that Mn, Zn and Cd do not form stable negative ions. The recent CAM method has been used to investigate the possible formation of stable negative ions through slow electron collisions with Mn, Zn and Cd atoms. From the imaginary parts of the CAM, we conclude that all these atoms form stable weakly bound anions as Regge resonances through slow electron collisions [10]. Binding energies, shape resonances and R-T minima have been obtained.

A.3 Low-energy electron scattering from atoms: Search for nanocatalysts

Manipulating the structure and the dynamics of metallic nanoparticles, attractive due to their optical, electronic and magnetic properties, including applications in catalysis, requires a fundamental understanding of the dynamic processes at the atomic level. The fundamental mechanism of catalysis at the atomic scale has already been proposed and demonstrated in the Au, Pd and Au-Pd catalysis of H_2O_2 through the scrutiny of low energy electron elastic TCSs [5]. The use of mixed precious metal catalysts can produce even higher activities compared to Au alone [11]. Here the Au TCSs are used as our benchmark for metal atom catalysts to identify nanoscale catalysts. Calculated, using the recent CAM methodology, electron elastic TCSs for Ag, Pt, Pd, Ru and Y atoms are presented as illustrations. It is concluded that these atoms are suitable candidates for nanocatalysts individually or in combinations [12]. It is now possible to systematically construct effective catalysts for various substances by putting together the catalysts Au, Ag, Pd, Pt, Ru and Y in various combinations [12]; Tl is another possible candidate.

A.4 Electron elastic cross sections for Ga, In and Tl atoms near threshold

Recently, Walter *et al.* [13] measured the EA of In to be 383.92(6) meV. The value compared very well with theoretical EAs but differed substantially from a previous measurement. For the Tl atom the calculated and measured EAs differ significantly, while for Ga theory and experiment agree reasonably well. Here we have investigated near-threshold electron scattering from In, Ga and Tl to understand the discrepancy between the various calculations and measurements. Also, we identify and delineate the resonance structures in the TCSs. From the characteristic dramatic resonances in the TCSs, we extract the EAs for these atoms and compare our values with the available data. A dramatically sharp resonance at 0.380 eV in our calculated elastic TCS for In corresponds to the negative ion formed during the collision and defines the EA of In, in excellent agreement with the measurement [13] and the calculation [14]. The TCS curve also exhibits a R-T minimum and a shape resonance. For Tl the EA value of 0.27 eV [14] compares excellently with our calculated BE of 0.281 eV. However, since our EA for Tl is 2.41 eV, we conclude that the 0.27eV [14] corresponds to the BE of an excited Tl^- anion and not to its EA.

B.1 Confinement Resonances in Photoionization of $Xe@C_{60}$ and $Xe^+@C_{60}$

Recently the photoionization of $Xe@C_{60}$ [15] and $Xe^+@C_{60}$ [16] have been measured in the energy region of the Xe 4d Giant resonance. The experiment [15] confirmed the predicted significant distortion of the Giant resonance by the C_{60} shell. Here the photoionization of both the $Xe@C_{60}$ and $Xe^+@C_{60}$ have been investigated using our recently developed C_{60} model potential [3] and the RPAE method for the former and the open-shell RPAE method for the latter. The calculation included all the intershell couplings among the transitions 4d- ϵ_f , 5s- ϵ_p , 5p- ϵ_s and 5p- ϵ_d . The results demonstrate significantly stronger correlated confinement resonances in the photoionization of $Xe@C_{60}$ and $Xe^+@C_{60}$. Also, our results yield better agreement with the measurements for $Xe@C_{60}$ [15] and for $Xe^+@C_{60}$ [16] and demonstrate strong intershell coupling between the 4d- ϵ_f and 5s- ϵ_p transitions.

B.2 Many-body Bethe- Salpeter equation and RPA investigation of $Ce@C_{82}$ endohedral fullerene

The geometry optimized Ce@C₈₂ endohedral fullerene, using the DMol3 software for all 550 electrons, has been investigated using various theoretical approaches. The charge distribution was calculated by Mulliken's equation, revealing that the Ce atom donates only 1.11 electrons to the cage. The band gap was evaluated using the GW approximation and compared with measurement; the obtained gap of 0.29 eV agrees well with the measured value of 0.33 eV. The amplitudes of the optical excitation have been calculated using the Bethe-Salpeter equation (BSE) and the RPA, GW-RPA and GW-BSE. The calculated peaks using the GW-BSE at 1.22 eV and 1.97 eV agree excellently with the measured ones [17], while the broad peak at 2.42-2.63 eV also matches with the measured peak.

C.1 Baryon asymmetry resulting from a quantum phase transition in the early universe

A novel mechanism for explaining the matter-antimatter asymmetry of the universe is considered. We assume that the universe starts from completely symmetric state and then, as it cools down, it undergoes a quantum-phase transition which in turn causes an asymmetry between matter and antimatter. The mechanism does not require the baryon-number-violating interactions or CP violation at a microscopic level. Our analysis of the matter-antimatter asymmetry is in the context of conspicuous experimental results obtained in the condensed-matter physics [18].

D.1 Fine-structure energy levels, oscillator strengths and lifetimes in Cu XVI

We have performed large-scale calculations of excitation energies from ground state for 69 fine-structure levels, oscillator strengths and radiative decay rates for all electric-dipole-allowed and intercombination transitions among the fine-structure levels belonging to the terms of $(1s^2 2s^2 2p^6 3s^2 3p^2, 3s3p^3, 3p^4, 3s^2 3p3d, 3s^2 3p4s, 3s^2 3p4p, 3s^2 3p4d, \text{ and } 3s^2 3p4f)$ configurations of Cu XVI [19]. Extensive CI wave functions obtained with the CIV3 code of Hibbert represent these states. The important relativistic effects in intermediate coupling are incorporated through the Breit-Pauli Hamiltonian. Small adjustments to the diagonal elements of the Hamiltonian matrices have been made so that the energy splittings are as close as possible to the NIST energy values. The mixing among several fine-structure levels is found to be very strong. We have also calculated radiative lifetimes of the fine-structure levels, obtaining excellent agreement with the experimental value [20] for the high spin level $3s3p^3(^5S_2)$. We also predict new data for several fine-structure levels where no experimental or other theoretical data are available.

FUTURE PLANS

We continue with the theoretical investigations of low-energy electron scattering from atoms/molecules and photoionization of endohedral fullerenes as delineated above. New accurate EAs for complex atoms will be obtained and nanocatalysts will be investigated and identified as well. Our recent CAM method will be employed as well as extended to investigate Feshbach resonances.

REFERENCES AND SOME PUBLICATIONS ACKNOWLEDGING GRANT

1. D. Sokolovski *et al*, Phys. Rev. A **76**, 012705 (2007).
2. "Complex angular momentum analysis of low-energy electron elastic scattering from lanthanide atoms", Z. Felfli, A.Z. Msezane and D. Sokolovski, Phys. Rev. A **81**, 042707 (2010).
3. "Photoionization of Ce³⁺@C₈₂", Zhifan Chen, R.A Phaneuf and A.Z. Msezane, J. Phys. B **43**, 215203 (2010)
4. "On Regge-pole trajectories for a rational function approximation of Thomas-Fermi potentials", S. Belov, K.-E. Thylwe, M. Marletta, A. Z. Msezane and S. Naboko, J. Phys. A **43**, 365301 (2010)
5. "Novel mechanism for nanoscale catalysis", A. Z. Msezane, Z. Felfli and D. Sokolovski, J. Phys. B **43**, 201001 (2010) (FAST TRACK); "Cold Fusion Mechanism in Nanoscale Catalysis?", *Europhysics.News* **41**, 11 (2010)
6. L. Pan and D.R. Beck, J. Phys. B **43**, 025002 (2010)
7. "Low-energy electron elastic collision cross sections for ground and excited Tm, Lu and Hf atoms", Z. Felfli, A.Z. Msezane and D. Sokolovski, *NIMB* **269** 1046-1052 (2011)

8. P. D. Burrow *et al*, J. Phys. B. **9**, 3225 (1976)
9. Z. J. Wu *et al*, Chem. Phys. Lett. **423**, 81 (2006); N.B. Balabanov *et al*, J. Chem. Phys. **125**,074110 (2006); ----**123**, 064107 (2005)
10. "Low-energy electron elastic scattering from Mn, Cu, Zn, Ni, Ag and Cd atoms", Z. Felfli, A.Z. Msezane and D. Sokolovski, Phys. Rev. A **83**, 052705 (2011)
11. D. T. Thompson, Nano Today **2**, 40 (2007).
12. "Elastic scattering of slow electrons from Y, Ru, Pd, Ag and Pt atoms: Search for nanocatalysts", Z. Felfli, A.Z. Msezane and D. Sokolovski, J. Phys. B **44**, 135204 (2011)
13. C.W. Walter *et al*, Phys. Rev. A **82**, 032507 (2010)
14. W.P. Wijesundera, Phys. Rev. A **55**, 1785 (1997).
15. A. L. D. Kilcoyne *et al*, Phys. Rev. Lett. **105**, 213001 (2010)
16. Yoh Itoh *et al*, J. Phys. B **34**, 3493 (2001)
17. "Electronic and Optical Properties of the Ce@C₈₂ Molecule", Zhifan Chen and A. Z. Msezane, The J. Phys. Chem., Submitted (2011)
18. "Baryon asymmetry resulting from a quantum phase transition in the early universe", V. R. Shaginyan, G. S. Japaridze, M. Ya. Amusia, A. Z. Msezane and K. G. Popov, Europhys. Lett. **94**, 69001 (2011)
19. "Fine-structure energy levels, oscillator strengths and lifetimes in Cu XVI", G. P. Gupta and A. Z. Msezane, Phys. Scr. **83**, 055301 (2011)
20. E. Trabert *et al*, J. Opt. Soc. Am. B **5**, 2173 (1988)

Additional Publications 2009-2011

1. "Low-Energy Electron Elastic Scattering from Complex Atoms: Nd, Eu and Tm", Z. Felfli, A.Z. Msezane and D. Sokolovski, Can. J. Phys. **87**, 321 (2009)
2. "Resonances in Low-Energy Electron Elastic Cross Sections for Lanthanide Atoms", Z. Felfli, A.Z. Msezane and D. Sokolovski, Phys. Rev. A **79**, 012714 (2009)
3. "Energy Scales and Magnetoresistance at a Quantum Critical Point", V.R. Shaginyan, M. Ya. Amusia, A.Z. Msezane, K.G. Popov and V.A. Stephanovich, Physics Letters A **373**, 986 (2009)
4. "[Ti II] lines observed in η Carinae Sr-filament and lifetimes of the metastable states of Ti⁺⁺", N. C. Deb, A. H. Hibbert, Z. Felfli and A. Z. Msezane, J. Phys. B **42**, 015701 (2009)
5. "Fast charged-particle impact ionization of endohedral atoms: e + He@C₆₀", A. S. Baltenkov, V. K. Dolmatov, S. T. Manson, and A. Z. Msezane, Phys. Rev. A **79**, 043201 (2009)
6. "Large scale CIV3 calculations of fine-structure energy levels and radiative rates in Al-like Copper", G. P. Gupta and A. Z. Msezane, Can. J. Phys. **87**, 895 (2009)
7. "Differential Cross Sections for Low-Energy Electron Elastic Scattering by Lanthanide Atoms: La, Ce, Pr, Nd, Eu, Gd, Dy and Tm", Z. Felfli, A.Z. Msezane and D. Sokolovski, Phys. Rev. A **79**, 062709 (2009)
8. "Photoionization of Ce³⁺ and Ce³⁺@C₆₀", Z. Chen and A. Z. Msezane, J. Phys. B **42**, 165206 (2009).
9. "Photoionization of the I⁺ Ion", Zhifan Chen and Alfred Z. Msezane, J. Phys. B **42**, 165203 (2009).
10. "Magnetic-Field-induced Reentrance of Fermi-Liquid Behavior and Spin-Lattice Relaxation Rates in YbCu_{5-x}Au_x", V.R. Shaginyan, A.Z. Msezane, K.G. Popov and V.A. Stephanovich, Phys. Letters A **373**, 3783 (2009)
11. "Fine-structure energy levels, oscillator strengths and lifetimes in Al-like Vanadium", G. P. Gupta and A. Z. Msezane, Phys. Scripta **81**, 045302 (2010).
12. "Low-energy electron elastic scattering cross sections for excited Au and Pt atoms", Z. Felfli, A. R. Eure*, A. Z. Msezane and D. Sokolovski, NIMB **268**, 1370 (2010)
13. "Effects of the fullerene (C₆₀) potential and position of the atom (A) on spectral characteristics of endohedral atoms A@C₆₀", A.S. Baltenkov, U. Becker, S. T. Manson and A. Z. Msezane, J. Phys. B **43**, 115102(2010)
14. "Scaling Behavior of Heavy Fermion Metals", V.R. Shaginyan, M.Ya. Amusia, A.Z. Msezane, K.G. Popov, Physics Reports **492**, 31-109 (2010)
15. "Density Functional Theory Investigation of Small Pt Clusters", Z. Chen and A. Z. Msezane, Fourth International Conference on Neural, Parallel and Scientific Computing, Eds. G.S. Ladde *et al*. (Dynamic Publishers, Inc., Atlanta, 2010), p. 104
16. "Nondipole Parameters of TDCS for Electron Impact Ionization and Drag Current", A.K. Baltenkov, S.T. Manson and A.Z. Msezane, Central European Journal of Physics, At Press (2011)

Theory and Simulations of Nonlinear X-ray Spectroscopy of Molecules

Shaul Mukamel

University of California, Irvine, CA 92697

Progress Report 2010, August 1, 2010

DOE DE-FG02-04ER15571

Program Scope

Theoretical and computational techniques are developed to describe coherent resonant nonlinear ultrafast x-ray spectroscopies in molecules, capable of probing the electronic and nuclear dynamics of molecules in the condensed phase with sub-femtosecond time and atomic spatial resolution. These techniques, which employ sequences of attosecond soft and hard x-ray pulses, will provide novel windows into the valence electronic structure and chemical dynamics with much higher resolution in space and time than possible in the visible regime. Electron wavepackets created by attosecond pulses generate coherent signals that may be described by extending concepts used for vibrational wavepackets in the femtosecond regime. Possible pulse sequences are analyzed and classified by their information content. Multidimensional signals obtained by creating multiple core excited states for controlled time periods will provide critical tests for electronic structure theory of molecules and highly correlated materials. Many-body coherence effects that may not be described by the charge density alone will be investigated. Green's function techniques are developed and applied for computing stimulated x-ray Raman techniques. These time-domain analogues of resonant inelastic x-ray scattering (RIXS) allow to control the excitation and observation windows by the pulse envelopes. Multidimensional time-resolved photoelectron signals are predicted. The creation and manipulation of entanglement of electrons and holes by attosecond pulses is investigated and schemes for controlling the pathways in matter by exploiting quantum properties of the x-ray fields are studied. Applications are made to amino acids, DNA bases, porphyrin arrays, and hydrogen bonding fluctuations in proteins.

Recent Progress

Simulation and visualization of attosecond stimulated x-ray Raman spectroscopy signals in trans-N-methylacetamide at the nitrogen and oxygen K-edges

The stimulated x-ray Raman spectroscopy (SXRS) signal of *trans*-N-methylacetamide (NMA), a small organic molecule used as a convenient model system for the peptide bond forming the backbones of proteins, was calculated using a higher level description of core excitations, the static-exchange (STEX) approximation, which offers a much improved description of orbital relaxation effects and of the virtual orbitals to which the core electrons are excited than the equivalent-core approximation (ECA) used earlier. The signal obtained in response to two soft x-ray pulses, reveals the dynamics of valence-electron wave packets prepared and detected in the vicinity of a selected atom (either nitrogen or oxygen).

Closed-time-path loop diagrams were developed for interpreting this signal. Orbital relaxation effects following core electronic excitations were studied by comparing the N and O K-edge x-ray absorption near-edge structure (XANES) at the ECA and STEX levels. Simulations of the stimulated Raman signals for the N1s pump/N1s probe and N1s pump/O1s probe pulse configurations are presented in Fig. 2. The evolving electronic charge densities, consisting of several entangled valence particle-hole pairs, as well as the electronic coherence of the doorway and the window created by the two pulses were visualized using a time-dependent basis set of natural orbitals. This picture goes beyond the time-resolved charge density of electron diffraction, and carries valuable many-body information about electron correlation as well.

NMA(trans): Nitrogen K-edge XANES

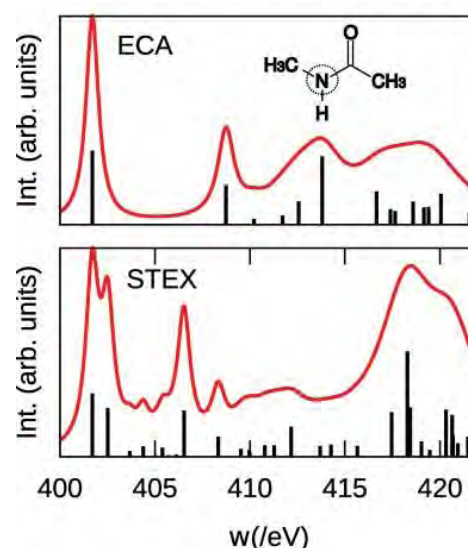


Figure 1: XANES N Kedge spectra of NMA computed at the ECA and STEX levels. STEX reveals additional low-energy peaks adjacent to the core edge in both figures, reflecting the relaxation effect of the occupied orbitals and its improved description of the virtual orbitals.

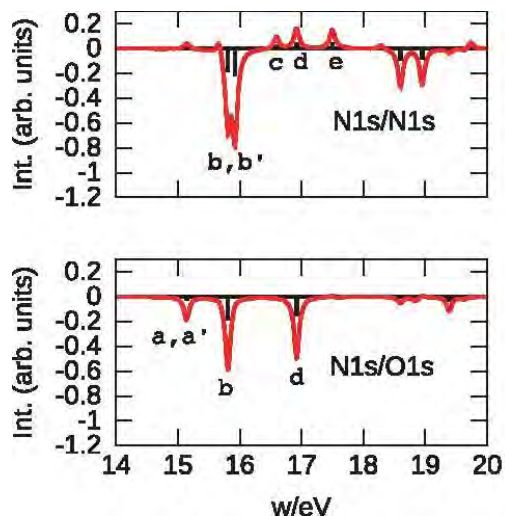


Figure 2: Stimulated Raman spectra of NMA for the N1s/N1s and N1s/O1s pump/probe pulse configurations.

The attosecond snapshots of electron dynamics provided by resonant x-ray techniques call for developing real time/real space visualization schemes. This visualization is not directly obtained from experimental data but is derived from simulations and should help the interpretation of experiments. Many-electron wavefunctions live in a high dimensional space which is impossible to visualize, we are developing techniques for display properties of these states in real space. These visualizations should help clarify the interpretation of X-ray experiments. We adopt an approximate electronic structure theory in which the reduced doorway-window representation carries the same information as the full many-electron wave packets of the signal, by assuming that only single-particle excitations dominate the signal. Valence excitations are efficiently visualized in terms of a few electron-hole pairs represented by natural orbitals. We have dissected the signal into individual doorway natural orbital contributions as shown in Fig. 3.

Multidimensional attosecond photoelectron spectroscopy with shaped pulses and quantum optical fields

Photoelectron spectroscopy is a powerful tool for probing orbital energies in molecules and crystals. In time resolved photoelectron spectroscopy (TRPES) the system is prepared in a nonequilibrium state by a laser pulse, evolves for a delay time t and is eventually probed by detecting the electrons generated by a second, ionizing, pulse. The distribution of the electron kinetic energy (ε) reveals underlying electronic and vibrational dynamics through a parametric dependence on the time delay. Multidimensional TRPES signals induced by a series of temporally-well separated pump pulses with variable delays followed by a final ionizing detection pulse were predicted and calculated. The technique was extended to attosecond electron dynamics. Here the pump ionizes the molecule to create one or several holes (core or valence type). The hole migration can then be probed by a second pulse and detected by either the generated photoelectrons or by directly looking at its absorption. Hole motion is very slow and negligible for deep core states and becomes faster for more shallow holes. Photoelectron signals induced by entangled optical or x-ray photons were predicted. Parameters of the photon wavefunction provide a new class of control knobs for multidimensional spectroscopy. The manipulation of multidimensional x-ray response by coherent control pulse shaping algorithms was explored.

We have calculated the photoelectron signal induced by a series of pump pulses with variable delays, followed by a final ionizing detection pulse. Correlation function expressions for multidimensional photoelectron signals obtained for the response of electrons and nuclei in molecules to multiple ultrafast optical or x-ray pulses are derived using a superoperator formalism. Multidimensional optical signals where fields are detected (e.g., wave mixing) are usually calculated in terms of nonlinear response function and susceptibilities. Photon counting measurements, on the other hand, are best described by sequences of transition amplitudes (generalized Fermi golden rule) using the celebrated formalism of Glauber. The connection of the two approaches was clarified. Since electron detection is more closely connected to photon counting, we recast these signals in terms of transition amplitudes, which are more intuitive and easier to calculate than susceptibilities.

The effective spectral and temporal resolution in multiple pulse experiments with shaped and chirped pulses was analyzed using Wigner spectrograms and used to describe recent stimulated Raman experiments in the visible regime. Collective two-particle resonances induced by photon entanglement were predicted. An assembly of non-interacting atoms may become correlated upon interaction with entangled photons, and certain elements of their joint density matrix can then show collective resonances. We explored experimental signatures of these resonances in the nonlinear response of a pair of two-level atoms. We found that these resonances are canceled out in stimulated signals such as pump-probe and two-photon absorption due to the destructive interference of two-photon-absorption and emission pathways in the joint two-particle space. However, they may be observed in photon statistics (Hanbury-Brown–Twiss) measurements through the attenuation of two-time intensity correlations.

Future Plans

Boson Representations of Electronic Relaxation and Dephasing in Attosecond Spectroscopy

Laser pulses shorter than typical molecular vibrational periods developed in the 1980s made it possible to excite vibrations impulsively and observe wavepackets in real time. Attosecond x-ray pulses are shorter than inverse valence electron transition frequencies and can similarly excite wavepackets of valence electrons impulsively, and observe motions of electrons in real space and time. We have used the formal analogy between vibrational and electronic wavepackets to design the CXRS technique. This analogy will be further extended to new computational schemes for ultrafast resonant x-ray techniques. Quasiboson oscillator representations of electronic excitations are widely used in many-body physics to describe elementary excitations in semiconductors and metals. Bosonization schemes can treat excitons as independent oscillators. X-ray absorption and photoelectron spectra in solids have been described phenomenologically using a quasiboson representation, the Bosons are obtained by fitting the computed or experimental dielectric functions. We will construct effective Boson oscillator Hamiltonians for x-ray transitions in molecules using parameters derived from ab-initio electronic structure codes. New expressions for nonlinear x-ray signals will be developed, building upon the analogy between attosecond electronic and femtosecond vibrational wavepackets. We will use this formalism to interpret spectra in terms of a few parameters as is commonly done in vibrational spectroscopy and identify the mechanism for pure dephasing of core transitions which controls the relative intensities and shapes of Raman vs. fluorescence signals.

Applications will be made to porphyrin aggregates and porphyrin containing proteins. The signal from pairs of linked porphyrins should contain signatures of energy and charge transfer between the metal centers. Electronic currents lasting for a few picoseconds can be induced in porphyrins by circularly polarized lasers. Possibilities for probing these currents by x-ray spectroscopy will be explored. Double quantum coherence spectroscopy on porphyrin arrays with different metals should give information on interactions between separate core-holes mediated by conjugated links.

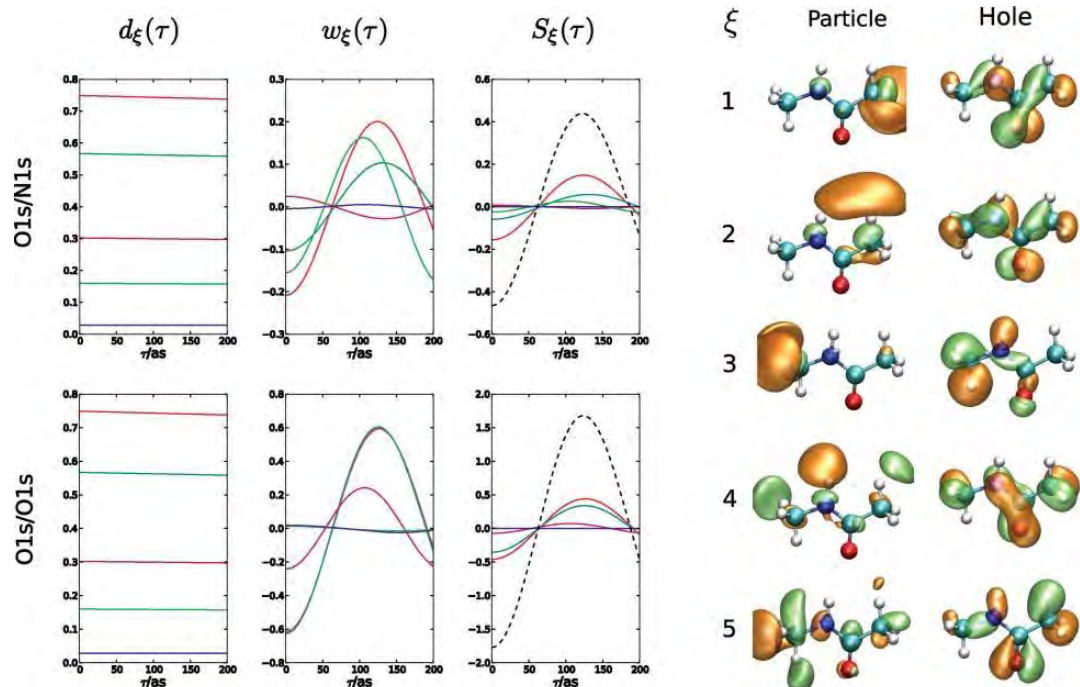


Figure 3: Time-dependent SXRS signal for NMA for a pump tuned to the oxygen K-edge, decomposed into contributions from: (first col) the time-dependent doorway weight for each natural orbital, (second col) the projection of the window operator onto each doorway natural orbital, and (third col) the contribution to the signal for each product: $S\xi = 2\text{Re } d\xi(\tau)w\xi(\tau)$. The dashed black line is the total signal $Stot(\tau) = S\xi(\tau)$. (Right) Nitrogen 1s doorway operator natural orbitals ξ at $\tau = 0$

Time-resolved Strong Field Photoelectron Spectroscopy

Much current research into many-body excited states revolves around effective mean-field approaches to the electronic response, by replacing the full interacting wavefunction with a single-particle effective field in which the interaction of other particles is treated like a bath. Similar approaches effectively describe the ground electronic state, and have been applied to excited states through the time-dependent Hartree-Fock(TDHF) and density functional theory(TDDFT) methods. Most assume weak oscillations in the charge density, so the Fock matrix around the ground state density matrix can be expanded order-by order. We propose an experiment in which a material system evolves under the influence of a strong pulse, whose time-resolved, one-electron density of states is probed by scanning an impulsive, ionizing, hard x-ray pulse through a delay relative to the center of the strong pulse envelope. The signal should contain direct information about the one-particle potential, through the peak positions, and the density matrix in this basis, through their amplitudes. This experiment will be simulated using real-time propagation of the single-particle density matrix, and use it to providing measurable tests for different functionals and memory functions in TDDFT and TDHF. Spectra may be simplified and the resolution improved by optimizing the temporal profiles of the pulses.

Publications Resulting from the Project

- P1. "Interplay of Slow Bath Fluctuations & Energy Transfer in 2D Spectroscopy of the FMO Light-Harvesting Complex Benchmarking of simulation protocols", B. Palmieri, D. Abramavicius and S. Mukamel, Phys. Chem. Chem. Phys. 12, 108-114 (2010).
- P2. "Two-Quantum Many-body Coherences in Two-Dimensional Fourier-Transform Spectra of Exciton Resonances in Semiconductor Quantum Wells", D. Karauskaj, A.D. Bristow, L. Yang, X. Dai, R.P. Mirin, S. Mukamel and S.T. Cundiff, Phys. Rev. Lett, 104, 117401 (2010).
- P3. "Stimulated Coherent Anti-Stokes Raman Spectroscopy (CARS) Resonances Originate from: Double-slit Interference of Two-photon Stokes Pathways" S.Rahav and S. Mukamel, PNAS 107, 4825-4829 (2010).
- P4. "Probing Many-Particle Correlations in Semiconductors Quantum Wells Using Double-Coherence Signals", L. Yang and S. Mukamel, Proc. of SPIE, 76001G (2010).
- P5. "Ultrafast Nonlinear Optical Signals Viewed from the Molecules Perspective; Kramers-Heisenberg Transition Amplitudes vs. Susceptibilities", S. Rahav and S. Mukamel, Advances in Atomic Molecular and Optical Physics, Vol. 59, Pages 223-263 (2010).
- P6. "Manipulating Quantum Entanglement of Quasiparticles in Many Electron Systems by Attosecond X-ray Pulses", S. Mukamel and H. Wang, Phys. Rev. A. 81, 062334(2010).
- P7. "Population and Coherence Transfer Signals Induced by 3-Exciton Correlation in the Nonlinear Optical Response of Photosynthetic Complexes", L. Yang, D.Abramavicius and S. Mukamel, New J. Phys., In Press (2010).
- P8. "Simulation of Attosecond Coherent Resonant Raman X-ray Spectroscopy of the Nitrogen & Oxygen K-Edges in Glycine", H. Wang and S. Mukamel, Phys. Rev. A. (Submitted, 2009).
- P9. "Spontaneous and Stimulated Coherent and Incoherent Nonlinear wave-mixing and Hyper-Raleigh Scattering", O. Roslyak and S. Mukamel, Lectures of virtual university on lasers, Max Born Institute, Berlin, Germany, <http://mitr.p.lodz.pl/evu/> European Virtual University Lecture Notes (2010).
- P10. "Multidimensional Attosecond Photoelectron Spectroscopy with Shaped Pulses and Quantum Optical Fields", S. Rahav and S. Mukamel, Phys. Rev. A.81, 063810 (2010).
- P11 "Effective Temporal Resolution in Pump-Probe Spectroscopy with Strongly Chirped Pulses", D. Polli, D. Brida, S. Mukamel, G. Lanzani and G. Cerullo, Phys. Rev. A, 82, 053809 (2010).
- P12 "Simulation and Visualization of Attosecond Stimulated X-ray Raman Spectroscopy(SXRS) Signals in trans-NMA at the Nitrogen & Oxygen K-Edges ", D. Healion, H. Wang and S. Mukamel, J. Chem. Phys. 134, 124101 (2011).
- P13 "Two-Photon Coincidence Fluorescence Spectra of Cavity Multi-Polaritons; Novel Signatures of Carrier Multiplication", O. Roslyak, G. Gumbs, G. Godfrey and S. Mukamel, Nanoletters, 10, 4253-4259 (2010).
- P14 "Multidimensional phase-sensitive Single-Molecule Spectroscopy with Time-and-Frequency-Gated Fluorescence Detection", S. Mukamel and M. Richter, Phys. Rev. A, 83,013815 (2011).
- P15 "Quantum Field, Interference, and Entanglement Effects in Nonlinear Optical Spectroscopy", S. Mukamel and Y. Nagata, Procedia. Chem. (In press, 2011).
- P16 "Collective Two-Particle Resonances Induced by Photon Entanglement", M. Richter, S. Mukamel, Phys.Rev. A. 83, 063805(2011).
- P17 "Exciton Dynamics in Chromophone Aggregates with Correlated Environment Fluctuations", D. Abramavicius, S. Mukamel, J. Chem. Phys.134, 174504(2011).
- P18 "Signatures of Carrier Multiplication in the Frequency Resolved Fluorescence Spectra from Polaritons", O. Roslyak, G. Gumbs, S. Mukamel, J. Modern Optics, 57, 2009-2019 (2010).
- P20 "Communication: Comment on the Effective Temporal and Spectral Resolution of Impulsive Stimulated Raman Signals". J. Biggs and S. Mukamel. J. Chem. Phys. 134, 161101 (2011).

Nonlinear Photoacoustic Spectroscopies Probed by Ultrafast EUV Light

Keith A. Nelson
Department of Chemistry
Massachusetts Institute of Technology
Cambridge, MA 02139
Email: kanelson@mit.edu

Henry C. Kapteyn, Margaret M. Murnane
JILA
University of Colorado and National Institutes of Technology
Boulder, CO 80309
E-mail: kapteyn@jila.colorado.edu, murnane@jila.colorado.edu

Program Scope

This project is aimed at direct spectroscopic characterization of phenomena that occur on mesoscopic (nanometer) length scales and ultrafast time scales in condensed matter, including non-diffusive thermal transport and the high-wavevector acoustic phonon propagation that mediates it, complex structural relaxation and the density and shear dynamics that mediate it, and nanostructure thermoelastic responses. A primary effort in the project is directed toward nonlinear time-resolved spectroscopy with coherent soft x-ray, or extreme ultraviolet (EUV), wavelengths. Time-resolved transient grating (TG) measurements are conducted in order to directly define an experimental length scale as the interference fringe spacing Λ (or wavevector magnitude $q = 2\pi/\Lambda$) formed by two crossed excitation pulses or by a fabricated spatially periodic pattern that is irradiated by a single excitation pulse. The dynamics of material responses at the selected wavevector, including thermoelastically induced surface acoustic waves and thermal diffusion or non-diffusive thermal transport, are recorded through time-resolved measurement of coherent scattering, i.e. diffraction, of variably delayed probe pulses from the transient grating pattern. Progress in high harmonic generation has yielded femtosecond EUV pulses with sufficient energy and focusability for use in TG experiments. EUV probe pulses provide far greater sensitivity than optical pulses to surface acoustic and thermal responses, since the surface modulations change the EUV phase by far more than the optical phase and thereby yield far higher EUV diffraction efficiencies. Crossed EUV excitation pulses will produce interference fringe spacings of tens of nanometers, far smaller than is possible with crossed optical pulses, providing access to mesoscopic length scales, very high acoustic frequencies, and non-ballistic thermal transport.

In complementary measurements, the frequency rather than the wavevector of an acoustic response is specified by using a sequence of femtosecond excitation pulses at a specified repetition rate, with each pulse thermoelastically driving a single acoustic cycle. In this case the acoustic wave propagates through the sample rather than along the surface, and detection is carried out at the opposite sample surface, i.e. multiple-pulsed excitation is at the front and detection is at the back of the sample. This approach provides access to high-frequency bulk acoustic waves, while the EUV measurements are used to examine surface acoustic waves. Bulk longitudinal and transverse waves can be excited and monitored. GHz-frequency shear waves can be observed in viscous fluids whose structural relaxation dynamics occur on nanosecond or slower timescales, permitting study of supercooled liquids and the liquid-glass transition.

Recent Progress

Nanoscale thermal transport: Understanding energy flow in nanostructures is very challenging because the basic models describing ballistic and quasi-ballistic transport are still under development, and more sophisticated simulations remain difficult to verify. Thermal energy is carried by phonons that travel ballistically away from a nanoscale heat source for a significant distance before experiencing collisions, leading to a non-local (i.e. non-diffusive) thermal energy distribution. In past work, we used ultrafast

coherent high harmonic (HHG) beams to directly measure the ballistic contribution to the transport of thermal energy from a 1D nanoscale heat source into its surroundings [1-3]. Despite considerable theoretical discussions and direct application to thermal management in nanoelectronics, nano-enabled energy systems, and nanomedicine, this non-Fourier heat dissipation had not been experimentally observed to date. We found a significant (as much as 3 times) decrease in energy transport away from the nanoscale heat source compared with Fourier law predictions. This work solved a controversy in the field, because two different theories were proposed, but only one agreed with our measurements.

In more recent experiments [4], we explored heat flow from 2D nickel squares-on-sapphire. Intuitively, 2D confinement of metal squares is stronger than for 1D wires of comparable size, that might lead to stronger ballistic effects. We also expect that ballistic effects would show up for larger dimensions in 2D. We can observe this experimentally - a simple comparison of 1D and 2D dynamic signals is shown for large (350nm) and small (80nm) nanostructures. On short time and length scales (80nm, <500ps), where the interface thermal transport dominates the signal, thermal decay in 2D (red curve) is much slower than that in 1D (blue curve), corresponding to a stronger ballistic effect for the 2D geometry. On longer timescales, where thermal dissipation in the substrate dominates the signal, thermal decay is identical for 1D and 2D, verifying that the sample substrate properties determine the heat flow. A three-dimensional thermal transport model is needed to understand thermal transport from an array of 2D metallic squares into the bulk substrate, and a finite element simulation framework is under development to fully understand our results.

Nanoscale high-frequency surface acoustic waves: We also extended ultrahigh frequency measurements of surface acoustic wave (SAW) propagation and dispersion studies from 1D [5, 6] to 2D nanostructured systems: Ni nanodots on sapphire, and multilayer nanostructures on silicon. The nanoscale periodicity of the 2D samples enabled us to excite surface acoustic waves with the shortest wavelength explored to date (35nm), corresponding to a penetration depth as low as 6 nm. Similar to 1D, the 2D samples have a slower SAW speed in the metal nanostructure than in the substrate. Therefore the nanostructure will slow down the SAW propagation. The effect is enhanced for shorter oscillation wavelengths, due to the stronger SAW confinement at the nanostructure/substrate interface. A deviation from the free substrate's SAW velocity is observed in the dispersion map over the entire range of grating sizes. We were also able to observe higher-order surface acoustic oscillations, especially in the 2D Ni-on-sapphire samples, which show even greater deviation compared to the fundamental SAW, due to their shorter wavelength and stronger surface confinement at the same wavenumber [7]. This method is suitable for characterizing mechanical and thermal properties of sub-10 nm films and interfaces.

Nanoscale high-frequency bulk acoustic waves: Compressional and shear acoustics

We have reported previously the first measurements of shear acoustic waves up to 50 GHz frequency in liquids [8-10]. These were generated through femtosecond optical pulse irradiation of thin metallic

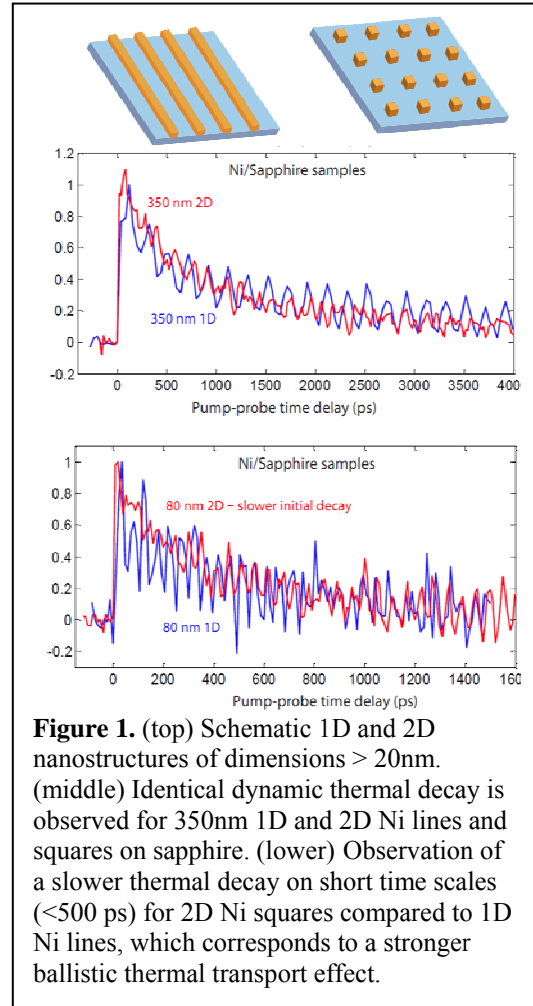


Figure 1. (top) Schematic 1D and 2D nanostructures of dimensions > 20nm. (middle) Identical dynamic thermal decay is observed for 350nm 1D and 2D Ni lines and squares on sapphire. (lower) Observation of a slower thermal decay on short time scales (<500 ps) for 2D Ni squares compared to 1D Ni lines, which corresponds to a stronger ballistic thermal transport effect.

crystalline films whose crystallographic axes were canted relative to the in-plane and through-plane directions so that the thermoelastic response upon sudden heating included a shear component that was transferred to the adjacent liquid medium. The shear waves were detected both in the liquid and after propagation into an adjacent solid substrate through coherent depolarized Brillouin scattering of optical probe pulses. Several papers are in advanced stages of preparation or recently published including descriptions of the shear wave excitation and detection mechanisms and of the results of shear and compressional wave measurements in silica and two supercooled liquids at variable temperatures [11-14].

A strong effort is under way to advance our capabilities for generation and detection of GHz-frequency shear and longitudinal waves and to reach higher acoustic frequencies extending into the THz range (with wavelengths well under 10 nm). The effort is crucial for an understanding of non-diffusive thermal transport since a significant amount of heat transport is mediated by phonons in the GHz-THz frequency ranges. This is a difficult effort for several reasons. Photoacoustic methods depend on the use of extremely thin films in order to reach the highest frequencies, and nearly atomically flat interfaces are required in order to transmit the acoustic waves from the generation layer into an

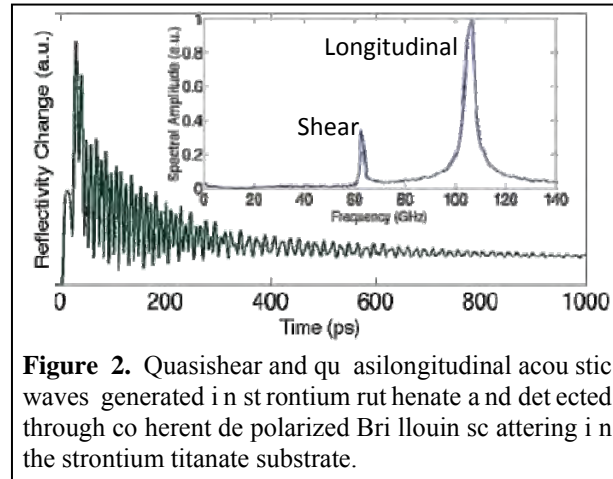


Figure 2. Quasishear and quasilongitudinal acoustic waves generated in strontium ruthenate and detected through coherent depolarized Brillouin scattering in the strontium titanate substrate.

adjacent material to be studied in a manner that preserves acoustic phase coherence for optical detection. Optical detection is difficult since coherent Brillouin scattering for high-frequency acoustic modes with nm wavelengths cannot be used with optical probe wavelengths. We have made progress in the generation of shear waves and in demonstration of atomically flat photoacoustic layers through the use of strontium ruthenate (SrRuO_3 , or SRO), which can be deposited in layers as thin as several nm over atomically flat strontium titanate (STO) substrates. In addition, the STO substrates can be cut off-axis so that the SRO film crystallographic axes are canted as described above. In this case both longitudinal and transverse waves are generated as shown in Fig. 2. Interferometric probing should reveal the full range of acoustic frequencies which is expected to extend far higher than 100 GHz. The use of SRO as a photoacoustic transducer has enabled several advances including photoacoustic study of highly scattering (e.g. biological) media [15].

We have reached higher acoustic frequencies using an InGaN/GaN superlattice (SL) structure whose 22 nm period defines the fundamental acoustic wavelength that is generated and whose interface sharpness allows multiple harmonics to be generated [16]. In this manner we have generated acoustic frequencies as high as 2.5 THz as shown in Fig. 3. The strategy is being replicated using multiple optical pulses to select individual high frequencies, and with SRO/STO superlattices with even sharper interfaces.

Nonlinear acoustics in the GHz frequency range

We have recently demonstrated nonlinear GHz acoustic wave propagation in solid and liquid samples [17,18], the latter a first in a photoacoustic measurement. This enables a very wide range of new prospects for study of anharmonic material responses and nonlinear relaxation phenomena.

Future Plans

In a continuation of the project, we plan to harness recently achieved EUV pulse energies for all-EUV TG measurements of non-diffusive thermal transport and GHz-frequency surface acoustic waves. Measurement of non-diffusive transport in a material with no thermal transfer between layers permits more straightforward analysis of the results. Similar measurements will be attempted using hard x-ray pulses at the LCLS. Success in these measurements will permit study of bulk non-diffusive thermal transport and extremely high-frequency bulk acoustic waves without the need for ultraflat interfaces for

acoustic transduction between different materials. It also will enable wide-ranging nonlinear spectroscopy measurements at hard x-ray frequencies. Finally, we plan to use recently generated strong THz pulses for direct piezoelectric interconversion to transverse and longitudinal acoustic waves in the GHz-THz frequency range in order to enable versatile tabletop study of bulk linear and nonlinear responses in this range.

Publications during Current Grant Period

1. M. Siemens et al., "Measurement of quasi-ballistic thermal transport from nanoscale interfaces using ultrafast coherent soft x-ray beams" *Nature Materials* **9**, 26 (2010).
2. "Nanoscale heat transport probed with ultrafast soft x-rays," M. Siemens, Q. Li, M. Murnane, H. Kapteyn, and K.A. Nelson, in *Ultrafast Phenomena XVI*, P. Corkum, S. De Silvestri, K. A. Nelson, E. Riedle, and R. W. Schoenlein, eds. (Springer-Verlag 2009), pp 149-151.
3. M. Siemens, Q. Li, R. Yang, K. Nelson, E. Anderson, M. Murnane, and H. Kapteyn, "Quasi-ballistic thermal transport from nanoscale interfaces observed using ultrafast coherent soft x-ray beams", proceeding of SPIE Photonics West 2011, 7937-41, in press (2011).
4. Q. Li et al., "Ballistic thermal transport from 2D nano-interfaces", in preparation (2011).
5. Siemens et al., "High-frequency surface acoustic wave propagation in nanostructures characterized by coherent extreme ultraviolet beams," *Appl. Phys. Lett.* **94**, 093103 (2009).
6. D. Nardi et al., "Probing Thermomechanics at the Nanoscale: Impulsively Excited Pseudosurface Acoustic Waves in Hypersonic Phononic Crystals", submitted (2011).
7. Q. Li et al., "Generation and Detection of Very Short-Wavelength 35nm Surface Acoustic Waves at Nano-interfaces", in preparation (2011).
8. T. Pezeril, C. Klieber, S. Andrieu, and K.A. Nelson, "Optical generation of gigahertz-frequency shear acoustic waves in liquid glycerol," *Physical Review Letters* **102**, 107402 (2009).
9. C. Klieber, T. Pezeril, S. Andrieu, and K.A. Nelson, "GHz longitudinal and transverse acoustic waves and structural relaxation dynamics in liquid glycerol," in *Ultrafast Phenomena XVI*, P. Corkum, S. De Silverstri, K.A. Nelson, E. Riedle, and R.W. Schoenlein, eds. (Springer-Verlag 2009), pp. 499-501.
10. T. Pezeril, C. Klieber, S. Andrieu, D. Chateigner, and K. A. Nelson, "Picosecond shear waves in nano-sized solids and liquids," *Proc. SPIE* **7214**, 721408 (2009).
11. C. Klieber, T. Pezeril, S. Andrieu, and K.A. Nelson, "Optical generation and detection of gigahertz-frequency longitudinal and shear acoustic waves in liquids: Detection theory and experiment," in preparation.
12. C. Klieber, T. Pezeril, D. Torchinsky, and K.A. Nelson, "Gigahertz-frequency longitudinal and shear acoustic dynamics in glycerol and DC704 studied by time-domain Brillouin scattering," in preparation.
13. D.H. Torchinsky, C. Klieber, J. A. Johnson, T. Hecksher, N.B. Olsen, T.E. Christensen, J. Dyre, and K.A. Nelson, "Millihertz through gigahertz structural relaxation dynamics in supercooled liquid tetrahydrofuran," in preparation.
14. C. Klieber, E. Peronne, K. Katayama, J. Choi, M. Yamaguchi, T. Pezeril, and K.A. Nelson, "Narrow-band acoustic attenuation measurements in vitreous silica at frequencies between 20 and 400 GHz," *Appl. Phys. Lett.* **98**, 211908-1 - 211908-3 (2011).
15. A.A. Maznev, K.J. Manke, K.A. Nelson, S.H. Baek, and C.-B. Eom, "Coherent Brillouin spectroscopy in a strongly scattering liquid by picosecond ultrasonics," *Opt. Lett.* **36**, in press (2011).
16. A.A. Maznev, K.J. Manke, K.-H. Lin, K.A. Nelson, C.-K. Sun, and J.-I. Chyi, "Broadband terahertz ultrasonic transducer based on a laser-driven piezoelectric semiconductor superlattice," *Ultrasonics*, in press.
17. V.V. Temnov, C. Klieber, K.A. Nelson, T. Thomay, A. Leitner, D. Makarov, M. Albrecht, and R. Bratschitsch, "Nonlinear femtosecond ultrasonics in gold probed with ultrashort surface plasmons," in preparation.
18. C. Klieber, V. Goussev, T. Pezeril, and K.A. Nelson, "Optical generation and detection of nonlinear acoustic wave propagation in a viscoelastic fluid across the glass transition," in preparation.

Antenna-Coupled Light-Matter Interactions

Lukas Novotny (novotny@optics.rochester.edu)

University of Rochester, The Institute of Optics, Rochester, NY, 14627.

1. Program Scope

We study antenna-coupled light emission on the single quantum emitter (molecule, atom, quantum dot, ..) level. We tailor the radiative properties of the quantum emitter by means of an optical antenna, - a device that converts localized energy to radiation, and *vice versa*. Optical antennas hold promise for enhancing the performance and efficiency of photodetection, light emission, and sensing.

2. Recent Progress

The objective of optical antenna design is equivalent to classical antenna design, namely to optimize the energy transfer between a localized source or receiver and the free radiation field. Antennas can enhance several distinct photophysical processes. In light-emitting devices, an electron-hole pair recombines to emit a photon. The reverse process takes place in photovoltaics, in which incoming light causes a charge separation in a material. In both cases, an optical antenna can be used to couple the propagating field and local electric field, making the transfer of energy between the two more efficient. In spectroscopy, incident light polarizes the material of interest, which generates outgoing radiation. The wavelength of the emitted light is related to the energy level structure of the material, allowing for chemical identification. In this case, the antenna serves to make both the excitation and emission more efficient. While the function of optical antennas is similar to their radiowave and microwave analogues, there are important differences due to their small size and the resonant properties of nanoscale materials.

At radio frequencies, metals have very large conductivities and are thus almost perfect reflectors. The *skin depth* is usually negligible compared to any relevant length scale of the antenna. However, at optical frequencies electrons in metals have considerable inertia and cannot respond instantaneously. The skin depth is consequently on the order of tens of nanometers, comparable to the dimensions of the antenna.

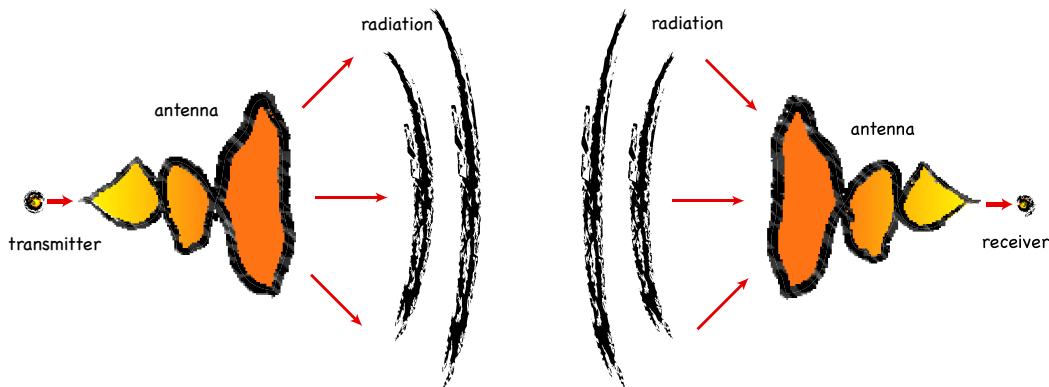


Figure 1: Conceptual illustration of a transmitting and a receiving optical antenna. Arrows indicate the direction of energy flow. The two configurations are related by the principle of reciprocity. In spectroscopy and microscopy, the two antenna concepts are combined; that is, the antenna is used both as a receiver and as a transmitter.

Traditional design rules that prescribe antenna parameters only in terms of an external wavelength are thus no longer valid. Rigorously treating the metal as a plasma is required, which leads to a reduced effective wavelength seen by the antenna [6]. This effective wavelength λ_{eff} is related to the external (incident) wavelength λ by the surprisingly simple relation

$$\lambda_{\text{eff}} = n_1 + n_2 \left[\frac{\lambda}{\lambda_p} \right], \quad (1)$$

where λ_p is the plasma wavelength of the metal and n_1 and n_2 are constants that depend on the geometry and dielectric parameters of the antenna. λ_{eff} is roughly a factor of 2 to 6 shorter than the free space λ for typical metals (Au, Ag, Al) and realistic antenna thicknesses [6].

In the traditional radiofrequency and microwave regime, antennas are usually employed to convert electromagnetic radiation into electric currents, and vice versa. However, most of the optical antennas studied to date operate on a light-in / light-out basis. To directly convert low-energy electrons into propagating photons we have started to study plasmon mediated two-step momentum downconversion. In our most recent work, surface plasmon polaritons (SPPs) propagating along an extended gold nanowire have been excited on one end by low-energy electron tunneling and were then converted to free-propagating photons at the other end [13]. The separation of excitation and outcoupling proves that tunneling electrons excite gap plasmons that subsequently couple to propagating plasmons.

The momentum of a non-relativistic free electron of mass m_e is a factor $\sqrt{2m_e c^2 / \hbar \omega} \sim 500$ greater than that of a visible photon of the same energy, which implies that the interaction between electrons and photons is weak for $\hbar \omega \ll m_e c^2$, since energy and momentum cannot be simultaneously conserved. One way to bridge this mismatch is to employ polariton modes (plasmons). They have the same energy as free space photons but arbitrarily high spatial localization (hence momentum), and can therefore couple efficiently to electrons. Fig. 2 shows the experimental configuration. A bias voltage is applied between a monocrystalline gold nanowire and a gold tip, whose position is held under feedback at a constant tunneling current. Light is collected on the substrate-side with a high numerical aperture (NA=1.4) objective, and the full angular distribution of emitted photons is recorded by imaging the back focal plane (Fourier

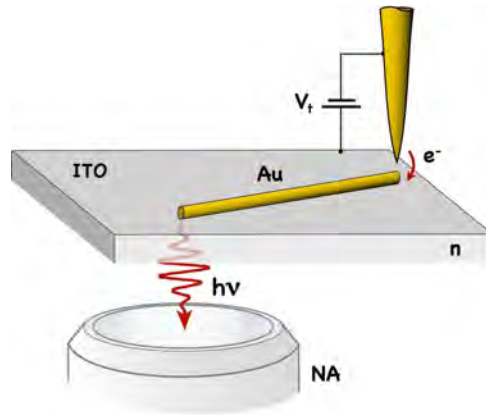


Figure 2: *Illustration of the experiment. Inelastic electron tunneling between a gold tip and a single-crystal gold nanorod gives rise to surface plasmon excitation. Locally excited surface plasmons propagate along the nanorod and scatter at the other end. Emitted photons are collected by an index-matched NA=1.4 objective and then analyzed.*

plane) of the objective on an electron-multiplying charge-coupled device (EMCCD) camera. Alternatively, the distribution of photons in real-space can be mapped by including another focusing lens in the imaging path.

The physical mechanism behind electron-excited SPP generation can be described by a two-step process. Inelastically tunneling electrons first couple to localized modes of the tip-sample junction (gap plasmons). The excited gap plasmons then couple to SPPs propagating along the gold nanowire. At the other end of the wire the excited SPPs are converted to propagating photons by scattering. Thus, the nanowire functions as a transmission line mediating between the electrical feed point and the optical outcoupling region.

Fig. 3 (b) shows the direct space photon map for the nanowire in Fig. 3 (a). SPPs are excited by electron tunneling at the left end of the wire. The bias voltage is $V_t = 2V$ and the tunnel current $I_t = 1nA$. The map indicates that no photons are emitted along the nanowire and that a remarkable fraction of photons emerges from the wire ends. Similar results have been recorded for other wires as well. Because of the strong localization at the nanowire end, the field distribution in the backfocal plane (Fourier plane) is very broad. measure $15,000 \text{ photons } s^{-1}$ emitted from the tunnel junction whereas the total counts from the opposite end are $750 \text{ photons } s^{-1}$. Thus, the overall coupling efficiency along the nanowire is $\sim 5\%$. The efficiency improves for shorter nanowires because of lower propagation losses. Further improvement requires optimization of the coupling between gap-plasmons and propagating SPPs and optimization of the SPP outcoupling on the opposite end of the nanowire.

The nanowire serves as a proof-of-principle geometry and is by no means an optimized configuration. Engineered plasmonic structures, such as optical antennas [10], will be able to improve the electron-photon conversion efficiency. Because of the spatial separation of SPP excitation and SPP outcoupling, the optimization can proceed in two separate steps: the optimization of the tunneling junction and the optimization of the photon emission region. The former is a function of both the electronic and electromagnetic density of states whereas the latter constitutes a canonical antenna problem.

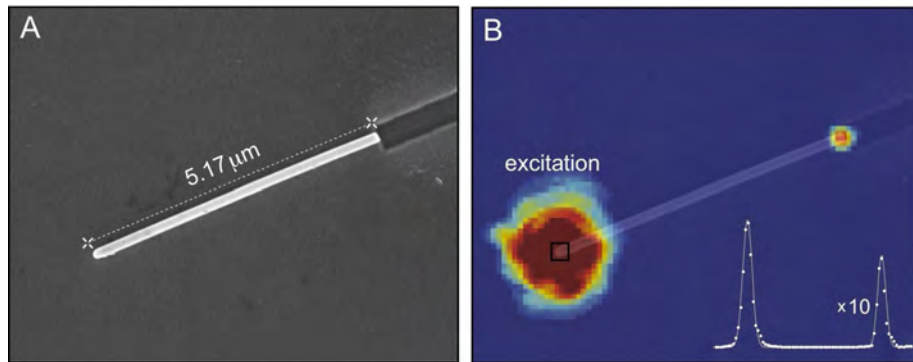


Figure 3: Electrical excitation of SPPs propagating along a monocrystalline gold nanowire. (A) SEM image of a gold nanowire of radius 87 nm and length $\sim 5\mu m$. (B) Photon emission map superimposed to the SEM image. SPPs excited at one end of the wire propagate to the other end where they are scattered and converted to propagating photons. Inset: Intensity map along the nanowire showing diffraction-limited emission peaks from both ends.

3. Future Plans

Our future experiments will build on the results and findings of the current project. In the next project period we are particularly interested in exploring the possibility of antenna-coupled electro-optical transduction and to optimize the conversion efficiency by suitable antenna designs.

4. DOE sponsored publications 2008-2011

- [1] R. J. Moerland, T. H. Taminiau, L. Novotny, N. F. van Hulst, and L. Kuipers, "Reversible polarization control of single molecule emission," *Nano Lett.* **8**, 606–610 (2008).
- [2] L. Novotny, "Optical antennas tuned to pitch," *Nature* **455**, 879 (2008).
- [3] L. Novotny and C. Henkel, "Van der Waals versus optical interaction between metal nanoparticles," *Opt. Lett.* **33**, 1029–1031 (2008).
- [4] S. Palomba and L. Novotny, "Nonlinear excitation of surface plasmon polaritons by four-wave mixing," *Phys. Rev. Lett.* **101**, 056802 (2008).
- [5] S. Palomba, M. Danckwerts, and L. Novotny, "Nonlinear Plasmonics with Gold Nanoparticle Antennas," *J. Opt. A: Pure and Appl. Opt.* **11**, 114030 (2009).
- [6] P. Bharadwaj, B. Deutsch, and L. Novotny, "Optical antennas," *Adv. Opt. Phot.* **1**, 438 – 483 (2009).
- [7] J. Renger, R. Quidant, N. V. Hulst, S. Palomba, and L. Novotny, "Free-space excitation of propagating surface plasmon polaritons by nonlinear four-wave mixing," *Phys. Rev. Lett.* **103**, 266802 (2009).
- [8] L. Novotny, "Optical antennas: A new technology that can enhance light-matter interactions," *The Bridge* **39**, 14–20 (2009).
- [9] L. Novotny, "Strong coupling, energy splitting, and level crossings: A classical perspective," *Am. J. Phys.* **78**, 1199-1202 (2010).
- [10] L. Novotny and N. F. van Hulst, "Antennas for light," *Nature Phot.* **5**, 83-90 (2011).
- [11] P. Bharadwaj and L. Novotny, "Plasmon enhanced photoemission from a single $Y_3N@C_{80}$ fullerene," *J. Phys. Chem. C* **114**, 7444–7447 (2010).
- [12] J. Renger, R. Quidant and L. Novotny, "Enhanced nonlinear response from metal surfaces," *Opt. Exp.* **19**, 1777-1785 (2011).
- [13] P. Bharadwaj, A. Bouhelier and L. Novotny, "Electrical excitation of surface plasmons," *Phys. Rev. Lett.* **106**, 226802 (2011).
- [14] S. Palomba, H. Harutyunyan, J. Renger, R. Quidant, N. F. van Hulst and L. Novotny, "Nonlinear plasmonics at planar metal surfaces," *Proc. Roy. Soc. B*, in print (2011).
- [15] P. Bharadwaj and L. Novotny, "Robustness of quantum dot power-law blinking," *Nano. Lett.* **11**, 2137-2141 (2011).
- [16] L. Novotny, "From near-field optics to optical antennas," *Physics Today*, July (2011).

Electron and Photon Excitation and Dissociation of Molecules

A. E. Orel
Department of Applied Science
University of California, Davis
Davis, CA 95616
aeorel@ucdavis.edu

Program Scope

This program will study how energy is interchanged in electron and photon collisions with molecules leading to excitation and dissociation. Modern *ab initio* techniques, both for the photoionization and electron scattering, and the subsequent nuclear dynamics studies, are used to accurately treat these problems. This work addresses vibrational excitation and dissociative attachment following electron impact, and the dynamics following inner shell photoionization. These problems are ones for which a full multi-dimensional treatment of the nuclear dynamics is essential and where non-adiabatic effects are expected to be important.

Recent Progress

Summary

We have carried out a number of calculations studying low-energy electron scattering and dissociative attachment. In addition, in order to explain some recent experiments, we began a series of studies of the dynamics following inner-shell photoionization. Much of this work has been done in collaboration with the AMO theory group at Lawrence Berkeley Laboratory headed by T. N. Rescigno and C. W. McCurdy.

Studies of Dissociative Electron Attachment

In response to the publication of a new experimental study[1] on the isotope effect in HCN vs DCN dissociative electron attachment, we returned to this system and carried out a new series of calculations, now going beyond the static-exchange level and adding the effects of polarization. The new results agree quite well with experiment. The results of the calculation are described in a paper published in Physical Review A (Publication 3). We have studied dissociative electron attachment (DEA) to HCCCN below 12 eV. We subdivided the molecule into three fragments (H), (CC) and (CN); therefore, four internal coordinates consisting in the distances between the center of masses of (H) and (CC) fragments, (CC) and (CN) fragments, the (H)-(CC) angle and the (CC)-(CN) angle were included in the calculation. We performed electron scattering calculations using the complex Kohn variational method to determine the resonance energies and autoionization widths for various geometries of the system and constructed the complex potential energy surfaces relevant to the metastable HCCCN⁻ ion. The nuclear dynamics was treated using the Multiconfiguration Time-Dependent Hartree (MCTDH) formalism and the flux of the propagating wavepacket is used to compute the DEA cross section relevant to the 4 channels in question[2]. Preliminary results have been published (Publication 4) and the full results of the calculation are described in a paper which will be submitted to Physical Review A.

Indirect Double Photoionization

Because of the long-range repulsive Coulomb interaction between singly charged ions, the vertical double ionization thresholds of small molecules generally lie above the dissociation limits corresponding to formation of singly charged fragments. This leads to the possibility of forming singly charged molecular ions by photoabsorption in the Franck-Condon region at energies below the lowest dication state, but above the dissociation limit for two singly charged fragment ions. These singly charged molecular ions can emit a second electron by autoionization, but only at larger internuclear separations where the ion falls into the electron+dication continuum. This process has been termed indirect double photoionization.

The AMO experimental group at LBL headed by A. Belkacen has carried out a kinetically complete experiment on the production of CO^+ autoionizing states following inner-valence photoionization of carbon monoxide below its double ionization threshold. Momentum imaging spectroscopy was used to measure the energies and body-frame angular distributions of both photo- and ejected electrons, as well as the kinetic energy release of the atomic ions. We have carried out *ab initio* theoretical calculations, calculating both the potential energy curves of the superexcited states and well as cross sections and molecular-frame photoelectron angular distributions in order to compare with experiment. This has provided insight into the nature of the molecular ion states produced and their subsequent dissociation into autoionizing atomic (O^*) fragments. The results of the calculation are described in a paper which was published in Physical Review A as a Rapid Communication (Publication 9).

In another set of experiments done at BESSY, H_2O was doubly photoionized at a photon energy of $h\nu = 43$ eV. To identify the states involved in the autoionization we carried out multi-reference configuration-interaction calculations for potential energy curves of H_2O^+ in this region. We found three excited H_2O^+ states of ${}^2A'$ symmetry which undergo several avoided crossings as the H-OH distance increases, and feed four states which dissociate to $\text{H}^+ + \text{OH}^*$. The OH^* states are autoionizing states of OH with a Rydberg electron attached to a bound, excited state of OH^+ . A simple classical scattering was developed, with electrons launched radially from a sphere of 1 a.u. centered at one Coulomb potential with a second one Coulomb potential simulating the proton was placed at a distance R. The starting kinetic energy of the electron is chosen such that the asymptotic energy matches the observed continuum energy. This classical modelling reproduced the observed angular distribution of the autoionizing electron almost exactly, with the distance R where autoionization occurs taken as a fitting parameter. When this distance is converted into a autoionization lifetime, it agreed with our calculations. The results of the calculation are described in a paper published in Physical Review Letters (Publication 10).

Electron interactions with complex targets - HOCO

A recent study of near-threshold angular resolved photodetachment of the hydroxyl formyl anion HOCO^- shows several striking features, namely, a sharp threshold peak that produces an apparently isotropic distribution of photoelectrons and a second low-energy peak that produces a dipole pattern of photoelectrons aligned along the polarization direction of the laser[3]. The isotropic threshold peak has been attributed to a dominance of s-wave scattering at very low electron energies, while the second peak has been interpreted as a low-energy p-wave shape resonance. This interpretation ignores the fact that the HOCO radical, which provides the field for the escaping photoelectron, has a large dipole moment which mixes partial waves at all energies. Electron scattering by strongly polar molecules is characterized by angular distributions that are strongly forward-peaked, not isotropic, and it would be unusual to find low-energy shape resonances in such systems. In collaboration with the group at LBL, we carried out fixed-nuclei variational electron-HOCO scattering calculations which were used to compute photodetachment cross sections and laboratory-frame photoelectron angular distributions. The calculations show a broad $A''(\pi^*)$ -shape resonance several eV above threshold. We found that the peaks, seen in the experiment, can be attributed to vibrational Feshbach resonances of dipole-bound trans- HOCO^- , and not s- and p-wave shape resonances as previously assumed. The results of the calculation are described in a paper published in Physical Review A (Publication 11).

Future Plans

Dissociative Electron Attachment

For dissociative electron attachment, the experimental AMO group at LBL, using the COLTRIMS method, can not only obtain total cross sections, but also information about partial cross sections into various vibrational states of the final fragments and the angular distributions of the fragments. These experiments would be a much more rigorous test of the theory, and yield more information about the process of dissociation in this system. Such experiments were carried out for water, and calculations[4] agreed well with experiment. Our initial studies will focus on formic acid and CO_2 . Considerable attention has been given to the lowest π^* negative ion shape resonance in formic acid.

Virtually nothing is known about the observed higher energy resonances between 7 and 9 eV, which evidently lead to production of O^- and OH^- . At this point it is unclear whether doubly-excited Feshbach resonances or possibly a quasi-bound dipole σ^* state is involved in the DEA dynamics. We plan to study this system in conjunction with planned experimental COLTRIMS studies at Lawrence Berkeley Laboratory. Recent experiments have been carried out on the dissociative attachment to CO_2 . Our preliminary studies have shown the existence of a Feshbach resonance $^2\Pi$ symmetry. This state has a conical intersection with the low-lying π^* shape resonance and leads to DEA. Fixed-nuclei calculations were used to obtain entrance amplitudes which gave the probability for an electron attaching to a target molecule as a function of its orientation in the laboratory frame. These calculations predicted ion angular distributions that agreed well with experiment. Other systems of interest include methanol and ethanol, which both undergo DEA via Feshbach resonances analogous to water, but evidently show some strikingly different dissociation dynamics which is not presently understood.

Highly correlated processes in diatomic photoionization An analog to dissociative attachment is dissociative recombination which has been well-studied due to its importance in applications such as planetary atmospheres, chemistry in interstellar clouds and combustion. Each electronic state of the molecular ion can support a series of neutral Rydberg states. Many of these states lie above the ground state of the ion and therefore are autoionizing resonant states. They appear in electron scattering calculations as resonances. These states can also be seen in photoionization. However, these generally carry little oscillator strength, have narrow widths and have potential energy curves that simply track their parent ion states. Some systems have non-Rydberg doubly excited states which are expected to have much larger oscillator strengths, since their spatial overlap with the initial state is large. The N_2 , CO and O_2 cases are particularly interesting since their doubly excited valence states, near the equilibrium target geometry, can decay into many open electronic channels. Moreover, some of the states are expected to be steeply dissociative. We propose to carry out high-level electronic structure and coupled-channel, fixed-nuclei electron-ion scattering calculations to obtain the energies and lifetimes of these states as a function of nuclear geometry. We will also compute photoionization cross sections and study the branching ratios into different final ion states and how these vary with internuclear distance. The primary motivation for undertaking these studies is to see if these states are interesting candidates for XUV pump/probe experiments, which we expect they will be, especially if the calculations show a rapid change in the branching ratios with increasing internuclear distance. This work will also form a basis for further time-dependent studies of these states in the ultrafast program.

Isomerization of HCCH: Snapshots of a chemical reaction The Moshhammer group at Heidelberg has begun studies of the dissociative photoionization of HCCH. These are two photon experiments. The first photon ionizes HCCH (below the double ionization limit), and then at a later variable time a second photon ionizes the $HCCH^+$. The experiment will focus on the (C^+, CH_2^+) channel. In order to reach this channel, the ion must isomerize, with one hydrogen moving into a vinyldyne-type configuration before dissociation. The plan for the experiment is to 'catch' this process by the time-delay for the second photon. We are performing calculations on the ion states and plan to carry out dynamics calculations to understand the isomerization that must occur to produce this channel. We will then compute molecular frame photoangular distributions (MFPADs) along the isomerization path. These will have to be appropriately averaged over the orientation of the fragment with respect to the axis of dissociation and compared to measured angular distributions taken at a series of time delays. The goal is to produce snapshots of the path to products.

Formation of autoionizing O^* following soft -ray induced O_2 dissociation As described in the subsection "Indirect Double Photoionization" in the section on "Recent Progress", we studied inner shell autoionizing states of CO^+ produced by inner-valence photoionization of carbon monoxide below its double ionization threshold. Another interesting example is autoionizing O^* following soft -ray induced O_2 dissociation. There has been experimental work on this system[5]. These experiments used an ultrashort pump beam with a photon energy of 42.7eV to ionize O_2 . For small internuclear separations, autoionization could not occur. At larger separations, >30 au, autoionization occurred. An IR probe pulse was used to 'interrupt' the autoionization. A COLTRIMS apparatus was used to determine the

momentum of all charged particles. We propose to calculate the potential curves involved in this process and study the subsequent dynamics.

References

- [1] O. May, D. Kubala and M. Allan *Phys. Rev. A* **82** 010701(R) (2010).
- [2] G. A. Worth, M. H. Beck, A. Jäckle, and H.-D. Meyer, The MCTDH Package, Version 8.2 (2000); H.-D. Meyer, Version 8.3; See <http://www.pci.uni-heidelberg.de/tc/usr/mctdh/>
- [3] Z. Lu and R. E. Continetti, *Phys. Rev. Lett.* **99**, 11305 (2007) and Z. Lu, Q. Hu, J. E. Oakman, and R. E. Continetti, *J. Chem. Phys.*, **126**, 194305 (2007).
- [4] D. J. Haxton, C. W. McCurdy and T. N. Rescigno, *Phys. Rev. A* **73** 062724 (2006).
- [5] A. S. Sandhu, *et al*, *Science*, **322**, 1081 (2008).

Publications

1. Improved calculation on the isotope effect in dissociative electron attachment to acetylene, (with S. T. Chourou) *Phys. Rev. A* **80** 034701 (2009).
2. Dissociative Electron Attachment to HCN and HNC, (with S. Chourou) *Phys. Rev. A* **80** 032709 (2009).
3. Isotope effect in dissociative electron attachment to HCN (with S. T. Chourou) *Phys. Rev. A* **83** 032709 (2011)
4. Dissociative Electron Attachment to HCN, HCCH and HCCCN (with S. T. Chourou) *J. Phys.: Conf. Ser.* **300** 012014 (2011)
5. Comment on "Electron-induced bond breaking at low energies in HCOOH and glycine: The role of very short-lived σ^* anion states", (with T. N. Rescigno and C. S. Trevisan) *Phys. Rev. A* **80** 046701 (2009).
6. Dissociative recombination of CF^+ : Experiment and theory (with O Novotny, O Motapon, M H Berg, D Bing, H Buhr, H Fadil, M Grieser, J Hoffmann, A S Jaroshevich, B Jordon-Thaden, C Krantz, M Lange, M Lestinsky, M Mendes, S Novotny, D A Orlov, A Petrigani, I F Schneider and A Wolf) *J. Phys.: Conf. Ser.* **192** 012021 (2009).
7. Asymmetric molecular-frame photoelectron angular distributions for C 1s photoejection from CO_2 ; a theoretical study, (with S. Miyabe, C. W. McCurdy and T. N. Rescigno) *J. Phys.: Conf. Ser.* **194** 012008 (2009).
8. Theoretical study of asymmetric molecular-frame photoelectron angular distributions for C 1s photoejection from CO_2 , (with S. Miyabe, C. W. McCurdy and T. N. Rescigno) *Phys. Rev. A* **79**, 053401 (2009)
9. Formation of inner-shell autoionizing CO^+ states below the CO^{2+} threshold (with T. Osipov, Th. Weber, T. N. Rescigno, S. Y. Lee, M. SchŽffler, F. P. Sturm, S. SchŽssler, U. Lenz, T. Havermeier, M. Kšhnel, T. Jahnke, J. B. Williams, D. Ray, A. Landers, R. Dorner, and A. Belkacem) *Phys. Rev. A* **81** 011402 (2010)
10. Electron diffraction self-imaging of molecular fragmentation in two-step double ionization of water (with H. Sann, T. Jahnke, T. Havermeier, K. Kreidi, C. Stuck, M. Meckel, M. Schöffler, N. Neumann, R. Wallauer, S. Voss, A. Czasch, O. Jagutzki, Th. Weber, H. Schmidt-Böcking, S. Miyabe, T. Rescigno and R. Dörner) *Phys. Rev. Lett.* **106** 133001 (2011).
11. Vibrational Feshbach resonances in near threshold $HOCO^-$ photodetachment; a theoretical study (with S. Miyabe, D. J. Haxton, K. V. Lawler, C. W. McCurdy and T. N. Rescigno, *Phys. Rev. A* **83** 043401 (2011).

“Low-Energy Electron Interactions with Liquid Interfaces and Biological Targets”

Thomas M. Orlando

School of Chemistry and Biochemistry and School of Physics,
Georgia Institute of Technology, Atlanta, GA 30332-0400

Thomas.Orlando@chemistry.gatech.edu, Phone: (404) 894-4012, FAX: (404) 894-7452

Project Scope: The primary objectives of this program are to investigate the fundamental physics and chemistry involved in low-energy (1-250 eV) electron interactions with i) condensed films of water adsorbed on rare-gas substrates, ii) condensed samples of complex biological targets (i.e. deoxyribonucleic acids (DNA), simple nucleic acids, nucleosides and nucleotides) and iii) aqueous solution surfaces and interfaces containing solvated ions and biomolecules. The program concentrates on the important issues dealing with electron initiated damage and energy exchange in the deep valence and shallow core regions of the collision targets. These types of excitations are extremely sensitive to many body interactions and changes in local potentials. We have continued using low-energy electron-scattering/ultrahigh vacuum surface science techniques to investigate intermolecular Coulomb Decay (ICD) and dissociative electron attachment (DEA) at complex interfaces. These investigations are useful in extracting details regarding non-thermal damage of heterogeneous systems which include hydrated biological interfaces.

Recent Progress:

Project 1. Intermolecular Coulomb decay at weakly interacting heterogeneous surfaces

We have continued our studies of shallow valence hole mediated Coulomb explosions and water cluster ion production/ejection at ice surfaces. The cluster ion yields are very sensitive to local hydrogen bonding interactions and are very good probes of hole exchange. We recently demonstrated that ejection of $H^+(H_2O)_{n=1-8}$ from low energy electron irradiated water clusters adsorbed on graphite and graphite with overlayers of Ar, Kr or Xe results from intermolecular Coulomb decay (ICD) at the mixed interface. Inner valence holes in water ($2a_1^{-1}$), Ar ($3s^{-1}$), Kr ($4s^{-1}$) and Xe ($5s^{-1}$) correlate with the cluster appearance thresholds and initiate ICD. Proton transfer occurs during or immediately after ICD and the resultant Coulomb explosion leads to $H^+(H_2O)_{n=1-8}$ desorption with kinetic energies that vary with initiating state, final state and inter-atomic/molecular

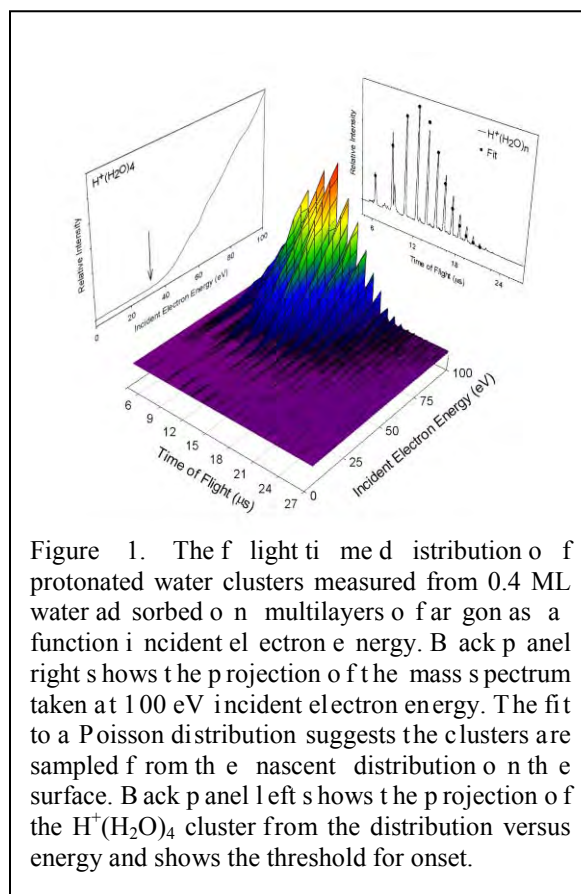


Figure 1. The flight time distribution of protonated water clusters measured from 0.4 ML water adsorbed on multilayers of argon as a function of incident electron energy. Back panel right shows the projection of the mass spectrum taken at 100 eV incident electron energy. The fit to a Poisson distribution suggests the clusters are sampled from the nascent distribution on the surface. Back panel left shows the projection of the $H^+(H_2O)_4$ cluster from the distribution versus energy and shows the threshold for onset.

distances. The color image in figure 1 shows the water cluster ion distribution as a function of incident electron energy. The dots in the back panel is a fit to a Poisson distribution and the left panels shows an example of the threshold data for $H^+(H_2O)_{n=4}$ formation and desorption from a $(H_2O)_n$:Ar/graphite substrate.

The threshold energies for direct ejection of $H^+(H_2O)_{n=4}$ from all the targets are shown in the left side panels of figure 2. The data are represented by solid symbols while results from an established threshold fitting procedure are shown with lines. The frames on the right of figure 2 show representative $H^+(H_2O)_4$ kinetic energy (KE) distributions. The low threshold energies and slow KE distributions (relative to multilayer water) indicate that formation/desorption of $H^+(H_2O)_n$ from < 0.5 ML of $(H_2O)_n$ on graphite and Ar, Kr and Xe covered graphite involves ICD.

Though the observed cluster sizes reflect the nascent deposited cluster distribution, the two-component energy distributions reflect the initial hole identities and charge locations produced via ICD.

Project 2. Low-energy electron-induced DNA damage

We have examined theoretically the elastic scattering of 5-30 eV electrons within the B-DNA 5'-CCGGCGCCGG-3' and A-DNA 5'-CGCGAATTCGCG-3' sequences using the separable representation of a free-space electron propagator and a curved wave multiple scattering formalism. The disorder brought about by the surrounding water and helical base stacking leads to featureless amplitude build-up of elastically scattered electrons on the sugars and phosphate groups for all energies between 5-30 eV. However, some constructive interference features arising from diffraction were revealed when examining the structural waters within the major groove. These are shown in figure 3 and appear at 5-10, 12-18 and 22-28 eV for the B-DNA target and at 7-11, 12-18 and 18-25 eV for the A-DNA target. Though the diffraction depends upon the base-pair sequence, the energy dependent elastic

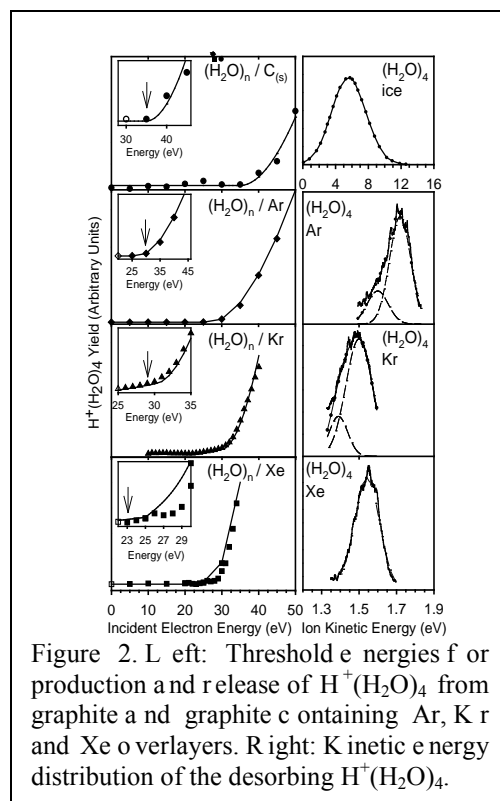


Figure 2. Left: Threshold energies for production and release of $H^+(H_2O)_4$ from graphite and graphite containing Ar, Kr and Xe overlayers. Right: Kinetic energy distribution of the desorbing $H^+(H_2O)_4$.

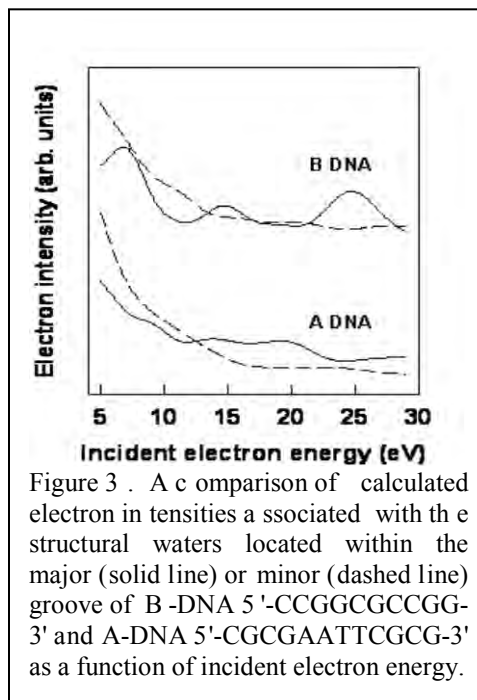


Figure 3. A comparison of calculated electron intensities associated with the structural waters located within the major (solid line) or minor (dashed line) groove of B-DNA 5'-CCGGCGCCGG-3' and A-DNA 5'-CGCGAATTCGCG-3' as a function of incident electron energy.

scattering features are primarily associated with the structural water molecules localized within 8-10 Å spheres surrounding the bases and/or the sugar-phosphate backbone. The electron density build-up occurs in regions of electron attachment resonances, direct electronic excitation and dissociative ionization. We correlated these scattering features with DNA single and double strand breaks and suggested that states involving major groove waters may be important in low-energy electron induced damage of DNA.

Project 3. Coulomb explosions at ionic-aqueous interfaces.

We have extended our studies of intermolecular Coulomb explosions of water

adsorbed on rare gases to aqueous interfaces containing dissolved ions. Specifically, we have studied solutions containing either NaCl, NaOH or HCl or using the liquid beam apparatus at Pacific Northwest National Laboratory. As shown in figure 4, laser excitation at 193 nm produced and removed cations of the form $H^+(H_2O)_n$ and $Na^+(H_2O)_m$ from liquid jet surfaces containing either NaCl or NaOH. The protonated water cluster yield varied inversely with increasing salt concentration, while the solvated sodium ion cluster yield varied by a non-type. We interpreted the production of the $H^+(H_2O)_n$ in terms of a localized ionization/Coulomb expulsion model. However, the UV desorption of $Na^+(H_2O)_m$ is not accounted for by this model. Rather it required the ionization of solvation shell waters and a contact ion/Coulomb expulsion mechanism.

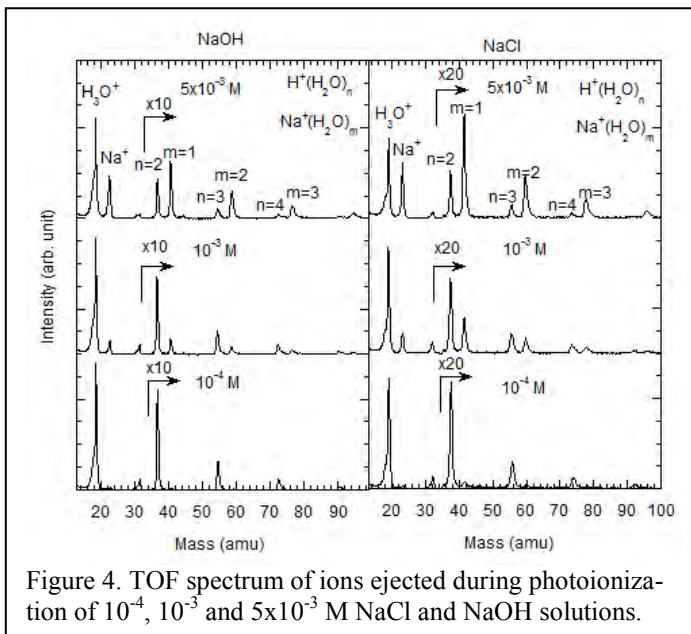


Figure 4. TOF spectrum of ions ejected during photoionization of 10^{-4} , 10^{-3} and 5×10^{-3} M NaCl and NaOH solutions.

Future Plans:

We plan to further examine the physics and chemistry involved in low-energy (5-250 eV) electron scattering with i) nanoscale films of simple hydrocarbons containing adsorbed water clusters and ii) nanoscale films of nucleic acids, and small oligonucleotide sequences containing well control amounts of co-adsorbed water, ions, and amino acids. We will also extend our studies by utilizing the attosecond x-ray capability in Boulder. Our approach provides a direct probe of the inelastic energy loss channels and scattering resonances which lead to ICD and DEA, electronic excitation and direct dissociation at complex heterogeneous surface and interfaces.

Presentations acknowledging support from this project (2008-2011).

1. T. M. Orlando, "Low-Energy Electron Interactions with Hydrated DNA and Complex Biological Interfaces", Department of Physics, University of Alabama, Jan. 25, 2008.
2. T. M. Orlando, "Probing the interfacial ion composition of low-temperature ice and aqueous salt solution interfaces using Coulomb ejection of cluster ions", Liquid and Solid Aqueous Surfaces and Interfaces Workshop, Telluride, CO, Aug. 10-16, 2008.

3. T. M. Orlando, "Non-thermal Surface Processes: From the Real to the Sublime", Department of Chemistry, University of Alabama, Tuscaloosa, Feb. 2, 2009.
4. T. M. Orlando, "Non-thermal Surface Processes: From the Real to the Sublime", Department of Chemistry, Louisiana State University, Baton Rouge Feb. 13, 2009.
5. T. M. Orlando, "Low-energy electron interactions with hydrated DNA", University of Notre Dame, Radiation Chemistry: A Visionary Meeting, July 2009.
6. T. M. Orlando, "Low-energy electron interactions with hydrated DNA", Radiation Research Society Meeting, Oct. 9, 2009.
7. T. M. Orlando, "The roles of resonances and diffraction in the electron-beam induced damage of DNA", International Physics Workshop on Dynamical Processes in Irradiated Systems, San Sebastian, Spain, July 26-28, 2010.
8. T. M. Orlando, "Low-energy electron interactions with hydrated DNA and complex biological targets. 240th ACS National Meeting, Boston, MA, United States, August 22-26, 2010.
9. T. M. Orlando, "The roles of resonances and diffraction in the electron-beam induced damage of DNA", International Conference on Ionizing Radiation of Polymers, Univ. of Maryland, Oct. 27-29, 2010.
10. T. M. Orlando, "Photoionization studies of aqueous salt solution interfaces", PacifiChem., Honolulu, HI, Dec 15-20, 2010.

Publications from this project (2008-2011).

1. Y. Chen, A. Aleksandrov and T. M. Orlando, "Low-energy Electron Induced Damage of Plasmid DNA", *Int. J. of Mass Spectrometry* **277**, 314 (2008).
2. T. M. Orlando, D. Oh, Y. Chen, and A. Alexandrov, "Low-energy Electron Diffraction and Induced Damage in Hydrated DNA", *J. Chem. Phys.* **128**, 195102 (2008).
3. G. A. Grieves, N. Petrik, J. Herring-Captain, B. Olanrewaju, A. Aleksandrov, R. G. Tonkyn, S. A. Barlow, G. A. Kimmel, and T. M. Orlando, "Photoionization of Sodium Salt Solutions in a Liquid Jet", *J. Phys. Chem. C.* **112**, 8359, (2008).
4. D. Oh, Ph.D. Thesis, (2009). "Low-energy electron diffraction effects at complex interfaces"
5. D. Oh, M. T. Sieger, and T. M. Orlando, "The Theoretical Description and Experimental Demonstration of Diffraction in Electron-stimulated Desorption", *J. of Physics: Condensed Matter*, **22**, 084001 (2010). **IOP - Special Recognition Paper**
6. G. A. Grieves, J. L. McLain, and T. M. Orlando, "Low-energy Stimulated Reactions in Nanoscale Water Films and Water:DNA interfaces", *Chapter 18, Charge Particle Interactions with Matter: Recent Advances, Applications and Interfaces*, Taylor, Francis Publishing Co. (2010).
7. B. Olanrewaju, J. Herring-Captain, G. A. Grieves, A. Aleksandrov and T. M. Orlando, "Probing the interaction of Hydrogen Chloride with low-temperature water ice surfaces using thermal and electron-stimulated desorption", *J. Phys. Chem. A*. dx.doi.org/10.1021/jp110332v (2011).
8. G. A. Grieves and T. M. Orlando, "Intermolecular Coulomb decay at weakly coupled heterogeneous interfaces", *Phys. Rev. Lett.* 10.1103/PhysRevLett.107.016104 (2011).
9. B. Olanrewaju, Ph.D. Thesis, (2011). "Nonthermal processes on ice and liquid microjet surfaces".

Structure from Fleeting Illumination of Faint Spinning Objects in Flight

Abbas Ourmazd and Peter Schwander

Dept. of Physics, University of Wisconsin Milwaukee
1900 E. Kenwood Blvd, Milwaukee, WI 53211
ourmazd@uwm.edu, pschwan@uwm.edu

It is now possible to intersect molecules, viruses, and cells “in flight” with intense short pulses of radiation, and record “snapshots” before the object is destroyed. We are developing a new generation of powerful algorithms to recover structure and dynamics from such ultra-low-signal random sightings. These techniques, based on concepts from differential geometry, general relativity, graph theory, and diffraction physics promise to revolutionize our understanding of structure and function in biological and energy-synthesis processes. Progress in five areas is reported below.

1. Computationally efficient 3D structure recovery from XFEL snapshots

Previous algorithms for single-particle structure recovery from random snapshots, including those developed by us, were based on computationally inefficient Bayesian inference. These techniques are able to reconstruct objects only eight times the spatial resolution, severely limiting the size and of amenable objects and the resolution to which they can be reconstructed. Using newly discovered symmetries underlying all image formation by scattering, we have demonstrated a computationally efficient approach able to reconstruct objects with computational complexities 10^4 x higher than previously possible, extending the amenable object size and resolution to objects of biological interest. Fig. 1, for example, shows the structure of the biologically important enzyme adenylate kinase from two million simulated snapshots of unknown orientation. We are thus in a position to recover structure from experimental snapshots of biologically interesting objects by scatter-and-destroy techniques, and await access to suitable datasets.

2. Efficient, unsupervised extraction of useful snapshots from large XFEL datasets

Ideally, XFEL scatter-and-destroy experiments intercept a succession of identical single-particles with a train of intense X-ray pulses to record diffraction snapshots before each particle is destroyed. In practice, several complications arise. a) Particle injectors are not synchronized with the X-ray pulses, resulting in a mixture of blank shots, where no injected object was intercepted, and exposures of injected objects. b) Injected objects can contain none, one, or multiple copies of the particle of interest. c) Unintentional contamination produces snapshots from a number of different species. d) The incident beam intensity varies from shot-to-shot. e) Only a part of the injected particle may be exposed to the incident beam. These factors give rise to unsorted datasets consisting of blank snapshots, and a variety of snapshots emanating from one or more particles belonging to a number of species. The fraction of snapshots from individual particles of one species is usually small (1-10% in our experiments), and must be extracted from large collections of $\sim 10^7$ snapshots. Experimental noise and stochastic processes, such as shot-to-shot variations in the beam intensity, make this task particularly challenging.

The need for snapshots from identical single-particles is an essential pre-requisite for current diffract-and-destroy 3D structure recovery techniques, severely limiting the number of “useful” snapshots.

We have developed and demonstrated an unbiased, accurate, and computationally efficient method for classifying experimental X-ray diffraction snapshots without recourse to operator supervision, specific noise models, or templates (see Fig. 2). The approach is based on spectral clustering, a kernel-based Principal Component Analysis (PCA) method, which uses the nonlinear correlations in the dataset over a variety of length scales to classify snapshots. Our primary results, obtained without supervision, can be summarized as follows. a) Experimental X-ray Free Electron Laser (XFEL) diffraction snapshots can be sorted with above 90% accuracy, as judged by manual expert assignment. b) We estimate a sorting capability of 10^6 snapshots in less than 10 hours with modest computing resources. Given the current experimental snapshot output of $\sim 10^6$ per day at 120Hz with 10% hit rate, this capability suffices for typical experimental runs until significantly higher source and injector repetition rates and/or source-injector synchronization become available.

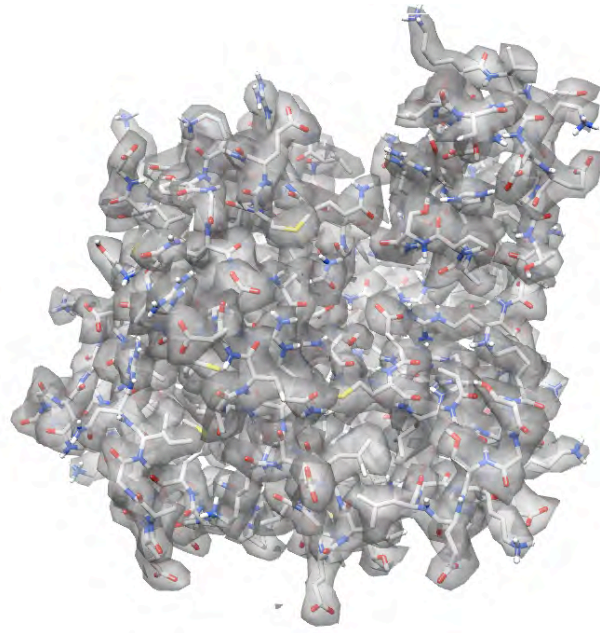


Fig. 1. 3D structure of the energy relevant enzyme adenylate kinase recovered from two million simulated diffracted snapshots.

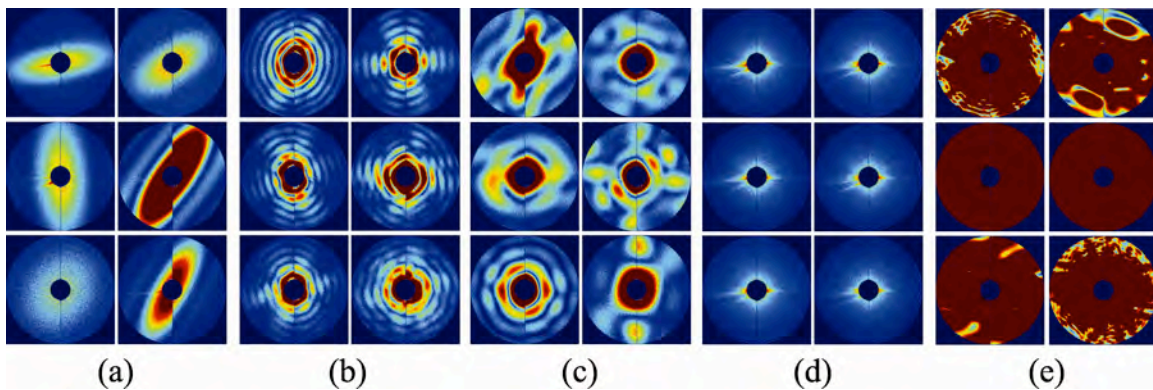


Fig. 2. Randomly selected representatives from sorted classes containing snapshots from: (a) nanorice; (b) mimivirus; (c) miscellaneous (possibly T4 virus); and (d) blank and (e) saturated snapshots. Assignment is correct to better than 90%.

3. Structure recovery from ultra-low-dose *image* snapshots.

Cryo-electron microscopy (Cryo-EM) currently sets the bar for 3D structure recovery from random snapshots in terms of spatial resolution ($\sim 0.3\text{nm}$) and has begun to produce dynamic information by mapping biologically important reactions. Radiation damage, however, limits the available information. Using the newly-discovered symmetries of image formation, we have demonstrated 3D structure recovery from cryo-EM snapshots at 12x lower dose than currently possible (Fig. 3). This allow us to advance structure recovery by cryo-EM, while preparing the way for high-resolution extraction of structure and dynamics from XFEL datasets anticipated to become available over the next five years.

4. 3D movies of biological entities (in progress).

There is mounting evidence that structural variability is common in biology and important to function, and that “structure” is neither static, nor immutable. The study of structural variability and dynamics represents an important, but difficult frontier in understanding biological processes. We are developing a new generation of algorithms to structure and dynamics (3D movies) from random sightings of heterogeneous ensembles, such as collections of molecules each at a different part of biological process. This would revolutionize our ability to understand the intimate connection between structure and function in life and energy synthesis processes.

5. Structure recovery for complex objects such as whole cells.

We have developed a conceptual framework for determining the structure of up to a million configurationally and compositionally heterogeneous cells with datasets expected from the Next Generation Light Source. This has formed a key part of the scientific case for the NGLS, of which one of us (AO) is a Principal Investigator.

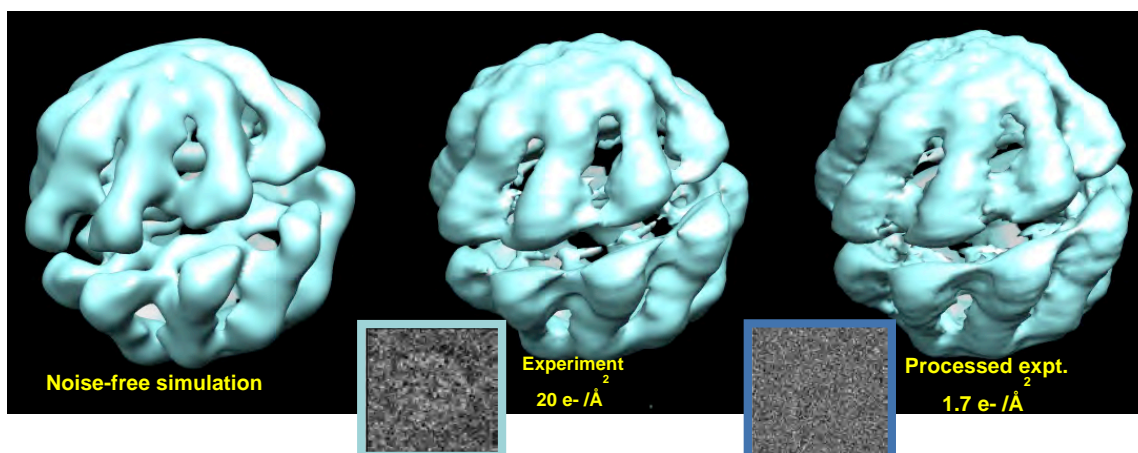


Fig. 3. 3D structure recovered from 2D cryo-EM micrographs. (*Left*) Noise-free simulated. (*Center*) Experimental, at typical dose of $20\text{ e}^-/\text{\AA}^2$. (*Right*) Experimental, pre-processed to represent dose of $1.7\text{ e}^-/\text{\AA}^2$. Insets show corresponding micrographs.

6. Ultrafast molecular processes beyond timing jitter

In conjunction with P. Bucksbaum et al., we have studied ultrafast, X-ray induced fragmentation of molecular nitrogen. Time-of-flight (ToF) spectra from pump-probe experiments using femtosecond IR-optical and X-ray pulses from the LCLS X-ray Free Electron Laser were analyzed to investigate the detailed processes underlying Coulomb explosion of N₂. The temporal resolution of these experiments is limited by timing jitter, measured to be ~ 300fs FWHM. Using advanced manifold-based analytical techniques, we have succeeded in revealing ultrafast processes much shorter than the timing jitter. These results have potentially broad implications for the study of ultrafast molecular processes.

Publications from DoE sponsored research

1. B. Moths, and A. Ourmazd, Bayesian algorithms for recovering structure from single-particle diffraction snapshots of unknown orientation: a comparison, *Acta Cryst A* (accepted).
2. D. Giannakis, P. Schwander, and A. Ourmazd, Symmetries of image formation: I. Theoretical framework, *Phys Rev E* (submitted).
3. P. Schwander, D. Giannakis, C.H. Yoon, and A. Ourmazd, Symmetries of image formation: II. Applications, *Phys Rev E* (submitted).
4. C.H. Yoon et al., Unsupervised classification of single-particle X-ray diffraction snapshots by spectral clustering, *Optics Express* (submitted).

Energetic Photon and Electron Interactions with Positive Ions

Ronald A. Phaneuf,
Department of Physics
University of Nevada
Reno NV 89557-0220
phaneuf@unr.edu

Program Scope

This experimental program investigates photon and electron initiated processes leading to ionization of positively charged atomic ions, as well as to ionization and fragmentation of molecular ions. The objective is a more complete and quantitative understanding of ionization mechanisms and of the collective dynamic response of bound electrons in atomic and molecular ions to incident EUV photons and electrons. Mono-energetic beams of photons and electrons are merged or crossed with mass/charge analyzed ion beams to probe their internal electronic structure and the dynamics of their interactions. The primary focus is on processes in which the behavior of bound electrons is highly correlated. This is manifested by giant dipole resonances in the ionization of atomic ions and also of fullerene molecular ions, whose quasi-spherical cage structures characterize them as structural intermediates between individual molecules and solids. In addition to precision spectroscopic data for understanding their internal electronic structure, high-resolution measurements of absolute cross sections for photoionization and electron-impact ionization of ions provide critical benchmarks for testing theoretical approximations such as those used to generate photon opacity databases. Their accuracy is critical to modeling and diagnostics of astrophysical, fusion-energy and laboratory plasmas. Of particular relevance to DOE are those produced by the Z pulsed-power facility at Sandia National Laboratories which is currently the world's most efficient high-intensity x-ray source, and the National Ignition Facility at Lawrence Livermore National Laboratory which is the world's most powerful laser system. Both facilities are dedicated to high-energy-density science as well as to research aimed at harnessing thermonuclear fusion as an energy source.

Recent Progress

The major research emphasis has been the application of an ion-photon-beam (IPB) research endstation to experimental studies of photoionization of singly and multiply charged positive ions using monochromatized synchrotron radiation at the Advanced Light Source (ALS). Measurements using the IPB endstation on beamline 10.0.1.2 define the state of the art in energy resolution and sensitivity for studies of photon-ion interactions in the 20 – 300 eV energy range. This program developed and retains partial responsibility for operation, maintenance and upgrades of this multi-user research endstation.

Due to their relatively large number of identical atoms, nanometer size and hollow spherical or quasi-spherical cage structures, fullerene molecular ions are of intrinsic interest as structural intermediates between individual molecules and solids, and exhibit some of the properties of each. As is the case for conducting solids, their large numbers of valence electrons may be collectively excited in strong plasmon modes with broad energy signatures in the photoionization cross section. Conversely, the excitation of core

electrons is spatially localized and of molecular character with narrower energy signatures characteristic of carbon-carbon bonding.

- An atom confined in a charged spherical shell is an intriguing quantum-mechanical system. Unusual phenomena associated with the interaction of EUV light with so-called endohedral fullerene molecules containing caged atoms have been predicted in numerous recent theoretical studies by M. Amusia, V. Dolmatov, S. Manson, A. Msezane, H. Chakraborty, A. Solov'yev and their collaborators, but remained untested by experiment. The single, giant 4d photoionization resonance in atomic Xe is predicted to be significantly distorted by the carbon cage in endohedral $\text{Xe}@C_{60}$, producing four distinct maxima termed confinement resonances. The predicted pattern is a multi-path interference effect caused by reflection of Xe 4d photoelectron waves by the C_{60} cage. Exchange of oscillator strength between plasmon modes of the fullerene cage and the trapped atom is also predicted. Previous measurements at ALS of photoionization of $\text{Ce}@C_{82}^+$ in the 70 – 160 eV photon energy range showed clear evidence of Ce 4d excitation, but neither interference structure nor exchange of oscillator strength. This was attributed to the fact that Ce forms ionic bonds and is not centered within the carbon cage. Reference photoionization measurements on ions of the Ce isonuclear sequence in the same photon energy range constituted the Ph.D. dissertation of M. Habibi and were published in Physical Review A [4]. Follow-up experiments with $\text{Ce}@C_{82}^+$ explored product photoion channels involving successive losses of two C atoms from the fullerene cage, which also exhibit significant Ce 4d oscillator strength. Product channels resulting in single and double ionization accompanied by loss of as many as 12 pairs of C atoms were found to have non-negligible cross sections with signatures of the Ce 4d resonance. The results of this collaborative investigation are being prepared for publication.
- A noble gas atom such as Xe is not expected to form ionic bonds and is predicted to be centered within a C_{60} fullerene cage. A measurement of photoionization of $\text{Xe}@C_{60}^+$ in the energy range of Xe 4d ionization therefore represents a critical test of the theory of confinement resonances. Such an experiment had not heretofore been possible because of extremely low yields of synthesized noble-gas endohedral fullerenes. At ALS during a period of several months, a 200 eV beam of Xe ions from an ion sputter-gun bombarded the surface of a rotating metal cylinder onto which C_{60} was being continuously deposited in vacuum by evaporation. The accumulated powder on the cylinder (few tens of mg) was scraped from the surface and placed into a small oven for subsequent re-evaporation into a low-power Ar discharge in an ECR ion source. A very small fraction ($\sim 10^{-5}$) of the C_{60} molecules in the accumulated samples containing a Xe atom was sufficient to produce a pure mass/charge analyzed beam of $\text{Xe}@C_{60}^+$ ions with a current of 0.06 – 0.3 pA. Proof-of-principle measurements of photoionization of $\text{Xe}@C_{60}^+$ made at ALS are presented in Figure 1. The data exhibit a clear signature of Xe 4d ionization in this photon energy range and structure strongly suggestive of confinement resonances. A report of this experiment was recently published in Physical Review Letters [1].
- Motivated by recent theoretical work of H. Chakraborty, an investigation of the n-dependence of photoionization cross sections of fullerene ions C_n^+ in the range $40 < n < 84$ was completed. The objective was to explore the effects of size, symmetry and shape of the fullerene cage on the strengths and widths of the collective plasmon modes. Subsequent measurements at ALS at higher mass resolution have indicated

that the cross section for single ionization accompanied by release of a pair of carbon atoms or a carbon dimer is as large as or larger than that for pure ionization at some photon energies. Previous measurements did not fully separate these two product channels. This project will comprise the M.S. thesis research of C.M. Thomas.

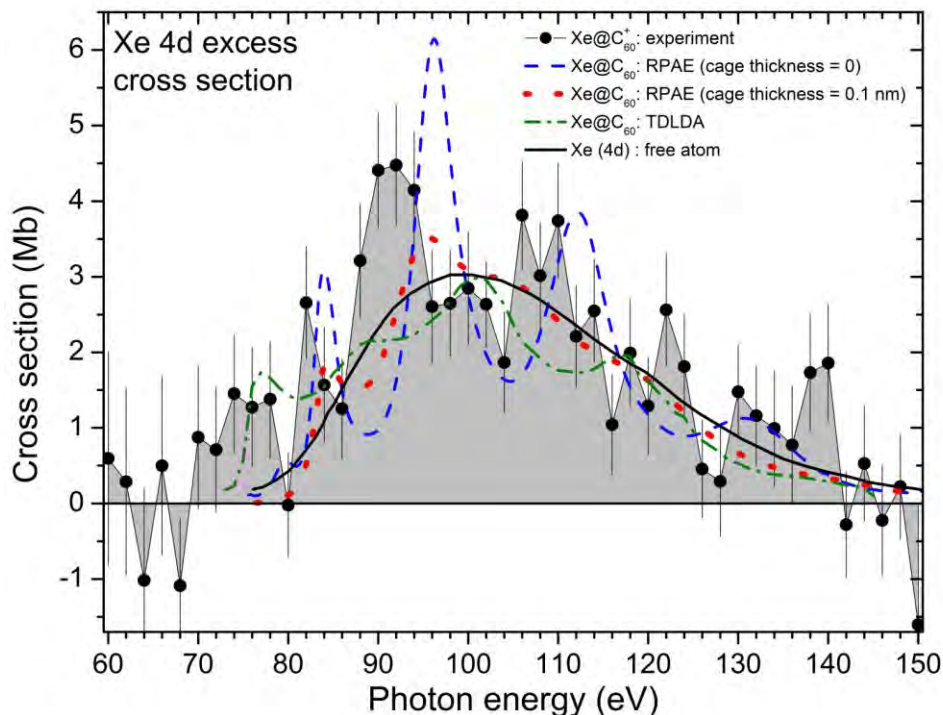


Figure 1. Measurements at ALS of excess cross section for Xe 4d ionization in double photoionization of endohedral Xe@C_{60}^+ with loss of 2 C atoms (solid circles) compared with different theoretical predictions of confinement resonances [1]. The theoretical curves have been divided by 10 for comparison.

Future Plans

The highest priority for future experiments at ALS will be more definitive experimental tests of numerous theoretical predictions of novel phenomena resulting from the exposure of fullerenes and endohedral fullerenes to EUV light.

- Building upon the proof-of-principle results for the Xe 4d signature in photoionization of Xe@C_{60}^+ , a priority will be to improve the statistics of measurements for different product ion channels. This will be done in close collaboration with the theorists. Better resolution of the frequency and phase of the interference patterns will provide new information about the molecular structure of endohedral fullerenes as well as the dynamics of confinement resonances.
- Measurements of the n-dependence of photoionization cross sections of fullerene ions C_n^+ in the range $30 < n < 90$ will be performed at higher mass resolution in the energy ranges of the plasmon oscillations (near 22 eV for the surface plasmon and 38 eV for the volume plasmon) to distinguish product channels involving pure ionization from those involving ionization plus loss of pairs of C atoms or C_2 dimers. These measurements will utilize a recently developed two-dimensional scanning technique to map out the ionized fullerene product mass distributions.

Publications of Research Fully or Partially Funded by DOE (2009-2011)

1. *Confinement Resonances in Photoionization of Xe@C₆₀⁺*, A.L.D. Kilcoyne, A. Aguilar, A. Müller, S. Schippers, C. Cisneros, G. Alna'Washi, N.B. Aryal, K.K. Baral, D.A. Esteves, C.M. Thomas and R.A. Phaneuf, Phys. Rev. Lett. 105, 213001 (2010).
2. *Plasmons in Fullerene Molecules*, R.A. Phaneuf, chapter 35 in "Handbook of Nanophysics," K. Sattler ed. (Taylor & Francis, 2010).
3. *Photoionization of the cerium isonuclear sequence and cerium endohedral fullerene*, M. Habibi, Ph.D. Dissertation, University of Nevada, 2009.
4. *Photoionization cross sections for the isonuclear sequence of cerium ions*, M. Habibi, D.A. Esteves, R.A. Phaneuf, A.L.D. Kilcoyne, A. Aguilar and C. Cisneros, Phys. Rev. A 80, 033407 (2009).
5. *K-shell photoionization of ground-state Li-like carbon ions [C³⁺]: experiment, theory and comparison with time-reversed photorecombination*, A. Müller, S. Schippers, R.A. Phaneuf, S.W.J. Scully, A. Aguilar, I Alvarez, C. Cisneros, E.D. Emmons, M.F. Gharaibeh, G. Hinojosa, A.S. Schlachter and B.M. McLaughlin, J. Phys. B: At. Mol. Opt. Phys. 42, 235602 (2009).
6. *Improved Neutron-Capture Element Abundances in Planetary Nebulae*, N.C. Sterling, H.L. Dinerstein, S. Hwang, S. Redfield, A. Aguilar, M.C. Witthoef, D. Esteves, A.L.D. Kilcoyne, M. Bautista, R. Phaneuf, R.C. Bilodeau, C.P. Balance, B. McLaughlin and P.H. Norrington, Pub. Astron. Soc. Australia 26, 339 (2009).
7. *Photoionization of Se ions for the determination of elemental abundances in astrophysical nebulae*, D.A. Esteves, Ph.D. Dissertation, University of Nevada, 2010.
8. *Valence-shell photoionization of the chlorine-like Ca³⁺ ion*, G. Alna'Washi, M. Lu, M. Habibi, R.A. Phaneuf, A.L.D. Kilcoyne, A.S. Schlachter, C. Cisneros and B.M. McLaughlin, Phys. Rev. A 81, 053416 (2010).
9. *Experimental photoionization cross-section measurements in the ground and metastable state threshold region of Se⁺*, N.C. Sterling, D.A. Esteves, R.C. Bilodeau, A.L.D. Kilcoyne, E.C. Red, R.A. Phaneuf and A. Aguilar, J. Phys. B: At. Mol. Opt. Phys. 44, 025701 (2011).
10. *Photoionization measurements for the iron isonuclear sequence: Fe³⁺, Fe⁵⁺ and Fe⁷⁺*, M.F. Gharaibeh, A. Aguilar, A.M. Covington, E.D. Emmons, S.W.J. Scully, R.A. Phaneuf, A.L.D. Kilcoyne, A.S. Schlachter, I Álvarez, C. Cisneros and G. Hinojosa, Phys. Rev. A 83, 043412 (2011).
11. *State-resolved valence shell photoionization of Be-like ions: experiment and theory*, A. Müller, S. Schippers, R.A. Phaneuf, A.L.D. Kilcoyne, H. Bräuning, A.S. Schlachter, M. Lu and B.M. McLaughlin, J. Phys. B: At. Mol. Opt. Phys. 43, 225201 (2010)
12. *K-shell photoionization of ground-state Li-like boron ions [B²⁺]: experiment and theory*, A. Müller, S. Schippers, S.W.J. Scully, A. Aguilar, C. Cisneros, M.F. Gharaibeh, A.S. Schlachter and B.M. McLaughlin, J. Phys. B: At. Mol. Opt. Phys. 44, 025701 (2011) J. Phys. B: At. Mol. Opt. Phys. 43, 135602 (2010).

Molecular photoionization studies of nucleobases and correlated systems

Erwin Poliakoff, Department of Chemistry, Louisiana State University, Baton Rouge, LA 70803, epoliak@lsu.edu

Robert R. Lucchese, Department of Chemistry, Texas A&M University, College Station, TX, 77843, lucchese@mail.chem.tamu.edu

Program Scope

Molecular photoionization provides an important probe of molecular structure and dynamics. In one-photon ionization the dipole matrix elements that control the ionization process contain information about the initial state, final ion-state, and the electron scattering continuum. Our main focus is to use vibrationally resolved photoelectron spectroscopy to probe the correlated motions of electrons and nuclei through the study of geometry and energy dependence of these dipole matrix elements. Experimentally, we acquire vibrationally resolved photoelectron spectra as a function of energy, using the capabilities of the high brightness Advanced Light Source at Lawrence Berkeley National Laboratory. On the theory side, we explicitly solve the electron-molecular ion scattering equations to compute the corresponding vibrationally specific matrix elements using the adiabatic approximation. We also explore applications of our knowledge of single-photon molecular photoionization to other processes. In collaboration with other groups, this includes studies of high-harmonic generation within the three-step model, photoelectron rescattering spectroscopy, and, with somewhat less intense sources, multiphoton ionization. This research benefits the Department of Energy because the results elucidate structure/spectra correlations that will be indispensable for probing complex and disordered systems of interest to DOE such as clusters, catalysts, reactive intermediates, transient species, and related species.

Recent Progress

Non-Franck-Condon Vibrational Branching Ratios in Complex Systems

In the simplest view of molecular photoionization, one assumes that vibrational and photoelectron motion are decoupled, which leads to the Franck-Condon approximation. The Franck-Condon principle has two predictions that are relevant to molecular ionization: (1) vibrational branching ratios are independent of photon energy, and (2) single quantum excitations of nontotally symmetric modes are forbidden. Nonresonant and resonant processes can result in coupling molecular vibration and photoelectron motion, with the result that vibrational branching ratios become dependent on photon energy, and that forbidden vibrations can be excited.

As a first step towards the study of the photoionization of nucleobases, we have begun a study of the ring molecule 2-bromothiophene. Experimentally, we have made considerable progress on this system. In the analysis of the $X a'' (1a_2)^{-1}$ state, we have identified 29 peaks resulting from the ν_6 , ν_7 and ν_{14} vibrations and their combination bands. The vibrations have been interpreted as follows: ν_6 is a ring stretching mode, ν_7 is a C-H in-plane bending mode and ν_{14} is a Br-sensitive mode. All of the branching ratio curves appear to show non-Franck-Condon behavior at low photon energies; specifically, there appears to be a sharp dip in branching ratio at $h\nu = 21\text{eV}$. We intend to collect more near-threshold data during future experiments ($h\nu = 17-$

21eV) in order to explore this feature. In some of the branching ratio curves, there also appears to be some possible deviations at higher photon energies, notably branching ratios for transitions with multiple quanta ν_6 . Supporting computational studies on this system are now being pursued.

Non-resonant effects in the vibrational branching ratios of XCN, X=Br,Cl

Earlier, we experimentally and computationally studied the non-Franck-Condon vibrational effects in the photoionization of ICN leading to its ground $X^2\Pi$ state. We have now extended our computational studies to explore similar effects in the ionization XCN ($X = \text{Cl}, \text{Br}$). The vibrational branching ratios for photoionization of the $X^2\Pi$ state in the XCN molecules for both non-degenerate vibrational stretching C–N and X–C modes have been computed employing the adiabatic approximation. Harmonic oscillator vibrational wave functions were used to calculate the vibrationally specific photoionization cross sections leading to the ground state of XCN^+ . In the case of the photoionization cross sections leading to the $X^2\Pi_{3/2,1/2}$ states of ICN^+ when q_1 (C–N stretching mode) or q_3 (I–CN stretching mode) are excited, significant non-Franck-Condon effects were seen at photon energies of 60-80. These differences arose from the sensitivity of the initial state orbital to the C–N bond length. In particular, the electron population in the highest occupied molecular orbital on the CN part of the ICN molecule increases as the C–N bond length increases. Similar effects have now been found in our computational study of the photoionization leading to the $X^2\Pi_{3/2,1/2}$ states of BrCN^+ and ClCN^+ . We find a breakdown of the Franck-Condon approximation due to strong geometry dependence of the transition moment coming from the geometry dependence of Cooper minima in the cross sections.

Vibrational Effects in the Initial State

We have studied the initial vibrational-state specific photoionization of CO_2 and N_2O in the shape resonance region above the K-shell ionization thresholds. This work is a collaborative project with experimental group of K. Ueda. For both molecules, significant diminution of the shape resonances by the bending excitation in the initial electronic ground state is observed in the experimental measurements. We have explained these observations using a one-dimensional adiabatic effective core Hartree-Fock model (ECHF), where the electronic wave function of the target was approximated by including the same number of electrons as in the initial molecule but increasing the charge by one unit on the nucleus where the $(1s)^{-1}$ hole is created. Within this model we see that there is a shape resonance that can be described as a valence σ_u^* state, where the ungerade label is only approximate in the case of N_2O . This state shifts to lower with bending and in most channels the peak in the cross section is reduced with bending. The resulting vibrationally averaged cross sections are in reasonable agreement with the experimental data supporting the conclusion that the adiabatic ECHF model can be used to explain the experimental observations. We found that the Hückel molecular orbital (HMO) model gives a qualitative explanation of the shifts in the resonance energies with bending angle observed in our calculations. We note that the HMO model also correctly describes the behavior of the resonance energy of the σ_g^* resonance which occurs at threshold in some of the ionization channels considered.

Rescattering Photoelectron Spectroscopy

We have collaborated with the group of K. Ueda in a study of the high-field elastic rescattering processes. Experimentally, large-angle elastic differential cross sections (DCSs) were obtained for scattering of free electrons by singly charged ions of partially aligned O₂ and CO₂ molecules from an analysis of the momentum distributions of rescattering photoelectrons generated by infrared laser pulses. The extracted DCSs are in good agreement with our computed *ab initio* results, confirming the validity of the extraction procedure. Noting that the double-slit-type interference includes information about the distances between the atoms of a molecule, the results of this study has a further implication that the rescattering electron spectroscopy is indeed potentially a powerful tool for determining the structure of molecules and thus may be employed for studying chemical reactions with a temporal resolution of femto- or subfemtoseconds and with atomic spatial resolution.

Future Plans

In addition to completing the project on 2-bromothiophene, the studies of the vibrationally resolved photoionization of complex systems will be extended both experimentally and theoretically to other systems including thymine and uracil. One possible constraint on these studies is the ability to obtain vibrationally resolved data on such systems with many modes. Theoretically, we will also consider vibrationally resolved photodetachment, for which there are new experimental data on the O₂⁻ system. This system is of interest because it will provide a test of the adiabatic approximation for the case of low kinetic energy ejected electrons and because electron correlation effects are more important in the case of photodetachment compared to photoionization. Finally we will extend our rescattering photoelectron spectroscopy computational studies to non-linear polyatomic systems including C₂H₄ and C₂H₆ to explore the sensitivity of the electron-molecular ion scattering DCSs to the structure of the molecule.

Publications in 2009-2011

1. A. Das, E. D. Poliakoff, R. R. Lucchese, and J. D. Bozek, Mode-specific photoionization dynamics of a simple asymmetric target: OCS, *J. Chem. Phys.* **130**, 044302:1-8 (2009).
2. A. T. Le, R. R. Lucchese, M. T. Lee, and C. D. Lin, Probing molecular frame photoionization via laser generated high-order harmonics from aligned molecules, *Phys. Rev. Lett.* **102**, 203001:1-4 (2009).
3. A. T. Le, R. R. Lucchese, and C. D. Lin, Uncovering multiple orbitals influence in high harmonic generation from aligned N₂, *J. Phys. B-At. Molec. Opt. Phys.* **42**, 211001:1-5 (2009).
4. A. T. Le, R. R. Lucchese, S. Tonzani, T. Morishita, and C. D. Lin, Quantitative rescattering theory for high-order harmonic generation from molecules, *Phys. Rev. A* **80**, 013401:1-23 (2009).
5. R. R. Lucchese, J. D. Bozek, A. Das, and E. D. Poliakoff, Vibrational Branching Ratios in the $(b_{2u})^{-1}$ Photoionization of C₆F₆, *J. Chem. Phys.* **131**, 044311:1-8 (2009).
6. C. Jin, A. T. Le, S. F. Zhao, R. R. Lucchese, and C. D. Lin, Theoretical study of photoelectron angular distributions in single-photon ionization of aligned N₂ and CO₂, *Phys. Rev. A* **81**, 033421:1-12 (2010).

7. R. R. Lucchese, R. Montuoro, K. Kotsis, M. Tashiro, M. Ehara, J. D. Bozek, A. Das, A. Landry, J. Rathbone, and E. D. Poliakoff, The effect of vibrational motion on the dynamics of shape resonant photoionization of BF_3 leading to the $E^2A'_1$ state of BF_3^+ , *Molec. Phys.* **108**, 1055-67 (2010).
8. C. D. Lin, Anh-Thu Le, Zhangjin Chen, Toru Morishita, and Robert Lucchese, Strong-field rescattering physics – self-imaging of a molecule by its own electrons, *J. Phys. B-At. Molec. Opt. Phys.* **43**, 122001:1-33 (2010).
9. Anh-Thu Le, R. R. Lucchese, and C. D. Lin, Polarization and ellipticity of high-order harmonics from aligned molecules generated by linearly polarized intense laser pulses, *Phys. Rev. A* **82**, 023814:1-6 (2010).
10. T. Tanaka, M. Hoshino, R. R. Lucchese, Y. Tamenori, H. Kato, H. Tanaka, K. Ueda, Bending-induced diminution of shape resonances in the core-level absorption region of hot CO_2 and N_2O , *New J. Phys.* **12**, 123017:1-18 (2010).
11. Misaki Okunishi, Hiromichi Niikura, R. R. Lucchese, Toru Morishita, and Kiyoshi Ueda, Extracting electron-ion differential scattering cross sections for partially aligned molecules by laser-induced rescattering photoelectron spectroscopy, *Phys. Rev. Lett.* **106**, 063001:1-14 (2011).
12. N. Berrah, R. C. Bilodeau, I. Dumitriu, D. Toffoli, R. R. Lucchese, Shape and Feshbach Resonances in Inner-Shell Photodetachment of Negative Ions, *J. Electron Spectrosc. Relat. Phenom.* **183**, 64-9 (2011).
13. Song-Feng Zhao, Cheng Jin, R. R. Lucchese, Anh-Thu Le, and C. D. Lin, High-order-harmonic generation using gas-phase H_2O molecules, *Phys. Rev. A* **83**, 033409:1-7 (2011).
14. Cheng Jin, Hans Jakob Wörner, V Tosa, Anh-Thu Le, Julien B. Bertrand, R. R. Lucchese, P. B. Corkum, D. M. Villeneuve, and C. D. Lin, Separation of target structure and medium propagation effects in high-harmonic generation, *J. Phys. B* **44**, 095601:1-5 (2011).
15. Bérenger Gans, Séverine Boyé-Péronne, Michel Broquier, Maxence Delsault, Stéphane Douin, Carlos E. Fellows, Philippe Halvick, Jean-Christophe Loison, Robert R. Lucchese, and Dolores Gauyacq, Photolysis of methane revisited at 121.6 nm and at 118.2 nm: quantum yields of the primary products, measured by mass spectrometry, *Phys. Chem. Chem. Phys.* **13**, 8140-52 (2011).

Control of Molecular Dynamics: Algorithms for Design and Implementation

Herschel Rabitz and Tak-San Ho, Princeton University
Frick Laboratory, Princeton, NJ 08540, hrabitz@princeton.edu, tsho@princeton.edu

- A. Program Scope:** This research is concerned with the conceptual and algorithmic developments addressing control over quantum dynamics phenomena. The research is theoretical and computational in nature, with a particular focus towards exploring basic principles of importance for laboratory studies, especially in conjunction with the use of optimal control theory and its realization in closed-loop learning experiments. This research program involves a set of interrelated components aiming at developing a deeper understanding of quantum control and providing new algorithms to extend the laboratory control capabilities.
- B. Research Progress:** In the past year several projects were pursued and the results are summarized below.

- 1. Attaining persistent field-free control of open and closed quantum systems[1]**
Persistent quantum control (PQC) aims to maintain an observable objective value over a period of time following the action of an applied field. Here we have given an assessment of the feasibility of achieving PQC for arbitrary finite-level systems and observables. The analysis has been carried out independent of the particular method used for state preparation. The PQC behavior has been optimized over the set of physically accessible prepared states for both open and closed systems. The quality of observable persistence value in the postcontrol period was found to vary with the required duration of persistence, the system temperature, the chosen observable operator, and the energy levels of the system. The alignment of a rigid diatomic rotor was studied as a model system. The theoretical estimates of PQC behavior were encouraging and suggested feasible exploration in the laboratory using currently available technology.
- 2. Exploring the top and bottom of the quantum control landscape[2]**
A controlled quantum system possesses a search landscape defined by the target physical objective as a function of the controls. In this work we have considered the landscape for the transition probability P_{if} between the states of a finite level quantum system. Traditionally, the controls are applied fields; here, we have extended the notion of control to also include the Hamiltonian structure, in the form of time independent matrix elements. Level sets of controls that produce the same transition probability value are shown to exist at the bottom $P_{if} = 0.0$ and top $P_{if} = 1.0$ of the landscape with the field and/or Hamiltonian structure as controls. We have presented an algorithm to continuously explore these level sets starting from an initial point residing at either extreme value of P_{if} . The technique can also identify control solutions that exhibit the desirable properties of (a) robustness at the top and (b) the ability to rapidly rise towards an optimal control from the bottom. Numerical simulations have been presented to illustrate the varied control behavior at the top and bottom of the landscape for several simple model systems.
- 3. Volume fractions of the kinematic near-critical sets of the quantum ensemble control landscape[3]**
We have derived an estimate of the volume fraction for a subset of $U(N)$ in the neighborhood of the critical set of the kinematic quantum ensemble

control landscape $J(U) = \text{Tr}(U\rho U^\dagger O)$, where U represents the unitary time evolution operator, ρ is the initial density matrix of the ensemble, and O is an observable operator. This estimate is based on the Hilbert-Schmidt geometry for the unitary group and a first-order approximation of $\|\nabla_U J(U)\|^2$. An upper bound on these near-critical volumes is conjectured and supported by numerical simulation, leading to an asymptotic analysis as the dimension N of the quantum system rises in which the volume fractions of these near-critical sets decrease to zero as N increases. This result helps explain the apparent lack of influence exerted by the many saddles of J over the gradient flow.

4. **Optimal laser control of molecular photoassociation along with vibrational stabilization**[4] This work has explored the optimization of laser pulses for the control of photoassociation and vibrational stabilization. Simulations are presented within a model system for the electronic ground-state collision of O + H. The goal was to drive the transition from a wave packet representing the colliding atoms to the vibrational ground level of the diatomic molecule. The optimized fields resulting from two distinct trial pulses were analyzed and compared. Very high yields were obtained in the molecular vibrational ground level.
5. **Why is chemical synthesis and property optimization easier than expected?**[5] We have formulated the OptiChem theory to assess the predicted characteristics of chemical fitness landscapes through a broad examination of the recent literature, which shows ample evidence of trap-free landscapes for many objectives. The fundamental and practical implications of OptiChem theory for chemistry has also been discussed. Specifically, identifying optimal conditions for chemical and material synthesis as well as optimizing the properties of the products is often much easier than simple reasoning would predict. The potential search space is infinite in principle and enormous in practice, yet optimal molecules, materials, and synthesis conditions for many objectives can often be found by performing a reasonable number of distinct experiments. Upon making simple physical assumptions, this work has demonstrated that the fitness landscape for chemical optimization contains no local sub-optimal maxima that may hinder attainment of the absolute best value of J . This feature provides a basis to explain the many reported efficient optimizations of synthesis conditions and molecular or material properties.
6. **A general formulation of monotonically convergent algorithms in the control of quantum dynamics beyond the linear dipole interaction**[6] This work has considered a general method to formulate monotonically convergent algorithms for identifying optimal control fields to manipulate quantum dynamics phenomena beyond the linear dipole interaction. The method, facilitated by a field-dependent dipole moment operator, was based on an integral equation of the first kind arising from the Heisenberg equation of motion for tracking a time-dependent, dynamical invariant observable associated with a reference control field.
7. **Search complexity and resource scaling for the quantum optimal control of unitary transformations**[7] Here we have introduced methods for quantifying Hamiltonian-dependent and kinematic effects on control optimization dynamics in order to classify quantum systems according to the search effort and control resources required to implement arbitrary unitary transformations. The optimal control of unitary transformations is a fundamental problem in quantum control theory and quantum information processing. The feasibility of performing such optimizations is deter-

mined by the computational and control resources required, particularly for systems with large Hilbert spaces. Prior work on unitary transformation control indicates that (i) for controllable systems, local extrema in the search landscape for optimal control of quantum gates have null measure, facilitating the convergence of local search algorithms, but (ii) the required time for convergence to optimal controls can scale exponentially with the Hilbert space dimension. Depending on the control-system Hamiltonian, the landscape structure and scaling may vary.

8. **Fidelity between unitary operators and the generation of robust gates against off-resonance perturbations**[8] We have performed a functional expansion of the fidelity between two unitary matrices in order to find necessary conditions for the robust implementation of a target gate. Comparison of these conditions with those obtained from the the Magnus expansion and Dyson series has shown that they are equivalent in the first order. By exploiting techniques from robust design optimization, we have accounted for issues of experimental feasibility by introducing an additional criterion to the search for control pulses. This search has been accomplished by exploring the competition between the multiple objectives in the implementation of the NOT gate by means of evolutionary multi-objective optimization

C. Future Plans: The research in the coming year will focus on the application of the recently developed general monotonically convergent algorithms beyond the linear dipole approximation [6]. Specifically, we plan to study various atomic and molecular dynamics control problems, including photo-association processes of atoms in thermal gases [4], and collective excitation of Bose-Einstein condensates. We also plan to (1) extend the current level-set study on the transition probability landscape [2] to investigate the quantum control landscape for any observable and for ensemble of systems using the density matrix formalism and (2) continue the application of the persistent quantum control concept [1] to the study of field-free molecular orientation/alignment control.

D. References:

1. Attaining persistent field-free control of open and closed quantum systems, E. Anson, V. Beltrani, and H. Rabitz, *J. Chem. Phys.*, 134, 124110 (2011).
2. Exploring the top and bottom of the quantum control landscape, V. Beltrani, J. Dominy, T.-S. Ho and H. Rabitz, *J. Chem. Phys.*, 134, 194106 (2011).
3. Volume fractions of the kinematic near-critical sets of the quantum ensemble control landscape, J. Dominy and H. Rabitz, *J. Phys. A*, 44, 255302 (2011).
4. Optimal laser control of molecular photoassociation along with vibrational stabilization, E. F. de Lima, T.-S. Ho, and H. Rabitz, *Chem. Phys. Lett.*, 501, 267 (2011).
5. Why is chemical synthesis and property optimization easier than expected? K. W. Moore, A. Pechen, X.-J. Feng, J. Dominy, V. J. Beltrani, and H. Rabitz, *Phys. Chem. Chem. Phys.*, 13, 10048 (2011).
6. A general formulation of monotonically convergent algorithms in the control of quantum dynamics beyond the linear dipole interaction, T.-S. Ho, H. Rabitz, and S.-I Chu, *Comp. Phys. Comm.*, 182, 14 (2011).

7. Search complexity and resource scaling for the quantum optimal control of unitary transformations, K. W. Moore, R. Chakrabarti, G. Riviello, and H. Rabitz, *Phys. Rev. A*, 83, 012326 (2011).
8. Fidelity between unitary operators and the generation of robust gates against off-resonance perturbations, R. Cabrera, O. M. Shir, R. Wu, and H. Rabitz, *J. Phys. A*, 44, 095302 (2011).
9. Accelerated monotonic convergence of optimal control over quantum dynamics, T.-S. Ho and H. Rabitz, *Phys. Rev E*, 82, 026703 (2010).
10. Features of quantum control in the sudden regime, M. Klein, V. Beltrani, and H. Rabitz, *Chem. Phys. Lett.*, 499, 161 (2010).
11. Control of quantum phenomena: past, present and future, C. Brif, R. Chakrabarti and H. Rabitz, *New J. Phys.*, 12, 075008 (2010).
12. The canonical coset decomposition of unitary matrices through Householder transformations, R. Cabrera, T. Strohecker, and H. Rabitz, *J. Math. Phys.*, 51, 082101 (2010).
13. Environment-invariant measure of distance between evolutions of an open quantum system, M. D. Grace, J. Dominy, R. L. Kosut, C. Brif, and H. Rabitz, *New J. Phys.* 12, 015001 (2010).
14. Multi-polarization quantum control of rotational motion through dipole coupling, G. Turinici and H. Rabitz, *J. Phys. A: Math. Theor.* 43, 105303 (2010).
15. The landscape of quantum transitions driven by single-qubit unitary transformations with implications for entanglement, R. Cabrera and H. Rabitz, *J. Phys. A: Math. Theor.* 42, 275303 (2009).
16. Gradient algorithm applied to laboratory quantum control, J. Roslund and H. Rabitz, *Phys. Rev. A* 79, 053417 (2009).
17. Experimental quantum control landscapes: Inherent monotonicity and artificial structure, J. Roslund and H. Rabitz, *Phys. Rev. A* 80, 013408 (2009).
18. Accelerated optimization and automated discovery with covariance matrix adaptation for experimental quantum control, J. Roslund, O. M. Shir, T. BŁck, and H. Rabitz, *Phys. Rev. A* 80, 043415 (2009).
19. Quantum optimal control of isomerization dynamics of a one-dimensional reaction-path model dominated by a competing dissociation channel, Yuzuru Kurosakia, Maxim Artamonov, Tak-San Ho, and Herschel Rabitz, *J. Chem. Phys.*, 131, 044306 (2009).
20. Landscape of unitary transformations in controlled quantum dynamics, T.-S. Ho, J. Dominy, and H. Rabitz, *Phys. Rev. A* 79, 013422 (2009).
21. Topology of the quantum control landscape for observables M. Hsieh, R. Wu, and H. Rabitz, *J. Chem. Phys.* 130, 104109 (2009).

Ultracold sodium and rubidium mixtures: collisions, interactions and heteronuclear molecule formation

Principal Investigator:

Dr. Chandra Raman
Assistant Professor
School of Physics
Georgia Institute of Technology Atlanta, GA 30332-0430
craman@gatech.edu

Program:

This program centers on quantum gases of ^{23}Na and ^{87}Rb , with the goal of observing collisions and interactions in binary mixtures. In the current period our research has focused on single species interactions and dynamics with a ^{23}Na Bose-Einstein condensate.

Recent Progress:

We have recently begun to explore the correspondence between a spinor Bose-Einstein condensate of sodium atoms and a quantum-mechanical rotor. Spinor BECs can offer unique insights into field-induced alignment in diatomic molecules. The role of the external aligning field is played by an external magnetic field through the quadratic Zeeman effect. Molecular rotation corresponds to rotations in spin space induced purely by interactions between atoms. For sodium atoms, with total hyperfine spin $F = 1$, the spin-dependent interactions are anti-ferromagnetic, leading to a nematic order parameter where spin alignment rather than orientation is the relevant degree of freedom. Thus a sodium BEC corresponds particularly closely to a homonuclear diatomic molecule. The moment of inertia is macroscopic in size, and therefore is very easily aligned by weak magnetic fields in the range of 0.1-1 Gauss. However, unlike a heavy diatomic, thermally occupied rotations are negligible, and the spinor BEC is very close to its energy ground state. Thus it offers insights into field induced alignment and wavepacket dynamics in a regime typically not easily accessed in other systems.

We observed the dynamics of the spinor BEC consisting of a pure $m=0$ spin projection as it was rapidly tuned from positive to negative quadratic energy shift q . The value $q = 0$ constitutes a quantum critical point. Negative q was realized using the AC Stark shift from a far-off resonance microwave field. By spatially imaging the 3 spin components of a sodium BEC, we observed a rapid dispersion of the initially localized wavepacket associated with the formation of pairs of atoms with spin projection ± 1 . These pairs appeared through a dynamical instability associated with the quantum phase transition as localized spin domains that grew in size, exhibiting coarsening dynamics.

Future Plans

Future work on spinor BEC will explore the correspondence more closely, including the possibility to observe wavepacket revivals and other nonclassical signatures of rotor dynamics.

“Coherent and Incoherent Transitions”

F. Robicheaux

Auburn University, Department of Physics, 206 Allison Lab, Auburn AL 36849
(robicfj@auburn.edu)

Program Scope

This theory project focuses on the time evolution of systems subjected to either coherent or incoherent interactions. This study is divided into three categories: (1) coherent evolution of highly excited quantum states, (2) incoherent evolution of highly excited quantum states, and (3) the interplay between ultra-cold plasmas and Rydberg atoms. Some of the techniques we developed have been used to study collision processes in ions, atoms and molecules. In particular, we have used these techniques to study the correlation between two (or more) continuum electrons.

Recent Progress 2010-2011

Transitions through a chaotic sea: Motivated by an experiment by T.F. Gallagher, we performed studies of microwave transitions when atoms were driven near, but not on, resonance.[5] The classical mechanism for the transition was an expansion of the chaotic sea to encompass the starting region of phase space; the surprise was that this classical mechanism could deliver the electron to a small range of n -states which is possible due to the stickiness of the edge the chaotic regions. We then investigated the case of kicked a Rydberg atom which we studied both classically and quantum mechanically.[18] During the past year we further extended this area by investigating molecular ro-vibrational energy transfer[20] and transfer of energy through an inflection point in the non-twist map[25]. For our molecular studies,[20] we used HF as a test system to show that we could transfer the molecule from the ground vibrational state to $v=4$ with near unit efficiency; we performed quantum calculations in full 3-D and showed that the final angular momentum distribution is restricted if the initial state is also restricted in J . We also performed calculations for a thermal distribution of J . For [25], we studied the situation where the energy and frequency do not have a monotonic relation. Systems with a monotonic relation are easy to manipulate with chirped pulses (quantum mechanically this corresponds to systems where the energy level spacing either decreases with increasing energy or the spacing increases with increasing energy). The inflection with energy prevents schemes like vibrational ladder climbing from working. We showed that adiabatically chirping through a multiphoton resonance between two states would allow us to transfer population through the inflection region.

Fluorescence as a probe of Ultracold plasmas: In a series of studies with Bergeson's experimental group, we have used experiments and simulations to investigate the early time properties of ultracold neutral plasmas. The technique uses fluorescence from excitation of the ionic core to measure the ion velocity using simulations as a guide. We focused on the earliest times, when the plasma equilibrium is evolving and before the plasma expands. To correctly model the fluorescence, we solved the optical Bloch equation for each ion in the simulation. In

the most recent paper[22], we investigated the density and temperature scaling of the disorder-induced heating of the ions. We did not find the expected scaling as the electron temperature was decreased to ~ 0 . The lack of scaling is interesting because our studies were at the earliest times where simple physics should be manifest.

Effect of plasmas on perturber states in Rydberg series: Collaboration with scientists interested in atomic processes in plasmas led to a novel idea about states imbedded in Rydberg series when the atom is in a plasma.[21,23] Resonance states in atoms or ions at low energies can control the rates of important plasma processes (e.g. dielectronic recombination). We examined the role of states at negative energies just below the ionization threshold of the recombined system and found that they can contribute as much, or more, to recombination as positive energy states because the Rydberg states are constantly being populated and mixed by the constituents of a plasma. We found that these states can substantially change thermally averaged rate coefficients and could remove much of the sensitivity of rates to the exact energy of states. The basic idea is described in Ref. [21] and the application of this idea to the experimentally accessible C^{3+} system is described in Ref. [23].

Electron impact double ionization/three electron continua: We continued our studies of electron impact double ionization of atoms. We studied the double ionization of B^+ ion[24] using the non-perturbative close-coupling method between the double-ionization threshold of 63.1 eV and the 1s ionization threshold of 218.4 eV. We computed the indirect single ionization-autoionization cross section using the perturbative distorted-wave method method between the 1s ionization threshold of 218.4 eV and 750 eV. We compared our results to a crossed-beam experiment over the entire range and found excellent agreement over the whole range.

Finally, this program has several projects that are strongly numerical but only require knowledge of classical mechanics. This combination is ideal for starting undergraduates on publication quality research. Since 2004, sixteen undergraduates have participated in this program. Most of these students have completed projects published in peer reviewed journals. One of these students, Michael Wall, was one of 5 undergraduates invited to give a talk on their research at the undergraduate session of the DAMOP 2006 meeting. The three students doing research during the 2010-11 school year will all return for research during the fall. One or two new undergraduates will be hired into the group at the beginning of the Fall 2011 semester and I expect they will continue the successful tradition of undergraduate research.

Future Plans

Global study of multiphoton ionization: T. Topcu recently started a large scale investigation of the multiphoton ionization of atoms from ground and highly excited states. For many situations, the Keldysh parameter is the only important quantity for characterizing the overall atom-strong laser interaction. We started calculations on a two dimensional grid of parameters looking for characteristic properties of the ionization rate. The two parameters we varied are the Keldysh parameter and the laser frequency divided by the classical frequency at the binding energy of the

atom. Preliminary results show that both parameters are equally important for characterizing ionization rates.

Ultra-cold plasmas The recent collaboration with Bergeson's group has raised some interesting questions about the early time evolution of ultracold plasmas. This involves the investigation of how low energy electrons scatter in the presence of ions. Extremely low temperatures, where naïve estimates give strongly coupled electrons, will be studied using collisional codes and molecular dynamics simulations. Experimental results from Bergeson and Killian's group indicate anomalous heating of the ions which we will investigate. There is also interesting results from Ed Grant's group where the positive ion is a molecule; they found substantially different behavior compared to atomic ions. We will investigate whether the electron interaction with the molecular ion could be affecting their measurements.

Anti-hydrogen motivated calculations The ALPHA group (of which FR is a member) has succeeded in trapping the antimatter version of the H atom. Thus, the main emphasis of this group has shifted to measuring the properties of the H atom which isn't directly helped by investigations supported by this grant. However, the ATRAP collaboration has been strongly pushing a double charge transfer scheme for making anti-hydrogen. Although ATRAP is a competing group, we could calculate the properties of the positronium formed in their first step as a way to help the general investigation of antimatter.

Coherent evolution Motivated by the collaboration with Landers,[7] we devoted substantial time to understanding how to simulate the interaction between two free electrons or the interaction between a free electron and a Rydberg atom. Recently, we have shown that a method for treating the Schrodinger equation is powerful and stable enough to accurately describe these extreme situations. We plan to use this program to study both a scattering situation like Ref. [7] and the dynamics of two weakly bound electrons as experimentally studied by R.R. Jones. This was the most speculative aspect of the proposal and the last major component of the original proposal that hasn't been investigated.

DOE Supported Publications (7/2008-7/2011)

- [1] S.D. Bergeson and F. Robicheaux, Phys. Rev. Lett. **101**, 073202 (2008).
- [2] F. Robicheaux, J. Phys. B **41**, 192001 (2008).
- [3] M.S. Pindzola, F. Robicheaux, and J. Colgan, J. Phys. B **41**, 235202 (2008).
- [4] J. Colgan, M.S. Pindzola, F. Robicheaux, C. Kaiser, A.J. Murray, and D.H. Madison, Phys. Rev. Lett. **101**, 233201 (2008).
- [5] T. Topcu and F. Robicheaux, J. Phys. B **42**, 044014 (2009).
- [6] T.-G. Lee, M.S. Pindzola, and F. Robicheaux, Phys. Rev. A **79**, 053420 (2009).
- [7] A.L. Landers, F. Robicheaux, T. Jahnke, M. Schoffler, T. Osipov, J. Titze, S.Y. Lee, H. Adaniya, M. Hertlein, P. Ranitovic, I. Bocharova, D. Akoury, A. Bhandary, Th. Weber, M.H. Prior, C.L. Cocke, R. Dorner, and A. Belkacem, Phys. Rev. Lett. **102**, 223001 (2009).
- [8] F. Robicheaux, J. Phys. B **42**, 195301 (2009).
- [9] A. Denning, S.D. Bergeson, and F. Robicheaux, Phys. Rev. A **80**, 033415 (2009).

- [10] G.B. Andresen et al. (ALPHA collaboration), *Phys. Plasmas* **16**, 100702 (2009).
- [11] S. Jonsell, D. P. van der Werf, M Charlton, and F. Robicheaux, *J. Phys. B* **42**, 215002 (2009).
- [12] M.S. Pindzola, J.A. Ludlow, F. Robicheaux, J. Colgan, and D.C. Griffin, *J. Phys. B* **42**, 215204 (2009).
- [13] J.A. Ludlow, J. Colgan, T.-G. Lee, M.S. Pindzola, and F. Robicheaux, *J. Phys. B* **42**, 225204 (2009).
- [14] M.S. Pindzola, J.A. Ludlow, F. Robicheaux, J. Colgan, and C.J. Fontes, *Phys. Rev. A* **80**, 052706 (2009).
- [15] F. Robicheaux, *J. Phys. B* **43**, 015202 (2010).
- [16] M. Jerkins, J.R. Klein, J.H. Majors, F. Robicheaux, and M.G. Raizen, *New J. Phys.* **12**, 043022 (2010).
- [17] M.S. Pindzola, C.P. Ballance, F. Robicheaux, and J. Colgan, *J. Phys. B* **43**, 105204 (2010).
- [18] T. Topcu and F. Robicheaux, *J. Phys. B* **43**, 115003 (2010).
- [19] T.-G. Lee, M.S. Pindzola, and F. Robicheaux, *J. Phys. B* **43**, 165601 (2010).
- [20] T. Topcu and F. Robicheaux, *J. Phys. B* **43**, 205101 (2010).
- [21] F. Robicheaux, S.D. Loch, M.S. Pindzola, and C.P. Ballance, *Phys. Rev. Lett.* **105**, 233201 (2010).
- [22] S.D. Bergeson, A. Denning, M. Lyon, and F. Robicheaux, *Phys. Rev. A* **83**, 023409 (2011).
- [23] M.S. Pindzola, S.D. Loch, and F. Robicheaux, *Phys. Rev. A* **83**, 042705 (2011).
- [24] M.S. Pindzola, J.A. Ludlow, C.P. Ballance, F. Robicheaux, and J. Colgan, *J. Phys. B* **44**, 105202 (2011).
- [25] T. Topcu and F. Robicheaux, *Phys. Rev. E* **83**, 046607 (2011).

Generation of Bright Soft X-ray Laser Beams

Jorge J. Rocca

Department of Electrical and Computer Engineering and Department of Physics

Colorado State University, Fort Collins, CO 80523-1373

rocca@engr.colostate.edu

Program description

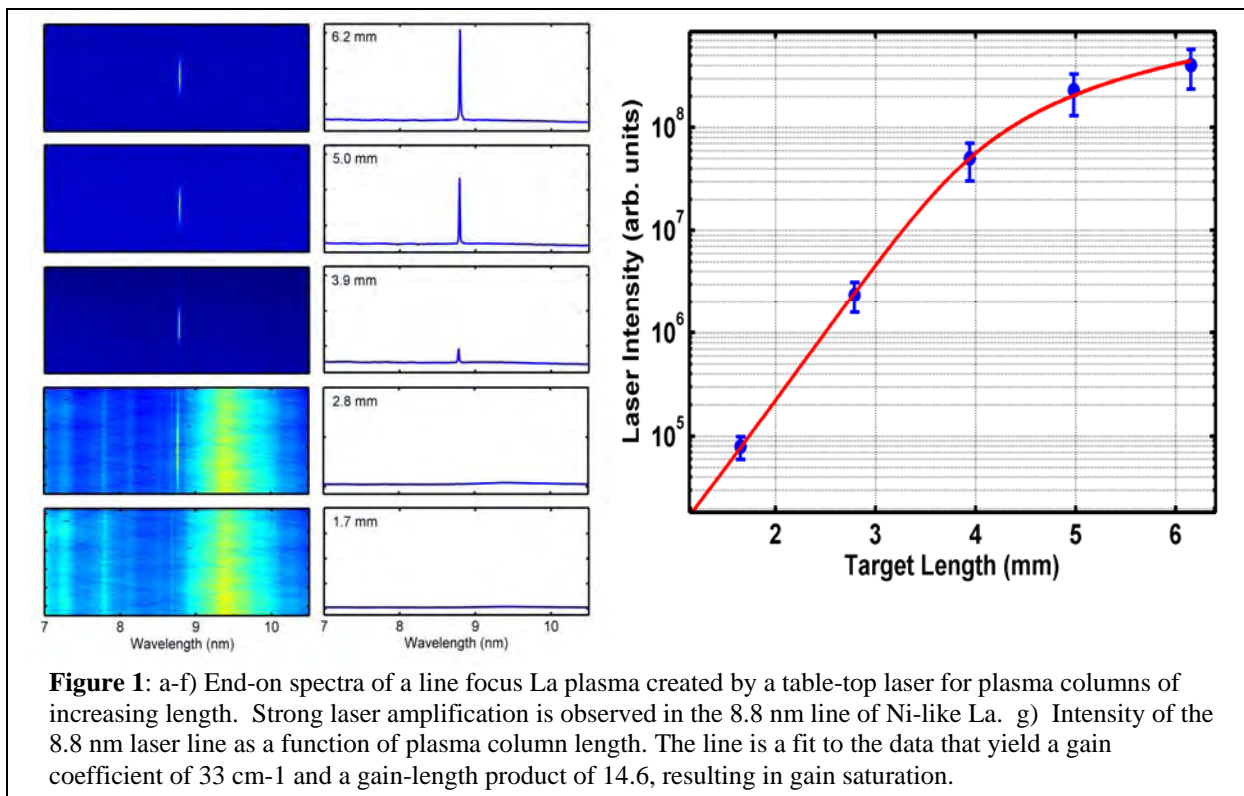
This project addresses the challenge of the efficient generation of bright x-ray laser beams. The widespread interest in the use of high intensity soft x-ray and x-ray light that has motivated the commissioning of free electron lasers also motivates the development of more compact and more readily accessible sources of intense soft x-ray laser light for applications. Table-top experiments are conducted at Colorado State University to advance the development of gain-saturated, high repetition rate, table-top plasma lasers towards shorter wavelengths. In 2010 we reported the demonstration of a gain-saturated table-top laser at $\lambda = 10.9$ nm. In more recent work we succeeded in extending gain-saturated table-top lasers to less than 10 nm for the first time. We have demonstrated a $\lambda = 8.8$ nm laser in a transition of nickel-like lanthanum, and subsequently observed lasing at increasingly shorter wavelengths by isoelectronic scaling to higher Z ions. Laser pulses of > 2 μJ energy were generated at 8.8 nm by collisional excitation in a laser-created plasma. Isoelectronic scaling of this result led to the observation of laser amplification at wavelengths down to 7.9 nm. The high plasma density at which these short wavelength soft x-ray amplifiers operate is computed to result in collisionally broaden lines that can support the amplification of sub-picosecond soft x-ray laser pulses. According to model simulations injection-seeding of these amplifiers will allow the generation of extremely intense, fully coherent, sub-picosecond soft x-ray laser pulses on a table top. Ultimately the size of compact soft x-ray lasers will be further reduced and their average power will be significantly increased using diode pump laser drivers.

Demonstration of a Gain-Saturated Table-Top Laser at $\lambda = 8.8$ nm

A goal of this project is to extend repetitive table-top soft x-ray lasers to sub-10nm wavelengths for applications. Of particular interest is the development of gain-saturated lasers producing high pulse energies and the average power required for many applications. The steep wavelength scaling of the energy necessary to pump such lasers imposes a challenge to the demonstration of gain-saturated high repetition rate lasers at sub-10 nm wavelengths. During this past year we have succeeded in extending gain-saturated table-top lasers to 8.8 nm by amplification of the $4d\ ^1S_0 \rightarrow 4p\ ^1P_1$ transition in 29 times ionized lanthanum atoms in a laser-created plasma using traveling wave excitation. This is the shortest wavelength gain-saturated table-top laser reported to date.

Lasing in nickel-like La had been first observed at Osaka using several hundred joules of optical laser pump energy to heat a collisionally pumped plasma. Subsequently another Japanese laboratory used a reduced energy of 18 J pulses from a Nd-glass laser firing a few times per hour to demonstrate lasing in this transition by transient collisional excitation. However, the gain-length product achieved was insufficient to reach the gain-saturated regime necessary for efficient amplifier operation. We have now demonstrated gain-saturate operation in this 8.8 nm laser line at 1 Hz repetition rate using significantly less pump energy. Model computations conducted using 1.5 and 2 dimension hydrodynamic/atomic physics codes developed in house suggested that gain-saturated lasing in the $\lambda = 8.8$ nm $4d\ ^1S_0 \rightarrow 4p\ ^1P_1$ transition of nickel-like La can be generated by irradiation of a solid La target with a sequence of pulses from a chirped pulse amplification laser with a total energy on target of only 7 J.

The experiment was conducted by rapidly heating a solid La slab target at 35 degrees grazing incidence with pulses from a chirped pulse amplification Ti:sapphire laser. The mismatch between the propagation velocities of the pump pulse and the amplified pulse significantly reduces the amplification of the



soft x-ray pulse, due to the short duration of the gain. To overcome this limitation an echelon mirror was used to achieve quasi-traveling wave excitation. Figure 1a shows a series of on-axis single-shot spectra and their corresponding vertical integrations for plasmas of different lengths between $L = 1.7$ and 6.2 mm. The soft x-ray laser intensity rapidly grows with target length to dominate the entire spectra, eventually reaching saturation. The corresponding measured soft x-ray laser intensity as a function of target length is shown in Figure 1b. The fit to the data shows a small signal gain of $g_0 = 33 \text{ cm}^{-1}$ and an integrated gain length product of 14.6. At about 4 mm, the intensity starts to show signs of saturation. Pumping a 8 mm wide La target with ~ 7.6 J of total laser pump energy produced laser pulses energies up to $2.7 \mu\text{J}$. The fact that collisional soft x-ray laser amplification at shorter wavelengths favors high plasma densities results in increased collisional line broadening, that can support the amplification of sub-picosecond soft x-ray laser pulses.

Observation of laser amplification at wavelengths down to 7.9 nm

Isoelectronic scaling using similar irradiation conditions resulted in lasing at shorter wavelengths. The spectra of Fig.2. shows lasing was also obtained at 8.5 nm in Ni-like Ce, at 8.2 nm in Ni-like Pr, and at 7.9 nm in Ni-like Nd. The latter is the shortest wavelength laser line reported to date from a table-top laser. The laser emission at 8.5 nm is strong and by comparison with the measurements for the 8.8 nm amplifier it is estimated to be not far from reaching gain saturation. Future plans also include efforts to demonstrate gain-saturated operation in these transitions. We are also working to obtain lasing on other transitions at wavelengths between 9 and 10 nm.

Study of spectral linewidth of a Ne-like Ar capillary discharge soft x-ray laser and its dependence on amplification

Capillary discharge lasers remain to date as the highest average power table-top source of coherent extreme ultraviolet radiation, and the 46.9 nm Ne-like Ar laser is the table-top soft x-ray laser most broadly utilized in applications. This very practical table-top laser has been widely characterized. However, the spectral line-width and the temporal coherence, which are important parameters for applications such as interferometry and large area nano-patterning, had not been measured. The

measurement of the line-width behavior is also of interest for fundamental reasons: this laser differs from collisional soft x-ray lasers created by laser heating of solid targets in that the inhomogeneous component of the linewidth greatly exceeds the homogenous component. The electron density in the capillary discharge lasers is typically up to two order of magnitude lower, while the ion temperature exceeds the electron temperature. Consequently the Doppler broadening contribution dominates the Voigt line profile, and the collisional component is less significant. This inhomogeneous line profile could be expected to lead to inhomogeneous Doppler saturation re-broadening not previously observed in studies of line amplification in soft x-ray amplifiers.

The relatively low electron density and moderate ion temperature that characterizes the capillary discharge plasma amplifiers gives origin to a small linewidth that is further narrowed in the amplification process well beyond the resolution of normal spectrometers. We have measured the line profile using a wavefront-division interferometer specifically designed to measure the temporal coherence of soft x-ray sources, and compared the results to model simulations.

The variation of the line-width as a function of amplifier plasma column was measured for plasma lengths between 18 cm and 36 cm. The line profile was inferred from the measurements of the fringe visibility as a function of path difference in the interferometer. The experimental set up is shown in Fig. 3a. Figure 3b shows the measured variation of the fringe visibility as a function of optical path difference for a 27 cm long capillary plasma column. The figure also shows raw interferograms corresponding to different path differences, along with a Gaussian fit to the data that yields a temporal coherence length of $\sim 700 \mu\text{m}$ (when defined as the e^{-1} point in the visibility curve), and a spectral bandwidth of $\Delta\lambda/\lambda = 3.5 \times 10^{-5}$. Figure 3c shows the measured variation of the laser line bandwidth as a function of plasma column length. This graph shows measurements for plasma column lengths that are shorter and longer than the gain saturation length of $L \sim 24$ cm. Figure 3c also compares the data with the result of model simulation that compute the line propagation along the amplifier taking into account gain saturation and refraction losses. The line corresponds to a plasma with an electron density of $2 \times 10^{18} \text{ cm}^{-3}$, derived from the beam divergence measured from far-field beam refraction pattern, to an electron temperature of 100 eV, and to an ion temperature of 150 eV. Line narrowing is observed to take place as the line is amplified. After saturation the line does not re-broaden, as could be expected for an inhomogeneously broadened line, but instead asymptotically reaches a linewidth of $\Delta\lambda/\lambda \sim 3 \times 10^{-5}$. Our line transport model simulations indicate that collisional redistribution, previously shown to affect the amplification dynamics of laser-pumped collisional soft x-ray lasers, also precludes saturation re-broadening in capillary discharge lasers even when these lasers operate at up to two orders of magnitude lower plasma density. In the absence of collisional redistribution the dominantly Gaussian profile is computed to result in re-broadening of the line after saturation. The inclusion of collisional redistribution results in good agreement with the experimental data.

The measured linewidth of this laser, $3-4 \times 10^{-5}$, corresponds to a coherence time of ~ 2 picoseconds that is significantly shorter than its pulse duration, of $\sim 1-1.5$ ns. The ratio of temporal coherence to laser

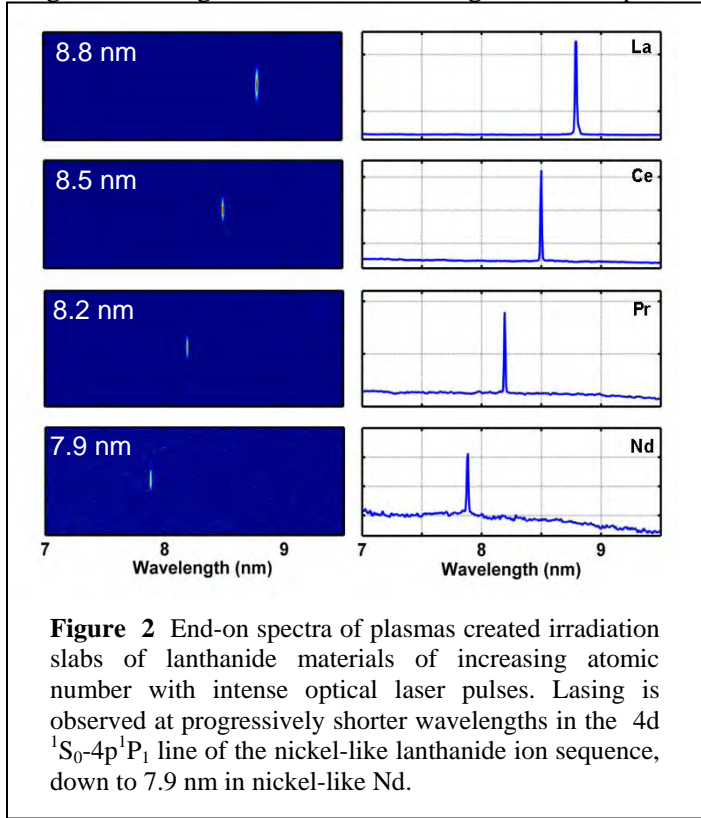


Figure 2 End-on spectra of plasmas created irradiation slabs of lanthanide materials of increasing atomic number with intense optical laser pulses. Lasing is observed at progressively shorter wavelengths in the $4d \ ^1S_0-4p \ ^1P_1$ line of the nickel-like lanthanide ion sequence, down to 7.9 nm in nickel-like Nd.

pulse duration for the capillary discharge 46.9 nm laser is thus significantly lower than those previously measured in transient collisional SXRLs created by laser irradiation of solid targets, due to the fact that the capillary discharge laser is essentially a quasi-CW laser with a laser pulse duration that is more than two orders of magnitude longer than both its upper laser level lifetime. Nevertheless, the temporal coherence length of 600-800 μm measured in this capillary discharge SXRL is among the largest from all soft x-ray lasers, which facilitates applications such as interferometry and large area nano-patterning that require a long coherence length.

Journal publications resulting from DOE-BES supported soft x-ray laser development work (2009-2011)

1. L.M. Meng, D. Alessi, O. Guilbaud, Y. Wang, M. Berrill, B.M. Luther, S.R. Domingue, D.H. Martz, D. Joyeux, S. De Rossi, J.J. Rocca, and A. Klisnick, "Temporal coherence and spectral linewidth of an injection-seeded transient collisional soft x-ray laser", *Optics Express*, **19**, 12087, (2011)
2. A.H. Curtis, B. A. Reagan, K. A. Wernsing, F. J. Furch, B. M. Luther, and J.J. Rocca, "Demonstration of a Compact 100 Hz, 0.1 J, Diode-Pumped Picosecond Laser", *Optics Letters*, **36**, 2164, (2011)
M. Berrill, B.M. Luther, and J.J. Rocca, "1 Hz Operation of a Gain-Saturated 10.9 nm Table-Top Laser in Nickel-like Te," *Optics Letters*, **35**, 414 (2010).
3. M. Berrill, D. Alessi, Y. Wang, S.R. Domingue, D.H. Martz, B.M.Luther, Y. Liu and J.J. Rocca; "Improved beam characteristics of solid-state target soft x-ray laser amplifiers by injection seeding with high harmonics", *Optics Letters*, **35**, 2317, (2010)
4. Y. Wang, M. Berrill, F. Pedaci, M.M. Shakya, S. Gilbertson, Z. Chang, E. Granados, B.M. Luther, M.A. Larotonda, and J.J. Rocca, "Measurement of 1 Picosecond Soft X-Ray Laser Pulses from an Injection-Seeded Plasma Amplifier," *Physical Review A* **79**, 023810 (2009)
5. F. Furch, B. Reagan, B. Luther, A. Curtis, S. Meehan, and J.J. Rocca, "Demonstration of an all-diode-pumped soft x-ray laser," *Optics Letters*, **34**, 3352 (2009)
6. L. Urbanski, M. Marconi, L.M. Meng, M. Berrill, O. Gilbaud, A. Klisnick and J.J. Rocca, "Spectral linewidth of a capillary discharge table-top soft x-ray laser and its dependence on amplification", submitted (2011) .

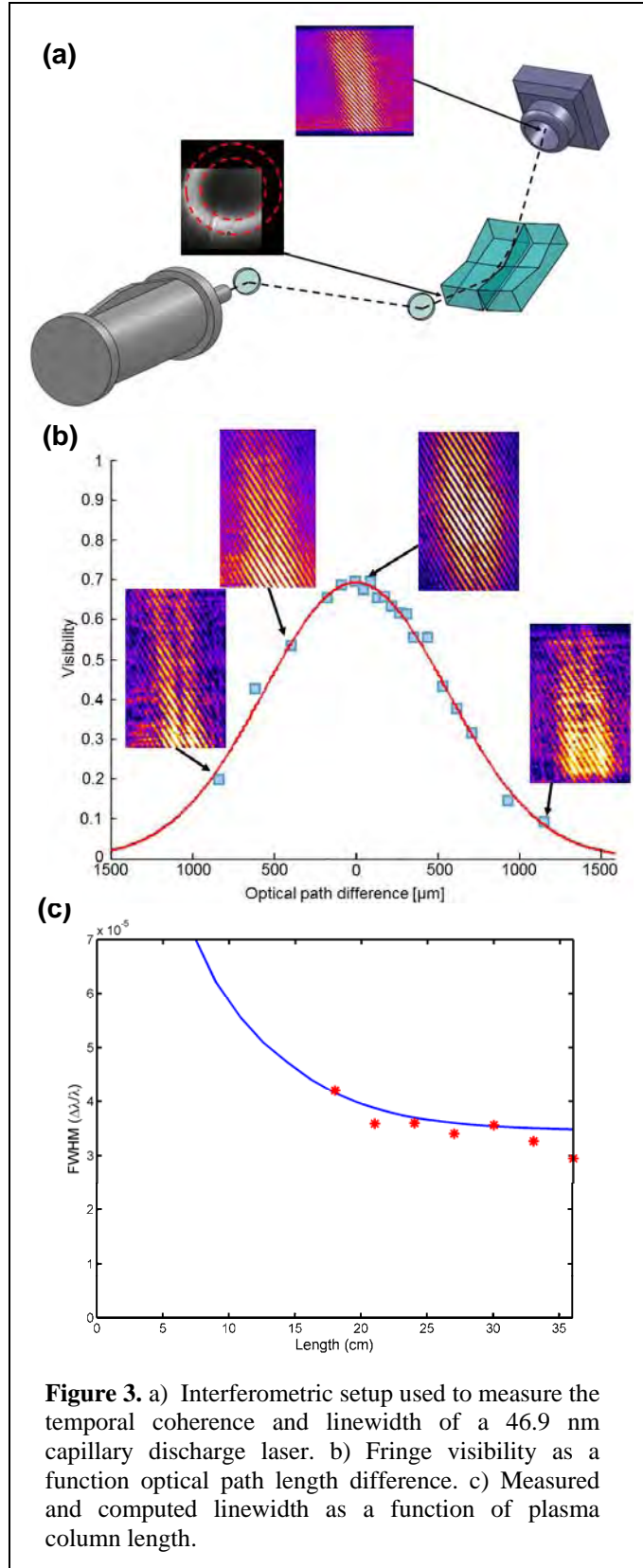


Figure 3. a) Interferometric setup used to measure the temporal coherence and linewidth of a 46.9 nm capillary discharge laser. b) Fringe visibility as a function optical path length difference. c) Measured and computed linewidth as a function of plasma column length.

Spatial Frequency X-ray Heterodyne Imaging of Micro and Nano structured Materials and their Time-resolved Dynamics

Christoph G. Rose-Petruck

Department of Chemistry, Box H, Brown University, Providence, RI 02912
phone: (401) 863-1533, fax: (401) 863-2594, Christoph_Rose-Petruck@brown.edu

Program Scope

Our previously completed work originally focused the x-ray phase contrast imaging of the dynamics of physical and chemical systems. During the course of the study new experimental opportunities and results emerged that somewhat changed the direction of the research project and resulted in several publications.¹⁻⁸ Specifically, a new x-ray absorption spectrometer was developed at the Advanced Photon Source, sector 7, ID-C and used for x-ray absorption measurements of the ligand substitution reaction of $\text{Fe}(\text{CO})_5$ in ethanol with 2ps temporal resolution.¹⁻³ Based on this work we applied for Partner-user status at the APS, which recently was granted for the period from the fall 2011 to the fall 2013. During this time we will receive 10% of the beamline's beamtime for further development and application of the picosecond x-ray instrument.

Our work on x-ray phase contrast imaging will be continued with the development of a novel x-ray imaging concept we named X-ray Spatial Frequency Heterodyne Imaging (XSFHI).⁴⁻⁶ As the name suggests the technique relies on the introduction of a "local oscillator" in the spatial frequency space of an x-ray image. Mathematical cross-terms between the local oscillator and the spatial frequency spectrum of the sample, lead to signal enhancements of selectable spatial frequency components that result in image contrast enhancements by orders of magnitude. In contrast to conventional or phase contrast x-ray imaging, a single exposure can be processed to obtain 1) the traditional x-ray absorption image and 2) an image formed exclusively by deflected or scattered x-rays. The signal in the scattered radiation image is depended on, for instance, the size and orientation of nanostructures or phase interfaces in the sample. We have demonstrated that the image contrast is several orders of magnitude larger than that of phase contrast, which itself typically is 3 orders of magnitude larger than for conventional x-ray absorption imaging. For high emittance x-ray sources or motion blurred samples, the XSFHI makes phase contrast features visible that would otherwise be undetectable. The method does not use any x-ray optics and is well-suited to time resolved imaging studies.

1 Recent Progress

During the last year progress has been made in three research topics funded by this DOE grant.

1.1 Time resolved XAFS at 7ID-C, APS

In collaboration with Dr. Bernhard Adams and Dr. Mathieu Chollet, Argonne National Laboratory, we have set up an UXAFS instrument at 7-ID-C. It consists of a high-speed x-ray chopper, liquid sample jet chamber with laser and x-ray beam diagnostic followed by an x-ray streak camera. Three papers describe the first experimental results as well as the technical advances.¹⁻³ The preliminary data analysis of the time-resolved data for the measurements of the chemical dynamics of $\text{Fe}(\text{CO})_5$ in ethanol has been described in last year's BES-AMOS abstract and is not further discussed here. The latest technical improvements of the ultrafast system are summarized below:

1. The streak camera and x-ray optics have been improved. The streak camera can now operate at any repetition rate. This has become possible by replacing the sweep voltage trigger based on a photoconductive switch, with a photodiode. Its signal is pulse shaped and amplified in microwave amplifiers yielding a sweep voltage that has no measurable laser-streak jitter. Since the photodiode needs only a very small amount of laser light (we use a stray reflection of an optical surface), the entire laser power can be used for sample excitation. The camera has been



Figure 1: Cover page of PCCP¹ showing a sketch of the 2-ps XAFS spectrometer at 7ID-C of the Advanced Photon Source.

successfully operated at about 80MHz repetition rate, driven by a Ti:Sapphire oscillator. As a consequence, the streak electronics is ready for making better use of the APS repetition rate and experiment repetition rates are now only limited by the available laser infrastructure.

2. An x-ray beam transport system consisting of refractive and reflective x-ray optics has been installed. Two refractive lenses with focal lengths of about 15 meters focus the beam to about $20 \times 50 \mu\text{m}$. At the focus position an additional curved x-ray mirror in von Hamos geometry is used to further focus the beam in horizontal direction, resulting in a spot of about $20 \times 10 \mu\text{m}$. We plan to insert 2 such mirrors this year to reduce the overall spot size to 5 to $10 \mu\text{m}$. As a consequence, the pump laser beam size could be reduced which improves the excitation yield of the samples.
3. The sample handling and pump system has been upgraded. It now consists of a glove box located next to the XAFS apparatus. Air-sensitive sample can be prepared in the box and filled into the sample pumping system installed in the glove box. Since the sample chamber where the liquid sample beam and the laser and x-ray beam intersect are purged with dry nitrogen, the integrity of sample throughout an experiment can be guaranteed.

1.2 Time resolved XSFH imaging of laser-induced carbon steam reaction

Spatial Harmonic Imaging uses the x-radiation scattered off the sample to form an image. A related method using single-crystal x-ray mirrors is known as diffraction-enhanced imaging. In SHI however, the deflection of x-rays from the primary beam direction is detected by placing an absorption grid between the sample and the camera as shown in the lower panel of Figure 3. The logarithm of the detected image intensity is proportional to the product of the absorbances of the sample and the grid. Fourier transformation of the image converts this product into a convolution. The grid, being a periodic structure, produces a series of peaks in the spatial frequency domain. Each peak is “surrounded” by the spatial frequency spectrum of the sample. An example is shown in Figure 2. The leftmost image in Figure 2 shows the x-ray absorption image of a liquid sample jet of water with 75-nm carbon nanoparticles at a concentration of 50 g / L. The jet has a diameter of 1 mm. An ultrafast-laser driven x-ray source emitted x-rays with emission lines in the 10-keV spectral range. The size of the x-ray emitting volume is $38 \mu\text{m}$ (horiz.) \times $13 \mu\text{m}$ (vert.). The source-sample distance was 30 cm, and the sample-detector distance was 70 cm. A commercial 2-dimensional wire mesh, henceforth referred to as grid, with $50.8\text{-}\mu\text{m}$ pitch was installed between the sample and the detector. The image was acquired with a liquid nitrogen-cooled x-ray CCD camera (Roper Scientific, model: 7382-0001). The CCD chip was directly exposed to the x-rays. In order to

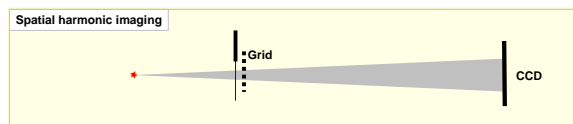


Figure 3: Layout of ultrafast imaging setups for XSFHI. A liquid beam serves a sample and the laser plasma source serves as an x-ray point source. A metal grid with $50.8\text{-}\mu\text{m}$ pitch is inserted between the sample and x-ray CCD.

avoid overexposure of the camera chip, short exposures were acquired and subsequently added until a total exposure time of 3600 s was achieved. The sample is illuminated with 200-ps, 800-nm, 200- μJ laser pulses at an incidence angle indicated by the arrow in Figure 2. With a laser repetition rate of 5 kHz, the evolution of the bubbles in the downward flowing jet is imaged in 200- μs steps. Owing to the simultaneous arrival of laser pump and x-ray probe pulses at the sample, no bubble is visible at time zero. The laser focus diameter is $75 \mu\text{m}$ and the absorption depth in the suspensions is $57 \mu\text{m}$. Thus, about 1.1 nmol of carbon atoms are within the laser focus. Upon laser pulse heating, the carbon nanoparticles undergo a carbon steam reaction and possibly further reactions such as the water-gas shift reaction. Considering the heating and evaporation of the water as well as the

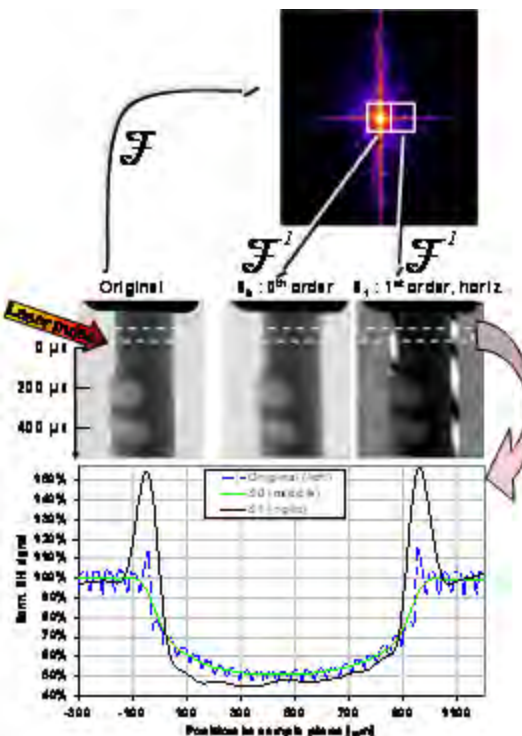


Figure 2: Diagram of the image processing steps of SHI. The original image of a liquid sample jet containing 75 nm carbon nanoparticles is reproduced on the left side. 200 ps laser pulses illuminate the jet at the position indicated by the straight arrow. The image is Fourier transformed yielding the spatial frequency spectrum at the top. Selecting the 0th and the 1st order areas and back transforming them yields S0, the 0th order harmonic image (middle) and S1, the 1st order harmonic image (right). The intensity profiles are shown at the bottom.

heating of the carbon to reaction temperature, the entire reaction is endothermic with an enthalpy of reaction of about 185 kJ / mol. The laser pulse provides just enough energy to convert completely all carbon particles within the laser focus volume into gas, producing a bubble with a theoretical maximum diameter of 0.5 mm. This size is in agreement with the bubble diameter shown in Figure 2. Since the nano particles are displaced by the expanding gas, we found that the higher particle concentration surrounding the bubble leads to an enhanced 1st order signal, which indicates that for the first time the concentration change of nanoparticles during chemical processes can be directly imaged. Owing to the particle heating and their subsequent chemical reaction, the particles should disappear during the laser-pulse exposure. This effect should result in a decrease of the 1st order signal on the time scale of hundreds of picoseconds, an effect that we attempt to observe in the coming year.

1.3 Theoretical description of XSFHI

We derived an expression for the electric field at the image plane from the Kirchhoff-Fresnel integral for a grating in contact with an object in an X-ray, in-line imaging configuration that shows the grating to give a heterodyning effect. We also show how image contrast in a harmonic of the grating is enhanced depending on the 1st space derivative of the phase function. Experiments were carried out where a Fourier component of the image intensity gives an improvement in contrast at the edge of an object that about 2 orders of magnitude larger than that found with conventional phase contrast imaging.

Consider a parallel beam of X-radiation whose intensity is recorded at a distance z from an object and absorption grating. The electric field $f(\vec{x})$ at the image plane for an object with a transmission function $q(\vec{X})$ that varies in one dimension only is described in the paraxial ray approximation by the Kirchhoff-Fresnel integral

$$f(\vec{x}, z, \lambda) = \sqrt{\frac{i}{\lambda z}} e^{-i\vec{k}z} \iint q(\vec{X}, \lambda) e^{-\frac{ik(\vec{x}-\vec{X})^2}{2z}} d\vec{X}. \quad (1)$$

k is the wave number of the x-radiation. It is possible to write the transmission function of the object and an absorption grating whose absorbance varies between zero and infinity as

$$q(\vec{X}) = \exp(i\varphi(\vec{X}) - \mu(\vec{X})) g(\vec{X}) \quad (2)$$

where g is the square wave function of a grating with a wavenumber k_g and φ and μ are the phase shift and absorbance of the object. After some algebra and considering that the x-ray intensity $I(\vec{x}) = |f(\vec{x})|^2$ we get

$$I(\vec{x}) = \frac{1}{2} (1 + \cos(2k_g x)) \left[\begin{aligned} & 1 - 2(\beta \sin(\beta) + \cos(\beta)) \mu(\vec{x}) + 2 \sin(\beta) \frac{\lambda z}{4\pi} \mu''(\vec{x}) \\ & - 2\beta \cos(\beta) \phi(\vec{x}) + 2 \sin(\beta) \phi(\vec{x}) + \frac{\lambda z}{2\pi} \cos(\beta) \phi''(\vec{x}) \end{aligned} \right], \quad (3)$$

$$+ \sin(2k_g x) \left[\frac{\lambda z}{4\pi} k_g (\sin(\beta) \mu'(\vec{x}) - \cos(\beta) \phi'(\vec{x})) \right]$$

with $\beta = \lambda z k_g^2 / 4\pi$. It can be seen that the image has only two heterodyned frequency components, a steady component and a second component modulated sinusoidally at a frequency $2k_g x$. Fourier transformation of (3), selection of the component at $2k_g$, back transformation of this component into coordinate space, division of this component by the identical quantity for the grating alone, and forming the magnitude of the resulting expression gives a normalized heterodyned image denoted I_{+2} . Assuming a pure phase object, i.e., $\mu \equiv 0$, we get

$$I_{+2} = \sqrt{\left[1 + 2(\sin(\beta) - \beta \cos(\beta)) \phi(\vec{x}) + \frac{\lambda z}{2\pi} \cos(\beta) \phi''(\vec{x}) \right]^2 + \left[\frac{\lambda z}{2\pi} k_g \cos(\beta) \phi'(\vec{x}) \right]^2}, \quad (4)$$

For typical experimental setups β is small and (4) simplifies to

$$I_{+2} = \sqrt{\left[1 + \frac{\lambda z}{2\pi} \phi''(\vec{x}) \right]^2 + \left[\frac{\lambda z}{2\pi} k_g \phi'(\vec{x}) \right]^2}, \quad (5)$$

which shows an altogether new dependence of image contrast on the first space derivative of the phase ϕ' with an amplitude enhancement factor of $\lambda z / 2\pi k_g$ arising from heterodyning of the spatial frequencies of the object with that of

the grating. The image contrast is expected to be dominated by ϕ' rather than ϕ'' because the latter is multiplied by the factor $\lambda z/2\pi$ which is small in the X-ray spectral region. Note that the intensity of the 1st derivative can be “amplified” by choosing a finer pitch, i.e., larger k_g , grating. Equation (5) is tested by imaging the edge of a 25 μm Kapton foil. The measurement was done with a microfocus x-ray tube (Trufocus, Inc., TFX-3110EW, x-ray spot diameter: 10 μm) with a tungsten anode operated at 96 kV. Considering the emission spectrum, the transmittances of all materials in the x-ray beam path, and the fluorescence efficiency of the camera’s phosphor screen, the maximum sensitivity is at an x-ray photon energy of approximately 17 keV. At this photon energy, the foil was a rather weak phase object (x-ray phase shift = 130°) with nearly no absorption. The results of the measurement are shown in Figure 4. The maximum of the phase contrast signal (which is proportional to ϕ'') is about 0.15%, which is less than the absorbance contrast. The maximum of I_{+2} normalized to the slight increase of the scatter signal between air and the Kapton foil is 21, i.e. more than 2 orders of magnitude larger. As expected, the I_{+2} signal has the shape of the a 1st derivative of the electron density step function convoluted with the resolution of the imaging system.

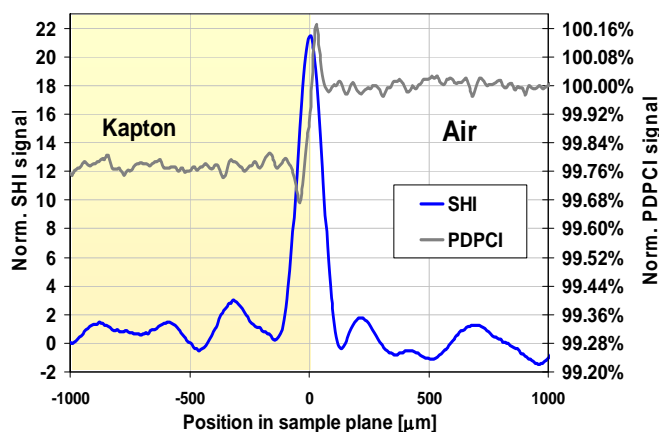


Figure 4: Phase-contrast (PDPCI) profile of an image of a 25 μm thick Kapton foil plotted on a logarithmic scale. I_{+2} : scatter image (SHI) profile extracted from the same exposure.

The maximum of the phase contrast signal (which is proportional to ϕ'') is about 0.15%, which is less than the absorbance contrast. The maximum of I_{+2} normalized to the slight increase of the scatter signal between air and the Kapton foil is 21, i.e. more than 2 orders of magnitude larger. As expected, the I_{+2} signal has the shape of the a 1st derivative of the electron density step function convoluted with the resolution of the imaging system.

Future plans

The goal of the present funding cycle is to continue the research on Spatial Frequency X-ray Heterodyne Imaging and related techniques using the setups at 7ID-C and at Brown University. Specifically, we will

1. continue the development of the theoretical framework of X-ray Spatial Frequency Heterodyne Imaging,
2. continue XSFHI experiments using the laser-driven plasma x-ray source at Brown University. The goal is to obtain information on the micro-scale structural dynamics during chemical reactions. Primary application: phase transitions in nanoparticle suspensions and in clathrate hydrate slurries.
3. Carry out ultrafast x-ray powder diffraction measurements on melting clathrate hydrates.
4. Implement XSFHI at 7 ID-C in order to carry out phase contrast and XSFH imaging experiments with high spatial resolution and in the anomalous dispersion regime of transition metals in preparation for future ultrafast oxidation state sensitive x-ray heterodyne imaging.

Papers acknowledging this DOE grant

1. "Picosecond x-ray absorption measurements of the ligand substitution dynamics of Fe(CO)₅ in ethanol," B. Ahr, M. Chollet, B. Adams, E. M. Lunny, C. M. Laperle and C. Rose-Petruck, Phys. Chem. Chem. Phys. 13 (Also PCCP Cover Page, April 2011) (13), 5590 (2011).
2. "2-ps Hard X-Ray Streak Camera Measurements at Sector 7 Beamline of the Advanced Photon Source (invited)," M. Chollet, B. Ahr, D. A. Walko, C. Rose-Petruck and B. Adams, Selected Topics in Quantum Electronics, IEEE Journal of in press (DOI: 10.1109/JSTQE.2011.2105464) (2011).
3. "Hard X-ray streak camera at the advanced photon source," M. Chollet, B. Ahr, D. A. Walko, C. Rose-Petruck and B. Adams, Nuclear Instruments and Methods in Physics Research Section A: Accelerators, Spectrometers, Detectors and Associated Equipment in press (DOI: 10.1109/JSTQE.2011.2105464) (2011).
4. "X-ray spatial harmonic imaging of phase objects," Y. Liu, B. Ahr, A. Linkin, J. D. Gerald and C. Rose-Petruck, Optics Letters 36, 2209 (2011).
5. "Gold Nanoparticle-Enhanced X-ray Detection of Liver Cancer Cells," D. Rand, V. Ortiz, Y. L. Z. Derdak, J. R. Wands, M. Tatfček and C. Rose-Petruck, Nanoletters Publication Date (Web): June 6 (2011).
6. "Spatial frequency x-ray heterodyne imaging," B. Wu, Y. Liu, J. D. Gerald and C. Rose-Petruck, Optics Express submitted (2011).
7. "X-ray Phase Contrast Imaging: Transmission Functions Separable in Cylindrical Coordinates," G. Cao, T. Hamilton, C. M. Laperle, C. Rose-Petruck and G. J. Diebold, J. Appl. Phys. 105, 102002 (2009).
8. "X-ray elastography: Modification of x-ray phase contrast images using ultrasonic radiation pressure," T. J. Hamilton, C. Bailat, S. Gehring, C. M. Laperle, J. Wands, C. Rose-Petruck and G. J. Diebold, Journal of Applied Physics 105 (10), 102001 (2009).

Tamar Seideman
Department of Chemistry, Northwestern University
2145 Sheridan Road, Evanston, IL 60208-3113
t-seideman@northwestern.edu

New Directions in Intense-Laser Alignment

1. Program Scope

Alignment by moderately intense laser pulses developed, during the past 15 years, from a theoretical dream into an active field of research with a rapidly growing range of applications in optics, physics and spectroscopy.

Our previous DOE-supported research in this area has successfully extended the concept of nonadiabatic alignment from the domain of isolated, rigid diatomic molecules to complex systems, including nonrigid molecules, large polyatomic molecules, solvated molecules, molecular assembly, and molecular junctions. Although part of this research has been continued during the past year, aimed at the extension of alignment from the domain of physics and optics to make a tool in material science, solution chemistry, and possibly engineering, our main effort this year has been devoted to the problem of high harmonic generation (HHG) from aligned molecules. This research was motivated by the intense interest of the AMOS Program in attosecond science and rescattering electrons physics, and has been mostly carried out in collaboration with AMOS colleagues.

Our work on methodology development and applications in the area of HHG from aligned molecules is discussed in Secs. 2.1–2.2 and its extension in future research is outlined in Sec. 3.1. Our work on laser alignment in complex materials is discussed in Sec. 2.3–2.4 and our future plans in this area are outlined in Sec. 3.2. Section. 2.5 summarizes briefly our recent and ongoing work on the role of alignment in laser filamentation.

2. Recent Progress

2.1 Extracting Electron Dynamics from Experimental High Harmonic Signals

In ongoing work in collaborations with AMOS colleagues Murnane and Kapteyn, we combine high quality HHG experimental signals with our previously developed exact theory of high harmonics from aligned molecules¹ to extract the fundamental electronic dipole elements that embody the complex electron dynamics giving rise to HHG. Our analysis points to a previously unexplored process in HHG, wherein the continuum electronic wavepacket gains angular momentum from the photon field to recombine at a higher angular momentum state than that with which it is ejected into the continuum. Such electron angular momentum non-conserving events dominate over angular momentum conserving processes for both CO₂ and N₂O, increasingly so as the harmonic order grows. Interestingly, our experimental data indicates that only a few electron partial waves contribute to the HHG dynamics. Clearly, our analysis provides needed benchmarking for numerical calculations of these fundamental electronic dipole elements. We showed also that the high-order nature and structural sensitivity of HHG make it particularly attractive as a means of studying rotational coherences. Although this was demonstrated in our theoretical work before,¹ the present work is the first to substantiate this argument with sufficiently high-accuracy data. A joint publication is in preparation.

2.2 Signatures of the Molecular Potential in the Ellipticity of High-Order Harmonics from Aligned Molecules

In recent work, we explore the information content of the polarization of high-order harmonics emitted from aligned molecules driven by a linearly polarized field. The study builds upon our previous publication,² which illustrated that the phase of the continuum electronic wavefunction,

and hence the underlying molecular potential, is responsible, at least in part, for the ellipticity observed in harmonic spectra. We use a simple model potential and systematically vary the potential parameters to investigate the sense in which, and the degree to which, the shape of the molecular potential is imprinted onto the polarization of the emitted harmonics. Strong ellipticity is observed over a wide range of potential parameters, suggesting that the emission of elliptically polarized harmonics is a general phenomenon, yet qualitatively determined by the molecular properties. The sensitivity of the ellipticity to the model parameters invites the use of ellipticity measurements as a probe of the continuum wavefunction and the underlying molecular potential. An article is in press in Physical Review A.³

2.4 Molecular Focusing and Alignment with Plasmon Fields

In a recent publication, we show the possibility of simultaneously aligning molecules and focusing their center-of-mass motion near a metal nanoparticle in the field intensity gradient created by the surface plasmon enhancement of incident light. The rotational motion is described quantum mechanically while the translation is treated classically. The effects of the nanoparticle shape on the alignment and focusing are explored. Sharp molecular focusing occurs in the plasmon-enhanced fields for all nanoparticle shapes. Our results suggest the potential application of metal nanoparticles and their arrays to create molecular nanopatterns with orientational and spatial order that are both subject to control. These results invite also the extension of our approach to trap atoms or ions in the plasmon-enhanced inhomogeneous field, with potential applications in logic and lithography. An article appeared in NanoLetters.⁵

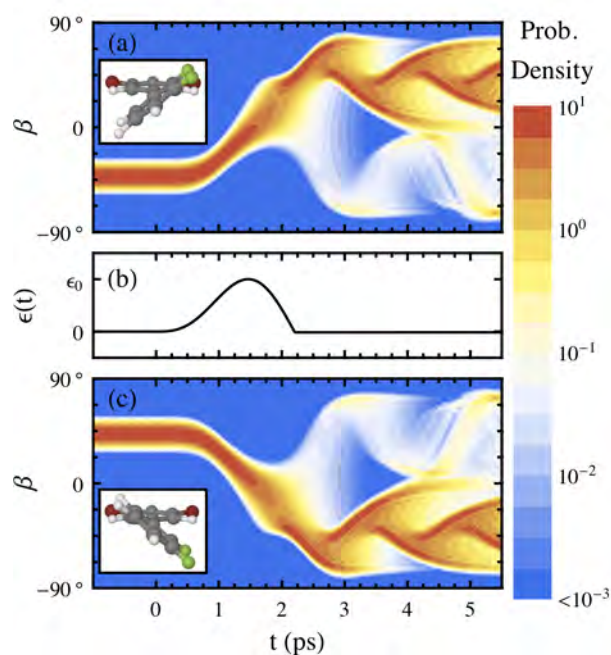


FIG. 1: Demonstration of stereochemistry inversion via torsional alignment. At $t = 0$ ps a half-cycle pulse inverts the molecular stereochemistry. (a) Inversion from “R” to “S”. (b) The half-cycle pulse envelope. (c) Inversion from “S” to “R”.

2.3 Coherent Torsional Alignment

In a recent study we extend the concept of nonadiabatic laser alignment to address the case of nonrigid polyatomics. Specifically, we propose a coherent, strong-field approach to control the torsional modes of polyatomic molecules, and develop a numerical scheme to simulate the torsional

dynamics. By choice of the field parameters, the method can be applied either to fix the torsion angle to an arbitrary configuration or to induce free internal rotation in a predetermined sense. Transient absorption spectroscopy is suggested as a general probe of torsional control and the usefulness of this approach is numerically explored. Several consequences of our ability to manipulate molecular torsional motions are considered. These include a method for the inversion of molecular chirality and an ultrafast chiral switch. The former application is briefly considered in Fig. 1, which illustrates the results of an “inversion” pulse. Analysis of the time-dependent probability density shows that immediately after the pulse, over 96 % of the wavefunction is successfully inverted (i.e. over 96 % of the “R” species is transformed into “S” and vice-versa) while an efficiency of more than 90 % is maintained for the duration of the simulation. The conversion efficiency could be enhanced with the aid of an optimal control method. An article was submitted for publication in the Journal of Chemical Physics.⁴

2.5 The Role of Nonadiabatic Alignment in Laser Filamentation

In recent studies, we combine short-pulse pump-probe experiments with alignment and rotational revivals calculations to explore fundamental processes in laser filamentation in air. Specifically, we study the fluorescence intensities from two bands as a function of the pump-probe time delay. Our experimental and numerical results are interpreted in terms of a universal phenomenon of population trapping of nitrogen molecules in highly excited states. Along with field induced alignment and rotational revivals of the nitrogen molecules, the population trapping gives rise to enhancement and periodic modulation of the signal, which are fully explained by our theory. An article appeared in J. Phys. B.⁶ A review article is in press.⁷

3. Future Plans

In the course of the next 3 years, we will continue to focus on attosecond science (Sec. 3.1), this topic being one of steadily growing interest to the AMOS program and a research field where there are opportunities for theoretical work to explore new physics. We will also continue and extend our work on the extension of alignment to address current problems in material science (Sec. 3.2). Although we will continue our research on the theory and applications of laser filamentation, this work will no longer be supported through our DOE grant, and hence is not discussed in this section.

3.1 High Harmonic Generation and Attosecond Science. A Time Dependent Density Functional Theory

Our short term goal in this area is to explore, in collaboration with the group of Murnane and Kapteyn, the problem of elliptical dichroism in HHG from aligned molecules. Our preliminary results, based on the combination of fully quantum calculations, a semiclassical theory, and measurements, unravel new and interesting physics in the dynamics of electrons driven by elliptically polarized laser fields with direct consequences on the observed dichroism. We hope to submit a joint publication within the next few months.

During the next 1–2 years, we will develop a new numerical method for calculation of HHG signals that will extend our current capabilities, Ref. 2, in a significant way. Our approach will be based on a real time time-dependent density functional theory (TDDFT), currently under development in my group. We will test the new method by application to the case of simple linear molecules, for which we currently have reliable results from solutions of the Schrödinger equation. It will be our main goal, however, to extend the method to polyatomic molecules. Here we will combine our (already tested) approach to establishing 3D alignment by means of elliptically polarized fields⁸ with a TDDFT solution of the driven electronic dynamics. These studies will be complemented by semiclassical trajectory calculations that will serve both to provide qualitative insights and to simplify aspects of the calculation. One of our long term goals will be to apply attosecond pulses to a condensed matter problem.

3.2 Alignment in Complex systems. Toward Applications in Material Science

Within the next 2 years, we will explore two new applications of intense laser alignment in material science. The first study, in collaboration with a Northwestern experimental group, will establish long-range orientational order in an assembly of semiconductor nanorods. The theoretical component will involve a molecular dynamics study using analytical polarizabilities and two-body interactions. The second study will apply torsional alignment to control transport via molecular heterojunctions. Here we will consider an array of substituted biphenyl molecules contacted to a semiconducting surface and a metal tip. We will account for the enhancement and spatial localization of the incident field by the tip using a three-dimensional finite-difference time-domain approach for the numerical solution of Maxwell's equations, and describe the current within the nonequilibrium Green Function framework. Work toward both goals has been initiated.

4. Publications from DOE sponsored research (past three years, in citation order)

1. S. Ramakrishna and T. Seideman, *High-Order Harmonic Generation as a Probe of Rotational Dynamics*, Phys. Rev. A, **77**, 053411 (2008).
2. S. Ramakrishna, P. Sherratt, A. Dutoi and T. Seideman, *Origin of Ellipticity in High Harmonic Generation from Aligned Molecules*, Phys. Rev. A Rapid Communication **81**, 021802(R) (2010).
3. P. Sherratt, S. Ramakrishna and T. Seideman, *Signatures of the Molecular Potential in the Ellipticity of High-Order Harmonics from Aligned Molecules*, Phys. Rev. A, in press.
4. S. M. Parker, M. A. Ratner and T. Seideman, *Coherent Control of Molecular Torsion*, submitted for publication in J. Chem. Phys.
5. M. Artamonov and T. Seideman, *Molecular Focusing and Alignment with Plasmon Fields*, Nano Letters, **10** 4908 (2010).
6. A. Azarm, S. Ramakrishna, A. Talebpour, S. Hosseini, Y. Teranishi, H. L. Xu, Y. Kamali, J. Bernhardt, S. H. Lin T. Seideman, and S. L. Chin, *Population Trapping and Rotational Revival of N₂ Molecules During Filamentation Of A Femtosecond Laser Pulse in Air*, J. Phys. B. **43**, 235602 (2010).
7. S. L. Chin, T. J. Wang, C. Marceau, J. Wu, J. S. Liu, O. Kosareva, N. Panov, Y. P. Chen, J-F Daigle, S. Yuan, A. Azarm, W. W. Liu, T. Seideman, H. P. Zeng, M. Richardson, R. Li, and Z. Z. Xu, *Advances in intense femtosecond laser filamentation in air*, Laser Physics, in press.
8. M. Artamonov and T. Seideman, *On the Optimal Approach to Field-Free 3D Alignment of Asymmetric Tops*, Phys. Rev. A **82**, 023413 (2010).
9. C. Marceau, S. Ramakrishna, S. Génier, T.-J. Wang, Y. Chen, F. Théberge, M. Châteauneuf, J. Dubois, T. Seideman, and S. L. Chin, *Femtosecond Filament Induced Birefringence in Argon and in Air: Ultrafast Refractive Index change*, Optics Communications **283**, 2732 (2010).
10. G. Pérez-Hernández, A. Pelzer, L. Gonzalez and T. Seideman, *Biologically Inspired Molecular Machines Driven by Coherent Light. A unidirectional Rotor*, Special Issue of New J.Phys. **12** 075007 (2010).
11. D. Shreenivas, A. Lee, N. Walter, D. Sampayo, S. Bennett and T. Seideman, *Alignment as a Route to Control of Surface Reactions*, J. Phys. Chem. **114**, 5674 (2010)
12. S. S. Viftrup, V. Kumarappan, L. Holmegaard, H. Stapelfeldt, M. Artamonov and T. Seideman, *Controlling the Rotation of Asymmetric Top Molecules by the Combination of A Long and A Short Laser Pulse*, Phys. Rev. A, **79**, 023404 (2009).
13. M. G. Reuter, M. Sukharev, and T. Seideman, *Laser Field Alignment of Organic Molecules on Semiconductor Surfaces: Toward Ultrafast Molecular Switches*, Phys. Rev. Lett. **101**, 208303 (2008).
14. I. Barth, L. Serrano-Andrés and T. Seideman, *Nonadiabatic Orientation, Toroidal Current, and Induced Magnetic Field in BeO Molecules*, J. Chem. Phys. **129**, 164303 (2008).
15. A. Pelzer, S. Ramakrishna and T. Seideman, *Optimal Control of Rotational Motions in Dissipative Media*, J. Chem. Phys. **129**, 134301 (2008).
16. M. Artamonov and T. Seideman, *Theory of Three-Dimensional Alignment by Intense Laser Pulses*, J. Chem. Phys. , **128** 154313 (2008).

New Scientific Opportunities through Inelastic X-ray Scattering at 3rd- and 4th-Generation Light Sources

PI: Gerald T. Seidler (seidler@uw.edu)
Department of Physics, University of Washington
Box 351560
Seattle WA 98195-1560

Program Scope

The goal of this program is to broaden the range of applications of resonant and nonresonant inelastic x-ray scattering and x-ray emission spectroscopies at both 3rd- and 4th-generation light sources. This includes the long-term goal of enabling and performing studies of x-ray nonlinear and/or nonequilibrium effects at XFEL facilities.

Recent Progress

Our recent progress divides into three categories: continued improved of the miniature x-ray spectrometers ("miniXS") that promise to greatly expand the use of x-ray emission spectroscopy (XES) at lightsources; use of these spectrometers over a wide range of scientific issues, often including penetration of the method into entirely new fields; new theoretical developments in the calculation of inelastic x-ray scattering from novel states of matter produced by extreme interactions of radiation with matter, such as at large-scale optical laser facilities or at the LCLS.

First, the refinement and construction of miniXS spectrometers has continued. Briefly, these instruments use arrays of flat-crystal analyzers placed relatively near to the sample in order to enable high collection solid angles while retaining energy resolutions generally better than the relevant core-hole lifetime of the species being excited. This approach is enabled by the high brilliance of synchrotron light sources and the availability of effectively zero-noise x-ray cameras. During FY2010-11 we have expanded the use of rapid prototype machining ("3D plastic printing") in miniXS fabrication, building several instruments where the entire spectrometer body and optical support is fabricated from "printed" plastic. [14,15] The net cost of these instruments has this been reduced to a few thousand dollars, less than 10% the cost of developing spectrometers with similar performance using traditional spherically-bent crystal analyzers. We have also initiated a side-project with the potential for order-of-magnitude improvement in collection efficiency. Plastically-deformed Si and Ge crystals have recently been investigated as possible optical components in hand-held commercial XRF units. [See, *e.g.*, Nakajima, et al., *Nature Mater.* 2005, Hayahsi, et al., *Rev. Sci. Instrum.* 2008] Unlike those studies, where the Si or Ge was hot-pressed at temperatures near their melting points, we are investigating the flash-heating by radio-frequency induction methods of

elastically-deformed Si to induce final plastic deformation. We have demonstrated radii of curvature as small as 5 cm for 0.3-mm thick Si wafers. If mosaicity is indeed suppressed by our process, as initial results indicate, then such miniature focusing x-ray optics can be used to dramatically improve the collection solid angle of miniXS instruments at little cost in energy resolution. Inexpensive, high-resolution x-ray emission spectrometers with collection angles of $\sim 1\text{-}2\%$ of 4π sr would thus become feasible.

Second, we have used miniXS spectrometers in numerous projects and collaborations aimed at improving the range of applications of high-resolution XES. Projects have included: micro-speciation and imaging of heterogeneous Co-rich catalysts seeing commercial use in the petroleum industry [20]; a comparative study of XANES and XES for determination of coordination populations in multi-phase and amorphous systems, such as fuel-cell catalytic membranes [19]; high-resolution studies of radiation-damage effects in photosystem-II [21]; investigation of core-hole effects and mixed-valency in f-electron compounds [16]; investigation of XES as a new method to determine the oxygen fugacity, and hence primary geophysical origin in the upper mantle, of igneous rocks [17]; investigation of the pressure-induced f-orbital volume collapse of Pr [15]. The PI's participation in the APS upgrade process and involvement in the ISS beamline at NSLS-II also involve popularization of XES, such as by miniXS spectrometers or other high-throughput optics. We anticipate that our first time-resolved XES studies at APS will occur in the 2011-3 beamrun.

Third, building on the highly-successful FEFF code of our colleague and collaborator John Rehr, we have extended the real-space full multiple scattering (RSFMS) approach to include calculation of Compton scattering profiles, *i.e.*, the probability density function for the electronic momenta in both valence and core levels. [12] This fills an important niche in IXS experiments on condensed phases performed under extreme conditions at laboratory-based high-power laser facilities (*i.e.*, NIF, LLE) and at LCLS. Whereas the Compton profile can be calculated with high-reliability and precision by band-structure methods for perfectly crystalline materials, there has not previously been a general tool to include truly condensed-phase effects for systems of limited spatial order but high densities. We find excellent agreement between theory and experiment for room-temperature and 'warm dense matter' Be, and are now extending the calculations for comparison to an experiment performed by an LLNL team at the AMO/LCLS endstation.

Future Plans

We will continue each of the above-mentioned thrusts in the coming year. An emphasis will be placed on submission of the several manuscripts that are nearing completion [12-21]. Anticipated highlights of new work in

FY2011-12 include: time-resolved XRD and XES studies of the metal-insulator transition of unstrained VO₂ single crystals, a system for which we have just completed the first polarization-dependent XANES study [13]; time-resolved XES studies of UV-active 'quantum cutting' phosphors; further application of the RSFMS Compton calculations to 'warm dense matter' systems, such as from experimental conditions of NIF or LLE; theoretical evaluation of plasmon damping effects on XANES in condensed phase systems with high electron temperatures induced by XFEL irradiation; and new LCLS proposals for instrument development and applications of ultrafast XES.

Publications during the term of this award

Submitted, accepted, or in print:

1. J.A. Bradley, A. Sakko, G.T. Seidler, et al, "Revisiting the Lyman-Birge-Hopfield Band of N₂," *accepted*, Physical Review A (2011).
2. Subhra Sen Gupta, J. A. Bradley, et al., "Coexistence of Bound and Virtual-bound States in Shallow-core to Valence Spectroscopies," *accepted*, Physical Review B (2011).
3. R.A. Gordon, G.T. Seidler, T.T. Fister, K.P. Nagle, "Studying low-energy core-valence transitions with bulk sensitivity using *q*-dependent NIXS," J. Elect. Spect. Related Phenom., **184**, 220 (2011).
4. A. F. Tillack, K. M. Noone, B. A. MacLeod, et al., "Surface Characterization of Polythiophene:Fullerene Blends on Different Electrodes using Near Edge X-ray Absorption Fine Structure," ACS Applied Materials and Interfaces **3**, 726 (2011).
5. D.W. Liu, Y.Y. Liu, A.Q. Pan, et al., "Enhanced Lithium-Ion Intercalation Properties of V₂O₅ Xerogel Electrodes with Surface Defects," Journal of Physical Chemistry C **115**, 4959 (2011).
6. J.A. Bradley, Ping Yang, E.R. Batista, et al., "Experimental and Theoretical Comparison of the O *K*-Edge Nonresonant Inelastic X-ray Scattering and X-ray Absorption Spectra of NaReO₄," Journal of the American Chemical Society **132**, 13914 (2010).
7. J.A. Bradley, G.T. Seidler, G. Cooper, M. Vos, A.P. Hitchcock, A.P. Sorini, C. Schlimmer, K.P. Nagle, "Comparative Study of the Valence Electronic Excitations of N₂ by Inelastic X-ray and Electron Scattering," Physical Review Letters **105**, 053202 (2010).
8. A. Sakko, C. Sternemann, Ch.J. Sahle, et al., "Suboxide interface in disproportionating α -SiO studied by x-ray Raman scattering," Physical Review B **81**, 205317 (2010).
9. J.A. Bradley, S. Sen Gupta, G.T. Seidler, et al., "Probing Electronic Correlations in Actinide Materials Using Multipolar Transitions," Physical Review B **81**, 193104 (2010).
10. O.M. Feroughi, C. Sternemann, C.J. Sahle, et al., "Phase separation and Si nanocrystal formation in bulk SiO studied by x-ray scattering," Applied Physics Letters **96**, 081912 (2010).
11. T. Gog, G.T. Seidler, D.M. Casa, et al., "Momentum-resolved Resonant and Nonresonant Inelastic X-ray Scattering at the Advanced Photon Source," Synchrotron Radiation News **22** (6), 12 (2009).

Manuscripts in preparation:

12. B.A. Mattern, G.T. Seidler, J. Kas, J.J. Rehr, "A Real-space Multiple-scattering Approach to Calculations of Compton Profiles From Ordered and Disordered Condensed Phases," *to be submitted*, Phys. Rev. B, 2011.
13. J.I. Pacold, J.T. Vinson, J.J. Kas, et al., "Polarization-dependent XANES through the metal-insulator transition in unstrained VO₂ single crystals," *in preparation*, Phys. Rev. Lett. 2011.
14. B.A. Mattern, G.T. Seidler, M. Haave, et al., "Fabrication of Miniature X-ray Spectrometers by Rapid Prototype Machining: Fe K β and valence emission," *to be submitted*, Rev. Sci. Instrum., 2011.
15. J.I. Pacold, G.T. Seidler, J.A. Bradley, et al., "A Miniature X-ray Spectrometer for High-Pressure Studies of the Pr Volume Collapse," *to be submitted*, Rev. Sci. Instrum., 2011.
16. R.A. Gordon, T.K. Sham, B. Mattern, et al., "Core-hole Effects and Nominal Mixed Valency of Ionic Ce Compounds Studied by Nonresonant and Resonant IXS," *to be submitted*, Phys. Rev. B, 2011.
17. J.I. Pacold, G.T. Seidler, C. Plummer, O. Bachmann, "Oxygen Fugacity and High-resolution X-ray Emission Spectromicroscopy of Igneous Rocks," *in preparation*, 2011.
18. G.T. Seidler, J.I. Pacold, "Plastic Deformation of Si by Rapid Thermal Treatment: Suppression of Polygonization," *in preparation*, J. Appl. Phys., 2011.
19. B. A. Mattern, G. T. Seidler, J. Kropf, D. Myers, C. Johnston, G. Wu, "Identifying the population of local metal-ion coordination in non-precious metal catalysts via a comparison of x-ray absorption and x-ray emission spectroscopies", *in preparation*, 2011.
20. S. Kelly, S. Bare, J.I. Pacold, G.T. Seidler, "Resonant and Nonresonant X-ray Emission Spectroscopy as a New Method for Micro-Speciation of Co in Catalysts for Production of low-sulfur Gasolines," *in preparation*, 2011.
21. K. , Y. Pushkar, J.I. Pacold, B.A. Mattern, G.T. Seidler, "A Room-Temperature Study of Radiation Damage Effects of Photosystem-II via High-Resolution Mn K β X-ray Emission Spectroscopy," *in preparation*, 2011.

DYNAMICS OF FEW-BODY ATOMIC PROCESSES

Anthony F. Starace

*The University of Nebraska
Department of Physics and Astronomy
855 North 16th Street, 208 Jorgensen Hall
Lincoln, NE 68588-0299*

Email: astarace1@unl.edu

PROGRAM SCOPE

The goals of this project are to understand, describe, control, and image processes involving energy transfers from intense electromagnetic radiation to matter as well as the time-dependent dynamics of interacting few-body, quantum systems. Investigations of current interest are in the areas of strong field (intense laser) physics, attosecond physics, high energy density physics, and multiphoton ionization processes. Nearly all proposed projects require large-scale numerical computations, involving, e.g., the direct solution of the full-dimensional time-dependent or time-independent Schrödinger equation for two-electron (or multi-electron) systems interacting with electromagnetic radiation. In some cases our studies are supportive of and/or have been stimulated by experimental work carried out by other investigators funded by the DOE AMOS physics program. Principal benefits and outcomes of this research are improved understanding of how to control atomic processes with electromagnetic radiation and how to transfer energy from electromagnetic radiation to matter.

RECENT PROGRESS

A. Perturbation Theory Analysis of Attosecond Photoionization

We have recently presented a detailed analysis of ionization of an atom by a few-cycle attosecond xuv pulse using perturbation theory (PT), keeping terms in the transition amplitude up to second order in the pulse electric field. Within the PT approach, we have presented an *ab initio* parametrization of the ionized electron angular distribution (AD) using rotational invariance and symmetry arguments. This parametrization gives analytically the dependence of the AD on the carrier envelope phase (CEP), the polarization of the pulse, and on the ionized electron momentum direction, \mathbf{p} . For the general case of an elliptically polarized pulse, we show that interference of the first- and second-order transition amplitudes causes a CEP-dependent asymmetry (with respect to $\mathbf{p} \rightarrow -\mathbf{p}$) and both elliptic and circular dichroism effects. All of these effects are maximal in the polarization plane and depend not only on the CEP but also on the phase of dynamical atomic parameters that enter our parametrization of the AD.

Within the single active electron model of an atom, for an initial *s* or *p* state we define all dynamical parameters in terms of radial matrix elements (analytic expressions for which are given for the Coulomb and zero-range potentials). For ionization of the H atom by linearly polarized pulses, our PT results are in excellent agreement with results of numerical solutions of the time-dependent Schrödinger equation of Peng *et al.* [1]. Also, our numerical results show that the asymmetries and dichroism effects at low electron energies have a *different physical origin* from those at high electron energies. Moreover, our results for Gaussian and cosine-squared pulse shapes are in good qualitative agreement. Finally, we show that our analytic formulas may prove useful for determining few-cycle extreme ultraviolet (xuv) pulse characteristics, such as the CEP and the polarization. (*See reference [6] in the publication list below.*)

B. Potential Barrier Features in Two-Photon Ionization Processes in Atoms

The development of novel, intense, and tunable X-ray sources opens a new regime in which nonlinear processes in the soft X-ray region can now be investigated. As was the case in single-photon ionization processes, in which many prominent features in photoionization cross sections and in photoelectron angular distributions were understood by means of a model potential approach (see, e.g., A.F. Starace, Theory of Atomic Photoionization, *Handbuch der Physik* **31**, ed. W. Mehlhorn (Springer-Verlag, Berlin, 1982), pp. 1-121), such an approach may be expected to provide similar understanding for multiphoton processes. We have obtained an extensive set of model potential results on the frequency dependence of two-photon ionization cross sections from inner subshells of rare gas and other closed-shell atoms. Our initial investigations have focused on potential barrier effects. We have used second order perturbation theory in the X-ray field and sum intermediate states using the well-known Dalgarno-Lewis method (A. Dalgarno and J.T. Lewis, *Proc. R. Soc. A* **233**, 70 (1955)). When one photon is above threshold, we employ a complex coordinate rotation method to calculate the two-photon amplitude (B. Gao and A.F. Starace, *Computers in Physics* **1**, 70 (1987)).

Our results for two-photon ionization of various subshells of Ar and Xe (as well as other results for Au, Ag, Cu, and Hg) indicate that potential barrier effects may be general features of multiphoton ionization processes. (We are currently investigating three-photon processes to confirm this expectation.) For the two-photon cases considered here, the most dramatic results occur in ATI processes when the intermediate-state electron wave packet having a high orbital angular momentum probes the corresponding potential barrier. Far from being merely a convenient way to sum over a complete set of intermediate states, the intermediate-state electron wave packet obtained by solving the Dalgarno-Lewis equation may be used to obtain insight into key features of two-photon processes. In the two-photon ionization case, in which the final-state electron probes the potential barrier, Cooper minima originating from rapid changes in the final-state phase shift are also likely to be common features, but require more systematic investigations. We emphasize that while electron correlations will alter these results quantitatively, the dramatic resonance-like enhancements that we predict represent a qualitatively correct guide for both experiments and also for more detailed theoretical calculations. (*See reference [7] in the publication list below.*)

C. Evidence of the $2s2p(^1P)$ Doubly-Excited State in the Harmonic Generation Spectrum of Helium

We have solved the fully dimensional time-dependent Schrödinger equation for a two-active-electron system (helium) in an intense and ultrashort laser field in order to study the role of electron correlation in the resonant enhancement of some harmonics in the HHG spectrum. Whereas in the tunneling regime the HHG rate has been shown to be proportional to the field-free photorecombination cross section (and hence to exhibit any correlation features in that cross section), the parameters of our present calculation are in the multiphoton regime, for which such a proportionality has not been predicted. However, based on perturbation theory arguments, electron correlations should be expected to play a role.

Our non-perturbative numerical calculations have focused on identifying signatures of the well-isolated He $2s2p(^1P)$ autoionizing state on the 9th, 11th, and 13th harmonics for a range of driving laser frequencies ω_L that put these harmonics in resonance with that state (from the ground state). Despite the fact that He is the simplest and most fundamental multi-electron system, our results show that isolating the resonant enhancement of the particular harmonics we investigated is complicated by both low-order multiphoton resonances with singly-excited states and also by resonant coupling between different autoionizing states. Nevertheless, our results show that when resonant coupling between doubly-excited states is absent, the resonant enhancement of the He $2s2p(^1P)$ autoionizing state on the 9th and 13th harmonics is clearly observable when one examines the ratio of the harmonic powers of these two harmonics with those of their lower order neighboring harmonics. These ratios serve to remove the effect

of low-order multiphoton resonances with singly-excited states and thus isolate the effect of the resonance with the autoionizing state.

Experimental observation of the results presented here seems feasible for experiments employing a spatially-shaped (flat-top) focus. However, even for a Gaussian-shaped driving laser pulse, our results show that resonance behavior as a function of driving laser frequency may be observable. We have shown results as a function of driving laser frequency in the narrow frequency range $4.6 \text{ eV} \leq \omega_L \leq 6.6 \text{ eV}$, within which lie the fundamental frequency of the KrF laser and the 3rd, 4th, and 5th harmonics of the tunable Ti:Sapphire laser. Only a small variation of the driving laser frequency is sufficient to scan the peak of the predicted resonances. Moreover, the predicted results appear to be reasonably insensitive to variations of intensity. In particular, the energy shifts of the resonance maxima with driving laser intensity appear to be smaller in magnitude than the widths of the resonance profiles. (*See reference [8] in the publication list below.*)

D. Perturbation Theory Analysis of Ionization by a Chirped Few-Cycle Attosecond Pulse

The angular distribution of electrons ionized from an atom by a chirped few-cycle attosecond pulse has been analyzed using the perturbation theory (PT) approach developed in Ref. [6], keeping terms in the transition amplitude up to second order in the pulse electric field. The dependence of the asymmetry in the ionized electron distributions on both the chirp and the carrier-envelope phase (CEP) of the pulse are explained physically using a simple analytical formula that approximates the exactly calculated PT result. This approximate formula (in which the chirp dependence is explicit) reproduces reasonably well the chirp-dependent oscillations of the electron angular distribution asymmetries found numerically by solving the time-dependent Schrödinger equation, as in Ref. [5]. It can also be used to determine the chirp rate of the attosecond pulse from the measured electron angular distribution asymmetry. (*See reference [9] in the publication list below.*)

FUTURE PLANS

Our group is currently carrying out research on the following additional projects:

(1) Attosecond Streaking in the Low-Energy Region

We have analyzed few-cycle XUV attosecond pulse carrier-envelope-phase effects on ionized electron momentum and energy distributions in the presence of a few-femtosecond IR laser pulse. Whereas attosecond streaking usually involves high-energy photoelectrons, when photoelectrons have low initial kinetic energies, the IR field can control the continuum-electron dynamics by deflecting the photoelectrons so that they scatter from the residual ion. Using a semiclassical model, we show that the various possible trajectories of the photoelectrons in the continuum can be revealed by the interference patterns exhibited in the low-energy photoelectron spectrum. Our analysis explains unusual asymmetric structures predicted previously by direct solution of the time-dependent Schrödinger equation [1]. This work has been submitted for publication.

(2) CEP Effects in Ionization Plus Excitation of He

We are currently modelling XUV attosecond pulse ionization plus excitation processes in He using codes that enable us to solve the two-electron, time-dependent Schrödinger equation in its full dimensionality; our preliminary results show large CEP-sensitive effects.

PUBLICATIONS STEMMING FROM DOE-SPONSORED RESEARCH (2008 – 2011)

- [1] L.Y. Peng, E.A. Pronin, and A.F. Starace, “Attosecond Pulse Carrier-Envelope Phase Effects on Ionized Electron Momentum and Energy Distributions: Roles of Frequency, Intensity, and an Additional IR Pulse,” *New J. Phys.* **10**, 025030 (2008).
- [2] N.L. Manakov, A.F. Starace, A.V. Flegel, and M.V. Frolov, “Threshold Phenomena in Electron-Atom Scattering in a Laser Field,” *JETP Lett.* **87**, 92 (2008).
- [3] L.-Y. Peng, Q. Gong, and A.F. Starace, “Angularly Resolved Electron Spectra of H⁺ by Few-Cycle Laser Pulses,” *Phys. Rev. A* **77**, 065403 (2008).
- [4] A. V. Flegel, M. V. Frolov, N. L. Manakov, and Anthony F. Starace, “Plateau Structure in Resonant Laser-Assisted Electron-Atom Scattering,” *Phys. Rev. Lett.* **102**, 103201 (2009).
- [5] L.Y. Peng, F. Tan, Q. Gong, E.A. Pronin, and A.F. Starace, “Few-Cycle Attosecond Pulse Chirp Effects on Asymmetries in Ionized Electron Momentum Distributions,” *Phys. Rev. A* **80**, 013407 (2009).
- [6] E. A. Pronin, A. F. Starace, M. V. Frolov and N. L. Manakov, “Perturbation Theory Analysis of Attosecond Photoionization,” *Phys. Rev. A* **80**, 063403 (2009).
- [7] L.-W. Pi and A.F. Starace, “Potential Barrier Effects in Two-Photon Ionization Processes,” *Phys. Rev. A* **82**, 053414 (2010).
- [8] J.M. Ngoko Djiokap and A.F. Starace, “Evidence of the $2s2p(^1P)$ Doubly Excited State in the Harmonic Generation Spectrum of He,” *Phys. Rev. A* (Accepted, in press).
- [9] E.A. Pronin, L.-Y. Peng, and A.F. Starace, “Perturbation Theory Analysis of Ionization by a Chirped, Few-Cycle Attosecond Pulse,” *Phys. Rev. A* (Accepted, in press).

FEMTOSECOND AND ATTOSECOND LASER-PULSE ENERGY TRANSFORMATION AND CONCENTRATION IN NANOSTRUCTURED SYSTEMS

DOE Grant No. DE-FG02-01ER15213

Mark I. Stockman, PI

Department of Physics and Astronomy, Georgia State University, Atlanta, GA 30303

E-mail: mstockman@gsu.edu, URL: <http://www.phy-astr.gsu.edu/stockman>

Annual Report for the three-year Grant Period of 2009-2011 (Publications 2009-2011)

1 Program Scope

The program is aimed at theoretical investigations of a wide range of phenomena induced by ultrafast laser-light excitation of nanostructured or nanosize systems, in particular, metal/semiconductor/dielectric nanocomposites and nanoclusters. Among the primary phenomena are processes of energy transformation, generation, transfer, and localization on the nanoscale and coherent control of such phenomena.

2 Recent Progress and Publications

During the current report period, the following papers have been supported by this DOE grant. Published in 2011 are: [1-4], in 2010 are: Refs. [5-10], and in 2009 are: Refs. [11-19]. Most of these publications are in top-level refereed journals [1-3, 5-10, 13, 15, 16]; there is also a book chapter [19] and an advance preprint publication in the ArXiv [4]. Below we highlight the recent publications that we consider the most significant.

2.1 Nanoplasmonics: The Physics behind the Application [3]

Nanoplasmonics is a relatively young science but it has already reached in phenomena that lead to important applications in physics, chemistry, biomedicine, environmental monitoring and national security. In this feature article [3] in the most widely read professional physics journal, *Physics Today*, we have considered the fundamental phenomena of nanoplasmonics in their relation to the applications that they have inspired and are underlying.

2.2 Metallization of Nanofilms in Strong Adiabatic Electric Fields [10]

We have introduced [10] an effect of metallization of dielectric nanofilms by strong, adiabatically varying electric fields normal to the film. The metallization causes optical properties of a dielectric film to become similar to those of a plasmonic metal (strong absorption and negative permittivity at low optical frequencies). This is a quantum effect, which is exponentially size-dependent, occurring at fields on the order of 0.1 V/\AA and pulse durations ranging from $\sim 1 \text{ fs}$ to $\sim 10 \text{ ns}$ for a film thickness of $2\text{--}10 \text{ nm}$. This effect can be used for devices that can be described as lightwave-controlled field effect transistors working in a bandwidth up to $\sim 100 \text{ THz}$. When the film is metallized, its optical properties change dramatically; in particular, the reflection coefficient of this film increases from almost zero to 10 percent. This predicted effect has stimulated at least one recent publication [1] – see Sec. 2.4.

2.3 Spaser Action, Loss Compensation, and Stability in Plasmonic Systems with Gain [2]

This work deals with one of the most important problems in nanooptics and nanoplasmonics: extremely high optical losses in existing plasmonic metamaterials render them practically unusable. One of the ways proposed to mitigate or even completely eliminate those losses is based on adding a gain medium and using quantum amplification to compensate those losses [20, 21]. This approach is based on our idea of spaser [8, 17, 18, 22].

We have developed [2] a general analytical theory of the loss compensation in dense resonance metamaterials, which all the existing optical metamaterials are. We have demonstrated that the conditions of spaser generation and the full loss compensation in a dense resonant plasmonic-gain medium (metamaterial) are identical. Consequently, attempting the full compensation or overcompensation of losses by gain will lead to instability and a transition to a spaser state. This will limit (clamp) the inversion and lead to the limitation on the maximum loss compensation achievable. The criterion of the loss overcompensation, leading to the instability and spasing, is given in an analytical and universal (independent from system's geometry) form.

2.4 Nearfield Enhanced Electron Acceleration from Dielectric Nanospheres by Intense Few-Cycle Laser Fields [1]

This work has been inspired to a significant degree by our recent work on metallization of dielectrics by intense optical fields [4, 10]. It is expected that in the optical fields of magnitude $\sim 1 \text{ V/\AA}$ dielectric may behave, under certain circumstances, as metals – see Sec. 2.2.

Collective electron motion in condensed matter typically unfolds on a sub-femtosecond timescale. The well-defined electric field evolution of intense, phase-stable few-cycle laser pulses provides an ideal tool for controlling this motion. The resulting manipulation of local electric fields at nanometer spatial and attosecond temporal scales offers unique spatio-temporal control of ultrafast nonlinear processes at the nanoscale, with important implications for the advancement of nanoelectronics. In this article [1] we have demonstrated the attosecond control of the collective electron motion and directional emission from isolated dielectric (SiO_2) nanoparticles with phase-stabilized few-cycle laser fields. A novel acceleration mechanism leading to the ejection of highly energetic electrons is identified by the comparison of the results to quasi-classical model calculations. The observed lightwave control in nanosized dielectrics has important implications for other material groups, including semiconductors and metals.

2.5 Spaser as a Nanoscopic Generator and Ultrafast Amplifier of Nanolocalized Optical Fields [8, 18]

The Surface Plasmon Amplification by Stimulated Emission of radiation (SPASER) has been introduced by us in the DOE-supported work [22-25]. The SPASER is the “missing link” of nanoplasmonics: a quantum generator of nanolocalized optical fields. Recently, the SPASER has been experimentally observed in a series of publications [26-28].

The SPASER is now recognized as an invention protected by a US Patent [18] just issued by USPTO. We have shown recently that SPASER is ultrafast (bandwidth over 10 THz) and can work as a logical amplifier [8, 17]. Thus, it is capable of performing the same function as MOSFET within the same $\sim 10 \text{ nm}$ form factor but ~ 1000 times faster. We anticipate that the SPASER will become as ubiquitous and important an element in nanooptics as a transistor is in microelectronics.

2.6 Surface-Plasmon-Induced Drag-Effect Rectification (SPIDER) [12, 13]

We have predicted a giant surface-plasmon-induced drag-effect rectification (SPIDER), a new effect that exists under conditions of the extreme nanoplasmonic confinement. In nanowires, this giant SPIDER generates rectified THz potential differences up to 10 V and extremely strong electric fields up to $\sim 10^5\text{--}10^6 \text{ V/cm}$. The giant SPIDER is an ultrafast effect whose bandwidth for nanometric wires is $\sim 20 \text{ THz}$. It opens up a new field of ultraintense THz nanooptics with wide potential applications in nanotechnology and nanoscience, including microelectronics, nanoplasmonics, and biomedicine.

2.7 Ultrafast Active Plasmonics [16]

Surface plasmon polaritons (SPPs), propagating bound oscillations of electrons and light at a metal surface, have great potential as information carriers for next-generation, highly integrated nanophotonic devices. A number of techniques for controlling the propagation of SPP signals have been demonstrated. However, with sub-microsecond or nanosecond response times at best, these techniques are too slow for future applications. We have reported that femtosecond optical frequency plasmon pulses can be modulated on the femtosecond timescale by direct ultrafast optical excitation of the metal, thereby offering unprecedented terahertz modulation bandwidth—a speed of many orders of magnitude faster than existing technologies. This work was done in collaboration with experimental group of Prof. N. Zheludev (University of Southampton, UK).

2.8 Coherent Control on the Nanoscale [5]

Our research has significantly focused on problem of controlling localization of the energy of ultrafast (femtosecond) optical excitation on the nanoscale. We have proposed and theoretically developed a distinct approach to solving this fundamental problem [29-35]. This approach, based on the using the relative phase of the light pulse as a functional degree of freedom, allows one to control the spatio-temporal distribution of the excitation energy on the nanometer-femtosecond scale. One of the most fundamental problems in nanoplasmonics and nanooptics generally is the spatio-temporal coherent control of nanoscale localization of optical energy. However, a key element was missing: an efficient and robust method to determine a shape of the controlling femtosecond pulse that would compel the femtosecond evolution of the nanoscale optical fields in a plasmonic system to result in the spatio-temporal concentration of the optical energy at a given nano-site within a required femtosecond interval of time.

We have solved this problem by using the idea of the time-reversal [36, 37]. We have shown that by exciting a system at a given spot, recording the produced wave in one direction in the far zone, time reversing it and sending the produced plane wave back to the system leads to the required spatio-temporal energy localization. This method can be used both

theoretically and experimentally to determine the required polarization, phase and amplitude modulation of the controlling pulses. Recently our idea of the time-reversal coherent control has been successfully tested in the microwave region experimentally [38]. Another significant development has been an ultrafast coherent control of the third-harmonic generation from a nanophotonic-plasmonic system [5]. This has been carried out in collaboration with University of Stuttgart and Max Planck Institute for Solid State Physics (Stuttgart, Germany).

2.9 Attosecond Nanoplasmonics [15, 19]

In collaboration with M. Kling, U. Kleineberg, and F. Krausz et al. from Max Planck Institute for Quantum Optics (Garching, Germany) and Ludwig Maximilian University (Munich, Germany), we have theoretically developed a novel concept called Attosecond Nanoplasmonic Field Microscope [39]. There has been a recent progress in this direction [15].

2.10 Directions of Work for the Next Period

We will develop the success in the optics of ultrastrong and ultrafast fields on the nanoscale. We have already developed a preliminary theory of the metallization of dielectric nanofilms by ultrafast (single-oscillation) optical fields [4]. One of the most important future directions will be the inclusion of phase-controlled attosecond pulses to study the metallization phenomena. We are also developing theory of metallization of bulk dielectrics by ultrastrong fields, which can be considered as a dynamic, ultrafast generalization of Zener's breakdown. The research mentioned above in this Section is being conducted in a close collaboration with the group of Prof. F. Krausz of the Max Planck Institute for Quantum Optics (Garching at Munich, Germany). We are also actively developing our collaboration with Italian Institute of Technology, group of Prof. E. Di Fabrizio. This work is directed to the achievement of control over the optical energy concentration and electron excitations in nanoplasmonic tapers. It has a great fundamental potential and promises important applications to nanoscopy.

References

1. S. Zherebtsov, T. Fennel, J. Plenge, E. Antonsson, I. Znakovskaya, A. Wirth, O. Herrwerth, F. Suessmann, C. Peltz, I. Ahmad, S. A. Trushin, V. Pervak, S. Karsch, M. J. J. Vrakking, B. Langer, C. Graf, M. I. Stockman, F. Krausz, E. Rühl, and M. F. Kling, *Controlled near-Field Enhanced Electron Acceleration from Dielectric Nanospheres with Intense Few-Cycle Laser Fields*, Nature Physics (2011). DOI: 10.1038/NPHYS1983.
2. M. I. Stockman, *Spaser Action, Loss Compensation, and Stability in Plasmonic Systems with Gain*, Phys. Rev. Lett. **106**, 156802-1-4 (2011). DOI: 10.1103/PhysRevLett.106.156802.
3. M. I. Stockman, *Nanoplasmonics: The Physics Behind the Applications*, Phys Today **64**, 39-44 (2011). DOI: 10.1063/1.3554315.
4. M. Durach, A. Rusina, M. Kling, and M. I. Stockman, *Ultrafast Dynamic Metallization of Dielectric Nanofilms by Strong Single-Cycle Optical Fields*, arXiv:1104.1642 (2011).
5. T. Utikal, M. I. Stockman, A. P. Heberle, M. Lippitz, and H. Giessen, *All-Optical Control of the Ultrafast Dynamics of a Hybrid Plasmonic System*, Phys. Rev. Lett. **104**, 113903-1-4 (2010). DOI: 10.1103/PhysRevLett.104.113903.
6. M. I. Stockman, *A Fluctuating Fractal Nanoworld*, Physics **3**, 90 (2010). DOI: 10.1103/Physics.3.90.
7. M. I. Stockman, *Dark-Hot Resonances*, Nature **467**, 541-542 (2010).
8. M. I. Stockman, *The Spaser as a Nanoscale Quantum Generator and Ultrafast Amplifier*, Journal of Optics **12**, 024004-1-13 (2010). doi: 10.1088/2040-8978/12/2/024004.
9. A. Rusina, M. Durach, and M. Stockman, *Theory of Spoof Plasmons in Real Metals*, Appl. Phys. A **100**, 375-1-4 (2010). DOI: 10.1007/s00339-010-5866-y.
10. M. Durach, A. Rusina, M. F. Kling, and M. I. Stockman, *Metallization of Nanofilms in Strong Adiabatic Electric Fields*, Phys. Rev. Lett. **105**, 086803-1-4 (2010).
11. A. Boardman, M. Brongersma, M. Stockman, and M. Wegener, *Plasmonics and Metamaterials: Introduction*, J. Opt. Soc. Am. B **26**, PM1-PM1 (2009). doi:10.1364/JOSAB.26.000PM1.
12. M. Durach, A. Rusina, and M. I. Stockman, *Giant Surface Plasmon Induced Drag Effect (Spider) in Metal Nanowires*, arXiv:0907.1621, 1-5 (2009). <http://arxiv.org/abs/0907.1621>.
13. M. Durach, A. Rusina, and M. I. Stockman, *Giant Surface-Plasmon-Induced Drag Effect in Metal Nanowires*, Phys. Rev. Lett. **103**, 186801-1-4 (2009).
14. A. S. Kirakosyan, M. I. Stockman, and T. V. Shahbazyan, *Surface Plasmon Lifetimes in Metal Nanoshells*, ArXiv:0908.0647 (2009).

15. J. Q. Lin, N. Weber, A. Wirth, S. H. Chew, M. Escher, M. Merkel, M. F. Kling, M. I. Stockman, F. Krausz, and U. Kleineberg, *Time of Flight-Photoemission Electron Microscope for Ultrahigh Spatiotemporal Probing of Nanoplasmonic Optical Fields*, *J. Phys.: Condens. Matter* **21**, 314005-1-7 (2009). doi:10.1088/0953-8984/21/31/314005.
16. K. F. MacDonald, Z. L. Samson, M. I. Stockman, and N. I. Zheludev, *Ultrafast Active Plasmonics*, *Nat. Phot.* **3**, 55-58 (2009).
17. M. I. Stockman, *Spaser as Nanoscale Quantum Generator and Ultrafast Amplifier*, arXiv:0908.3559 (2009).
18. M. I. Stockman and D. J. Bergman, *Surface Plasmon Amplification by Stimulated Emission of Radiation (Spaser) [US Patent 7,569,188]*, USA Patent No. 7,569,188 (August 4, 2009).
19. M. I. Stockman, M. F. Kling, U. Kleineberg, and F. Krausz, *Attosecond Nanoplasmonic Field Microscope*, in *Ultrafast Phenomena XVI (Proceedings of the 16th International Conference, Palazzo Dei Congressi Stresa, Italy, June 9-13, 2008)*, edited by P. Corkum, S. D. Silvestri, K. A. Nelson, E. Riedle and R. W. Schoenlein (Springer, Heidelberg, London, New York, 2009), p. 696-698.
20. V. M. Shalaev, *Optical Negative-Index Metamaterials*, *Nat. Phot.* **1**, 41-48 (2007).
21. S. Xiao, V. P. Drachev, A. V. Kildishev, X. Ni, U. K. Chettiar, H.-K. Yuan, and V. M. Shalaev, *Loss-Free and Active Optical Negative-Index Metamaterials*, *Nature* **466**, 735-738 (2010). <http://www.nature.com/nature/journal/v466/n7307/abs/nature09278.html#supplementary-information>.
22. D. J. Bergman and M. I. Stockman, *Surface Plasmon Amplification by Stimulated Emission of Radiation: Quantum Generation of Coherent Surface Plasmons in Nanosystems*, *Phys. Rev. Lett.* **90**, 027402-1-4 (2003).
23. M. I. Stockman and D. J. Bergman, in Proceedings of SPIE: Complex Mediums IV: Beyond Linear Isotropic Dielectrics, edited by M. W. McCall and G. Dewar, *Surface Plasmon Amplification through Stimulated Emission of Radiation (Spaser)* (SPIE, San Diego, California, 2003), Vol. 5221, p. 93-102.
24. D. J. Bergman and M. I. Stockman, *Can We Make a Nanoscopic Laser?*, *Laser Phys.* **14**, 409-411 (2004).
25. K. Li, X. Li, M. I. Stockman, and D. J. Bergman, *Surface Plasmon Amplification by Stimulated Emission in Nanolenses*, *Phys. Rev. B* **71**, 115409-1-4 (2005).
26. M. T. Hill, M. Marell, E. S. P. Leong, B. Smalbrugge, Y. Zhu, M. Sun, P. J. van Veldhoven, E. J. Geluk, F. Karouta, Y.-S. Oei, R. Nötzel, C.-Z. Ning, and M. K. Smit, *Lasing in Metal-Insulator-Metal Sub-Wavelength Plasmonic Waveguides*, *Opt. Express* **17**, 11107-11112 (2009).
27. R. F. Oulton, V. J. Sorger, T. Zentgraf, R.-M. Ma, C. Gladden, L. Dai, G. Bartal, and X. Zhang, *Plasmon Lasers at Deep Subwavelength Scale*, *Nature* **461**, 629-632 (2009). doi:10.1038/nature08364.
28. M. A. Noginov, G. Zhu, A. M. Belgrave, R. Bakker, V. M. Shalaev, E. E. Narimanov, S. Stout, E. Herz, T. Suteewong, and U. Wiesner, *Demonstration of a Spaser-Based Nanolaser*, *Nature* **460**, 1110-1112 (2009).
29. M. I. Stockman, S. V. Faleev, and D. J. Bergman, *Coherent Control of Femtosecond Energy Localization in Nanosystems*, *Phys. Rev. Lett.* **88**, 67402-1-4 (2002).
30. M. I. Stockman, S. V. Faleev, and D. J. Bergman, *Coherently Controlled Femtosecond Energy Localization on Nanoscale*, *Appl. Phys. B* **74**, S63-S67 (2002).
31. M. I. Stockman, S. V. Faleev, and D. J. Bergman, *Coherently-Controlled Femtosecond Energy Localization on Nanoscale*, *Appl. Phys. B* **74**, 63-67 (2002).
32. M. I. Stockman, D. J. Bergman, and T. Kobayashi, in Proceedings of SPIE: Plasmonics: Metallic Nanostructures and Their Optical Properties, edited by N. J. Halas, *Coherent Control of Ultrafast Nanoscale Localization of Optical Excitation Energy* (SPIE, San Diego, California, 2003), Vol. 5221, p. 182-196.
33. M. I. Stockman, S. V. Faleev, and D. J. Bergman, in Ultrafast Phenomena XIII, *Coherently-Controlled Femtosecond Energy Localization on Nanoscale* (Springer, Berlin, Heidelberg, New York, 2003).
34. M. I. Stockman, D. J. Bergman, and T. Kobayashi, *Coherent Control of Nanoscale Localization of Ultrafast Optical Excitation in Nanosystems*, *Phys. Rev. B* **69**, 054202-10 (2004).
35. M. I. Stockman and P. H. Hwang, *Nanocalibrated Nonlinear Electron Photoemission under Coherent Control*, *Nano Lett.* **5**, 2325-2329 (2005).
36. X. Li and M. I. Stockman, *Time-Reversal Coherent Control in Nanoplasmonics*, arXiv:0705.0553 (2007).
37. X. Li and M. I. Stockman, *Highly Efficient Spatiotemporal Coherent Control in Nanoplasmonics on a Nanometer-Femtosecond Scale by Time Reversal*, *Phys. Rev. B* **77**, 195109-1-10 (2008).
38. F. Lemoult, G. Lerosey, J. de Rosny, and M. Fink, *Resonant Metalenses for Breaking the Diffraction Barrier*, *Phys. Rev. Lett.* **104**, 203901-1-4 (2010). Doi 10.1103/Physrevlett.104.203901.
39. M. I. Stockman, M. F. Kling, U. Kleineberg, and F. Krausz, *Attosecond Nanoplasmonic Field Microscope*, *Nat. Phot.* **1**, 539-544 (2007). doi:10.1038/nphoton.2007.169.

Laser-Produced Coherent X-Ray Sources

Donald Umstadter, *Physics and Astronomy Department, 257 Behlen Laboratory, University of Nebraska, Lincoln, NE 68588-0111, dpu@unlserve.unl.edu*

Program Scope

In this project, we experimentally and theoretically explore the physics of novel x-ray sources, based on the interactions of ultra-high-intensity laser light with matter. Laser-accelerated electron beams are used to produce x-rays in the energy range 1-100 keV using techniques such as Thomson scattering off a second laser pulse, or betatron oscillations in a laser-produced ion channel. Such photon sources can provide information on the structure of matter with atomic-scale resolution, on both the spatial and temporal scale lengths—simultaneously. Moreover, because the electron beam is accelerated by the ultra-high gradient of a laser-driven wakefield, the combined length of both the accelerator and wiggler regions is only a few millimeters. The x-ray source design parameters are sub-angstrom wavelength, femtosecond pulse duration, and university-laboratory—scale footprint. The required components, laser system (delivering peak power >100 TW at a repetition rate of 10 Hz) and electron accelerator (delivering beams with energy up to 800 MeV and divergence of 2 mrad) have been developed and characterized.

This project involves the physics at the forefront of relativistic plasma physics and beams, as well as relativistic nonlinear optics. Applications include the study of ultrafast chemical, biological and physical processes, such as inner-shell electronic or phase transitions. Industrial applications include non-destructive evaluation, large-standoff—distance imaging of cracks, remote sensing and the detection of shielded nuclear materials.

Recent Results

Improvement of the laser wakefield accelerator by controlling the energy spread and tunability

The quality of electron-beam-driven x-rays obviously depends critically on the quality of the electron-beam driver. For this reason we invested considerable effort into improving our understanding of, and control of, the electron beam dynamics in laser-wakefield accelerators (LWA).

Our table-top-sized laser wakefield electron accelerator is based on the focusing of high-power (20 - 100 TW), short pulses (30 fs) of light onto mm-cm long supersonic helium gas jets. The focused laser pulse, with intensity 10^{18} - 10^{19} W cm⁻², ionizes the medium and drives relativistic plasma waves. Electrons are self-injected into the plasma wave, and accelerated by strong longitudinal GeV cm⁻¹ electrostatic fields. The resulting electron beams have excellent characteristics in terms of stability (energy and pointing), energy spread, charge, and divergence as well as negligible dark current. Even greater stability and tunability is obtained by optically injecting electrons into the wakefield using a counter propagating injection pulse.

A detailed parametric study was used to control the energy spread of the electron beams and tune the electron energy over a broad range. The energy resolution is better than 10% at 300 MeV, and rapidly degrades beyond 400 MeV.

The position of the laser focal plane with respect to the nozzle was kept constant over the entire series of shots. The evolution of single-shot energy spectra is presented in Fig. 1. Multi-shot electron beam statistics for each set of parameters are summarized in Table 1. The dark current component of the beam is quantified by computing the *contrast*, defined as the ratio of the charge within the FWHM of the quasi-monoenergetic peak to the total charge on the LANEX. If significant dark current is present, the contrast would be low, and vice versa. As demonstrated by the data of column C of Table 1, the optimal beams have the highest contrast, 0.75 (same as for an ideal Gaussian distribution). Hence, all the charge is contained in the monoenergetic peak, with no detectable charge at other energies – the beam is dark-current-free. The presence of a low-energy tail noticeably reduces the contrast; at higher densities, when the beam becomes polychromatic, the contrast is the lowest.

This near-threshold operating regime is scalable: an optimal density can be found for different

laser powers, and acceleration lengths, leading to a stable, dark-current-free, quasi-monoenergetic electron beam (similar to that shown in Fig.1(d)). Example of such optimal beams obtained over a broad range of laser, and plasma parameters are shown in Fig.2.

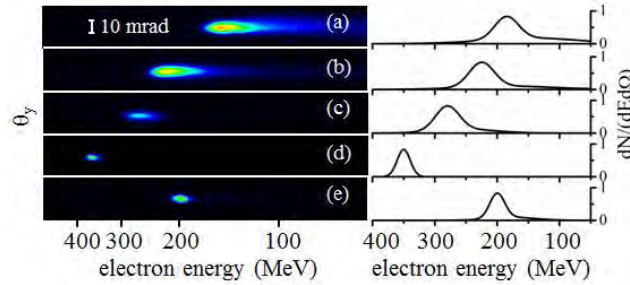


Figure 1: Spectrally dispersed electron beams at the exit of magnetic spectrometer and corresponding line outs of electron spectra, convolved using the GPT code, taking into account the spectrometer response function and electron beam divergence. Statistics and brightness for these beams are shown in Table 1. Panels (a)–(e) correspond to plasma densities 12; 9; 7.2; 6; or $4.8 \times 10^{18} \text{cm}^{-3}$, respectively. The jet length is 3 mm. The laser power on target is 42 TW.

The pointing stability of electron beams is found to be sensitive to the pulse contrast. Reduction of shot-to-shot pointing variation to a few milliradians requires nanosecond contrast of 2×10^{-8} , which is achieved by optimizing the timing of the Pockels cells in the laser chain, and the time delay between the pump, and seed beams in all amplification stages. Table 1 shows that the pointing angle fluctuation is below the beam divergence in the entire range of densities $(4.8 - 12) \times 10^{18} \text{cm}^{-3}$, which is opposite to the observations made in earlier experiments with high-density plasmas. At the optimal operational point, the measured pointing fluctuation reaches the minimum, ± 1.1 mrad.

	E	ΔE	D	P	Q	B	C
(a)	185	0.24	4.3	± 3	240	19	0.46
(b)	225	0.21	3.9	± 2.8	85	7.5	0.55
(c)	280	0.16	2.7	± 1.8	27	5.5	0.64
(d)	350	0.07	2.3	± 1.1	7	8.5	0.75
(e)	200	0.12	3.1	± 1.7	20	4.4	0.62

Table 1: Electron beam characteristics for the parameters of Fig.1 averaged over 10-30 shots; E is the central energy in MeV; $\Delta E/E$ is the normalized energy spread (FWHM); D is the FWHM divergence in mrad; P is the pointing stability in mrad; Q is the charge in pC; B is the brightness (per shot) in units of 10^{10} electrons $\text{MeV}^{-1} \text{mm}^{-2} \text{mrad}^{-2}$; and C is the ratio of the charge within FWHM in energy to the total beam charge. The measured beam charge fluctuation is 50%.

The results of Fig. 1 imply that a self-injection threshold corresponds to the laser power ten times higher than the critical power for relativistic self-focusing. In all cases presented in Fig.1 and 2, beam loading is too weak to suppress self-injection. Thus, the only way to terminate injection is to limit the plasma length. Reducing the plasma density slows focusing of the pulse, delaying formation of the bubble. Below the cutoff density, the bubble does not form during the laser transit through the plasma, and self-injection into the first bucket does not occur. At the optimal density, the bubble forms before the end of the plasma, experiences minimal evolution, and creates a quasi-monoenergetic electron bunch. The plasma ends before either the laser waist oscillates or pulse self-compresses; hence, injection into the bubble does not resume, and the continuous low-energy tail does not form.

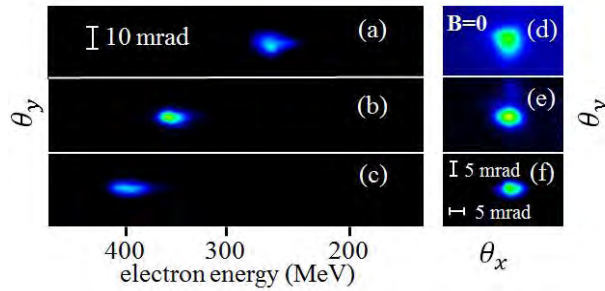


Figure 2: Images of spectrally dispersed (left) and undeflected (right) background-free electron beams as a function of laser power and plasma density: (a, d) $P = 34$ TW, $n_{e0} = 7.8 \times 10^{18} \text{ cm}^{-3}$; (b, e) $P = 42$ TW, $n_{e0} = 6 \times 10^{18} \text{ cm}^{-3}$; (c, f) $P = 58$ TW, $n_{e0} = 5.3 \times 10^{18} \text{ cm}^{-3}$; the halo in panel (b) is produced by low-energy background (< 10 MeV) present at high-densities, which is not seen after the magnet. Images (a) and (c) are obtained with a 3mm jet. Image (e) is obtained with a 4-mm jet and a higher-resolution spectrometer. θ_x and θ_y denote the divergence angle in the horizontal and vertical direction.

This interpretation has been confirmed with three-dimensional particle-in-cell (3D PIC) simulations using pre-ionized helium plasma with a trapezoidal profile (0.5-mm linear entrance, and exit ramps and a 2-mm plateau) and a Gaussian laser pulse with 42-TW power, central wavelength $0.805 \mu\text{m}$, duration 30 fs, and waist $13.6 \mu\text{m}$. In all simulations, the plasma extends from $z = 0$ to 3 mm. The simulated beam characteristics are found to be in good agreement with experimental observations, and confirm the postulated mechanism describe above.

Upgrade of laser system to the petawatt peak power level

Our laser facility has recently been upgraded to increase its power rate by a factor of ten. This project also featured a reduction of the laser pulse duration. The project supported applications of the laser, to improve the quality of laser-driven electron beams and x-rays, integrate radiation sources with suitable detectors and imaging techniques, and develop techniques for imaging through dense thicknesses of steel.

The central feature was the development of a petawatt high-energy laser amplifier, by the addition of a multi-pass amplifier and a pulse compression system for the amplified laser pulse. The original system comprised of an oscillator, stretcher, and 4 multi-pass amplifiers produced 5 J per pulse at 10-Hz repetition rate. The amplified pulse was compressed to 30-fs pulse duration in a standard two-grating pulse compressor and resulted in a peak power of > 100 TW. The laser system has been upgraded to the 1-PW peak power level with an additional power amplifier and pulse compressor. The upgrade to the system consists of the following: (a) high-energy pump lasers, (b) power amplifier, (c) pulse compressor, and (d) diagnostics.

At the 100 TW laser power level, the energy of the laser-wakefield accelerated electron beam was increased to 0.8 GeV, while maintaining the qualities of the lower energy beams (e.g., low angular divergence: 2 mrad). The electron and x-ray detection systems were cross-calibrated by means of an absolutely calibrated beam from a conventional accelerator.

Modeling of x-ray source and detection system

Schematic diagrams of the laser-driven monochromatic x-ray source system have been defined for use in modeling the detection system. An initial version of the Monte Carlo detector response model has been developed using MCNPX version 2.6.0. Cesium iodide emits an average of 54 visible photons per keV of energy deposited. This response will be used to calculate the CsI(Tl) detector response that will be measured by the CCD camera.

To model the x-ray source, we seek to identify optimal laser and electron beam parameters and benchmark ongoing experiments on the generation of x-rays from inverse Compton scattering of an intense laser field by a relativistic electron beam. To a 0th-order approximation, where the laser field is described by a monochromatic plane wave field and mono-energetic collimated electron beam, the efficiency of x-ray generation from inverse Compton scattering of an 800 nm laser light may be obtained with the formula given by

$$\frac{N_x}{N_e} = 127.8832 \times \frac{E_{\text{laser}} \text{ (J)}}{\pi \times s_0^2 \text{ (}\mu\text{m}^2\text{)'}}$$

where E_{laser} , s_0 , N_e , and N_x represent laser energy, laser focus beam waist radius, number of electrons and x-ray photons, respectively. The most striking implication of this 0th-order estimate is that the number of Compton scattered x-ray photons is independent of the scattering laser pulse temporal width and depends solely on the energy flux of the scattering laser field. With the aid of this simple formula we deduce the highest number of x-ray photons which are generated by using the maximum possible laser energy focused to a spot size as small as the electron beam size and choosing the laser pulse duration such that the laser strength parameter, $a_0 < 1$. For instance, a x-ray photon number of the order of 10^9 could be generated from the scattering of an 800-nm, 25-J, 10- μm (FWHM) laser focus by a relativistic electron beam that has a charge of 10 pC.

It is clear that treating the laser as a monochromatic plane wave field, and the electron beam as a mono-energetic and collimated beam, is an idealization; the validity of these approximations has to be checked for given realistic experimental electron and laser beam parameters. To check the validity of these idealizations, and benchmark realistic experimental conditions, we have developed an exact and fully relativistic three-dimensional x-ray source model. In the model, the laser field could be calculated with high degree of accuracy (without the plane wave approximation), and parameters of the electron beam could be imported from experimental measurements of the LWA. The code has already been benchmarked against the 0th-order analytic solutions of inverse Compton scattering, and has been proven to be consistent.

The optimal laser and electron beam parameters required for x-ray generation have been analytically determined. Work has been completed on the single particle model. Optimizing the multiple-particle model, by developing binning and interpolating algorithms to increase the computational efficiency, is currently under way.

Future efforts

We will model and calibrate our x-ray detection over the range of experimental x-ray parameters.

Further, we will study the effects of finite electron-beam size on x-ray efficiency, such as: a) finite temporal duration of the scattering laser pulse, b) 3-dimensional focused geometry, c) electron-beam energy spread, d) electron-beam divergence, e) temporal width of the electron beam.

Besides continuing our research on the development of ultrashort x-ray probes, we also intend to apply our newly improved laser capability to the study high-field physics in the highly relativistic regime.

DOE-Sponsored Publications (published within last three years)

1. S.Y. Kalmykov et al., "Electron self-injection into an evolving plasma bubble: Quasi-monoenergetic laser-plasma acceleration in the blowout regime," *Phys. Plasmas* **18**, 056704 (2011).
2. V. Ramanathan, S. Banerjee, N. Powers et al., "Sub-millimeter-resolution radiography of shielded structures with laser-accelerated electron beams," *Phys. Rev. ST Accel. Beams* **13**, 104701 (2010).
3. D. Umstadter, S. Banerjee, V. Ramanathan et al., "Development of a source of quasi-monochromatic MeV energy photons," CP1099, *Application of Accelerators in Research and Industry: 20th International Conference*, edited by F. D. McDaniel and B. L. Doyle (AIP, 2009), p. 606.

Cold and ultracold polar molecules

Jun Ye

JILA, National Institute of Standards and Technology and University of Colorado

Boulder, Colorado 80309-0440

Ye@jila.colorado.edu

Below I discuss a number of recent breakthroughs in the study and control of cold and ultracold polar molecules over the last 12 months.

In joint work with Debbie Jin and building on the previous success of producing a rovibronic ground-state molecular quantum gas in a single hyperfine state, we have demonstrated quantum stereodynamics of ultracold bimolecular reactions. We achieve suppression of the bimolecular chemical reaction rate by nearly two orders of magnitude when we use an optical lattice trap to confine the fermionic polar molecules in a quasi-two-dimensional, pancake-like geometry, with the dipoles oriented along the tight confinement direction. With the combination of sufficiently tight confinement and Fermi statistics of the molecules, two polar molecules can approach each other only in a ‘side-by-side’ collision under repulsive dipole–dipole interactions. The suppression of chemical reactions is a prerequisite for the realization of new molecule-based quantum systems.

We have recently loaded ultracold KRb molecules into a three dimensional optical lattice and demonstrated a dipole-moment-independent lifetime exceeding 25 s, limited only by photon scattering of the trapping light. We have also measured the real part of the complex polarizability of molecules confined in our optical trap. This knowledge has allowed us to achieve control of molecular rotations at long coherence times.

On the cold molecule work, we have studied for the first time dipolar effects for hetero-molecular collisions. This work is in collaboration with John Doyle of Harvard. By combining for the first time the techniques of Stark deceleration, magnetic trapping, and cryogenic buffer gas cooling, we have made the first experimental observation of cold collisions between two different species of state-selected neutral polar molecules. This has enabled an absolute measurement of the total trap loss cross sections between OH and ND₃ at a mean collision energy of 5 K. Due to the dipolar interaction, the total cross section increases upon application of an external polarizing electric field. Cross sections computed from *ab initio* potential energy surfaces are in good agreement with the measured value at zero external electric field.

To study the effect on dipolar collisions by different orientation configurations (OH and ND₃ can be polarized parallel or anti-parallel with respect to each other), we have made a systematic study of coherent population transfer of OH molecules from one of its Lambda-doublet states to the other, thus flipping its dipole orientation. In fact, cold and ultracold polar molecules with nonzero electronic angular momentum such as OH are of great interest to the community. However, in mixed electric and magnetic fields, these molecules are generically subject to a large set of avoided crossings among their Zeeman sublevels; in magnetic traps, these crossings lead to distorted potentials and trap losses. We have characterized these crossings in OH by microwave-pumping trapped OH molecules from the electrically weak field-seeking state (upper doublet state) to the strong-field seeking state (lower doublet state) under an applied electric bias field. Our observations are very well described by a simple Landau-Zener model.

Publications:

D. S. Jin and J. Ye, "Polar molecules in the quantum regime," *Physics Today* 64, 27 – 31 (May, 2011). (Invited Review)

M. H. G. de Miranda, A. Choat, B. Neyenhuis, D. Wang, G. Quémener, S. Ospelkaus, J. L. Bohn, J. Ye, and D. S. Jin, "Controlling the quantum stereodynamics of ultracold bimolecular reactions," *Nature Phys.* 7, 502 – 507 (2011).

B. C. Sawyer, B. K. Stuhl, M. Yeo, T. V. Tscherbul, M. T. Hummon, Y. Xia, J. Klos, D. Patterson, J. M. Doyle, and J. Ye, "Cold heteromolecular dipolar collisions," *Phys. Chem. Chem. Phys.*, in press (2011).

*Author Index
and
List of Participants*

Principal Investigator Index

Agostini, P.	3, 141,145
Becker, A.	52,101
Belkacem, A.	32, 63, 64, 73
Ben-Itzhak, I.	21, 23, 24, 31, 32, 53
Berrah, N.	2, 3, 5, 105
Bogan, M.	83, 94
Bohn, J.	109
Bucksbaum, P.	2, 3, 83, 86, 90
Buth, C.	1, 6, 7, 8, 9
Centurion, M.	113
Chang, Z.	21, 27, 28
Chu, S.I.	117
Cocke, C.L.	21, 31, 32, 53
Côté, R.	121
Cundiff, S.T.	125
Dalgarno, A.	129
Dantus, M.	133
DeMille, D.	137
DiMauro, L.	2, 3, 4, 141, 145
Ditmire, T.	149
Doumy, G.	1, 2, 3, 4, 5, 10, 11, 12
Doyle, J.	153
Dunford, R.W.	1, 12, 14
Dürr, H.	15, 83, 92
Eberly, J.H.	157
Elser, V.	161
Esry, B.D.	21, 23, 35
Feagin, J.M.	165
Gaffney, K.	83, 98
Gallagher, T.F.	169
Gessner, O.	73
Gould, P.	173
Greene, C.H.	177
Gühr, M.	83, 90
Haxton, D.	63
Head-Gordon, M.	73
Ho, T.S.	249
Jones, R.R.	181
Kanter, E.P.	1, 2, 3, 5, 10, 11, 12, 14
Kapteyn, H.C.	185, 221
Klimov, V.	59
Kling, M.	21, 24, 31, 32, 39, 53
Krässig, B.	1, 2, 3, 5, 10, 11, 14
Kumarappan, V.	21, 43
Landers, A.	32, 189
Leone, S.	73
Lin, C.D.	21, 47
Lindenberg, A.	83
Lucchese, R.	245
Lundeen, S.R.	193
Macek, J.H.	197

Principal Investigator Index

Manson, S.T.	201
Martínez, T.J.	83, 90
Matsika, S.	205
McCurdy, C.W.	63, 68, 73
McKoy, V.	209
Miller, T.A.	145
Msezane, A.Z.	213
Mukamel, S.	217
Murnane, M.M.	185, 221
Nelson, K.A.	221
Neumark, D.	73
Novotny, L.	225
Orel, A.E.	32, 229
Orlando, T.M.	233
Ourmazd, A.	237
Pelton, M.	13
Phaneuf, R.A.	241
Poliakoff, E.	245
Rabitz, H.	249
Raman, C.	253
Reis, D.	2, 3, 15, 83, 86
Rescigno, T.N.	32, 63, 68
Robicheaux, F.	255
Rocca, J.J.	259
Rose-Petruck, C.G.	15, 263
Santra, R.	2, 3, 5, 6, 9, 14
Scherer, N.	13
Schoenlein, R.W.	73
Schwander, P.	237
Seideman, T.	267
Seidler, G.T.	271
Southworth, S.H.	1, 2, 5, 10, 11, 12, 14, 15
Starace, A.F.	275
Stockman, M.I.	279
Stöhr, J.	83
Thumm, U.	21, 28, 31, 51
Trallero, C.A.	21, 55
Umstadter, D.	283
Weber, Th.	63, 64, 73
Weinacht, T.	205
Ye, J.	287
Young, L.	1, 2, 3, 5, 6, 10, 11, 12, 13, 14, 15

Participants

Pierre Agostini
Ohio State University
191 W. Woodruff Ave.
Columbus, OH 43210
Phone: 614-247-4734
E-Mail: agostini@mps.ohio-state.edu

Paul Baker
Army Research Office
4300 S. Miami Blvd.
Durham, NC 27703-9142
Phone: 919-549-4202
E-Mail: Paul.M.Baker1@us.army.mil

Andreas Becker
JILA and Department of Physics
440 UCB, University of Colorado
Boulder, CO 80309-0440
Phone: 303-492-7825
E-Mail: andreas.becker@colorado.edu

Ali Belkacem
Lawrence Berkeley National Laboratory
Mail Stop 2R0100
Berkeley, CA 94720
Phone: 510-486-7778
E-Mail: abelkacem@lbl.gov

Michael Bogan
SLAC National Accelerator Laboratory
2575 Sand Hill Road
Menlo Park, CA 94025
Phone: 650-926-2731
E-Mail: mbogan@slac.stanford.edu

John Bohn
JILA
UCB 440
Boulder, CO 80305
Phone: 202-492-5426
E-Mail: bohn@murphy.colorado.edu

Philip Bucksbaum
Stanford PULSE Institute
SLAC, 2575 Sand Hill Road, M.S. 59
Menlo Park, CA 94025
Phone: 650-926-5337
E-Mail: phb@slac.stanford.edu

Christian Buth
Argonne National Laboratory
9700 South Cass Avenue
Argonne, IL 60439
Phone: 630-252-1397
E-Mail: cbuth@anl.gov

Michael Casassa
Department of Energy
19901 Germantown Rd.
Germantown, MD 20874
Phone: 301-903-0448
E-Mail: michael.casassa@science.doe.gov

Martin Centurion
University of Nebraska - Lincoln
Jorgensen Hall, 855 North 16th Street
Lincoln, NE 68588
Phone: 402-472-5810
E-Mail: mcenturion2@unl.edu

Zenghu Chang
KSU and UCF
4000 Central Florida Blvd., PS430
Orlando, FL 32816
Phone: 407-823-4442
E-Mail: Zenghu.Chang@ucf.edu

Shih-I Chu
University of Kansas
Department of Chemistry, Malott Hall
Lawrence, KS 66045
Phone: 785-864-4094
E-Mail: sichu@ku.edu

Participants

C.L. Cocke
Kansas State University
Physics Dept., , Cardwell Hall
Manhattan, KS 66506
Phone: 785-532-1609
E-Mail: cocke@phys.ksu.edu

Robin Côté
University of Connecticut
2152 Hillside Road, U-3046
Storrs, CT 06269
Phone: 860-486-4912
E-Mail: rcote@phys.uconn.edu

Steven Cundiff
JILA
440 UCB
Boulder, CO 80309
Phone: 303-492-7858
E-Mail: cundiff@jila.colorado.edu

Marcos Dantus
Michigan State University
58 Chemistry Building
East Lansing, MI 48823
Phone: 517-881-4562
E-Mail: dantus@msu.edu

Matthew DeCamp
University of Delaware
217 Sharp Laboratory
Newark, DE 19716
Phone: 302-831-2671
E-Mail: mdecamp@udel.edu

David DeMille
Yale University
Physics Dept., P.O. Box 208120
New Haven, CT 06520
Phone: 203-432-3833
E-Mail: david.demille@yale.edu

Louis DiMauro
The Ohio State University
191 W. Woodruff Ave. #4178
Columbus, OH 43210
Phone: 614-688-5726
E-Mail: jackson.1926@osu.edu

Todd Ditmire
University of Texas at Austin
1 University Station #C1600
Austin, TX 78712
Phone: 512-471-3296
E-Mail: tditmire@physics.utexas.edu

Gilles Doumy
Argonne National Laboratory
9700 S. Cass Ave.
Argonne, IL 60439
Phone: 630-252-2588
E-Mail: gdoumy@aps.anl.gov

John Doyle
Harvard University
17 Oxford St.
Cambridge, MA 02138
Phone: 617-495-3201
E-Mail: doyle@physics.harvard.edu

Robert Dunford
Argonne National Laboratory
9700 S. Cass Ave.
Argonne, IL 60439
Phone: 630-252-4052
E-Mail: dunford@anl.gov

Joseph Eberly
University of Rochester
600 Wilson Blvd.
Rochester, NY 14627
Phone: 585-275-4351
E-Mail: eberly@pas.rochester.edu

Veit Elser
Cornell University
426 PSB
Ithaca, NY 14853
Phone: 607-255-2340
E-Mail: ve10@cornell.edu

Brett Esry
J.R. Macdonald Lab, Kansas State
University
116 Cardwell Hall
Manhattan, KS 66506
Phone: 785-532-1620
E-Mail: esry@phys.ksu.edu

Participants

Roger Falcone
Lawrence Berkeley National Laboratory
One Cyclotron Road Mailstop 80R0114
Berkeley, CA 94720
Phone: 510-486-6692
E-Mail: RWFalcone@lbl.gov

Jim Feagin
California State University, Fullerton
800 North State College Blvd.
Fullerton, CA 92834
Phone: 657-278-4827
E-Mail: jfeagin@fullerton.edu

Kelly Gaffney
SLAC and Stanford University
2575 Sand Hill Road
Menlo Park, CA 94306
Phone: 650-926-2382
E-Mail: kgaffney@slac.stanford.edu

Thomas Gallagher
University of Virginia
Department of Physics
Charlottesville, VA 22904
Phone: 434-924-6817
E-Mail: tfg@virginia.edu

Oliver Gessner
Lawrence Berkeley National Laboratory
1 Cyclotron Rd.
Berkeley, CA 94720
Phone: 510-486-6929
E-Mail: ogessner@lbl.gov

Phillip Gould
University of Connecticut
Physics Dept. U-3046, 2152 Hillside Rd.
Storrs, CT 06269-3046
Phone: 860-486-2950
E-Mail: phillip.gould@uconn.edu

Chris Greene
University of Colorado
JILA
Boulder, CO 80309-0440
Phone: 303-731-2824
E-Mail: chris.greene@colorado.edu

Daniel Haxton
Lawrence Berkeley National Laboratory
1 Cyclotron Road Mail Stop 2R0100
Berkeley, CA 94720
Phone: 415-412-9508
E-Mail: djhaxton@lbl.gov

Robert Jones
University of Virginia
382 McCormick Road
Charlottesville, VA 22904-4714
Phone: 434-924-3088
E-Mail: bjones@virginia.edu

Elliot Kanter
Argonne National Laboratory
X-ray Science Division
Argonne, IL 60439
Phone: 908-617-1622
E-Mail: kanter@anl.gov

Henry Kapteyn
JILA, University of Colorado at Boulder
UCB 440
Boulder, CO 80309
Phone: 303-492-8198
E-Mail: kapteyn@jila.colorado.edu

Victor Klimov
Los Alamos National Laboratory
MS-J567, Chemistry Division
Los Alamos, NM 87545
Phone: 505-661-6161
E-Mail: klimov@lanl.gov

Matthias Kling
Kansas State University
116 Cardwell Hall
Manhattan, KS 66506
Phone: 785-532-6786
E-Mail: kling@phys.ksu.edu

Bertold Kraessig
Argonne National Laboratory
437 7th Ave
La Grange, IL 60525
Phone: 708-482-3891
E-Mail: kraessig@anl.gov

Participants

Jeffrey Krause
Department of Energy
19901 Germantown Rd.
Germantown, MD 20874
Phone: 301-903-5827
E-Mail: Jeff.Krause@science.doe.gov

Vinod Kumarappan
Kansas State University
328 Cardwell Hall
Manhattan, KS 66506
Phone: 785-532-3415
E-Mail: vinod@phys.ksu.edu

Allen Landers
Auburn University
206 Allison Laboratory, Physics
Auburn, AL 36849
Phone: 334-844-4048
E-Mail: landers@physics.auburn.edu

Stephen Leone
Lawrence Berkeley National Laboratory
209 Gilman Hall
Berkeley, CA 94720
Phone: 510-643-5467
E-Mail: srl@berkeley.edu

Chii Dong Lin
Kansas State University
Department of Physics, Cardwell Hall
Manhattan, KS 66506
Phone: 785-532-1617
E-Mail: cdlin@phys.ksu.edu

Robert Lucchese
Texas A&M University
Department of Chemistry
College Station, TX 77843-3255
Phone: 979-845-0187
E-Mail: lucchese@mail.chem.tamu.edu

Stephen Lundeen
Colorado State University
Dept. of Physics, Colorado State Univ.
Fort Collins, CO 80523-1875
Phone: 970-491-6647
E-Mail: lundeen@lamar.colostate.edu

Joseph Macek
University of Tennessee
401 Nielsen Physics Bldg.
Knoxville, TN 37996-1200
Phone: 865-675-5541
E-Mail: jmacek@utk.edu

Steven Manson
Georgia State University
Dept. of Physics & Astronomy
Atlanta, GA 30303
Phone: 404-824-0625
E-Mail: smanson@gsu.edu

William McCurdy
Lawrence Berkeley National Laboratory
One Cyclotron Road
Berkeley, CA 94720
Phone: 510-486-4283
E-Mail: cwmccurdy@lbl.gov

Vincent McKoy
California Institute of Technology
120 Noyes, Caltech Chemistry 127-72
Pasadena, CA 91125
Phone: 626-395-6545
E-Mail: mckoy@caltech.edu

Terry Miller
Ohio State University
Dept. of Chemistry
Columbus, OH 43210
Phone: 614-292-2569
E-Mail: tamiller@chemistry.ohio-state.edu

Alfred Z. Msezane
Clark Atlanta University
223 James P. Brawley Dr. SW
Atlanta, GA 30314
Phone: 404-880-8663
E-Mail: amsezane@cau.edu

Shaul Mukamel
University of California, Irvine
1102 Natural Sciences II
Irvine, CA 92697-2025
Phone: 949-824-7600
E-Mail: smukamel@uci.edu

Participants

Margaret Murnane
JILA, Univ of Colorado at Boulder
UCB 440
Boulder, CO 80309
Phone: 303-492-8198
E-Mail: murnane@jila.colorado.edu

Keith Nelson
Massachusetts Institute of Technology
MIT Room 6-235
Cambridge, MA 02139
Phone: 617-253-1423
E-Mail: kanelson@mit.edu

Lukas Novotny
University of Rochester
The Institute of Optics
Rochester, NY 14627
Phone: 585-275-5767
E-Mail: novotny@optics.rochester.edu

Ann Orel
University of California, Davis
One Shields Ave.
Davis, CA 95616
Phone: 925-980-9245
E-Mail: aeorel@ucdavis.edu

Thomas Orlando
Georgia Institute of Technology
901 Atlantic Drive
Atlanta, GA 30332
Phone: 404-385-6047
E-Mail: nicole.williams@chemistry.gatech.edu

Abbas Ourmazd
University of Wisconsin
Physics, 1900 E. Kenwood Blvd.
Milwaukee, WI 53211
Phone: 414-229-2610
E-Mail: ourmazd@uwm.edu

Enrique Parra
Air Force Office of Scientific Research
875 North Randolph St., Suite 325
Arlington, VA 22203
Phone: 703-696-8571
E-Mail: enrique.parra@afosr.af.mil

Mark Pederson
Basic Energy Sciences
1000 Independence Ave., SW
Washington, DC 20585-1290
Phone: 301-903-9956
E-Mail: mark.pederson@science.doe.gov

Matthew Pelton
Argonne National Laboratory
9700 S. Cass Ave.
Argonne, IL 60439
Phone: 630-252-4598
E-Mail: pelton@anl.gov

Ronald Phaneuf
University of Nevada
Department of Physics
Reno, NV 89557-0220
Phone: 775-784-6818
E-Mail: phaneuf@unr.edu

Erwin Poliakoff
Louisiana State University
Chemistry Department
Baton Rouge, LA 70803
Phone: 225-578-2933
E-Mail: epoliak@lsu.edu

Herschel Rabitz
Princeton University
Frick Laboratory
Princeton, NJ 08544
Phone: 609-258-3917
E-Mail: hrabitz@princeton.edu

Chandra Raman
Georgia Institute of Technology
837 State St.
Atlanta, GA 30332-0430
Phone: 404-894-9062
E-Mail: craman@gatech.edu

Thomas Rescigno
Lawrence Berkeley National Laboratory
1 Cyclotron Rd. MS 2-100
Berkeley, CA 94720
Phone: 510-486-8652
E-Mail: tnrescigno@lbl.gov

Participants

Francis Robicheaux
Auburn University
206 Allison Lab
Auburn University, AL 36849
Phone: 334-844-4366
E-Mail: robicfj@auburn.edu

Jorge Rocca
Colorado State University
Dept. of Electrical and Computer Eng.
Fort Collins, CO 80523
Phone: 970-491-8371
E-Mail: rocca@engr.colostate.edu

Christoph Rose-Petruck
Brown University
324 Brook Street
Providence, RI 02912
Phone: 401-863-1533
E-Mail: crosepet@brown.edu

Robert Schoenlein
Lawrence Berkeley National Laboratory
1 Cyclotron Rd. MS: 80-114
Berkeley, CA 94720
Phone: 510-486-6557
E-Mail: rwschoenlein@lbl.gov

Tamar Seideman
Northwestern University
2145 Sheridan Road
Evanston, IL 60208-3113
Phone: 847-467-4979
E-Mail: t-seideman@northwestern.edu

Gerald Seidler
University of Washington
Box 351560
Seattle, WA 98195-1560
Phone: 206-427-8045
E-Mail: seidler@uw.edu

Stephen Southworth
Argonne National Laboratory
Bldg. 401
Argonne, IL 60439
Phone: 630-252-3894
E-Mail: southworth@anl.gov

Anthony F. Starace
University of Nebraska
855 North 16th St, 208 Jorgensen Hall
Lincoln, NE 68588-0299
Phone: 402-472-2795
E-Mail: astarace1@unl.edu

Mark Stockman
Georgia State University
29 Peachtree Center Ave.
Atlanta, GA 30302
Phone: 678-457-4739
E-Mail: mstockman@gsu.edu

Uwe Thumm
Kansas State University
Dept. of Physics
Manhattan, KS 66506
Phone: 785-532-1613
E-Mail: thumm@phys.ksu.edu

Carlos Trallero
J.R. Macdonald Lab
116 Cardwell Hall
Manhattan, KS 66506
Phone: 785-532-0846
E-Mail: trallero@phys.ksu.edu

Donald Umstadter
University of Nebraska-Lincoln
208 Jorgensen Hall
Lincoln, NE 68588-0299
Phone: 402-472-8115
E-Mail: dpu@hfsserve.unl.edu

Thorsten Weber
Lawrence Berkeley National Laboratory
1 Cyclotron Road
Berkeley, CA 94720
Phone: 510-486-5588
E-Mail: TWeber@lbl.gov

Thomas Weinacht
Stony Brook University
Dept. of Physics and Astronomy
Stony Brook, NY 11794-3800
Phone: 631-632-8163
E-Mail: thomas.weinacht@stonybrook.edu

Participants

Jun Ye
JILA, University of Colorado
440 UCB
Boulder, CO 80309-0440
Phone: 303-735-3171
E-Mail: ye@jila.colorado.edu

Linda Young
Argonne National Laboratory
9700 S. Cass Ave.
Argonne, IL 60439
Phone: 630-252-8878
E-Mail: young@anl.gov